

UNIVERSITA' DEGLI STUDI DI ROMA "LA SAPIENZA"



SAPIENZA
UNIVERSITÀ DI ROMA

Facoltà di Ingegneria Civile ed Industriale

Dip. di Ingegneria Aeronautica, Elettrica ed Energetica

Corso di Dottorato in Energia e Ambiente

**Predictive Modeling Analysis
of a Wet Cooling Tower**

**Adjoint Sensitivity Analysis, Uncertainty Quantification,
Data Assimilation, Model Calibration
Best-Estimate Predictions with Reduced Uncertainties**

Coordinatori:

Prof. Gianfranco Caruso

Prof. Antonio Naviglio

Supervisor:

Prof. Dan Gabriel Cacuci

Dottorando:

Federico Di Rocco

1258714

Anno Accademico 2016–2017

Contents

Abstract	1
1 Introduction	3
1.1 State-of-the-art of sensitivity and uncertainty analysis, data assimilation, model calibration, model validation, best-estimate predictions with reduced uncertainties	3
1.2 Aim and outline of the work	7
2 Description of the system	11
2.1 Context on cooling towers	11
2.2 Description of the cooling tower model	13
2.3 Governing equations of the mathematical models and cases selected	16
2.3.1 Mathematical Model for Case 1a: Natural Draft Cooling Tower operated in Saturated Outlet Air Condition, with Inlet Air Unsaturated	17
2.3.2 Mathematical Model for Case 1b: Natural Draft Cooling Tower operated in Saturated Outlet Air Condition, with Inlet Air Saturated	28
2.3.3 Mathematical Model for Case 2: Natural Draft Cooling Tower operated in Unsaturated Outlet Air Condition, with Inlet Air Unsaturated	34

CONTENTS

3	Description of the mathematical framework	40
3.1	Development of the Adjoint Sensitivity Model with the Adjoint Sensitivity Analysis Methodology (ASAM)	40
3.1.1	Development of the Cooling Tower Adjoint Sensitivity Model for Case 1a: Fan Off, Saturated Outlet Air Conditions, with Inlet Air Unsaturated	40
3.1.2	Development of the Cooling Tower Adjoint Sensitivity Model for Case 1b: Fan Off, Saturated Outlet Air Conditions, with Inlet Air Saturated	53
3.1.3	Development of the Cooling Tower Adjoint Sensitivity Model for Case 2: Fan Off, Unsaturated Air Conditions	62
3.2	Data assimilation, model calibration and best-estimate predictions with reduced uncertainties: Predictive Modeling for Coupled Multi-Physics Systems (PM_CMPS)	70
4	Results	78
4.1	Adjoint Sensitivity Analysis of the cooling tower cases of interest	78
4.1.1	Adjoint Sensitivity Analysis of Case 1a: Fan Off, Saturated Outlet Air Conditions, with Inlet Air Unsaturated	80
4.1.1.1	Relative sensitivities of the outlet air temperature, $T_a^{(1)}$	80
4.1.1.2	Relative sensitivities of the outlet water temperature, $T_w^{(50)}$	82
4.1.1.3	Relative sensitivities of the outlet water mass flow rate, $m_w^{(50)}$	83
4.1.1.4	Relative sensitivities of the outlet air relative humidity, $RH^{(1)}$	83
4.1.1.5	Relative sensitivities of the air mass flow rate, m_a	84

CONTENTS

4.1.2	Adjoint Sensitivity Analysis of Case 1b: Fan Off, Saturated Outlet Air Conditions, with Inlet Air Saturated	86
4.1.2.1	Relative sensitivities of the outlet air temperature, $T_a^{(1)}$	86
4.1.2.2	Relative sensitivities of the outlet water temperature, $T_w^{(50)}$	88
4.1.2.3	Relative sensitivities of the outlet water mass flow rate, $m_w^{(50)}$	89
4.1.2.4	Relative sensitivities of the outlet air relative humidity, $RH^{(1)}$	89
4.1.2.5	Relative sensitivities of the air mass flow rate, m_a	90
4.1.3	Adjoint Sensitivity Analysis of Case 2: Fan Off, Unsaturated Air Conditions	92
4.1.3.1	Relative sensitivities of the outlet air temperature, $T_a^{(1)}$	92
4.1.3.2	Relative sensitivities of the outlet water temperature, $T_w^{(50)}$	94
4.1.3.3	Relative sensitivities of the outlet water mass flow rate, $m_w^{(50)}$	95
4.1.3.4	Relative sensitivities of the outlet air relative humidity, $RH^{(1)}$	95
4.1.3.5	Relative sensitivities of the air mass flow rate, m_a	97
4.2	Cross-comparison of the most relevant sensitivities	98
4.2.1	Relative sensitivities of the outlet air temperature, $T_a^{(1)}$	99
4.2.2	Relative sensitivities of the outlet water temperature, $T_w^{(50)}$	100
4.2.3	Relative sensitivities of the outlet water mass flow rate, $m_w^{(50)}$	101
4.2.4	Relative sensitivities of the outlet air relative humidity, $RH^{(1)}$	103

CONTENTS

4.2.5	Relative sensitivities of the air mass flow rate, m_a	104
4.3	Uncertainty Analysis and Predictive Modeling of the cooling tower cases of interest	105
4.3.1	Uncertainty Analysis and Predictive Modeling of Case 1a: Fan Off, Saturated Outlet Air Conditions, with Inlet Air Unsaturated	106
4.3.1.1	Model Calibration: Predicted Best-Estimated Parameter Values with Reduced Predicted Standard Deviations	107
4.3.1.2	Predicted Best-Estimated Response Values with Reduced Predicted Standard Deviations	111
4.3.2	Uncertainty Analysis and Predictive Modeling of Case 1b: Fan Off, Saturated Outlet Air Conditions, with Inlet Air Saturated	113
4.3.2.1	Model Calibration: Predicted Best-Estimated Parameter Values with Reduced Predicted Standard Deviations	114
4.3.2.2	Predicted Best-Estimated Response Values with Reduced Predicted Standard Deviations	118
4.3.3	Uncertainty Analysis and Predictive Modeling of Case 2: Fan Off, Unsaturated Air Conditions	120
4.3.3.1	Model Calibration: Predicted Best-Estimated Parameter Values with Reduced Predicted Standard Deviations	121
4.3.3.2	Predicted Best-Estimated Response Values with Reduced Predicted Standard Deviations	125

CONTENTS

4.4	Uncertainty Analysis and Predictive Modeling of Mechanical Draft Cases	127
4.4.1	Predicted Best-Estimated Response Values with Reduced Predicted Standard Deviations for Case 3a	128
4.4.2	Predicted Best-Estimated Response Values with Reduced Predicted Standard Deviations for Case 3b	130
4.4.3	Predicted Best-Estimated Response Values with Reduced Predicted Standard Deviations for Case 3b	131
5	Discussion and Conclusions	134
	Appendix A Statistical Analysis of Measured Responses	139
A.1	Statistical Analysis of experimentally measured responses for Case 1a: Fan Off, Saturated Outlet Air Conditions, with Inlet Air Unsaturated	141
A.2	Statistical Analysis of experimentally measured responses for Case 1b: Fan Off, Saturated Outlet Air Conditions, with Inlet Air Saturated	148
A.3	Statistical Analysis of experimentally measured responses for Case 2: Fan Off, Unsaturated Air Conditions	154
	Appendix B Parameters for the SRNL F-Area Cooling Towers	160
B.1	Model Parameters for Case 1a: Fan Off, Saturated Outlet Air Conditions, with Inlet Air Unsaturated	160
B.2	Model Parameters for Case 1b: Fan Off, Saturated Outlet Air Conditions, with Inlet Air Saturated	168
B.3	Model Parameters for Case 2: Fan Off, Unsaturated Air Conditions	174
	Appendix C Derivative Matrix (Jacobian) of the Model Equations	

CONTENTS

with Respect to the State Functions	181
C.1 Jacobian Matrix of Case 1a: Fan Off, Saturated Outlet Air Conditions, with Inlet Air Unsaturated	184
C.1.1 Derivatives of the liquid continuity equations with respect to the state variables	184
C.1.2 Derivatives of the liquid energy balance equations with respect to the state variables	189
C.1.3 Derivatives of the water vapor continuity equations with respect to the state variables	192
C.1.4 Derivatives of the air/water vapor energy balance equations with respect to the state variables	195
C.1.5 Derivatives of the mechanical energy equation with respect to the state variables	199
C.2 Jacobian Matrix of Case 1b: Fan Off, Saturated Outlet Air Conditions, with Inlet Air Saturated	201
C.2.1 Derivatives of the liquid continuity equations with respect to the state variables	201
C.2.2 Derivatives of the liquid energy balance equations with respect to the state variables	205
C.2.3 Derivatives of the water vapor continuity equations with respect to the state variables	205
C.2.4 Derivatives of the air/water vapor energy balance equations with respect to the state variables	205
C.2.5 Derivatives of the mechanical energy equation with respect to the state variables	206
C.3 Jacobian Matrix of Case 2: Fan Off, Unsaturated Air Conditions .	206

CONTENTS

C.3.1	Derivatives of the liquid continuity equations with respect to the state variables	207
C.3.2	Derivatives of the liquid energy balance equations with respect to the state variables	210
C.3.3	Derivatives of the water vapor continuity equations with respect to the state variables	210
C.3.4	Derivatives of the air/water vapor energy balance equations with respect to the state variables	211
C.3.5	Derivatives of the mechanical energy equation with respect to the state variables	211
Appendix D Verification of the Model Adjoint Functions		212
D.1	Verification of the Model Adjoint Functions for Case 1a: Fan Off, Saturated Outlet Air Conditions, with Inlet Air Unsaturated . . .	213
D.1.1	Verification of the Adjoint Functions for the Outlet Air Temperature Response $T_a^{(1)}$	213
D.1.1.1	Verification of the adjoint function μ_a	213
D.1.1.2	Verification of the adjoint function $o^{(49)}$	215
D.1.1.3	Verification of the adjoint function $\tau_a^{(49)}$	217
D.1.1.4	Verification of the adjoint function $\tau_w^{(1)}$	218
D.1.1.5	Verification of the adjoint function $\mu_w^{(1)}$	220
D.1.2	Verification of the Adjoint Functions for the Outlet Water Temperature Response $T_w^{(50)}$	222
D.1.2.1	Verification of the adjoint function μ_a	222
D.1.2.2	Verification of the adjoint function $o^{(49)}$	223
D.1.2.3	Verification of the adjoint function $\tau_a^{(49)}$	225
D.1.2.4	Verification of the adjoint function $\tau_w^{(1)}$	227
D.1.2.5	Verification of the adjoint function $\mu_w^{(1)}$	228

CONTENTS

D.1.3	Verification of the Adjoint Functions for the Outlet Air	
	Relative Humidity $RH^{(1)}$	230
D.1.3.1	Verification of the adjoint function μ_a	231
D.1.3.2	Verification of the adjoint function $o^{(49)}$	232
D.1.3.3	Verification of the adjoint function $\tau_a^{(49)}$	234
D.1.3.4	Verification of the adjoint function $\tau_w^{(1)}$	235
D.1.3.5	Verification of the adjoint function $\mu_w^{(1)}$	237
D.1.4	Verification of the Adjoint Functions for the Outlet Water	
	Mass Flow Rate $m_w^{(50)}$	239
D.1.4.1	Verification of the adjoint function μ_a	239
D.1.4.2	Verification of the adjoint function $o^{(49)}$	241
D.1.4.3	Verification of the adjoint function $\tau_a^{(49)}$	242
D.1.4.4	Verification of the adjoint function $\tau_w^{(1)}$	244
D.1.4.5	Verification of the adjoint function $\mu_w^{(1)}$	245
D.1.5	Verification of the Adjoint Functions for the Outlet Air	
	Mass Flow Rate m_a	247
D.1.5.1	Verification of the adjoint function μ_a	248
D.1.5.2	Verification of the adjoint function $o^{(49)}$	249
D.1.5.3	Verification of the adjoint function $\tau_a^{(49)}$	251
D.1.5.4	Verification of the adjoint function $\tau_w^{(1)}$	253
D.1.5.5	Verification of the adjoint function $\mu_w^{(1)}$	254
D.2	Verification of the Model Adjoint Functions for Case 1b: Fan Off, Saturated Outlet Air Conditions, with Inlet Air Saturated	257
D.2.1	Verification of the adjoint function μ_a for all responses . .	257
D.2.2	Verification of the adjoint function $o^{(49)}$ for all responses .	259
D.2.3	Verification of the adjoint function $\tau_a^{(49)}$ for all responses .	262
D.2.4	Verification of the adjoint function $\tau_w^{(1)}$ for all responses . .	265

CONTENTS

D.2.5	Verification of the adjoint function $\mu_w^{(1)}$ for all responses . .	268
D.3	Verification of the Model Adjoint Functions for Case 2: Fan Off, Unsaturated Air Conditions	272
D.3.1	Verification of the adjoint function μ_a for all responses . .	272
D.3.2	Verification of the adjoint function $o^{(49)}$ for all responses .	274
D.3.3	Verification of the adjoint function $\tau_a^{(49)}$ for all responses .	277
D.3.4	Verification of the adjoint function $\tau_w^{(1)}$ for all responses . .	280
D.3.5	Verification of the adjoint function $\mu_w^{(1)}$ for all responses . .	283
 Appendix E Derivatives of the Model Equations with respect to the Model Parameters		 287
E.1	Derivatives of the Model Equations with respect to the Model Pa- rameters for Case 1a: Fan Off, Saturated Outlet Air Conditions, with Inlet Air Unsaturated	287
E.1.1	Derivatives of the liquid continuity equations with respect to the parameters	288
E.1.2	Derivatives of the liquid energy balance equations with re- spect to the parameters	303
E.1.3	Derivatives of the water vapor continuity equations with respect to the parameters	313
E.1.4	Derivatives of the air/water vapor energy balance equations with respect to the parameters	322
E.1.5	Derivatives of the mechanical energy equations with respect to the parameters	333
E.2	Derivatives of the Model Equations with respect to the Model Pa- rameters for Case 1b: Fan Off, Saturated Outlet Air Conditions, with Inlet Air Saturated	342

E.2.1	Derivatives of the liquid continuity equations with respect to the parameters	342
E.3	Derivatives of the Model Equations with respect to the Model Pa- rameters for Case 2: Fan Off, Unsaturated Air Conditions	353
E.3.1	Derivatives of the liquid continuity equations with respect to the parameters	354
Bibliography		365

Abstract

The present work focuses on performing sensitivity and uncertainty analysis, data assimilation, model calibration, model validation and best-estimate predictions with reduced uncertainties on a counter-flow, wet cooling tower model developed by SRNL. The methodologies are part of two distinct mathematical frameworks: the Adjoint Sensitivity Analysis Methodology (ASAM) is used to compute the adjoint sensitivities of the model quantities of interest (called “model responses”) with respect to the model parameters; the Predictive Modeling of Coupled Multi-Physics Systems (PM_CMPS) simultaneously combines all of the available computed information and experimentally measured data to yield optimal values of the system parameters and responses, while simultaneously reducing the corresponding uncertainties in parameters and responses. A cooling tower discharges waste heat produced by an industrial plant to the external environment. The amount of thermal energy discharged into the environment can be determined by measurements of quantities representing the external conditions, such as outlet air temperature, outlet water temperature, and outlet air relative humidity, in conjunction with computational models that simulate numerically the cooling tower behavior. Variations in the model parameters (e.g., material properties, model correlations, boundary conditions) cause variations in the model response. The functional derivatives of the model response with respect to the model parameters (called “sensitivities”) are needed to quantify such response variations

CONTENTS

changes. In this work, the comprehensive adjoint sensitivity analysis methodology for nonlinear systems is applied to compute the sensitivities of the cooling tower responses to all of the model parameters. These sensitivities are used in this work for (i) ranking the model parameters according to the magnitude of their contribution to response uncertainties; (ii) propagating the uncertainties in the model parameters to quantify the uncertainties in the model responses; (iii) performing model validation and predictive modeling, combining computational and experimental information, including the respective uncertainties, to obtain optimally predicted best-estimate nominal values for the model parameters and responses, with reduced predicted uncertainties.

Chapter 1

Introduction

1.1 State-of-the-art of sensitivity and uncertainty analysis, data assimilation, model calibration, model validation, best-estimate predictions with reduced uncertainties

It is common practice, in the modern era, to base the process of understanding and eventually predicting the behavior of complex physical systems on simulating operational situations through system codes. In order to provide a more thorough and accurate comprehension of the system dynamics, these numerical simulations are often and preferably flanked by experimental measurements. In practice, repeated measurements of the same physical quantity produce values differing from each other and from the measured quantity's true value, which remains unknown; the errors leading to this variation in results can be of methodological, instrumental or personal nature.

It is not feasible to obtain experimental results devoid of uncertainty, and this

CHAPTER 1. INTRODUCTION

means that a range of values possibly representative of the true value always exists around any value stemming from experimental measurements. A quantification of this range is critical to any practical application of the measured data, whose nominal measured values are insufficient for applications unless the quantitative uncertainties associated to the experimental data are also provided. Not even numerical models can reveal the true value of the investigated quantity, for two reasons: first, any numerical model is imperfect, meaning that it constitutes an inevitable simplification of the real world system it aims to represent; in second place, a hypothetically perfect model would still have uncertain values for its model parameters - such as initial conditions, boundary conditions and material properties - and the stemming results would therefore still be differing from the true value and from the experimental measurements of the quantity.

With both computational and experimental results at hand, the final aim is to obtain a probabilistic description of possible future outcomes based on all recognized errors and uncertainties. This operation falls within the scope of *predictive modeling* procedures, which rely on three key elements: *model calibration*, *model extrapolation* and *estimation of the validation domain*. The first step of the procedure involves the adjustment of the numerical model parameters accordingly to the experimental results; this aim is achieved by integrating computed and measured data, and the associated procedure is known as *model calibration*. In order for this operation to be properly executed, all errors and uncertainties at any level of the modeling path leading to numerical results have to be identified and characterized, including errors and uncertainties on the model parameters, numerical discretization errors and possible incomplete knowledge of the physical process being modeled. Calibration of models is performed through the mathematical framework provided by *data assimilation* procedures; these procedures strongly rely on *sensitivity analysis*, and for this reason are often cumbersome in

CHAPTER 1. INTRODUCTION

terms of computational load.

Generally speaking, sensitivity analyses can be conducted with two different techniques, respectively known as *direct* or *forward* methods and *adjoint* methods. The forward methods calculate the finite difference of a small perturbation in a parameter by means of differences between the responses of two independent calculations, and are advantageous only for systems in which the number of responses exceeds the number of model parameters; unfortunately this is seldom the case in real large-scale systems. In this work, this problem has been overcome by using the *adjoint sensitivity analysis methodology* (ASAM) by Cacuci [1-4]: as opposed to forward methods, the ASAM is most efficient for systems in which the number of parameters is greater than the number of responses, such as the model investigated in this thesis and many others currently used for numerical simulations of industrial systems. This methodology has been recently extended to second-order sensitivities (2^{nd} -ASAM) by Cacuci for linear [5-6] and nonlinear systems [7-8], for computing exactly and efficiently the second-order functional derivatives of system responses to the system model parameters. *Model extrapolation* addresses the prediction of uncertainty in new environments or conditions of interest, including both untested parts of the parameter space and higher levels of system complexity in the validation hierarchy. *Estimation of the validation domain* addresses the estimation of contours of constant uncertainty in the high-dimensional space that characterizes the application of interest.

The first systematic studies focused on obtaining best-estimate values for model parameters were produced almost simultaneously in the mid 1960s by independent groups of scientists all around the world [9-11], with the aim of possibly improving the cross section values by means of experiments conducted in order to measure reaction rates and multiplication factors. In the 1970s, Rowlands [12] and Gandini [13] used a weighted least-square procedure - response sensitiv-

CHAPTER 1. INTRODUCTION

ities being used as weights - to combine uncertainties in the model parameters with uncertainties in the experimental data, typifying a trend which had been developing under the name of “cross-section adjustment”. Best-estimate system responses such as reaction rates, multiplication factors and Doppler coefficients were predicted by making use of the “adjusted” parameters and uncertainties in the investigated reactor physics models. By the late-1970s the weighting functions values, obtained as the first-order response sensitivities, started being computed by means of adjoint neutron fluxes, as in Kuroi [14], Dragt [15] and Weisbin [16]. It is worth noting that all of the abovementioned works addressed merely the time-independent linear neutron transport or diffusion problem, a mathematically well-known case for which the corresponding adjoint equations were already known and readily available. The general adjoint method for computing efficiently sensitivities for nonlinear, time-dependent or stationary problems was formulated in 1981 by Cacuci [1]; just one year later, Barhen presented the first general formulation of a “data adjustment” for time-dependent nonlinear problems [17]. This methodology regrettably failed to spread to other scientific fields, and after a stagnation period was rediscovered in its basic ideas to be adapted to the geophysical sciences, under the name of “data assimilation”. Since then, well over a thousand works on data assimilation have been published in the geophysical sciences alone, under the name of “3D-VAR” (for time-independent problems, and “4D-VAR” for time-dependent problems). Although too numerous to cite extensively here, representative works can be found cited in the books by Lewis [18], Lahoz [19] and Cacuci [20]. A comprehensive mathematical methodology aimed at yielding best-estimate predictions for large-scale nonlinear time-dependent systems has been recently published by Cacuci and Ionescu-Bujor [21]. Besides extending the results yielded from the standard data assimilation procedures, this methodology provides quantitative indicators, stemming from sensitivities and

CHAPTER 1. INTRODUCTION

covariances, for the evaluation of the consistency among the computational and experimental values of parameters and responses. This comprehensive predictive modeling methodology, which has already yielded successful results when applied to large-scale experimental cases and to the validation of nuclear reactor system codes related to reactor physics [22]-[23], light water reactors [24] and sodium-cooled fast reactors [25], has been used in this work to perform the assimilation of experimental measurements and the calibration of model parameters for the cooling tower model under investigation.

1.2 Aim and outline of the work

This work concentrates on a counter-flow cooling tower operated as a natural draft/wind-aided cooling tower, under saturated and unsaturated conditions. A model for the steady-state simulation of both cross-flow and counter-flow wet cooling towers has been developed by Savannah River National Laboratory, implemented in the “CTTool” system code and presented in [26]. In this thesis, a relevantly more efficient numerical method has been developed and applied to the cooling tower model presented in [26], leading to the accurate computation of the steady-state distributions for the following quantities: (i) the water mass flow rates at the exit of each control volume along the height of the fill section of the cooling tower; (ii) the water temperatures at the exit of each control volume along the height of the fill section of the cooling tower; (iii) the air temperatures at the exit of each control volume along the height of the fill section of the cooling tower; (iv) the humidity ratios at the exit of each control volume along the height of the fill section of the cooling tower; and (v) the air mass flow rates at the exit of the cooling tower. As shown in the foregoing of the thesis, the application of the numerical method selected eliminates the convergence issues experienced when applying the solution method implemented in [26], yielding accurate results for

CHAPTER 1. INTRODUCTION

all the control volumes of the cooling tower and for all the data set of interest.

The development of the *adjoint sensitivity model* for the cooling tower has been realized by applying the general *adjoint sensitivity analysis methodology* (ASAM) *for nonlinear systems* [1-4]. The first critical topic of this work is represented by the development of the adjoint sensitivity model for the cooling tower system, with the aim of allowing the computation of the sensitivities (functional derivatives) of the model responses to all the model parameters in an efficient and exact way, eliminating repeated calculations and approximations introduced by using finite difference methods. The forward cooling tower model presents nonlinearity in their state functions; the adjoint sensitivity model possesses the relevant feature of being instead linear in the adjoint state functions, whose one-to-one correspondence to the forward state functions is essential for the calculation of the adjoint sensitivities. Moreover, the utilization of the adjoint state functions allows the simultaneous computation of the sensitivities of each model response to all of the 47 independent model parameters just by means of a single adjoint model run; obtaining the same results making use of finite-difference forward methods would require 47 separate computations, with the relevant disadvantage of leading to approximate results of the sensitivities, as opposed to the exact ones yielded by applying the adjoint procedure. For all the cases the following five model responses have been selected: (i) the water mass flow rate at the outlet of the bottom control volume of the fill section of the cooling tower, $m_w^{(50)}$; (ii) the water temperature at the outlet of the bottom control volume of the fill section of the cooling tower, $T_w^{(50)}$; (iii) the air temperature at the outlet of the top control volume of the fill section of the cooling tower, $T_a^{(1)}$; (iv) the humidity ratio at the outlet of the top control volume of the fill section of the cooling tower, $RH^{(1)}$; and (v) the air mass flow rate at the outlet of the cooling tower, m_a . Hence, the nonlinear model analyzed in this work has 47 independent parameters and

CHAPTER 1. INTRODUCTION

5 responses, and this would cause a sensitivity analysis conducted with forward methods not only to yield approximate results, but to be extremely cumbersome in terms of computational time. For this reason, the application of the ASAM to this specific cooling tower model is extremely convenient.

The adjoint sensitivities are necessary to realize many operations, such as: (i) ranking the model parameters according to the magnitude of their contribution to response uncertainties; (ii) determine the propagation of uncertainties, in form of variances and covariances, of the parameters in the model in order to quantify the uncertainties of the model responses; (iii) allow predictive modeling operations, such as experimental data assimilation and model parameters calibration, with the aim to yield best-estimate predicted nominal values both for model parameters and responses, with correspondently reduced values for the predicted uncertainties associated. After being calculated, sensitivities are subsequently used for the application of the PM_CMPS methodology, aimed at yielding best-estimate predicted nominal values and uncertainties for model parameters and responses. This methodology simultaneously combines all of the available computed information and experimentally measured data for the counter-flow cooling tower operating under saturated and unsaturated conditions. The best-estimate results predicted by the “predictive modeling for coupled multi-physics systems” (PM_CMPS) methodology reveal that the predicted values of the standard deviations of the model responses, even those for which no experimental data have been recorded, are smaller than the smallest value between either the computed or the measured standard deviations for the respective responses. As a result of the data assessment, model calibration and model validation procedures applied, the CTTool code will be validated in this thesis. The CTTool is foreseen to be part of a facility modeling program suite, which is envisaged to encompass modules simulating chemical processes and atmospheric transport of pollutants.

CHAPTER 1. INTRODUCTION

This work is organized as follows: Chapter 2 provides a description of the physical system simulated, along with presenting the governing equations underlying the model used in this work for simulating a counter-flow cooling tower operating under saturated and unsaturated conditions. The three cases and subcases analyzed in this work and their corresponding mathematical models are hereby detailed, as well as the new solution scheme implemented and applied to the model and the accurate steady-state distributions for the model responses. Chapter 3 presents the development of the adjoint sensitivity model for the counter-flow cooling tower operating under saturated and unsaturated conditions using the general adjoint sensitivity analysis methodology (ASAM) for nonlinear systems [1-4]. The mathematical framework of the PM_CMPS [27] is also detailed. Chapter 4 presents the results of applying the ASAM and PM_CMPS methodologies to all the cases listed in Chapter 2. This thesis concludes with Chapter 5 by discussing the significance of these predicted results and by indicating possible further generalizations of the adjoint sensitivity analysis and PM_CMPS methodologies.

Chapter 2

Description of the system

2.1 Context on cooling towers

An unavoidable necessity of any energy-producing plant housing an industrial process is to release waste heat into the external environment. The most popular solution to accomplish this task is through the use of a cooling tower, which can provide a temperature decrease of the operational fluid of the plant by evaporation and sensible heat transfer. Cooling tower can be generally classified by heat transfer method in dry cooling towers and wet cooling towers. Dry cooling towers foresee a physical separation between the working fluid (e.g. water) and the external ambient air; due to the lack of direct contact between the two streams, in these towers convective heat transfer is the dominating heat exchange mechanic. Wet cooling towers present no physical barrier between the working fluid and the ambient air; this allows wet cooling towers to be operated on the principle of evaporative cooling. According to the different flow regimes in the fill, the cooling tower can be further divided into cross-flow type (in which the air flow is directed perpendicular to the water flow, with the induced air moving horizontally while the water falls vertically) or counter-flow type (in which the air flow is directly

CHAPTER 2. DESCRIPTION OF THE SYSTEM

opposite of the water flow).

The amount of thermal energy discharged into the atmosphere can be determined by making coupled use of a model simulating the cooling tower behavior and experimental measurements of the quantities representing the external conditions, such as outlet air temperature, outlet water temperature and outlet air relative humidity. In the case of a thermal imagery-based cooling tower model, an inner model and an outer model are necessary in order to fulfil the need to relate a remotely measured cooling tower throat or area-weighted temperature to a cooling water inlet temperature. The inner model has the aim of quantifying the water temperature decrease in relation to the inlet water temperature and air temperature and humidity, while the outer model addresses iteratively the inlet water temperature using the remotely measured throat or area-weighted temperature in order to match the desired temperature value.

The cooling tower model analyzed and studied in this work has been developed by Savannah River National Laboratory (SRNL), implemented in the “CTTool” system code and presented in [26]. The “CTTool” code simulates steady-state thermal performance for both cross-flow and counter-flow wet cooling towers. The needed inputs are the water temperature and mass flow rate at the inlet of the cooling tower and the temperature and humidity ratio of the external air at the inlet of the cooling tower; the computed responses are the exhaust air temperature and relative humidity, the outlet water temperature and the outlet water mass flow rate. If the cooling tower fans are on, the mass flow rate of water and air is known, and the system is referred to as a mechanical draft cooling tower. If the fans are off - and the air mass flow rate becomes therefore an additional unknown - an additional mechanical energy equation is instead used to solve for the mass flow rate of air through the cooling tower, with the system being operated as a natural draft/wind aided cooling tower.

2.2 Description of the cooling tower model

The counter-flow cooling tower considered in this work has been originally developed in [26] and has been thoroughly described in [28], from which Figures 2.1 - 2.3 have been taken. Natural draft air enters the tower through the “rain section” above the water basin, passes through the fill section and the drift eliminator, and exits the tower at the top through an exhaust comprising a fan. Hot water flows downward, entering the tower above the fill section and being sprayed over the fill section, with the result of creating a uniform film flow through the fill.

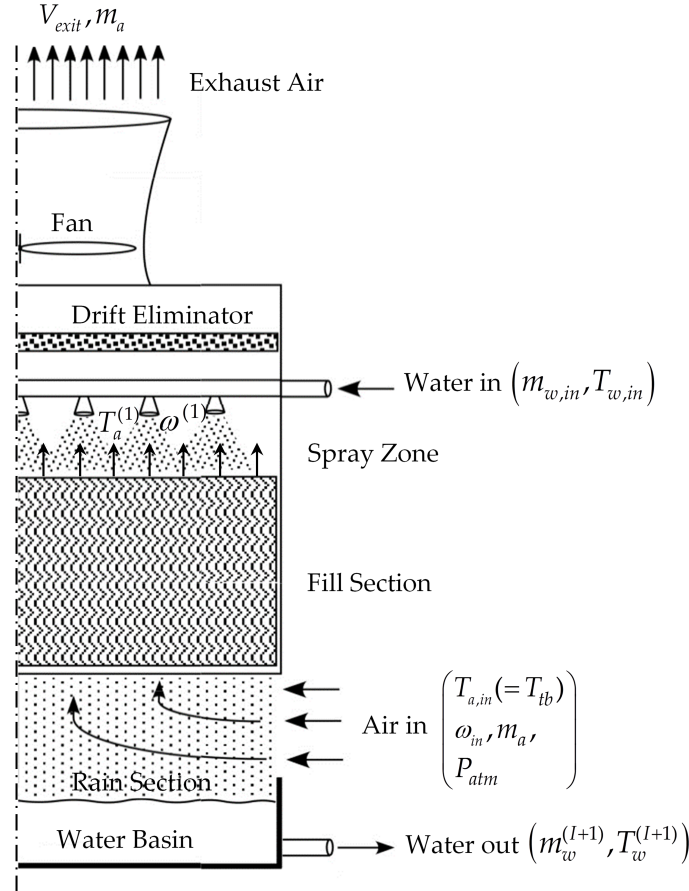


Figure 2.1: Flow through a counter-flow cooling tower

CHAPTER 2. DESCRIPTION OF THE SYSTEM

At the interface between water and air phenomena of both heat and mass transfer occur; these processes are mostly occurring in the fill section. The drift eliminator is aimed to retain water droplets from the air flow; just below the fill section, water droplets fall into a collection basin, located at the bottom of the cooling tower.

The mathematical quantification of the heat and mass transfer processes occurring in the counter-flow cooling tower of interest is accomplished by solving the following balance equations: (A) liquid continuity; (B) liquid energy balance; (C) water vapor continuity; (D) air/water vapor energy balance; (E) mechanical energy balance. In deriving these equations, several assumptions have been made, namely:

1. air and water stream temperatures are uniform at any cross section;
2. the cross-sectional area of the cooling tower is assumed to be uniform;
3. the heat and mass transfer only occur in the direction normal to flows;
4. the heat and mass transfer through tower walls to the environment is neglected;
5. the heat transfer from the cooling tower fan and motor assembly to the air is neglected;
6. the air and water vapor is considered a mixture of ideal gasses;
7. the flow between flat plates is saturated through the fill section.

The assumptions listed above have been made by the CTTool code developers at SRNL, and do not affect the general accuracy of the model. This work addresses cooling towers of moderate size, for which the contribution of the heat and mass transfer phenomena occurring in the rain section is negligible. Figure 2.2 shows

CHAPTER 2. DESCRIPTION OF THE SYSTEM

how the fill section is nodalized in vertically stacked control volumes. A closer picture of the heat and mass transfer processes occurring at the free surface between the water film and the air flow within a control volume is shown in Figure 2.3.

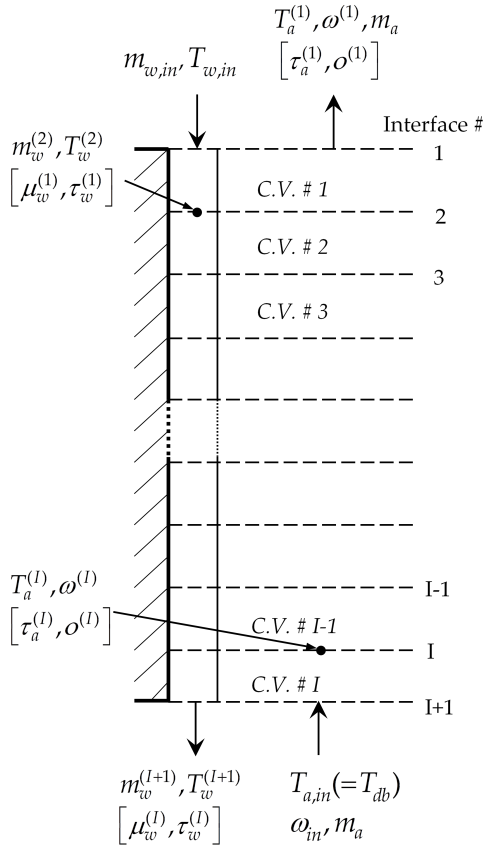


Figure 2.2: Vertically stacked control volumes ($i = 1, \dots, I$) constituting the fill section of the cooling tower, together with the symbols denoting forward state functions $(m_w^{(i)}, T_w^{(i)}, T_a^{(i)}, \omega^{(i)}, m_a; i = 1, \dots, I)$ and adjoint state functions $(\mu_w^{(i)}, \tau_w^{(i)}, \tau_a^{(i)}, o^{(i)}, \mu_a; i = 1, \dots, I)$.

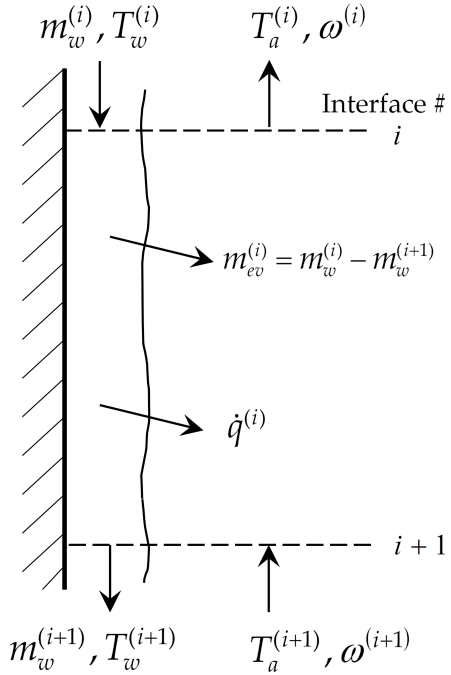


Figure 2.3: Heat and mass transfer phenomena occurring between falling water film and rising air in a typical control volume of the cooling tower fill section.

CHAPTER 2. DESCRIPTION OF THE SYSTEM

As for the counter-flow cooling tower under saturated condition, the analysis has been further divided into two subcases, based on the air inlet boundary conditions at the fill section entrance. The first subcase describes a situation in which air enters the fill section in unsaturated condition, but it gets saturated before reaching the outlet of the fill section; in the second subcase air enters the fill section already saturated, exiting the fill section also saturated. For both subcases, the outlet air flow from the fill section is saturated; the difference lies in the inlet air conditions. The measured benchmark data sets for F-area cooling towers (counter-flow cooling tower, fan-on and fan-off mode) at SRNL [33] also support such a separation. Those two subcases are treated separately for the mathematical model and the adjoint sensitivity model, since the governing equations for the two subcases are different, as described in the following.

2.3 Governing equations of the mathematical models and cases selected

This work aims to investigate the behavior of the cooling tower in the regime of the normally occurring operating conditions. The cases of interest have been divided depending on:

1. the air condition (saturated or unsaturated) at the inlet of the cooling tower;
2. the air condition (saturated or unsaturated) at the outlet of the cooling tower;

These criteria led to the following cases:

- **Case 1:** the cooling tower is operated in fan-off mode (natural draft) and the outlet air is in saturated conditions; this case is split into two subcases

CHAPTER 2. DESCRIPTION OF THE SYSTEM

according to the inlet air conditions:

- **Subcase I:** the inlet air is in unsaturated conditions; this means that unsaturated inlet air becomes saturated at a certain control volume of the fill section along the height of the cooling tower. This subcase will be referred to as **case 1a**;
- **Subcase II:** the inlet air is in saturated conditions: in this subcase, air is in saturated condition from the inlet through the outlet of the fill section, i.e., air is saturated in all the 49 control volumes. This subcase will be referred to as **case 1b**.
- **Case 2:** the cooling tower is operated in fan-off mode (natural draft) and the outlet air is in unsaturated conditions; in this case, it is only possible for inlet air to be in unsaturated conditions as well, hence there is no need for subcases.

The most general case in terms of the governing equations underlying the model is case 1a, in which the air saturation point is located somewhere inside the cooling tower; mathematically speaking case 1b and case 2 are particular cases of case 1a, in which the air saturation point is located, on the air path, outside of the cooling tower, respectively before the inlet and after the outlet of the cooling tower itself.

2.3.1 Mathematical Model for Case 1a: Natural Draft Cooling Tower operated in Saturated Outlet Air Condition, with Inlet Air Unsaturated

In this subcase, unsaturated inlet air becomes saturated at a certain control volume of the fill section. Assuming air gets saturated at the exit of the K^{th}

CHAPTER 2. DESCRIPTION OF THE SYSTEM

control volume, where $1 < K \leq I$, then in control volumes between #1 to # K air is in saturated condition; in control volumes between # $K + 1$ to # I air is in unsaturated condition. Note that the flow direction of air is upward from the # I control volume to the #1 control volume, as illustrated in Figure 2.2.

In the natural draft/wind-aided mode, the mass flowrate of dry air is unknown. With the fan off and hot water flowing through the cooling tower, air will continue to flow through the tower due to buoyancy. Wind pressure at the air inlet to the cooling tower will also enhance air flow through the tower. The air flowrate is determined from the overall mechanical energy equation for the dry air flow. The state functions underlying the cooling tower model (cf. Figures 2.1 - 2.3) are as follows:

1. the water mass flow rates, denoted as $m_w^{(i)}$ ($i = 2, \dots, 50$), at the exit of each control volume, i , along the height of the fill section of the cooling tower;
2. the water temperatures, denoted as $T_w^{(i)}$ ($i = 2, \dots, 50$), at the exit of each control volume, i , along the height of the fill section of the cooling tower;
3. the air temperatures, denoted as $T_a^{(i)}$ ($i = 1, \dots, 49$), at the exit of each control volume, i , along the height of the fill section of the cooling tower;
4. the humidity ratios, denoted as $\omega^{(i)}$ ($i = 1, \dots, 49$), at the exit of each control volume, i , along the height of the fill section of the cooling tower;
5. the air mass flow rate, denoted as m_a , constant along the height of the fill section of the cooling tower.

It is convenient to consider the above state functions to be components of the following (column) vectors:

$$\begin{aligned} \mathbf{m}_w &\equiv [m_w^{(2)}, \dots, m_w^{(I+1)}]^\dagger, & \mathbf{T}_w &\equiv [T_w^{(2)}, \dots, T_w^{(I+1)}]^\dagger, \\ \mathbf{T}_a &\equiv [T_a^{(1)}, \dots, T_a^{(I)}]^\dagger, & \boldsymbol{\omega} &\equiv [\omega^{(1)}, \dots, \omega^{(I)}]^\dagger, & m_a \end{aligned} \quad (2.1)$$

CHAPTER 2. DESCRIPTION OF THE SYSTEM

In this work, the dagger (\dagger) will be used to denote “transposition”, and all vectors will be considered to be column vectors. The governing conservation equations within the total of $I = 49$ control volumes represented in Figure 2.2 are as follows [26]:

A. Liquid continuity equations:

(i) Control Volume $i = 1$:

$$\begin{aligned} N_1^{(1)}(\mathbf{m}_w, \mathbf{T}_w, \mathbf{T}_a, \boldsymbol{\omega}, m_a; \boldsymbol{\alpha}) &\triangleq m_w^{(2)} - m_{w,in} \\ &+ \frac{M(m_a, \boldsymbol{\alpha})}{\bar{R}} \left[\frac{P_{vs}^{(2)}(T_w^{(2)}, \boldsymbol{\alpha})}{T_w^{(2)}} - \frac{P_{vs}^{(1)}(T_a^{(1)}, \boldsymbol{\alpha})}{T_a^{(1)}} \right] = 0 \end{aligned} \quad (2.2)$$

(ii) Control Volumes $i = 2, \dots, K$:

$$\begin{aligned} N_1^{(i)}(\mathbf{m}_w, \mathbf{T}_w, \mathbf{T}_a, \boldsymbol{\omega}, m_a; \boldsymbol{\alpha}) &\triangleq m_w^{(i+1)} - m_w^{(i)} \\ &+ \frac{M(m_a, \boldsymbol{\alpha})}{\bar{R}} \left[\frac{P_{vs}^{(i+1)}(T_w^{(i+1)}, \boldsymbol{\alpha})}{T_w^{(i+1)}} - \frac{P_{vs}^{(i)}(T_a^{(i)}, \boldsymbol{\alpha})}{T_a^{(i)}} \right] = 0 \end{aligned} \quad (2.3)$$

where K is the control volume at which its outlet air is saturated.

(iii) Control Volumes $i = K + 1, \dots, I - 1$:

$$\begin{aligned} N_1^{(i)}(\mathbf{m}_w, \mathbf{T}_w, \mathbf{T}_a, \boldsymbol{\omega}, m_a; \boldsymbol{\alpha}) &\triangleq m_w^{(i+1)} - m_w^{(i)} \\ &+ \frac{M(m_a, \boldsymbol{\alpha})}{\bar{R}} \left[\frac{P_{vs}^{(i+1)}(T_w^{(i+1)}, \boldsymbol{\alpha})}{T_w^{(i+1)}} - \frac{\omega^{(i)} P_{atm}}{T_a^{(i)} (0.622 + \omega^{(i)})} \right] = 0 \end{aligned} \quad (2.4)$$

(iv) Control Volume $i = I$:

$$\begin{aligned} N_1^{(I)}(\mathbf{m}_w, \mathbf{T}_w, \mathbf{T}_a, \boldsymbol{\omega}, m_a; \boldsymbol{\alpha}) &\triangleq m_w^{(I+1)} - m_w^{(I)} \\ &+ \frac{M(m_a, \boldsymbol{\alpha})}{\bar{R}} \left[\frac{P_{vs}^{(I+1)}(T_w^{(I+1)}, \boldsymbol{\alpha})}{T_w^{(I+1)}} - \frac{\omega^{(I)} P_{atm}}{T_a^{(I)} (0.622 + \omega^{(I)})} \right] = 0 \end{aligned} \quad (2.5)$$

CHAPTER 2. DESCRIPTION OF THE SYSTEM

B. Liquid energy balance equations:

(i) Control Volume $i = 1$:

$$\begin{aligned} N_2^{(1)}(\mathbf{m}_w, \mathbf{T}_w, \mathbf{T}_a, \boldsymbol{\omega}, m_a; \boldsymbol{\alpha}) &\triangleq m_{w,in} h_f(T_{w,in}, \boldsymbol{\alpha}) \\ &- (T_w^{(2)} - T_a^{(1)}) H(m_a, \boldsymbol{\alpha}) - m_w^{(2)} h_f^{(2)}(T_w^{(2)}, \boldsymbol{\alpha}) \\ &- (m_{w,in} - m_w^{(2)}) h_{g,w}^{(2)}(T_w^{(2)}, \boldsymbol{\alpha}) = 0 \end{aligned} \quad (2.6)$$

(ii) Control Volumes $i = 2, \dots, I - 1$:

$$\begin{aligned} N_2^{(i)}(\mathbf{m}_w, \mathbf{T}_w, \mathbf{T}_a, \boldsymbol{\omega}, m_a; \boldsymbol{\alpha}) &\triangleq m_w^{(i)} h_f^{(i)}(T_w^{(i)}, \boldsymbol{\alpha}) \\ &- (T_w^{(i+1)} - T_a^{(i)}) H(m_a, \boldsymbol{\alpha}) - m_w^{(i+1)} h_f^{(i+1)}(T_w^{(i+1)}, \boldsymbol{\alpha}) \\ &- (m_w^{(i)} - m_w^{(i+1)}) h_{g,w}^{(i+1)}(T_w^{(i+1)}, \boldsymbol{\alpha}) = 0 \end{aligned} \quad (2.7)$$

(iii) Control Volume $i = I$:

$$\begin{aligned} N_2^{(I)}(\mathbf{m}_w, \mathbf{T}_w, \mathbf{T}_a, \boldsymbol{\omega}, m_a; \boldsymbol{\alpha}) &\triangleq m_w^{(I)} h_f^{(I)}(T_w^{(I)}, \boldsymbol{\alpha}) \\ &- (T_w^{(I+1)} - T_a^{(I)}) H(m_a, \boldsymbol{\alpha}) - m_w^{(I+1)} h_f^{(I+1)}(T_w^{(I+1)}, \boldsymbol{\alpha}) \\ &- (m_w^{(I)} - m_w^{(I+1)}) h_{g,w}^{(I+1)}(T_w^{(I+1)}, \boldsymbol{\alpha}) = 0 \end{aligned} \quad (2.8)$$

C. Water vapor continuity equations:

(i) Control Volume $i = 1$:

$$N_3^{(1)}(\mathbf{m}_w, \mathbf{T}_w, \mathbf{T}_a, \boldsymbol{\omega}, m_a; \boldsymbol{\alpha}) \triangleq \omega^{(2)} - \omega^{(1)} + \frac{m_{w,in} - m_w^{(2)}}{|m_a|} = 0 \quad (2.9)$$

(ii) Control Volumes $i = 2, \dots, I - 1$:

$$N_3^{(i)}(\mathbf{m}_w, \mathbf{T}_w, \mathbf{T}_a, \boldsymbol{\omega}, m_a; \boldsymbol{\alpha}) \triangleq \omega^{(i+1)} - \omega^{(i)} + \frac{m_w^{(i)} - m_w^{(i+1)}}{|m_a|} = 0 \quad (2.10)$$

(iii) Control Volume $i = I$:

$$N_3^{(I)}(\mathbf{m}_w, \mathbf{T}_w, \mathbf{T}_a, \boldsymbol{\omega}, m_a; \boldsymbol{\alpha}) \triangleq \omega_{in} - \omega^{(I)} + \frac{m_w^{(I)} - m_w^{(I+1)}}{|m_a|} = 0 \quad (2.11)$$

CHAPTER 2. DESCRIPTION OF THE SYSTEM

D. Air/water vapor energy balance equations:

(i) Control Volume $i = 1$:

$$\begin{aligned}
 N_4^{(1)}(\mathbf{m}_w, \mathbf{T}_w, \mathbf{T}_a, \boldsymbol{\omega}, m_a; \boldsymbol{\alpha}) &\triangleq (T_a^{(2)} - T_a^{(1)}) C_p^{(1)} \left(\frac{T_a^{(1)} + 273.15}{2}, \boldsymbol{\alpha} \right) \\
 &\quad - \omega^{(1)} h_{g,a}^{(1)}(T_a^{(1)}, \boldsymbol{\alpha}) + \frac{(T_w^{(2)} - T_a^{(1)}) H(m_a, \boldsymbol{\alpha})}{|m_a|} \\
 &\quad + \frac{(m_{w,in} - m_w^{(2)}) h_{g,w}^{(2)}(T_w^{(2)}, \boldsymbol{\alpha})}{|m_a|} + \omega^{(2)} h_{g,a}^{(2)}(T_a^{(2)}, \boldsymbol{\alpha}) = 0
 \end{aligned} \tag{2.12}$$

(ii) Control Volumes $i = 2, \dots, I - 1$:

$$\begin{aligned}
 N_4^{(i)}(\mathbf{m}_w, \mathbf{T}_w, \mathbf{T}_a, \boldsymbol{\omega}, m_a; \boldsymbol{\alpha}) &\triangleq (T_a^{(i+1)} - T_a^{(i)}) C_p^{(i)} \left(\frac{T_a^{(i)} + 273.15}{2}, \boldsymbol{\alpha} \right) \\
 &\quad - \omega^{(i)} h_{g,a}^{(i)}(T_a^{(i)}, \boldsymbol{\alpha}) + \frac{(T_w^{(i+1)} - T_a^{(i)}) H(m_a, \boldsymbol{\alpha})}{|m_a|} \\
 &\quad + \frac{(m_w^{(i)} - m_w^{(i+1)}) h_{g,w}^{(i+1)}(T_w^{(i+1)}, \boldsymbol{\alpha})}{|m_a|} + \omega^{(i+1)} h_{g,a}^{(i+1)}(T_a^{(i+1)}, \boldsymbol{\alpha}) = 0
 \end{aligned} \tag{2.13}$$

(iii) Control Volume $i = I$:

$$\begin{aligned}
 N_4^{(I)}(\mathbf{m}_w, \mathbf{T}_w, \mathbf{T}_a, \boldsymbol{\omega}, m_a; \boldsymbol{\alpha}) &\triangleq (T_{a,in} - T_a^{(I)}) C_p^{(I)} \left(\frac{T_a^{(I)} + 273.15}{2}, \boldsymbol{\alpha} \right) \\
 &\quad - \omega^{(I)} h_{g,a}^{(I)}(T_a^{(I)}, \boldsymbol{\alpha}) + \frac{(T_w^{(I+1)} - T_a^{(I)}) H(m_a, \boldsymbol{\alpha})}{|m_a|} \\
 &\quad + \frac{(m_w^{(I)} - m_w^{(I+1)}) h_{g,w}^{(I+1)}(T_w^{(I+1)}, \boldsymbol{\alpha})}{|m_a|} + \omega_{in} h_{g,a}(T_{a,in}, \boldsymbol{\alpha}) = 0
 \end{aligned} \tag{2.14}$$

CHAPTER 2. DESCRIPTION OF THE SYSTEM

E. Mechanical energy equation:

$$\begin{aligned}
 N_5(\mathbf{m}_w, \mathbf{T}_w, \mathbf{T}_a, \boldsymbol{\omega}, m_a; \boldsymbol{\alpha}) \triangleq & \left[\frac{1}{2\rho(T_{tdb}, \boldsymbol{\alpha})} \left(\frac{1}{A_{out}(\boldsymbol{\alpha})^2} - \frac{1}{A_{in}(\boldsymbol{\alpha})^2} + \frac{k_{sum}}{A_{fill}^2} \right) \right. \\
 & \left. + \frac{f}{2\rho(T_{tdb}, \boldsymbol{\alpha})} \frac{96}{\text{Re}(m_a, \boldsymbol{\alpha})} \frac{L_{fill}(\boldsymbol{\alpha})}{A_{fill}^2 D_h} \right] |m_a| m_a - gZ(\boldsymbol{\alpha}) \rho(T_{tdb}, \boldsymbol{\alpha}) \\
 & - \frac{V_w^2 \rho(T_{tdb}, \boldsymbol{\alpha})}{2} + \Delta z_{rain} g \rho(T_{tdb}, \boldsymbol{\alpha}) + g \rho(T_a^{(1)}, \boldsymbol{\alpha}) \Delta z_{4-2}(\boldsymbol{\alpha}) \\
 & + g \Delta z(\boldsymbol{\alpha}) \frac{P_{atm}}{R_{air}} \left[\frac{1}{2T_{a,in}} + \frac{1}{2T_a^{(1)}} + \sum_{i=2}^I \frac{1}{T_a^{(i)}} \right] = 0
 \end{aligned} \tag{2.15}$$

The components of the vector $\boldsymbol{\alpha}$, which appears in Eqs. (2.2)-(2.15), are the model parameters which are referred to as α_i , i.e.,

$$\boldsymbol{\alpha} \triangleq (\alpha_1, \dots, \alpha_{N_\alpha}) \tag{2.16}$$

where $N_\alpha = 47$ represents the total number of model parameters. These model parameters are quantities which have been derived experimentally, and their distributions are only partially known; the first four moments (mean, variance/covariance, skewness, and kurtosis) of these parameter distributions have nevertheless been determined, as detailed in Appendix B.

In the original work [26], the solution of Eqs. (2.2)-(2.15) was achieved by making use of a two-stage iterative method including an “inner-iteration” which utilized Newton’s method inside each control volume, coupled with an outer iteration supposed to guarantee the convergence of the whole model. Unfortunately, this procedure could not achieve convergence for all the data points taken into consideration; several alternatives from [34] and [35] were therefore analyzed and tested, and the original solution method in [26] was in the end substituted with a more accurate and efficient one, based on the joint use of Newton’s method and the GMRES linear iterative solver for sparse matrices [36] comprised in the

CHAPTER 2. DESCRIPTION OF THE SYSTEM

NSPCG package [35]. The GMRES method selected [36] computes an approximated solution of the linear system of interest making use of the Arnoldi iteration, minimizing the norm of the vector of the residuals over a Krylov subspace. More in detail, the single computational steps are hereby listed:

(a) Eqs. (2.2)-(2.15) are written in vector form as

$$\mathbf{N}(\mathbf{u}) = \mathbf{0} \quad (2.17)$$

where the following definitions were used:

$$\begin{aligned} \mathbf{N} &\triangleq \left(N_1^{(1)}, \dots, N_2^{(I)}, \dots, N_3^{(1)}, \dots, N_4^{(I)}, \dots, N_5 \right)^\dagger, \\ \mathbf{u} &\triangleq (\mathbf{m}_w, \mathbf{T}_w, \mathbf{T}_a, \boldsymbol{\omega}, m_a)^\dagger \end{aligned} \quad (2.18)$$

- (b) Initial solution guess, \mathbf{u}_0 , is set to be the inlet boundary conditions;
- (c) Outer iteration loop comprises steps (d) through (g); iterate over these steps until convergence for $n = 0, 1, 2, \dots$;
- (d) Inner iteration loop: for $m = 1, 2, \dots$, use the iterative GMRES linear solver coupled with the Modified Incomplete Cholesky (MIC) preconditioner, to solve, until convergence, the following system to compute the vector $\delta\mathbf{u}$:

$$\mathbf{J}(\mathbf{u}_n) \delta\mathbf{u} = -\mathbf{N}(\mathbf{u}_n), \quad (2.19)$$

where with n the current outer loop iteration number is denoted, and $\mathbf{J}(\mathbf{u}_n)$ indicates the Jacobian matrix of derivatives of Eqs. (2.2)-(2.15) with respect to the state functions:

$$\mathbf{J}(\mathbf{u}_n) \triangleq \begin{pmatrix} \mathbf{A}_1 & \mathbf{B}_1 & \mathbf{C}_1 & \mathbf{D}_1 & \mathbf{E}_1 \\ \mathbf{A}_2 & \mathbf{B}_2 & \mathbf{C}_2 & \mathbf{D}_2 & \mathbf{E}_2 \\ \mathbf{A}_3 & \mathbf{B}_3 & \mathbf{C}_3 & \mathbf{D}_3 & \mathbf{E}_3 \\ \mathbf{A}_4 & \mathbf{B}_4 & \mathbf{C}_4 & \mathbf{D}_4 & \mathbf{E}_4 \\ \mathbf{A}_5 & \mathbf{B}_5 & \mathbf{C}_5 & \mathbf{D}_5 & \mathbf{E}_5 \end{pmatrix}; \quad (2.20)$$

CHAPTER 2. DESCRIPTION OF THE SYSTEM

components of this block matrix are detailed in Subsection C.1 of Appendix C. More in detail, $\mathbf{J}(\mathbf{u}_n)$ is a non-symmetric sparse matrix of order 197 by 197, with 166 nonzero diagonals because of the presence of the column vectors $(\mathbf{E}_1, \dots, \mathbf{E}_4)$ and of the row vectors $(\mathbf{A}_5, \dots, \mathbf{D}_5)$, which are responsible for 142 diagonals of the Jacobian matrix to contain just one non-zero element; this would have led to a massive efficiency loss of the diagonal storage format, which is the one selected for the GMRES linear solver, with the “condensed” Jacobian Matrix having dimensions 197 by 166. By producing the approximation of setting vectors $(\mathbf{E}_1, \dots, \mathbf{E}_4)$ and $(\mathbf{A}_5, \dots, \mathbf{D}_5)$ to zero the Jacobian matrix becomes a non-symmetric sparse matrix of order 197 by 197, with just 14 nonzero diagonals. The non-symmetric diagonal storage format is used to store the respective 14 nonzero diagonals, so that the “condensed” Jacobian matrix has dimensions 197 by 14. Since the Jacobian is highly non-symmetric, the computational cost of the GMRES solver iterations grows as $O(m^2)$, where m is the number of iterations performed within the GMRES solver. The restart feature allows to configure the GMRES solver in order to reduce this computational cost: for the specific application, an optimized value of 10 is chosen for the restart frequency. The convergence of the GMRES solver can be sped up by tuning the values of the parameters OMEGA and LVFILL [35] in the modified incomplete factorization methods for the MIC preconditioner; for the application of interest, the chosen optimal values were: OMEGA = 0.000000001 and LVFILL = 1. The sparse GMRES solver does not perform an internal update of the Jacobian matrix. The following criterion is used to test the default convergence of GMRES [35],

$$\left[\frac{\langle \tilde{\mathbf{z}}^{(m)}, \tilde{\mathbf{z}}^{(m)} \rangle}{\langle \delta \mathbf{u}^{(m)}, \delta \mathbf{u}^{(m)} \rangle} \right]^{\frac{1}{2}} < \zeta \quad (2.21)$$

where $\tilde{\mathbf{z}}^{(m)}$ is used to indicate the pseudo-residual at m^{th} -iteration of the

CHAPTER 2. DESCRIPTION OF THE SYSTEM

GMRES solver, $\delta \mathbf{u}^{(m)}$ is the solution of Eq. (2.19) at m^{th} -iteration, and ζ denotes the stopping test value for the GMRES solver;

(e) Set

$$\mathbf{u}_{n+1} = \mathbf{u}_n + \delta \mathbf{u} \quad (2.22)$$

where n is the number of the current outer loop iteration, and update the Jacobian;

(f) The outer loop convergence has to be tested until the solution error is less than a specified maximum value. For the solution of Eqs. (2.2)-(2.15), the following maximum error criterion has been used:

$$error = \max \left(\frac{|\delta m_w^{(i)}|}{m_w^{(i)}}, \frac{|\delta T_w^{(i)}|}{T_w^{(i)}}, \frac{|\delta T_a^{(i)}|}{T_a^{(i)}}, \frac{|\delta \omega^{(i)}|}{\omega^{(i)}}, \frac{|\delta m_a|}{m_a} \right) < 10^{-6} \quad (2.23)$$

(g) Set $n = n + 1$ and return to step (d).

For all the 377 saturated benchmark data sets taken into consideration for case 1a, the above strategy for the solution of Eqs. (2.2)-(2.15) has reached convergence.

As mentioned above and vastly reported in Appendix A, each of these data sets comprises measurements of the following quantities: (i) outlet air temperature measured with the “Tidbit” sensor; (ii) outlet air temperature measured with the “Hobo” sensor; (iii) outlet water temperature; (iv) outlet air relative humidity. For each of the 377 benchmark data sets, the outer loop iterations detailed above (i.e., steps (c) through (g)) reaches convergence in 4 iterations; for each outer loop iteration, the GMRES solver needs 12 iterations for solving Eq. (2.19). The solution accuracy is tested through a “zero-to-zero” verification, which yields an error of the order of 10^{-5} .

CHAPTER 2. DESCRIPTION OF THE SYSTEM

Based on the above-mentioned measured quantities comprised in the benchmark data sets, the quantities computed by solving the governing system are:

- (a) the vector $\mathbf{m}_w \triangleq [m_w^{(2)}, \dots, m_w^{(I+1)}]^\dagger$ of water mass flow rates at the exit of each control volume i , ($i = 1, \dots, 49$);
- (b) the vector $\mathbf{T}_w \triangleq [T_w^{(2)}, \dots, T_w^{(I+1)}]^\dagger$ of water temperatures at the exit of each control volume i , ($i = 1, \dots, 49$);
- (c) the vector $\mathbf{T}_a \triangleq [T_a^{(1)}, \dots, T_a^{(I)}]^\dagger$ of air temperatures at the exit of each control volume i , ($i = 1, \dots, 49$);
- (d) the vector $\mathbf{RH} \triangleq [RH^{(1)}, \dots, RH^{(I)}]^\dagger$, having as components the air relative humidity at the exit of each control volume i , ($i = 1, \dots, 49$);
- (e) the scalar m_a , representing the air mass flow rate along the height of the cooling tower.

It is worth specifying that the water mass flow rates $m_w^{(i)}$, the water temperatures $T_w^{(i)}$, the air temperatures $T_a^{(i)}$ and the air mass flow rate m_a are obtained directly as the solutions of Eqs. (2.2)-(2.15); the air relative humidity value, $RH^{(i)}$, is calculated instead, for each control volume, by means of the following expression:

$$RH^{(i)} = \frac{P_v(\omega^{(i)}, \boldsymbol{\alpha})}{P_{vs}(T_a^{(i)}, \boldsymbol{\alpha})} \times 100 = \frac{\left(\frac{\omega^{(i)} P_{atm}}{\omega^{(i)} + 0.622}\right)}{\left(e^{a_0 + \frac{a_1}{T_a^{(i)}}}\right)} \times 100 \quad (2.24)$$

The nominal values of the model parameters (α_i), used in solving Eqs. (2.2)-(2.15), are listed in Table B.1 of Subsection B.1.1, Appendix B. It is important to note that the nominal values for the first five parameters α_1 through α_5 (i.e., the dry bulb air temperature, dew point temperature, inlet water temperature, atmospheric pressure and wind speed) are obtained through a statistic mean of the values of the respective quantities in the 377 saturated data sets which fall in

CHAPTER 2. DESCRIPTION OF THE SYSTEM

case 1a. This solution strategy with Eqs. (2.17) through (2.23) has been applied to cases 1a, 1b and 2, i.e. all the cases in which the cooling tower is operated in natural draft mode.

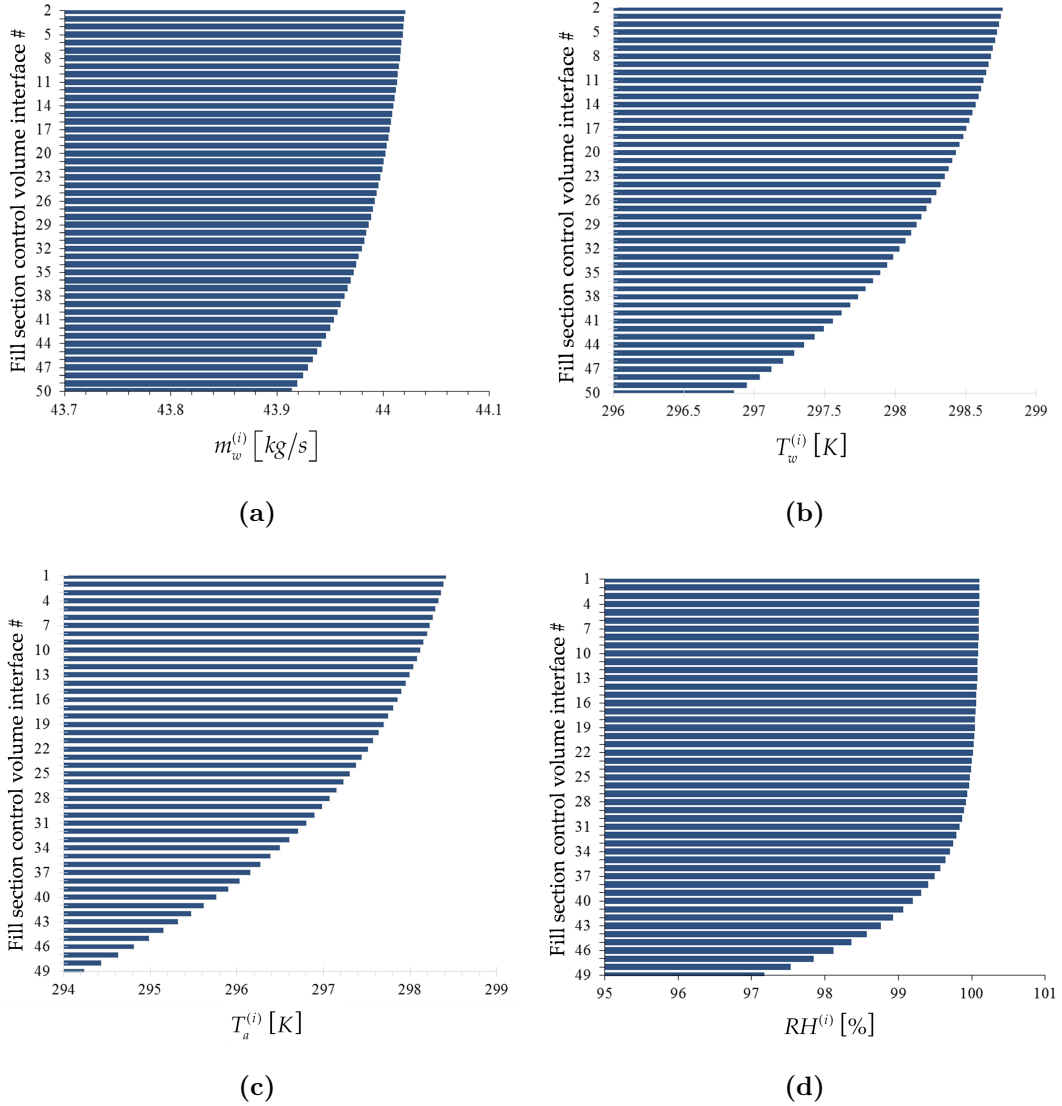


Figure 2.4: Bar plots of the state functions for **(a)** $m_w^{(i)}$, ($i = 2, \dots, 50$); **(b)** $T_w^{(i)}$, ($i = 2, \dots, 50$); **(c)** $T_a^{(i)}$, ($i = 1, \dots, 49$); **(d)** $RH^{(i)}$, ($i = 1, \dots, 49$) at the exit of each control volume along the height of the fill section of the cooling tower (for case 1a: fan off, saturated outlet air condition, with inlet air unsaturated).

The bar plots presented above in Figure 2.4 display the respective values of the water mass flow rates $m_w^{(i)}$, the water temperatures $T_w^{(i)}$, the air temperatures

CHAPTER 2. DESCRIPTION OF THE SYSTEM

$T_a^{(i)}$, and the air relative humidity, $RH^{(i)}$, at the exit of each of the 49 control volumes.

As shown in Figure 2.4, water mass flow rate $m_w^{(i)}$ decreases around 0.10 kg/s along the height of the fill section, from 44.021 kg/s at the inlet to 43.914 kg/s at the outlet; water temperature $T_w^{(i)}$ decreases around 1.9 K, from 298.77 K at the inlet to 296.86 K at the outlet; air temperature $T_a^{(i)}$ increases around 4.38 K, from 294.03 K at the inlet to 298.41 K at the outlet; and the air relative humidity $RH^{(i)}$ increases around 3.32%, from 96.78% at the inlet to 100.11% at the outlet. It is worth noting that the increase and decrease of the responses of interest are nonlinear along the height of the fill section. Air becomes saturated at the exit of the 23rd control volume, as shown in Figure 2.4(d). Thus air is in unsaturated condition from the inlet of the fill section (i.e., the 49th control volume) to the 24th control volume; it is in saturated condition from the 23rd control volume to the outlet of the fill section (i.e., the 1st control volume).

2.3.2 Mathematical Model for Case 1b: Natural Draft Cooling Tower operated in Saturated Outlet Air Condition, with Inlet Air Saturated

In this subcase, air is in saturated condition from the inlet through the outlet of the fill section, i.e., air is saturated in all the 49 control volumes. The state functions for the water mass flow rates $m_w^{(i)}$ ($i = 2, \dots, 50$), the water temperatures $T_w^{(i)}$ ($i = 2, \dots, 50$), the air temperatures $T_a^{(i)}$ ($i = 1, \dots, 49$), the humidity ratios $\omega^{(i)}$ ($i = 1, \dots, 49$), and the air mass flow rate are defined the same way as in case 1a, as described in Subsection 2.3.1.

The governing conservation equations within the total of I=49 control volumes represented in Figure 2.2 are the following [26]:

CHAPTER 2. DESCRIPTION OF THE SYSTEM

A. Liquid continuity equations:

(i) Control Volume $i = 1$:

$$\begin{aligned} N_1^{(1)}(\mathbf{m}_w, \mathbf{T}_w, \mathbf{T}_a, \boldsymbol{\omega}, m_a; \boldsymbol{\alpha}) &\triangleq m_w^{(2)} - m_{w,in} \\ &+ \frac{M(m_a, \boldsymbol{\alpha})}{\bar{R}} \left[\frac{P_{vs}^{(2)}(T_w^{(2)}, \boldsymbol{\alpha})}{T_w^{(2)}} - \frac{P_{vs}^{(1)}(T_a^{(1)}, \boldsymbol{\alpha})}{T_a^{(1)}} \right] = 0 \end{aligned} \quad (2.25)$$

(ii) Control Volumes $i = 2, \dots, I - 1$:

$$\begin{aligned} N_1^{(i)}(\mathbf{m}_w, \mathbf{T}_w, \mathbf{T}_a, \boldsymbol{\omega}, m_a; \boldsymbol{\alpha}) &\triangleq m_w^{(i+1)} - m_w^{(i)} \\ &+ \frac{M(m_a, \boldsymbol{\alpha})}{\bar{R}} \left[\frac{P_{vs}^{(i+1)}(T_w^{(i+1)}, \boldsymbol{\alpha})}{T_w^{(i+1)}} - \frac{P_{vs}^{(i)}(T_a^{(i)}, \boldsymbol{\alpha})}{T_a^{(i)}} \right] = 0 \end{aligned} \quad (2.26)$$

(iii) Control Volume $i = I$:

$$\begin{aligned} N_1^{(I)}(\mathbf{m}_w, \mathbf{T}_w, \mathbf{T}_a, \boldsymbol{\omega}, m_a; \boldsymbol{\alpha}) &\triangleq m_w^{(I+1)} - m_w^{(I)} \\ &+ \frac{M(m_a, \boldsymbol{\alpha})}{\bar{R}} \left[\frac{P_{vs}^{(I+1)}(T_w^{(I+1)}, \boldsymbol{\alpha})}{T_w^{(I+1)}} - \frac{P_{vs}^{(I)}(T_a^{(I)}, \boldsymbol{\alpha})}{T_a^{(I)}} \right] = 0 \end{aligned} \quad (2.27)$$

B. Liquid energy balance equations:

(i) Control Volume $i = 1$:

$$\begin{aligned} N_2^{(1)}(\mathbf{m}_w, \mathbf{T}_w, \mathbf{T}_a, \boldsymbol{\omega}, m_a; \boldsymbol{\alpha}) &\triangleq m_{w,in} h_f(T_{w,in}, \boldsymbol{\alpha}) \\ &- (T_w^{(2)} - T_a^{(1)}) H(m_a, \boldsymbol{\alpha}) - m_w^{(2)} h_f^{(2)}(T_w^{(2)}, \boldsymbol{\alpha}) \\ &- (m_{w,in} - m_w^{(2)}) h_{g,w}^{(2)}(T_w^{(2)}, \boldsymbol{\alpha}) = 0 \end{aligned} \quad (2.28)$$

(ii) Control Volumes $i = 2, \dots, I - 1$:

$$\begin{aligned} N_2^{(i)}(\mathbf{m}_w, \mathbf{T}_w, \mathbf{T}_a, \boldsymbol{\omega}, m_a; \boldsymbol{\alpha}) &\triangleq m_w^{(i)} h_f^{(i)}(T_w^{(i)}, \boldsymbol{\alpha}) \\ &- (T_w^{(i+1)} - T_a^{(i)}) H(m_a, \boldsymbol{\alpha}) - m_w^{(i+1)} h_f^{(i+1)}(T_w^{(i+1)}, \boldsymbol{\alpha}) \\ &- (m_w^{(i)} - m_w^{(i+1)}) h_{g,w}^{(i+1)}(T_w^{(i+1)}, \boldsymbol{\alpha}) = 0 \end{aligned} \quad (2.29)$$

CHAPTER 2. DESCRIPTION OF THE SYSTEM

(iii) Control Volume $i = I$:

$$\begin{aligned}
 N_2^{(I)}(\mathbf{m}_w, \mathbf{T}_w, \mathbf{T}_a, \boldsymbol{\omega}, m_a; \boldsymbol{\alpha}) &\triangleq m_w^{(I)} h_f^{(I)}(T_w^{(I)}, \boldsymbol{\alpha}) \\
 - (T_w^{(I+1)} - T_a^{(I)}) H(m_a, \boldsymbol{\alpha}) - m_w^{(I+1)} h_f^{(I+1)}(T_w^{(I+1)}, \boldsymbol{\alpha}) &\quad (2.30) \\
 - (m_w^{(I)} - m_w^{(I+1)}) h_{g,w}^{(I+1)}(T_w^{(I+1)}, \boldsymbol{\alpha}) &= 0
 \end{aligned}$$

C. Water vapor continuity equations:

(i) Control Volume $i = 1$:

$$N_3^{(1)}(\mathbf{m}_w, \mathbf{T}_w, \mathbf{T}_a, \boldsymbol{\omega}, m_a; \boldsymbol{\alpha}) \triangleq \omega^{(2)} - \omega^{(1)} + \frac{m_{w.in} - m_w^{(2)}}{|m_a|} = 0 \quad (2.31)$$

(ii) Control Volumes $i = 2, \dots, I - 1$:

$$N_3^{(i)}(\mathbf{m}_w, \mathbf{T}_w, \mathbf{T}_a, \boldsymbol{\omega}, m_a; \boldsymbol{\alpha}) \triangleq \omega^{(i+1)} - \omega^{(i)} + \frac{m_w^{(i)} - m_w^{(i+1)}}{|m_a|} = 0 \quad (2.32)$$

(iii) Control Volume $i = I$:

$$N_3^{(I)}(\mathbf{m}_w, \mathbf{T}_w, \mathbf{T}_a, \boldsymbol{\omega}, m_a; \boldsymbol{\alpha}) \triangleq \omega_{in} - \omega^{(I)} + \frac{m_w^{(I)} - m_w^{(I+1)}}{|m_a|} = 0 \quad (2.33)$$

D. Air/water vapor energy balance equations:

(i) Control Volume $i = 1$:

$$\begin{aligned}
 N_4^{(1)}(\mathbf{m}_w, \mathbf{T}_w, \mathbf{T}_a, \boldsymbol{\omega}, m_a; \boldsymbol{\alpha}) &\triangleq (T_a^{(2)} - T_a^{(1)}) C_p^{(1)} \left(\frac{T_a^{(1)} + 273.15}{2}, \boldsymbol{\alpha} \right) \\
 - \omega^{(1)} h_{g,a}^{(1)}(T_a^{(1)}, \boldsymbol{\alpha}) &+ \frac{(T_w^{(2)} - T_a^{(1)}) H(m_a, \boldsymbol{\alpha})}{|m_a|} \\
 + \frac{(m_{w.in} - m_w^{(2)}) h_{g,w}^{(2)}(T_w^{(2)}, \boldsymbol{\alpha})}{|m_a|} &+ \omega^{(2)} h_{g,a}^{(2)}(T_a^{(2)}, \boldsymbol{\alpha}) = 0
 \end{aligned} \quad (2.34)$$

CHAPTER 2. DESCRIPTION OF THE SYSTEM

(ii) Control Volumes $i = 2, \dots, I - 1$:

$$\begin{aligned}
 N_4^{(i)}(\mathbf{m}_w, \mathbf{T}_w, \mathbf{T}_a, \boldsymbol{\omega}, m_a; \boldsymbol{\alpha}) &\triangleq (T_a^{(i+1)} - T_a^{(i)}) C_p^{(i)} \left(\frac{T_a^{(i)} + 273.15}{2}, \boldsymbol{\alpha} \right) \\
 &- \omega^{(i)} h_{g,a}^{(i)}(T_a^{(i)}, \boldsymbol{\alpha}) + \frac{(T_w^{(i+1)} - T_a^{(i)}) H(m_a, \boldsymbol{\alpha})}{|m_a|} \\
 &+ \frac{(m_w^{(i)} - m_w^{(i+1)}) h_{g,w}^{(i+1)}(T_w^{(i+1)}, \boldsymbol{\alpha})}{|m_a|} + \omega^{(i+1)} h_{g,a}^{(i+1)}(T_a^{(i+1)}, \boldsymbol{\alpha}) = 0
 \end{aligned} \tag{2.35}$$

(iii) Control Volume $i = I$:

$$\begin{aligned}
 N_4^{(I)}(\mathbf{m}_w, \mathbf{T}_w, \mathbf{T}_a, \boldsymbol{\omega}, m_a; \boldsymbol{\alpha}) &\triangleq (T_{a,in} - T_a^{(I)}) C_p^{(I)} \left(\frac{T_a^{(I)} + 273.15}{2}, \boldsymbol{\alpha} \right) \\
 &- \omega^{(I)} h_{g,a}^{(I)}(T_a^{(I)}, \boldsymbol{\alpha}) + \frac{(T_w^{(I+1)} - T_a^{(I)}) H(m_a, \boldsymbol{\alpha})}{|m_a|} \\
 &+ \frac{(m_w^{(I)} - m_w^{(I+1)}) h_{g,w}^{(I+1)}(T_w^{(I+1)}, \boldsymbol{\alpha})}{|m_a|} + \omega_{in} h_{g,a}(T_{a,in}, \boldsymbol{\alpha}) = 0
 \end{aligned} \tag{2.36}$$

E. Mechanical energy equation:

$$\begin{aligned}
 N_5(\mathbf{m}_w, \mathbf{T}_w, \mathbf{T}_a, \boldsymbol{\omega}, m_a; \boldsymbol{\alpha}) &\triangleq \left[\frac{1}{2\rho(T_{tdb}, \boldsymbol{\alpha})} \left(\frac{1}{A_{out}(\boldsymbol{\alpha})^2} - \frac{1}{A_{in}(\boldsymbol{\alpha})^2} + \frac{k_{sum}}{A_{fill}^2} \right) \right. \\
 &+ \frac{f}{2\rho(T_{tdb}, \boldsymbol{\alpha})} \frac{96}{\text{Re}(m_a, \boldsymbol{\alpha})} \frac{L_{fill}(\boldsymbol{\alpha})}{A_{fill}^2 D_h} \left. \right] |m_a| m_a - gZ(\boldsymbol{\alpha}) \rho(T_{tdb}, \boldsymbol{\alpha}) \\
 &- \frac{V_w^2 \rho(T_{tdb}, \boldsymbol{\alpha})}{2} + \Delta z_{rain} g \rho(T_{tdb}, \boldsymbol{\alpha}) + g \rho(T_a^{(1)}, \boldsymbol{\alpha}) \Delta z_{4-2}(\boldsymbol{\alpha}) \\
 &+ g \Delta z(\boldsymbol{\alpha}) \frac{P_{atm}}{R_{air}} \left[\frac{1}{2T_{a,in}} + \frac{1}{2T_a^{(1)}} + \sum_{i=2}^I \frac{1}{T_a^{(i)}} \right] = 0
 \end{aligned} \tag{2.37}$$

CHAPTER 2. DESCRIPTION OF THE SYSTEM

The differences between the governing equations for case 1a and case 1b are in the “liquid continuity equations”. Specifically, for case 1a, the “liquid continuity equations” are defined in Eqs. (2.2)-(2.5); whereas for case 1b, they are defined in Eqs. (2.25)-(2.27). Other governing equations (i.e., liquid energy balance equations; water vapor continuity equations; and the air/water vapor energy balance equations) are the same for both cases 1a and 1b.

The components of the model parameter vector α , which appears in Eqs. (2.25)-(2.37), are the same as that of case 1a. The nominal values of the model parameters (α_i) are listed in Table B.9 of Subsection B.1.2, Appendix B. Again, the nominal values for the first five parameters α_1 through α_5 are the statistic mean values of the respective quantities in the 290 saturated data sets which are considered in case 1b. These model parameters (i.e., α_1 through α_5) are experimentally derived quantities, and their complete distributions are not known; however, the first four moments (means, variance/covariance, skewness, and kurtosis) of each of these parameter distributions have been calculated, as detailed in Appendix B, Subsection B.1.2.

Similarly, the above-mentioned solution strategy, i.e. Newton’s method together with the GMRES linear iterative solver for sparse matrices, already used in solving Eqs. (2.2)-(2.15) for case 1a, is also used to solve Eqs. (2.25)-(2.37) for case 1b. The procedure converged successfully for all the 290 saturated benchmark data sets which are considered in case 1b. For each of these benchmark data sets, the outer loop iterations converge in 4 iterations; for each outer loop iteration, the GMRES solver used for solving Eq. (2.19) converges in 12 iterations. The “zero-to-zero” verification of the solution accuracy using Eqs. (2.25) through (2.37) gives an error of the order of 10^{-5} .

The responses of interest such as the water mass flow rates $m_w^{(i)}$, the water temperatures $T_w^{(i)}$, the air temperatures $T_a^{(i)}$, and the air mass flow rate m_a are

CHAPTER 2. DESCRIPTION OF THE SYSTEM

obtained directly as the solutions of Eqs. (2.25)-(2.37), while the air relative humidity, $RH^{(i)}$, is computed for each control volume using Eq. (2.24). The bar plots presented in Figure 2.5 display the respective values of the water mass flow rates $m_w^{(i)}$, the water temperatures $T_w^{(i)}$, the air temperatures $T_a^{(i)}$, and the air relative humidity, $RH^{(i)}$, at the exit of each of the 49 control volumes.

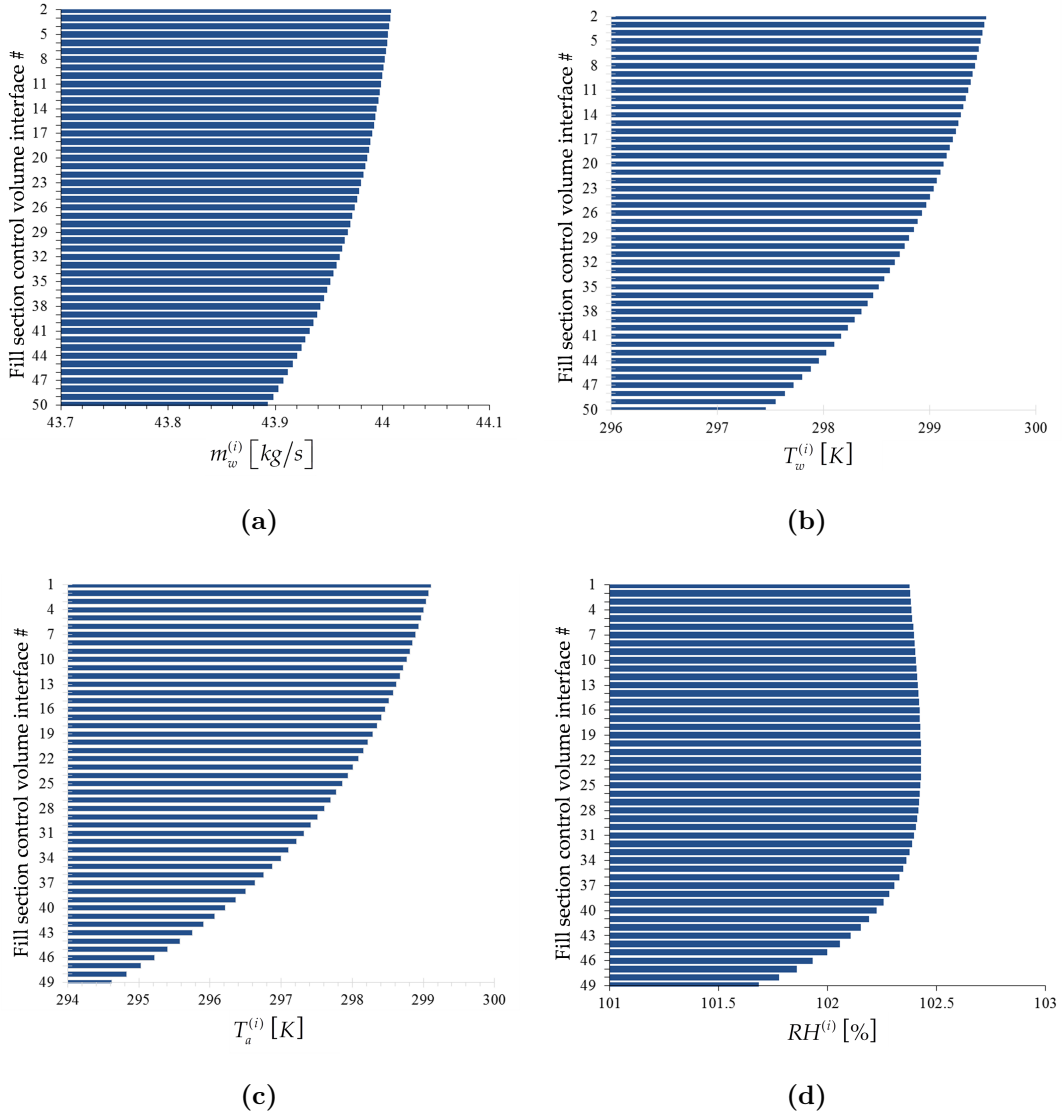


Figure 2.5: Bar plots of the state functions for **(a)** $m_w^{(i)}$, ($i = 2, \dots, 50$); **(b)** $T_w^{(i)}$, ($i = 2, \dots, 50$); **(c)** $T_a^{(i)}$, ($i = 1, \dots, 49$); **(d)** $RH^{(i)}$, ($i = 1, \dots, 49$) at the exit of each control volume along the height of the fill section of the cooling tower (for case 1b: fan off, saturated outlet air condition, with inlet air saturated).

CHAPTER 2. DESCRIPTION OF THE SYSTEM

As shown in the Figure 2.5, water mass flow rate $m_w^{(i)}$ decreases around 0.11 kg/s along the height of the fill section, from 44.01 kg/s at the inlet to 43.89 kg/s at the outlet; water temperature $T_w^{(i)}$ decreases around 2.1 K, from 299.54 K at the inlet to 297.46 K at the outlet; air temperature $T_a^{(i)}$ increases around 4.7 K, from 294.40 K at the inlet to 299.1 K at the outlet; and the air relative humidity $RH^{(i)}$ increases around 0.80%, from 101.58% at the inlet to 102.38% at the outlet. As shown in Figure 2.5(d), air is in saturated condition from the inlet through the outlet of the fill section.

2.3.3 Mathematical Model for Case 2: Natural Draft Cooling Tower operated in Unsaturated Outlet Air Condition, with Inlet Air Unsaturated

In this case, air is in unsaturated condition from the inlet through the outlet of the fill section, i.e., air is unsaturated in all the 49 control volumes.

The state functions for the the water mass flow rates $m_w^{(i)}$ ($i = 2, \dots, 50$), the water temperatures $T_w^{(i)}$ ($i = 2, \dots, 50$), the air temperatures $T_a^{(i)}$ ($i = 1, \dots, 49$), the humidity ratios $\omega^{(i)}$ ($i = 1, \dots, 49$), and the mass flow rates are defined the same way as in cases 1a and 1b, Sections 2.3.1 and 2.3.2.

The governing conservation equations within the total of I=49 control volumes represented in Figure 2.2 are the following [26]:

A. Liquid continuity equations:

(i) Control Volume $i = 1$:

$$N_1^{(1)}(\mathbf{m}_w, \mathbf{T}_w, \mathbf{T}_a, \boldsymbol{\omega}, m_a; \boldsymbol{\alpha}) \triangleq m_w^{(2)} - m_{w,in} + \frac{M(m_a, \boldsymbol{\alpha})}{\bar{R}} \left[\frac{P_{vs}^{(2)}(T_w^{(2)}, \boldsymbol{\alpha})}{T_w^{(2)}} - \frac{\omega^{(1)} P_{atm}}{T_a^{(1)} (0.622 + \omega^{(1)})} \right] = 0 \quad (2.38)$$

CHAPTER 2. DESCRIPTION OF THE SYSTEM

(ii) Control Volumes $i = 2, \dots, I - 1$:

$$N_1^{(i)}(\mathbf{m}_w, \mathbf{T}_w, \mathbf{T}_a, \boldsymbol{\omega}, m_a; \boldsymbol{\alpha}) \triangleq m_w^{(i+1)} - m_w^{(i)} + \frac{M(m_a, \boldsymbol{\alpha})}{\bar{R}} \left[\frac{P_{vs}^{(i+1)}(T_w^{(i+1)}, \boldsymbol{\alpha})}{T_w^{(i+1)}} - \frac{\omega^{(i)} P_{atm}}{T_a^{(i)} (0.622 + \omega^{(i)})} \right] = 0 \quad (2.39)$$

(iii) Control Volume $i = I$:

$$N_1^{(I)}(\mathbf{m}_w, \mathbf{T}_w, \mathbf{T}_a, \boldsymbol{\omega}, m_a; \boldsymbol{\alpha}) \triangleq m_w^{(I+1)} - m_w^{(I)} + \frac{M(m_a, \boldsymbol{\alpha})}{\bar{R}} \left[\frac{P_{vs}^{(I+1)}(T_w^{(I+1)}, \boldsymbol{\alpha})}{T_w^{(I+1)}} - \frac{\omega^{(I)} P_{atm}}{T_a^{(I)} (0.622 + \omega^{(I)})} \right] = 0 \quad (2.40)$$

B. Liquid energy balance equations:

(i) Control Volume $i = 1$:

$$N_2^{(1)}(\mathbf{m}_w, \mathbf{T}_w, \mathbf{T}_a, \boldsymbol{\omega}, m_a; \boldsymbol{\alpha}) \triangleq m_{w,in} h_f(T_{w,in}, \boldsymbol{\alpha}) - (T_w^{(2)} - T_a^{(1)}) H(m_a, \boldsymbol{\alpha}) - m_w^{(2)} h_f^{(2)}(T_w^{(2)}, \boldsymbol{\alpha}) - (m_{w,in} - m_w^{(2)}) h_{g,w}^{(2)}(T_w^{(2)}, \boldsymbol{\alpha}) = 0 \quad (2.41)$$

(ii) Control Volumes $i = 2, \dots, I - 1$:

$$N_2^{(i)}(\mathbf{m}_w, \mathbf{T}_w, \mathbf{T}_a, \boldsymbol{\omega}, m_a; \boldsymbol{\alpha}) \triangleq m_w^{(i)} h_f^{(i)}(T_w^{(i)}, \boldsymbol{\alpha}) - (T_w^{(i+1)} - T_a^{(i)}) H(m_a, \boldsymbol{\alpha}) - m_w^{(i+1)} h_f^{(i+1)}(T_w^{(i+1)}, \boldsymbol{\alpha}) - (m_w^{(i)} - m_w^{(i+1)}) h_{g,w}^{(i+1)}(T_w^{(i+1)}, \boldsymbol{\alpha}) = 0 \quad (2.42)$$

(iii) Control Volume $i = I$:

$$N_2^{(I)}(\mathbf{m}_w, \mathbf{T}_w, \mathbf{T}_a, \boldsymbol{\omega}, m_a; \boldsymbol{\alpha}) \triangleq m_w^{(I)} h_f^{(I)}(T_w^{(I)}, \boldsymbol{\alpha}) - (T_w^{(I+1)} - T_a^{(I)}) H(m_a, \boldsymbol{\alpha}) - m_w^{(I+1)} h_f^{(I+1)}(T_w^{(I+1)}, \boldsymbol{\alpha}) - (m_w^{(I)} - m_w^{(I+1)}) h_{g,w}^{(I+1)}(T_w^{(I+1)}, \boldsymbol{\alpha}) = 0 \quad (2.43)$$

CHAPTER 2. DESCRIPTION OF THE SYSTEM

C. Water vapor continuity equations:

(i) Control Volume $i = 1$:

$$N_3^{(1)}(\mathbf{m}_w, \mathbf{T}_w, \mathbf{T}_a, \boldsymbol{\omega}, m_a; \boldsymbol{\alpha}) \triangleq \omega^{(2)} - \omega^{(1)} + \frac{m_{w.in} - m_w^{(2)}}{|m_a|} = 0 \quad (2.44)$$

(ii) Control Volumes $i = 2, \dots, I - 1$:

$$N_3^{(i)}(\mathbf{m}_w, \mathbf{T}_w, \mathbf{T}_a, \boldsymbol{\omega}, m_a; \boldsymbol{\alpha}) \triangleq \omega^{(i+1)} - \omega^{(i)} + \frac{m_w^{(i)} - m_w^{(i+1)}}{|m_a|} = 0 \quad (2.45)$$

(iii) Control Volume $i = I$:

$$N_3^{(I)}(\mathbf{m}_w, \mathbf{T}_w, \mathbf{T}_a, \boldsymbol{\omega}, m_a; \boldsymbol{\alpha}) \triangleq \omega_{in} - \omega^{(I)} + \frac{m_w^{(I)} - m_w^{(I+1)}}{|m_a|} = 0 \quad (2.46)$$

D. Air/water vapor energy balance equations:

(i) Control Volume $i = 1$:

$$\begin{aligned} N_4^{(1)}(\mathbf{m}_w, \mathbf{T}_w, \mathbf{T}_a, \boldsymbol{\omega}, m_a; \boldsymbol{\alpha}) \triangleq & (T_a^{(2)} - T_a^{(1)}) C_p^{(1)} \left(\frac{T_a^{(1)} + 273.15}{2}, \boldsymbol{\alpha} \right) \\ & - \omega^{(1)} h_{g,a}^{(1)}(T_a^{(1)}, \boldsymbol{\alpha}) + \frac{(T_w^{(2)} - T_a^{(1)}) H(m_a, \boldsymbol{\alpha})}{|m_a|} \\ & + \frac{(m_{w.in} - m_w^{(2)}) h_{g,w}^{(2)}(T_w^{(2)}, \boldsymbol{\alpha})}{|m_a|} + \omega^{(2)} h_{g,a}^{(2)}(T_a^{(2)}, \boldsymbol{\alpha}) = 0 \end{aligned} \quad (2.47)$$

(ii) Control Volumes $i = 2, \dots, I - 1$:

$$\begin{aligned} N_4^{(i)}(\mathbf{m}_w, \mathbf{T}_w, \mathbf{T}_a, \boldsymbol{\omega}, m_a; \boldsymbol{\alpha}) \triangleq & (T_a^{(i+1)} - T_a^{(i)}) C_p^{(i)} \left(\frac{T_a^{(i)} + 273.15}{2}, \boldsymbol{\alpha} \right) \\ & - \omega^{(i)} h_{g,a}^{(i)}(T_a^{(i)}, \boldsymbol{\alpha}) + \frac{(T_w^{(i+1)} - T_a^{(i)}) H(m_a, \boldsymbol{\alpha})}{|m_a|} \\ & + \frac{(m_w^{(i)} - m_w^{(i+1)}) h_{g,w}^{(i+1)}(T_w^{(i+1)}, \boldsymbol{\alpha})}{|m_a|} + \omega^{(i+1)} h_{g,a}^{(i+1)}(T_a^{(i+1)}, \boldsymbol{\alpha}) = 0 \end{aligned} \quad (2.48)$$

CHAPTER 2. DESCRIPTION OF THE SYSTEM

(iii) *Control Volume $i = I$:*

$$\begin{aligned}
 N_4^{(I)}(\mathbf{m}_w, \mathbf{T}_w, \mathbf{T}_a, \boldsymbol{\omega}, m_a; \boldsymbol{\alpha}) &\triangleq (T_{a,in} - T_a^{(I)}) C_p^{(I)} \left(\frac{T_a^{(I)} + 273.15}{2}, \boldsymbol{\alpha} \right) \\
 &\quad - \omega^{(I)} h_{g,a}^{(I)}(T_a^{(I)}, \boldsymbol{\alpha}) + \frac{(T_w^{(I+1)} - T_a^{(I)}) H(m_a, \boldsymbol{\alpha})}{|m_a|} \\
 &\quad + \frac{(m_w^{(I)} - m_w^{(I+1)}) h_{g,w}^{(I+1)}(T_w^{(I+1)}, \boldsymbol{\alpha})}{|m_a|} + \omega_{in} h_{g,a}(T_{a,in}, \boldsymbol{\alpha}) = 0
 \end{aligned} \tag{2.49}$$

E. Mechanical energy equation:

$$\begin{aligned}
 N_5(\mathbf{m}_w, \mathbf{T}_w, \mathbf{T}_a, \boldsymbol{\omega}, m_a; \boldsymbol{\alpha}) &\triangleq \left[\frac{1}{2\rho(T_{tdb}, \boldsymbol{\alpha})} \left(\frac{1}{A_{out}(\boldsymbol{\alpha})^2} - \frac{1}{A_{in}(\boldsymbol{\alpha})^2} + \frac{k_{sum}}{A_{fill}^2} \right) \right. \\
 &\quad \left. + \frac{f}{2\rho(T_{tdb}, \boldsymbol{\alpha})} \frac{96}{\text{Re}(m_a, \boldsymbol{\alpha})} \frac{L_{fill}(\boldsymbol{\alpha})}{A_{fill}^2 D_h} \right] |m_a| m_a - gZ(\boldsymbol{\alpha}) \rho(T_{tdb}, \boldsymbol{\alpha}) \\
 &\quad - \frac{V_w^2 \rho(T_{tdb}, \boldsymbol{\alpha})}{2} + \Delta z_{rain} g \rho(T_{tdb}, \boldsymbol{\alpha}) + g \rho(T_a^{(1)}, \boldsymbol{\alpha}) \Delta z_{4-2}(\boldsymbol{\alpha}) \\
 &\quad + g \Delta z(\boldsymbol{\alpha}) \frac{P_{atm}}{R_{air}} \left[\frac{1}{2T_{a,in}} + \frac{1}{2T_a^{(1)}} + \sum_{i=2}^I \frac{1}{T_a^{(i)}} \right] = 0
 \end{aligned} \tag{2.50}$$

The differences with the governing equations of cases 1a and 1b listed above are, again, in the “liquid continuity equations”. All the other governing equations (i.e., liquid energy balance equations; water vapor continuity equations; and the air/water vapor energy balance equations) remain unaltered.

The components of the model parameter vector $\boldsymbol{\alpha}$, which appears in Eqs. (2.38)-(2.50), are the same as that of cases 1a and 1b. The nominal values of the model parameters (α_i) are listed in Table B.15 of Subsection B.1.3, Appendix B. Again, the nominal values for the first five parameters α_1 through α_5 are the statistic mean values of the respective quantities in the 6717 unsaturated data sets considered. These model parameters (i.e., α_1 through α_5) are experimentally

CHAPTER 2. DESCRIPTION OF THE SYSTEM

derived quantities, and their complete distributions are not known; however, the first four moments (means, variance/covariance, skewness, and kurtosis) of each of these parameter distributions have been calculated, as detailed in Appendix B, Subsection B.1.3.

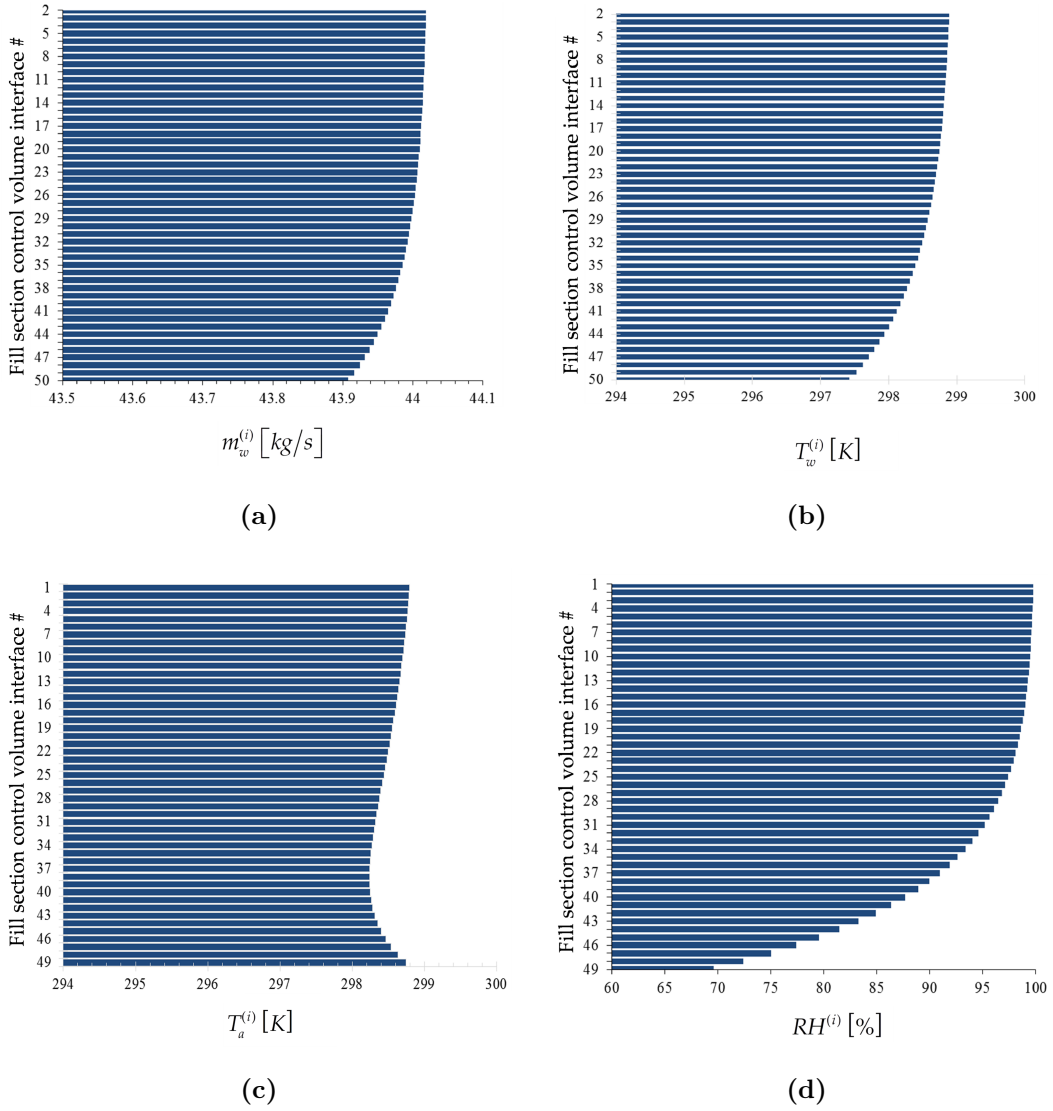


Figure 2.6: Bar plots of the state functions for (a) $m_w^{(i)}$, ($i = 2, \dots, 50$); (b) $T_w^{(i)}$, ($i = 2, \dots, 50$); (c) $T_a^{(i)}$, ($i = 1, \dots, 49$); (d) $RH^{(i)}$, ($i = 1, \dots, 49$) at the exit of each control volume along the height of the fill section of the cooling tower (for case 2: fan off, unsaturated air conditions).

CHAPTER 2. DESCRIPTION OF THE SYSTEM

The solution strategy mentioned in Subsection 2.1.1, i.e. Newton’s method together with the GMRES linear iterative solver for sparse matrices, already used for cases 1a and 1b, is also used to solve Eqs. (2.38)-(2.50) for case 2. The procedure converged successfully for all the 6717 unsaturated benchmark data sets. The outer loop converge in 4 iterations; for each outer loop iteration, the GMRES solver used for solving Eq. (2.19) converges in 8 iterations. The “zero-to-zero” verification of the solution accuracy using Eqs. (2.38) through (2.50) gives an error of the order of 10^{-5} . The bar plots presented in Figure 2.6 display the respective values of the water mass flow rates $m_w^{(i)}$, the water temperatures $T_w^{(i)}$, the air temperatures $T_a^{(i)}$, and the air relative humidity, $RH^{(i)}$, at the exit of each of the 49 control volumes.

Chapter 3

Description of the mathematical framework

3.1 Development of the Adjoint Sensitivity Model with the Adjoint Sensitivity Analysis Methodology (ASAM)

This section presents the development of the cooling tower adjoint sensitivity model, along with the solution method for computing the adjoint state functions.

3.1.1 Development of the Cooling Tower Adjoint Sensitivity Model for Case 1a: Fan Off, Saturated Outlet Air Conditions, with Inlet Air Unsaturated

The experimentally measured and/or computed responses of case 1a listed in Section 2.3.1 can be represented in the functional form $R(\mathbf{m}_w, \mathbf{T}_w, \mathbf{T}_a, \boldsymbol{\omega}, m_a; \boldsymbol{\alpha})$, where R denotes a known functional of the model state functions and parame-

CHAPTER 3. DESCRIPTION OF THE MATHEMATICAL FRAMEWORK

ters. As generally proved in [1], it is possible to compute the sensitivity of this functional to arbitrary variations in the model parameters $\delta\boldsymbol{\alpha} \triangleq (\delta\alpha_1, \dots, \delta\alpha_{N_\alpha})$ and state functions $\delta\mathbf{m}_w, \delta\mathbf{T}_w, \delta\mathbf{T}_a, \delta\boldsymbol{\omega}, \delta m_a$ by means of the response Gâteaux (G-)differential $DR(\mathbf{m}_w^0, \mathbf{T}_w^0, \mathbf{T}_a^0, \boldsymbol{\omega}^0, m_a^0; \boldsymbol{\alpha}^0; \delta\mathbf{m}_w, \delta\mathbf{T}_w, \delta\mathbf{T}_a, \delta\boldsymbol{\omega}, \delta m_a; \delta\boldsymbol{\alpha})$, which is defined as:

$$\begin{aligned} DR(\mathbf{m}_w^0, \mathbf{T}_w^0, \mathbf{T}_a^0, \boldsymbol{\omega}^0, m_a^0; \boldsymbol{\alpha}^0; \delta\mathbf{m}_w, \delta\mathbf{T}_w, \delta\mathbf{T}_a, \delta\boldsymbol{\omega}, \delta m_a; \delta\boldsymbol{\alpha}) &\triangleq \\ \frac{d}{d\varepsilon} [R(\mathbf{m}_w^0 + \varepsilon\delta\mathbf{m}_w, \mathbf{T}_w^0 + \varepsilon\delta\mathbf{T}_w, \mathbf{T}_a^0 + \varepsilon\delta\mathbf{T}_a, \boldsymbol{\omega}^0 + \varepsilon\delta\boldsymbol{\omega}, m_a^0 + \varepsilon\delta m_a; \boldsymbol{\alpha}^0 + \varepsilon\delta\boldsymbol{\alpha})]_{\varepsilon=0} \\ &= DR_{direct} + DR_{indirect} \end{aligned} \quad (3.1)$$

where the so-called “direct effect” term, DR_{direct} , and the so-called “indirect effect” term, $DR_{indirect}$, are respectively defined as follows:

$$\begin{aligned} DR_{direct} &\triangleq \sum_{i=1}^{N_\alpha} \left(\frac{\partial R}{\partial \alpha_i} \delta \alpha_i \right) \\ DR_{indirect} &\triangleq \sum_{i=1}^I \left(\frac{\partial R}{\partial m_w^{(i+1)}} \delta m_w^{(i+1)} + \frac{\partial R}{\partial T_w^{(i+1)}} \delta T_w^{(i+1)} + \frac{\partial R}{\partial T_a^{(i)}} \delta T_a^{(i)} + \frac{\partial R}{\partial \omega^{(i)}} \delta \omega^{(i)} \right) \\ &\quad + \frac{\partial R}{\partial m_a} \delta m_a = \mathbf{R}_1 \cdot \delta\mathbf{m}_w + \mathbf{R}_2 \cdot \delta\mathbf{T}_w + \mathbf{R}_3 \cdot \delta\mathbf{T}_a + \mathbf{R}_4 \cdot \delta\boldsymbol{\omega} + R_5 \cdot \delta m_a \end{aligned} \quad (3.3)$$

where the components of the vectors $\mathbf{R}_\ell \triangleq (r_\ell^{(1)}, \dots, r_\ell^{(I)})$, $\ell = 1, 2, 3, 4$ are defined as follows:

$$r_1^{(i)} \triangleq \frac{\partial R}{\partial m_w^{(i+1)}}; \quad r_2^{(i)} \triangleq \frac{\partial R}{\partial T_w^{(i+1)}}; \quad r_3^{(i)} \triangleq \frac{\partial R}{\partial T_a^{(i)}}; \quad r_4^{(i)} \triangleq \frac{\partial R}{\partial \omega^{(i)}}; \quad i = 1, \dots, I. \quad (3.4)$$

CHAPTER 3. DESCRIPTION OF THE MATHEMATICAL FRAMEWORK

and where R_5 is defined as follows:

$$R_5 \triangleq \frac{\partial R}{\partial m_a} \quad (3.5)$$

Since Eqs. (2.2) - (2.15) relate the model parameters to the model state functions, changes in the model parameters will cause changes in the state variables. More in detail, it has been found in [1-4] that to first-order in the parameter variations, the respective change in the state variables values can be obtained by solving the G-differentiated model equations, namely:

$$\frac{d}{d\varepsilon} [\mathbf{N}(\mathbf{u}^0 + \varepsilon \delta \mathbf{u}; \boldsymbol{\alpha}^0 + \varepsilon \delta \boldsymbol{\alpha})]_{\varepsilon=0} = \mathbf{0}. \quad (3.6)$$

Differentiating as above Eqs. (2.2) through (2.15) yields the following forward sensitivity system:

$$\begin{pmatrix} \mathbf{A}_1 & \mathbf{B}_1 & \mathbf{C}_1 & \mathbf{D}_1 & \mathbf{E}_1 \\ \mathbf{A}_2 & \mathbf{B}_2 & \mathbf{C}_2 & \mathbf{D}_2 & \mathbf{E}_2 \\ \mathbf{A}_3 & \mathbf{B}_3 & \mathbf{C}_3 & \mathbf{D}_3 & \mathbf{E}_3 \\ \mathbf{A}_4 & \mathbf{B}_4 & \mathbf{C}_4 & \mathbf{D}_4 & \mathbf{E}_4 \\ \mathbf{A}_5 & \mathbf{B}_5 & \mathbf{C}_5 & \mathbf{D}_5 & \mathbf{E}_5 \end{pmatrix} \begin{pmatrix} \delta \mathbf{m}_w \\ \delta \mathbf{T}_w \\ \delta \mathbf{T}_a \\ \delta \boldsymbol{\omega} \\ \delta m_a \end{pmatrix} = \begin{pmatrix} \mathbf{Q}_1 \\ \mathbf{Q}_2 \\ \mathbf{Q}_3 \\ \mathbf{Q}_4 \\ Q_5 \end{pmatrix}, \quad (3.7)$$

where the components of the vectors $\mathbf{Q}_\ell \triangleq (q_\ell^{(1)}, \dots, q_\ell^{(I)})$, $\ell = 1, 2, 3, 4$ are defined as follows:

$$q_\ell^{(i)} \triangleq \sum_{j=1}^{N_\alpha} \left(\frac{\partial N_\ell^{(i)}}{\partial \alpha_j} \delta \alpha_j \right); \quad i = 1, \dots, I; \quad \ell = 1, 2, 3, 4. \quad (3.8)$$

and where Q_5 is defined as follows:

$$Q_5 \triangleq \sum_{j=1}^{N_\alpha} \left(\frac{\partial N_5}{\partial \alpha_j} \delta \alpha_j \right). \quad (3.9)$$

CHAPTER 3. DESCRIPTION OF THE MATHEMATICAL FRAMEWORK

The system in Eq. (3.7) is referred to as the *forward sensitivity system*, which can be generally solved to calculate the variations induced in the state functions values by any change in the model parameters values. The “indirect effect” term in Eq. (3.3), $DR_{indirect}$, can in turn be obtained by using the solution of Eq. (3.7). Practically though, since the parameter variations to be considered are usually a large number, computing $DR_{indirect}$ by repeatedly solving Eq. (3.7) happens to become computationally very expensive.

The application of the Adjoint Sensitivity Analysis Procedure (ASAM) formulated in [1-4] allows to avoid the need for repeatedly solving Eq. (3.7): the ASAM proceeds by forming the inner-product of Eq. (3.7) with a yet unspecified vector of the form $[\boldsymbol{\mu}_w, \boldsymbol{\tau}_w, \boldsymbol{\tau}_a, \mathbf{o}, \mu_a]^\dagger$, presenting the same structure as the vector $\mathbf{u} \triangleq (\mathbf{m}_w, \mathbf{T}_w, \mathbf{T}_a, \boldsymbol{\omega}, m_a)^\dagger$, transposing the resulting scalar equation and using Eq. (3.3). Furthermore, the procedure requires that the vector $[\boldsymbol{\mu}_w, \boldsymbol{\tau}_w, \boldsymbol{\tau}_a, \mathbf{o}, \mu_a]^\dagger$ satisfies the following adjoint sensitivity system:

$$\begin{pmatrix} \mathbf{A}_1^\dagger & \mathbf{A}_2^\dagger & \mathbf{A}_3^\dagger & \mathbf{A}_4^\dagger & \mathbf{A}_5^\dagger \\ \mathbf{B}_1^\dagger & \mathbf{B}_2^\dagger & \mathbf{B}_3^\dagger & \mathbf{B}_4^\dagger & \mathbf{B}_5^\dagger \\ \mathbf{C}_1^\dagger & \mathbf{C}_2^\dagger & \mathbf{C}_3^\dagger & \mathbf{C}_4^\dagger & \mathbf{C}_5^\dagger \\ \mathbf{D}_1^\dagger & \mathbf{D}_2^\dagger & \mathbf{D}_3^\dagger & \mathbf{D}_4^\dagger & \mathbf{D}_5^\dagger \\ \mathbf{E}_1^\dagger & \mathbf{E}_2^\dagger & \mathbf{E}_3^\dagger & \mathbf{E}_4^\dagger & \mathbf{E}_5^\dagger \end{pmatrix} \begin{pmatrix} \boldsymbol{\mu}_w \\ \boldsymbol{\tau}_w \\ \boldsymbol{\tau}_a \\ \mathbf{o} \\ \mu_a \end{pmatrix} = \begin{pmatrix} \mathbf{R}_1 \\ \mathbf{R}_2 \\ \mathbf{R}_3 \\ \mathbf{R}_4 \\ R_5 \end{pmatrix} ; \quad (3.10)$$

it therefore ultimately follows that the “indirect effect” term can be expressed as:

$$DR_{indirect} \triangleq \boldsymbol{\mu}_w \cdot \mathbf{Q}_1 + \boldsymbol{\tau}_w \cdot \mathbf{Q}_2 + \boldsymbol{\tau}_a \cdot \mathbf{Q}_3 + \mathbf{o} \cdot \mathbf{Q}_4 + \mu_a \cdot Q_5 \quad (3.11)$$

The system in Eq. (3.10) is called the *adjoint sensitivity system*, which - notably - is independent of parameter variations. This means, as already mentioned before, that the adjoint sensitivity system needs to be solved just once to allow

CHAPTER 3. DESCRIPTION OF THE MATHEMATICAL FRAMEWORK

computing the selected adjoint functions $[\boldsymbol{\mu}_w, \boldsymbol{\tau}_w, \boldsymbol{\tau}_a, \mathbf{o}, \mu_a]^\dagger$. The adjoint functions are then used to compute $DR_{indirect}$, in an efficient and exact way, by using Eq. (3.11).

In order to provide an illustrative example of computing the response sensitivities through the adjoint sensitivity system, let's assume that the model response of interest is the air relative humidity, $RH^{(i)}$, in a generic control volume i , as in Eq. (2.24). For this model response, the “direct effect” term, indicated as $D[RH^{(i)}]_{direct}$, is directly obtained in the form:

$$D[RH^{(i)}]_{direct} = \frac{\partial (RH^{(i)})}{\partial P_{atm}} (\delta P_{atm}) + \frac{\partial (RH^{(i)})}{\partial a_0} (\delta a_0) + \frac{\partial (RH^{(i)})}{\partial a_1} (\delta a_1),$$

$$i = 1, \dots, I;$$
(3.12)

where:

$$\frac{\partial (RH^{(i)})}{\partial P_{atm}} = \frac{\partial}{\partial P_{atm}} \left[\frac{P_v(\omega^{(i)}, \boldsymbol{\alpha})}{P_{vs}(T_a^{(i)}, \boldsymbol{\alpha})} \times 100 \right] = \frac{0.622}{(0.622 + \omega^{(i)}) e^{\frac{a_0 + \frac{a_1}{T_a^{(i)}}}} \times 100;$$

$$i = 1, \dots, I;$$
(3.13)

$$\frac{\partial (RH^{(i)})}{\partial a_0} = \frac{\partial}{\partial a_0} \left[\frac{P_v(\omega^{(i)}, \boldsymbol{\alpha})}{P_{vs}(T_a^{(i)}, \boldsymbol{\alpha})} \times 100 \right] = - \frac{0.622 P_{atm}}{(0.622 + \omega^{(i)}) e^{\frac{a_0 + \frac{a_1}{T_a^{(i)}}}} \times 100;$$

$$i = 1, \dots, I;$$
(3.14)

$$\frac{\partial (RH^{(i)})}{\partial a_1} = \frac{\partial}{\partial a_1} \left[\frac{P_v(\omega^{(i)}, \boldsymbol{\alpha})}{P_{vs}(T_a^{(i)}, \boldsymbol{\alpha})} \times 100 \right] = - \frac{0.622 P_{atm}}{(0.622 + \omega^{(i)}) e^{\frac{a_0 + \frac{a_1}{T_a^{(i)}}}} \frac{-1}{T_a^{(i)}} \times 100;$$

$$i = 1, \dots, I.$$
(3.15)

CHAPTER 3. DESCRIPTION OF THE MATHEMATICAL FRAMEWORK

On the other side, the “indirect effect” term, indicated as $D[RH^{(i)}]_{indirect}$, is promptly obtained in the form:

$$D[RH^{(i)}]_{indirect} = \frac{\partial (RH^{(i)})}{\partial \omega^{(i)}} (\delta \omega^{(i)}) + \frac{\partial (RH^{(i)})}{\partial T_a^{(i)}} (\delta T_a^{(i)}); \quad i = 1, \dots, I; \quad (3.16)$$

where:

$$\begin{aligned} \frac{\partial (RH^{(i)})}{\partial \omega^{(i)}} &= \frac{\partial}{\partial \omega^{(i)}} \left[\frac{P_v(\omega^{(i)}, \alpha)}{P_{vs}(T_a^{(i)}, \alpha)} \times 100 \right] = \frac{100}{P_{vs}(T_a^{(i)}, \alpha)} \frac{\partial P_v(\omega^{(i)}, \alpha)}{\partial \omega^{(i)}} \\ &= \frac{0.622 P_{atm}}{(0.622 + \omega^{(i)})^2 e^{a_0 + \frac{a_1}{T_a^{(i)}}}} \times 100; \quad i = 1, \dots, I; \end{aligned} \quad (3.17)$$

$$\begin{aligned} \frac{\partial (RH^{(i)})}{\partial T_a^{(i)}} &= \frac{\partial}{\partial T_a^{(i)}} \left[\frac{P_v(\omega^{(i)}, \alpha)}{P_{vs}(T_a^{(i)}, \alpha)} \times 100 \right] \\ &= 100 \times P_v(\omega^{(i)}, \alpha) \frac{\partial}{\partial T_a^{(i)}} \left[\frac{1}{P_{vs}(T_a^{(i)}, \alpha)} \right] \\ &= \frac{0.622 P_{atm}}{(0.622 + \omega^{(i)}) e^{a_0 + \frac{a_1}{T_a^{(i)}}}} \frac{a_1}{[T_a^{(i)}]^2} \times 100; \quad i = 1, \dots, I. \end{aligned} \quad (3.18)$$

Dimensional analysis allows to determine the units of the adjoint functions from Eq. (3.11). More in detail, the units for the adjoint functions must satisfy the following relations:

$$[\mu_w^{(i)}] = \frac{[R]}{[N_1]}; \quad [\tau_w^{(i)}] = \frac{[R]}{[N_2]}; \quad [\tau_a^{(i)}] = \frac{[R]}{[N_3]}; \quad [o^{(i)}] = \frac{[R]}{[N_4]}; \quad [\mu_a] = \frac{[R]}{[N_5]} \quad (3.19)$$

where $[R]$ indicates the unit of the response R , while the units for the respective governing equations are the following:

$$[N_1] = \frac{kg}{s}; \quad [N_2] = \frac{J}{s}; \quad [N_3] = [-]; \quad [N_4] = \frac{J}{kg}; \quad [N_5] = \frac{J}{m^3} \quad (3.20)$$

CHAPTER 3. DESCRIPTION OF THE MATHEMATICAL FRAMEWORK

Table 3.1 below lists the units of the adjoint functions for five responses of interest: $R \triangleq T_a^{(1)}$, $R \triangleq T_w^{(50)}$, $R \triangleq RH^{(1)}$, $R \triangleq m_w^{(50)}$ and $R \triangleq m_a$, respectively, in which, $T_a^{(1)}$ denotes exit air temperature; $T_w^{(50)}$ denotes exit water temperature; $RH^{(1)}$ denotes exit air relative humidity; $m_w^{(50)}$ denotes exit water mass flow rate; and m_a denotes air mass flow rate.

Responses	$[\mu_w^{(i)}]$	$[\tau_w^{(i)}]$	$[\tau_a^{(i)}]$	$[o^{(i)}]$	$[\mu_a]$
$R \triangleq T_a^{(1)}$	$K/(kg/s)$	$K/(J/s)$	K	$K/(J/kg)$	$K/(J/m^3)$
$R \triangleq T_w^{(50)}$	$K/(kg/s)$	$K/(J/s)$	K	$K/(J/kg)$	$K/(J/m^3)$
$R \triangleq RH^{(1)}$	$(kg/s)^{-1}$	$(J/s)^{-1}$	—	$(J/kg)^{-1}$	$(J/m^3)^{-1}$
$R \triangleq m_w^{(50)}$	—	$(J/kg)^{-1}$	kg/s	$(kg/s)/(J/kg)$	$(kg/s)/(J/m^3)$
$R \triangleq m_a$	—	$(J/kg)^{-1}$	kg/s	$(kg/s)/(J/kg)$	$(kg/s)/(J/m^3)$

Table 3.1: Units of the adjoint functions for different responses in natural draft cases.

Remembering that the adjoint sensitivity system in Eq. (3.10) is linear in the adjoint state functions, it follows that numerical methods appropriate for large-scale sparse linear systems can be used to solve it. Namely, the selected numerical method was NSPCG, a “Package for Solving Large Sparse Linear Systems by Various Iterative Methods” [35]; 12 to 18 iterations were sufficient for the solution of the adjoint system within convergence criterion of $\zeta = 10^{-12}$.

Figures 3.1 through 3.5 below display the bar plots of the adjoint functions corresponding to the five measured responses of interest, namely: (i) the exit air temperature $R \triangleq T_a^{(1)}$; (ii) the outlet (exit) water temperature $R \triangleq T_w^{(50)}$; (iii) the exit air humidity ratio $R \triangleq RH^{(1)}$; (iv) the outlet (exit) water mass flow rate $R \triangleq m_w^{(50)}$; and (v) the air mass flow rate $R \triangleq m_a$.

CHAPTER 3. DESCRIPTION OF THE MATHEMATICAL FRAMEWORK

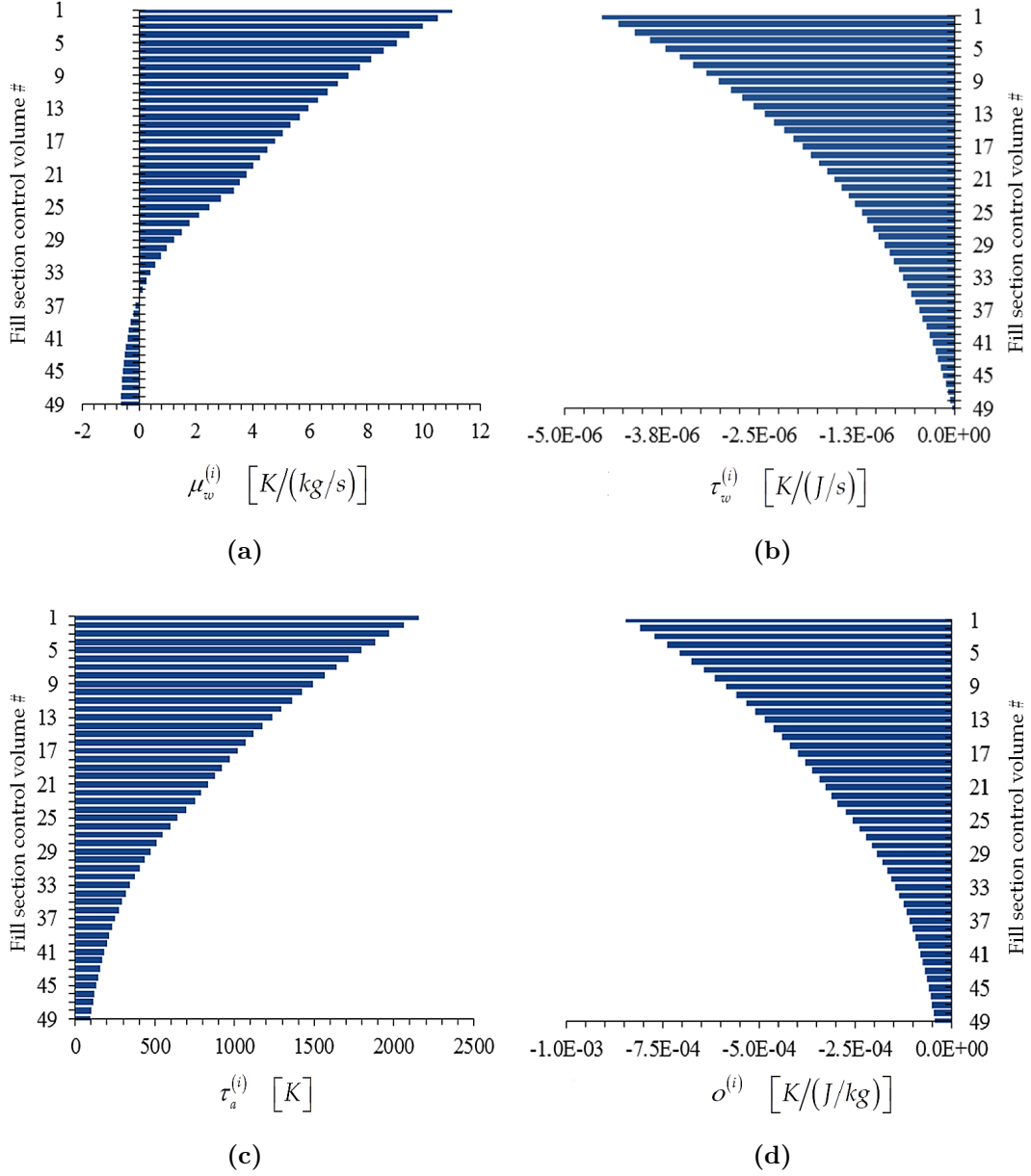


Figure 3.1: Bar plots of adjoint functions for the response $R \triangleq T_a^{(1)}$ as functions of the height of the cooling tower fill section: (a) $\mu_w \triangleq (\mu_w^{(1)}, \dots, \mu_w^{(49)})$, (b) $\tau_w \triangleq (\tau_w^{(1)}, \dots, \tau_w^{(49)})$, (c) $\tau_a \triangleq (\tau_a^{(1)}, \dots, \tau_a^{(49)})$, (d) $o \triangleq (o^{(1)}, \dots, o^{(49)})$, for case 1a: fan off, saturated outlet air condition, with inlet air unsaturated.

For the response $R \triangleq T_a^{(1)}$, the value of μ_a is -0.24204 .

CHAPTER 3. DESCRIPTION OF THE MATHEMATICAL FRAMEWORK

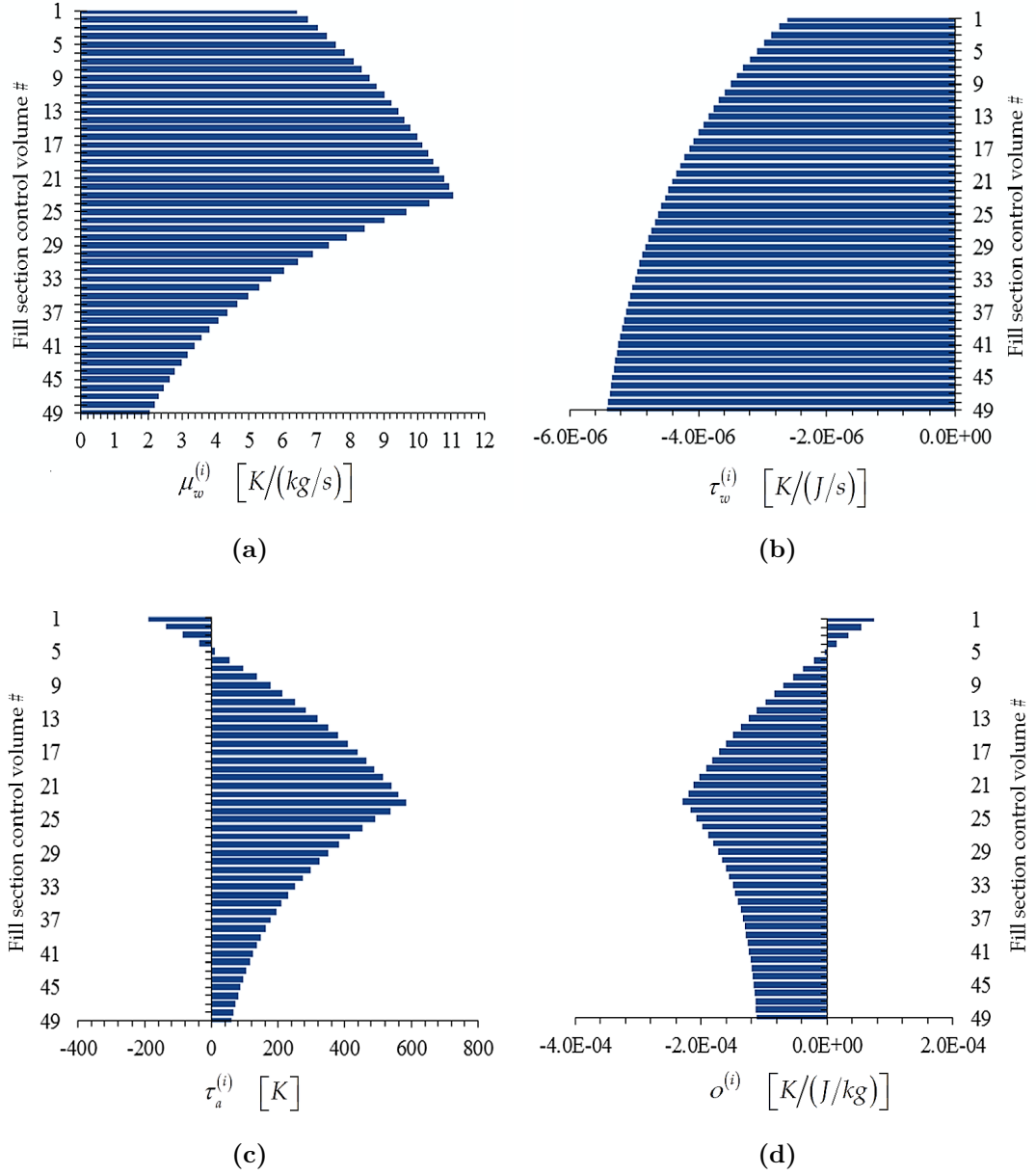


Figure 3.2: Bar plots of adjoint functions for the response $R \triangleq T_w^{(50)}$ as functions of the height of the cooling tower fill section: (a) $\mu_w \triangleq (\mu_w^{(1)}, \dots, \mu_w^{(49)})$, (b) $\tau_w \triangleq (\tau_w^{(1)}, \dots, \tau_w^{(49)})$, (c) $\tau_a \triangleq (\tau_a^{(1)}, \dots, \tau_a^{(49)})$, (d) $o \triangleq (o^{(1)}, \dots, o^{(49)})$, for case 1a: fan off, saturated outlet air condition, with inlet air unsaturated.

For the response $R \triangleq T_w^{(50)}$, the value of μ_a is -0.31664 .

CHAPTER 3. DESCRIPTION OF THE MATHEMATICAL FRAMEWORK

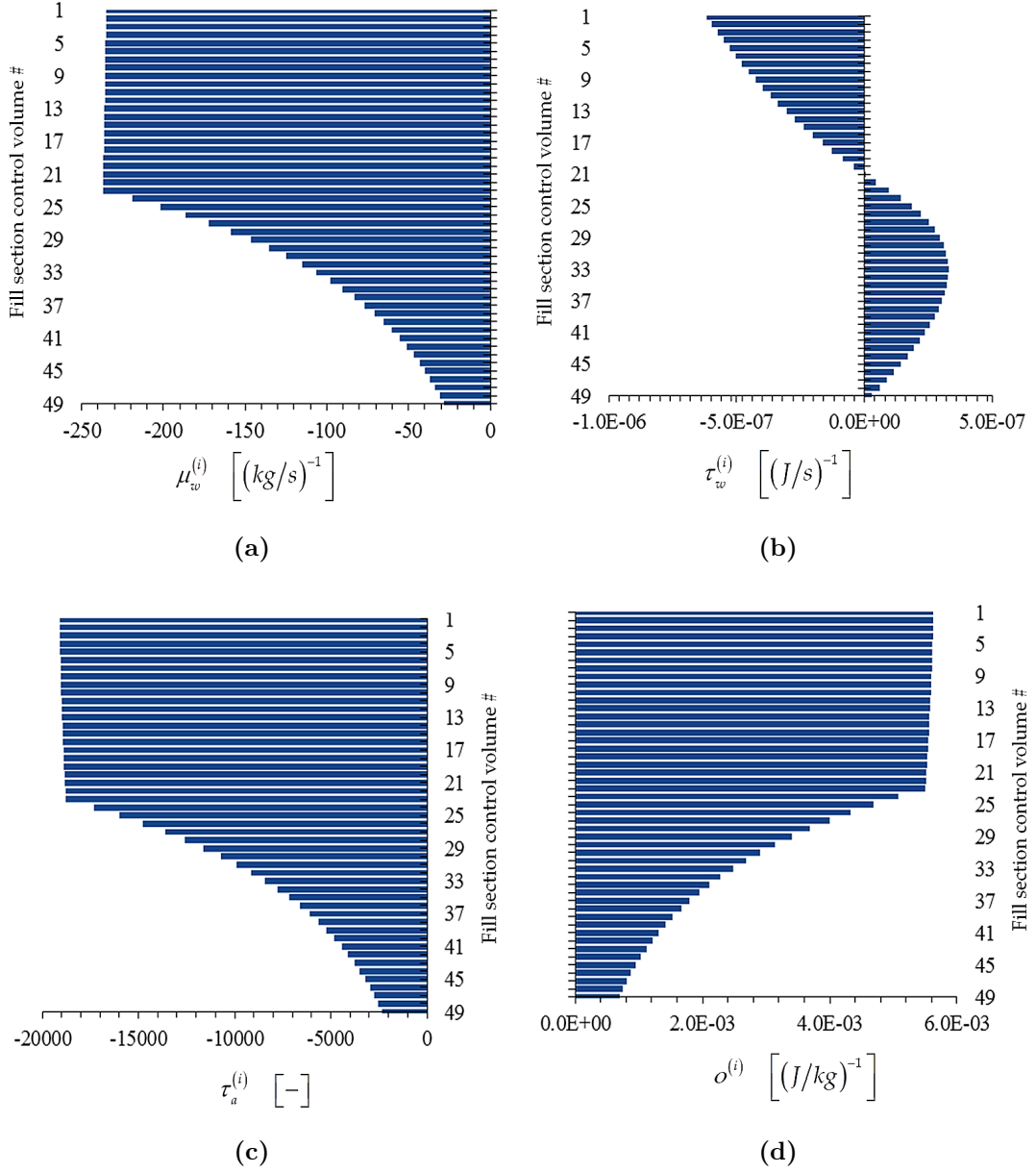


Figure 3.3: Bar plots of adjoint functions for the response $R \triangleq RH^{(1)}$ as functions of the height of the cooling tower fill section: (a) $\mu_w \triangleq (\mu_w^{(1)}, \dots, \mu_w^{(49)})$, (b) $\tau_w \triangleq (\tau_w^{(1)}, \dots, \tau_w^{(49)})$, (c) $\tau_a \triangleq (\tau_a^{(1)}, \dots, \tau_a^{(49)})$, (d) $o \triangleq (o^{(1)}, \dots, o^{(49)})$, for case 1a: fan off, saturated outlet air condition, with inlet air unsaturated.

For the response $R \triangleq RH^{(1)}$, the value of μ_a is -0.00603 .

CHAPTER 3. DESCRIPTION OF THE MATHEMATICAL FRAMEWORK

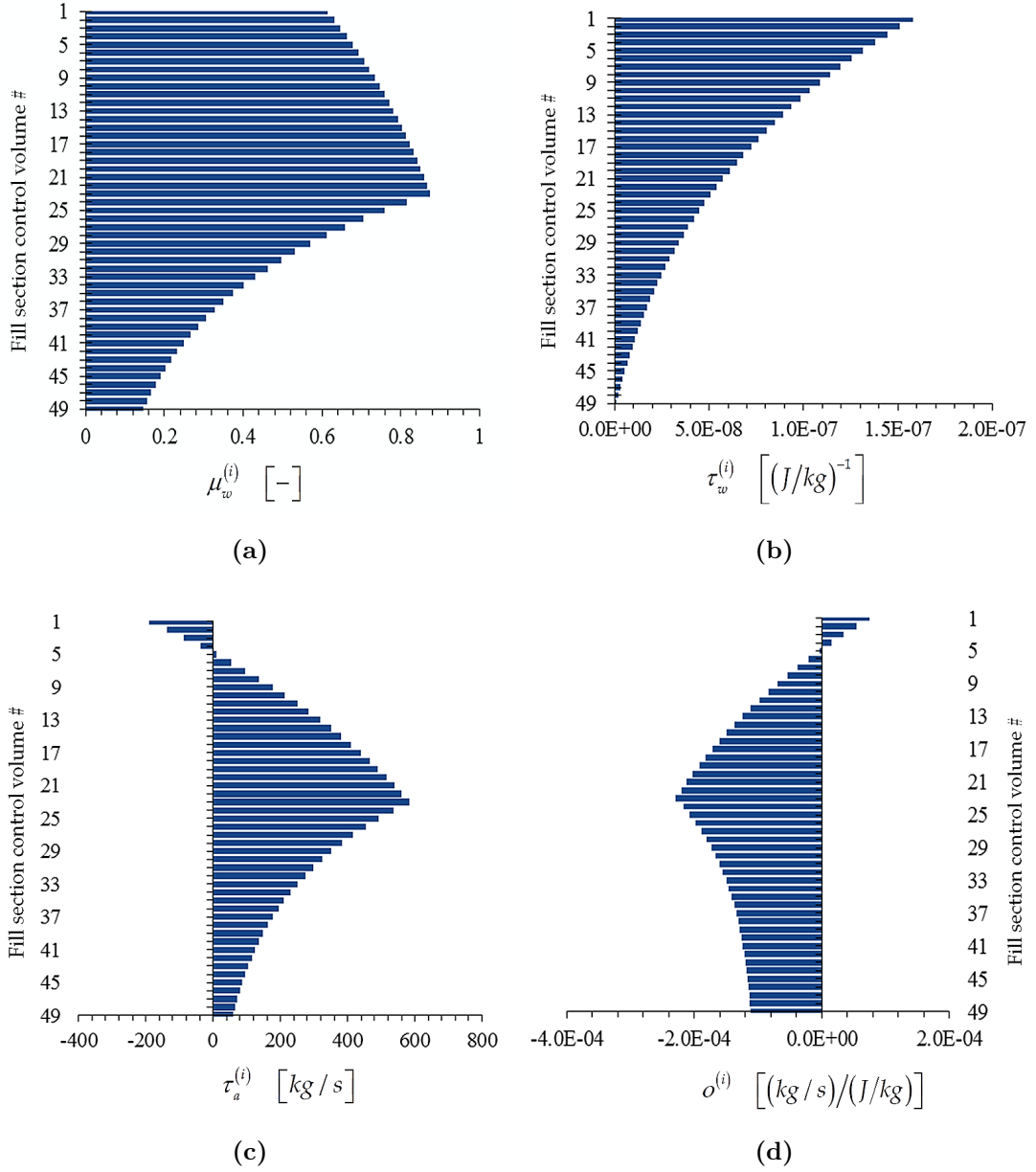


Figure 3.4: Bar plots of adjoint functions for the response $R \triangleq m_w^{(50)}$ as functions of the height of the cooling tower fill section: (a) $\mu_w \triangleq (\mu_w^{(1)}, \dots, \mu_w^{(49)})$, (b) $\tau_w \triangleq (\tau_w^{(1)}, \dots, \tau_w^{(49)})$, (c) $\tau_a \triangleq (\tau_a^{(1)}, \dots, \tau_a^{(49)})$, (d) $o \triangleq (o^{(1)}, \dots, o^{(49)})$, for case 1a: fan off, saturated outlet air condition, with inlet air unsaturated.

For the response $R \triangleq m_w^{(50)}$, the value of μ_a is -0.01765 .

CHAPTER 3. DESCRIPTION OF THE MATHEMATICAL FRAMEWORK

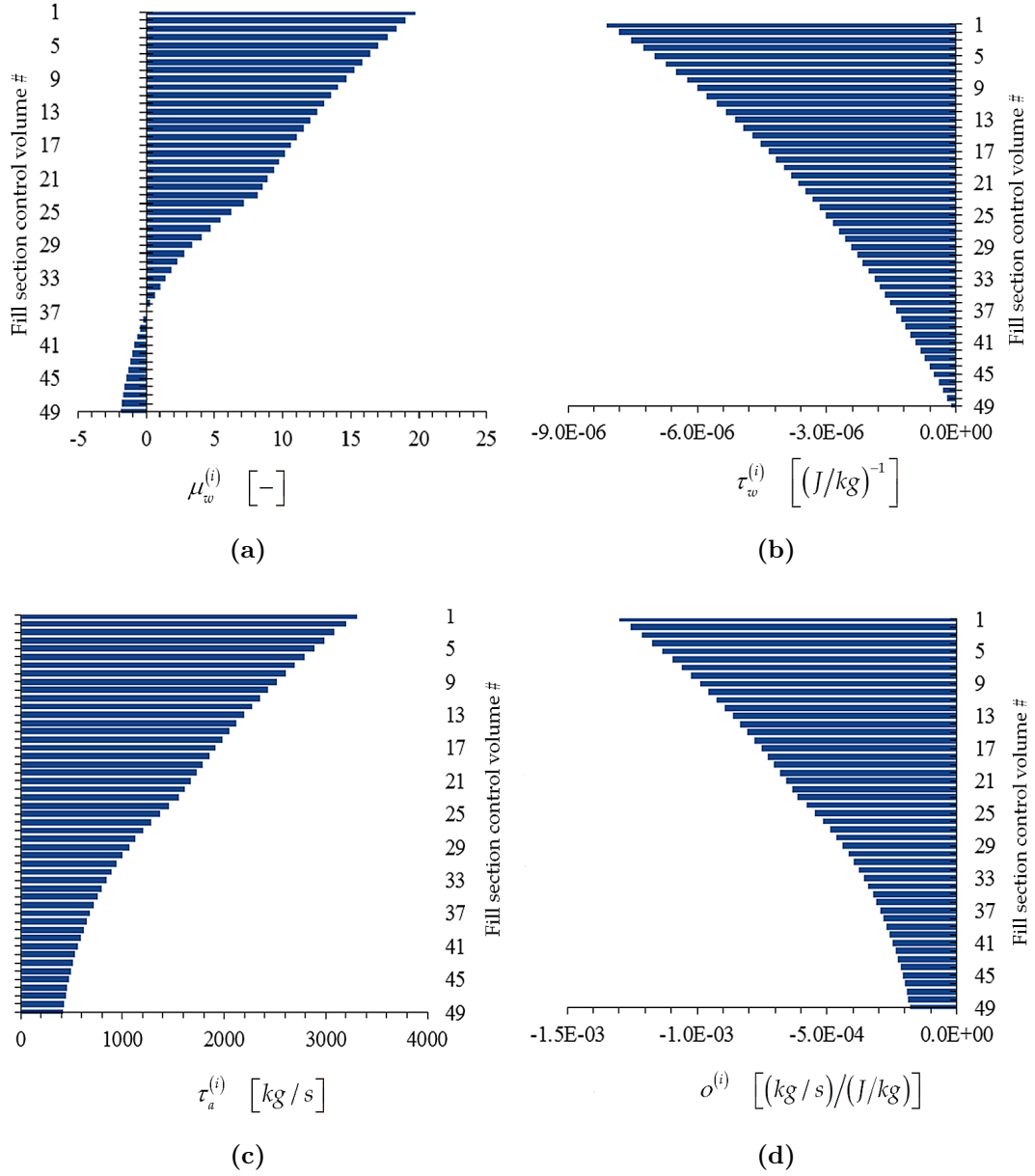


Figure 3.5: Bar plots of adjoint functions for the response $R \triangleq m_a$ as functions of the height of the cooling tower fill section: (a) $\mu_w \triangleq (\mu_w^{(1)}, \dots, \mu_w^{(49)})$, (b) $\tau_w \triangleq (\tau_w^{(1)}, \dots, \tau_w^{(49)})$, (c) $\tau_a \triangleq (\tau_a^{(1)}, \dots, \tau_a^{(49)})$, (d) $o \triangleq (o^{(1)}, \dots, o^{(49)})$, for case 1a: fan off, saturated outlet air condition, with inlet air unsaturated.

For the response $R \triangleq m_a$, the value of μ_a is 4.4364.

An independent verification of the numerical accuracy of the computed adjoint functions can be performed by first noting that from Eqs. (3.1), (3.2) and (3.11)

CHAPTER 3. DESCRIPTION OF THE MATHEMATICAL FRAMEWORK

follows that

$$DR(\mathbf{m}_w^0, \mathbf{T}_w^0, \mathbf{T}_a^0, \boldsymbol{\omega}^0, m_a^0; \boldsymbol{\alpha}^0; \delta \mathbf{m}_w, \delta \mathbf{T}_w, \delta \mathbf{T}_a, \delta \boldsymbol{\omega}, \delta m_a; \delta \boldsymbol{\alpha}) = \sum_{j=1}^{N_\alpha} S_j \delta \alpha_j, \quad (3.21)$$

where N_α indicates the total number of model parameters, and where S_j represents the “absolute sensitivity” of the response R with respect to the parameter α_j , defined as:

$$S_j \triangleq \frac{\partial R}{\partial \alpha_j} - \left[\sum_{i=1}^I \left(\mu_w^{(i)} \frac{\partial N_1^{(i)}}{\partial \alpha_j} + \tau_w^{(i)} \frac{\partial N_2^{(i)}}{\partial \alpha_j} + \tau_a^{(i)} \frac{\partial N_3^{(i)}}{\partial \alpha_j} + o^{(i)} \frac{\partial N_4^{(i)}}{\partial \alpha_j} \right) + \mu_a \frac{\partial N_5}{\partial \alpha_j} \right] \quad (3.22)$$

All the derivatives with respect to the model parameter α_j on the right side of Eq. (3.22) are known quantities. The absolute response sensitivity S_j can be also computed independently, as follows:

1. consider an arbitrarily small perturbation $\delta \alpha_j$ to the model parameter α_j ;
2. re-compute the perturbed response $R(\alpha_j^0 + \delta \alpha_j)$, where α_j^0 denotes the unperturbed parameter value;
3. use the finite difference formula

$$S_j^{FD} \cong \frac{R(\alpha_j^0 + \delta \alpha_j) - R(\alpha_j^0)}{\delta \alpha_j} + O(\delta \alpha_j)^2; \quad (3.23)$$

4. use the approximate equality between Eqs. (3.23) and (3.22) to obtain independently the respective values of the adjoint function(s) being verified.

The independent verification methodology discussed in steps (1)-(4) above will be vastly illustrated in Section D.1 of Appendix D, where the adjoint functions depicted in Figures 3.1 - 3.5 will be verified.

3.1.2 Development of the Cooling Tower Adjoint Sensitivity Model for Case 1b: Fan Off, Saturated Outlet Air Conditions, with Inlet Air Saturated

The procedure for deriving the cooling tower adjoint sensitivity model for case 1b is the same as that for case 1a, described in Section 3.1.1. The responses of interest can be represented in the functional form $R(\mathbf{m}_w, \mathbf{T}_w, \mathbf{T}_a, \boldsymbol{\omega}, m_a; \boldsymbol{\alpha})$. The sensitivity of this response to arbitrary variations in the model parameters $\delta\boldsymbol{\alpha} \triangleq (\delta\alpha_1, \dots, \delta\alpha_{N_\alpha})$ and state functions $\delta\mathbf{m}_w, \delta\mathbf{T}_w, \delta\mathbf{T}_a, \delta\boldsymbol{\omega}, \delta m_a$ is defined as follows:

$$\begin{aligned} DR(\mathbf{m}_w^0, \mathbf{T}_w^0, \mathbf{T}_a^0, \boldsymbol{\omega}^0, m_a^0; \boldsymbol{\alpha}^0; \delta\mathbf{m}_w, \delta\mathbf{T}_w, \delta\mathbf{T}_a, \delta\boldsymbol{\omega}, \delta m_a; \delta\boldsymbol{\alpha}) &\triangleq \\ \frac{d}{d\varepsilon} [R(\mathbf{m}_w^0 + \varepsilon\delta\mathbf{m}_w, \mathbf{T}_w^0 + \varepsilon\delta\mathbf{T}_w, \mathbf{T}_a^0 + \varepsilon\delta\mathbf{T}_a, \boldsymbol{\omega}^0 + \varepsilon\delta\boldsymbol{\omega}, m_a^0 + \varepsilon\delta m_a; \boldsymbol{\alpha}^0 + \varepsilon\delta\boldsymbol{\alpha})]_{\varepsilon=0} & \\ = DR_{direct} + DR_{indirect}, & \end{aligned} \quad (3.24)$$

$$DR_{direct} \triangleq \sum_{i=1}^{N_\alpha} \left(\frac{\partial R}{\partial \alpha_i} \delta\alpha_i \right), \quad (3.25)$$

where the “direct effect” term, DR_{direct} , and the “indirect effect” term, $DR_{indirect}$, are as follows:

$$\begin{aligned} DR_{indirect} &\triangleq \sum_{i=1}^I \left(\frac{\partial R}{\partial m_w^{(i+1)}} \delta m_w^{(i+1)} + \frac{\partial R}{\partial T_w^{(i+1)}} \delta T_w^{(i+1)} + \frac{\partial R}{\partial T_a^{(i)}} \delta T_a^{(i)} + \frac{\partial R}{\partial \omega^{(i)}} \delta \omega^{(i)} \right) \\ &+ \frac{\partial R}{\partial m_a} \delta m_a = \mathbf{R}_1 \cdot \delta\mathbf{m}_w + \mathbf{R}_2 \cdot \delta\mathbf{T}_w + \mathbf{R}_3 \cdot \delta\mathbf{T}_a + \mathbf{R}_4 \cdot \delta\boldsymbol{\omega} + R_5 \cdot \delta m_a, \end{aligned} \quad (3.26)$$

where the components of the vectors $\mathbf{R}_\ell \triangleq (r_\ell^{(1)}, \dots, r_\ell^{(I)})$, $\ell = 1, 2, 3, 4$ are defined as follows:

CHAPTER 3. DESCRIPTION OF THE MATHEMATICAL FRAMEWORK

$$r_1^{(i)} \triangleq \frac{\partial R}{\partial m_w^{(i+1)}}; \quad r_2^{(i)} \triangleq \frac{\partial R}{\partial T_w^{(i+1)}}; \quad r_3^{(i)} \triangleq \frac{\partial R}{\partial T_a^{(i)}}; \quad r_4^{(i)} \triangleq \frac{\partial R}{\partial \omega^{(i)}}; \quad i = 1, \dots, I. \quad (3.27)$$

and where R_5 is defined as follows:

$$R_5 \triangleq \frac{\partial R}{\partial m_a} \quad (3.28)$$

Since Eqs. (2.25) - (2.37) relate the model parameters to the model state functions, changes in the model parameters will cause changes in the state variables. More in detail, it has been found in [1-4] that to first-order in the parameter variations, the respective change in the state variables values can be obtained by solving the G-differentiated model equations, namely:

$$\frac{d}{d\varepsilon} [\mathbf{N}(\mathbf{u}^0 + \varepsilon \delta \mathbf{u}; \boldsymbol{\alpha}^0 + \varepsilon \delta \boldsymbol{\alpha})]_{\varepsilon=0} = \mathbf{0}, \quad (3.29)$$

Performing the above differentiation on Eqs. (2.25) through (2.37) yields the following forward sensitivity system:

$$\begin{pmatrix} \mathbf{A}_1^I & \mathbf{B}_1^I & \mathbf{C}_1^I & \mathbf{D}_1^I & \mathbf{E}_1^I \\ \mathbf{A}_2 & \mathbf{B}_2 & \mathbf{C}_2 & \mathbf{D}_2 & \mathbf{E}_2 \\ \mathbf{A}_3 & \mathbf{B}_3 & \mathbf{C}_3 & \mathbf{D}_3 & \mathbf{E}_3 \\ \mathbf{A}_4 & \mathbf{B}_4 & \mathbf{C}_4 & \mathbf{D}_4 & \mathbf{E}_4 \\ \mathbf{A}_5 & \mathbf{B}_5 & \mathbf{C}_5 & \mathbf{D}_5 & \mathbf{E}_5 \end{pmatrix} \begin{pmatrix} \delta \mathbf{m}_w \\ \delta \mathbf{T}_w \\ \delta \mathbf{T}_a \\ \delta \boldsymbol{\omega} \\ \delta m_a \end{pmatrix} = \begin{pmatrix} \mathbf{Q}_1^I \\ \mathbf{Q}_2 \\ \mathbf{Q}_3 \\ \mathbf{Q}_4 \\ Q_5 \end{pmatrix}, \quad (3.30)$$

where the components of the vectors $\mathbf{Q}_1^I \triangleq (q_1^{(1)}, \dots, q_1^{(I)})$ and $\mathbf{Q}_\ell \triangleq (q_\ell^{(1)}, \dots, q_\ell^{(I)})$, $\ell = 2, 3, 4$ are defined as:

$$q_\ell^{(i)} \triangleq \sum_{j=1}^{N_\alpha} \left(\frac{\partial N_\ell^{(i)}}{\partial \alpha_j} \delta \alpha_j \right); \quad i = 1, \dots, I; \quad \ell = 1, 2, 3, 4. \quad (3.31)$$

and where Q_5 is defined as follows:

CHAPTER 3. DESCRIPTION OF THE MATHEMATICAL FRAMEWORK

$$Q_5 \triangleq \sum_{j=1}^{N_\alpha} \left(\frac{\partial N_5}{\partial \alpha_j} \delta \alpha_j \right). \quad (3.32)$$

The vector \mathbf{Q}_1^I on the right hand side of Eq. (3.30) is denoted separately from others to highlight the difference of this source term from the one in case 1a. As mentioned earlier in Section 2.3.2, the differences between the governing equations for cases 1a and 1b are in the “liquid continuity equations”. Other governing equations (i.e., liquid energy balance equations; water vapor continuity equations; the air/water vapor energy balance equations; and the mechanical energy equation) are the same for both subcases. As a result, the Jacobian matrix presented in Eq. (3.30), which represents the derivatives of Eqs. (2.25) - (2.37) with respect to the state functions, is different from the Jacobian matrix presented in Eq. (3.7), which represents the derivatives of Eqs. (2.2) - (2.15) with respect to the state functions. More specifically, the Jacobian matrix-components in the first row, namely $\mathbf{A}_1^I, \mathbf{B}_1^I, \mathbf{C}_1^I, \mathbf{D}_1^I$ and \mathbf{E}_1^I , are changed as defined in Section C.2 of Appendix C. Other matrix-components are kept the same as that in the Jacobian matrix in Eq. (3.7).

Apply then the ASAM proceeding by forming the inner-product of Eq. (3.30) with a yet unspecified vector of the form $[\boldsymbol{\mu}_w, \boldsymbol{\tau}_w, \boldsymbol{\tau}_a, \mathbf{o}, \mu_a]^\dagger$, presenting the same structure as the vector $\mathbf{u} \triangleq (\mathbf{m}_w, \mathbf{T}_w, \mathbf{T}_a, \boldsymbol{\omega}, m_a)^\dagger$, transposing the resulting scalar equation and using Eq. (3.26). Furthermore, the procedure requires that the vector $[\boldsymbol{\mu}_w, \boldsymbol{\tau}_w, \boldsymbol{\tau}_a, \mathbf{o}, \mu_a]^\dagger$ satisfies the following adjoint sensitivity system:

$$\begin{pmatrix} \mathbf{A}_1^{I\dagger} & \mathbf{A}_2^\dagger & \mathbf{A}_3^\dagger & \mathbf{A}_4^\dagger & \mathbf{A}_5^\dagger \\ \mathbf{B}_1^{I\dagger} & \mathbf{B}_2^\dagger & \mathbf{B}_3^\dagger & \mathbf{B}_4^\dagger & \mathbf{B}_5^\dagger \\ \mathbf{C}_1^{I\dagger} & \mathbf{C}_2^\dagger & \mathbf{C}_3^\dagger & \mathbf{C}_4^\dagger & \mathbf{C}_5^\dagger \\ \mathbf{D}_1^{I\dagger} & \mathbf{D}_2^\dagger & \mathbf{D}_3^\dagger & \mathbf{D}_4^\dagger & \mathbf{D}_5^\dagger \\ \mathbf{E}_1^{I\dagger} & \mathbf{E}_2^\dagger & \mathbf{E}_3^\dagger & \mathbf{E}_4^\dagger & \mathbf{E}_5^\dagger \end{pmatrix} \begin{pmatrix} \boldsymbol{\mu}_w \\ \boldsymbol{\tau}_w \\ \boldsymbol{\tau}_a \\ \mathbf{o} \\ \mu_a \end{pmatrix} = \begin{pmatrix} \mathbf{R}_1 \\ \mathbf{R}_2 \\ \mathbf{R}_3 \\ \mathbf{R}_4 \\ R_5 \end{pmatrix}; \quad (3.33)$$

CHAPTER 3. DESCRIPTION OF THE MATHEMATICAL FRAMEWORK

it ultimately results that the “indirect effect” term can be expressed in the form

$$DR_{indirect} \triangleq \boldsymbol{\mu}_w \cdot \mathbf{Q}_1^I + \boldsymbol{\tau}_w \cdot \mathbf{Q}_2 + \boldsymbol{\tau}_a \cdot \mathbf{Q}_3 + \mathbf{o} \cdot \mathbf{Q}_4 + \mu_a \cdot Q_5 \quad (3.34)$$

The adjoint sensitivity system, as defined in Eq. (3.33), is independent of parameter variations. Therefore, the adjoint sensitivity system needs to be solved only once to compute the adjoint functions $[\boldsymbol{\mu}_w, \boldsymbol{\tau}_w, \boldsymbol{\tau}_a, \mathbf{o}, \mu_a]^\dagger$. In turn, the adjoint functions are used to compute $DR_{indirect}$, efficiently and exactly, using Eq. (3.34). For case 1b, the units of the adjoint functions are listed in Table 3.1.

Since the adjoint sensitivity system represented by Eq. (3.33) is linear in the adjoint state functions, it can be solved by using numerical methods appropriate for large-scale sparse linear systems. As in case 1a, it was solved by using NSPCG, a “Package for Solving Large Sparse Linear Systems by Various Iterative Methods” [35]; 12 to 18 iterations sufficed for solving the adjoint system within convergence criterion of $\zeta = 10^{-12}$.

The bar plots presented in Figures 3.6 - 3.10 display the trend of the adjoint functions corresponding to the five measured responses of interest, namely: (i) the exit air temperature $R \triangleq T_a^{(1)}$; (ii) the outlet (exit) water temperature $R \triangleq T_w^{(50)}$; (iii) the exit air humidity ratio $R \triangleq RH^{(1)}$; (iv) the outlet (exit) water mass flow rate $R \triangleq m_w^{(50)}$; and (v) the air mass flow rate $R \triangleq m_a$.

For case 1b, the verification of the adjoint functions depicted in Figures 3.6 - 3.10 has been performed with the same methodology as for case 1a, and it is included in Section D.2 of Appendix D.

CHAPTER 3. DESCRIPTION OF THE MATHEMATICAL FRAMEWORK

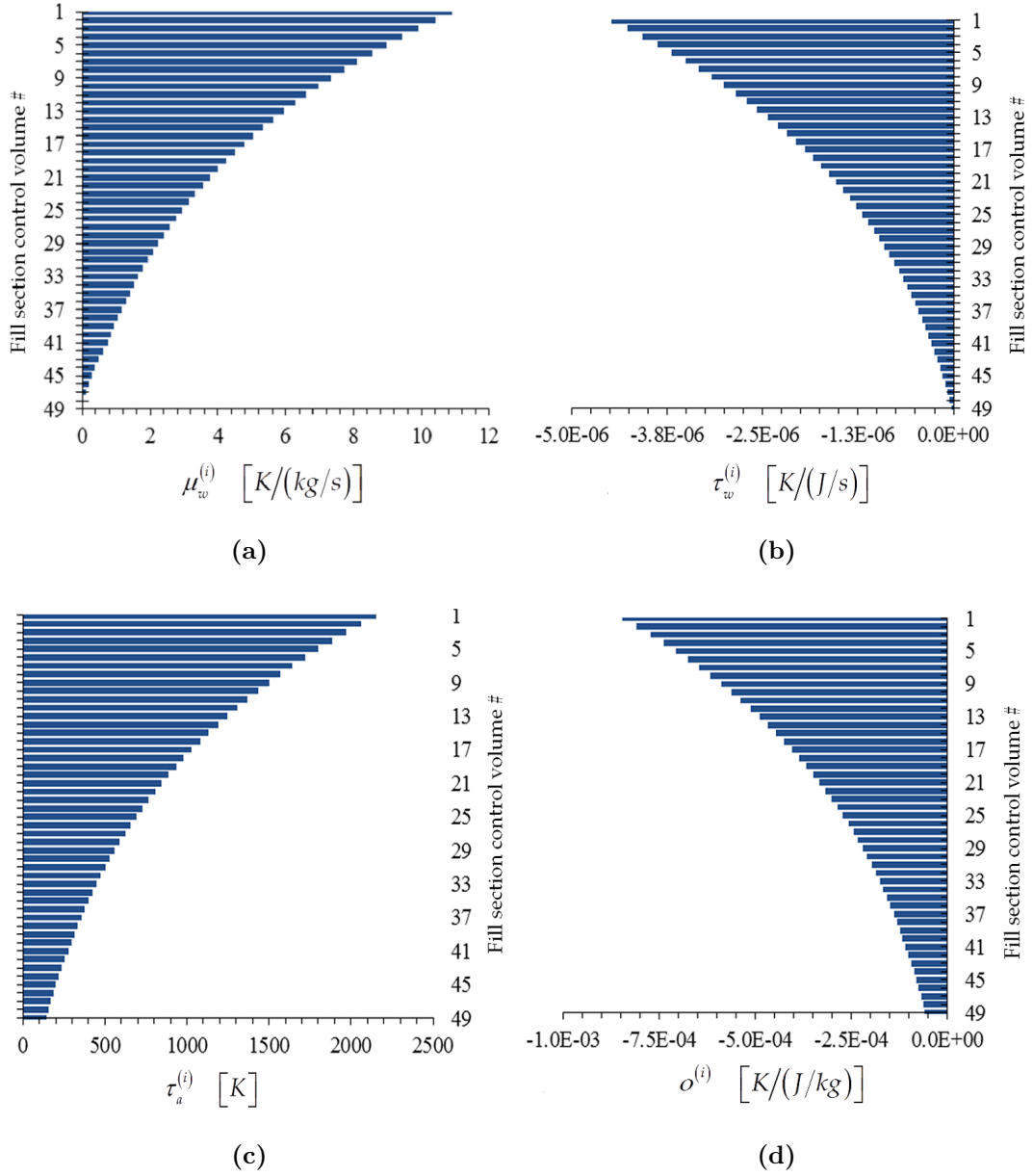


Figure 3.6: Bar plots of adjoint functions for the response $R \triangleq T_a^{(1)}$ as functions of the height of the cooling tower fill section: (a) $\mu_w \triangleq (\mu_w^{(1)}, \dots, \mu_w^{(49)})$, (b) $\tau_w \triangleq (\tau_w^{(1)}, \dots, \tau_w^{(49)})$, (c) $\tau_a \triangleq (\tau_a^{(1)}, \dots, \tau_a^{(49)})$, (d) $\mathbf{o} \triangleq (o^{(1)}, \dots, o^{(49)})$, for case 1b: fan off, saturated outlet air condition, with inlet air saturated.

For the response $R \triangleq T_a^{(1)}$, the value of μ_a is -0.2627 .

CHAPTER 3. DESCRIPTION OF THE MATHEMATICAL FRAMEWORK

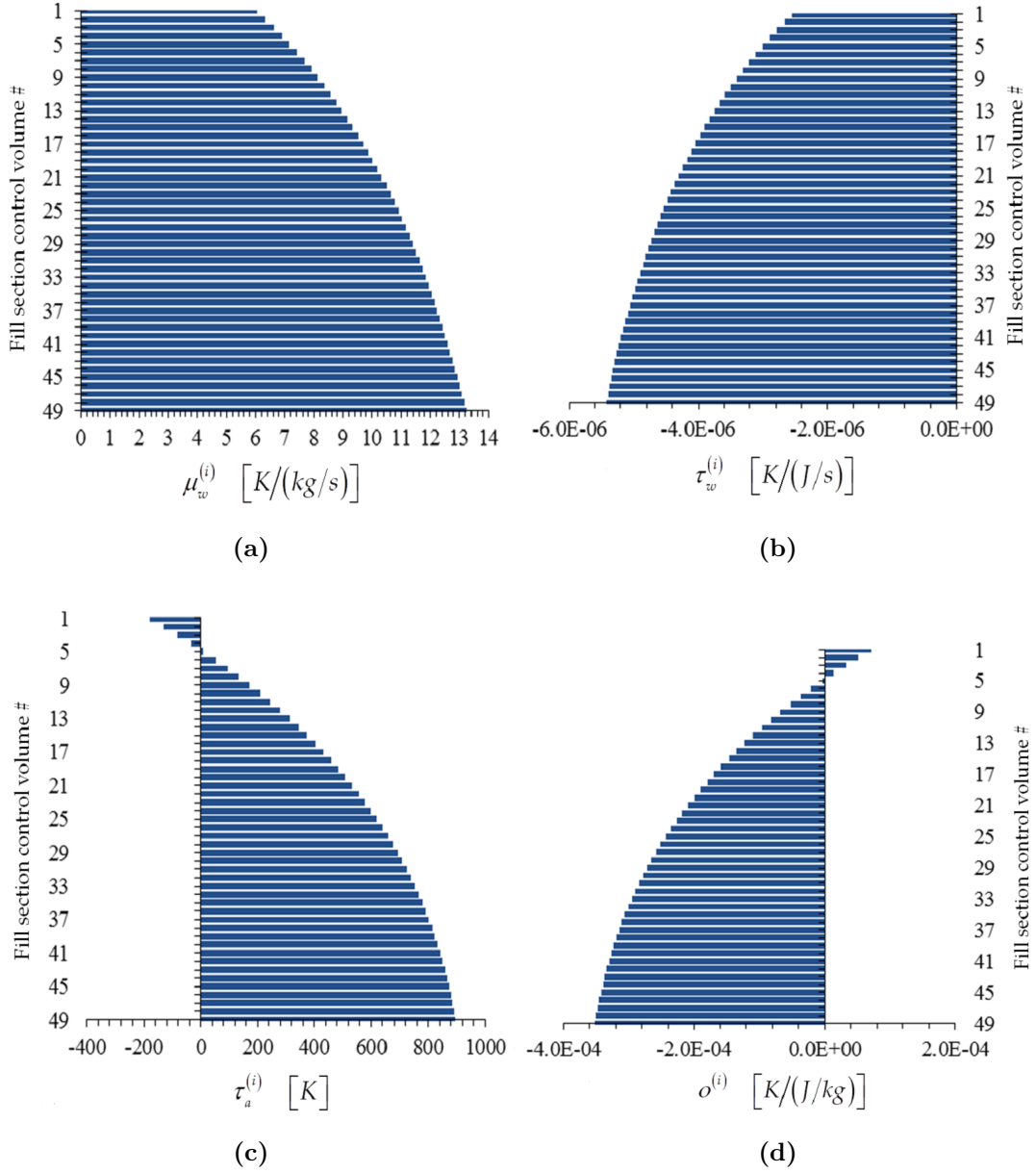


Figure 3.7: Bar plots of adjoint functions for the response $R \triangleq T_w^{(50)}$ as functions of the height of the cooling tower fill section: (a) $\mu_w \triangleq (\mu_w^{(1)}, \dots, \mu_w^{(49)})$, (b) $\tau_w \triangleq (\tau_w^{(1)}, \dots, \tau_w^{(49)})$, (c) $\tau_a \triangleq (\tau_a^{(1)}, \dots, \tau_a^{(49)})$, (d) $o \triangleq (o^{(1)}, \dots, o^{(49)})$, for case 1b: fan off, saturated outlet air condition, with inlet air saturated.

For the response $R \triangleq T_w^{(50)}$, the value of μ_a is -0.30696 .

CHAPTER 3. DESCRIPTION OF THE MATHEMATICAL FRAMEWORK

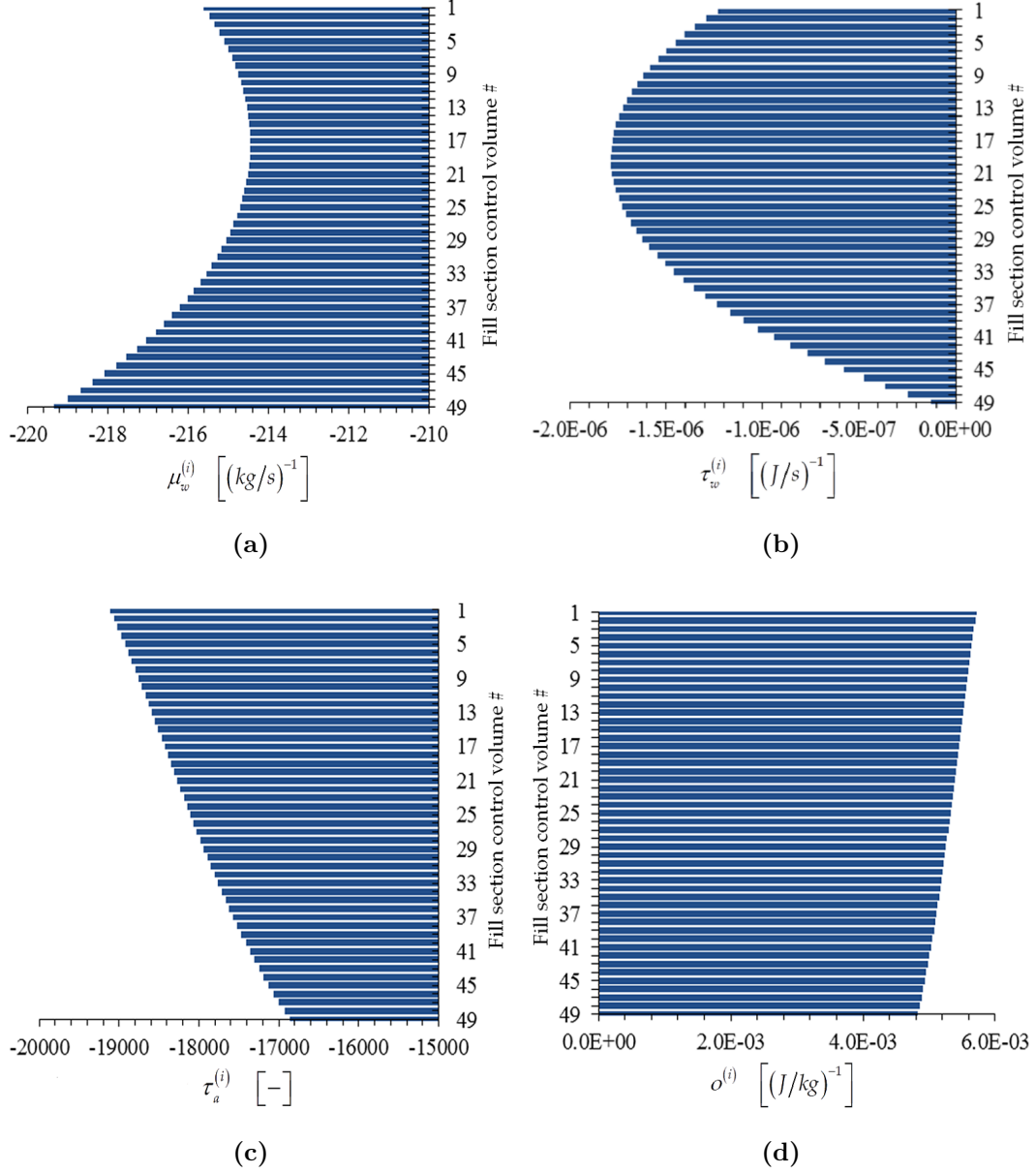


Figure 3.8: Bar plots of adjoint functions for the response $R \triangleq RH^{(1)}$ as functions of the height of the cooling tower fill section: (a) $\mu_w \triangleq (\mu_w^{(1)}, \dots, \mu_w^{(49)})$, (b) $\tau_w \triangleq (\tau_w^{(1)}, \dots, \tau_w^{(49)})$, (c) $\tau_a \triangleq (\tau_a^{(1)}, \dots, \tau_a^{(49)})$, (d) $o \triangleq (o^{(1)}, \dots, o^{(49)})$, for case 1b: fan off, saturated outlet air condition, with inlet air saturated.

For the response $R \triangleq RH^{(1)}$, the value of μ_a is -0.03451 .

CHAPTER 3. DESCRIPTION OF THE MATHEMATICAL FRAMEWORK

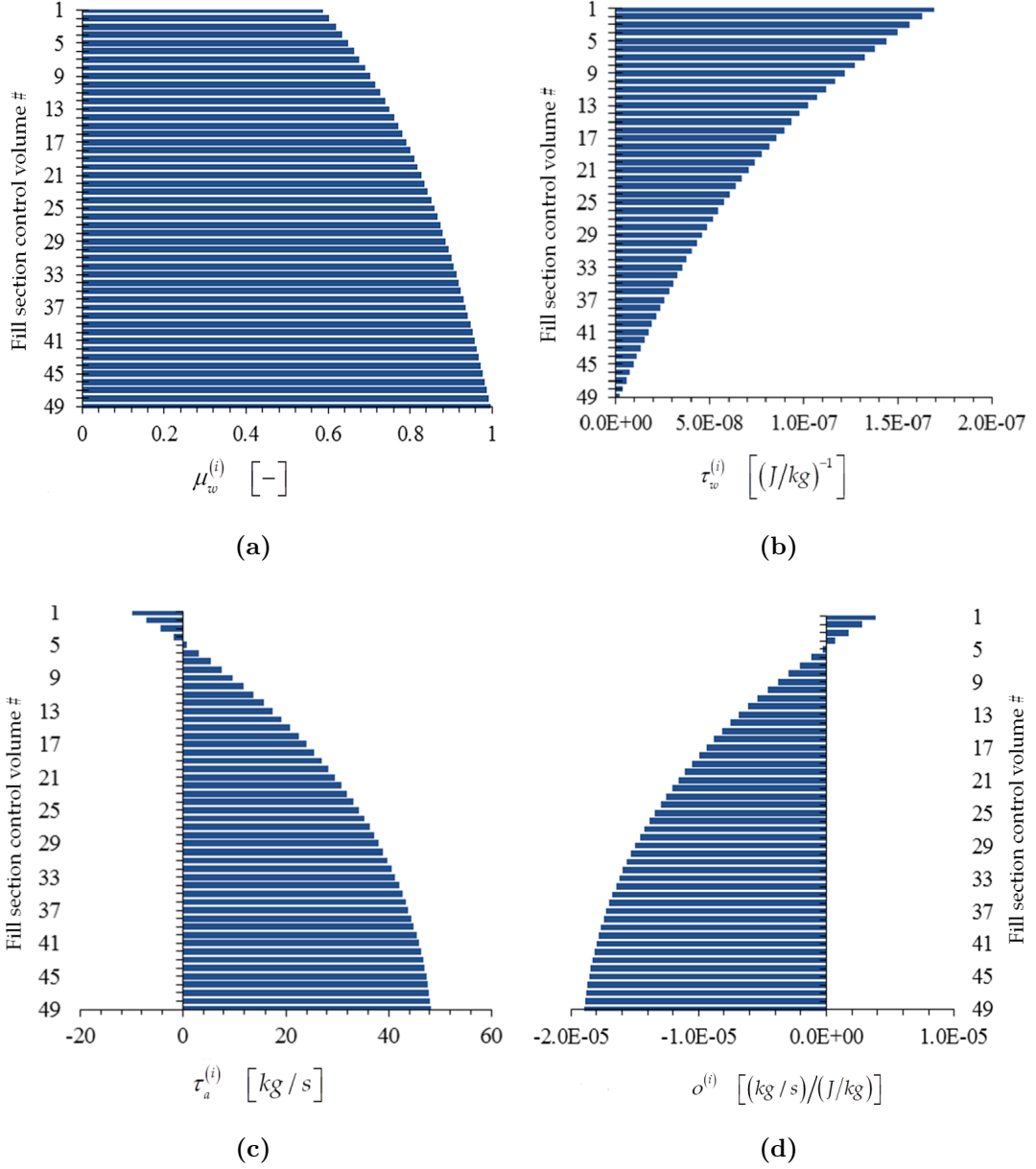


Figure 3.9: Bar plots of adjoint functions for the response $R \triangleq m_w^{(50)}$ as functions of the height of the cooling tower fill section: (a) $\mu_w \triangleq (\mu_w^{(1)}, \dots, \mu_w^{(49)})$, (b) $\tau_w \triangleq (\tau_w^{(1)}, \dots, \tau_w^{(49)})$, (c) $\tau_a \triangleq (\tau_a^{(1)}, \dots, \tau_a^{(49)})$, (d) $o \triangleq (o^{(1)}, \dots, o^{(49)})$, for case 1b: fan off, saturated outlet air condition, with inlet air saturated.

For the response $R \triangleq m_w^{(50)}$, the value of μ_a is -0.01664 .

CHAPTER 3. DESCRIPTION OF THE MATHEMATICAL FRAMEWORK

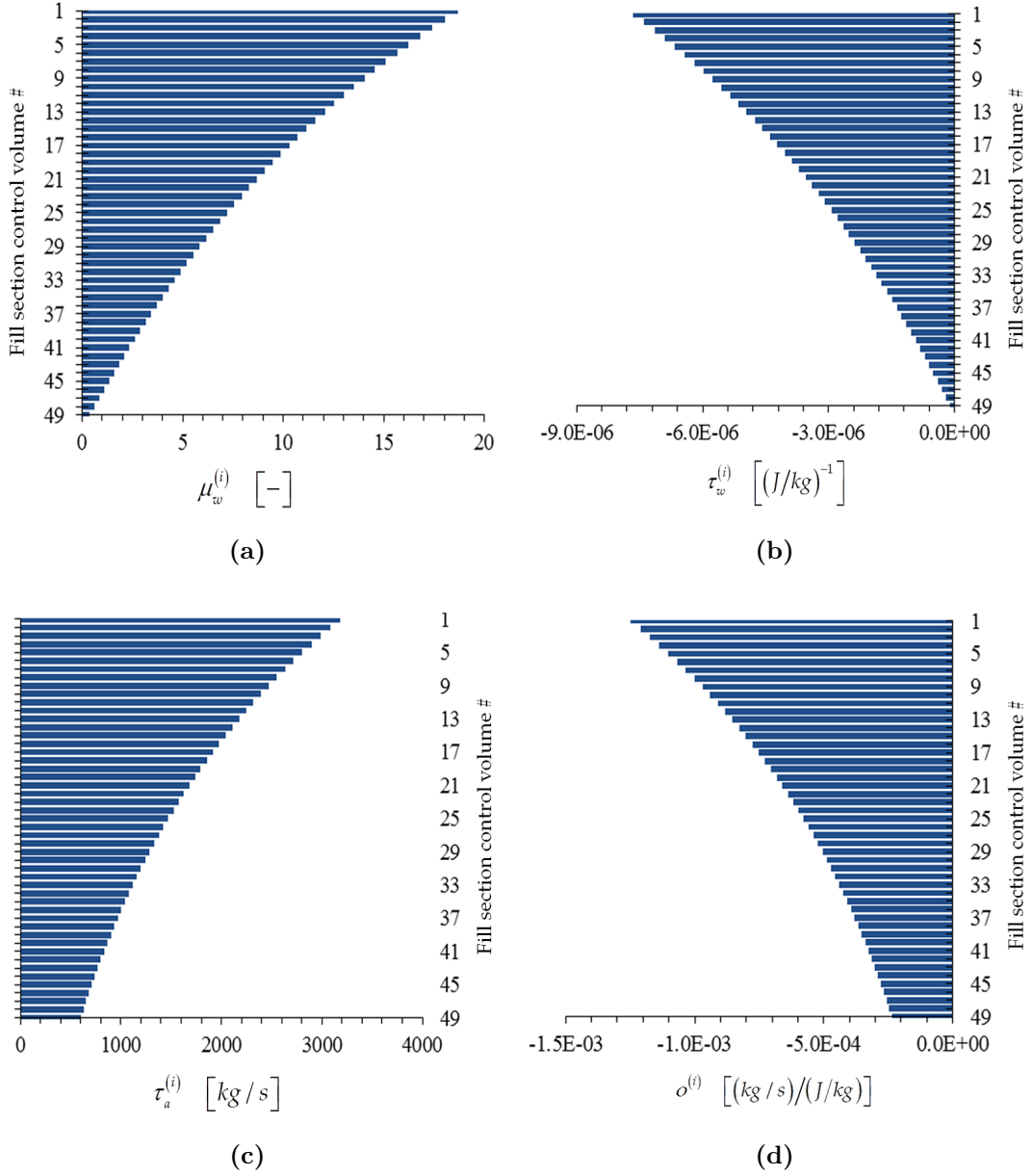


Figure 3.10: Bar plots of adjoint functions for the response $R \triangleq m_a$ as functions of the height of the cooling tower fill section: (a) $\mu_w \triangleq (\mu_w^{(1)}, \dots, \mu_w^{(49)})$, (b) $\tau_w \triangleq (\tau_w^{(1)}, \dots, \tau_w^{(49)})$, (c) $\tau_a \triangleq (\tau_a^{(1)}, \dots, \tau_a^{(49)})$, (d) $o \triangleq (o^{(1)}, \dots, o^{(49)})$, for case 1b: fan off, saturated outlet air condition, with inlet air saturated.

For the response $R \triangleq m_a$, the value of μ_a is 4.29938.

3.1.3 Development of the Cooling Tower Adjoint Sensitivity Model for Case 2: Fan Off, Unsaturated Air Conditions

The development of the cooling tower adjoint sensitivity model follows the same path as detailed in Section 3.1.1 for case 1a. The total sensitivity of a model response $R(\mathbf{m}_w, \mathbf{T}_w, \mathbf{T}_a, \boldsymbol{\omega}, m_a; \boldsymbol{\alpha})$, with respect to arbitrary variations in the model parameters $\delta\boldsymbol{\alpha} \triangleq (\delta\alpha_1, \dots, \delta\alpha_{N_\alpha})$ and state functions $\delta\mathbf{m}_w, \delta\mathbf{T}_w, \delta\mathbf{T}_a, \delta\boldsymbol{\omega}, \delta m_a$, around the nominal values $(\mathbf{m}_w^0, \mathbf{T}_w^0, \mathbf{T}_a^0, \boldsymbol{\omega}^0, m_a^0; \boldsymbol{\alpha}^0)$ of the parameters and state functions, is obtained by means of the G-differential of the model response to these changes. This G-differential is referred to as $DR(\mathbf{m}_w^0, \mathbf{T}_w^0, \mathbf{T}_a^0, \boldsymbol{\omega}^0, m_a^0; \boldsymbol{\alpha}^0; \delta\mathbf{m}_w, \delta\mathbf{T}_w, \delta\mathbf{T}_a, \delta\boldsymbol{\omega}, \delta m_a; \delta\boldsymbol{\alpha})$, and introducing the adjoint sensitivity functions it becomes:

$$\begin{aligned} DR(\mathbf{m}_w^0, \mathbf{T}_w^0, \mathbf{T}_a^0, \boldsymbol{\omega}^0, m_a^0; \boldsymbol{\alpha}^0; \delta\mathbf{m}_w, \delta\mathbf{T}_w, \delta\mathbf{T}_a, \delta\boldsymbol{\omega}, \delta m_a; \delta\boldsymbol{\alpha}) \\ = \sum_{i=1}^{N_\alpha} \left(\frac{\partial R}{\partial \alpha_i} \delta\alpha_i \right) + DR_{indirect} \end{aligned} \quad (3.35)$$

where the “indirect effect” term, $DR_{indirect}$, is again obtained as:

$$DR_{indirect} \triangleq \boldsymbol{\mu}_w \cdot \mathbf{Q}_1 + \boldsymbol{\tau}_w \cdot \mathbf{Q}_2 + \boldsymbol{\tau}_a \cdot \mathbf{Q}_3 + \mathbf{o} \cdot \mathbf{Q}_4 + \mu_a \cdot Q_5 \quad (3.36)$$

Performing the differentiation in Eq. (3.29) on Eqs. (2.39) - (2.51), and reminding the differences between the governing equation systems of case 1a and case 2 (see Section 2.3.3), the forward sensitivity system for case 2 is as follows:

$$\begin{pmatrix} \mathbf{A}_1^{II} & \mathbf{B}_1^{II} & \mathbf{C}_1^{II} & \mathbf{D}_1^{II} & \mathbf{E}_1^{II} \\ \mathbf{A}_2 & \mathbf{B}_2 & \mathbf{C}_2 & \mathbf{D}_2 & \mathbf{E}_2 \\ \mathbf{A}_3 & \mathbf{B}_3 & \mathbf{C}_3 & \mathbf{D}_3 & \mathbf{E}_3 \\ \mathbf{A}_4 & \mathbf{B}_4 & \mathbf{C}_4 & \mathbf{D}_4 & \mathbf{E}_4 \\ \mathbf{A}_5 & \mathbf{B}_5 & \mathbf{C}_5 & \mathbf{D}_5 & \mathbf{E}_5 \end{pmatrix} \begin{pmatrix} \delta\mathbf{m}_w \\ \delta\mathbf{T}_w \\ \delta\mathbf{T}_a \\ \delta\boldsymbol{\omega} \\ \delta m_a \end{pmatrix} = \begin{pmatrix} \mathbf{Q}_1^{II} \\ \mathbf{Q}_2 \\ \mathbf{Q}_3 \\ \mathbf{Q}_4 \\ Q_5 \end{pmatrix}, \quad (3.37)$$

CHAPTER 3. DESCRIPTION OF THE MATHEMATICAL FRAMEWORK

where the components of the vectors $\mathbf{Q}_1^{II} \triangleq (q_1^{(1)}, \dots, q_1^{(I)})$ and $\mathbf{Q}_\ell \triangleq (q_\ell^{(1)}, \dots, q_\ell^{(I)})$, $\ell = 2, 3, 4$ are defined as:

$$q_\ell^{(i)} \triangleq \sum_{j=1}^{N_\alpha} \left(\frac{\partial N_\ell^{(i)}}{\partial \alpha_j} \delta \alpha_j \right); \quad i = 1, \dots, I; \quad \ell = 1, 2, 3, 4. \quad (3.38)$$

and where Q_5 is defined as follows:

$$Q_5 \triangleq \sum_{j=1}^{N_\alpha} \left(\frac{\partial N_5}{\partial \alpha_j} \delta \alpha_j \right). \quad (3.39)$$

The vector \mathbf{Q}_1^{II} on the right hand side of Eq. (3.37) is denoted separately from others to highlight the difference of this source term from the one in case 1a. As mentioned earlier in Section 2.3.3, the differences between the governing equations for cases 1a and 2 are only in the “liquid continuity equations”. As a result, the Jacobian matrix presented in Eq. (3.37), which represents the derivatives of Eqs. (2.39) - (2.51) with respect to the state functions, is different from the Jacobian matrix presented in Eq. (3.7), which represents the derivatives of Eqs. (2.2) - (2.15) with respect to the state functions. More specifically, the Jacobian matrix-components in the first row, namely \mathbf{A}_1^{II} , \mathbf{B}_1^{II} , \mathbf{C}_1^{II} , \mathbf{D}_1^{II} and \mathbf{E}_1^{II} , are changed as defined in Section C.3 of Appendix C. Other matrix-components are kept the same as that in the Jacobian matrix in the RHS of Eq. (3.7). Hence, the vector $[\boldsymbol{\mu}_w, \boldsymbol{\tau}_w, \boldsymbol{\tau}_a, \mathbf{o}, \mu_a]^\dagger$ is required to be the solution of the following adjoint sensitivity system:

$$\begin{pmatrix} \mathbf{A}_1^{II\dagger} & \mathbf{A}_2^\dagger & \mathbf{A}_3^\dagger & \mathbf{A}_4^\dagger & \mathbf{A}_5^\dagger \\ \mathbf{B}_1^{II\dagger} & \mathbf{B}_2^\dagger & \mathbf{B}_3^\dagger & \mathbf{B}_4^\dagger & \mathbf{B}_5^\dagger \\ \mathbf{C}_1^{II\dagger} & \mathbf{C}_2^\dagger & \mathbf{C}_3^\dagger & \mathbf{C}_4^\dagger & \mathbf{C}_5^\dagger \\ \mathbf{D}_1^{II\dagger} & \mathbf{D}_2^\dagger & \mathbf{D}_3^\dagger & \mathbf{D}_4^\dagger & \mathbf{D}_5^\dagger \\ \mathbf{E}_1^{II\dagger} & \mathbf{E}_2^\dagger & \mathbf{E}_3^\dagger & \mathbf{E}_4^\dagger & \mathbf{E}_5^\dagger \end{pmatrix} \begin{pmatrix} \boldsymbol{\mu}_w \\ \boldsymbol{\tau}_w \\ \boldsymbol{\tau}_a \\ \mathbf{o} \\ \mu_a \end{pmatrix} = \begin{pmatrix} \mathbf{R}_1 \\ \mathbf{R}_2 \\ \mathbf{R}_3 \\ \mathbf{R}_4 \\ R_5 \end{pmatrix}; \quad (3.40)$$

CHAPTER 3. DESCRIPTION OF THE MATHEMATICAL FRAMEWORK

it ultimately results that the “indirect effect” term can be expressed in the form

$$DR_{indirect} \triangleq \boldsymbol{\mu}_w \cdot \mathbf{Q}_1^{II} + \boldsymbol{\tau}_w \cdot \mathbf{Q}_2 + \boldsymbol{\tau}_a \cdot \mathbf{Q}_3 + \mathbf{o} \cdot \mathbf{Q}_4 + \mu_a \cdot Q_5 \quad (3.41)$$

The vectors $\mathbf{R}_\ell \triangleq (r_\ell^{(1)}, \dots, r_\ell^{(I)})$, $\ell = 1, 2, 3, 4$ in Eq. (3.40) comprise the functional derivatives of the model responses with respect to the state functions, i.e.,:

$$r_1^{(i)} \triangleq \frac{\partial R}{\partial m_w^{(i+1)}}; \quad r_2^{(i)} \triangleq \frac{\partial R}{\partial T_w^{(i+1)}}; \quad r_3^{(i)} \triangleq \frac{\partial R}{\partial T_a^{(i)}}; \quad r_4^{(i)} \triangleq \frac{\partial R}{\partial \omega^{(i)}}; \quad i = 1, \dots, I. \quad (3.42)$$

and where R_5 is defined as follows:

$$R_5 \triangleq \frac{\partial R}{\partial m_a} \quad (3.43)$$

It is worth reminding that the adjoint sensitivity system in Eq. (3.40) is independent of parameter variations. This feature allows the selected adjoint functions $[\boldsymbol{\mu}_w, \boldsymbol{\tau}_w, \boldsymbol{\tau}_a, \mathbf{o}, \mu_a]^\dagger$ to be computed by solving the adjoint sensitivity system just once. For case 2, the units of the adjoint functions are the same as that listed in Table 1. Since the adjoint sensitivity system represented by Eq. (3.40) is linear in the adjoint state functions, it can be solved by using numerical methods appropriate for large-scale sparse linear systems. As in case 1, it was solved by using NSPCG, a “Package for Solving Large Sparse Linear Systems by Various Iterative Methods” [35]; 12 to 18 iterations sufficed for solving the adjoint system within convergence criterion of $\zeta = 10^{-12}$. The bar plots presented in Figures 3.11 - 3.15 display the trend of the adjoint functions corresponding to the five measured responses of interest, namely: (i) the exit air temperature $R \triangleq T_a^{(1)}$; (ii) the outlet (exit) water temperature $R \triangleq T_w^{(50)}$; (iii) the exit air humidity ratio $R \triangleq RH^{(1)}$; (iv) the outlet (exit) water mass flow rate $R \triangleq m_w^{(50)}$; and (v) the air mass flow rate $R \triangleq m_a$. For case 2, the verification of the adjoint functions depicted in Figures 3.11 - 3.15 has been performed with the same methodology as for case 1a, Section 3.1.1, and it is included in Section D.3 of Appendix D.

CHAPTER 3. DESCRIPTION OF THE MATHEMATICAL FRAMEWORK

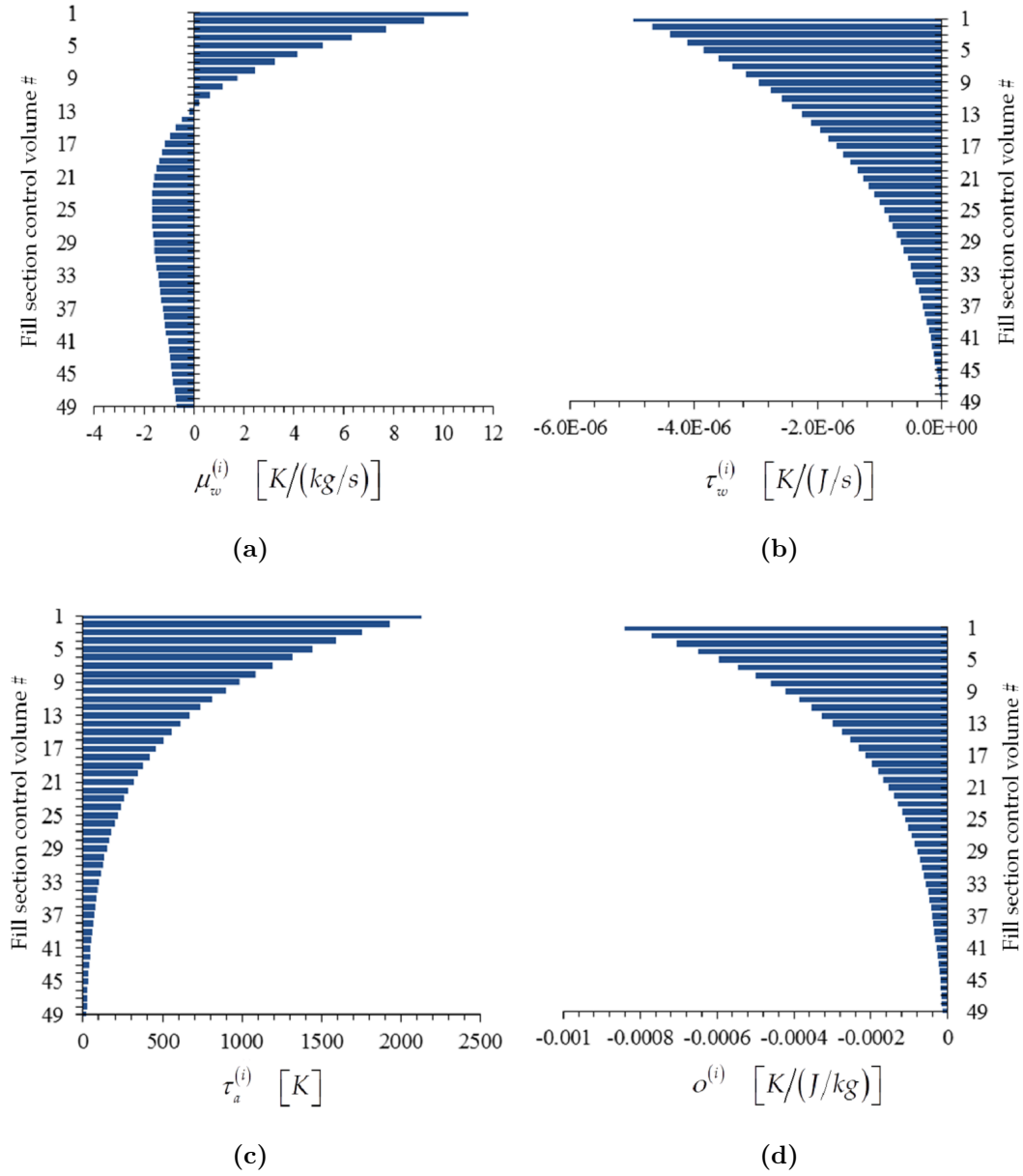


Figure 3.11: Bar plots of adjoint functions for the response $R \triangleq T_a^{(1)}$ as functions of the height of the cooling tower fill section: (a) $\mu_w \triangleq (\mu_w^{(1)}, \dots, \mu_w^{(49)})$, (b) $\tau_w \triangleq (\tau_w^{(1)}, \dots, \tau_w^{(49)})$, (c) $\tau_a \triangleq (\tau_a^{(1)}, \dots, \tau_a^{(49)})$, (d) $o \triangleq (o^{(1)}, \dots, o^{(49)})$, for case 2: fan off, unsaturated air conditions.

For the response $R \triangleq T_a^{(1)}$, the value of μ_a is -0.12651 .

CHAPTER 3. DESCRIPTION OF THE MATHEMATICAL FRAMEWORK

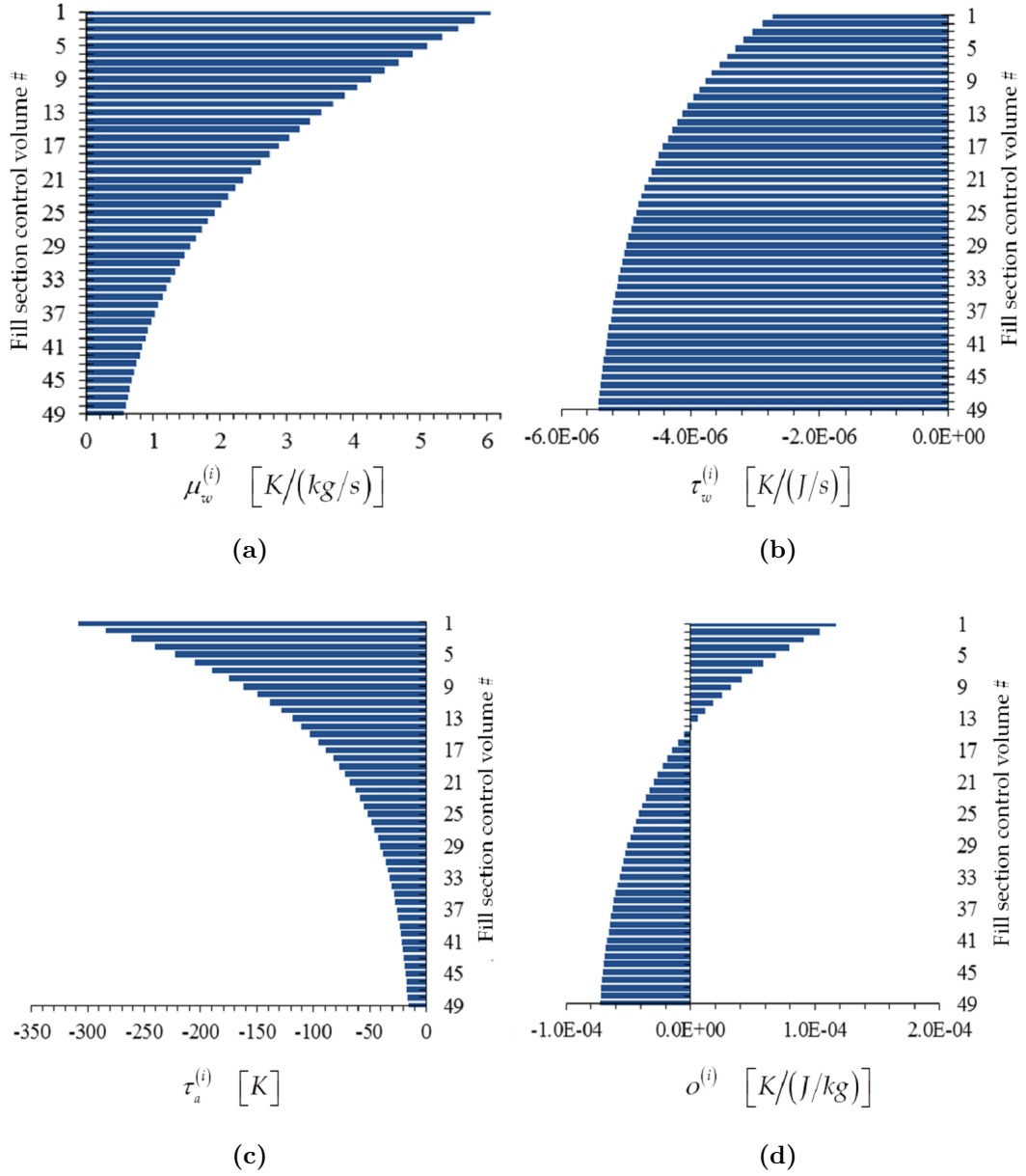


Figure 3.12: Bar plots of adjoint functions for the response $R \triangleq T_w^{(50)}$ as functions of the height of the cooling tower fill section: (a) $\mu_w \triangleq (\mu_w^{(1)}, \dots, \mu_w^{(49)})$, (b) $\tau_w \triangleq (\tau_w^{(1)}, \dots, \tau_w^{(49)})$, (c) $\tau_a \triangleq (\tau_a^{(1)}, \dots, \tau_a^{(49)})$, (d) $o \triangleq (o^{(1)}, \dots, o^{(49)})$, for case 2: fan off, unsaturated air conditions.

For the response $R \triangleq T_w^{(50)}$, the value of μ_a is -0.3771 .

CHAPTER 3. DESCRIPTION OF THE MATHEMATICAL FRAMEWORK

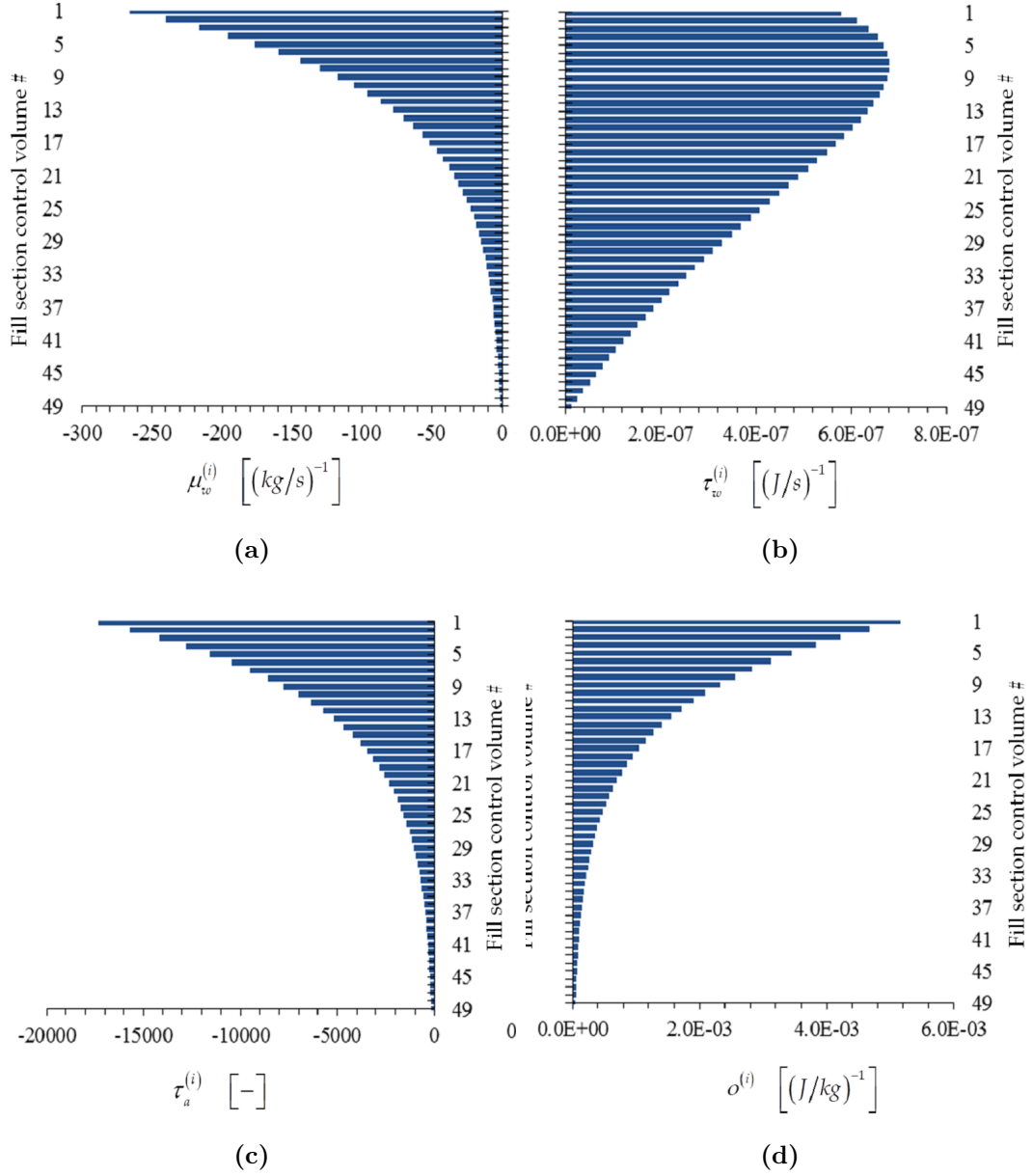


Figure 3.13: Bar plots of adjoint functions for the response $R \triangleq RH^{(1)}$ as functions of the height of the cooling tower fill section: (a) $\mu_w \triangleq (\mu_w^{(1)}, \dots, \mu_w^{(49)})$, (b) $\tau_w \triangleq (\tau_w^{(1)}, \dots, \tau_w^{(49)})$, (c) $\tau_a \triangleq (\tau_a^{(1)}, \dots, \tau_a^{(49)})$, (d) $o \triangleq (o^{(1)}, \dots, o^{(49)})$, for case 2: fan off, unsaturated air conditions.

For the response $R \triangleq RH^{(1)}$, the value of μ_a is -0.00743 .

CHAPTER 3. DESCRIPTION OF THE MATHEMATICAL FRAMEWORK

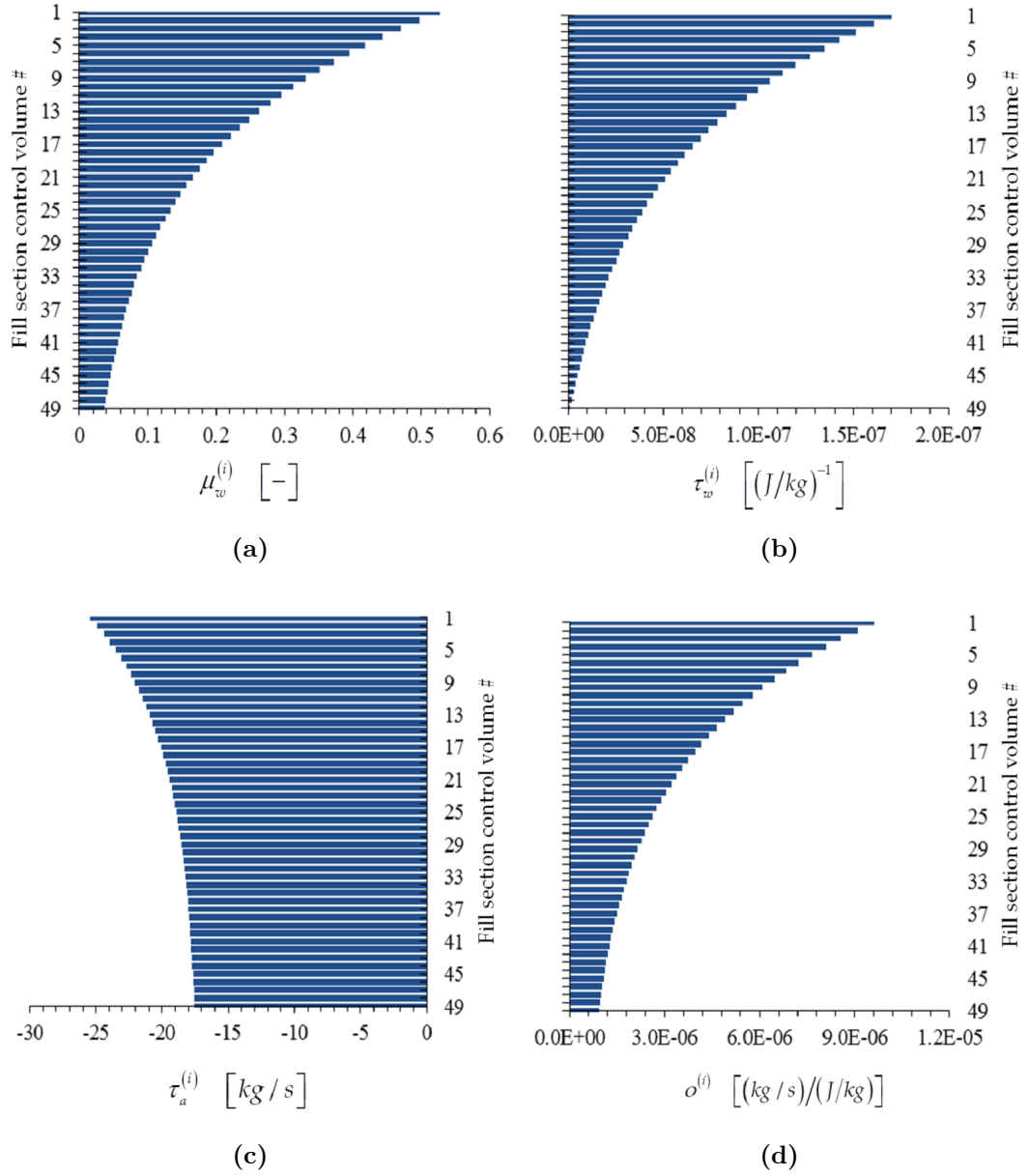


Figure 3.14: Bar plots of adjoint functions for the response $R \triangleq m_w^{(50)}$ as functions of the height of the cooling tower fill section: (a) $\mu_w \triangleq (\mu_w^{(1)}, \dots, \mu_w^{(49)})$, (b) $\tau_w \triangleq (\tau_w^{(1)}, \dots, \tau_w^{(49)})$, (c) $\tau_a \triangleq (\tau_a^{(1)}, \dots, \tau_a^{(49)})$, (d) $o \triangleq (o^{(1)}, \dots, o^{(49)})$, for case 2: fan off, unsaturated air conditions.

For the response $R \triangleq m_w^{(50)}$, the value of μ_a is -0.0306 .

CHAPTER 3. DESCRIPTION OF THE MATHEMATICAL FRAMEWORK

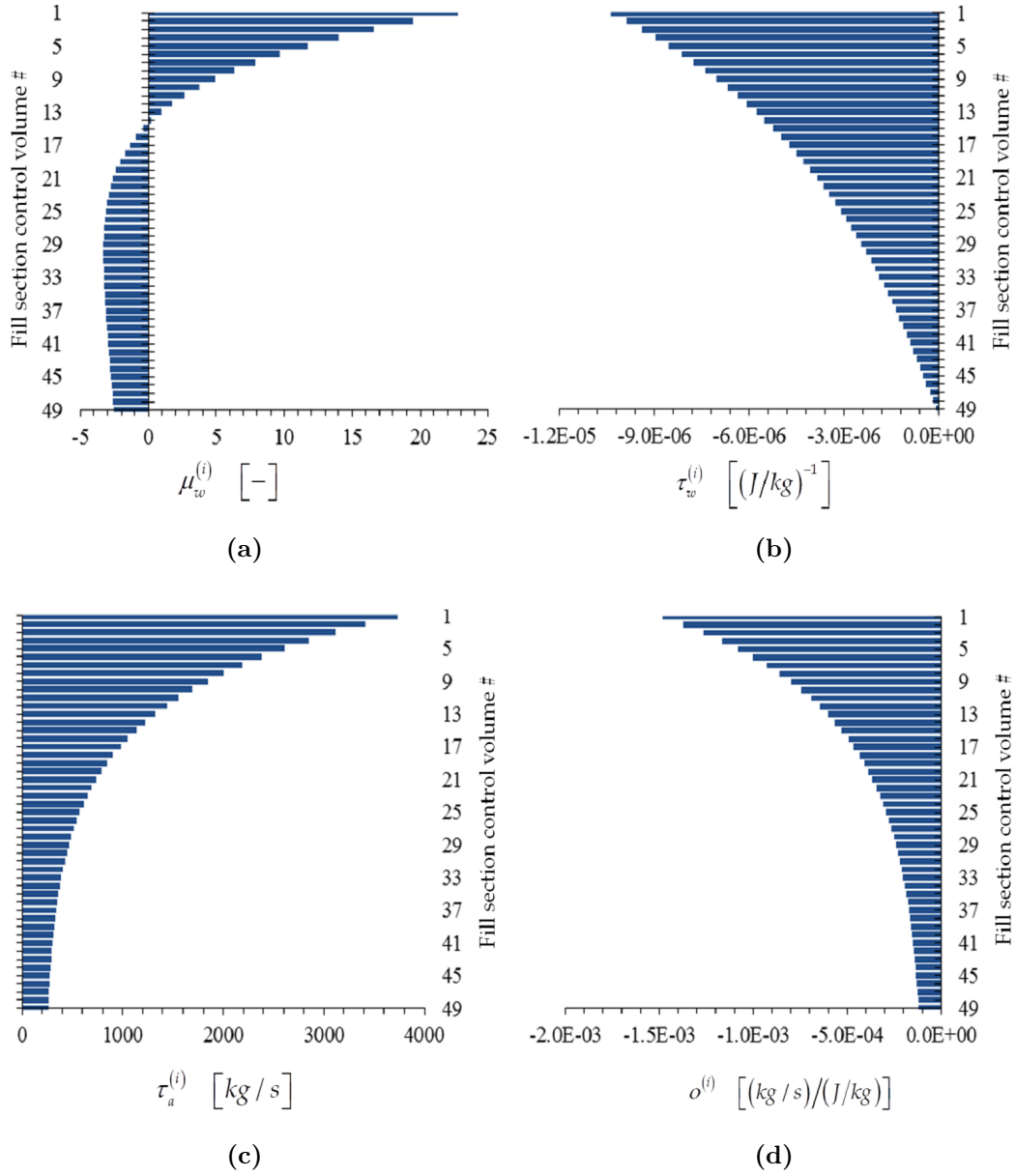


Figure 3.15: Bar plots of adjoint functions for the response $R \triangleq m_a$ as functions of the height of the cooling tower fill section: (a) $\mu_w \triangleq (\mu_w^{(1)}, \dots, \mu_w^{(49)})$, (b) $\tau_w \triangleq (\tau_w^{(1)}, \dots, \tau_w^{(49)})$, (c) $\tau_a \triangleq (\tau_a^{(1)}, \dots, \tau_a^{(49)})$, (d) $o \triangleq (o^{(1)}, \dots, o^{(49)})$, for case 2: fan off, unsaturated air conditions.

For the response $R \triangleq m_a$, the value of μ_a is 5.805.

3.2 Data assimilation, model calibration and best-estimate predictions with reduced uncertainties: Predictive Modeling for Coupled Multi-Physics Systems (PM_CMPS)

In this subsection the mathematical framework of the Predictive Modeling of Coupled Multi-Physics Systems (PM_CMPS) methodology [21] is described. The PM_CMPS methodology [21] comprises both the ideas of “forward” and “inverse” modeling within a mathematically and conceptually consolidated framework, which includes data assimilation, model calibration and prediction of best-estimate values for model parameters and responses, with optimized reduced uncertainties.

In general, a physical system subject in which experimental measurements can be made can be modeled with the following elements:

- A system of linear/nonlinear governing equations relating the system independent variables and parameters to the state functions of the system;
- (In)equality constraints that bound the range of the system parameters;
- One or more quantities of interest, referred to as system responses, obtained by solving the mathematical model;
- Experimental values of the system responses, accompanied by their respective nominal values and uncertainties.

The mathematical framework for the PM_CMPS methodology has been presented by Cacuci and Ionescu-Bujor in [21] for time-dependent systems; in this

CHAPTER 3. DESCRIPTION OF THE MATHEMATICAL FRAMEWORK

chapter the notation has been simplified to consider only time-independent systems, since the one system analyzed in this work falls within this category.

Generally, a time-independent physical system will comprise N_α not exactly known model parameters, α_n , referred to as the components of a (column) vector, $\boldsymbol{\alpha}$, denoted as:

$$\boldsymbol{\alpha} = \{\alpha_n | n = 1, \dots, N_\alpha\} \quad (3.44)$$

The mean values of the model parameters α_n are defined as $\alpha_n^0 \triangleq \langle \alpha_n \rangle$, while the covariances between two generic parameters α_i and α_j are denoted as $\text{cov}(\alpha_i, \alpha_j)$. The mean values α_n^0 are treated as being known a priori; from that follows that the vector $\boldsymbol{\alpha}^0$, referred to as $\boldsymbol{\alpha}^0 = \{\alpha_n^0 | n = 1, \dots, N_\alpha\}$ is considered to be known a priori as well. The covariances $\text{cov}(\alpha_i, \alpha_j)$ are also treated as being known a priori; these covariances are regarded to be the elements of the a priori known parameter covariance matrix, denoted as $\mathbf{C}_{\alpha\alpha}^{(N_\alpha \times N_\alpha)}$ and defined as:

$$\begin{aligned} \mathbf{C}_{\alpha\alpha}^{(N_\alpha \times N_\alpha)} &\triangleq [\text{cov}(\alpha_i, \alpha_j)]_{N_\alpha \times N_\alpha} \triangleq \langle (\alpha_i - \alpha_i^0) (\alpha_j - \alpha_j^0) \rangle_{N_\alpha \times N_\alpha}; \\ &i, j = 1, \dots, N_\alpha \end{aligned} \quad (3.45)$$

Generally, the model will also comprise N_r experimentally measured responses, r_i , regarded as the components of the column vector:

$$\mathbf{r} = \{r_i | i = 1, \dots, N_r\} \quad (3.46)$$

The mean values of the experimentally measured responses, r_i , denoted as r_i^m , as well as the covariances between two measured responses r_i and r_j , denoted as $\langle (r_i - r_i^m) (r_j - r_j^m) \rangle$, are regarded to be a priori known. The mean measured values r_i^m are organized as the components of the vector \mathbf{r}^m defined as:

$$\mathbf{r}^m = \{r_i^m | i = 1, \dots, N_r\}, \quad r_i^m \triangleq \langle r_i \rangle, \quad i = 1, \dots, N_r, \quad (3.47)$$

CHAPTER 3. DESCRIPTION OF THE MATHEMATICAL FRAMEWORK

while the covariances $\langle (r_i - r_i^m) (r_j - r_j^m) \rangle$ of the experimentally measured responses are treated as being the components of the a priori known measured covariance matrix, denoted as $\mathbf{C}_{rr}^{(N_r \times N_r)}$, and defined as:

$$\mathbf{C}_{rr}^{(N_r \times N_r)} \triangleq \langle (r_i - r_i^m) (r_j - r_j^m) \rangle_{N_r \times N_r}, \quad i, j = 1, \dots, N_r. \quad (3.48)$$

Parameters and responses may be also generically correlated to each other; such correlations are computed through a priori known parameter-response matrices, denoted as $\mathbf{C}_{\alpha r}^{(N_\alpha \times N_r)}$, and defined as follows:

$$\mathbf{C}_{\alpha r}^{(N_\alpha \times N_r)} \triangleq \langle (\boldsymbol{\alpha} - \boldsymbol{\alpha}^0) (\mathbf{r} - \mathbf{r}^m)^\dagger \rangle = [\mathbf{C}_{r\alpha}^{(N_r \times N_\alpha)}]^\dagger \quad (3.49)$$

For notation clarity reasons, the size of the vectors and matrices in the following will not be shown in the subsequent formulas. In general, a response computed using the model can depend nonlinearly and implicitly on the model parameters. Uncertainties due to parameters induce uncertainties in the responses which, in this case, can be computed deterministically using propagation of moments method. The computed response is linearized via a functional Taylor-series expansion around the nominal parameter values $\boldsymbol{\alpha}^0$ as:

$$\mathbf{r}(\boldsymbol{\alpha}) = \mathbf{R}(\boldsymbol{\alpha}^0) + \mathbf{S}(\boldsymbol{\alpha} - \boldsymbol{\alpha}^0) + \text{higher order terms} \quad (3.50)$$

where $\mathbf{R}(\boldsymbol{\alpha}^0)$ represents the vector of computed responses at the nominal parameter values $\boldsymbol{\alpha}^0$ and \mathbf{S} denotes the $N_r \times N_\alpha$ dimensional matrix containing the first Gâteaux derivatives of the computed responses with respect to the parameters:

$$\mathbf{S}_{r\alpha}^{N_r \times N_\alpha} \triangleq \begin{pmatrix} \frac{\partial r_1}{\partial \alpha_1} & \dots & \frac{\partial r_1}{\partial \alpha_{N_\alpha}} \\ \vdots & \ddots & \vdots \\ \frac{\partial r_{N_r}}{\partial \alpha_1} & \dots & \frac{\partial r_{N_r}}{\partial \alpha_{N_\alpha}} \end{pmatrix}. \quad (3.51)$$

CHAPTER 3. DESCRIPTION OF THE MATHEMATICAL FRAMEWORK

The expectation value $\langle \mathbf{r} \rangle$ is computed by integrating the expansion of the responses over the unknown joint probability distribution $p(\boldsymbol{\alpha}, \mathbf{r})$:

$$\langle \mathbf{r} \rangle = \int_{D_\alpha} \mathbf{r}(\boldsymbol{\alpha}) p(\boldsymbol{\alpha}, \mathbf{r}) d\boldsymbol{\alpha} \quad (3.52)$$

where D_α is the domain of all α values. Substituting the first-order Taylor expansion of Eq. (3.76) into Eq. (3.78) yields

$$\langle \mathbf{r} \rangle = \int_{D_\alpha} \mathbf{R}(\boldsymbol{\alpha}^0) p(\boldsymbol{\alpha}, \mathbf{r}) d\boldsymbol{\alpha} + \int_{D_\alpha} \sum_{i_1=1}^{N_\alpha} \left. \frac{\partial \mathbf{R}}{\partial \alpha_{i_1}} \right|_{\alpha^0} \delta \alpha_{i_1} p(\boldsymbol{\alpha}, \mathbf{r}) d\boldsymbol{\alpha} \quad (3.53)$$

The terms independent of $\boldsymbol{\alpha}$ can be pulled out of the integral, to have:

$$\langle \mathbf{r} \rangle = \mathbf{R}(\boldsymbol{\alpha}^0) \int_{D_\alpha} p(\boldsymbol{\alpha}, \mathbf{r}) d\boldsymbol{\alpha} + \sum_{i_1=1}^{N_\alpha} \left. \frac{\partial \mathbf{R}}{\partial \alpha_{i_1}} \right|_{\alpha^0} \int_{D_\alpha} \delta \alpha_{i_1} p(\boldsymbol{\alpha}, \mathbf{r}) d\boldsymbol{\alpha} \quad (3.54)$$

The result of the integral in the first term is 1, since $p(\boldsymbol{\alpha}, \mathbf{r})$ is a probability distribution integrated over the whole domain. The integrand in the second term is the first central moment, which is zero. The expectation value is therefore:

$$\langle \mathbf{r} \rangle = \mathbf{R}(\boldsymbol{\alpha}^0) \quad (3.55)$$

The computed responses covariance matrix can be calculated as follows:

$$\begin{aligned} \mathbf{C}_{rr}^{comp} &\triangleq \left\langle [\mathbf{r}(\boldsymbol{\alpha}) - \mathbf{R}(\boldsymbol{\alpha}^0)] [\mathbf{r}(\boldsymbol{\alpha}) - \mathbf{R}(\boldsymbol{\alpha}^0)]^T \right\rangle \\ &= [\mathbf{S}(\boldsymbol{\alpha}^0)] \left\langle [\boldsymbol{\alpha} - \boldsymbol{\alpha}^0] [\boldsymbol{\alpha} - \boldsymbol{\alpha}^0]^T \right\rangle [\mathbf{S}(\boldsymbol{\alpha}^0)]^T \\ &= [\mathbf{S}(\boldsymbol{\alpha}^0)] \mathbf{C}_\alpha [\mathbf{S}(\boldsymbol{\alpha}^0)]^T \end{aligned} \quad (3.56)$$

The application of the maximum entropy algorithm described in [21] to the computational and experimental information listed above yields that the most objective probability distribution for this information is a multivariate Gaussian of the

CHAPTER 3. DESCRIPTION OF THE MATHEMATICAL FRAMEWORK

form:

$$p(\mathbf{z}|\mathbf{C})d\mathbf{z} = \frac{e^{-\frac{1}{2}Q(\mathbf{z})}}{|2\pi\mathbf{C}|^{\frac{1}{2}}}d\mathbf{z}, \quad (3.57)$$

where:

$$Q(\mathbf{z}) \triangleq \mathbf{z}^\dagger \mathbf{C}^{-1} \mathbf{z}, \quad -\infty < z_j < \infty \quad (3.58)$$

$$\mathbf{z} \triangleq \begin{pmatrix} \boldsymbol{\alpha} - \boldsymbol{\alpha}^0 \\ \mathbf{r} - \mathbf{r}_m \end{pmatrix}, \quad (3.59)$$

$$\mathbf{C} = \begin{pmatrix} \mathbf{C}_\alpha & \mathbf{C}_{\alpha r} \\ \mathbf{C}_{\alpha r}^T & \mathbf{C}_{rr} \end{pmatrix}. \quad (3.60)$$

If no specific loss function is provided, the recommended best-estimate mean vector \mathbf{z}^{BE} and its respective best-estimate posterior covariance matrix are usually computed assuming quadratic loss. The bulk of the contribution in Eq. (3.84) is extracted by computing it at the point where Q attains a minimum subject to Eq. (3.76). When higher-order terms as well as numerical errors are neglected this relation can be conveniently written in the form:

$$\mathbf{Z}(\boldsymbol{\alpha}^0)\mathbf{z} + \mathbf{d} = 0, \quad (3.61)$$

where:

$$\mathbf{d} \triangleq \mathbf{R}(\boldsymbol{\alpha}^0) - \mathbf{r}_m \quad (3.62)$$

and \mathbf{Z} denotes the partitioned matrix:

$$\mathbf{Z} \triangleq (\mathbf{S} \mathbf{I}), \quad (3.63)$$

where \mathbf{I} is a $N_r \times N_r$ identity matrix. Finding the minimum of $Q(\mathbf{z})$ subject to Eq. (3.87) is a constrained minimization problem that may be solved by introducing

CHAPTER 3. DESCRIPTION OF THE MATHEMATICAL FRAMEWORK

Lagrange multipliers λ to construct an augmented functional:

$$P(\mathbf{z}, \lambda) \triangleq Q(\mathbf{z}) + 2\lambda^\dagger [\mathbf{Z}(\boldsymbol{\alpha}^0) \mathbf{z} + \mathbf{d}] = \min \quad (3.64)$$

at

$$\mathbf{z} = \mathbf{z}^{BE} \triangleq \begin{pmatrix} \boldsymbol{\alpha}^{BE} - \boldsymbol{\alpha}^0 \\ \mathbf{r}^{BE} - \mathbf{r}_m \end{pmatrix}. \quad (3.65)$$

The point where the functional $P(\mathbf{z}, \lambda)$ reaches its minimum may be found through the conditions:

$$\nabla_{\mathbf{z}} P(\mathbf{z}, \lambda) = 0, \quad \nabla_{\lambda} P(\mathbf{z}, \lambda) = 0, \quad \text{at } \mathbf{z} = \mathbf{z}^{BE}. \quad (3.66)$$

The solution to this constrained minimization problem is presented in detail in the Appendix of [21]. The resulting best-estimate parameters, responses and reduced uncertainties covariance matrix are listed in the following.

A. Optimally predicted “best-estimate” nominal values, $\boldsymbol{\alpha}^{pred}$, for the model parameters:

$$\boldsymbol{\alpha}^{pred} = \boldsymbol{\alpha}^0 - (\mathbf{C}_{\alpha\alpha} \mathbf{S}_{r\alpha}^\dagger - \mathbf{C}_{\alpha r}) [\mathbf{D}_{rr}]^{-1} [\mathbf{r}^c(\boldsymbol{\alpha}^0, \beta^0) - \mathbf{r}^m], \quad (3.67)$$

where the matrix \mathbf{D}_{rr} is defined as

$$\mathbf{D}_{rr} = \mathbf{S}_{r\alpha} \mathbf{C}_{\alpha\alpha} \mathbf{S}_{r\alpha}^\dagger - \mathbf{S}_{r\alpha} \mathbf{C}_{\alpha r} - \mathbf{C}_{\alpha r}^\dagger \mathbf{S}_{r\alpha}^\dagger + \mathbf{C}_{rr}, \quad (3.68)$$

and the elements of the matrix $\mathbf{S}_{r\alpha}^{N_r \times N_\alpha}$ are the first-order sensitivities of all model responses with respect to all model parameters, defined as follows:

$$\mathbf{S}_{r\alpha}^{N_r \times N_\alpha} \triangleq \begin{pmatrix} \frac{\partial r_1}{\partial \alpha_1} & \dots & \frac{\partial r_1}{\partial \alpha_{N_\alpha}} \\ \vdots & \ddots & \vdots \\ \frac{\partial r_{N_r}}{\partial \alpha_1} & \dots & \frac{\partial r_{N_r}}{\partial \alpha_{N_\alpha}} \end{pmatrix}. \quad (3.69)$$

CHAPTER 3. DESCRIPTION OF THE MATHEMATICAL FRAMEWORK

It is worth noticing that, in case just the first-order sensitivities are being considered, the first term on the right side of Eq. (3.94) corresponds to the covariance matrix of the computed responses, \mathbf{C}_{rr}^{comp} , i.e.,

$$\mathbf{C}_{rr}^{comp} = \mathbf{S}_{r\alpha} \mathbf{C}_{\alpha\alpha} \mathbf{S}_{r\alpha}^\dagger \quad (3.70)$$

B. Reduced predicted uncertainties, $\mathbf{C}_{\alpha\alpha}^{pred}$, for the predicted nominal parameter values, given by the expression below:

$$\mathbf{C}_{\alpha\alpha}^{pred} = \mathbf{C}_{\alpha\alpha} - (\mathbf{C}_{\alpha\alpha} \mathbf{S}_{r\alpha}^\dagger - \mathbf{C}_{\alpha r}) [\mathbf{D}_{rr}]^{-1} (\mathbf{C}_{\alpha\alpha} \mathbf{S}_{r\alpha}^\dagger - \mathbf{C}_{\alpha r})^\dagger; \quad (3.71)$$

C. Optimally predicted “best-estimate” nominal values, \mathbf{r}^{pred} , for the model responses, given by the expression below:

$$\mathbf{r}^{pred} = \mathbf{r}^m - (\mathbf{C}_{\alpha r}^\dagger \mathbf{S}_{r\alpha}^\dagger - \mathbf{C}_{rr}) [\mathbf{D}_{rr}]^{-1} [\mathbf{r}^c(\boldsymbol{\alpha}^0, \beta^0) - \mathbf{r}^m]; \quad (3.72)$$

D. Reduced predicted uncertainties, \mathbf{C}_{rr}^{pred} , for the predicted nominal parameter values, given by the expression below:

$$\mathbf{C}_{rr}^{pred} = \mathbf{C}_{rr} - (\mathbf{C}_{\alpha r}^\dagger \mathbf{S}_{r\alpha}^\dagger - \mathbf{C}_{rr}) [\mathbf{D}_{rr}]^{-1} (\mathbf{C}_{\alpha r}^\dagger \mathbf{S}_{r\alpha}^\dagger - \mathbf{C}_{rr})^\dagger; \quad (3.73)$$

E. Predicted correlations, $\mathbf{C}_{\alpha r}^{pred}$, between the predicted model parameters and responses, given by the expression below:

$$\mathbf{C}_{\alpha r}^{pred} = \mathbf{C}_{\alpha r} - (\mathbf{C}_{\alpha\alpha} \mathbf{S}_{r\alpha}^\dagger - \mathbf{C}_{\alpha r}) [\mathbf{D}_{rr}]^{-1} (\mathbf{C}_{\alpha r}^\dagger \mathbf{S}_{r\alpha}^\dagger - \mathbf{C}_{rr})^\dagger. \quad (3.74)$$

It is important to notice that in the case of a perfect model (which means that $\mathbf{C}_{\alpha\alpha} = \mathbf{0}$ and $\mathbf{C}_{\alpha r} = \mathbf{0}$), Eqs. (3.70) through (3.100) would yield

$$\boldsymbol{\alpha}^{pred} = \boldsymbol{\alpha}^0 \quad (3.75)$$

and

$$\mathbf{r}^{pred} = \mathbf{r}^c(\boldsymbol{\alpha}^0, \beta^0), \quad (3.76)$$

CHAPTER 3. DESCRIPTION OF THE MATHEMATICAL FRAMEWORK

with all accompanying uncertainties being null (i.e., $\mathbf{C}_{rr}^{pred} = \mathbf{0}$, $\mathbf{C}_{\alpha\alpha}^{pred} = \mathbf{0}$, $\mathbf{C}_{\alpha r}^{pred} = \mathbf{0}$).

Practically, a perfect model would get from the PM_CMPS methodology predicted values for the parameters and responses that would exactly match the model original parameters and computed responses values (considered as perfect); on the other side the experimental data would not influence the predictions whatsoever (as it is logical, since imperfect measurements could in no way improve “perfect” model predictions).

On the other hand, if the measurements were perfect, (i.e., $\mathbf{C}_{rr} = \mathbf{0}$ and $\mathbf{C}_{\alpha r} = \mathbf{0}$), but the model were imperfect, then Eqs. (3.70) through (3.100) would yield

$$\boldsymbol{\alpha}^{pred} = \boldsymbol{\alpha}^0 - \mathbf{C}_{\alpha\alpha} \mathbf{S}_{r\alpha}^\dagger [\mathbf{S}_{r\alpha} \mathbf{C}_{\alpha\alpha} \mathbf{S}_{r\alpha}^\dagger]^{-1} \mathbf{r}^d (\boldsymbol{\alpha}^0), \quad (3.77)$$

$$\mathbf{r}^{pred} = \mathbf{r}^m, \quad (3.78)$$

$$\mathbf{C}_{rr}^{pred} = \mathbf{0}, \mathbf{C}_{\alpha r}^{pred} = \mathbf{0}, \mathbf{C}_{\alpha\alpha}^{pred} = \mathbf{C}_{\alpha\alpha} - \mathbf{C}_{\alpha\alpha} \mathbf{S}_{r\alpha}^\dagger [\mathbf{S}_{r\alpha} \mathbf{C}_{\alpha\alpha} \mathbf{S}_{r\alpha}^\dagger]^{-1} \mathbf{S}_{r\alpha} \mathbf{C}_{\alpha\alpha}. \quad (3.79)$$

In case the measurement were perfect, the PM_CMPS predicted values for the responses would therefore match the measured values (considered as perfect), while the model uncertain parameters would be optimized by considering the respective measurements in order to lead to improved nominal values and reduced parameters uncertainties.

Chapter 4

Results

This chapter presents the results stemming from the application of the ASAM and of the PM_CMPS methodologies described in Chapter 3 to the cooling tower model of interest. Every case listed in Chapter 2 has been treated separately, to provide to the reader the numeric results for all the operating conditions analyzed; a cross-comparison of the most relevant results has been performed and is detailed in Section 4.2.

4.1 Adjoint Sensitivity Analysis of the cooling tower cases of interest

As it can be found detailed in Appendix A, there are a total of 8079 measured benchmark data sets for the cooling tower model with the “fan-off”. Out of the 8079 total data sets, 667 benchmark data sets present outlet air in “saturated conditions”, falling therefore within case 1. In Appendix A it is shown that these 667 data sets are further separated based on their air inlet boundary conditions at the fill section entrance. Case 1a describes a situation in which air enters the

CHAPTER 4. RESULTS

fill section in unsaturated condition, but it gets saturated before reaching the outlet of the fill section; in case 1b air enters the fill section already saturated, exiting the fill section also saturated. For both cases, air exits the fill section in saturated conditions, and only the inlet air conditions are different. Among the 667 saturated data sets, 377 of them have unsaturated air inlet boundary conditions, and therefore are grouped into case 1a; the other 290 data sets have saturated air inlet boundary conditions, and therefore are grouped into case 1b. Out of the 8079 total data sets, 6717 benchmark data sets present outlet air in unsaturated conditions, and are therefore relevant to case 2.

The nominal values for boundary and atmospheric conditions used for the sensitivity analysis were obtained, as described in Appendix A, from the statistics of the aforementioned groups of 377 data sets for case 1a, 290 data sets for case 1b and 6717 data sets for case 2. In turn, these “saturated” boundary and atmospheric conditions were used to obtain the sensitivity results reported, below, in Subsections 4.1.1 - 4.1.3. Subsections 4.1.1 - 4.1.3 provide the numerical values and rankings, in descending order, of the relative sensitivities computed using the adjoint sensitivity analysis methodology for the five model responses $T_a^{(1)}$, $T_w^{(50)}$, $m_w^{(50)}$, $RH^{(1)}$ and m_a of case 1a, case 1b and case 2, respectively.

Note that the relative sensitivity, $RS(\alpha_i)$, of a response $R(\alpha_i)$ to a parameter α_i is defined as $RS(\alpha_i) \triangleq [dR(\alpha_i)/d\alpha_i][\alpha_i/R(\alpha_i)]$. Thus, the relative sensitivities are unit-less and are very useful in ranking the sensitivities to highlight their relative importance for the respective response. A relative sensitivity of 1.00 indicates that a change of 1% in the respective parameter will induce a 1% change in a response that is linear in the respective sensitivity. The higher the relative sensitivity, the more important the respective parameter to the respective response.

CHAPTER 4. RESULTS

4.1.1 Adjoint Sensitivity Analysis of Case 1a: Fan Off, Saturated Outlet Air Conditions, with Inlet Air Un-saturated

4.1.1.1 Relative sensitivities of the outlet air temperature, $T_a^{(1)}$

The sensitivities of the air outlet temperature with respect to all of the model parameters for case 1a have been computed using Eq. (3.22). The numerical results and ranking of the relative sensitivities, in descending order of their magnitudes, are provided in Table 4.1, below, along with their respective relative standard deviations.

Table 4.1: Ranked relative sensitivities of the outlet air temperature, $T_a^{(1)}$, for case 1a.

Rank #	Parameter (α_i)	Nominal Value	Rel. Sens. $RS(\alpha_i)$	Rel. std. dev. (%)
1	Inlet water temperature, $T_{w,in}$	298.77 K	0.8346	0.47
2	Air temperature (dry bulb), T_{db}	294.03 K	0.1436	0.61
3	Inlet air temperature, $T_{a,in}$	294.03 K	0.1429	0.61
4	$P_{vs}(T)$ parameters, a_0	25.5943	-0.0231	0.04
5	$P_{vs}(T)$ parameters, a_1	-5229.89	0.0151	0.08
6	Dew point temperature, T_{dp}	293.49 K	0.0127	0.55
7	Fill section equivalent diameter, D_h	0.0381 m	-0.0045	1
8	Atmospheric pressure, P_{atm}	100853 Pa	-0.0041	0.28
9	Fan shroud inner diameter, D_{fan}	4.1 m	-0.0031	1
10	$C_{pa}(T)$ parameters, $a_{0,cpa}$	1030.5	-0.003	0.03
11	Thermal conductivity of air at T=300 K, k_{air}	0.02624 W/(m·K)	0.0027	6.04
12	Heat transfer coefficient multiplier, f_{ht}	1	0.0027	50
13	Nusselt parameters, $a_{0,Nu}$	8.235	0.0022	25
14	Wetted fraction of fill surface area, w_{tsa}	1	0.0022	0
15	Fill section surface area, A_{surf}	14221 m ²	0.0022	25
16	Wind speed, V_w	1.352 m/s	-0.0018	46.15
17	Fill section flow area, A_{fill}	67.29 m ²	-0.0018	10
18	Water enthalpy $h_f(T)$ parameters, a_{1f}	4186.51	0.0015	0.04
19	Cooling tower deck height above ground, Δz_{dk}	10.0 m	-0.0014	1

CHAPTER 4. RESULTS

Rank #	Parameter (α_i)	Nominal Value	Rel. Sens. $RS(\alpha_i)$	Rel. std. dev. (%)
20	Fill section height, Δz_{fill}	2.013 m	0.0012	1
21	Dynamic viscosity of air at T=300 K, μ	$1.983 \cdot 10^{-5}$ kg/(m·s)	0.0012	4.88
22	Fill section frictional loss multiplier, f	4	0.0012	50
23	Inlet water mass flow rate, $m_{w,in}$	44.0213 kg/s	0.0011	5
24	Inlet air humidity ratio, ω_{in}	0.01552	0.00069	8.15
25	D _{av} (T) parameters, $a_{1,dav}$	2.65322	0.00067	0.11
26	h _g (T) parameters, a_{0g}	2005743	-0.00065	0.05
27	Mass transfer coefficient multiplier, f_{mt}	1	-0.00053	50
28	D _{av} (T) parameters, $a_{2,dav}$	$-6.1681 \cdot 10^{-3}$	-0.00045	0.37
29	Fan shroud height, Δz_{fan}	3.0 m	-0.00042	1
30	h _f (T) parameters, a_{0f}	-1143423	-0.00037	0.05
31	D _{av} (T) parameters, $a_{0,dav}$	$7.06085 \cdot 10^{-9}$	-0.00035	0
32	Sum of loss coefficients above fill, k_{sum}	10	0.0003	50
33	h _g (T) parameters, a_{1g}	1815.437	-0.00027	0.19
34	Rain section height, Δz_{rain}	1.633 m	0.00023	1
35	Kinematic viscosity of air at T=300 K, ν	$1.568 \cdot 10^{-5}$ m ² /s	-0.00018	12.09
36	Prandtl number of air at T=80 °C, P_r	0.708	0.00018	0.71
37	Schmidt number, Sc	0.6188	-0.00018	1.19
38	C _{pa} (T) parameters, $a_{1,cpa}$	-0.19975	0.00017	1
39	Basin section height, Δz_{bs}	1.168 m	0.00016	1
40	D _{av} (T) parameters, $a_{3,dav}$	$6.55265 \cdot 10^{-6}$	0.00014	0.58
41	C _{pa} (T) parameters, $a_{2,cpa}$	$3.9734 \cdot 10^{-4}$	-0.00009	0.84
42	Drift eliminator thickness, Δz_{de}	0.1524 m	0.00008	1
43	Cooling tower deck width in x-dir, W_{dkx}	8.5 m	0.00005	1
44	Cooling tower deck width in y-dir, W_{dky}	8.5 m	0.00005	1
45	Nusselt parameters, $a_{1,Nu}$	0.0031498	0.0011	31.75
46	Nusselt parameters, $a_{2,Nu}$	0.9902987	0.00008	33.02
47	Nusselt parameters, $a_{3,Nu}$	0.023	0	38.26

As the results in Table 4.1 indicate, the first 3 parameters (i.e., $T_{w,in}$, T_{db} and $T_{a,in}$) have relative sensitivities between ca. 15% and 83%, and are therefore the most important for the air outlet temperature response, $T_a^{(1)}$. The largest sensitivity has a value ca. 83%, which means that a 1% change in $T_{w,in}$ would induce a

CHAPTER 4. RESULTS

0.83% change in $T_a^{(1)}$. The next three parameters (i.e., a_0 , a_1 and T_{dp}) have relative sensitivities between 1% and 3%, and are therefore somewhat important. The remaining 41 parameters are relatively unimportant for this response, having relative sensitivities smaller than 1% of the largest relative sensitivity (with respect to $T_{a,in}$) for this response. Positive sensitivities imply that a positive change in the respective parameter would cause an increase in the response, while negative sensitivities imply that a positive change in the respective parameter would cause a decrease in the response.

4.1.1.2 Relative sensitivities of the outlet water temperature, $T_w^{(50)}$

The results and ranking of the relative sensitivities of the outlet water temperature with respect to the most important 9 parameters for this response are listed in Table 4.2. The largest sensitivity of $T_w^{(50)}$ is to the parameter $T_{w,in}$, and has the value of 0.4856; this means that a 1% increase in $T_{w,in}$ would induce a 0.4856% increase in $T_w^{(50)}$. The sensitivities to the remaining 38 model parameters have not been listed since they are smaller than 1% of the largest sensitivity (with respect to $T_{w,in}$) for this response.

Table 4.2: Ranked relative sensitivities of the outlet water temperature, $T_w^{(50)}$, for case 1a.

Rank #	Parameter (α_i)	Nominal Value	Rel. Sens. $RS(\alpha_i)$	Rel. std. dev. (%)
1	Inlet water temperature, $T_{w,in}$	298.77 K	0.4856	0.47
2	Inlet air temperature, $T_{a,in}$	294.03 K	0.246	0.61
3	Air temperature (dry bulb), T_{db}	294.03 K	0.2434	0.61
4	Dew point temperature, T_{dp}	293.49 K	0.2074	0.55
5	$P_{vs}(T)$ parameters, a_0	25.5943	-0.114	0.04
6	$P_{vs}(T)$ parameters, a_1	-5229.89	0.0742	0.08
7	Inlet air humidity ratio, ω_{in}	0.01552	0.0114	8.15
8	Water enthalpy $h_f(T)$ parameters, a_{1f}	4186.51	0.0079	0.04
9	Inlet water mass flow rate, $m_{w,in}$	44.01 kg/s	0.0058	5

CHAPTER 4. RESULTS

4.1.1.3 Relative sensitivities of the outlet water mass flow rate, $m_w^{(50)}$

The results and ranking of the relative sensitivities of the outlet water mass flow rate with respect to the most important 7 parameters for this response are listed in Table 4.3. This response is most sensitive to $m_{w,in}$ (a 1% increase in this parameter would cause a 1.00% increase in the response) and the second largest sensitivity is to the parameter $T_{w,in}$ (a 1% increase in this parameter would cause a 0.198% decrease in the response). The sensitivities to the remaining 40 model parameters have not been listed since they are smaller than 1% of the largest sensitivity (with respect to $m_{w,in}$) for this response.

Table 4.3: Ranked relative sensitivities of the outlet water temperature, $T_w^{(50)}$, for case 1a.

Rank #	Parameter (α_i)	Nominal Value	Rel. Sens. $RS(\alpha_i)$	Rel. std. dev. (%)
1	Inlet water mass flow rate, $m_{w,in}$	44.0213 kg/s	1.0021	5
2	Inlet water temperature, $T_{w,in}$	298.77 K	-0.1983	0.47
3	Dew point temperature, T_{dp}	293.49 K	0.1069	0.55
4	P _{vs} (T) parameters, a_0	25.5943	-0.0593	0.04
5	Inlet air temperature, $T_{a,in}$	294.03 K	0.0557	0.61
6	Air temperature (dry bulb), T_{db}	294.03 K	0.0543	0.61
7	P _{vs} (T) parameters, a_1	-5229.89	0.0386	0.08

4.1.1.4 Relative sensitivities of the outlet air relative humidity, $RH^{(1)}$

The results and ranking of the relative sensitivities of the outlet air relative humidity with respect to the most important 19 parameters for this response are listed in Table 4.4. The first three sensitivities of this response are quite large. In particular, an increase of 1% in $T_{a,in}$ or T_{db} would cause a decrease in the response of 2.11% or 1.95%, respectively. On the other hand, an increase of 1% in T_{dp} would cause an increase of 1.58% in the response. The sensitivities to the

CHAPTER 4. RESULTS

remaining 28 model parameters have not been listed since they are smaller than 1% of the largest sensitivity (with respect to $T_{a,in}$) for this response.

Table 4.4: Ranked relative sensitivities of the outlet air relative humidity, $RH^{(1)}$, for case 1a.

Rank #	Parameter (α_i)	Nominal Value	Rel. Sens. $RS(\alpha_i)$	Rel. std. dev. (%)
1	Inlet air temperature, $T_{a,in}$	294.03 K	-2.1108	0.61
2	Air temperature (dry bulb), T_{db}	294.03 K	-1.9468	0.61
3	Dew point temperature, T_{dp}	293.49 K	1.5759	0.55
4	Inlet water temperature, $T_{w,in}$	298.77 K	0.3398	0.47
5	D _{av} (T) parameters, $a_{1,dav}$	2.653	-0.1559	0.11
6	Atmospheric pressure, P_{atm}	100853 Pa	0.1276	0.28
7	Mass transfer coefficient multiplier, f_{mt}	1	0.1239	50
8	Thermal conductivity of air at T=300 K, k_{air}	0.02624 W/(m·K)	-0.1238	6.04
9	Heat transfer coefficient multiplier, f_{ht}	1	-0.1238	50
10	C _{pa} (T) parameters, $a_{0,cpa}$	1030.5	0.1231	0.03
11	D _{av} (T) parameters, $a_{2,dav}$	-6.1681·10 ⁻³	0.1066	0.37
12	Inlet air humidity ratio, ω_{in}	0.01552	0.0863	8.15
13	P _{vs} (T) parameters, a_0	25.5943	-0.0847	0.04
14	D _{av} (T) parameters, $a_{0,dav}$	7.06085·10 ⁻⁹	0.0826	0
15	P _{vs} (T) parameters, a_1	-5229.89	0.071	0.08
16	Prandlt number of air at T=80 °C, Pr	0.708	-0.0413	0.71
17	Kinematic viscosity of air at T=300 K, ν	1.568·10 ⁻⁵ m ² /s	0.0413	12.09
18	Schmidt number, Sc	0.6188	0.0413	1.19
19	D _{av} (T) parameters, $a_{3,dav}$	6.55265·10 ⁻⁶	-0.0333	0.58

4.1.1.5 Relative sensitivities of the air mass flow rate, m_a

The results and ranking of the relative sensitivities of the outlet air relative humidity with respect to the most important 15 parameters for this response are listed in Table 4.5. The first three sensitivities of this response are very large (relative sensitivities much larger than unity are customarily considered to be very significant). In particular, an increase of 1% in T_{db} or $T_{a,in}$ would cause a

CHAPTER 4. RESULTS

decrease in the response of 24.48% or 24.45%, respectively. On the other hand, an increase of 1% in $T_{w,in}$ would cause an increase of 22.21% in the response. The sensitivities to the remaining 32 model parameters have not been listed since they are smaller than 1% of the largest sensitivity (with respect to T_{db}) for this response.

Table 4.5: Ranked relative sensitivities of the air mass flow rate, m_a , for case 1a.

Rank #	Parameter (α_i)	Nominal Value	Rel. Sens. $RS(\alpha_i)$	Rel. std. dev. (%)
1	Air temperature (dry bulb), T_{db}	294.03 K	-24.478	0.61
2	Inlet air temperature, $T_{a,in}$	294.03 K	-24.456	0.61
3	Inlet water temperature, $T_{w,in}$	298.77 K	22.209	0.47
4	Atmospheric pressure, P_{atm}	100853 Pa	1.2204	0.28
5	Fan shroud inner diameter, D_{fan}	4.1 m	0.8567	1
6	P _{vs} (T) parameters, a_0	25.5943	-0.8069	0.04
7	Dew point temperature, T_{dp}	293.49 K	0.5673	0.55
8	Fill section equivalent diameter, D_h	0.0381 m	0.5568	1
9	P _{vs} (T) parameters, a_1	-5229.89	0.5259	0.08
10	Wind speed, V_w	1.352 m/s	0.4825	46.15
11	Fill section flow area, A_{fill}	67.29 m ²	0.4783	10
12	Cooling tower deck height above ground, Δz_{dk}	10.0 m	0.3797	1
13	Fill section height, Δz_{fill}	2.013 m	-0.317	1
14	Dynamic viscosity of air at T=300 K, μ	$1.983 \cdot 10^{-5}$ kg/(m·s)	-0.3134	4.88
15	Fill section frictional loss multiplier, f	4	-0.3134	50

Overall, the air mass flow rate, m_a , displays the largest sensitivities, so this response is the most sensitive to parameter variations. The other responses, namely the outlet air temperature, the outlet water temperature, the outlet water mass flow rate and the outlet air relative humidity display sensitivities of comparable magnitude.

CHAPTER 4. RESULTS

4.1.2 Adjoint Sensitivity Analysis of Case 1b: Fan Off, Saturated Outlet Air Conditions, with Inlet Air Saturated

4.1.2.1 Relative sensitivities of the outlet air temperature, $T_a^{(1)}$

The sensitivities of the air outlet temperature with respect to all of the model parameters for case 1b have been computed using Eq. (3.22). The numerical results and ranking of the relative sensitivities, in descending order of their magnitudes, are provided in Table 4.6, below, along with their respective relative standard deviations.

Table 4.6: Ranked relative sensitivities of the outlet air temperature, $T_a^{(1)}$, for case 1b.

Rank #	Parameter (α_i)	Nominal Value	Rel. Sens. $RS(\alpha_i)$	Rel. std. dev. (%)
1	Inlet water temperature, $T_{w,in}$	299.54 K	0.8161	0.36
2	Inlet air temperature, $T_{a,in}$	294.40 K	0.1753	0.34
3	Air temperature (dry bulb), T_{db}	294.40 K	0.1741	0.34
4	P _{vs} (T) parameters, a_0	25.5943	-0.0272	0.04
5	P _{vs} (T) parameters a_1	-5229.89	0.0176	0.08
6	Fill section equivalent diameter, D_h	0.0381 m	-0.0051	1
7	Atmospheric pressure, P_{atm}	100606 Pa	-0.0049	0.31
8	C _{pa} (T) parameters, $a_{0,cpa}$	1030.5	-0.0037	0.03
9	Fan shroud inner diameter, D_{fan}	4.1 m	-0.0036	1
10	Thermal conductivity of air at T=300 K, k_{air}	0.02624 W/(m·K)	0.0035	6.04
11	Heat transfer coefficient multiplier, f_{ht}	1	0.0035	50
12	Fill section surface area, A_{surf}	14221 m ²	0.0025	25
13	Wetted fraction of fill surface area, w_{tsa}	1	0.0025	0
14	Nusselt parameters, $a_{0,Nu}$	8.235	0.0025	25
15	Fill section flow area, A_{fill}	67.29 m ²	-0.002	10
16	Wind speed, V_w	1.80 m/s	-0.002	10
17	Dew point temperature, T_{dp}	294.66 K	-0.0019	0.37
18	Water enthalpy h _f (T) parameters, a_{1f}	4186.51	0.0017	0.04
19	Cooling tower deck height above ground, Δz_{dk}	10.0 m	-0.0016	1

CHAPTER 4. RESULTS

Rank #	Parameter (α_i)	Nominal Value	Rel. Sens. $RS(\alpha_i)$	Rel. std. dev. (%)
20	Fill section height, Δz_{fill}	2.013 m	0.0013	1
21	Fill section frictional loss multiplier, f	4	0.0013	50
22	Dynamic viscosity of air at T=300 K, μ	$1.983 \cdot 10^{-5}$ kg/(m·s)	0.0013	4.88
23	Inlet water mass flow rate, $m_{w,in}$	44.01 kg/s	0.0013	5
24	D _{av} (T) parameters, $a_{1,dav}$	2.65322	0.0012	0.11
25	Mass transfer coefficient multiplier, f_{mt}	1	-0.00095	50
26	D _{av} (T) parameters, $a_{2,dav}$	$-6.1681 \cdot 10^{-3}$	-0.00082	0.37
27	h _g (T) parameters, a_{0g}	2005743	-0.00077	0.05
28	D _{av} (T) parameters, $a_{0,dav}$	$7.06085 \cdot 10^{-9}$	-0.00064	0
29	Fan shroud height, Δz_{fan}	3.0 m	-0.00048	1
30	Water enthalpy h _f (T) parameters, a_{0f}	-1143423	-0.00044	0.05
31	Sum of loss coefficients above fill, k_{sum}	10	0.00035	50
32	h _g (T) parameters, a_{1g}	1815.437	-0.00033	0.19
33	Prandlt number of air at T=80 °C, P_r	0.708	0.00032	0.71
34	Schmidt number, Sc	0.619	-0.00032	12.12
35	Kinematic viscosity of air at T=300 K, ν	$1.568 \cdot 10^{-5}$ m ² /s	-0.00032	12.09
36	Rain section height, Δz_{rain}	1.633 m	0.00026	1
37	D _{av} (T) parameters, $a_{3,dav}$	$6.55265 \cdot 10^{-6}$	0.00026	0.58
38	C _{pa} (T) parameters, $a_{1,cpa}$	-0.19975	0.00021	1
39	Basin section height, Δz_{bs}	1.168 m	0.00019	1
40	C _{pa} (T) parameters, $a_{2,cpa}$	$3.9734 \cdot 10^{-4}$	-0.00012	0.84
41	Inlet air humidity ratio, ω_{in}	0.01588	-0.00011	8.08
42	Drift eliminator thickness, Δz_{de}	0.1524 m	0.00009	1
43	Cooling tower deck width in x-dir, W_{dkx}	8.5 m	0.00006	1
44	Cooling tower deck width in y-dir, W_{dky}	8.5 m	0.00006	1
45	Nusselt parameters, $a_{1,Nu}$	0.0031498	0	31.75
46	Nusselt parameters, $a_{2,Nu}$	0.9902987	0	33.02
47	Nusselt parameters, $a_{3,Nu}$	0.023	0	38.26

As the results in Table 4.6 indicate, the first 3 parameters (i.e., $T_{w,in}$, $T_{a,in}$ and T_{db}) have relative sensitivities between ca. 17% and 81%, and are therefore the most important for the air outlet temperature response, $T_a^{(1)}$. The largest sensitivity has a value of 0.8161, which means that a 1% change in $T_{w,in}$ would

CHAPTER 4. RESULTS

induce a 0.81% change in $T_a^{(1)}$. The next two parameters (i.e., a_0 and a_1) have relative sensitivities between 1% and 3%, and are therefore somewhat important. The remaining 42 parameters are relatively unimportant for this response, having relative sensitivities smaller than 1% of the largest relative sensitivity (with respect to $T_{w,in}$) for this response.

4.1.2.2 Relative sensitivities of the outlet water temperature, $T_w^{(50)}$

The results and ranking of the relative sensitivities of the outlet water temperature with respect to the most important 9 parameters for this response are listed in Table 4.7. The largest two sensitivities of $T_w^{(50)}$ are to the parameters $T_{a,in}$ and T_{db} . An increase of 1% in $T_{a,in}$ or T_{db} would cause an increase in the response of 0.486% or 0.480%, respectively. The sensitivities to the remaining 38 model parameters have not been listed since they are smaller than 1% of the largest sensitivity (with respect to $T_{a,in}$) for this response.

Table 4.7: Ranked relative sensitivities of the outlet water temperature, $T_w^{(50)}$, for case 1b.

Rank #	Parameter (α_i)	Nominal Value	Rel. Sens. $RS(\alpha_i)$	Rel. std. dev. (%)
1	Inlet air temperature, $T_{a,in}$	294.40 K	0.4858	0.34
2	Air temperature (dry bulb), T_{db}	294.40 K	0.48	0.34
3	Inlet water temperature, $T_{w,in}$	299.54 K	0.4567	0.36
4	$P_{vs}(T)$ parameters, a_0	25.5943	-0.117	0.04
5	$P_{vs}(T)$ parameters, a_1	-5229.89	0.0756	0.08
6	Water enthalpy $h_f(T)$ parameters, a_{1f}	4186.51	0.0083	0.04
7	Inlet water mass flow rate, $m_{w,in}$	44.01 kg/s	0.006	5
8	Atmospheric pressure, P_{atm}	100606 Pa	-0.0058	0.31
9	$D_{av}(T)$ parameters, $a_{1,dav}$	2.65322	0.0056	0.11

CHAPTER 4. RESULTS

4.1.2.3 Relative sensitivities of the outlet water mass flow rate, $m_w^{(50)}$

The results and ranking of the relative sensitivities of the outlet water mass flow rate with respect to the most important 6 parameters for this response are listed in Table 4.8. This response is most sensitive to $m_{w,in}$ (a 1% increase in this parameter would cause a 1.00% increase in the response) and the second largest sensitivity is to the parameter $T_{w,in}$ (a 1% increase in this parameter would cause a 0.213% decrease in the response). The sensitivities to the remaining 41 model parameters have not been listed since they are smaller than 1% of the largest sensitivity (with respect to $m_{w,in}$) for this response.

Table 4.8: Ranked relative sensitivities of the outlet water temperature, $T_w^{(50)}$, for case 1b.

Rank #	Parameter (α_i)	Nominal Value	Rel. Sens. $RS(\alpha_i)$	Rel. std. dev. (%)
1	Inlet water mass flow rate, $m_{w,in}$	44.01 kg/s	1.0022	5
2	Inlet water temperature, $T_{w,in}$	299.54 K	-0.2129	0.36
3	Inlet air temperature, $T_{a,in}$	294.40 K	0.1783	0.34
4	Air temperature (dry bulb), T_{db}	294.40 K	0.1752	0.34
5	P _{vs} (T) parameters, a_0	25.5943	-0.0613	0.04
6	P _{vs} (T) parameters, a_1	-5229.89	0.0396	0.08

4.1.2.4 Relative sensitivities of the outlet air relative humidity, $RH^{(1)}$

The results and ranking of the relative sensitivities of the outlet air relative humidity with respect to the most important 15 parameters for this response are listed in Table 4.9. The first three sensitivities of this response are quite large. In particular, an increase of 1% in $T_{a,in}$ or T_{db} would cause a decrease in the response of 14.35% or 14.02%, respectively. On the other hand, an increase of 1% in T_{dp} would cause an increase of 13.22% in the response. The sensitivities to the

CHAPTER 4. RESULTS

remaining 32 model parameters have not been listed since they are smaller than 1% of the largest sensitivity (with respect to $T_{a,in}$) for this response.

Table 4.9: Ranked relative sensitivities of the outlet air relative humidity, $RH^{(1)}$, for case 1b.

Rank #	Parameter (α_i)	Nominal Value	Rel. Sens. $RS(\alpha_i)$	Rel. std. dev. (%)
1	Inlet air temperature, $T_{a,in}$	294.40 K	-14.347	0.34
2	Air temperature (dry bulb), T_{db}	294.40 K	-14.024	0.34
3	Dew point temperature, T_{dp}	294.66 K	13.216	0.37
4	Inlet air humidity ratio, ω_{in}	0.0162	0.7257	8.07
5	Inlet water temperature, $T_{w,in}$	299.54 K	0.6619	0.36
6	$D_{av}(T)$ parameters, $a_{1,dav}$	2.653	-0.3078	0.11
7	$P_{vs}(T)$ parameters, a_0	25.5943	-0.2779	0.04
8	Atmosphere pressure, P_{atm}	100606 Pa	0.2535	0.31
9	Thermal conductivity of air at T=300 K, k_{air}	0.02624 W/(m·K)	-0.2475	6.04
10	Heat transfer coefficient multiplier, f_{ht}	1	-0.2475	50
11	$C_{pa}(T)$ parameters, $a_{0,cpa}$	1030.5	0.2449	0.03
12	Mass transfer coefficient multiplier, f_{mt}	1	0.2446	50
13	$P_{vs}(T)$ parameters, a_1	-5229.89	0.2324	0.08
14	$D_{av}(T)$ parameters, $a_{2,dav}$	-6.1681·10 ⁻³	0.2107	0.37
15	$D_{av}(T)$ parameters, $a_{0,dav}$	7.06085·10 ⁻⁹	0.163	0

4.1.2.5 Relative sensitivities of the air mass flow rate, m_a

The results and ranking of the relative sensitivities of the outlet air relative humidity with respect to the most important 14 parameters for this response are listed in Table 4.10. The first three sensitivities of this response are very large (relative sensitivities much larger than unity are customarily considered to be very significant). In particular, an increase of 1% in T_{db} or $T_{a,in}$ would cause a decrease in the response of 22.04% or 22.00%, respectively. On the other hand, an increase of 1% in $T_{w,in}$ would cause an increase of 20.37% in the response.

CHAPTER 4. RESULTS

The sensitivities to the remaining 33 model parameters have not been listed since they are smaller than 1% of the largest sensitivity (with respect to T_{db}) for this response.

Table 4.10: Ranked relative sensitivities of the air mass flow rate, m_a , for case 1b.

Rank #	Parameter (α_i)	Nominal Value	Rel. Sens. $RS(\alpha_i)$	Rel. std. dev. (%)
1	Air temperature (dry bulb), T_{db}	294.40 K	-22.043	0.34
2	Inlet air temperature, $T_{a,in}$	294.40 K	-22.002	0.34
3	Inlet water temperature, $T_{w,in}$	299.54 K	20.375	0.36
4	Atmospheric pressure, P_{atm}	100606 Pa	1.1942	0.31
5	P _{vs} (T) parameters, a_0	25.5943	-0.8716	0.04
6	Fan shroud inner diameter, D_{fan}	4.1 m	0.86	1
7	P _{vs} (T) parameters, a_1	-5229.89	0.5649	0.08
8	Fill section equivalent diameter, D_h	0.0381 m	0.5365	1
9	Fill section flow area, A_{fill}	67.29 m ²	0.4704	10
10	Wind speed, V_w	1.80 m/s	0.4676	10
11	Cooling tower deck height above ground, Δz_{dk}	10.0 m	0.3804	1
12	Fill section height, Δz_{fill}	2.013 m	-0.3097	1
13	Fill section frictional loss multiplier, f	4	-0.3048	50
14	Dynamic viscosity of air at T=300 K, μ	$1.983 \cdot 10^{-5}$ kg/(m·s)	-0.3048	4.88

The air mass flow rate, m_a , together with the outlet air relative humidity, $RH^{(1)}$, displays the largest sensitivities, so these two responses are the most sensitive to parameter variations. The other responses, namely the outlet air temperature, the outlet water temperature, and the outlet water mass flow rate display sensitivities of comparable magnitudes.

CHAPTER 4. RESULTS

4.1.3 Adjoint Sensitivity Analysis of Case 2: Fan Off, Unsaturated Air Conditions

4.1.3.1 Relative sensitivities of the outlet air temperature, $T_a^{(1)}$

Table 4.11 lists the sensitivities, computed using Eq. (3.22), of the air outlet temperature with respect to all of the model parameters. The parameters have been ranked according to the descending order of their relative sensitivities.

Table 4.11: Ranked relative sensitivities of the outlet air temperature, $T_a^{(1)}$, for case 2.

Rank #	Parameter (α_i)	Nominal Value	Rel. Sens. $RS(\alpha_i)$	Rel. std. dev. (%)
1	Inlet water temperature, $T_{w,in}$	298.893 K	0.91878	0.56
2	Air temperature (dry bulb), T_{db}	298.882 K	0.06522	1.35
3	Inlet air temperature, $T_{a,in}$	298.882 K	0.06478	1.35
4	$P_{vs}(T)$ parameters, a_0	25.5943	-0.01266	0.04
5	Dew point temperature, T_{dp}	292.077 K	0.01005	0.78
6	$P_{vs}(T)$ parameters, a_1	-5229.89	0.00828	0.08
7	Wind speed, V_w	1.859 m/s	-0.00172	50.7
8	Fill section equivalent diameter, D_h	0.0381 m	-0.00168	1
9	Fan shroud inner diameter, D_{fan}	4.1 m	-0.00104	1
10	Atmospheric pressure, P_{atm}	100588 Pa	-0.00084	0.41
11	Water enthalpy $h_f(T)$ parameters, a_{1f}	4186.51	0.0007	0.04
12	Nusselt parameter, $a_{0,Nu}$	8.235	0.0007	25
13	Fill section surface area, A_{surf}	14221 m ²	0.0007	25
14	Wetted fraction of fill surface area, w_{tsa}	1	0.0007	0
15	Fill section flow area, A_{fill}	67.29 m ²	-0.00068	10
16	Inlet air humidity ratio, ω_{in}	0.0139	0.00055	13.8
17	Inlet water mass flow rate, $m_{w,in}$	44.0193 kg/s	0.00048	5
18	Dynamic viscosity of air at T=300 K, μ	$1.983 \cdot 10^{-5}$ kg/(m·s)	0.00048	4.88
19	Fill section frictional loss multiplier, f	4	0.00048	50
20	Fill section height, Δz_{fill}	2.013 m	0.00046	1
21	$D_{av}(T)$ parameters, $a_{1,dav}$	2.65322	-0.00043	0.11
22	$C_{pa}(T)$ parameters, $a_{0,cpa}$	1030.5	-0.00041	0.03
23	Thermal conductivity of air at T=300 K, k_{air}	0.02624 W/(m·K)	0.00037	6.04

CHAPTER 4. RESULTS

Rank #	Parameter (α_i)	Nominal Value	Rel. Sens. $RS(\alpha_i)$	Rel. std. dev. (%)
24	Heat transfer coefficient multiplier, f_{ht}	1	0.00037	50
25	$h_g(T)$ parameters, a_{0g}	2005744	-0.00036	0.05
26	Mass transfer coefficient multiplier, f_{mt}	1	0.00034	50
27	$D_{av}(T)$ parameters, $a_{2,dav}$	$-6.17 \cdot 10^{-3}$	0.0003	0.37
28	$D_{av}(T)$ parameters, $a_{0,dav}$	$7.06 \cdot 10^{-9}$	0.00022	0
29	$h_f(T)$ parameters, a_{0f}	-1143423	-0.0002	0.05
30	Kinematic viscosity of air at T=300 K, ν	$1.568 \cdot 10^{-5} \text{ m}^2/\text{s}$	0.00011	12.09
31	Prandlt number of air at T=80 °C, Pr	0.708	-0.00011	0.71
32	Schmidt number, Sc	0.5998	0.00011	2.66
33	$h_g(T)$ parameters, a_{1g}	1815.437	-0.00011	0.19
34	Sum of loss coefficients above fill, k_{sum}	10	0.0001	50
35	$D_{av}(T)$ parameters, $a_{3,dav}$	$6.55 \cdot 10^{-6}$	-0.000094	0.58
36	Drift eliminator thickness, Δz_{de}	0.1524 m	0.000034	1
37	$C_{pa}(T)$ parameter, $a_{1,cpa}$	-0.19975	0.000023	1
38	Cooling tower deck width in x-dir, W_{dkx}	8.5 m	0.000017	1
39	Cooling tower deck width in y-dir, W_{dky}	8.5 m	0.000017	1
40	Cooling tower deck height above ground, Δz_{dk}	10.0 m	0.000014	1
41	$C_{pa}(T)$ parameter, $a_{2,cpa}$	$3.97 \cdot 10^{-4}$	-0.000013	0.84
42	Fan shroud height, Δz_{fan}	3.0 m	0.000004	1
43	Rain section height, Δz_{rain}	1.633 m	-0.000002	1
44	Basin section height, Δz_{bs}	1.168 m	-0.000001	1
45	Nusselt parameters, $a_{1,Nu}$	0.0031498	0	31.75
46	Nusselt parameters, $a_{2,Nu}$	0.9902987	0	33.02
47	Nusselt parameters, $a_{3,Nu}$	0.023	0	38.26

As the results in Table 4.11 indicate, the first parameter (i.e., $T_{w,in}$) has a relative sensitivity around 90%, and is therefore the most important for the air outlet temperature response, $T_a^{(1)}$, since that means that a 1% change in $T_{w,in}$ would induce a 0.91% change in $T_a^{(1)}$. The next four parameters (i.e., T_{db} , $T_{a,in}$, a_0 , T_{dp}) have relative sensitivities between 1% and 6%, and are therefore somewhat important. Parameters #6 through #9 (i.e., a_1 , V_w , D_h , D_{fan}) have relative sensitivities between 0.1% and 0.8%. The remaining 38 parameters are relatively

CHAPTER 4. RESULTS

unimportant for this response, having relative sensitivities smaller than 1% of the largest relative sensitivity (with respect to $T_{a,in}$) for this response. Positive sensitivities imply that a positive change in the respective parameter would cause an increase in the response, while negative sensitivities imply that a positive change in the respective parameter would cause a decrease in the response.

4.1.3.2 Relative sensitivities of the outlet water temperature, $T_w^{(50)}$

The results and ranking of the relative sensitivities of the outlet water temperature with respect to the most important 9 parameters for this response are listed in Table 4.12. The largest sensitivity of $T_w^{(50)}$ is to the parameter $T_{w,in}$, and has the value of 0.5055; this means that a 1% increase in $T_{w,in}$ would induce a 0.5055% increase in $T_w^{(50)}$. The sensitivities to the remaining 38 model parameters have not been listed since they are smaller than 1% of the largest sensitivity (with respect to $T_{w,in}$) for this response.

Table 4.12: Ranked relative sensitivities of the outlet water temperature, $T_w^{(50)}$, for case 2.

Rank #	Parameter (α_i)	Nominal Value	Rel. Sens. $RS(\alpha_i)$	Rel. std. dev. (%)
1	Inlet water temperature, $T_{w,in}$	298.893 K	0.50556	0.56
2	Inlet air temperature, $T_{a,in}$	298.882 K	0.25323	1.35
3	Air temperature (dry bulb), T_{db}	298.882 K	0.25263	1.35
4	Dew point temperature, T_{dp}	292.077 K	0.171	0.78
5	$P_{vs}(T)$ parameters, a_0	25.5943	-0.12617	0.04
6	$P_{vs}(T)$ parameters, a_1	-5229.89	0.08251	0.08
7	Inlet air humidity ratio, ω_{in}	0.0139	0.00934	13.8
8	Water enthalpy $h_f(T)$ parameter, a_{1f}	4186.50768	0.00704	0.04
9	Wind speed, V_w	1.859 m/s	-0.00595	50.7

CHAPTER 4. RESULTS

4.1.3.3 Relative sensitivities of the outlet water mass flow rate, $m_w^{(50)}$

The results and ranking of the relative sensitivities of the outlet water mass flow rate with respect to the most important 12 parameters for this response are listed in Table 4.13. This response is most sensitive to $m_{w,in}$ (a 1% increase in this parameter would cause a 1.01% increase in the response) and the second largest sensitivity is to the parameter $T_{w,in}$ (a 1% increase in this parameter would cause a 0.214% decrease in the response). The sensitivities to the remaining 35 model parameters have not been listed since they are smaller than 1% of the largest sensitivity (with respect to $m_{w,in}$) for this response.

Table 4.13: Ranked relative sensitivities of the outlet water temperature, $T_w^{(50)}$, for case 2.

Rank #	Parameter (α_i)	Nominal Value	Rel. Sens. $RS(\alpha_i)$	Rel. std. dev. (%)
1	Inlet water mass flow rate, $m_{w,in}$	44.0193 kg/s	1.0024	5
2	Inlet water temperature, $T_{w,in}$	298.893 K	-0.21368	0.56
3	Dew point temperature, T_{dp}	292.077 K	0.08748	0.78
4	Inlet air temperature, $T_{a,in}$	298.882 K	0.08692	1.35
5	Air temperature (dry bulb), T_{db}	298.882 K	0.08663	1.35
6	P _{vs} (T) parameters, a_0	25.5943	-0.06479	0.04
7	P _{vs} (T) parameters, a_1	-5229.89	0.04238	0.08
8	Inlet air humidity ratio, ω_{in}	0.0139	0.00478	13.8
9	Wind speed, V_w	1.859 m/s	-0.00313	50.7
10	Fan shroud inner diameter, D_{fan}	4.1 m	-0.00189	1
11	Fill section equivalent diameter, D_h	0.0381 m	-0.00152	1
12	Fill section flow area, A_{fill}	67.29 m ²	0.00124	10

4.1.3.4 Relative sensitivities of the outlet air relative humidity, $RH^{(1)}$

The results and ranking of the relative sensitivities of the outlet air relative humidity with respect to the most important 29 parameters for this response are listed in Table 4.14. The first three sensitivities of this response are the most

CHAPTER 4. RESULTS

relevant ; in particular, an increase of 1% in T_{db} or $T_{a,in}$ would cause an increase in the response of 0.27% or 0.25%, respectively. On the other hand, an increase of 1% in $T_{w,in}$ would cause a decrease of 0.32% in the response. The sensitivities to the remaining 18 model parameters have not been listed since they are smaller than 1% of the largest sensitivity (with respect to $T_{w,in}$) for this response.

Table 4.14: Ranked relative sensitivities of the outlet air relative humidity, $RH^{(1)}$, for case 2.

Rank #	Parameter (α_i)	Nominal Value	Rel. Sens. $RS(\alpha_i)$	Rel. std. dev. (%)
1	Inlet water temperature, $T_{w,in}$	298.893 K	-0.31903	0.56
2	Air temperature (dry bulb), T_{db}	298.882 K	0.27111	1.35
3	Inlet air temperature, $T_{a,in}$	298.882 K	0.24914	1.35
4	Dew point temperature, T_{dp}	292.077 K	0.062	0.78
5	D _{av} (T) parameters, $a_{1,dav}$	2.65322	-0.21076	0.11
6	Fill section equivalent diameter, D_h	0.0381 m	-0.01753	1
7	Mass transfer coefficient multiplier, f_{mt}	1	0.01662	50
8	D _{av} (T) parameters, $a_{2,dav}$	-0.006168	0.01464	0.37
9	Wind speed, V_w	1.859 m/s	-0.01353	50.7
10	D _{av} (T) parameters, $a_{0,dav}$	$7.06 \cdot 10^{-9}$	0.01108	0
11	Fill section surface area, A_{surf}	14221 m ²	0.00991	25
12	Wetted fraction of fill surface area, w_{tsa}	1	0.00991	0
13	Nusselt parameters, $a_{0,Nu}$	8.235	0.00991	25
14	Fan shroud inner diameter, D_{fan}	4.1 m	-0.0082	1
15	Thermal conductivity of air at T=300 K, k_{air}	0.02624 W/(m·K)	-0.00671	6.04
16	Heat transfer coefficient multiplier, f_{ht}	1	-0.00671	50
17	C _{pa} (T) parameters, $a_{0,cpa}$	1030.5	0.0067	0.03
18	P _{vs} (T) parameters, a_0	25.5943	-0.00656	0.04
19	Kinematic viscosity of air at T=300 K, ν	$1.568 \cdot 10^{-5}$ m ² /s	0.00554	12.09
20	Prandlt number of air at T=80 °C, Pr	0.708	-0.00554	0.71
21	Schmidt number, Sc	0.5998	0.00554	2.66
22	Fill section flow area, A_{fill}	67.29 m ²	-0.00539	10
23	D _{av} (T) parameters, $a_{3,dav}$	$6.55 \cdot 10^{-6}$	-0.00465	0.58
24	Dynamic viscosity of air at T=300 K, μ	$1.983 \cdot 10^{-5}$ kg/(m·s)	0.00381	4.88
25	Fill section frictional loss multiplier, f	4	0.00381	50
26	P _{vs} (T) parameters, a_1	-5229.89	0.00379	0.08

CHAPTER 4. RESULTS

Rank #	Parameter (α_i)	Nominal Value	Rel. Sens. $RS(\alpha_i)$	Rel. std. dev. (%)
27	Atmosphere pressure, P_{atm}	100588 Pa	0.00372	0.41
28	Fill section height, Δz_{fill}	2.013 m	0.00362	1
29	Inlet air humidity ratio, ω_{in}	0.0139	0.00339	13.8

4.1.3.5 Relative sensitivities of the air mass flow rate, m_a

The results and ranking of the relative sensitivities of the air mass flow rate with respect to the most important 14 parameters for this response are listed in Table 4.15. The first three sensitivities of this response are very large (relative sensitivities larger than unity are customarily considered to be very significant). In particular, an increase of 1% in $T_{a,in}$ or T_{db} would cause a decrease in the response of 38.51% or 38.49%, respectively. On the other hand, an increase of 1% in $T_{w,in}$ would cause an increase of 36% in the response. The sensitivities to the remaining 33 model parameters have not been listed since they are smaller than 1% of the largest sensitivity (with respect to $T_{a,in}$) for this response.

Table 4.15: Ranked relative sensitivities of the air mass flow rate, m_a , for case 2.

Rank #	Parameter (α_i)	Nominal Value	Rel. Sens. $RS(\alpha_i)$	Rel. std. dev. (%)
1	Inlet air temperature, $T_{a,in}$	298.882 K	-38.51406	1.35
2	Air temperature (dry bulb), T_{db}	298.882 K	-38.49249	1.35
3	Inlet water temperature, $T_{w,in}$	298.893 K	36.0013	0.56
4	Atmosphere pressure, P_{atm}	100588 Pa	1.37474	0.41
5	Wind speed, V_w	1.859 m/s	1.36609	50.7
6	Fan shroud inner diameter, D_{fan}	4.1 m	0.8279	1
7	P _{vs} (T) parameters, a_0	25.5943	-0.767	0.04
8	Fill section equivalent diameter, D_h	0.0381 m	0.74221	1
9	Dew point temperature, T_{dp}	292.077 K	0.70105	0.78

CHAPTER 4. RESULTS

Rank #	Parameter (α_i)	Nominal Value	Rel. Sens. $RS(\alpha_i)$	Rel. std. dev. (%)
10	Fill section flow area, A_{fill}	67.29 m ²	0.54384	10
11	P _{vs} (T) parameters, a_1	-5229.89	0.50156	0.08
12	Dynamic viscosity of air at T=300 K, μ	1.983·10 ⁻⁵ kg/(m·s)	-0.38448	4.88
13	Fill section frictional loss multiplier, f	4	-0.38448	50
14	Fill section height, Δz_{fill}	2.013 m	-0.36512	1

Overall, the air mass flow rate, m_a , displays the largest sensitivities, so this response is the most sensitive to parameter variations. The other responses, namely the outlet air temperature, the outlet water temperature, the outlet water mass flow rate and the outlet air relative humidity display sensitivities of comparable magnitude for case 2.

4.2 Cross-comparison of the most relevant sensitivities

In Tables 4.16 through 4.20, the ranked relative sensitivities for each response are compared side-by-side between the three natural draft operating conditions, i.e., case 1a, case 1b and case 2. Among the three operating conditions, case 2 is defined as a working condition in which air is unsaturated from the inlet to outlet of the cooling tower; while in the saturated case 1b, on the contrary, air is saturated from inlet to outlet of the cooling tower; the saturated case 1a is the combination of the these two cases, i.e., air in the lower portion of the fill section of the cooling tower is in unsaturated conditions, reaching saturation at some point along the height of the tower and remaining saturated in the upper part of the cooling tower. Cross-comparison of sensitivity results reveals the sensitivity variations between the three operating conditions.

CHAPTER 4. RESULTS

4.2.1 Relative sensitivities of the outlet air temperature,

$$T_a^{(1)}$$

The relative sensitivities and corresponding parameters listed in Table 4.16 are extracted from Table 4.1 in Paragraph 4.1.1.1, from Table 4.6 in Paragraph 4.1.2.1, and from Table 4.11 in Paragraph 4.1.3.1.

Table 4.16: Cross-comparison of the top 5 relative sensitivities for the response of outlet air temperature, $T_a^{(1)}$, between the natural draft cases 1a, 1b and 2.

Rank #	Rel. Sens. in Unsaturated	Rel. Sens. in Saturated Conditions	
	Conditions - Case 2 (based on 6717 unsaturated data sets)	Case 1a (based on 377 data sets with inlet air unsaturated)	Case 1b (based on 290 data sets with inlet air unsaturated)
1	0.9179 $T_{w,in}$	0.8346 $T_{w,in}$	0.8161 $T_{w,in}$
2	0.0652 T_{db}	0.1436 $T_{a,in}$	0.1754 $T_{a,in}$
3	0.0648 $T_{a,in}$	0.1429 T_{db}	0.1741 T_{db}
4	-0.0127 a_0	-0.0231 a_0	-0.0272 a_0
5	0.0101 T_{dp}	0.0151 a_1	0.0176 a_1

As shown in Table 4.16, for all three operating conditions, the first most sensitive parameters of the response of air outlet temperature, $T_a^{(1)}$, is the same (i.e., $T_{w,in}$). The 2nd and 3rd most sensitive parameter are inverted in the case 2 with respect to cases 1a and 1b, but with values very close between the two parameters. The parameters that ranks in 4th place for this response is the same for all cases (i.e., a_0). The 5th parameter is a_0 for cases 1a and 1b and T_{dp} for the case 2. For the first parameter (i.e., $T_{w,in}$), case 2 displays the largest

CHAPTER 4. RESULTS

sensitivity for this response; case 1b has the smallest sensitivity; while case 1a has an intermediate value of sensitivity between the two. This is expected since case 1a is a mixed case between case 2 and the saturated case 1b. For all the remaining parameters in the table the situation is reversed, with case 1b showing the largest sensitivity values and the unsaturated case presenting the smallest ones, with case 1a still in the middle. Generally, the sensitivity magnitude of case 1a is slightly closer to that of case 1b. This can be explained by the fact that air remains unsaturated less than half of the height of the fill section, and flows in saturated conditions for more than half of the height of the fill section, as analyzed in Section 2.3.1.

4.2.2 Relative sensitivities of the outlet water temperature, $T_w^{(50)}$

The relative sensitivities and corresponding parameters listed in Table 4.17 are extracted from Table 4.2 in Paragraph 4.1.1.2, from Table 4.7 in Paragraph 4.1.2.2, and from Table 4.12 in Paragraph 4.1.3.2.

Table 4.17: Cross-comparison of the top 5 relative sensitivities for the response of outlet water temperature, $T_w^{(50)}$, between the natural draft cases 1a, 1b and 2.

Rank #	Rel. Sens. in Unsaturated	Rel. Sens. in Saturated Conditions	
	Conditions - Case 2 (based on 6717 unsaturated data sets)	Case 1a (based on 377 data sets with inlet air unsaturated)	Case 1b (based on 290 data sets with inlet air unsaturated)
1	0.9179 $T_{w,in}$	0.8346 $T_{w,in}$	0.8161 $T_{w,in}$
2	0.0652 T_{db}	0.1436 $T_{a,in}$	0.1754 $T_{a,in}$
3	0.0648 $T_{a,in}$	0.1429 T_{db}	0.1741 T_{db}

CHAPTER 4. RESULTS

Rank #	Rel. Sens. in Unsaturated	Rel. Sens. in Saturated Conditions	
	Conditions - Case 2	Case 1a	Case 1b
	(based on 6717 unsaturated data sets)	(based on 377 data sets with inlet air unsaturated)	(based on 290 data sets with inlet air unsaturated)
4	-0.0127 a_0	-0.0231 a_0	-0.0272 a_0
5	0.0101 T_{dp}	0.0151 a_1	0.0176 a_1

As shown in Table 4.17, for the response of water outlet temperature, $T_w^{(50)}$, both case 2 and case 1a are most sensitive to the parameter $T_{w,in}$, whereas case 1b is most sensitive to the parameter $T_{a,in}$. As a comparison, the response of water outlet temperature to the parameter $T_{w,in}$ ranks in 3rd place, with a value comparable to the other two cases. The next two most sensitive parameters that rank from 2nd to 3rd places of this response are also different between the operating conditions: for both case 2 and case 1a, parameters $T_{a,in}$ and T_{db} rank in 2nd and 3rd places, respectively; however, for case 1b, parameters that take the 2nd and 3rd places are T_{db} and $T_{w,in}$, respectively. The parameters that take the 4th and 5th places are also different between the operating conditions, as shown in the table. Overall, for the response of water outlet temperature, $T_w^{(50)}$, the sensitivity behavior of case 1a is more similar to that of the case 2.

4.2.3 Relative sensitivities of the outlet water mass flow rate, $m_w^{(50)}$

The relative sensitivities and corresponding parameters listed in Table 4.18 are extracted from Table 4.3 in Paragraph 4.1.1.3, from Table 4.8 in Paragraph 4.1.2.3, and from Table 4.13 in Paragraph 4.1.3.3.

CHAPTER 4. RESULTS

Table 4.18: Cross-comparison of the top 5 relative sensitivities for the response of outlet water mass flow rate, $m_w^{(50)}$, between the natural draft cases 1a, 1b and 2.

Rank #	Rel. Sens. in Unsaturated	Rel. Sens. in Saturated Conditions	
	Conditions - Case 2 (based on 6717 unsaturated data sets)	Case 1a (based on 377 data sets with inlet air unsaturated)	Case 1b (based on 290 data sets with inlet air unsaturated)
1	1.002 $m_{w,in}$	1.002 $m_{w,in}$	1.002 $m_{w,in}$
2	-0.2137 $T_{w,in}$	-0.1983 $T_{w,in}$	-0.2129 $T_{w,in}$
3	0.0875 T_{dp}	0.1069 T_{dp}	0.1783 $T_{a,in}$
4	0.0869 $T_{a,in}$	-0.0593 a_0	0.1751 T_{db}
5	0.0867 T_{db}	0.0557 $T_{a,in}$	-0.0613 a_0

As shown in Table 4.18, for all three operating conditions, the first two most sensitive parameters of the response of water outlet mass flow rate, $m_w^{(50)}$, are the same (i.e., $m_{w,in}$ and $T_{w,in}$, respectively). In addition, for each of the first two parameters, all three operating conditions have comparable sensitivity magnitudes. This indicates that the sensitivities of the first two parameters are insensitive to the operating condition change. The third most sensitive parameter of this response is different between the operating conditions: for both case 2 and case 1a, this parameter is T_{dp} ; whereas, for case 1b, this parameter is $T_{a,in}$. Similarly, the parameters that take the 4th and 5th places are also different between the operating conditions, as shown in the table.

4.2.4 Relative sensitivities of the outlet air relative humidity, $RH^{(1)}$

The relative sensitivities and corresponding parameters listed in Table 4.19 are extracted from Table 4.4 in Paragraph 4.1.1.4, from Table 4.9 in Paragraph 4.1.2.4, and from Table 4.14 in Paragraph 4.1.3.4.

Table 4.19: Cross-comparison of the top 5 relative sensitivities for the response of outlet air relative humidity, $RH^{(1)}$, between the natural draft cases 1a, 1b and 2.

Rank #	Rel. Sens. in Unsaturated	Rel. Sens. in Saturated Conditions	
	Conditions - Case 2	Case 1a	Case 1b
	(based on 6717 unsaturated data sets)	(based on 377 data sets with inlet air unsaturated)	(based on 290 data sets with inlet air unsaturated)
1	-0.3190 $T_{w,in}$	-2.1108 $T_{a,in}$	-14.347 $T_{a,in}$
2	0.2711 T_{db}	-1.9469 T_{db}	-14.024 T_{db}
3	0.2491 $T_{a,in}$	1.5759 T_{dp}	13.216 T_{dp}
4	0.0620 T_{dp}	0.3398 $T_{w,in}$	0.7257 ω_{in}
5	-0.2108 $a_{1,dav}$	-0.1559 $a_{1,dav}$	0.6619 $T_{w,in}$

As shown in Table 4.19, for cases 1a and 1b, the first three most sensitive parameters of the response of air outlet relative humidity, $RH^{(1)}$, are the same (i.e., $T_{a,in}$, T_{db} and T_{dp} , respectively); the order is different for case 2. The next two most sensitive parameters that rank the 4th and 5th places of this response are different between the operating conditions.

For each of the first three parameters, all three operating conditions are sensitive to the parameter changes. In which, case 1b is the most sensitive case; and

CHAPTER 4. RESULTS

case 2 is the least sensitive case comparatively. For instance, 1% change in $T_{a,in}$, T_{db} or T_{dp} will cause around 0.2% change in $RH^{(1)}$ for case 2, around 2% change in $RH^{(1)}$ for case 1a; and nearly 15% change in $RH^{(1)}$ for case 1b, respectively. Overall, for the response of air outlet relative humidity, $RH^{(1)}$, the sensitivity behavior of case 1a is also more similar to that of case 1b, as also the signs of most of the sensitivity values, inverted in case 2 with respect to case 1a and 1b, show in Table 4.19.

4.2.5 Relative sensitivities of the air mass flow rate, m_a

The relative sensitivities and corresponding parameters listed in Table 4.20 are extracted from Table 4.5 in Paragraph 4.1.1.5, from Table 4.10 in Paragraph 4.1.2.5, and from Table 4.15 in Paragraph 4.1.3.5.

Table 4.20: Cross-comparison of the top 5 relative sensitivities for the response of water outlet temperature, $T_w^{(50)}$, between the natural draft cases 1a, 1b and 2.

Rank #	Rel. Sens. in Unsaturated	Rel. Sens. in Saturated Conditions	
	Conditions - Case 2	Case 1a	Case 1b
	(based on 6717 unsaturated data sets)	(based on 377 data sets with inlet air unsaturated)	(based on 290 data sets with inlet air unsaturated)
1	-38.514 $T_{a,in}$	-24.478 T_{db}	-22.043 T_{db}
2	-38.492 T_{db}	-24.456 $T_{a,in}$	-22.002 $T_{a,in}$
3	36.001 $T_{w,in}$	22.209 $T_{w,in}$	20.375 $T_{w,in}$
4	1.3747 P_{atm}	1.2204 P_{atm}	1.1942 P_{atm}
5	1.3661 V_w	0.8567 D_{fan}	-0.8716 a_0

CHAPTER 4. RESULTS

As shown in Table 4.20, for all the operating conditions, the first three most sensitive parameters of the response of air mass flow rate, m_a , are the same (i.e., T_{db} , $T_{a,in}$ and $T_{w,in}$, respectively) with the order of the first two being swapped for the unsaturated case. P_{atm} is the 4th more sensitive parameter in all operating conditions, and with values comparable between the three cases; the parameters ranking in 5th place are different for the three operating conditions.

For each of the first three parameters, all three operating conditions are sensitive to the parameter changes. Differently from the response $RH^{(1)}$, case 1b is this time the least sensitive case, while case 2 is the most sensitive case comparatively. For instance, 1% change in $T_{a,in}$, T_{db} or $T_{w,in}$ will cause around 38% change in m_a for case 2, around 24% change in m_a for case 1a; and nearly 22% change in m_a for case 1b, respectively. Overall, for the response of air mass flow rate, m_a , the sensitivity behavior of case 1a is also more similar to that of case 1b.

4.3 Uncertainty Analysis and Predictive Modeling of the cooling tower cases of interest

The results of the application of the “predictive modeling for coupled multi-physics systems” (PM_CMPS) methodology, simultaneously combining all of the available computed information and experimentally measured data for the counter-flow cooling tower, are reported in this section for all the selected cases of interest. Previously computed adjoint sensitivities are hereby used for yielding best-estimate predicted nominal values and uncertainties for model parameters and responses.

4.3.1 Uncertainty Analysis and Predictive Modeling of Case 1a: Fan Off, Saturated Outlet Air Conditions, with Inlet Air Unsaturated

The a priori response-parameter covariance matrix, $\mathbf{C}_{r\alpha}$, for case 1a, is computed in Appendix A, Eq. (A.5), and is reproduced in Eq. (4.1):

$$\begin{aligned} \mathbf{C}_{r\alpha} &\equiv Cov(T_{a,out}^{meas}, T_{w,out}^{meas}, RH^{meas}, \alpha_1, \dots, \alpha_{47}) \\ &= \begin{pmatrix} 1.53 & 1.01 & 0.76 & -104.46 & 0.11 & 0 & \dots & 0 \\ 1.10 & 1.08 & 1.28 & -111.01 & 0.12 & 0 & \dots & 0 \\ 0.05 & 0.34 & -0.75 & 76.60 & -0.25 & 0 & \dots & 0 \end{pmatrix} \end{aligned} \quad (4.1)$$

where the measured correlated parameters are: $\alpha_1 \triangleq T_{db}$, $\alpha_2 \triangleq T_{dp}$, $\alpha_3 \triangleq T_{w,in}$, $\alpha_4 \triangleq P_{atm}$, and $\alpha_5 \triangleq V_w$.

The a priori parameter covariance matrix, $\mathbf{C}_{\alpha\alpha}$, for case 1a, is partly computed in Appendix B, Eq. (B.1), and is reproduced in Eq. (4.2).

$$\begin{aligned} \mathbf{C}_{\alpha\alpha} &\equiv \begin{pmatrix} Var(\alpha_1) & Cov(\alpha_1, \alpha_2) & \bullet & Cov(\alpha_1, \alpha_{47}) \\ Cov(\alpha_2, \alpha_1) & Var(\alpha_2) & \bullet & Cov(\alpha_2, \alpha_{47}) \\ \bullet & \bullet & \bullet & \bullet \\ Cov(\alpha_{47}, \alpha_1) & \bullet & \bullet & Var(\alpha_{47}) \end{pmatrix} \\ &= \begin{pmatrix} 3.18 & 2.17 & 1.19 & -187.06 & 0.26 & 0 & \bullet & 0 \\ 2.17 & 2.58 & 1.26 & -178.24 & 0.28 & 0 & \bullet & 0 \\ 1.19 & 1.26 & 2.00 & -184.39 & 0.26 & 0 & \bullet & 0 \\ -187.06 & -178.24 & -184.39 & 82133 & 0.42 & 0 & \bullet & 0 \\ 0.26 & 0.28 & 0.26 & 0.42 & 0.39 & 0 & \bullet & 0 \\ 0 & 0 & 0 & 0 & 0 & 0 & \bullet & 0 \\ \bullet & \bullet & \bullet & \bullet & \bullet & \bullet & \bullet & \bullet \\ 0 & 0 & 0 & 0 & 0 & 0 & \bullet & 5.33 \times 10^{-5} \end{pmatrix} \end{aligned} \quad (4.2)$$

CHAPTER 4. RESULTS

The a priori covariance matrix of the computed responses, \mathbf{C}_{rr}^{comp} , for case 1a, is obtained by using Eqs. (3.96) and (4.2) together with the sensitivity results presented in Tables 4.1 - 4.5 ; the end result is:

$$\begin{aligned} \mathbf{C}_{rr}^{comp} &\equiv Cov(T_a^{(1)}, T_w^{(50)}, RH^{(1)}) = \mathbf{S}_{r\alpha} \mathbf{C}_{\alpha\alpha} \mathbf{S}_{r\alpha}^\dagger \\ &= \begin{pmatrix} \frac{\partial T_a^{(1)}}{\partial \alpha_1}, \dots, \frac{\partial T_a^{(1)}}{\partial \alpha_{N\alpha}} \\ \frac{\partial T_w^{(50)}}{\partial \alpha_1}, \dots, \frac{\partial T_w^{(50)}}{\partial \alpha_{N\alpha}} \\ \frac{\partial RH^{(1)}}{\partial \alpha_1}, \dots, \frac{\partial RH^{(1)}}{\partial \alpha_{N\alpha}} \end{pmatrix} \begin{pmatrix} Var(\alpha_1) & Cov(\alpha_1, \alpha_2) & \bullet & Cov(\alpha_1, \alpha_{47}) \\ Cov(\alpha_2, \alpha_1) & Var(\alpha_2) & \bullet & Cov(\alpha_2, \alpha_{47}) \\ \bullet & \bullet & \bullet & \bullet \\ Cov(\alpha_{52}, \alpha_1) & \bullet & \bullet & Var(\alpha_{47}) \end{pmatrix} \begin{pmatrix} \frac{\partial T_a^{(1)}}{\partial \alpha_1}, \dots, \frac{\partial T_a^{(1)}}{\partial \alpha_{N\alpha}} \\ \frac{\partial T_w^{(50)}}{\partial \alpha_1}, \dots, \frac{\partial T_w^{(50)}}{\partial \alpha_{N\alpha}} \\ \frac{\partial RH^{(1)}}{\partial \alpha_1}, \dots, \frac{\partial RH^{(1)}}{\partial \alpha_{N\alpha}} \end{pmatrix}^\dagger \\ &= \begin{pmatrix} 1.98 & 1.60 & -3.42 \\ 1.60 & 1.88 & -2.82 \\ -3.42 & -2.82 & 80.71 \end{pmatrix}. \end{aligned} \quad (4.3)$$

The a priori covariance matrix, $Cov(T_{a,out}^{meas}, T_{w,out}^{meas}, RH_{out}^{meas}) \triangleq \mathbf{C}_{rr}$, of the measured responses (namely: the outlet air temperature, $T_{a,out}^{meas} \equiv [T_a^{(1)}]^{measured}$; the outlet water temperature, $T_{w,out}^{meas} \equiv [T_w^{(50)}]^{measured}$, and the outlet air relative humidity, $RH_{out}^{meas} \equiv [RH^{(1)}]^{measured}$) for case 1a is computed in Appendix A, Eq. (A.4), and is as follows:

$$\mathbf{C}_{rr} \equiv Cov(T_{a,out}^{meas}, T_{w,out}^{meas}, RH_{out}^{meas}) = \begin{pmatrix} 1.10 & 0.61 & -0.04 \\ 0.61 & 1.25 & -0.64 \\ -0.04 & -0.64 & 3.68 \end{pmatrix}. \quad (4.4)$$

4.3.1.1 Model Calibration: Predicted Best-Estimated Parameter Values with Reduced Predicted Standard Deviations

The best-estimate nominal parameter values have been calculated using Eq. (3.93) coupled with the a priori matrices given in Eqs. (4.1) - (4.4) and the sensitivities listed in Tables 4.1 - 4.5. The resulting best-estimate nominal values are listed in Table 4.21. The best-estimate absolute standard deviations of the parameters are also listed in this table. These values are obtained as the square-roots

CHAPTER 4. RESULTS

of the diagonal elements of the matrix $\mathbf{C}_{\alpha\alpha}^{pred}$, which is computed using Eq. (3.97) together with the a priori matrices presented in Eqs. (4.1) - (4.4) and the sensitivities listed in Tables 4.1 - 4.5. For a more direct comparison, the original nominal parameter values and original absolute standard deviations are also listed. As shown in Table 4.21, all the best-estimate standard deviations are smaller or at most equal to the original standard deviations. The variations in the parameters values are proportional to the magnitudes of their corresponding sensitivities: the parameters undergoing the largest reductions in their best-estimate standard deviations are those characterized by the largest sensitivities.

Table 4.21: Best-estimated nominal parameter values and their standard deviations for case 1a.

i	Model Independent Scalar Parameters (α_i)	Math. Notation	Original Nominal Value	Original Absolute Std. Dev.	Best- estimate Nominal Value	Best- estimate Absolute Std. Dev.
1	Air temperature (dry bulb), (K)	T_{db}	294.03	1.79	294.954	1.7
2	Dew point temperature (K)	T_{dp}	293.49	1.61	293.68	1.51
3	Inlet water temperature (K)	$T_{w,in}$	298.78	1.42	298.533	1.09
4	Atmospheric pressure (Pa)	P_{atm}	100853	287	100883	269
5	Wind speed (m/s)	V_w	1.42	0.62	1.274	0.62
6	Sum of loss coefficients above fill	k_{sum}	10	5	10.061	5
7	Dynamic viscosity of air at T=300 K (kg/m·s)	μ	$1.98 \cdot 10^{-5}$	$9.68 \cdot 10^{-7}$	$1.98 \cdot 10^{-5}$	$9.66 \cdot 10^{-7}$
8	Kinematic viscosity of air at T=300 K (m ² /s)	ν	$1.57 \cdot 10^{-5}$	$1.89 \cdot 10^{-6}$	$1.57 \cdot 10^{-5}$	$1.89 \cdot 10^{-6}$
9	Thermal conductivity of air at T=300 K (W/m·K)	k_{air}	0.02624	$1.58 \cdot 10^{-3}$	0.02611	$1.58 \cdot 10^{-3}$
10	Heat transfer coefficient multiplier	f_{ht}	1	0.5	0.6603	0.346
11	Mass transfer coefficient multiplier	f_{mt}	1	0.5	0.9671	0.364

CHAPTER 4. RESULTS

i	Model Independent Scalar Parameters (α_i)	Math. Notation	Original Nominal Value	Original Absolute Std. Dev.	Best- estimate Nominal Value	Best- estimate Absolute Std. Dev.
12	Fill section frictional loss multiplier	f	4	2	4.093	1.92
13	P _{vs} (T) parameters	a_0	25.5943	0.01	25.5942	0.01
14		a_1	-5229.89	4.4	-5229.97	4.4
15	C _{pa} (T) parameters	$a_{0,cpa}$	1030.5	0.294	1030.5	0.294
16		$a_{1,cpa}$	-0.19975	0.002	-0.19975	0.002
17		$a_{2,cpa}$	$3.97 \cdot 10^{-4}$	$3.40 \cdot 10^{-6}$	$3.97 \cdot 10^{-4}$	$3.35 \cdot 10^{-6}$
18	D _{av} (T) parameters	$a_{0,dav}$	$7.06 \cdot 10^{-9}$	0	$7.06 \cdot 10^{-9}$	0
19		$a_{1,dav}$	2.65322	0.003	2.65322	0.003
20		$a_{2,dav}$	$-6.17 \cdot 10^{-3}$	$2.30 \cdot 10^{-5}$	$-6.17 \cdot 10^{-3}$	$2.30 \cdot 10^{-5}$
21		$a_{3,dav}$	$6.55 \cdot 10^{-6}$	$3.80 \cdot 10^{-8}$	$6.55 \cdot 10^{-6}$	$3.80 \cdot 10^{-8}$
22	h _f (T) parameters	a_{0f}	-1143423	543	-1143423	543
23		a_{1f}	4186.50768	1.8	4186.50955	1.8
24	h _g (T) parameters	a_{0g}	2005743.99	1046	2005743.4	1046
25		a_{1g}	1815.437	3.5	1815.43526	3.5
26	Nusselt parameters	$a_{0,Nu}$	8.235	2.059	7.46776	2.024
27		$a_{1,Nu}$	0.00314987	0.00105	0.00314987	0.001
28		$a_{2,Nu}$	0.9902987	0.329	0.9902987	0.327
29		$a_{3,Nu}$	0.023	0.0088	0.023	0.0088
30	Cooling tower deck width in x-dir (m)	W_{dkx}	8.5	0.085	8.5	0.085
31	Cooling tower deck width in y-dir (m)	W_{dky}	8.5	0.085	8.5	0.085
32	Cooling tower deck height above ground (m)	Δz_{dk}	10	0.1	10	0.1
33	Fan shroud height (m)	Δz_{fan}	3	0.03	3	0.03

CHAPTER 4. RESULTS

i	Model Independent Scalar Parameters (α_i)	Math. Notation	Original Nominal Value	Original Absolute Std. Dev.	Best- estimate Nominal Value	Best- estimate Absolute Std. Dev.
34	Fan shroud inner diameter (m)	D_{fan}	4.1	0.041	4.1	0.041
35	Fill section height (m)	Δz_{fill}	2.013	0.02013	2.013	0.02013
36	Rain section height (m)	Δz_{rain}	1.633	0.01633	1.633	0.01633
37	Basin section height (m)	Δz_{bs}	1.168	0.01168	1.168	0.01168
38	Drift eliminator thickness (m)	Δz_{de}	0.1524	0.00152	0.1524	0.00152
39	Fill section equivalent diam- eter (m)	D_h	0.0381	0.00038	0.0381	0.00038
40	Fill section flow area (m ²)	A_{fill}	67.29	6.729	67.1945	6.705
41	Fill section surface area (m ²)	A_{surf}	14221	3555.3	12896	3495
42	Prandtl number of air at T=80 °C	P_r	0.708	0.005	0.708	0.005
43	Wetted fraction of fill sur- face area	w_{tsa}	1	0	1	0
i	Boundary Parameters (α_i)	Math. Notation	Original Nominal Value	Original Absolute Std. Dev.	Best- estimate Nominal Value	Best- estimate Absolute Std. Dev.
44	Inlet water mass flow rate (kg/s)	$m_{w,in}$	44.02	2.20	44.2145	2.192
45	Inlet air temperature (K)	$T_{a,in}$	294.03	1.79	294.3174	1.57
46	Inlet air humidity ratio	ω_{in}	0.01552	0.00149	0.01567	0.00136
i	Special Dependent Parameters (α_i)	Math. Notation	Original Nominal Value	Original Absolute Std. Dev.	Best- estimate Nominal Value	Best- estimate Absolute Std. Dev.
47	Schmidt number	Sc	0.619	0.0073	0.6193	0.0073

CHAPTER 4. RESULTS

4.3.1.2 Predicted Best-Estimated Response Values with Reduced Predicted Standard Deviations

Using the a priori matrices in Eqs. (4.1) - (4.4) together with the sensitivities listed in Tables 4.1 - 4.5 in Eq. (3.99), the following predicted response covariance matrix, \mathbf{C}_{rr}^{pred} , is obtained:

$$\mathbf{C}_{rr}^{pred} \equiv Cov \left([T_a^{(1)}]^{be}, [T_w^{(50)}]^{be}, [RH^{(1)}]^{be} \right) = \begin{pmatrix} 0.953 & 0.795 & -0.291 \\ 0.795 & 0.939 & -0.283 \\ -0.291 & -0.283 & 3.130 \end{pmatrix}. \quad (4.5)$$

The best-estimate response-parameter correlation matrix, $\mathbf{C}_{\alpha r}^{pred}$, is obtained by means of Eq. (3.100) in conjunction with the a priori matrices presented in Eqs. (4.1) - (4.4) and the sensitivities listed in Tables 4.1 - 4.5.

The best-estimate nominal values of the outlet air temperature, $T_a^{(1)}$; outlet water temperature $T_w^{(50)}$; and outlet air relative humidity, $RH^{(1)}$, have been computed using Eq. (3.98) coupled with the a priori matrices given in Eqs. (4.1) - (4.4) and the sensitivities listed in Tables 4.1 - 4.5. The resulting best-estimate nominal values are displayed in Table 4.22. To facilitate comparison, the corresponding measured and computed nominal values are also presented in this table. Note that there are no direct measurements for the outlet water flow rate, $m_w^{(50)}$ and the air mass flow rate m_a . For these two responses, therefore, the predicted best-estimate nominal values have been obtained by a forward re-computation using the best-estimate nominal parameter values listed in Table 4.21, while the predicted best estimate standard deviation for this response has been obtained by using “best-estimate” values in Eq. (3.96), i.e.,

$$[\mathbf{C}_{rr}^{comp}]^{be} = [\mathbf{S}_{r\alpha}]^{be} [\mathbf{C}_{\alpha\alpha}]^{be} [\mathbf{S}_{r\alpha}^\dagger]^{be} \quad (4.6)$$

CHAPTER 4. RESULTS

Table 4.22: Computed, measured, and optimal best-estimate nominal values and standard deviations for the outlet air temperature, outlet water temperature, outlet air relative humidity, outlet water mass flow rate and air mass flow rate responses for case 1a.

Nominal Values and Standard Deviations		$T_a^{(1)}$ [K]	$T_w^{(50)}$ [K]	$RH^{(1)}$ [%]	$m_w^{(50)}$ [kg/s]	m_a [kg/s]
Measured						
	nominal value	296.45	297.91	102.28	—	—
	standard deviation	± 1.05	± 1.12	± 1.92	—	—
Computed						
	nominal value	298.41	296.86	100.11	43.91	20.11
	standard deviation	± 1.41	± 1.37	± 8.98	± 2.20	± 6.97
Best-estimate						
	nominal value	297.86	296.94	103.48	44.12	16.15
	standard deviation	± 0.97	± 0.96	± 1.77	± 2.19	± 5.73

The results presented in Table 4.22 indicate that, as anticipated, the predicted standard deviations are smaller than either the computed or the experimentally measured ones. This is consequential to utilizing the PM_CMPS methodology together with *consistent* computational and experimental information. Unspotted errors can often make the used information inconsistent; methods to confront these situations are discussed in [37]. It is also worth noting that the PM_CMPS methodology has reduced the predicted standard deviation for the water mass flow rate and for the air mass flow rate responses, despite the lack of experimentally measure data. This is due to the *global* characteristics of the PM_CMPS methodology to foresee a *simultaneous* combination of all the available data in the phase-space, yielding this way the aforementioned best-estimate predicted results; currently used data assimilation methodologies, on the other hand, proceed by combine the available information in a sequential way [38, 39].

4.3.2 Uncertainty Analysis and Predictive Modeling of Case 1b: Fan Off, Saturated Outlet Air Conditions, with Inlet Air Saturated

The a priori response-parameter covariance matrix, $\mathbf{C}_{r\alpha}$, for case 1b, is computed in Appendix A, Eq. (A.9), and is reproduced in Eq. (4.7).

$$\begin{aligned} \mathbf{C}_{r\alpha} &\equiv Cov(T_{a,out}^{meas}, T_{w,out}^{meas}, RH^{meas}, \alpha_1, \dots, \alpha_{47}) \\ &= \begin{pmatrix} 0.45 & 0.52 & 0.52 & 1.12 & 0.007 & 0 & \dots & 0 \\ 0.50 & 0.55 & 0.60 & -51.14 & -0.13 & 0 & \dots & 0 \\ 0.02 & 0.08 & 0.06 & 123.51 & -0.23 & 0 & \dots & 0 \end{pmatrix} \end{aligned} \quad (4.7)$$

where the measured correlated parameters are: $\alpha_1 \triangleq T_{db}$, $\alpha_2 \triangleq T_{dp}$, $\alpha_3 \triangleq T_{w,in}$, $\alpha_4 \triangleq P_{atm}$, and $\alpha_5 \triangleq V_w$.

The a priori parameter covariance matrix, $\mathbf{C}_{\alpha\alpha}$, for case 1b, is partly computed in Appendix B, Eq. (B.4), and is reproduced in Eq. (4.8).

$$\begin{aligned} \mathbf{C}_{\alpha\alpha} &\equiv \begin{pmatrix} Var(\alpha_1) & Cov(\alpha_1, \alpha_2) & \bullet & Cov(\alpha_1, \alpha_{47}) \\ Cov(\alpha_2, \alpha_1) & Var(\alpha_2) & \bullet & Cov(\alpha_2, \alpha_{47}) \\ \bullet & \bullet & \bullet & \bullet \\ Cov(\alpha_{47}, \alpha_1) & \bullet & \bullet & Var(\alpha_{47}) \end{pmatrix} \\ &= \begin{pmatrix} 0.97 & 1.04 & 0.60 & -128.15 & 0.07 & 0 & \bullet & 0 \\ 1.04 & 1.16 & 0.66 & -138.34 & 0.06 & 0 & \bullet & 0 \\ 0.60 & 0.66 & 1.14 & -51.83 & 0.02 & 0 & \bullet & 0 \\ -128.15 & -138.34 & -51.83 & 97463 & 30.66 & 0 & \bullet & 0 \\ 0.07 & 0.06 & 0.02 & 30.66 & 0.52 & 0 & \bullet & 0 \\ 0 & 0 & 0 & 0 & 0 & 0 & \bullet & 0 \\ \bullet & \bullet & \bullet & \bullet & \bullet & \bullet & \bullet & \bullet \\ 0 & 0 & 0 & 0 & 0 & 0 & \bullet & 1.68 \times 10^{-5} \end{pmatrix} \end{aligned} \quad (4.8)$$

CHAPTER 4. RESULTS

The a priori covariance matrix of the computed responses, \mathbf{C}_{rr}^{comp} , for case 1a, is obtained by using Eqs. (3.96) and (4.8) together with the sensitivity results presented in Tables 4.6 - 4.10 ; the end result is:

$$\begin{aligned} \mathbf{C}_{rr}^{comp} &\equiv Cov(T_a^{(1)}, T_w^{(50)}, RH^{(1)}) = \mathbf{S}_{r\alpha} \mathbf{C}_{\alpha\alpha} \mathbf{S}_{r\alpha}^\dagger \\ &= \begin{pmatrix} \frac{\partial T_a^{(1)}}{\partial \alpha_1}, \dots, \frac{\partial T_a^{(1)}}{\partial \alpha_{N\alpha}} \\ \frac{\partial T_w^{(50)}}{\partial \alpha_1}, \dots, \frac{\partial T_w^{(50)}}{\partial \alpha_{N\alpha}} \\ \frac{\partial RH^{(1)}}{\partial \alpha_1}, \dots, \frac{\partial RH^{(1)}}{\partial \alpha_{N\alpha}} \end{pmatrix} \begin{pmatrix} Var(\alpha_1) & Cov(\alpha_1, \alpha_2) & \bullet & Cov(\alpha_1, \alpha_{47}) \\ Cov(\alpha_2, \alpha_1) & Var(\alpha_2) & \bullet & Cov(\alpha_2, \alpha_{47}) \\ \bullet & \bullet & \bullet & \bullet \\ Cov(\alpha_{52}, \alpha_1) & \bullet & \bullet & Var(\alpha_{47}) \end{pmatrix} \begin{pmatrix} \frac{\partial T_a^{(1)}}{\partial \alpha_1}, \dots, \frac{\partial T_a^{(1)}}{\partial \alpha_{N\alpha}} \\ \frac{\partial T_w^{(50)}}{\partial \alpha_1}, \dots, \frac{\partial T_w^{(50)}}{\partial \alpha_{N\alpha}} \\ \frac{\partial RH^{(1)}}{\partial \alpha_1}, \dots, \frac{\partial RH^{(1)}}{\partial \alpha_{N\alpha}} \end{pmatrix}^\dagger \\ &= \begin{pmatrix} 1.46 & 1.27 & -9.01 \\ 1.27 & 1.76 & -15.75 \\ -9.01 & -15.75 & 370.72 \end{pmatrix}. \end{aligned} \quad (4.9)$$

The a priori covariance matrix, $Cov(T_{a,out}^{meas}, T_{w,out}^{meas}, RH_{out}^{meas}) \triangleq \mathbf{C}_{rr}$, of the measured responses (namely: the outlet air temperature, $T_{a,out}^{meas} \equiv [T_a^{(1)}]^{measured}$; the outlet water temperature, $T_{w,out}^{meas} \equiv [T_w^{(50)}]^{measured}$, and the outlet air relative humidity, $RH_{out}^{meas} \equiv [RH^{(1)}]^{measured}$) for case 1b is computed in Appendix A, Eq. (A.8), and is as follows:

$$\mathbf{C}_{rr} \equiv Cov(T_{a,out}^{meas}, T_{w,out}^{meas}, RH_{out}^{meas}) = \begin{pmatrix} 0.75 & 0.18 & 0.14 \\ 0.18 & 0.79 & 0.21 \\ 0.14 & 0.21 & 1.65 \end{pmatrix}. \quad (4.10)$$

4.3.2.1 Model Calibration: Predicted Best-Estimated Parameter Values with Reduced Predicted Standard Deviations

The best-estimate nominal parameter values have been calculated using Eq. (3.93) coupled with the a priori matrices given in Eqs. (4.7) - (4.10) and the sensitivities listed in Tables 4.6 - 4.10. The resulting best-estimate nominal values are listed in Table 4.23. The best-estimate absolute standard deviations of the parameters are also listed in this table. These values are obtained as the square-

CHAPTER 4. RESULTS

roots of the diagonal elements of the matrix $\mathbf{C}_{\alpha\alpha}^{pred}$, which is computed using Eq. (3.97) coupled with the a priori matrices presented in Eqs. (4.7) - (4.10) and the sensitivities listed in Tables 4.6 - 4.10. For a more direct comparison, the original nominal parameter values and original absolute standard deviations are also listed. As shown in Table 4.23, all the best-estimate standard deviations are smaller or at most equal to the original standard deviations. The variations in the parameters values are proportional to the magnitudes of their corresponding sensitivities: the parameters undergoing the largest reductions in their best-estimate standard deviations are those characterized by the largest sensitivities.

Table 4.23: Best-estimated nominal parameter values and their standard deviations for case 1b.

i	Model Independent Scalar Parameters (α_i)	Math. Notation	Original Nominal Value	Original Absolute Std. Dev.	Best- estimate Nominal Value	Best- estimate Absolute Std. Dev.
1	Air temperature (dry bulb), (K)	T_{db}	294.4	0.98	294.115	0.93
2	Dew point temperature (K)	T_{dp}	294.661	1.08	294.41	1.02
3	Inlet water temperature (K)	$T_{w,in}$	299.543	1.07	298.411	0.9
4	Atmospheric pressure (Pa)	P_{atm}	100605	312	100767	292
5	Wind speed (m/s)	V_w	1.377	0.72	1.803	0.69
6	Sum of loss coefficients above fill	k_{sum}	10	5	9.613	4.98
7	Dynamic viscosity of air at T=300 K (kg/m·s)	μ	$1.98 \cdot 10^{-5}$	$9.68 \cdot 10^{-7}$	$1.98 \cdot 10^{-5}$	$9.67 \cdot 10^{-7}$
8	Kinematic viscosity of air at T=300 K (m ² /s)	ν	$1.57 \cdot 10^{-5}$	$1.89 \cdot 10^{-6}$	$1.56 \cdot 10^{-5}$	$1.89 \cdot 10^{-6}$
9	Thermal conductivity of air at T=300 K (W/m·K)	k_{air}	0.02624	$1.58 \cdot 10^{-3}$	0.02611	$1.58 \cdot 10^{-3}$
10	Heat transfer coefficient multiplier	f_{ht}	1	0.5	0.6711	0.36
11	Mass transfer coefficient multiplier	f_{mt}	1	0.5	0.7223	0.36

CHAPTER 4. RESULTS

i	Model Independent Scalar Parameters (α_i)	Math. Notation	Original Nominal Value	Original Absolute Std. Dev.	Best- estimate Nominal Value	Best- estimate Absolute Std. Dev.
12	Fill section frictional loss multiplier	f	4	2	3.4307	1.88
13	$P_{vs}(T)$ parameters	a_0	25.5943	0.01	25.5943	0.01
14		a_1	-5229.89	4.4	-5229.92	4.4
15	$C_{pa}(T)$ parameters	$a_{0,cpa}$	1030.5	0.294	1030.5	0.294
16		$a_{1,cpa}$	-0.19975	0.002	-0.19975	0.002
17		$a_{2,cpa}$	$3.97 \cdot 10^{-4}$	$3.40 \cdot 10^{-6}$	$3.97 \cdot 10^{-4}$	$3.35 \cdot 10^{-6}$
18	$D_{av}(T)$ parameters	$a_{0,dav}$	$7.06 \cdot 10^{-9}$	0	$7.06 \cdot 10^{-9}$	0
19		$a_{1,dav}$	2.65322	0.003	2.65322	0.003
20		$a_{2,dav}$	$-6.17 \cdot 10^{-3}$	$2.30 \cdot 10^{-5}$	$-6.17 \cdot 10^{-3}$	$2.30 \cdot 10^{-5}$
21		$a_{3,dav}$	$6.55 \cdot 10^{-6}$	$3.80 \cdot 10^{-8}$	$6.55 \cdot 10^{-6}$	$3.80 \cdot 10^{-8}$
22	$h_f(T)$ parameters	a_{0f}	-1143423	543	-1143423	543
23		a_{1f}	4186.50768	1.8	4186.5085	1.8
24	$h_g(T)$ parameters	a_{0g}	2005743.99	1046	2005743.74	1046
25		a_{1g}	1815.437	3.5	1815.43646	3.5
26	Nusselt parameters	$a_{0,Nu}$	8.235	2.059	6.98576	2
27		$a_{1,Nu}$	0.00314987	0.00105	0.00314987	0.001
28		$a_{2,Nu}$	0.9902987	0.329	0.9902987	0.327
29		$a_{3,Nu}$	0.023	0.0088	0.023	0.0088
30	Cooling tower deck width in x-dir (m)	W_{dkx}	8.5	0.085	8.5	0.085
31	Cooling tower deck width in y-dir (m)	W_{dky}	8.5	0.085	8.5	0.085
32	Cooling tower deck height above ground (m)	Δz_{dk}	10	0.1	10	0.1
33	Fan shroud height (m)	Δz_{fan}	3	0.03	3	0.03

CHAPTER 4. RESULTS

i	Model Independent Scalar Parameters (α_i)	Math. Notation	Original Nominal Value	Original Absolute Std. Dev.	Best- estimate Nominal Value	Best- estimate Absolute Std. Dev.
34	Fan shroud inner diameter (m)	D_{fan}	4.1	0.041	4.1	0.041
35	Fill section height (m)	Δz_{fill}	2.013	0.02013	2.013	0.02013
36	Rain section height (m)	Δz_{rain}	1.633	0.01633	1.633	0.01633
37	Basin section height (m)	Δz_{bs}	1.168	0.01168	1.168	0.01168
38	Drift eliminator thickness (m)	Δz_{de}	0.1524	0.00152	0.1524	0.00152
39	Fill section equivalent diam- eter (m)	D_h	0.0381	0.00038	0.0381	0.00038
40	Fill section flow area (m ²)	A_{fill}	67.29	6.729	67.881	6.692
41	Fill section surface area (m ²)	A_{surf}	14221	3555.3	12064	3455
42	Prandtl number of air at T=80 °C	P_r	0.708	0.005	0.708	0.005
43	Wetted fraction of fill sur- face area	w_{tsa}	1	0	1	0
i	Boundary Parameters (α_i)	Math. Notation	Original Nominal Value	Original Absolute Std. Dev.	Best- estimate Nominal Value	Best- estimate Absolute Std. Dev.
44	Inlet water mass flow rate (kg/s)	$m_{w,in}$	44.0089	2.20	44.0939	2.188
45	Inlet air temperature (K)	$T_{a,in}$	294.40	0.98	294.524	0.89
46	Inlet air humidity ratio	ω_{in}	0.0162008	0.00131	0.016083	0.001
i	Special Dependent Parameters (α_i)	Math. Notation	Original Nominal Value	Original Absolute Std. Dev.	Best- estimate Nominal Value	Best- estimate Absolute Std. Dev.
47	Schmidt number	Sc	0.6178	0.0041	0.6178	0.004

CHAPTER 4. RESULTS

4.3.2.2 Predicted Best-Estimated Response Values with Reduced Predicted Standard Deviations

Using the a priori matrices in Eqs. (4.7) - (4.10) together with the sensitivities listed in Tables 4.6 - 4.10 in Eq. (3.99), the following predicted response covariance matrix, \mathbf{C}_{rr}^{pred} , is obtained:

$$\mathbf{C}_{rr}^{pred} \equiv Cov \left([T_a^{(1)}]^{be}, [T_w^{(50)}]^{be}, [RH^{(1)}]^{be} \right) = \begin{pmatrix} 0.59 & 0.37 & 0.17 \\ 0.37 & 0.53 & 0.18 \\ 0.17 & 0.18 & 1.62 \end{pmatrix}. \quad (4.11)$$

The best-estimate response-parameter correlation matrix, \mathbf{C}_{ar}^{pred} , is obtained by means of Eq. (3.100) in conjunction with the a priori matrices presented in Eqs. (4.7) - (4.10) and the sensitivities listed in Tables 4.6 - 4.10.

The best-estimate nominal values of the outlet air temperature, $T_a^{(1)}$; outlet water temperature $T_w^{(50)}$; and outlet air relative humidity, $RH^{(1)}$, have been computed using Eq. (3.98) coupled with the a priori matrices given in Eqs. (4.7) - (4.10) and the sensitivities listed in Tables 4.6 - 4.10. The resulting best-estimate nominal values are displayed in Table 4.24. To facilitate comparison, the corresponding measured and computed nominal values are also presented in this table. Note that there are no direct measurements for the outlet water flow rate, $m_w^{(50)}$ and the air mass flow rate m_a . For these two responses, therefore, the predicted best-estimate nominal values have been obtained by a forward re-computation using the best-estimate nominal parameter values listed in Table 4.23, while the predicted best estimate standard deviation for this response has been obtained by using “best-estimate” values in Eq. (3.96), i.e.,

$$[\mathbf{C}_{rr}^{comp}]^{be} = [\mathbf{S}_{r\alpha}]^{be} [\mathbf{C}_{\alpha\alpha}]^{be} [\mathbf{S}_{r\alpha}^\dagger]^{be} \quad (4.12)$$

CHAPTER 4. RESULTS

Table 4.24: Computed, measured, and optimal best-estimate nominal values and standard deviations for the outlet air temperature, outlet water temperature, outlet air relative humidity, outlet water mass flow rate and air mass flow rate responses for case 1b.

Nominal Values and Standard Deviations		$T_a^{(1)}$ [K]	$T_w^{(50)}$ [K]	$RH^{(1)}$ [%]	$m_w^{(50)}$ [kg/s]	m_a [kg/s]
Measured						
	nominal value	299.10	297.46	102.37	—	—
	standard deviation	± 0.86	± 0.89	± 1.28	—	—
Computed						
	nominal value	296.50	298.21	102.83	43.89	20.75
	standard deviation	± 1.21	± 1.33	± 19.25	± 2.20	± 6.54
Best-estimate						
	nominal value	297.41	296.82	102.76	44.02	23.18
	standard deviation	± 0.77	± 0.73	± 1.27	± 2.19	± 7.20

The results presented in Table 4.24 indicate that the predicted standard deviations are smaller than either the computed or the experimentally measured ones, except for the air mass flow rate. This exception is due to the simultaneous use of all the available data, which causes the responses nominal values (and their respective standard deviations) to be mutually correlated because of the covariances between model parameters and responses ($\mathbf{C}_{r\alpha} \neq 0$). In order to verify the correctness of the calculation performed, a separate case without considering the covariances between model parameters and responses ($\mathbf{C}_{r\alpha} = 0$) has been developed and analyzed, and the results confirmed the theory expectations, yielding all predicted standard deviations smaller than either the computed or the experimentally measured ones, even for the air mass flow rate. In the PM_CMPS framework, the standard deviation values of the responses for which no experimental data are available are only influenced by the correlations to the other responses' values, both experimental and computed. For this reason, the results of the fully-correlated model (with $\mathbf{C}_{r\alpha} \neq 0$) have been chosen: in fact, despite the slightly bigger standard deviation for the air mass flow rate, which is the con-

CHAPTER 4. RESULTS

sequence of all the information simultaneously used in the PM_CMPS methodology, those results are to be considered the most accurate, since they were obtained by means of the simultaneous using of all the available data.

4.3.3 Uncertainty Analysis and Predictive Modeling of Case 2: Fan Off, Unsaturated Air Conditions

The a priori response-parameter covariance matrix, $\mathbf{C}_{r\alpha}$, for case 2, is computed in Appendix A, Eq. (A.13), and is reproduced in Eq. (4.7).

$$\begin{aligned} \mathbf{C}_{r\alpha} &\equiv Cov(T_{a,out}^{meas}, T_{w,out}^{meas}, RH^{meas}, \alpha_1, \dots, \alpha_{47}) \\ &= \begin{pmatrix} 10.36 & 2.81 & 2.22 & -232.64 & 1.30 & 0 & \dots \\ 1.58 & 1.96 & 2.01 & -23.76 & -0.10 & 0 & \dots \\ -35.89 & 2.43 & -0.79 & 720.11 & -5.48 & 0 & \dots \end{pmatrix} \end{aligned} \quad (4.13)$$

where the measured correlated parameters are: $\alpha_1 \triangleq T_{db}$, $\alpha_2 \triangleq T_{dp}$, $\alpha_3 \triangleq T_{w,in}$, $\alpha_4 \triangleq P_{atm}$, and $\alpha_5 \triangleq V_w$. The a priori parameter covariance matrix, $\mathbf{C}_{\alpha\alpha}$, for case 2, is partly computed in Appendix B, Eq. (B.5), and is reproduced in Eq. (4.14).

$$\begin{aligned} \mathbf{C}_{\alpha\alpha} &\equiv \begin{pmatrix} Var(\alpha_1) & Cov(\alpha_1, \alpha_2) & \bullet & Cov(\alpha_1, \alpha_{47}) \\ Cov(\alpha_2, \alpha_1) & Var(\alpha_2) & \bullet & Cov(\alpha_2, \alpha_{47}) \\ \bullet & \bullet & \bullet & \bullet \\ Cov(\alpha_{47}, \alpha_1) & \bullet & \bullet & Var(\alpha_{47}) \end{pmatrix} \\ &= \begin{pmatrix} 16.27 & 3.56 & 2.13 & -494.48 & 2.45 & 0 & \bullet & 0 \\ 3.56 & 5.23 & 2.22 & -138.46 & 0.28 & 0 & \bullet & 0 \\ 2.13 & 2.22 & 2.85 & -58.63 & 0.12 & 0 & \bullet & 0 \\ -494.48 & -138.46 & -58.63 & 166678.40 & -49.62 & 0 & \bullet & 0 \\ 2.45 & 0.28 & 0.12 & -49.62 & 0.89 & 0 & \bullet & 0 \\ 0 & 0 & 0 & 0 & 0 & 0 & \bullet & 0 \\ \bullet & \bullet & \bullet & \bullet & \bullet & \bullet & \bullet & \bullet \\ 0 & 0 & 0 & 0 & 0 & 0 & \bullet & 0.00025 \end{pmatrix} \end{aligned} \quad (4.14)$$

CHAPTER 4. RESULTS

The a priori covariance matrix of the computed responses, \mathbf{C}_{rr}^{comp} , for case 2, is obtained by using Eqs. (3.96) and (4.14) together with the sensitivity results presented in Tables 4.11 - 4.15; the end result is:

$$\begin{aligned} \mathbf{C}_{rr}^{comp} &\equiv Cov(T_a^{(1)}, T_w^{(50)}, RH^{(1)}) = \mathbf{S}_{r\alpha} \mathbf{C}_{\alpha\alpha} \mathbf{S}_{r\alpha}^\dagger \\ &= \begin{pmatrix} \frac{\partial T_a^{(1)}}{\partial \alpha_1}, \dots, \frac{\partial T_a^{(1)}}{\partial \alpha_{N\alpha}} \\ \frac{\partial T_w^{(50)}}{\partial \alpha_1}, \dots, \frac{\partial T_w^{(50)}}{\partial \alpha_{N\alpha}} \\ \frac{\partial RH^{(1)}}{\partial \alpha_1}, \dots, \frac{\partial RH^{(1)}}{\partial \alpha_{N\alpha}} \end{pmatrix} \begin{pmatrix} Var(\alpha_1) & Cov(\alpha_1, \alpha_2) & \bullet & Cov(\alpha_1, \alpha_{47}) \\ Cov(\alpha_2, \alpha_1) & Var(\alpha_2) & \bullet & Cov(\alpha_2, \alpha_{47}) \\ \bullet & \bullet & \bullet & \bullet \\ Cov(\alpha_{52}, \alpha_1) & \bullet & \bullet & Var(\alpha_{47}) \end{pmatrix} \begin{pmatrix} \frac{\partial T_a^{(1)}}{\partial \alpha_1}, \dots, \frac{\partial T_a^{(1)}}{\partial \alpha_{N\alpha}} \\ \frac{\partial T_w^{(50)}}{\partial \alpha_1}, \dots, \frac{\partial T_w^{(50)}}{\partial \alpha_{N\alpha}} \\ \frac{\partial RH^{(1)}}{\partial \alpha_1}, \dots, \frac{\partial RH^{(1)}}{\partial \alpha_{N\alpha}} \end{pmatrix}^\dagger \\ &= \begin{pmatrix} 2.78 & 2.64 & 0.11 \\ 2.64 & 3.85 & 0.56 \\ 0.11 & 0.56 & 1.37 \end{pmatrix}. \end{aligned} \quad (4.15)$$

The a priori covariance matrix, $Cov(T_{a,out}^{meas}, T_{w,out}^{meas}, RH_{out}^{meas}) \triangleq \mathbf{C}_{rr}$, of the measured responses (namely: the outlet air temperature, $T_{a,out}^{meas} \equiv [T_a^{(1)}]^{measured}$; the outlet water temperature, $T_{w,out}^{meas} \equiv [T_w^{(50)}]^{measured}$, and the outlet air relative humidity, $RH_{out}^{meas} \equiv [RH^{(1)}]^{measured}$) for case 2 is computed in Appendix A, Eq. (A.12), and is as follows:

$$\mathbf{C}_{rr} \equiv Cov(T_{a,out}^{meas}, T_{w,out}^{meas}, RH_{out}^{meas}) = \begin{pmatrix} 8.09 & 1.91 & -27.74 \\ 1.91 & 1.94 & -1.97 \\ -27.74 & -1.97 & 195.81 \end{pmatrix}. \quad (4.16)$$

4.3.3.1 Model Calibration: Predicted Best-Estimated Parameter Values with Reduced Predicted Standard Deviations

The best-estimate nominal parameter values have been calculated using Eq. (3.93) coupled with the a priori matrices given in Eqs. (4.13) - (4.16) and the sensitivities listed in Tables 4.11 - 4.15. The resulting best-estimate nominal values are listed in Table 4.25, below. The best-estimate absolute standard deviations of these parameters are also listed in this table. These values have been obtained as the square-roots of the diagonal elements of the matrix $\mathbf{C}_{\alpha\alpha}^{pred}$, which is computed

CHAPTER 4. RESULTS

using Eq. (3.97) together with the a priori matrices presented in Eqs. (4.13) - (4.16) and the sensitivities listed in Tables 4.11 - 4.15. For a more direct comparison, the original nominal parameter values and original absolute standard deviations are also listed. As it is clear from Table 4.25, all the predicted best-estimate standard deviations are smaller or at most equal to the original standard deviations. The variations in the parameters values are proportional to the magnitudes of their corresponding sensitivities: the parameters undergoing the largest reductions in their best-estimate standard deviations are those characterized by the largest sensitivities.

Table 4.25: Best-estimated nominal parameter values and their standard deviations for case 2.

i	Model Independent Scalar Parameters (α_i)	Math. Notation	Original Nominal Value	Original Absolute Std. Dev.	Best- estimate Nominal Value	Best- estimate Absolute Std. Dev.
1	Air temperature (dry bulb), (K)	T_{db}	298.882	4.034	298.799	2.23
2	Dew point temperature (K)	T_{dp}	292.077	2.287	292.803	2.16
3	Inlet water temperature (K)	$T_{w,in}$	298.893	1.687	298.712	1.63
4	Atmospheric pressure (Pa)	P_{atm}	100588	408.26	100566	397.57
5	Wind speed (m/s)	V_w	1.859	0.941	1.794	0.783
6	Sum of loss coefficients above fill	k_{sum}	10	5	10.045	4.996
7	Dynamic viscosity of air at T=300 K (kg/m·s)	μ	$1.98 \cdot 10^{-5}$	$9.68 \cdot 10^{-7}$	$1.98 \cdot 10^{-5}$	$9.67 \cdot 10^{-7}$
8	Kinematic viscosity of air at T=300 K (m ² /s)	ν	$1.57 \cdot 10^{-5}$	$1.90 \cdot 10^{-6}$	$1.57 \cdot 10^{-5}$	$1.90 \cdot 10^{-6}$
9	Thermal conductivity of air at T=300 K (W/m·K)	k_{air}	0.02624	$1.58 \cdot 10^{-3}$	0.02624	$1.58 \cdot 10^{-3}$
10	Heat transfer coefficient multiplier	f_{ht}	1	0.5	1.00532	0.5
11	Mass transfer coefficient multiplier	f_{mt}	1	0.5	0.9342	0.496

CHAPTER 4. RESULTS

i	Model Independent Scalar Parameters (α_i)	Math. Notation	Original Nominal Value	Original Absolute Std. Dev.	Best- estimate Nominal Value	Best- estimate Absolute Std. Dev.
12	Fill section frictional loss multiplier	f	4	2	4.088	1.96
13	P _{vs} (T) parameters	a_0	25.5943	0.01	25.5943	0.01
14		a_1	-5229.89	4.4	-5229.92	4.4
15	C _{pa} (T) parameters	$a_{0,cpa}$	1030.5	0.294	1030.5	0.294
16		$a_{1,cpa}$	-0.19975	0.002	-0.19975	0.002
17		$a_{2,cpa}$	$3.97 \cdot 10^{-4}$	$3.35 \cdot 10^{-6}$	$3.97 \cdot 10^{-4}$	$3.35 \cdot 10^{-6}$
18	D _{av} (T) parameters	$a_{0,dav}$	$7.06 \cdot 10^{-9}$	0	$7.06 \cdot 10^{-9}$	0
19		$a_{1,dav}$	2.65322	0.003	2.65322	0.003
20		$a_{2,dav}$	$-6.17 \cdot 10^{-3}$	$2.30 \cdot 10^{-5}$	$-6.17 \cdot 10^{-3}$	$2.30 \cdot 10^{-5}$
21		$a_{3,dav}$	$6.55 \cdot 10^{-6}$	$3.80 \cdot 10^{-8}$	$6.55 \cdot 10^{-6}$	$3.80 \cdot 10^{-8}$
22	h _f (T) parameters	a_{0f}	-1143423	543	-1143423	543
23		a_{1f}	4186.50768	1.8	4186.50822	1.8
24	h _g (T) parameters	a_{0g}	2005743.99	1046	2005743.78	1046
25		a_{1g}	1815.437	3.5	1815.4363	3.5
26	Nusselt parameters	$a_{0,Nu}$	8.235	2.059	8.11039	2.055
27		$a_{1,Nu}$	0.00314987	0.00105	0.00314987	0.001
28		$a_{2,Nu}$	0.9902987	0.329	0.9902987	0.327
29		$a_{3,Nu}$	0.023	0.0088	0.023	0.0088
30	Cooling tower deck width in x-dir (m)	W_{dkx}	8.5	0.085	8.5	0.085
31	Cooling tower deck width in y-dir (m)	W_{dky}	8.5	0.085	8.5	0.085
32	Cooling tower deck height above ground (m)	Δz_{dk}	10	0.1	10	0.1
33	Fan shroud height (m)	Δz_{fan}	3	0.03	3	0.03

CHAPTER 4. RESULTS

i	Model Independent Scalar Parameters (α_i)	Math. Notation	Original Nominal Value	Original Absolute Std. Dev.	Best- estimate Nominal Value	Best- estimate Absolute Std. Dev.
34	Fan shroud inner diameter (m)	D_{fan}	4.1	0.041	4.1	0.041
35	Fill section height (m)	Δz_{fill}	2.013	0.02013	2.013	0.02013
36	Rain section height (m)	Δz_{rain}	1.633	0.01633	1.633	0.01633
37	Basin section height (m)	Δz_{bs}	1.168	0.01168	1.168	0.01168
38	Drift eliminator thickness (m)	Δz_{de}	0.1524	0.00152	0.1524	0.00152
39	Fill section equivalent diam- eter (m)	D_h	0.0381	0.00038	0.0381	0.00038
40	Fill section flow area (m ²)	A_{fill}	67.29	6.729	67.207	6.72
41	Fill section surface area (m ²)	A_{surf}	14221	3555.3	14005	3548.6
42	Prandtl number of air at T=80 °C	P_r	0.708	0.005	0.708	0.005
43	Wetted fraction of fill sur- face area	w_{tsa}	1	0	1	0
i	Boundary Parameters (α_i)	Math. Notation	Original Nominal Value	Original Absolute Std. Dev.	Best- estimate Nominal Value	Best- estimate Absolute Std. Dev.
44	Inlet water mass flow rate (kg/s)	$m_{w,in}$	44.0193	2.201	44.0696	2.199
45	Inlet air temperature (K)	$T_{a,in}$	294.40	4.034	299.841	2.73
46	Inlet air humidity ratio	ω_{in}	0.01379	0.00192	0.01406	0.00191
i	Special Dependent Parameters (α_i)	Math. Notation	Original Nominal Value	Original Absolute Std. Dev.	Best- estimate Nominal Value	Best- estimate Absolute Std. Dev.
47	Schmidt number	Sc	0.5999	0.0159	0.5999	0.0159

CHAPTER 4. RESULTS

4.3.3.2 Predicted Best-Estimated Response Values with Reduced Predicted Standard Deviations

Using the a priori matrices in Eqs. (4.13) - (4.16) together with the sensitivities listed in Tables 4.11 - 4.15 in Eq. (3.99), the following predicted response covariance matrix, \mathbf{C}_{rr}^{pred} , is obtained:

$$\mathbf{C}_{rr}^{pred} \equiv Cov \left([T_a^{(1)}]^{be}, [T_w^{(50)}]^{be}, [RH^{(1)}]^{be} \right) = \begin{pmatrix} 6.71 & 2.73 & -22.80 \\ 2.73 & 2.37 & -1.79 \\ -22.80 & -1.79 & 145.19 \end{pmatrix}. \quad (4.17)$$

The best-estimate response-parameter correlation matrix, $\mathbf{C}_{\alpha r}^{pred}$, is obtained by means of Eq. (3.100) in conjunction with the a priori matrices presented in Eqs. (4.13) - (4.16) and the sensitivities listed in Tables 4.11 - 4.15.

The best-estimate nominal values of the outlet air temperature, $T_a^{(1)}$; outlet water temperature $T_w^{(50)}$; and outlet air relative humidity, $RH^{(1)}$, have been computed using Eq. (3.98) coupled with the a priori matrices given in Eqs. (4.13) - (4.16) and the sensitivities listed in Tables 4.11 - 4.15. The resulting best-estimate nominal values are displayed in Table 4.26. To facilitate comparison, the corresponding measured and computed nominal values are also presented in this table. Note that there are no direct measurements for the outlet water flow rate, $m_w^{(50)}$ and the air mass flow rate m_a . For these two responses, therefore, the predicted best-estimate nominal values have been obtained by a forward re-computation using the best-estimate nominal parameter values listed in Table 4.25, while the predicted best estimate standard deviation for this response has been obtained by using “best-estimate” values in Eq. (3.96), i.e.,

$$[\mathbf{C}_{rr}^{comp}]^{be} = [\mathbf{S}_{r\alpha}]^{be} [\mathbf{C}_{\alpha\alpha}]^{be} [\mathbf{S}_{r\alpha}^\dagger]^{be} \quad (4.18)$$

CHAPTER 4. RESULTS

Table 4.26: Computed, measured, and optimal best-estimate nominal values and standard deviations for the outlet air temperature, outlet water temperature, outlet air relative humidity, outlet water mass flow rate and air mass flow rate responses for case 2.

Nominal Values and Standard Deviations		$T_a^{(1)}$ [K]	$T_w^{(50)}$ [K]	$RH^{(1)}$ [%]	$m_w^{(50)}$ [kg/s]	m_a [kg/s]
Measured						
	nominal value	299.11	298.10	89.61	—	—
	standard deviation	± 2.84	± 1.39	± 13.62	—	—
Computed						
	nominal value	298.79	297.42	99.80	43.91	15.84
	standard deviation	± 1.67	± 1.96	± 1.17	± 2.20	± 12.20
Best-estimate						
	nominal value	298.65	297.52	99.69	43.97	14.86
	standard deviation	± 1.57	± 1.38	± 1.09	± 2.19	± 8.34

The results presented in Table 4.26 indicate that, as anticipated, the predicted standard deviations are smaller than either the computed or the experimentally measured ones. This is consequential to utilizing the PM_CMPS methodology together with *consistent* computational and experimental information. Unspotted errors can often make the used information inconsistent; methods to confront these situations are discussed in [37]. It is also worth noting that the PM_CMPS methodology has reduced the predicted standard deviation for the water mass flow rate and for the air mass flow rate responses, despite the lack of experimentally measure data. This is due to the *global* characteristics of the PM_CMPS methodology to foresee a *simultaneous* combination of all the available data in the phase-space, yielding this way the aforementioned best-estimate predicted results; currently used data assimilation methodologies, on the other hand, proceed by combine the available information in a sequential way [38, 39].

4.4 Uncertainty Analysis and Predictive Modeling of Mechanical Draft Cases

The results of particular cases of case 1 and case 2 are shown, for verification purposes, in this section: the air conditions are in fact the same as in case 1 and 2, but the difference consists in the cooling tower being operated in mechanical draft mode, determining *a priori* the air mass flow rate through the cooling tower and therefore simplifying the governing equations system. The results shown are from [31, 32].

Following the same naming criteria used for case 1 and 2 in Chapter 2, we can list them as:

- **Case 3:** the cooling tower is operated in fan-on mode (mechanical draft) and the outlet air is in saturated conditions; just as case 1, this case is split into two subcases according to the inlet air conditions:
 - **Subcase I:** the inlet air is in unsaturated conditions; this means that unsaturated inlet air becomes saturated at a certain control volume of the fill section along the height of the cooling tower. This particular case of case 1a will be referred to as **case 3a**;
 - **Subcase II:** the inlet air is in saturated conditions: in this subcase, air is in saturated condition from the inlet through the outlet of the fill section, i.e., air is saturated in all the 49 control volumes. This particular case of case 1b will be referred to as **case 3b**.
- **Case 4:** the cooling tower is operated in fan-on mode (mechanical draft) and the outlet air is in unsaturated conditions; this is a particular case of case 2. Just as for case 2, in this case it is only possible for inlet air to be in unsaturated conditions as well, hence there is no need for subcases.

CHAPTER 4. RESULTS

For brevity reasons, only the predicted best-estimated response values with the relative reduced predicted standard deviations are hereby reported.

4.4.1 Predicted Best-Estimated Response Values with Reduced Predicted Standard Deviations for Case 3a

The *a priori* matrices for Case 3a are detailed in [32]. The four system responses are $T_a^{(1)}$, $T_w^{(50)}$, $RH^{(1)}$ and $m_w^{(50)}$. The air mass flow rate m_a is no longer a response, since its value is known being the cooling tower operated in mechanical draft mode.

The resulting best-estimate nominal values are displayed in Table 4.27. To facilitate comparison, the corresponding measured and computed nominal values are also presented in this table. Note that there are no direct measurements for the outlet water flow rate, $m_w^{(50)}$. For this response, therefore, the predicted best-estimate nominal value has been obtained by a forward re-computation using the best-estimate nominal parameter values listed in [32], while the predicted best estimate standard deviation for this response has been obtained by using “best-estimate” values in Eq. (3.96), i.e.,

$$[\mathbf{C}_{rr}^{comp}]^{be} = [\mathbf{S}_{r\alpha}]^{be} [\mathbf{C}_{\alpha\alpha}]^{be} [\mathbf{S}_{r\alpha}^\dagger]^{be} \quad (4.19)$$

The results presented in Table 4.27 indicate that, as anticipated, the predicted standard deviations are smaller than either the computed or the experimentally measured ones. More specifically, comparing to the best-estimated standard deviations, the experimentally measured standard deviations associated with the measured quantities for $T_a^{(1)}$, $T_w^{(50)}$ and $RH^{(1)}$ are reduced by 2.3%, 1.8% and 5.9%, respectively; whereas, the computed standard deviations associated with the computed quantities for $T_a^{(1)}$, $T_w^{(50)}$ and $RH^{(1)}$ are reduced by 22%, 38%, and 68%,

CHAPTER 4. RESULTS

respectively. As it can be seen, the improvements to the computed standard deviations are quite large, especially to the standard deviation of the computed outlet air relative humidity response. This is consequential to utilizing the PM_CMPS methodology together with consistent computational and experimental information. Unspotted errors can often make the used information inconsistent; methods to confront these situations are discussed in [37]. It is also worth noting that the PM_CMPS methodology has reduced the predicted standard deviation for the water mass flow rate response, despite the lack of experimentally measure data. This is due to the peculiar characteristic of the PM_CMPS methodology to foresee a simultaneous combination of all the available data in the phase-space, yielding this way the aforementioned best-estimate predicted results; currently used data assimilation methodologies, on the other hand, proceed by combine the available information in a sequential way [38, 39].

Table 4.27: Computed, measured, and optimal best-estimate nominal values and standard deviations for the outlet air temperature, outlet water temperature, outlet air relative humidity, and outlet water mass flow rate responses for case 3a.

Nominal Values and Standard Deviations		$T_a^{(1)}$ [K]	$T_w^{(50)}$ [K]	$RH^{(1)}$ [%]	$m_w^{(50)}$ [kg/s]
Measured					
	nominal value	294.24	294.71	101.14	—
	standard deviation	± 1.28	± 1.10	± 2.70	—
Computed					
	nominal value	295.22	294.24	100.29	43.75
	standard deviation	± 1.60	± 1.75	± 7.94	± 2.20
Best-estimate					
	nominal value	294.53	294.73	101.54	43.66
	standard deviation	± 1.25	± 1.08	± 2.54	± 2.19

4.4.2 Predicted Best-Estimated Response Values with Reduced Predicted Standard Deviations for Case 3b

The *a priori* matrices for Case 3b are detailed in [32]. The four system responses are $T_a^{(1)}$, $T_w^{(50)}$, $RH^{(1)}$ and $m_w^{(50)}$. The air mass flow rate m_a is no longer a response, since its value is known being the cooling tower operated in mechanical draft mode.

The resulting best-estimate nominal values are displayed in Table 4.28. To facilitate comparison, the corresponding measured and computed nominal values are also presented in this table. Note that there are no direct measurements for the outlet water flow rate, $m_w^{(50)}$. For this response, therefore, the predicted best-estimate nominal value has been obtained by a forward re-computation using the best-estimate nominal parameter values listed in [32], while the predicted best estimate standard deviation for this response has been obtained by using “best-estimate” values in Eq. (3.96), i.e.,

$$[\mathbf{C}_{rr}^{comp}]^{be} = [\mathbf{S}_{r\alpha}]^{be} [\mathbf{C}_{\alpha\alpha}]^{be} [\mathbf{S}_{r\alpha}^\dagger]^{be} \quad (4.20)$$

Table 4.28: Computed, measured, and optimal best-estimate nominal values and standard deviations for the outlet air temperature, outlet water temperature, outlet air relative humidity, and outlet water mass flow rate responses for case 3b.

Nominal Values and Standard Deviations		$T_a^{(1)}$ [K]	$T_w^{(50)}$ [K]	$RH^{(1)}$ [%]	$m_w^{(50)}$ [kg/s]
Measured					
	nominal value	294.77	295.17	101.73	—
	standard deviation	± 0.90	± 0.86	± 2.48	—
Computed					
	nominal value	295.84	294.97	101.99	43.76
	standard deviation	± 1.33	± 1.49	± 11.57	± 2.19
Best-estimate					
	nominal value	294.99	295.18	102.03	43.62
	standard deviation	± 0.88	± 0.85	± 2.41	± 2.18

CHAPTER 4. RESULTS

The results presented in Table 4.28 indicate that the predicted standard deviations are smaller than either the computed or the experimentally measured ones. More specifically, comparing to the best-estimated standard deviations, the experimentally measured standard deviations associated with the measured quantities for $T_a^{(1)}$, $T_w^{(50)}$ and $RH^{(1)}$ are reduced by 2.2%, 1.2% and 2.8%, respectively; whereas, the computed standard deviations associated with the computed quantities for $T_a^{(1)}$, $T_w^{(50)}$ and $RH^{(1)}$ are reduced by 34%, 43%, and 79%, respectively. Again, the computed standard deviations are substantially improved by the PM_CMPS methodology. Moreover, the standard deviation associated with the computed outlet water mass flow rate, $m_w^{(50)}$, is also reduced by 0.5%, even though the measurements are not available for this response. Unspotted errors can often make the used information inconsistent; methods to confront these situations are discussed in [37]. It is also worth noting that the PM_CMPS methodology has reduced the predicted standard deviation for the water mass flow rate response, despite the lack of experimentally measure data. This is due to the peculiar characteristic of the PM_CMPS methodology to foresee a simultaneous combination of all the available data in the phase-space, yielding this way the aforementioned best-estimate predicted results; currently used data assimilation methodologies, on the other hand, proceed by combine the available information in a sequential way [38, 39].

4.4.3 Predicted Best-Estimated Response Values with Reduced Predicted Standard Deviations for Case 3b

The *a priori* matrices for Case 4 are detailed in [31]. The four system responses are $T_a^{(1)}$, $T_w^{(50)}$, $RH^{(1)}$ and $m_w^{(50)}$. The air mass flow rate m_a is no longer a response, since its value is known being the cooling tower operated in mechanical draft mode.

CHAPTER 4. RESULTS

The resulting best-estimate nominal values are displayed in Table 4.29. To facilitate comparison, the corresponding measured and computed nominal values are also presented in this table. Note that there are no direct measurements for the outlet water flow rate, $m_w^{(50)}$. For this response, therefore, the predicted best-estimate nominal value has been obtained by a forward re-computation using the best-estimate nominal parameter values listed in [31], while the predicted best estimate standard deviation for this response has been obtained by using “best-estimate” values in Eq. (3.96), i.e.,

$$[\mathbf{C}_{rr}^{comp}]^{be} = [\mathbf{S}_{r\alpha}]^{be} [\mathbf{C}_{\alpha\alpha}]^{be} [\mathbf{S}_{r\alpha}^\dagger]^{be} \quad (4.21)$$

Table 4.29: Computed, measured, and optimal best-estimate nominal values and standard deviations for the outlet air temperature, outlet water temperature, outlet air relative humidity, and outlet water mass flow rate responses for case 4.

Nominal Values and Standard Deviations		$T_a^{(1)}$ [K]	$T_w^{(50)}$ [K]	$RH^{(1)}$ [%]	$m_w^{(50)}$ [kg/s]
Measured					
	nominal value	298.34	295.68	81.98	—
	standard deviation	± 3.36	± 1.59	± 15.89	—
Computed					
	nominal value	297.46	294.58	86.12	43.60
	standard deviation	± 3.30	± 2.78	± 14.90	± 2.21
Best-estimate					
	nominal value	298.45	295.67	82.12	43.67
	standard deviation	± 2.59	± 1.54	± 12.05	± 2.20

The results presented in Table 4.29 indicate that the predicted standard deviations are smaller than either the computed or the experimentally measured ones; again, the computed standard deviations are substantially improved by the PM_CMPS methodology. Moreover, the standard deviation associated with the computed outlet water mass flow rate, $m_w^{(50)}$, is also reduced by 0.5%, even though

CHAPTER 4. RESULTS

the measurements are not available for this response. Unspotted errors can often make the used information inconsistent; methods to confront these situations are discussed in [37]. It is also worth noting that the PM_CMPS methodology has reduced the predicted standard deviation for the water mass flow rate response, despite the lack of experimentally measure data. This is due to the peculiar characteristic of the PM_CMPS methodology to foresee a simultaneous combination of all the available data in the phase-space, yielding this way the aforementioned best-estimate predicted results; currently used data assimilation methodologies, on the other hand, proceed by combine the available information in a sequential way [38, 39].

Chapter 5

Discussion and Conclusions

The CTTool model, which has been validated in this thesis, is foreseen to be part of a facility modeling program suite, within which it is envisaged to be coupled to modules simulating the chemical processes which would provide the input for the cooling tower model, as well as to atmospheric transport models, which would couple the output of the cooling tower model to the external environment. Within this framework, the present work focused on performing sensitivity and uncertainty analysis, data assimilation, model calibration, model validation and best-estimate predictions with reduced uncertainties on a counter-flow, wet cooling tower model developed by Savannah River National Laboratory.

A relevantly more refined and efficient numerical method was developed and applied to the cooling tower model originally presented in [26]; this allowed to reach convergence for all the data sets, and increased the accuracy in computing the steady state distributions of the model's quantities of interest. The behavior of the cooling tower has been investigated under several different operating conditions; more specifically, three cases have been selected depending on the air conditions at the inlet of the cooling tower and the air conditions at the outlet of the cooling tower. For all the cases the following five model responses have been

CHAPTER 5. DISCUSSION AND CONCLUSIONS

selected: (i) the water mass flow rate at the outlet of the bottom control volume of the fill section of the cooling tower, $m_w^{(50)}$; (ii) the water temperature at the outlet of the bottom control volume of the fill section of the cooling tower, $T_w^{(50)}$; (iii) the air temperature at the outlet of the top control volume of the fill section of the cooling tower, $T_a^{(1)}$; (iv) the humidity ratio at the outlet of the top control volume of the fill section of the cooling tower, $RH^{(1)}$; and (v) the air mass flow rate at the outlet of the cooling tower, m_a .

Applying the general adjoint sensitivity analysis methodology, the sensitivities of the model responses to all the model parameters were calculated in an efficient and exact way by implementing the adjoint cooling tower sensitivity model. While the cooling tower governing system presents nonlinearity in the forward state function, the adjoint sensitivity model possesses the relevant feature of being linear in the adjoint functions, whose one-to-one correspondence to the forward state functions has been pointed out. As discussed, the utilization of the adjoint functions allows the simultaneous computation of the sensitivities of each model response to all of the 47 model parameters just running a single adjoint model computation; obtaining the same results making use of the forward model together with finite-differences methods would require 47 separate computations, with the relevant disadvantage of leading to approximate results of the sensitivities, as opposed to the exact ones yielded by applying the adjoint procedure.

The aforementioned adjoint functions have been obtained, by solving the adjoint sensitivity system, and thoroughly verified, in order to pave the way to the specific calculations necessary to yield the response sensitivities. These sensitivities have then been numerically computed for the subsequent realization of several operations, such as: (i) ranking the model parameters according to the magnitude of their contribution to response uncertainties; (ii) determining the propagation of uncertainties, in form of variances and covariances, of the parameters in the model

CHAPTER 5. DISCUSSION AND CONCLUSIONS

in order to quantify the uncertainties of the model responses; (iii) allowing predictive modeling operations, such as experimental data assimilation and model parameters calibration, with the aim to yield best-estimate predicted nominal values both for model parameters and responses, with correspondently reduced values for the predicted uncertainties associated.

More specifically, the ASAM was used to efficiently obtain the sensitivities of all the model responses to the model parameters, and therefore list, for each case, the magnitude of all the model parameters' contributions to the model responses' uncertainties. These sensitivities, whose exact values would have been impossible to obtain by using forward methods, and whose approximate values would have still been very computationally expensive to compute without the application of the ASAM, showed that the three cases analyzed yield sensitivity values very different from each other, despite the three cooling tower governing systems appearing very similar to each other. This phenomenon is particularly evident when analyzing and ranking the sensitivity values of the air humidity ratio and of the air mass flow rate responses with respect to the model parameters; the values of these sensitivities are shown in fact to change up to one order of magnitude from one case to the other. It was also shown that the air humidity ratio and of the air mass flow rate are not only the responses presenting the highest sensitivity values with respect to a few key-parameters, but also those showing non-negligible sensitivity values to the highest number of parameters.

By making use of the computed sensitivities within the framework of the “predictive modeling for coupled multi-physics systems” (PM_CMPS) methodology, explicit mathematical formulations have been derived for the best-estimate nominal values of the model parameters and responses, together with the best-estimate reduced standard deviations of the predicted model parameters and responses. The results stemming from this work show that the PM_CMPS procedure allows

CHAPTER 5. DISCUSSION AND CONCLUSIONS

to improve the predicted standard deviation reducing them to values smaller than the smallest between the standard deviation values relative to computed and measured results, even in the case of responses for which experimentally measured values are not available. The only exception to what just stated occurred in the framework of the mixed, partially saturated case: the best-estimate standard deviation value for the air mass flow rate response is slightly bigger than the standard deviation value relative to the computed response. This exception is due to the simultaneous use of all the available data, which causes the responses nominal values (and their respective standard deviations) to be mutually correlated because of the covariances between model parameters and responses ($\mathbf{C}_{r\alpha} \neq 0$). In order to verify the correctness of the calculation performed, a separate case without considering the covariances between model parameters and responses ($\mathbf{C}_{r\alpha} = 0$) has been developed and analyzed, and the results confirmed the theory expectations, yielding all predicted standard deviations smaller than either the computed or the experimentally measured ones, even for the air mass flow rate.

In the PM_CMPS framework, the standard deviation values of the responses for which no experimental data are available are only influenced by the correlations to the other responses' values, both experimental and computed. For this reason, therefore, the results of the fully-correlated model (with $\mathbf{C}_{r\alpha} \neq 0$) have been chosen: in fact, despite the slightly bigger standard deviation for the air mass flow rate, which can be interpreted as a consequence of all the information simultaneously used in the PM_CMPS methodology, those results are to be considered the most accurate, since they were obtained by means of the simultaneous using of all the available data. All the responses for which both experimental and computational results are available have their standard deviations reduced by the application of the predictive modeling methodology. This is due to the peculiar characteristic of the PM_CMPS methodology to foresee a simultaneous

CHAPTER 5. DISCUSSION AND CONCLUSIONS

combination of all the available data in the phase-space, yielding this way the aforementioned best-estimate predicted results; currently used data assimilation methodologies, on the other hand, proceed by combining the available information in a sequential way [40, 41]. The reduced standard deviation values have to be attributed to the coupled application of the PM_CMPS methodology together with consistent (as opposed to discrepant) computational and experimental information. Unspotted errors can often make the used information inconsistent; methods to confront these situations are discussed in [39].

The adjoint sensitivity analysis methodology utilized for the exact and efficient computation of the 1st-order response sensitivities to model parameters has been recently extended to calculate the 2nd-order response sensitivities with respect to parameters for linear [5, 6] and nonlinear [7, 8] large-scale systems. As discussed in [5-8], the major effects of the 2nd-order response sensitivities on the computed moments of the response distribution are: (a) causing the “response expected value” to differ from the “response nominal value”; and (b) a decisive contribution in causing asymmetries in the distribution of the model response. It is worth noting that ignoring second-order sensitivities would void the third-order response correlations, causing the skewness of the response to be overlooked. As a natural consequence, any occurrence falling in a response’s long/short tails, as it happens for uncommon but relevant events (e.g., major accidents, catastrophes), would most probably be ignored. Current efforts are aimed at extending the adjoint sensitivity analysis and the PM_CMPS methodologies to further generalized applications, in order to make possible the computation of 3rd- and higher-order sensitivities and response distributions. The possibility to exactly and efficiently compute high-order response sensitivities for large-scale systems is expected to provide a relevant contribution to the areas of uncertainty quantification, model validation, reduced-order modeling, and predictive modeling/data assimilation.

Appendix A

Statistical Analysis of Experimentally Measured Responses

Starting from April, 2004 to August, 2004, a total of 8079 benchmark data sets for F-area cooling towers (fan-off mode) were measured and recorded at SRNL (Savannah River National Laboratory) for F-Area Cooling Towers, one every fifteen minutes [33]. In each one of these data sets the following (four) measured quantities are contained: (i) outlet air temperature measured with the “Tidbit” sensor, which will be referred to in the following as $T_{a,out(Tidbit)}$; (ii) outlet air temperature measured with the “Hobo” sensor, which will be referred to in the following as $T_{a,out(Hobo)}$; (iii) outlet water temperature, which will be referred to as $T_{w,out}^{meas}$; (iv) outlet air relative humidity, which will be referred to as RH^{meas} . SRNL compared these measurements to the numerical results obtained by using their CTTool code [26] as far the air exit relative humidity (RH) is regarded; a data set is intended as saturated if the computed value of RH falls in the super saturation range (equal to or greater than 100%). With this procedure, 667 data

APPENDIX A. STATISTICAL ANALYSIS OF MEASURED RESPONSES

sets out of the 8079 complexively measured have been identified as “saturated”.

These 667 saturated points are further separated into two subcases based on the air inlet boundary conditions at the fill section entrance. As already mentioned, case 1a describes a situation in which air enters the fill section in unsaturated condition, but it gets saturated before reaching the outlet of the fill section; in case 1b air enters the fill section already saturated, exiting the fill section also saturated. Among the 667 saturated data sets, 377 of them have unsaturated air inlet boundary conditions, thus they are grouped into case 1a; whereas the other 290 data sets have saturated air inlet boundary conditions at the fill section entrance, thus they are grouped into case 1b. In other 6717 benchmark data sets the air conditions are always unsaturated; hence these data sets are considered to belong to case 2.

Histogram plots of these measurement sets (each set containing measurements of $T_{a,out(Tidbit)}$, $T_{a,out(Hobo)}$, $T_{w,out}^{meas}$, and RH^{meas}), together with statistical analyses thereof are presented in Section A.1 for case 1a, in Section A.2 for case 1b and in Section A.3 for case 2. The measured outlet (exit) air relative humidity, RH^{meas} , was obtained using Hobo humidity sensors. The accuracy of these sensors is depicted in Figure A.1, which indicates the following tolerances (standard deviations): $\pm 2.5\%$ for relative humidity from 10 to 90%; between $\pm 2.5\%$ and $\pm 3.5\%$ for relative humidity from 90% to 95%; and $\pm 3.5\% \sim \pm 4.0\%$ from 95 to 100%. However, when exposed to relative humidity above 95%, the maximum sensor error may temporally increase by an additional 1%, so that the error can reach values between $\pm 4.5\%$ to $\pm 5.0\%$ for relative humidity from 95 to 100%.

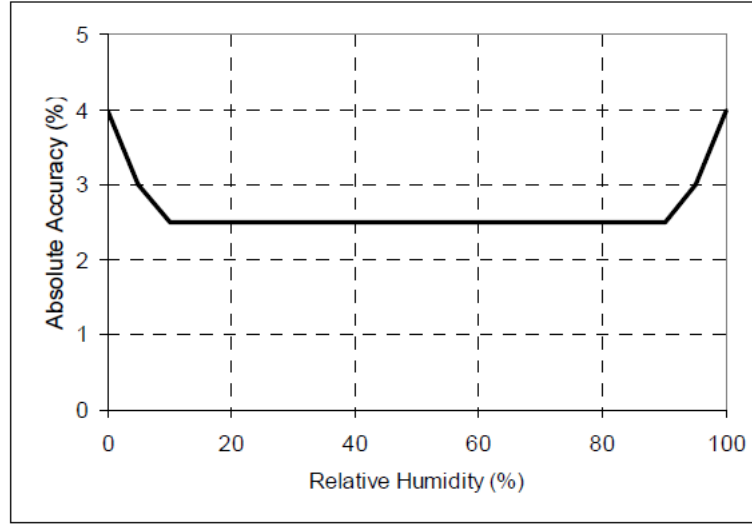


Figure A.1: Humidity sensor accuracy plot (adopted from the specification of HOBO Pro v2).

A.1 Statistical Analysis of experimentally measured responses for Case 1a: Fan Off, Saturated Outlet Air Conditions, with Inlet Air Unsaturated

A total of 377 measured data sets are grouped into case 1a, as they are considered according to the results produced by CTTool code to be “saturated” at the outlet of the fill section, and for each data set, air enters the fill section in unsaturated condition. Although the computed relative humidity for each of the 377 data sets is greater than 100%, the measured relative humidity RH^{meas} actually spans the range from 95.5% to 104.1%. However, if the humidity sensor’s tolerance (standard deviation, as shown in Figure A.1) is taken into account, it would make it possible for a measurement with RH^{meas} in the range of 95% \sim 105% to be nevertheless “saturated”. Figure A.2 shows the histogram plot of the

APPENDIX A. STATISTICAL ANALYSIS OF MEASURED RESPONSES

measured outlet air relative humidity for the 377 benchmark data sets which were considered as “saturated”. This plot, as well as all of the other histogram plots in this work, has its total respective area normalized to unity. As shown in this figure, the measured relative humidity RH^{meas} values fall in a range spanning from 95.5% to 104.1% (which are both within the 95% \sim 105% range limit).

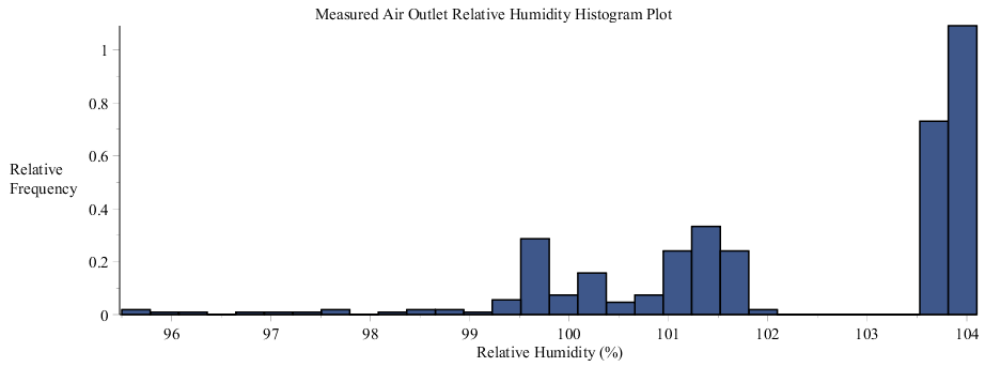


Figure A.2: Histogram plot of the measured air outlet relative humidity, within the 377 data sets collected by SRNL from F-Area cooling towers for case 1a.

The statistical properties of the (measured air outlet relative humidity) distribution shown in Figure A.2 have been computed using standard packages, and are presented in Table A.1. These statistical properties will be needed for the uncertainty quantification and predictive modeling computations presented in the main body of this work.

Table A.1: Statistics of the air outlet relative humidity distribution [%] for case 1a.

Minimum	Maximum	Range	Mean	Std.Dev.	Variance	Skewness	Kurtosis
95.5	104.1	8.6	102.28	1.92	3.68	-0.83	3.03

The histogram plots and their corresponding statistical characteristics of the 377 data sets for the other measurements, namely for: the outlet air temperature $[T_{a,out}(Tidbit)]$ measured using the “Tidbit” sensors; the outlet air temperature

APPENDIX A. STATISTICAL ANALYSIS OF MEASURED RESPONSES

$[T_{a,out(Hobo)}]$ measured using the “Hobo” sensors; and the outlet water temperature $[T_{w,out}^{meas}]$ are reported below in Figures A.3 through A.6, and Tables A.2 through A.5, respectively.

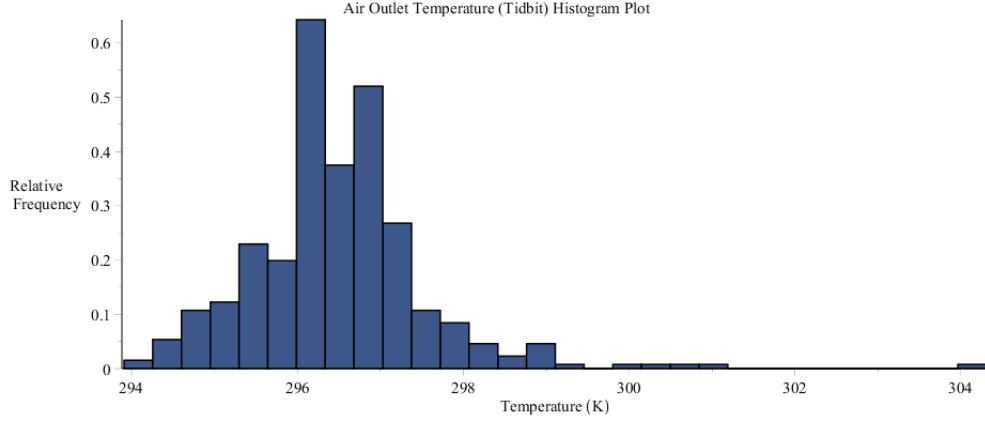


Figure A.3: Histogram plot of the air outlet temperature measured using “Tidbit” sensors, within the 377 data sets collected by SRNL from F-Area cooling towers for case 1a.

Table A.2: Statistics of the air outlet temperature distribution [K], measured using “Tidbit” sensors for case 1a.

Minimum	Maximum	Range	Mean	Std.Dev.	Variance	Skewness	Kurtosis
293.91	304.31	10.4	296.79	1.06	1.12	1.71	12.18

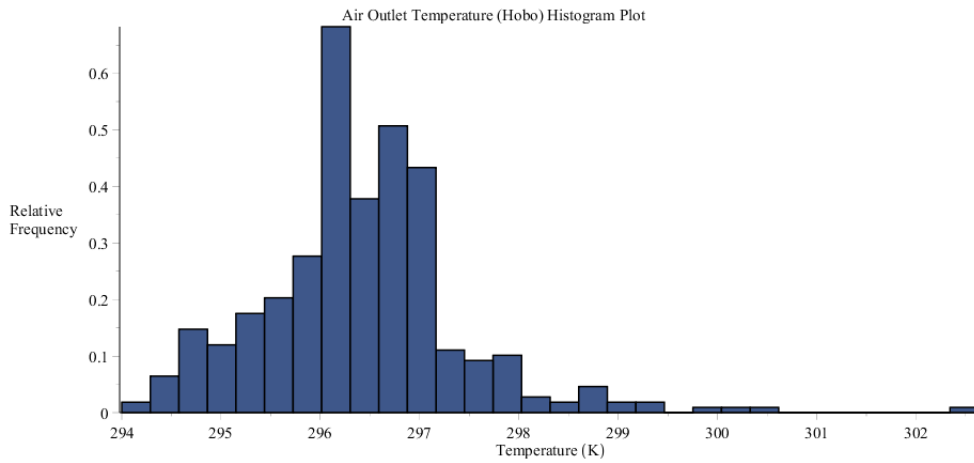


Figure A.4: Histogram plot of the air outlet temperature measured using “Hobo” sensors, within the 377 data sets collected by SRNL from F-Area cooling towers for case 1a.

APPENDIX A. STATISTICAL ANALYSIS OF MEASURED RESPONSES

Table A.3: Air outlet temperature distribution statistics [K], measured using “Hobo” sensors for case 1a.

Minimum	Maximum	Range	Mean	Std.Dev.	Variance	Skewness	Kurtosis
294.00	302.63	8.63	296.41	1.01	1.02	1.08	7.68

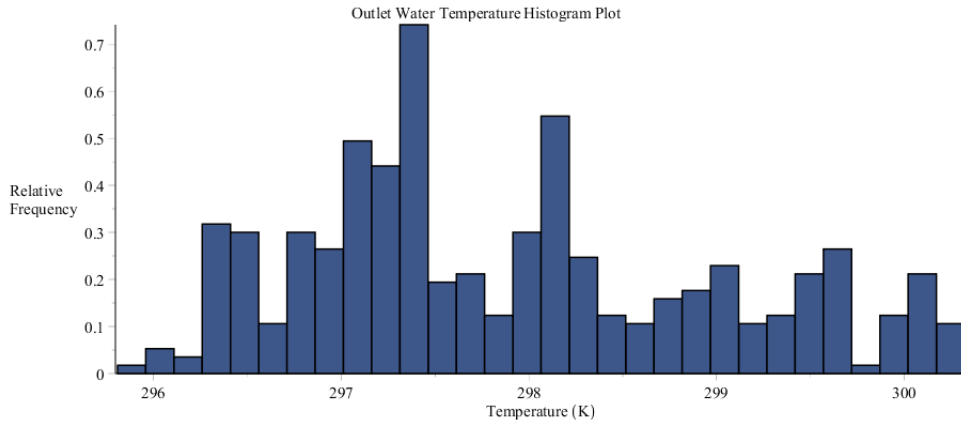


Figure A.5: Histogram plot of water outlet temperature measurements, within the 377 data sets collected by SRNL from F-Area cooling towers for case 1a.

Table A.4: Water outlet temperature [K] distribution statistics for case 1a.

Minimum	Maximum	Range	Mean	Std.Dev.	Variance	Skewness	Kurtosis
295.81	300.32	4.51	297.91	1.10	1.21	0.46	2.25

Putting the above-mentioned four measured responses in the following order:
 (i) outlet air temperature $T_{a,out(Tidbit)}$; (ii) outlet air temperature $T_{a,out(Hobo)}$; (iii) outlet water temperature $T_{w,out}^{meas}$; and (iv) outlet air relative humidity RH_{out}^{meas} , yields the following “measured response covariance matrix”, denoted as:

APPENDIX A. STATISTICAL ANALYSIS OF MEASURED RESPONSES

$$\begin{aligned}
& Cov(T_{a,out(Tidbit)}, T_{a,out(Hobo)}, T_{w,out}^{meas}, RH_{out}^{meas}) \\
&= \begin{pmatrix} 1.12 & 1.05 & 0.62 & -0.07 \\ 1.05 & 1.02 & 0.59 & -0.003 \\ 0.62 & 0.59 & 1.21 & -0.64 \\ -0.07 & -0.003 & -0.64 & 3.68 \end{pmatrix} \quad (A.1)
\end{aligned}$$

For the future purposes of uncertainty quantification, data assimilation, model calibration and predictive modeling, the data measurements provided by the “Tidbit” and “Hobo” temperature sensors can be combined into an “averaged” data set of measured air outlet temperatures, which will be indicated as $T_{a,out}^{meas}$. The histogram plot and corresponding statistical characteristics of this averaged quantity are shown in Figure A.6 and Table A.5, respectively.

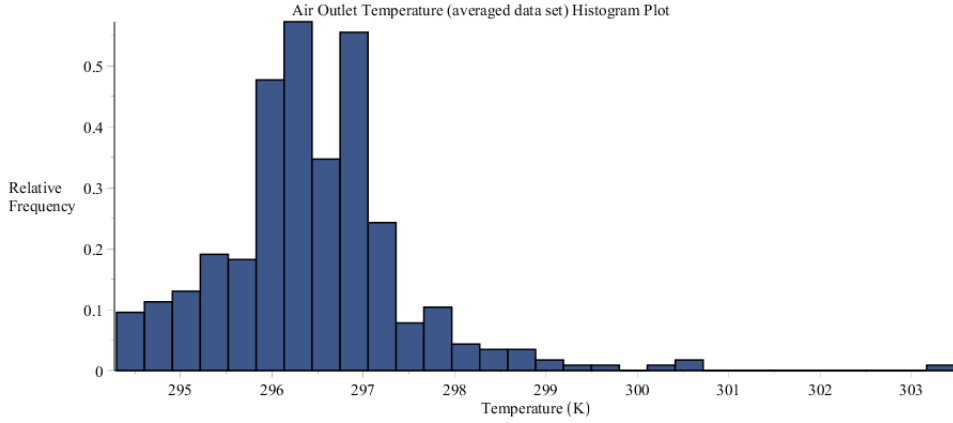


Figure A.6: Histogram plot of air outlet temperatures averaged from Figures A.3 and A.4.

Table A.5: Statistics of the averaged air outlet temperature distribution [K] for case 1a.

Minimum	Maximum	Range	Mean	Std.Dev.	Variance	Skewness	Kurtosis
294.3	303.47	9.17	296.45	1.03	1.06	1.40	9.76

APPENDIX A. STATISTICAL ANALYSIS OF MEASURED RESPONSES

Calculating the covariance matrix, denoted as $[Cov(T_{a,out}^{meas}, T_{w,out}^{meas}, RH_{out}^{meas})]_{data}$, for all of the considered experimental data points for the averaged outlet air temperature $[T_{a,out}^{meas}]$, the outlet water temperature $[T_{w,out}^{meas}]$, and the outlet air relative humidity $[RH_{out}^{meas}]$, yields the following covariance matrix:

$$[Cov(T_{a,out}^{meas}, T_{w,out}^{meas}, RH_{out}^{meas})]_{data} = \begin{pmatrix} 1.06 & 0.61 & -0.04 \\ 0.61 & 1.21 & -0.65 \\ -0.04 & -0.65 & 3.68 \end{pmatrix} \quad (A.2)$$

A comparison between the results in Eqs. (A.1) and (A.2) makes clear that the elimination of the second column and row in Eq. (A.1) yields a 3-by-3 matrix which has entries basically equivalent to the covariance matrix shown in Eq. (A.2). Therefore, this means that the temperature distributions measured by the “Tidbit” and “Hobo” sensors do not need to be dealt with as separate data sets for the purposes of uncertainty quantification and predictive modeling.

The standard deviation of the humidity sensor utilized for the measurements ($\sigma_{sensor} = 5.0\%$ for the response $RH^{(1)}$) have been already considered for the data at the 100%-saturation point by including in the category of the “saturated” data sets those that have their respective measured relative humidity, RH^{meas} , between 95.5% and 104.1%. In addition to that, the respective uncertainties of the temperature sensors (standard deviations, $\sigma_{sensor} = 0.2K$ for both responses $T_a^{(1)}$ and $T_w^{(50)}$) must also be taken into consideration for the 377 data sets. The measuring methods and devices are not dependent with respect to each other, therefore the data standard deviation $\sigma_{statistic}$, stemming from the statistical analysis of the 377 benchmark data sets, and the sensor standard deviation, σ_{sensor} , stemming from the instrument’s uncertainty, must stack according to the well-known formula of “addition of the variances of uncorrelated variates”, i.e.:

$$\sigma = \sqrt{\sigma_{statistic}^2 + \sigma_{sensor}^2} \quad (A.3)$$

APPENDIX A. STATISTICAL ANALYSIS OF MEASURED RESPONSES

Coupling the above relation with the result presented in Eq. (A.2) will lead to incremented values of the variances on the diagonal of the respective “measured covariance matrix”; this new form of the covariance matrix which will be denoted as $Cov(T_{a,out}^{meas}, T_{w,out}^{meas}, RH_{out}^{meas})$. The obtained result is:

$$Cov(T_{a,out}^{meas}, T_{w,out}^{meas}, RH_{out}^{meas}) = \begin{pmatrix} 1.10 & 0.61 & -0.04 \\ 0.61 & 1.25 & -0.64 \\ -0.04 & -0.64 & 3.68 \end{pmatrix} \quad (A.4)$$

In the predictive modeling formalism (which includes uncertainty quantification, data assimilation, and model calibration) the covariance matrix between the measured parameters and responses is required as an input. In the case of interest, all the parameters and responses can be considered as uncorrelated, excepting the measured responses considered in this Appendix and the measured parameters listed in Appendix B. The “parameter-response” covariance matrix in Eq. (A.5), indicated as $Cov(T_{a,out}^{meas}, T_{w,out}^{meas}, RH_{out}^{meas}, \alpha_1, \dots, \alpha_{47})$, refers to the above mentioned parameters (namely: dry-bulb air temperature, T_{db} ; dew-point air temperature, T_{dp} , inlet water temperature, $T_{w,in}$, atmospheric pressure, P_{atm} and wind speed V_w) and responses (i.e., average outlet air temperature, outlet water temperature, and outlet air relative humidity):

$$Cov(T_{a,out}^{meas}, T_{w,out}^{meas}, RH_{out}^{meas}, \alpha_1, \dots, \alpha_{47}) = \begin{pmatrix} 1.53 & 1.01 & 0.76 & -104.46 & 0.11 & 0 & \dots & 0 \\ 1.10 & 1.08 & 1.28 & -111.01 & 0.12 & 0 & \dots & 0 \\ 0.05 & 0.34 & -0.75 & 76.60 & -0.25 & 0 & \dots & 0 \end{pmatrix} \quad (A.5)$$

A.2 Statistical Analysis of experimentally measured responses for Case 1b: Fan Off, Saturated Outlet Air Conditions, with Inlet Air Saturated

A total of 290 measured data sets are grouped into case 1b, as they are considered according to the results produced by CTTool code to be “saturated” at the outlet of the fill section, and for each data set, air enters the fill section in saturated condition. Although the computed relative humidity for each of the 290 data sets is greater than 100%, the measured relative humidity RH^{meas} actually spans the range from 98.8% to 104.1%. However, if the humidity sensor’s tolerance (standard deviation, as shown in Figure A.1) is taken into account, it would make it possible for a measurement with RH^{meas} in the range of 95% \sim 105% to be nevertheless “saturated”. Consequently, all the 290 benchmark data sets have their RH^{meas} falling into the 95% \sim 105% range, therefore they were all considered as valid “saturated” data sets.

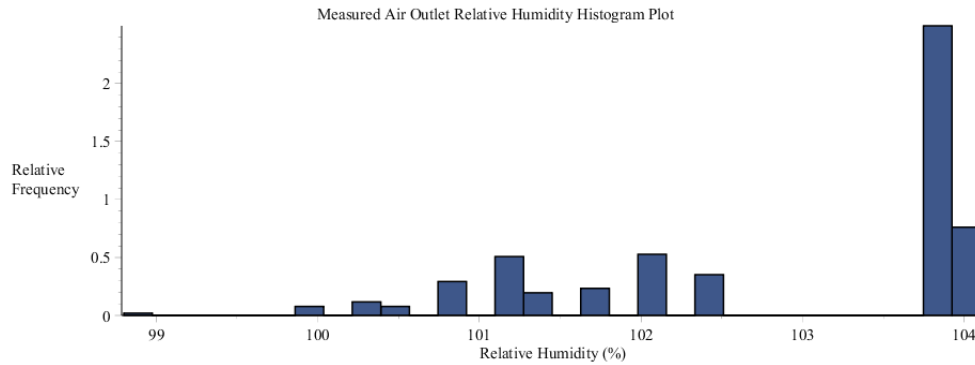


Figure A.7: Histogram plot of the measured air outlet relative humidity, within the 290 data sets collected by SRNL from F-Area cooling towers for case 1b.

Figure A.7 shows the histogram plot of the measured air outlet relative hu-

APPENDIX A. STATISTICAL ANALYSIS OF MEASURED RESPONSES

midity for the 290 benchmark data sets, which were considered as “saturated”. As shown in this figure, the measured relative humidity RH^{meas} spans the range from 98.8% to 104.1%.

The statistical properties of the (measured air outlet relative humidity) distribution shown in Figure A.7 have been computed using standard packages, and are presented in Table A.6. These statistical properties will be needed for the uncertainty quantification and predictive modeling computations presented in the main body of this work.

Table A.6: Statistics of the air outlet relative humidity distribution [%] for case 1b.

Minimum	Maximum	Range	Mean	Std.Dev.	Variance	Skewness	Kurtosis
98.8	104.1	5.3	102.83	1.28	1.65	-0.72	2.07

The histogram plots and their corresponding statistical characteristics of the 290 data sets for the other measurements, namely for: the outlet air temperature $[T_{a,out}(Tidbit)]$ measured using the “Tidbit” sensors; the outlet air temperature $[T_{a,out}(Hobo)]$ measured using the “Hobo” sensors; and the outlet water temperature $[T_{w,out}^{meas}]$ are reported below in Figures A.8 through A.10, and Tables A.7 through A.9, respectively.

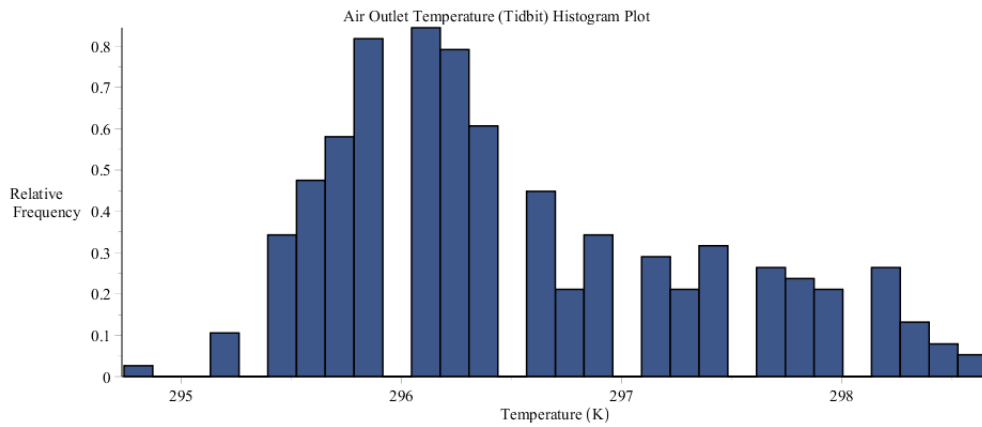


Figure A.8: Histogram plot of the air outlet temperature measured using “Tidbit” sensors, within the 290 data sets collected by SRNL from F-Area cooling towers for case 1b.

APPENDIX A. STATISTICAL ANALYSIS OF MEASURED RESPONSES

Table A.7: Statistics of the air outlet temperature distribution [K], measured using “Tidbit” sensors for case 1b.

Minimum	Maximum	Range	Mean	Std.Dev.	Variance	Skewness	Kurtosis
294.74	298.66	3.92	296.53	0.84	0.70	0.66	2.51

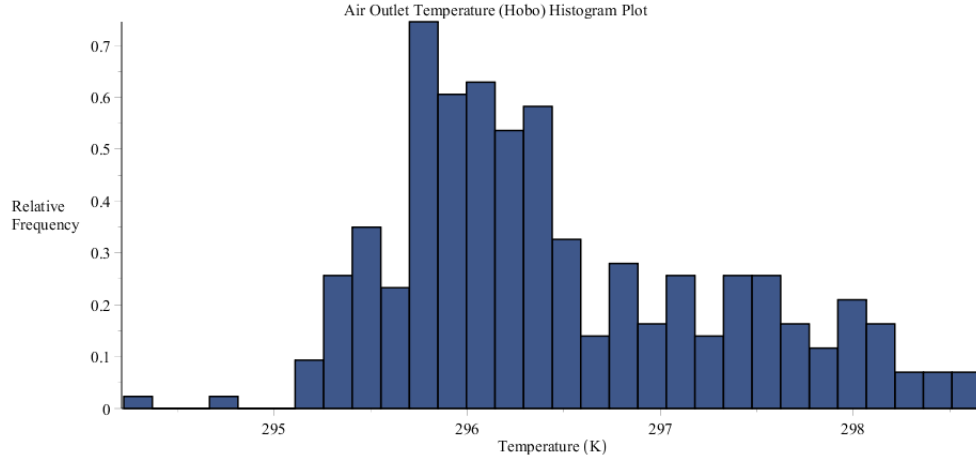


Figure A.9: Histogram plot of the air outlet temperature measured using “Hobo” sensors, within the 290 data sets collected by SRNL from F-Area cooling towers for case 1b.

Table A.8: Air outlet temperature distribution statistics [K], measured using “Hobo” sensors for case 1a.

Minimum	Maximum	Range	Mean	Std.Dev.	Variance	Skewness	Kurtosis
294.22	298.66	4.44	296.47	0.85	0.72	0.62	2.63

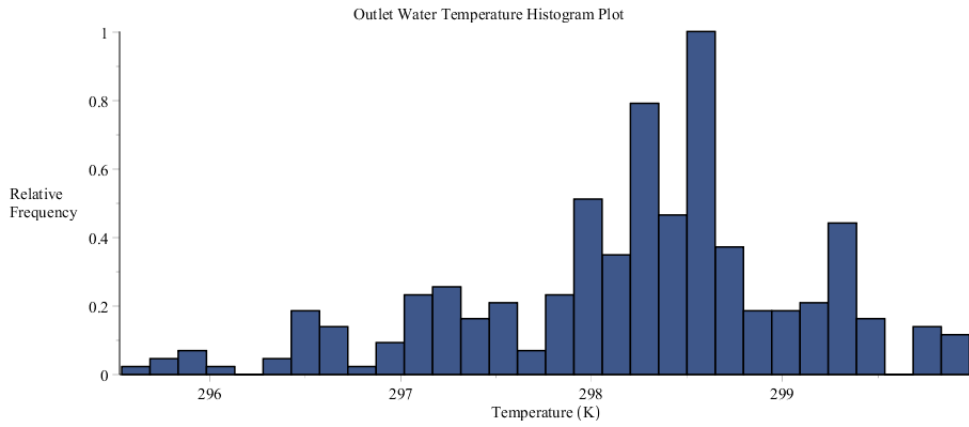


Figure A.10: Histogram plot of water outlet temperature measurements, within the 290 data sets collected by SRNL from F-Area cooling towers for case 1b.

APPENDIX A. STATISTICAL ANALYSIS OF MEASURED RESPONSES

Table A.9: Water outlet temperature [K] distribution statistics for case 1a.

Minimum	Maximum	Range	Mean	Std.Dev.	Variance	Skewness	Kurtosis
295.54	299.98	4.44	298.21	0.87	0.75	-0.60	3.34

Putting the above-mentioned four measured responses in the following order:
 (i) outlet air temperature $T_{a,out(Tidbit)}$; (ii) outlet air temperature $T_{a,out(Hobo)}$; (iii)
 outlet water temperature $T_{w,out}^{meas}$; and (iv) outlet air relative humidity RH_{out}^{meas} ,
 yields the following “measured response covariance matrix”, denoted as:

$$\begin{aligned}
 &Cov(T_{a,out(Tidbit)}, T_{a,out(Hobo)}, T_{w,out}^{meas}, RH_{out}^{meas}) \\
 &= \begin{pmatrix} 0.70 & 0.71 & 0.19 & 0.13 \\ 0.71 & 0.72 & 0.18 & 0.14 \\ 0.19 & 0.18 & 0.75 & 0.21 \\ 0.13 & 0.14 & 0.21 & 1.65 \end{pmatrix} \quad (A.6)
 \end{aligned}$$

For the future purposes of uncertainty quantification, data assimilation, model calibration and predictive modeling, the data measurements provided by the “Tidbit” and “Hobo” temperature sensors can be combined into an “averaged” data set of measured air outlet temperatures, which will be indicated as $T_{a,out}^{meas}$.

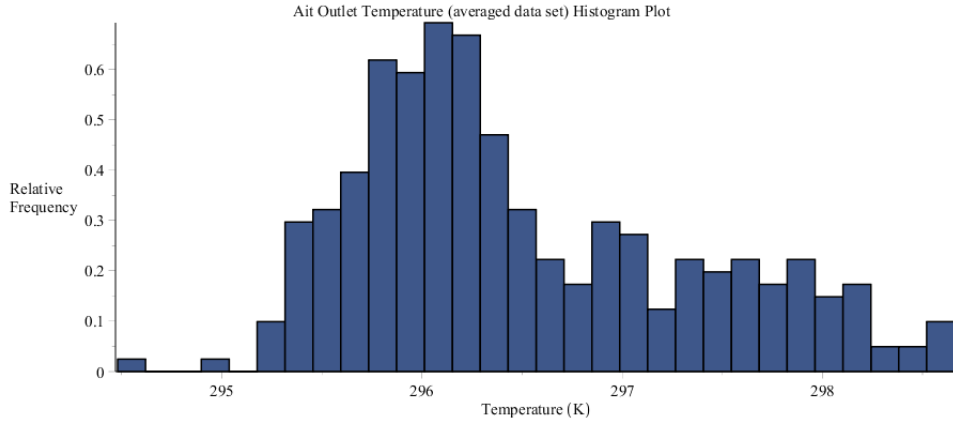


Figure A.11: Histogram plot of air outlet temperatures averaged from Figures A.8 and A.9.

APPENDIX A. STATISTICAL ANALYSIS OF MEASURED RESPONSES

Table A.10: Statistics of the averaged air outlet temperature distribution [K] for case 1b.

Minimum	Maximum	Range	Mean	Std.Dev.	Variance	Skewness	Kurtosis
294.48	298.66	4.18	296.50	0.84	0.71	0.65	2.56

The histogram plot and corresponding statistical characteristics of the averaged temperature $T_{a,out}^{meas}$ are shown in Figure A.11 and Table A.10, respectively.

Calculating the covariance matrix, denoted as $[Cov(T_{a,out}^{meas}, T_{w,out}^{meas}, RH_{out}^{meas})]_{data}$, for all of the considered experimental data points for the averaged outlet air temperature $[T_{a,out}^{meas}]$, the outlet water temperature $[T_{w,out}^{meas}]$, and the outlet air relative humidity $[RH_{out}^{meas}]$, yields the following covariance matrix:

$$[Cov(T_{a,out}^{meas}, T_{w,out}^{meas}, RH_{out}^{meas})]_{data} = \begin{pmatrix} 0.71 & 0.18 & 0.14 \\ 0.18 & 0.75 & 0.21 \\ 0.14 & 0.21 & 1.65 \end{pmatrix} \quad (A.7)$$

A comparison between the results in Eqs. (A.6) and (A.7) makes clear that the elimination of the second column and row in Eq. (A.6) yields a 3-by-3 matrix which has entries basically equivalent to the covariance matrix shown in Eq. (A.7). Therefore, this means that the temperature distributions measured by the “Tidbit” and “Hobo” sensors do not need to be dealt with as separate data sets for the purposes of uncertainty quantification and predictive modeling.

The standard deviation of the humidity sensor utilized for the measurements ($\sigma_{sensor} = 5.0\%$ for the response $RH^{(1)}$) have been already considered for the data at the 100%-saturation point by including in the category of the “saturated” data sets those that have their respective measured relative humidity, RH^{meas} , between 95.5% and 104.1%. In addition to that, the respective uncertainties of the temperature sensors (standard deviations, $\sigma_{sensor} = 0.2K$ for both responses $T_a^{(1)}$ and $T_w^{(50)}$) must also be taken into consideration for the 290 data sets. Using

APPENDIX A. STATISTICAL ANALYSIS OF MEASURED RESPONSES

the relation in the above Eq. (A.3) in conjunction with the result presented in Eq. (A.7) will lead to an increase of the variances on the diagonal of the respective “measured covariance matrix”. The final result obtained is:

$$Cov(T_{a,out}^{meas}, T_{w,out}^{meas}, RH_{out}^{meas}) = \begin{pmatrix} 0.75 & 0.18 & 0.14 \\ 0.18 & 0.79 & 0.21 \\ 0.14 & 0.21 & 1.65 \end{pmatrix} \quad (A.8)$$

In the predictive modeling formalism (which includes uncertainty quantification, data assimilation, and model calibration) the covariance matrix between the measured parameters and responses is required as an input. In the case of interest, all the parameters and responses can be considered as uncorrelated, excepting the measured responses considered in this Appendix and the measured parameters listed in Appendix B. The “parameter-response” covariance matrix in Eq. (A.9), indicated as $Cov(T_{a,out}^{meas}, T_{w,out}^{meas}, RH_{out}^{meas}, \alpha_1, \dots, \alpha_{47})$, refers to the above mentioned parameters (namely: dry-bulb air temperature, T_{db} ; dew-point air temperature, T_{dp} , inlet water temperature, $T_{w,in}$, atmospheric pressure, P_{atm} and wind speed V_w) and responses (i.e., average outlet air temperature, outlet water temperature, and outlet air relative humidity):

$$Cov(T_{a,out}^{meas}, T_{w,out}^{meas}, RH_{out}^{meas}, \alpha_1, \dots, \alpha_{47}) = \begin{pmatrix} 0.45 & 0.52 & 0.52 & 1.12 & 0.007 & 0 & \dots & 0 \\ 0.50 & 0.55 & 0.60 & -51.14 & -0.13 & 0 & \dots & 0 \\ 0.02 & 0.08 & 0.06 & 123.51 & -0.23 & 0 & \dots & 0 \end{pmatrix} \quad (A.9)$$

A.3 Statistical Analysis of experimentally measured responses for Case 2: Fan Off, Unsaturated Air Conditions

Histogram plots of the 6717 measurement sets considered for case 2 (each set containing measurements of $T_{\alpha,out(Tidbit)}$, $T_{\alpha,out(Hobo)}$, $T_{w,out}^{meas}$, and RH^{meas}), together with statistical analyses thereof are presented in this section of the Appendix A. As shown in Figure A.12, although the computed relative humidity for each of the 6717 data sets is less than 100%, the measured relative humidity RH^{meas} actually spans the range from 33.0% to 104.1%; in this range, 4925 data sets have their respective RH^{meas} less than 100% while the other 1792 data sets have their respective RH^{meas} over 100%. This situation is nevertheless consistent with the range of the sensors when their tolerances (standard deviations) are taken into account, which would make it possible for a measurement with $RH^{meas} = 105\%$ to be nevertheless “unsaturated”. Consequently, all the 6717 benchmark data sets plotted in Figure A.12, were considered as “unsaturated”, since their respective RH^{meas} was below the 105% threshold.

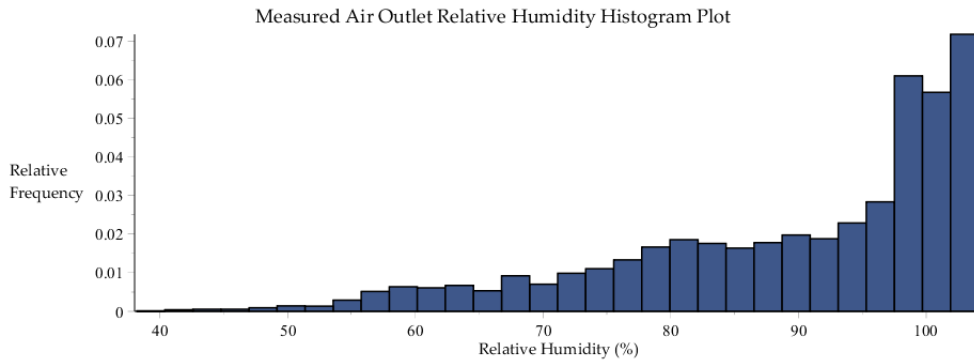


Figure A.12: Histogram plot of the measured air outlet relative humidity, within the 6717 data sets collected by SRNL from F-Area cooling towers for case 2.

APPENDIX A. STATISTICAL ANALYSIS OF MEASURED RESPONSES

The statistical properties of the (measured air outlet relative humidity) distribution shown in Figure A.12 have been computed using standard packages, and are presented in Table A.11. These statistical properties will be needed for the uncertainty quantification and predictive modeling computations presented in the main body of this work.

Table A.11: Statistics of the air outlet relative humidity distribution [%] for case 2.

Minimum	Maximum	Range	Mean	Std.Dev.	Variance	Skewness	Kurtosis
38.2	104.1	65.9	89.61	13.63	185.72	-1.01	3.22

The histogram plots and their corresponding statistical characteristics of the 290 data sets for the other measurements, namely for: the outlet air temperature $[T_{a,out}(Tidbit)]$ measured using the “Tidbit” sensors; the outlet air temperature $[T_{a,out}(Hobo)]$ measured using the “Hobo” sensors; and the outlet water temperature $[T_{w,out}^{meas}]$ are reported below in Figures A.13 through A.15, and Tables A.12 through A.14, respectively.

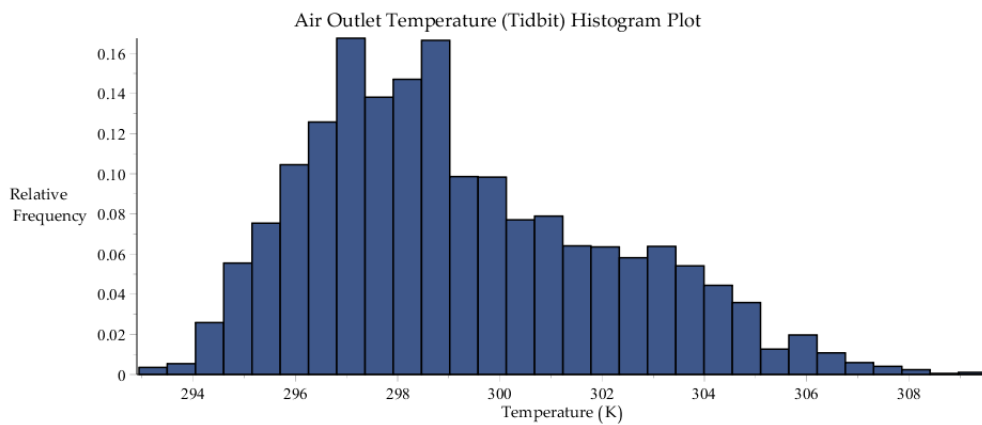


Figure A.13: Histogram plot of the air outlet temperature measured using “Tidbit” sensors, within the 6717 data sets collected by SRNL from F-Area cooling towers for case 2.

APPENDIX A. STATISTICAL ANALYSIS OF MEASURED RESPONSES

Table A.12: Statistics of the air outlet temperature distribution [K], measured using “Tidbit” sensors for case 2.

Minimum	Maximum	Range	Mean	Std.Dev.	Variance	Skewness	Kurtosis
292.94	309.52	16.58	299.21	2.92	8.55	0.59	2.71

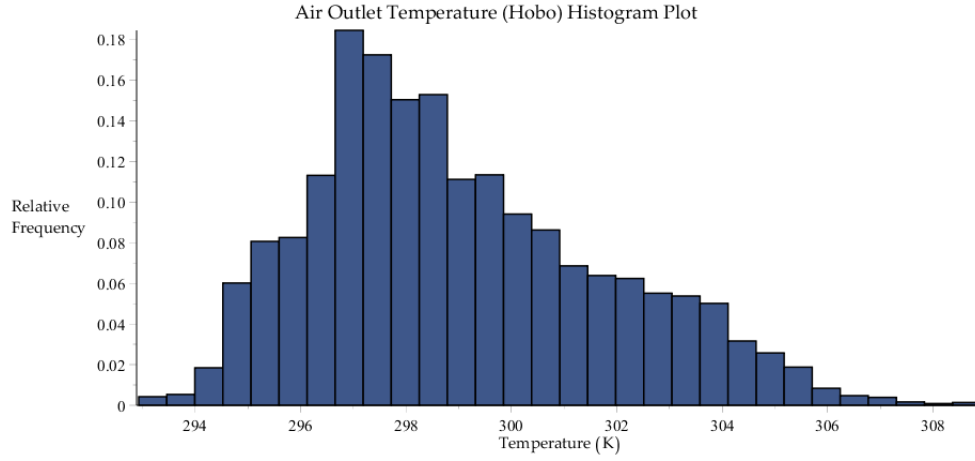


Figure A.14: Histogram plot of the air outlet temperature measured using “Hobo” sensors, within the 6717 data sets collected by SRNL from F-Area cooling towers for case 2.

Table A.13: Air outlet temperature distribution statistics [K], measured using “Hobo” sensors for case 2.

Minimum	Maximum	Range	Mean	Std.Dev.	Variance	Skewness	Kurtosis
292.93	308.90	15.97	299.00	2.77	7.68	0.58	2.75

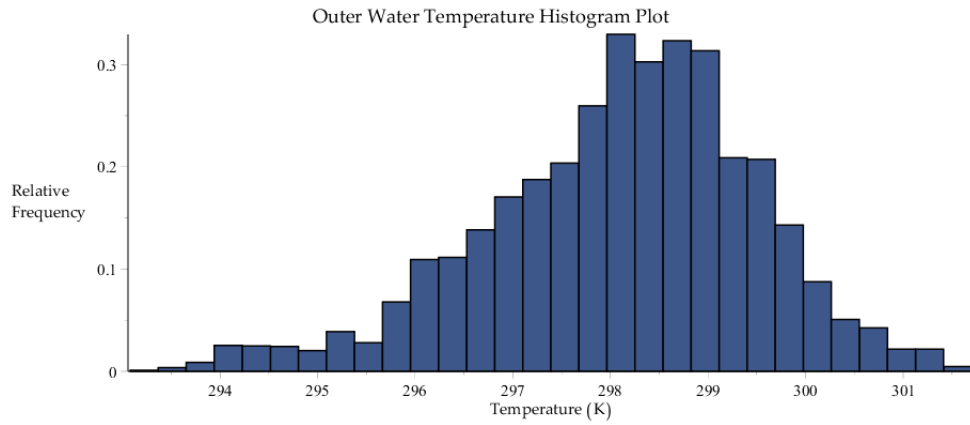


Figure A.15: Histogram plot of water outlet temperature measurements, within the 6717 data sets collected by SRNL from F-Area cooling towers for case 2.

APPENDIX A. STATISTICAL ANALYSIS OF MEASURED RESPONSES

Table A.14: Water outlet temperature [K] distribution statistics for case 2.

Minimum	Maximum	Range	Mean	Std.Dev.	Variance	Skewness	Kurtosis
293.08	301.70	8.62	298.10	1.39	1.94	-0.51	3.31

Ordering the above-mentioned four measured responses as follows: (i) outlet air temperature $T_{a,out(Tidbit)}$; (ii) outlet air temperature $T_{a,out(Hobo)}$; (iii) outlet water temperature $T_{w,out}^{meas}$; and (iv) outlet air relative humidity RH_{out}^{meas} , yields the following “measured response covariance matrix”, denoted as:

$$Cov(T_{a,out(Tidbit)}, T_{a,out(Hobo)}, T_{w,out}^{meas}, RH_{out}^{meas}) = \begin{pmatrix} 8.55 & 8.06 & 1.92 & -28.43 \\ 8.06 & 7.68 & 1.91 & -27.04 \\ 1.92 & 1.91 & 1.94 & -1.97 \\ -28.43 & -27.04 & -1.97 & 185.72 \end{pmatrix} \quad (A.10)$$

For the future purposes of uncertainty quantification, data assimilation, model calibration and predictive modeling, the data measurements provided by the “Tidbit” and “Hobo” temperature sensors can be combined into an “averaged” data set of measured air outlet temperatures, which will be indicated as $T_{a,out}^{meas}$.

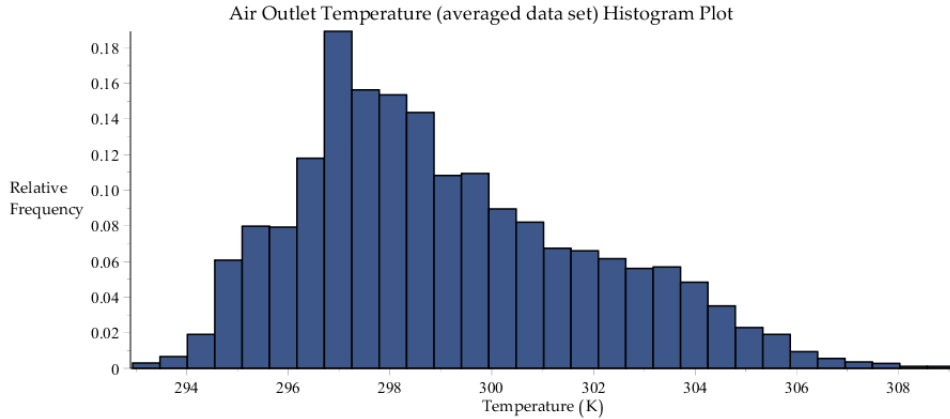


Figure A.16: Histogram plot of air outlet temperatures averaged from Figures A.13 and A.14.

APPENDIX A. STATISTICAL ANALYSIS OF MEASURED RESPONSES

Table A.15: Statistics of the averaged air outlet temperature distribution [K] for case 2.

Minimum	Maximum	Range	Mean	Std.Dev.	Variance	Skewness	Kurtosis
292.93	309.10	16.17	299.11	2.84	8.09	0.58	2.71

The histogram plot and corresponding statistical characteristics of the averaged temperature $T_{a,out}^{meas}$ are shown in Figure A.16 and Table A.15, respectively.

Calculating the covariance matrix, denoted as $[Cov(T_{a,out}^{meas}, T_{w,out}^{meas}, RH_{out}^{meas})]_{data}$, for all of the considered experimental data points for the averaged outlet air temperature $[T_{a,out}^{meas}]$, the outlet water temperature $[T_{w,out}^{meas}]$, and the outlet air relative humidity $[RH_{out}^{meas}]$, yields the following covariance matrix:

$$[Cov(T_{a,out}^{meas}, T_{w,out}^{meas}, RH_{out}^{meas})]_{data} = \begin{pmatrix} 8.09 & 1.91 & -27.74 \\ 1.91 & 1.94 & -1.97 \\ -27.74 & -1.97 & 185.72 \end{pmatrix} \quad (A.11)$$

A comparison between the results in Eqs. (A.10) and (A.11) makes clear that the elimination of the second column and row in Eq. (A.10) yields a 3-by-3 matrix which has entries basically equivalent to the covariance matrix shown in Eq. (A.11). Therefore, this means that the temperature distributions measured by the “Tidbit” and “Hobo” sensors do not need to be dealt with as separate data sets for the purposes of uncertainty quantification and predictive modeling.

The standard deviation of the humidity sensor utilized for the measurements ($\sigma_{sensor} = 5.0\%$ for the response $RH^{(1)}$) have been already considered by including in the category of the “unsaturated” data sets those that have their respective measured relative humidity, RH^{meas} , up to 105.0%. In addition to that, the respective uncertainties of the temperature sensors (standard deviations, $\sigma_{sensor} = 0.2K$ for both responses $T_a^{(1)}$ and $T_w^{(50)}$) must also be taken into consideration for the 6717 data sets.

APPENDIX A. STATISTICAL ANALYSIS OF MEASURED RESPONSES

Coupling Eq. (A.3) with the result presented in Eq. (A.11) will lead to incremented values of the variances on the diagonal of the respective “measured covariance matrix”. The obtained result is:

$$Cov(T_{a,out}^{meas}, T_{w,out}^{meas}, RH_{out}^{meas}) = \begin{pmatrix} 8.09 & 1.91 & -27.74 \\ 1.91 & 1.94 & -1.97 \\ -27.74 & -1.97 & 195.81 \end{pmatrix} \quad (A.12)$$

In the predictive modeling formalism (which includes uncertainty quantification, data assimilation, and model calibration) the covariance matrix between the measured parameters and responses is required as an input. In the case of interest, all the parameters and responses can be considered as uncorrelated, excepting the measured responses considered in this Appendix and the measured parameters listed in Appendix B. The “parameter-response” covariance matrix in Eq. (A.13), indicated as $Cov(T_{a,out}^{meas}, T_{w,out}^{meas}, RH^{meas}, \alpha_1, \dots, \alpha_{47})$, refers to the above mentioned parameters (namely: dry-bulb air temperature, T_{db} ; dew-point air temperature, T_{dp} , inlet water temperature, $T_{w,in}$, atmospheric pressure, P_{atm} and wind speed V_w) and responses (i.e., average outlet air temperature, outlet water temperature, and outlet air relative humidity):

$$Cov(T_{a,out}^{meas}, T_{w,out}^{meas}, RH^{meas}, \alpha_1, \dots, \alpha_{47}) = \begin{pmatrix} 10.36 & 2.81 & 2.22 & -232.64 & 1.30 & 0 & \dots & 0 \\ 1.58 & 1.96 & 2.01 & -23.76 & -0.10 & 0 & \dots & 0 \\ -35.89 & 2.43 & -0.79 & 720.11 & -5.48 & 0 & \dots & 0 \end{pmatrix} \quad (A.13)$$

Appendix B

Model Parameters for the SRNL F-Area Cooling Towers

B.1 Model Parameters for Case 1a: Fan Off, Saturated Outlet Air Conditions, with Inlet Air Unsaturated

The mean values and standard deviations for the independent model parameters α_i , ($i = 1, \dots, N_\alpha = 47$), presented in Table B.1 have been derived in collaboration with Dr. Sebastian Aleman of SRNL (private communications, 2016).

Table B.1: Model Parameters for SRNL F-area Cooling Towers for case 1a.

i	Model Independent Scalar Parameters (α_i)	Math. Notation	Nominal Value	Absolute Std. Dev.	Relative Std. Dev.
1	Air temperature (dry bulb), (K)	T_{db}	294.03	1.79	0.61
2	Dew point temperature (K)	T_{dp}	293.49	1.61	0.55
3	Inlet water temperature (K)	$T_{w,in}$	298.78	1.42	0.47
4	Atmospheric pressure (Pa)	P_{atm}	100853	287	0.28
5	Wind speed (m/s)	V_w	1.42	0.62	42.52

APPENDIX B. PARAMETERS FOR THE F-AREA COOLING TOWERS

i	Model Independent Scalar Parameters (α_i)	Math. Notation	Nominal Value	Absolute Std. Dev.	Relative Std. Dev.
6	Sum of loss coefficients above fill	k_{sum}	10	5	50
7	Dynamic viscosity of air at T=300 K (kg/m·s)	μ	$1.98 \cdot 10^{-5}$	$9.68 \cdot 10^{-7}$	4.88
8	Kinematic viscosity of air at T=300 K (m ² /s)	ν	$1.57 \cdot 10^{-5}$	$1.89 \cdot 10^{-6}$	12.09
9	Thermal conductivity of air at T=300 K (W/m·K)	k_{air}	0.02624	$1.58 \cdot 10^{-3}$	6.04
10	Heat transfer coefficient multiplier	f_{ht}	1	0.5	50
11	Mass transfer coefficient multiplier	f_{mt}	1	0.5	50
12	Fill section frictional loss multiplier	f	4	2	50
13	P _{vs} (T) parameters	a_0	25.5943	0.01	0.04
14		a_1	-5229.89	4.4	0.08
15		$a_{0,cpa}$	1030.5	0.294	0.03
16	C _{pa} (T) parameters	$a_{1,cpa}$	-0.19975	0.002	1.00
17		$a_{2,cpa}$	$3.97 \cdot 10^{-4}$	$3.40 \cdot 10^{-6}$	0.84
18		$a_{0,dav}$	$7.06 \cdot 10^{-9}$	0	0
19	D _{av} (T) parameters	$a_{1,dav}$	2.65322	0.003	0.11
20		$a_{2,dav}$	$-6.17 \cdot 10^{-3}$	$2.30 \cdot 10^{-5}$	0.37
21		$a_{3,dav}$	$6.55 \cdot 10^{-6}$	$3.80 \cdot 10^{-8}$	0.58
22	h _f (T) parameters	a_{0f}	-1143423	543	0.05
23		a_{1f}	4186.50768	1.8	0.04
24	h _g (T) parameters	a_{0g}	2005743.99	1046	0.05
25		a_{1g}	1815.437	3.5	0.19
26	Nusselt parameters	$a_{0,Nu}$	8.235	2.059	25
27		$a_{1,Nu}$	0.00314987	0.00105	33.25
28		$a_{2,Nu}$	0.9902987	0.329	33.25
29		$a_{3,Nu}$	0.023	0.0088	38.26

APPENDIX B. PARAMETERS FOR THE F-AREA COOLING TOWERS

i	Model Independent Scalar Parameters (α_i)	Math. Notation	Nominal Value	Absolute Std. Dev.	Relative Std. Dev.
30	Cooling tower deck width in x-dir (m)	W_{dkx}	8.5	0.085	1
31	Cooling tower deck width in y-dir (m)	W_{dky}	8.5	0.085	1
32	Cooling tower deck height above ground (m)	Δz_{dk}	10	0.1	1
33	Fan shroud height (m)	Δz_{fan}	3	0.03	1
34	Fan shroud inner diameter (m)	D_{fan}	4.1	0.041	1
35	Fill section height (m)	Δz_{fill}	2.013	0.02013	1
36	Rain section height (m)	Δz_{rain}	1.633	0.01633	1
37	Basin section height (m)	Δz_{bs}	1.168	0.01168	1
38	Drift eliminator thickness (m)	Δz_{de}	0.1524	0.00152	1
39	Fill section equivalent diameter (m)	D_h	0.0381	0.00038	1
40	Fill section flow area (m ²)	A_{fill}	67.29	6.729	10
41	Fill section surface area (m ²)	A_{surf}	14221	3555.3	25
42	Prandtl number of air at T=80 °C	P_r	0.708	0.005	0.71
43	Wetted fraction of fill surface area	w_{tsa}	1	0	0
i	Boundary Parameters (α_i)	Math. Notation	Nominal Value	Absolute Std. Dev.	Relative Std. Dev.
44	Inlet water mass flow rate (kg/s)	$m_{w,in}$	44.02	2.20	5
45	Inlet air temperature (K)	$T_{a,in}$	294.03	1.79	0.61
46	Inlet air humidity ratio	ω_{in}	0.01552	0.00149	8.15
i	Special Dependent Parameters (α_i)	Math. Notation	Nominal Value	Absolute Std. Dev.	Relative Std. Dev.
47	Schmidt number	Sc	0.619	0.0073	1.19

The above *independent* model parameters are used for computing various *dependent* model parameters and thermal material properties, as shown in Tables B.2 and B.3.

APPENDIX B. PARAMETERS FOR THE F-AREA COOLING TOWERS

Table B.2: Dependent Scalar Model Parameters.

Dependent Scalar Parameters	Math. Notation	Defining Equation or Correlation
Mass diffusivity of water vapor in air (m ² /s)	$D_{av}(T_a, \alpha)$	$\frac{a_{0,dav} T^{1.5}}{a_{1,dav} + (a_{2,dav} + a_{3,dav} T) T}$
Heat transfer coefficient (W/m ² ·K)	$h(\alpha)$	$\frac{f_{ht} N_u k_{air}}{D_h}$
Mass transfer coefficient (m/s)	$k_m(\alpha)$	$\frac{f_{mt} S_h D_{av}(T_{db}, \alpha)}{D_h}$
Heat transfer term (W/K)	$H(m_a, \alpha)$	$h(\alpha) w_{tsa} A_{ff}$
Mass transfer term (m ³ /s)	$M(m_a, \alpha)$	$M_{H_2O} k_m(\alpha) w_{tsa} A_{ff}$
Density of dry air (kg/m ³)	$\rho(\alpha)$	$\frac{P_{atm}}{R_{air} T_{db}}$
Air velocity in the fill section (m/s)	$v_a(m_a, \alpha)$	$\frac{ m_a }{\rho(\alpha) A_{fill}}$
Fill falling-film surface area per vertical section (m ²)	A_{ff}	$\frac{A_{surf}}{I}$
Rain section inlet flow area (m ²)	A_{in}	$W_{dkx} W_{dky}$
Height for natural convection (m)	Z	$\Delta z_{dk} + \Delta z_{fan} - \Delta z_{bs}$
Height above fill section (m)	Δz_{4-2}	$Z - \Delta z_{fill} - \Delta z_{rain}$
Fill section control volume height (m)	Δz	$\frac{\Delta z_{fill}}{I}$
Fill section length, including drift eliminator (m)	L_{fill}	$\Delta z_{fill} + \Delta z_{de}$
Fan shroud inner radius (m)	r_{fan}	$0.5 D_{fan}$
Fan shroud flow area (m ²)	A_{out}	πr_{fan}^2

Table B.3: Thermal Properties (Dependent Scalar Model Parameters).

Thermal Properties (functions of state variables)	Math. Notation	Defining Equation or Correlation
$h_f(T_w)$ = saturated liquid enthalpy (J/kg)	$h_f(T_w, \alpha)$	$a_{0f} + a_{1f} T_w$
$H_g(T_w)$ = saturated vapor enthalpy (J/kg)	$h_{g,w}(T_w, \alpha)$	$a_{0g} + a_{1g} T_w$
$H_g(T_a)$ = saturated vapor enthalpy (J/kg)	$h_{g,a}(T_a, \alpha)$	$a_{0g} + a_{1g} T_a$
$C_{pa}(T)$ = specific heat of dry air (J/kg·K)	$C_p(T, \alpha)$	$a_{0,cpa} + (a_{1,cpa} + a_{2,cpa} T) T$
$P_{vs}(T_w)$ = saturation pressure (Pa)	$P_{vs}(T_w, \alpha)$	$P_c \cdot e^{a_0 + \frac{a_1}{T_w}}$, in which $P_c = 1.0$ Pa
$P_{vs}(T_a)$ = saturation pressure (Pa)	$P_{vs}(T_a, \alpha)$	$P_c \cdot e^{a_0 + \frac{a_1}{T_a}}$, in which $P_c = 1.0$ Pa.

Note 1: The measurements of parameters α_1 through α_5 (i.e., the dry bulb air temperature, dew point temperature, inlet water temperature, atmospheric pressure and wind speed) were taken at the SRNL site, where the F-area cooling towers are located. Out of the 8079 total benchmark data sets [33], 377 data sets have been considered in case 1a; through these data sets the statistical properties

APPENDIX B. PARAMETERS FOR THE F-AREA COOLING TOWERS

(means, variance and covariance, skewness and kurtosis) for these model parameters have been derived, as shown in Figures B.1 through B.5 and Tables B.4 through B.8.

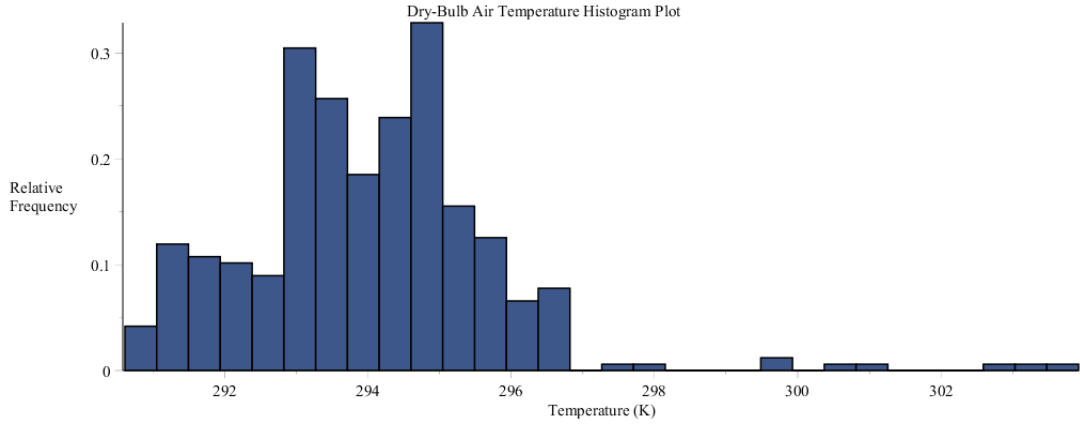


Figure B.1: Histogram plot of dry-bulb air temperature data collected by SRNL from F-Area cooling towers for case 1a.

Table B.4: Statistics of the dry-bulb air temperature distribution [K] for case 1a.

Minimum	Maximum	Range	Mean	Std.Dev.	Variance	Skewness	Kurtosis
290.61	303.92	13.31	294.03	1.78	3.18	1.38	8.67

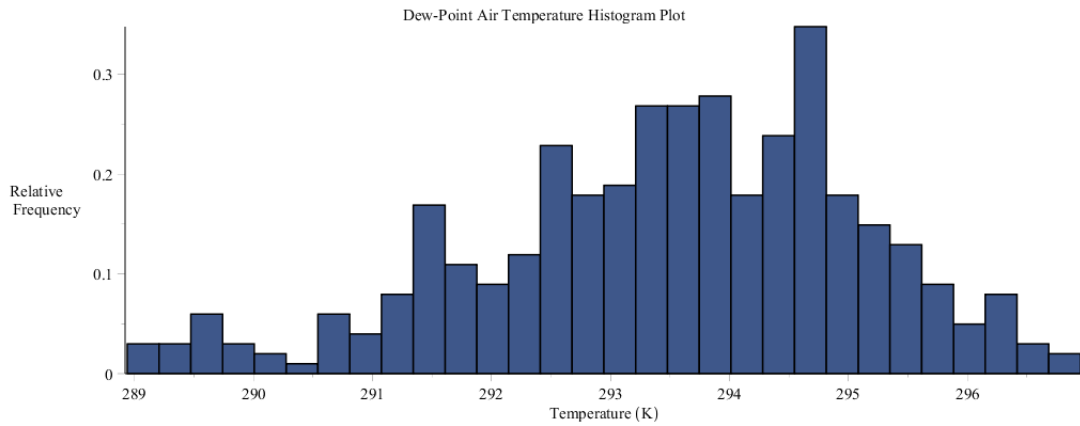


Figure B.2: Histogram plot of dew-point air temperature data collected by SRNL from F-Area cooling towers for case 1a.

APPENDIX B. PARAMETERS FOR THE F-AREA COOLING TOWERS

Table B.5: Statistics of the dew-point air temperature distribution [K] for case 1a.

Minimum	Maximum	Range	Mean	Std.Dev.	Variance	Skewness	Kurtosis
288.94	296.95	8.01	293.49	1.61	2.58	-0.49	2.97

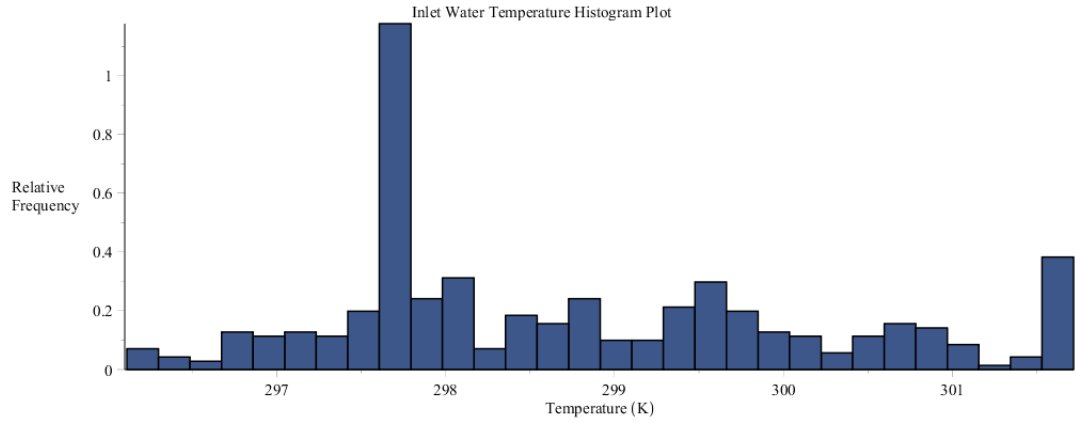


Figure B.3: Histogram plot of inlet water temperature data collected by SRNL from F-Area cooling towers for case 1a.

Table B.6: Statistics of the inlet water temperature distribution [K] for case 1a.

Minimum	Maximum	Range	Mean	Std.Dev.	Variance	Skewness	Kurtosis
296.11	301.72	5.61	298.77	1.41	2.00	0.49	2.21

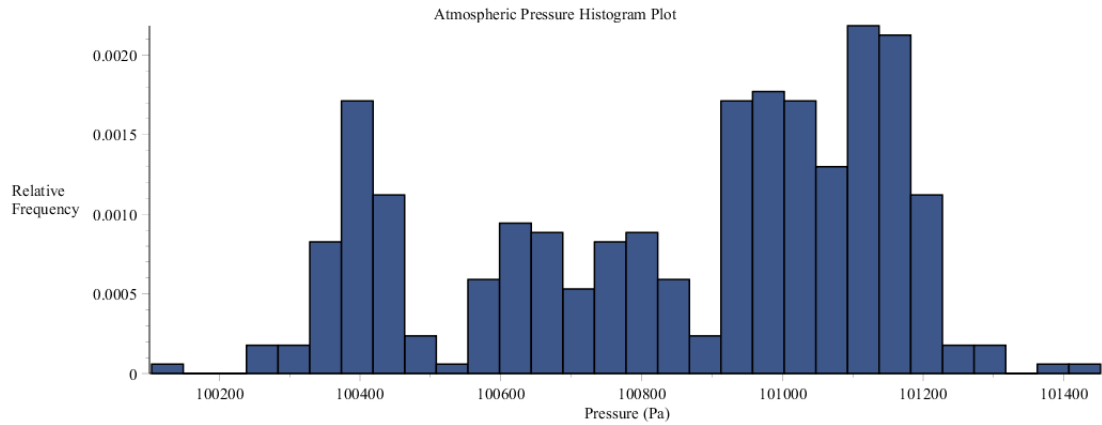


Figure B.4: Histogram plot of atmospheric pressure data collected by SRNL from F-Area cooling towers for case 1a.

APPENDIX B. PARAMETERS FOR THE F-AREA COOLING TOWERS

Table B.7: Statistics of the atmospheric pressure distribution [Pa] for case 1a.

Minimum	Maximum	Range	Mean	Std.Dev.	Variance	Skewness	Kurtosis
100104	101452	1348	100853	286.59	82133	-0.49	1.99

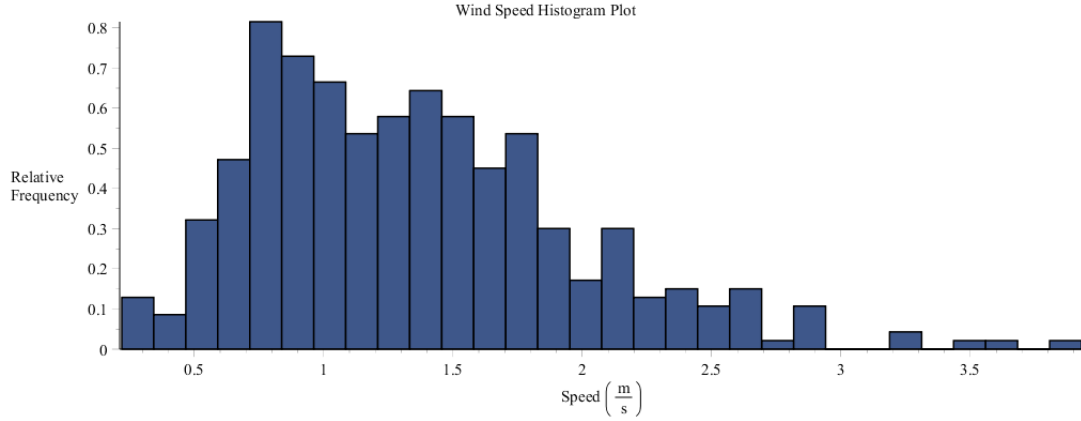


Figure B.5: Histogram plot of wind speed data collected by SRNL from F-Area cooling towers for case 1a.

Table B.8: Statistics of the wind speed distribution [m/s] for case 1a.

Minimum	Maximum	Range	Mean	Std.Dev.	Variance	Skewness	Kurtosis
0.22	3.93	3.71	1.35	0.62	0.39	0.90	4.00

The 5-by-5 covariance matrix for the above experimental data has also been computed and is provided below, with the five model parameters ordered as follows: dry-bulb air temperature T_{db} , dew-point air temperature T_{dp} , inlet water temperature $T_{w,in}$, atmospheric air pressure P_{atm} , and wind speed V_w .

$$Cov(T_{db}; T_{dp}; T_{w,in}; P_{atm}; V_w) = \begin{pmatrix} 3.18 & 2.17 & 1.19 & -187.06 & 0.26 \\ 2.17 & 2.58 & 1.26 & -178.24 & 0.28 \\ 1.19 & 1.26 & 2.00 & -184.39 & 0.26 \\ -187.06 & -178.24 & -184.39 & 82133 & 0.42 \\ 0.26 & 0.28 & 0.26 & 0.42 & 0.39 \end{pmatrix} \quad (B.1)$$

APPENDIX B. PARAMETERS FOR THE F-AREA COOLING TOWERS

The covariance matrix in Eq. (B.1) neglects the uncertainty associated with sensor readings throughout the data collection period. When combining uncertainties by adding variances, the contribution from the sensors is 0.04 K for each of the first three parameters, which accounts for a maximum of ca. 2% of the total variance (for the dry-bulb air temperature, specifically). The uncertainty in the atmospheric pressure sensor is at this time unknown. For these reasons, their contribution to overall uncertainty is considered insignificant at this time.

Note 2: Temperature and pressure values are initially input in units of [°C] and [mb], respectively, but are internally converted to [K] and [Pa] for computational purposes.

Note 3: Inlet air humidity ratio is defined as follows:

$$\omega_{in} = \frac{0.622P_{vs}(T_{dp}, \alpha)}{P_{atm} - P_{vs}(T_{dp}, \alpha)} = \frac{0.622e^{a_0 + \frac{a_1}{T_{dp}}}}{P_{atm} - e^{a_0 + \frac{a_1}{T_{dp}}}} \quad (B.2)$$

Note 4: The Nusselt number is defined as follows:

$$Nu = \begin{cases} a_{0,Nu} & Re_d < 2300 \\ a_{1,Nu} \cdot Re_d + a_{2,Nu} & 2300 \leq Re_d \leq 10000 \\ a_{3,Nu} \cdot Re_d^{0.8} \cdot Pr^{\frac{1}{3}} & Re_d > 10000 \end{cases} \quad (B.3)$$

B.2 Model Parameters for Case 1b: Fan Off, Saturated Outlet Air Conditions, with Inlet Air Saturated

The mean values and standard deviations for the independent model parameters α_i , ($i = 1, \dots, N_\alpha = 47$), presented in Table B.1 have been derived in collaboration with Dr. Sebastian Aleman of SRNL (private communications, 2016).

Table B.9: Model Parameters for SRNL F-area Cooling Towers for case 1a.

i	Model Independent Scalar Parameters (α_i)	Math. Notation	Nominal Value	Absolute Std. Dev.	Relative Std. Dev.
1	Air temperature (dry bulb), (K)	T_{db}	294.4	0.98	0.34
2	Dew point temperature (K)	T_{dp}	294.661	1.08	0.37
3	Inlet water temperature (K)	$T_{w,in}$	299.543	1.07	0.36
4	Atmospheric pressure (Pa)	P_{atm}	100605	312	0.31
5	Wind speed (m/s)	V_w	1.377	0.72	52.40
6	Sum of loss coefficients above fill	k_{sum}	10	5	50
7	Dynamic viscosity of air at T=300 K (kg/m·s)	μ	$1.98 \cdot 10^{-5}$	$9.68 \cdot 10^{-7}$	4.88
8	Kinematic viscosity of air at T=300 K (m ² /s)	ν	$1.57 \cdot 10^{-5}$	$1.89 \cdot 10^{-6}$	12.09
9	Thermal conductivity of air at T=300 K (W/m·K)	k_{air}	0.02624	$1.58 \cdot 10^{-3}$	6.04
10	Heat transfer coefficient multiplier	f_{ht}	1	0.5	50
11	Mass transfer coefficient multiplier	f_{mt}	1	0.5	50
12	Fill section frictional loss multiplier	f	4	2	50
13	P _{vs} (T) parameters	a_0	25.5943	0.01	0.04
14		a_1	-5229.89	4.4	0.08

APPENDIX B. PARAMETERS FOR THE F-AREA COOLING TOWERS

i	Model Independent Scalar Parameters (α_i)	Math. Notation	Nominal Value	Absolute Std. Dev.	Relative Std. Dev.
15	$C_{pa}(T)$ parameters	$a_{0,cpa}$	1030.5	0.294	0.03
16		$a_{1,cpa}$	-0.19975	0.002	1
17		$a_{2,cpa}$	$3.97 \cdot 10^{-4}$	$3.40 \cdot 10^{-6}$	0.84
18	$D_{av}(T)$ parameters	$a_{0,dav}$	$7.06 \cdot 10^{-9}$	0	0
19		$a_{1,dav}$	2.65322	0.003	0.11
20		$a_{2,dav}$	$-6.17 \cdot 10^{-3}$	$2.30 \cdot 10^{-5}$	0.37
21		$a_{3,dav}$	$6.55 \cdot 10^{-6}$	$3.80 \cdot 10^{-8}$	0.58
22	$h_f(T)$ parameters	a_{0f}	-1143423	543	0.05
23		a_{1f}	4186.50768	1.8	0.04
24	$h_g(T)$ parameters	a_{0g}	2005743.99	1046	0.05
25		a_{1g}	1815.437	3.5	0.19
26	Nusselt parameters	$a_{0,Nu}$	8.235	2.059	25
27		$a_{1,Nu}$	0.00314987	0.00105	31.75
28		$a_{2,Nu}$	0.9902987	0.329	34.09
29		$a_{3,Nu}$	0.023	0.0088	38.26
30	Cooling tower deck width in x-dir (m)	W_{dkx}	8.5	0.085	1
31	Cooling tower deck width in y-dir (m)	W_{dky}	8.5	0.085	1
32	Cooling tower deck height above ground (m)	Δz_{dk}	10	0.1	1
33	Fan shroud height (m)	Δz_{fan}	3	0.03	1
34	Fan shroud inner diameter (m)	D_{fan}	4.1	0.041	1
35	Fill section height (m)	Δz_{fill}	2.013	0.02013	1
36	Rain section height (m)	Δz_{rain}	1.633	0.01633	1
37	Basin section height (m)	Δz_{bs}	1.168	0.01168	1
38	Drift eliminator thickness (m)	Δz_{de}	0.1524	0.00152	1
39	Fill section equivalent diameter (m)	D_h	0.0381	0.00038	1
40	Fill section flow area (m ²)	A_{fill}	67.29	6.729	10

APPENDIX B. PARAMETERS FOR THE F-AREA COOLING TOWERS

i	Model Independent Scalar Parameters (α_i)	Math. Notation	Nominal Value	Absolute Std. Dev.	Relative Std. Dev.
41	Fill section surface area (m ²)	A_{surf}	14221	3555.3	25
42	Prandtl number of air at T=80 °C	P_r	0.708	0.005	071
43	Wetted fraction of fill surface area	w_{tsa}	1	0	0
i	Boundary Parameters (α_i)	Math. Notation	Nominal Value	Absolute Std. Dev.	Relative Std. Dev.
44	Inlet water mass flow rate (kg/s)	$m_{w,in}$	44.0089	2.20	5
45	Inlet air temperature (K)	$T_{a,in}$	294.40	0.98	0.34
46	Inlet air humidity ratio	ω_{in}	0.0162008	0.00131	6.75
i	Special Dependent Parameters (α_i)	Math. Notation	Nominal Value	Absolute Std. Dev.	Relative Std. Dev.
47	Schmidt number	Sc	0.6178	0.0041	0.66

The above *independent* model parameters are used for computing various *dependent* model parameters and thermal material properties, as shown in Tables B.2 and B.3.

Note 1: The measurements of parameters α_1 through α_5 (i.e., the dry bulb air temperature, dew point temperature, inlet water temperature, atmospheric pressure and wind speed) were taken at the SRNL site, where the F-area cooling towers are located. Out of the 8079 total benchmark data sets [33], 290 data sets have been considered in case 1b; through these data sets the statistical properties (means, variance and covariance, skewness and kurtosis) for these model parameters have been derived, as shown in Figures B.6 through B.10 and Tables B.10 through B.14.

APPENDIX B. PARAMETERS FOR THE F-AREA COOLING TOWERS

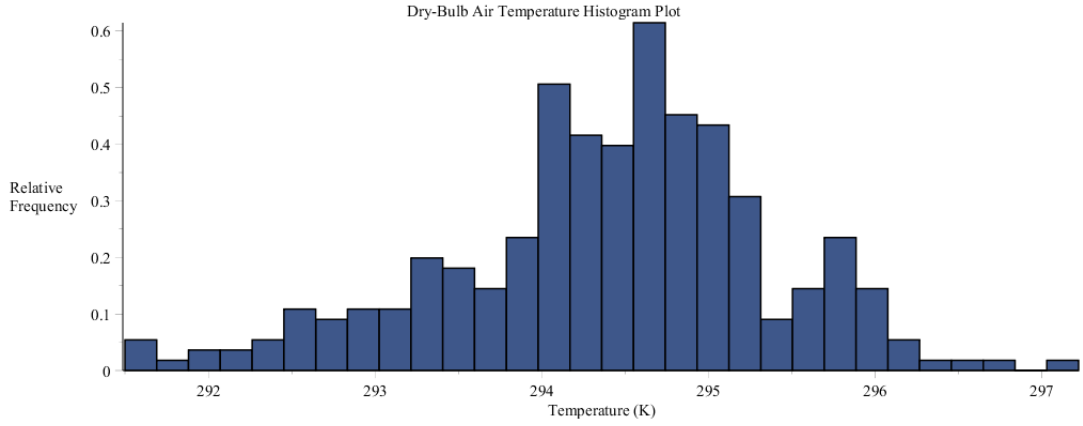


Figure B.6: Histogram plot of dry-bulb air temperature data collected by SRNL from F-Area cooling towers for case 1b.

Table B.10: Statistics of the dry-bulb air temperature distribution [K] for case 1b.

Minimum	Maximum	Range	Mean	Std.Dev.	Variance	Skewness	Kurtosis
291.50	297.22	5.72	294.40	0.98	0.97	-0.43	3.37

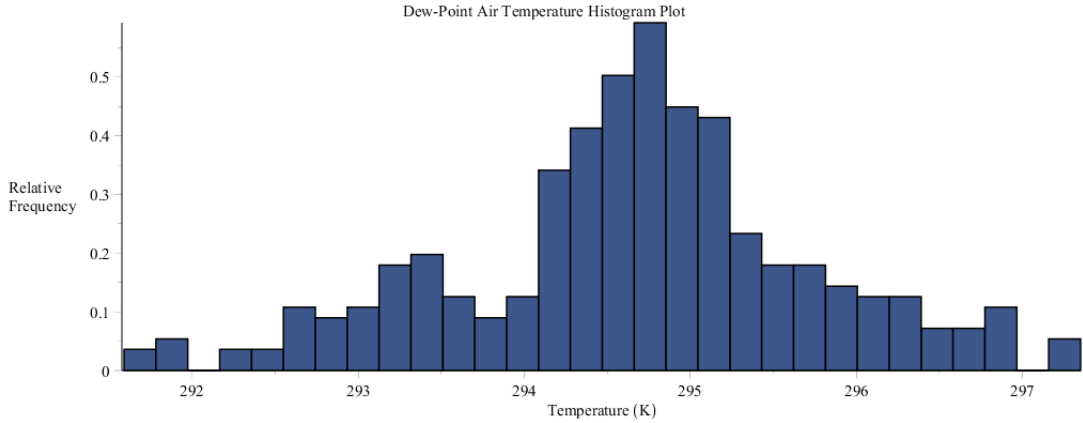


Figure B.7: Histogram plot of dew-point air temperature data collected by SRNL from F-Area cooling towers for case 1b.

Table B.11: Statistics of the dew-point air temperature distribution [K] for case 1b.

Minimum	Maximum	Range	Mean	Std.Dev.	Variance	Skewness	Kurtosis
291.59	297.35	5.76	294.66	1.08	1.16	-0.22	3.24

APPENDIX B. PARAMETERS FOR THE F-AREA COOLING TOWERS

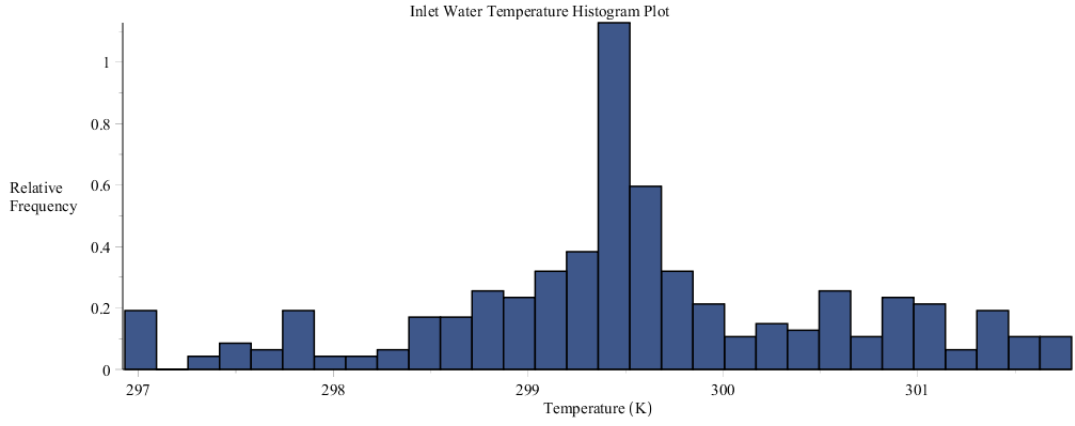


Figure B.8: Histogram plot of inlet water temperature data collected by SRNL from F-Area cooling towers for case 1b.

Table B.12: Statistics of the inlet water temperature distribution [K] for case 1b.

Minimum	Maximum	Range	Mean	Std.Dev.	Variance	Skewness	Kurtosis
296.93	301.79	4.86	299.54	1.07	1.14	-0.15	3.01

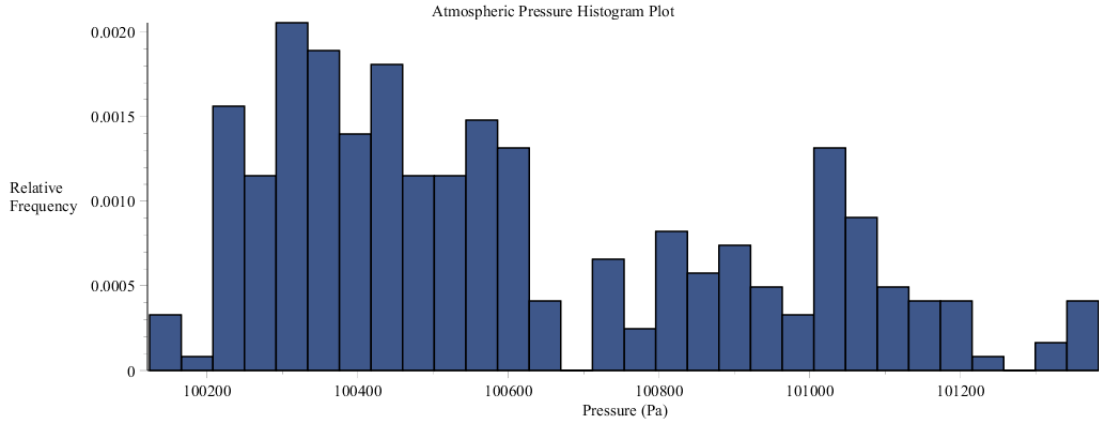


Figure B.9: Histogram plot of atmospheric pressure data collected by SRNL from F-Area cooling towers for case 1b.

Table B.13: Statistics of the atmospheric pressure distribution [Pa] for case 1b.

Minimum	Maximum	Range	Mean	Std.Dev.	Variance	Skewness	Kurtosis
100124	101383	1259	100605	312	97463	0.66	2.29

APPENDIX B. PARAMETERS FOR THE F-AREA COOLING TOWERS

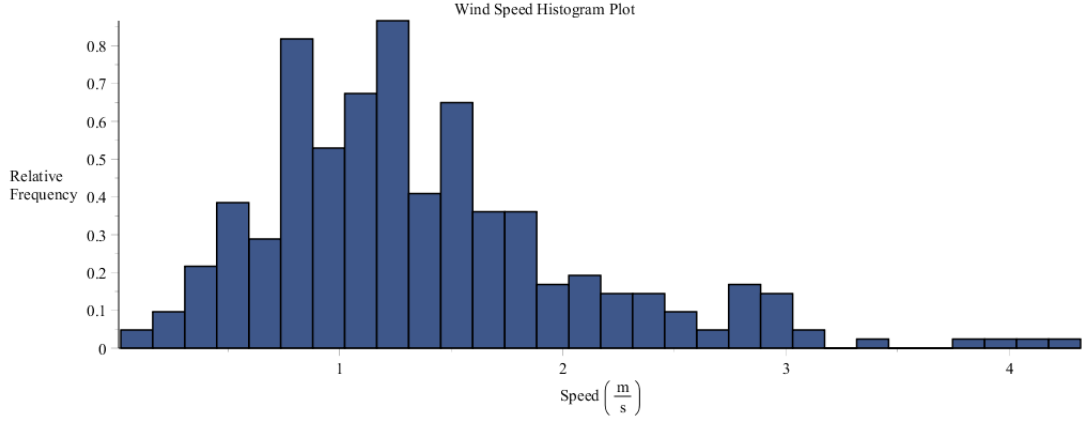


Figure B.10: Histogram plot of wind speed data collected by SRNL from F-Area cooling towers for case 1b.

Table B.14: Statistics of the wind speed distribution [m/s] for case 1b.

Minimum	Maximum	Range	Mean	Std.Dev.	Variance	Skewness	Kurtosis
0.02	4.32	4.30	1.38	0.72	0.52	1.15	4.72

The 5-by-5 covariance matrix for the above experimental data has also been computed and is provided below, with the five model parameters ordered as follows: dry-bulb air temperature T_{db} , dew-point air temperature T_{dp} , inlet water temperature $T_{w,in}$, atmospheric air pressure P_{atm} , and wind speed V_w .

$$Cov(T_{db}; T_{dp}; T_{w,in}; P_{atm}; V_w) = \begin{pmatrix} 0.97 & 1.04 & 0.60 & -128.15 & 0.07 \\ 1.04 & 1.16 & 0.66 & -138.34 & 0.06 \\ 0.60 & 0.66 & 1.14 & -51.83 & 0.02 \\ -128.15 & -138.34 & -51.83 & 97463 & 30.66 \\ 0.07 & 0.06 & 0.02 & 30.66 & 0.52 \end{pmatrix} \quad (\text{B.4})$$

The covariance matrix in Eq. (B.4) neglects the uncertainty associated with sensor readings throughout the data collection period. When combining uncertainties by adding variances, the contribution from the sensors is 0.04 K for each of the first three parameters, which accounts for a maximum of ca. 4% of the

APPENDIX B. PARAMETERS FOR THE F-AREA COOLING TOWERS

total variance (for the dry-bulb air temperature, specifically). The uncertainty in the atmospheric pressure sensor is at this time unknown. For these reasons, their contribution to overall uncertainty is considered insignificant at this time.

B.3 Model Parameters for Case 2: Fan Off, Unsaturated Air Conditions

The mean values and standard deviations for the independent model parameters α_i , ($i = 1, \dots, N_\alpha = 47$), presented in Table B.1 have been derived in collaboration with Dr. Sebastian Aleman of SRNL (private communications, 2016).

Table B.15: Model Parameters for SRNL F-area Cooling Towers for case 1a.

i	Model Independent Scalar Parameters (α_i)	Math. Notation	Nominal Value	Absolute Std. Dev.	Relative Std. Dev.
1	Air temperature (dry bulb), (K)	T_{db}	298.882	4.034	1.35
2	Dew point temperature (K)	T_{dp}	292.077	2.287	0.78
3	Inlet water temperature (K)	$T_{w,in}$	298.893	1.687	0.56
4	Atmospheric pressure (Pa)	P_{atm}	100588	408.26	0.41
5	Wind speed (m/s)	V_w	1.859	0.941	50.7
6	Sum of loss coefficients above fill	k_{sum}	10	5	50
7	Dynamic viscosity of air at T=300 K (kg/m·s)	μ	$1.98 \cdot 10^{-5}$	$9.68 \cdot 10^{-7}$	4.88
8	Kinematic viscosity of air at T=300 K (m ² /s)	ν	$1.57 \cdot 10^{-5}$	$1.90 \cdot 10^{-6}$	12.09
9	Thermal conductivity of air at T=300 K (W/m·K)	k_{air}	0.02624	$1.58 \cdot 10^{-3}$	6.04
10	Heat transfer coefficient multiplier	f_{ht}	1	0.5	50
11	Mass transfer coefficient multiplier	f_{mt}	1	0.5	50
12	Fill section frictional loss multiplier	f	4	2	50

APPENDIX B. PARAMETERS FOR THE F-AREA COOLING TOWERS

i	Model Independent Scalar Parameters (α_i)	Math. Notation	Nominal Value	Absolute Std. Dev.	Relative Std. Dev.
13	$P_{vs}(T)$ parameters	a_0	25.5943	0.01	0.04
14		a_1	-5229.89	4.4	0.08
15		$a_{0,cpa}$	1030.5	0.294	0.03
16	$C_{pa}(T)$ parameters	$a_{1,cpa}$	-0.19975	0.002	1
17		$a_{2,cpa}$	$3.97 \cdot 10^{-4}$	$3.35 \cdot 10^{-6}$	0.84
18		$a_{0,dav}$	$7.06 \cdot 10^{-9}$	0	0
19	$D_{av}(T)$ parameters	$a_{1,dav}$	2.65322	0.003	0.11
20		$a_{2,dav}$	$-6.17 \cdot 10^{-3}$	$2.30 \cdot 10^{-5}$	0.37
21		$a_{3,dav}$	$6.55 \cdot 10^{-6}$	$3.80 \cdot 10^{-8}$	0.58
22	$h_f(T)$ parameters	a_{0f}	-1143423	543	0.05
23		a_{1f}	4186.50768	1.8	0.04
24	$h_g(T)$ parameters	a_{0g}	2005743.99	1046	0.05
25		a_{1g}	1815.437	3.5	0.19
26	Nusselt parameters	$a_{0,Nu}$	8.235	2.059	25
27		$a_{1,Nu}$	0.00314987	0.00105	31.75
28		$a_{2,Nu}$	0.9902987	0.329	33.02
29		$a_{3,Nu}$	0.023	0.0088	38.26
30	Cooling tower deck width in x-dir (m)	W_{dkx}	8.5	0.085	1
31	Cooling tower deck width in y-dir (m)	W_{dky}	8.5	0.085	1
32	Cooling tower deck height above ground (m)	Δz_{dk}	10	0.1	1
33	Fan shroud height (m)	Δz_{fan}	3	0.03	1
34	Fan shroud inner diameter (m)	D_{fan}	4.1	0.041	1
35	Fill section height (m)	Δz_{fill}	2.013	0.02013	1
36	Rain section height (m)	Δz_{rain}	1.633	0.01633	1
37	Basin section height (m)	Δz_{bs}	1.168	0.01168	1
38	Drift eliminator thickness (m)	Δz_{de}	0.1524	0.00152	1

APPENDIX B. PARAMETERS FOR THE F-AREA COOLING TOWERS

i	Model Independent Scalar Parameters (α_i)	Math. Notation	Nominal Value	Absolute Std. Dev.	Relative Std. Dev.
39	Fill section equivalent diameter (m)	D_h	0.0381	0.00038	1
40	Fill section flow area (m ²)	A_{fill}	67.29	6.729	10
41	Fill section surface area (m ²)	A_{surf}	14221	3555.3	25
42	Prandtl number of air at T=80 °C	P_r	0.708	0.005	0.71
43	Wetted fraction of fill surface area	w_{tsa}	1	0	0
i	Boundary Parameters (α_i)	Math. Notation	Nominal Value	Absolute Std. Dev.	Relative Std. Dev.
44	Inlet water mass flow rate (kg/s)	$m_{w,in}$	44.0193	2.201	5
45	Inlet air temperature (K)	$T_{a,in}$	294.40	4.034	1.35
46	Inlet air humidity ratio	ω_{in}	0.01379	0.00192	13.80
i	Special Dependent Parameters (α_i)	Math. Notation	Nominal Value	Absolute Std. Dev.	Relative Std. Dev.
47	Schmidt number	Sc	0.5999	0.0159	2.66

The above *independent* model parameters are used for computing various *dependent* model parameters and thermal material properties, as shown in Tables B.2 and B.3.

Note 1: The measurements of parameters α_1 through α_5 (i.e., the dry bulb air temperature, dew point temperature, inlet water temperature, atmospheric pressure and wind speed) were taken at the SRNL site, where the F-area cooling towers are located. Out of the 8079 total benchmark data sets [33], 6717 data sets have been considered in case 2; through these data sets the statistical properties (means, variance and covariance, skewness and kurtosis) for these model parameters have been derived, as shown in Figures B.11 through B.15 and Tables B.16 through B.20.

APPENDIX B. PARAMETERS FOR THE F-AREA COOLING TOWERS

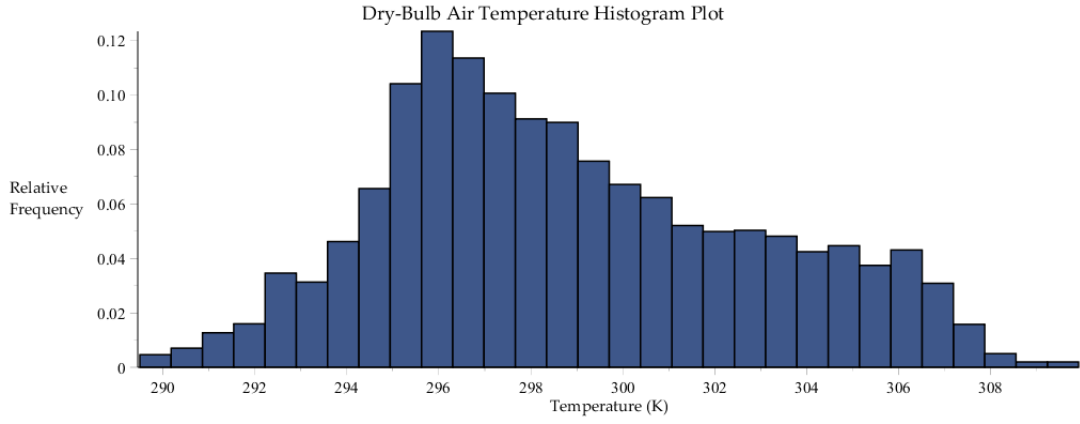


Figure B.11: Histogram plot of dry-bulb air temperature data collected by SRNL from F-Area cooling towers for case 2.

Table B.16: Statistics of the dry-bulb air temperature distribution [K] for case 2.

Minimum	Maximum	Range	Mean	Std.Dev.	Variance	Skewness	Kurtosis
289.50	309.91	20.41	298.88	4.03	16.27	0.36	2.38

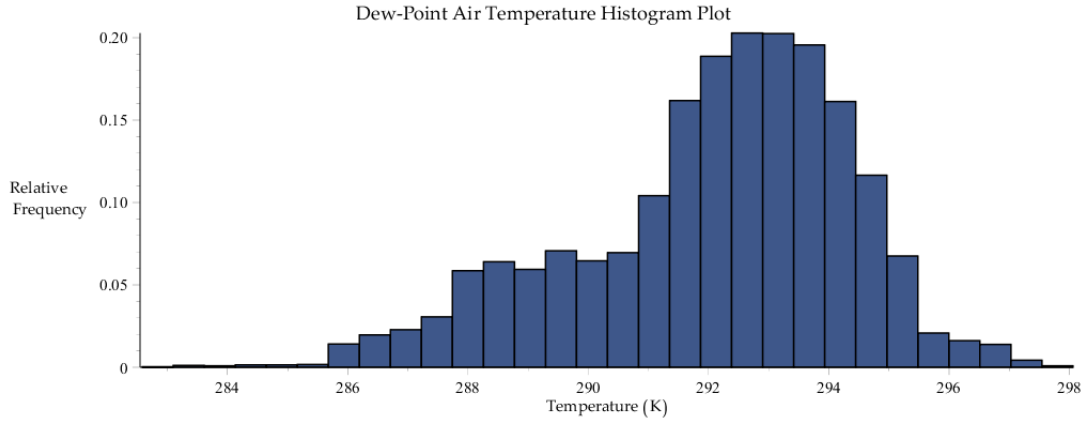


Figure B.12: Histogram plot of dew-point air temperature data collected by SRNL from F-Area cooling towers for case 2.

Table B.17: Statistics of the dew-point air temperature distribution [K] for case 2.

Minimum	Maximum	Range	Mean	Std.Dev.	Variance	Skewness	Kurtosis
282.58	298.06	15.48	292.08	2.29	5.23	-0.66	3.11

APPENDIX B. PARAMETERS FOR THE F-AREA COOLING TOWERS

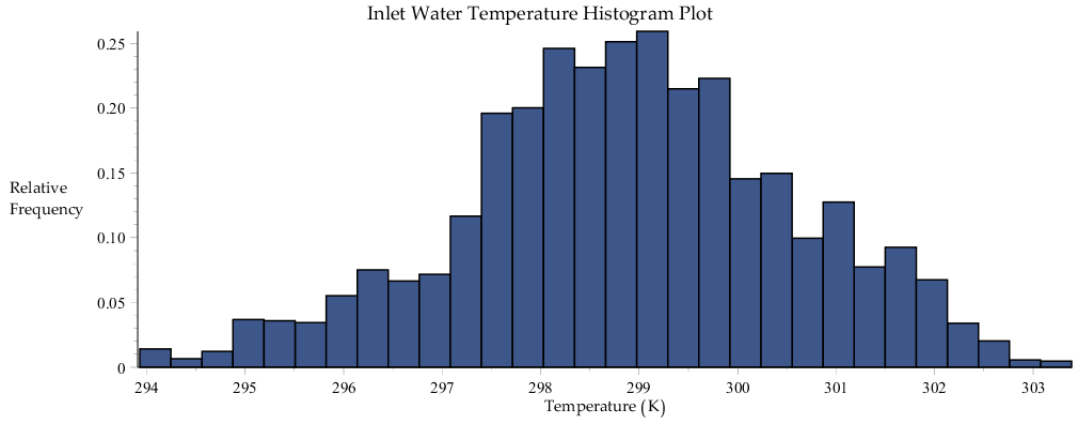


Figure B.13: Histogram plot of inlet water temperature data collected by SRNL from F-Area cooling towers for case 2.

Table B.18: Statistics of the inlet water temperature distribution [K] for case 2.

Minimum	Maximum	Range	Mean	Std.Dev.	Variance	Skewness	Kurtosis
293.93	303.39	9.46	298.89	1.69	2.85	-0.16	2.91

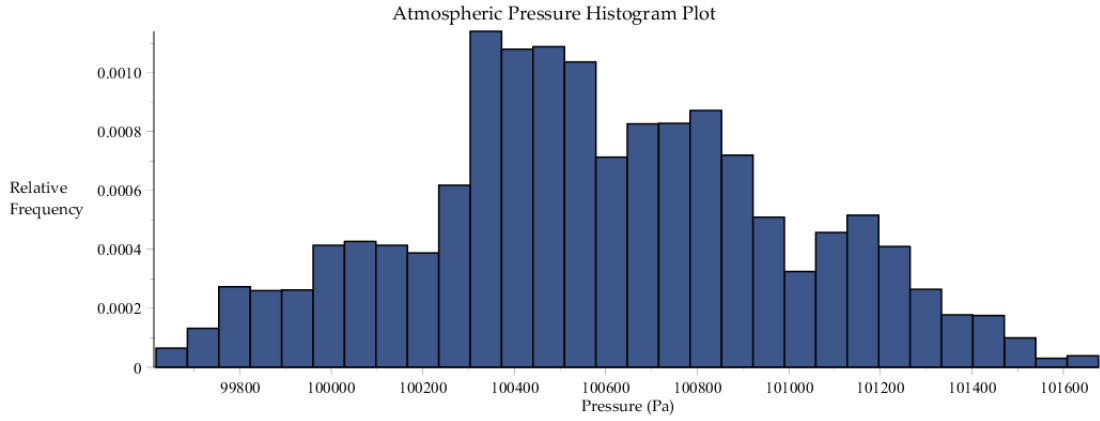


Figure B.14: Histogram plot of atmospheric pressure data collected by SRNL from F-Area cooling towers for case 2.

Table B.19: Statistics of the atmospheric pressure distribution [Pa] for case 2.

Minimum	Maximum	Range	Mean	Std.Dev.	Variance	Skewness	Kurtosis
99617	101677	2060	100588	408.6	166678	0.079	2.57

APPENDIX B. PARAMETERS FOR THE F-AREA COOLING TOWERS

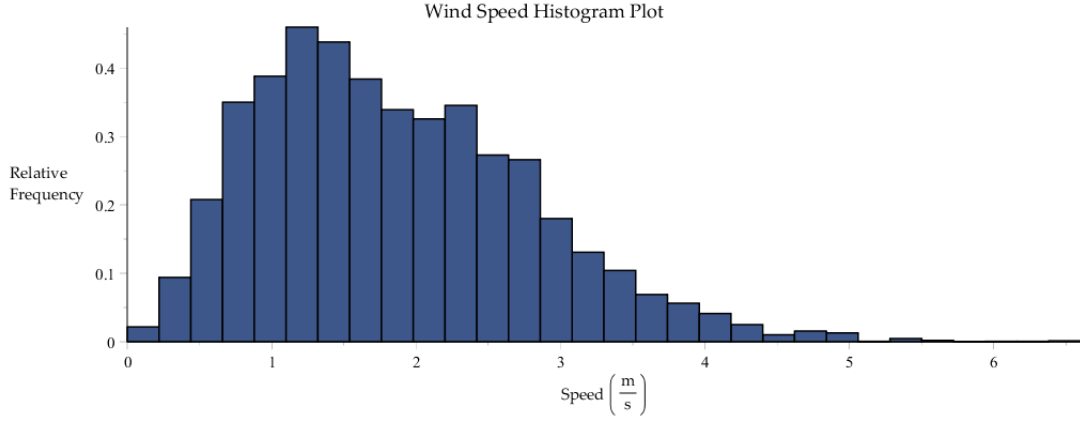


Figure B.15: Histogram plot of wind speed data collected by SRNL from F-Area cooling towers for case 2.

Table B.20: Statistics of the wind speed distribution [m/s] for case 2.

Minimum	Maximum	Range	Mean	Std.Dev.	Variance	Skewness	Kurtosis
0.00	6.60	6.60	1.859	0.94	0.89	0.71	3.42

The 5-by-5 covariance matrix for the above experimental data has also been computed and is provided below, with the five model parameters ordered as follows: dry-bulb air temperature T_{db} , dew-point air temperature T_{dp} , inlet water temperature $T_{w,in}$, atmospheric air pressure P_{atm} , and wind speed V_w .

$$Cov(T_{db}; T_{dp}; T_{w,in}; P_{atm}; V_w) = \begin{pmatrix} 16.27 & 3.56 & 2.13 & -494.48 & 2.45 \\ 3.56 & 5.23 & 2.22 & -138.46 & 0.28 \\ 2.13 & 2.22 & 2.85 & -58.63 & 0.12 \\ -494.48 & -138.46 & -58.63 & 166678.40 & -49.62 \\ 2.45 & 0.28 & 0.12 & -49.62 & 0.89 \end{pmatrix} \quad (B.5)$$

The covariance matrix in Eq. (B.5) neglects the uncertainty associated with sensor readings throughout the data collection period. When combining uncertainties by adding variances, the contribution from the sensors is 0.04 K for each of the first three parameters, which accounts for a maximum of ca. 4% of the total variance (for the dry-bulb air temperature, specifically). The uncertainty in

APPENDIX B. PARAMETERS FOR THE F-AREA COOLING TOWERS

the atmospheric pressure sensor is at this time unknown. For these reasons, their contribution to overall uncertainty is considered insignificant at this time.

Appendix C

Derivative Matrix (Jacobian) of the Model Equations with Respect to the State Functions

This section presents the functional derivatives of the model governing equations with respect to the vector-values state function $\mathbf{u} \triangleq (\mathbf{m}_w, \mathbf{T}_w, \mathbf{T}_a, \boldsymbol{\omega}, m_a)^\dagger$.

The notation for the derivatives of (i) the liquid continuity equations, (ii) the liquid energy balance equations, (iii) the water vapor continuity equations, and (iv) the air/water vapor energy balance equations with respect to the state (i.e., dependent) variables will be as follows:

$$a_\ell^{i,j} \equiv \frac{\partial N_\ell^{(i)}}{\partial m_w^{(j+1)}}; \ell = 1, 2, 3, 4; i = 1, \dots, I; j = 1, \dots, I; \quad (\text{C.1})$$

$$b_\ell^{i,j} \equiv \frac{\partial N_\ell^{(i)}}{\partial T_w^{(j+1)}}; \ell = 1, 2, 3, 4; i = 1, \dots, I; j = 1, \dots, I; \quad (\text{C.2})$$

$$c_\ell^{i,j} \equiv \frac{\partial N_\ell^{(i)}}{\partial T_a^{(j)}}; \ell = 1, 2, 3, 4; i = 1, \dots, I; j = 1, \dots, I; \quad (\text{C.3})$$

APPENDIX C. DERIVATIVE MATRIX (JACOBIAN) OF THE MODEL EQUATIONS WITH RESPECT TO THE STATE FUNCTIONS

$$d_\ell^{i,j} \equiv \frac{\partial N_\ell^{(i)}}{\partial \omega^{(j)}}; \quad \ell = 1, 2, 3, 4; \quad i = 1, \dots, I; \quad j = 1, \dots, I; \quad (\text{C.4})$$

$$e_\ell^i \equiv \frac{\partial N_\ell^{(i)}}{\partial m_a}; \quad \ell = 1, 2, 3, 4; \quad i = 1, \dots, I; \quad (\text{C.5})$$

The notation for the derivatives of the mechanical energy equations with respect to the state (i.e., dependent) variables will be as follows:

$$a_5^j \equiv \frac{\partial N_5}{\partial m_w^{(j+1)}}; \quad j = 1, \dots, I; \quad (\text{C.6})$$

$$b_5^j \equiv \frac{\partial N_5}{\partial T_w^{(j+1)}}; \quad j = 1, \dots, I; \quad (\text{C.7})$$

$$c_5^j \equiv \frac{\partial N_5}{\partial T_a^{(j)}}; \quad j = 1, \dots, I; \quad (\text{C.8})$$

$$d_5^j \equiv \frac{\partial N_5}{\partial \omega^{(j)}}; \quad j = 1, \dots, I; \quad (\text{C.9})$$

$$e_5 \equiv \frac{\partial N_5}{\partial m_a}; \quad (\text{C.10})$$

Used in the following of the document, the partial derivatives of $H(m_a, \alpha)$ with respect to m_a are listed as follows:

1) For $\text{Re}_d < 2300$:

$$\frac{\partial H_1}{\partial m_a} = \frac{\partial \left[\frac{f_{ht} a_{0,Nu} K_{air} w_{tsa} A_{surf}}{D_h I} \right]}{\partial m_a} = 0; \quad (\text{C.11})$$

APPENDIX C. DERIVATIVE MATRIX (JACOBIAN) OF THE MODEL EQUATIONS WITH RESPECT TO THE STATE FUNCTIONS

2) For $2,300 \leq \text{Re}_d \leq 10,000$:

$$\begin{aligned} \frac{\partial H_2}{\partial m_a} &= \frac{\partial \left[\frac{f_{ht} \cdot \left(a_{1,Nu} \frac{D_h \cdot |m_a|}{\mu_{air} A_{fill}} + a_{2,Nu} \right) K_{air} w_{tsa} A_{surf}}{D_h I} \right]}{\partial m_a} \\ &= \frac{f_{ht} a_{1,Nu} K_{air} w_{tsa} A_{surf}}{\mu_{air} A_{fill} I} \cdot \text{sgn}(m_a); \end{aligned} \quad (\text{C.12})$$

3) For $\text{Re}_d > 10,000$:

$$\begin{aligned} \frac{\partial H_3}{\partial m_a} &= \frac{\partial \left[\frac{f_{ht} a_{3,Nu} \cdot \left(\frac{D_h \cdot |m_a|}{\mu_{air} A_{fill}} \right)^{0.8} \text{Pr}^{\frac{1}{3}} K_{air} w_{tsa} A_{surf}}{D_h I} \right]}{\partial m_a} \\ &= \frac{4}{5} \frac{f_{ht} a_{3,Nu} \text{Pr}^{\frac{1}{3}} K_{air} w_{tsa} A_{surf}}{(\mu_{air} A_{fill})^{0.8} \cdot (D_h m_a)^{0.2} \cdot I} \cdot \text{sgn}(m_a); \end{aligned} \quad (\text{C.13})$$

Used in the following of the document, the partial derivatives of $M(m_a, \alpha)$ with respect to m_a are listed as follows:

1) For $\text{Re}_d < 2300$:

$$\frac{\partial M_1}{\partial m_a} = \frac{\partial \left[\frac{M_{h2o} f_{mt} a_{0,Nu} \nu_{air}^{\frac{1}{3}} D_{av}^{\frac{2}{3}} w_{tsa} A_{surf}}{\text{Pr}^{\frac{1}{3}} D_h I} \right]}{\partial m_a} = 0; \quad (\text{C.14})$$

APPENDIX C. DERIVATIVE MATRIX (JACOBIAN) OF THE MODEL EQUATIONS WITH RESPECT TO THE STATE FUNCTIONS

2) For $2,300 \leq \text{Re}_d \leq 10,000$:

$$\begin{aligned} \frac{\partial M_2}{\partial m_a} &= \frac{\partial \left[\frac{M_{h2o} f_{mt} \cdot \left(\frac{D_h \cdot |m_a| \cdot a_{1,Nu}}{A_{fill} \nu_{air}} + a_{2,Nu} \right) \nu_{air}^{\frac{1}{3}} D_{av}^{\frac{2}{3}} w_{tsa} A_{surf}}{\text{Pr}^{\frac{1}{3}} D_h I} \right]}{\partial m_a} \\ &= \frac{M_{h2o} f_{mt} \cdot a_{1,Nu} D_{av}^{\frac{2}{3}} w_{tsa} A_{surf}}{A_{fill} \nu_{air}^{\frac{2}{3}} \text{Pr}^{\frac{1}{3}} I} \cdot \text{sgn}(m_a); \end{aligned} \quad (\text{C.15})$$

3) For $\text{Re}_d > 10,000$:

$$\begin{aligned} \frac{\partial M_3}{\partial m_a} &= \frac{\partial \left[\frac{M_{h2o} f_{mt} \cdot a_{1,Nu} \left(\frac{D_h \cdot |m_a|}{A_{fill} \nu_{air}} \right)^{0.8} \nu_{air}^{\frac{1}{3}} D_{av}^{\frac{2}{3}} w_{tsa} A_{surf}}{D_h I} \right]}{\partial m_a} \\ &= \frac{4}{5} \frac{M_{h2o} f_{mt} \cdot a_{3,Nu} \nu_{air}^{\frac{1}{3}} D_{av}^{\frac{2}{3}} w_{tsa} A_{surf}}{(m_a D_h)^{0.2} (A_{fill} \nu_{air})^{0.8} I} \cdot \text{sgn}(m_a); \end{aligned} \quad (\text{C.16})$$

C.1 Jacobian Matrix of Case 1a: Fan Off, Saturated Outlet Air Conditions, with Inlet Air Unsaturated

C.1.1 Derivatives of the liquid continuity equations with respect to the state variables

The derivatives of the “liquid continuity equations” [cf. Eqs. (2.2) - (2.5)] with respect to $m_w^{(j)}$ are as follows:

APPENDIX C. DERIVATIVE MATRIX (JACOBIAN) OF THE MODEL EQUATIONS WITH RESPECT TO THE STATE FUNCTIONS

$$\frac{\partial N_1^{(i)}}{\partial m_w^{(j+1)}} \equiv a_1^{i,j} = 0; \quad i = 1, \dots, I; \quad j = 1, \dots, I; \quad j \neq i - 1, \quad i; \quad (C.17)$$

$$\frac{\partial N_1^{(i)}}{\partial m_w^{(i)}} \equiv a_1^{i,i-1} = -1; \quad i = 2, \dots, I; \quad j = i - 1; \quad (C.18)$$

$$\frac{\partial N_1^{(i)}}{\partial m_w^{(i+1)}} \equiv a_1^{i,i} = 1; \quad i = 1, \dots, I; \quad j = i. \quad (C.19)$$

For subsequent use, the above quantities are considered to be the components of the $I \times I$ matrix \mathbf{A}_1 defined as follows:

$$\mathbf{A}_1 \equiv (a_1^{i,j})_{I \times I} = \begin{pmatrix} 1 & 0 & . & 0 & 0 \\ -1 & 1 & . & 0 & 0 \\ . & . & . & . & . \\ 0 & 0 & . & 1 & 0 \\ 0 & 0 & . & -1 & 1 \end{pmatrix} \quad (C.20)$$

The derivatives of the “liquid continuity equations” [cf. Eqs. (2.2) - (2.5)] with respect to $T_w^{(j)}$ are as follows:

$$\frac{\partial N_1^{(i)}}{\partial T_w^{(j+1)}} \equiv b_1^{i,j} = 0; \quad (C.21)$$

$$i = 1, \dots, I; \quad j = 1, \dots, I; \quad j \neq i;$$

$$\frac{\partial N_1^{(i)}}{\partial T_w^{(i+1)}} \equiv b_1^{i,i} = -\frac{M(m_a, \boldsymbol{\alpha})}{\bar{R}} \frac{P_{vs}^{(i+1)}(T_w^{(i+1)}, \boldsymbol{\alpha})}{[T_w^{(i+1)}]^2} \left\{ \frac{a_1}{T_w^{(i+1)}} + 1 \right\}; \quad (C.22)$$

$$i = 1, \dots, I; \quad j = i.$$

APPENDIX C. DERIVATIVE MATRIX (JACOBIAN) OF THE MODEL EQUATIONS WITH RESPECT TO THE STATE FUNCTIONS

For subsequent use, the above quantities are considered to be the components of the $I \times I$ diagonal matrix \mathbf{B}_1 defined as follows:

$$\mathbf{B}_1 \equiv (b_1^{i,j})_{I \times I} = \begin{pmatrix} b_1^{1,1} & 0 & . & 0 & 0 \\ 0 & b_1^{2,2} & . & 0 & 0 \\ . & . & . & . & . \\ 0 & 0 & . & b_1^{I-1,I-1} & 0 \\ 0 & 0 & . & 0 & b_1^{I,I} \end{pmatrix} \quad (\text{C.23})$$

The derivatives of the “liquid continuity equations” [cf. Eqs. (2.2) - (2.5)] with respect to $T_a^{(j)}$ are as follows:

$$\frac{\partial N_1^{(i)}}{\partial T_a^{(j)}} \equiv c_1^{i,j} = 0; \quad i = 1, \dots, I; \quad j = 1, \dots, I; \quad j \neq i; \quad (\text{C.24})$$

$$\frac{\partial N_1^{(i)}}{\partial T_a^{(i)}} \equiv c_1^{i,i} = \frac{M(m_a, \boldsymbol{\alpha})}{\bar{R}} \frac{P_{vs}^{(i)}(T_a^{(i)}, \boldsymbol{\alpha})}{[T_a^{(i)}]^2} \left[1 + \frac{a_1}{T_a^{(i)}} \right]; \quad i = 1, \dots, K; \quad j = i. \quad (\text{C.25})$$

$$\frac{\partial N_1^{(i)}}{\partial T_a^{(i)}} \equiv c_1^{i,i} = \frac{M(m_a, \boldsymbol{\alpha})}{\bar{R}} \frac{\omega^{(i)} P_{atm}}{[T_a^{(i)}]^2 (0.622 + \omega^{(i)})}; \quad i = K + 1, \dots, I; \quad j = i. \quad (\text{C.26})$$

For subsequent use, the above quantities are considered to be the components of the $I \times I$ diagonal matrix \mathbf{C}_1 defined as follows:

$$\mathbf{C}_1 \equiv (c_1^{i,j})_{I \times I} = \begin{pmatrix} c_1^{1,1} & 0 & . & 0 & 0 \\ 0 & c_1^{2,2} & . & 0 & 0 \\ . & . & . & . & . \\ 0 & 0 & . & c_1^{I-1,I-1} & 0 \\ 0 & 0 & . & 0 & c_1^{I,I} \end{pmatrix} \quad (\text{C.27})$$

APPENDIX C. DERIVATIVE MATRIX (JACOBIAN) OF THE MODEL EQUATIONS WITH RESPECT TO THE STATE FUNCTIONS

The derivatives of the “liquid continuity equations” [cf. Eqs. (2.2) - (2.5)] with respect to $\omega^{(j)}$ are as follows:

$$\frac{\partial N_1^{(i)}}{\partial \omega^{(j)}} \equiv d_1^{i,j} = 0; \quad i = 1, \dots, I; \quad j = 1, \dots, I; \quad j \neq i; \quad (\text{C.28})$$

$$\frac{\partial N_1^{(i)}}{\partial \omega^{(i)}} \equiv d_1^{i,i} = 0; \quad i = 1, \dots, K; \quad j = i. \quad (\text{C.29})$$

$$\frac{\partial N_1^{(i)}}{\partial \omega^{(i)}} \equiv d_1^{i,i} = \frac{M(m_a, \boldsymbol{\alpha})}{\bar{R}} \frac{P_{atm}}{[0.622 + \omega^{(i)}] T_a^{(i)}} \left\{ \frac{\omega^{(i)}}{[0.622 + \omega^{(i)}]} - 1 \right\}; \quad (\text{C.30})$$

$$i = K + 1, \dots, I; \quad j = i.$$

For subsequent use, the above quantities are considered to be the components of the $I \times I$ diagonal matrix \mathbf{D}_1 defined as follows:

$$\mathbf{D}_1 \equiv (d_1^{i,j})_{I \times I} = \begin{pmatrix} d_1^{1,1} & 0 & . & 0 & 0 \\ 0 & d_1^{2,2} & . & 0 & 0 \\ . & . & . & . & . \\ 0 & 0 & . & d_1^{I-1,I-1} & 0 \\ 0 & 0 & . & 0 & d_1^{I,I} \end{pmatrix} \quad (\text{C.31})$$

The derivatives of the “liquid continuity equations” [cf. Eqs. (2.2) - (2.5)] with respect to m_a are:

1) For $\text{Re}_d < 2300$

$$\frac{\partial N_1^{(i)}}{\partial m_a} \equiv e_1^i = 0; \quad i = 1, \dots, I; \quad (\text{C.32})$$

APPENDIX C. DERIVATIVE MATRIX (JACOBIAN) OF THE MODEL EQUATIONS WITH RESPECT TO THE STATE FUNCTIONS

2) For $2,300 \leq \text{Re}_d \leq 10,000$

$$\frac{\partial N_1^{(i)}}{\partial m_a} \equiv e_1^i = \left[\frac{P_{vs}(T_w^{(i+1)}, \boldsymbol{\alpha})}{\bar{R} \cdot T_w^{(i+1)}} - \frac{P_{vs}^{(i)}(T_a^{(i)}, \boldsymbol{\alpha})}{T_a^{(i)}} \right] \cdot \frac{\partial M_2(m_a, \boldsymbol{\alpha})}{\partial m_a}; \quad (\text{C.33})$$

$$i = 1, \dots, K;$$

$$\frac{\partial N_1^{(i)}}{\partial m_a} \equiv e_1^i = \left[\frac{P_{vs}(T_w^{(i+1)}, \boldsymbol{\alpha})}{\bar{R} \cdot T_w^{(i+1)}} - \frac{\omega^{(i)} P_{atm}}{\bar{R} \cdot T_a^{(i)} (0.622 + \omega^{(i)})} \right] \cdot \frac{\partial M_2(m_a, \boldsymbol{\alpha})}{\partial m_a}; \quad (\text{C.34})$$

$$i = K + 1, \dots, I;$$

3) For $\text{Re}_d > 10,000$

$$\frac{\partial N_1^{(i)}}{\partial m_a} \equiv e_1^i = \left[\frac{P_{vs}(T_w^{(i+1)}, \boldsymbol{\alpha})}{\bar{R} \cdot T_w^{(i+1)}} - \frac{P_{vs}^{(i)}(T_a^{(i)}, \boldsymbol{\alpha})}{T_a^{(i)}} \right] \cdot \frac{\partial M_3(m_a, \boldsymbol{\alpha})}{\partial m_a}; \quad (\text{C.35})$$

$$i = 1, \dots, K;$$

$$\frac{\partial N_1^{(i)}}{\partial m_a} \equiv e_1^i = \left[\frac{P_{vs}(T_w^{(i+1)}, \boldsymbol{\alpha})}{\bar{R} \cdot T_w^{(i+1)}} - \frac{\omega^{(i)} P_{atm}}{\bar{R} \cdot T_a^{(i)} (0.622 + \omega^{(i)})} \right] \cdot \frac{\partial M_3(m_a, \boldsymbol{\alpha})}{\partial m_a}; \quad (\text{C.36})$$

$$i = K + 1, \dots, I;$$

For subsequent use, the above quantities are considered to be the components of the I column vector \mathbf{E}_1 defined as follows:

$$\mathbf{E}_1 \equiv (e_1^i)_I = \begin{pmatrix} e_1^1 \\ e_1^2 \\ \vdots \\ e_1^{I-1} \\ e_1^I \end{pmatrix} \quad (\text{C.37})$$

APPENDIX C. DERIVATIVE MATRIX (JACOBIAN) OF THE MODEL EQUATIONS WITH RESPECT TO THE STATE FUNCTIONS

C.1.2 Derivatives of the liquid energy balance equations with respect to the state variables

Derivatives of the liquid energy balance equations [cf. Eqs. (2.6) - (2.8)] with respect to $m_w^{(j)}$ are as follows:

$$\frac{\partial N_2^{(i)}}{\partial m_w^{(j+1)}} \equiv a_2^{i,j} = 0; \quad i = 1, \dots, I; \quad j = 1, \dots, I; \quad j \neq i - 1, \quad i; \quad (\text{C.38})$$

$$\frac{\partial N_2^{(i)}}{\partial m_w^{(i)}} \equiv a_2^{i,i-1} = h_f^{(i)}(T_w^{(i)}, \boldsymbol{\alpha}) - h_g^{(i+1)}(T_w^{(i+1)}, \boldsymbol{\alpha}); \quad i = 2, \dots, I; \quad j = i - 1; \quad (\text{C.39})$$

$$\frac{\partial N_2^{(i)}}{\partial m_w^{(i+1)}} \equiv a_2^{i,i} = h_g^{(i+1)}(T_w^{(i+1)}, \boldsymbol{\alpha}) - h_f^{(i+1)}(T_w^{(i+1)}, \boldsymbol{\alpha}); \quad i = 1, \dots, I; \quad j = i. \quad (\text{C.40})$$

For subsequent use, the above quantities are considered to be the components of the $I \times I$ matrix \mathbf{A}_2 defined as follows:

$$\mathbf{A}_2 \equiv (a_2^{i,j})_{I \times I} = \begin{pmatrix} a_2^{1,1} & 0 & . & 0 & 0 \\ a_2^{2,1} & a_2^{2,2} & . & 0 & 0 \\ . & . & . & . & . \\ 0 & 0 & . & a_2^{I-1,I-1} & 0 \\ 0 & 0 & . & a_2^{I,I-1} & a_2^{I,I} \end{pmatrix} \quad (\text{C.41})$$

Derivatives of the liquid energy balance equations [cf. Eqs. (2.6) - (2.8)] with respect to $T_w^{(j)}$ are as follows:

$$\frac{\partial N_2^{(i)}}{\partial T_w^{(j+1)}} \equiv b_2^{i,j} = 0; \quad i = 1, \dots, I; \quad j = 1, \dots, I; \quad j \neq i - 1, \quad i; \quad (\text{C.42})$$

$$\frac{\partial N_2^{(i)}}{\partial T_w^{(i)}} \equiv b_2^{i,i-1} = m_w^{(i)} \frac{\partial h_f^{(i)}}{\partial T_w^{(i)}}; \quad i = 2, \dots, I; \quad j = i - 1; \quad (\text{C.43})$$

APPENDIX C. DERIVATIVE MATRIX (JACOBIAN) OF THE MODEL EQUATIONS WITH RESPECT TO THE STATE FUNCTIONS

$$\frac{\partial N_2^{(i)}}{\partial T_w^{(i+1)}} \equiv b_2^{i,i} = -m_w^{(i+1)} \frac{\partial h_f^{(i+1)}}{\partial T_w^{(i+1)}} - (m_w^{(i)} - m_w^{(i+1)}) \frac{\partial h_{g,w}^{(i+1)}}{\partial T_w^{(i+1)}} \quad (\text{C.44})$$

$$-H(m_a, \boldsymbol{\alpha}); \quad i = 1, \dots, I; \quad j = i.$$

For subsequent use, the above quantities are considered to be the components of the $I \times I$ diagonal matrix \mathbf{B}_2 defined as follows:

$$\mathbf{B}_2 \equiv (b_2^{i,j})_{I \times I} = \begin{pmatrix} b_2^{1,1} & 0 & . & 0 & 0 \\ b_2^{2,1} & b_2^{2,2} & . & 0 & 0 \\ . & . & . & . & . \\ 0 & 0 & . & b_2^{I-1,I-1} & 0 \\ 0 & 0 & . & b_2^{I,I-1} & b_2^{I,I} \end{pmatrix} \quad (\text{C.45})$$

Derivatives of the liquid energy balance equations [cf. Eqs. (2.6) - (2.8)] with respect to $T_a^{(j)}$ are as follows:

$$\frac{\partial N_2^{(i)}}{\partial T_a^{(j)}} \equiv c_2^{i,j} = 0; \quad i = 1, \dots, I; \quad i = 1, \dots, I; \quad j \neq i; \quad (\text{C.46})$$

$$\frac{\partial N_2^{(i)}}{\partial T_a^{(i)}} \equiv c_2^{i,i} = H(m_a, \boldsymbol{\alpha}); \quad i = 1, \dots, I; \quad j = i. \quad (\text{C.47})$$

For subsequent use, the above quantities are considered to be the components of the $I \times I$ diagonal matrix \mathbf{C}_2 defined as follows:

$$\mathbf{C}_2 \equiv (c_2^{i,j})_{I \times I} = \begin{pmatrix} c_2^{1,1} & 0 & . & 0 & 0 \\ 0 & c_2^{2,2} & . & 0 & 0 \\ . & . & . & . & . \\ 0 & 0 & . & c_2^{I-1,I-1} & 0 \\ 0 & 0 & . & 0 & c_2^{I,I} \end{pmatrix} \quad (\text{C.48})$$

APPENDIX C. DERIVATIVE MATRIX (JACOBIAN) OF THE MODEL EQUATIONS WITH RESPECT TO THE STATE FUNCTIONS

The derivatives of the liquid energy balance equations [cf. Eqs. (2.6) - (2.8)] with respect to $\omega^{(j)}$ are as follows:

$$\frac{\partial N_2^{(i)}}{\partial \omega^{(j)}} \equiv d_2^{i,j} = 0; \quad i = 1, \dots, I; \quad j = 1, \dots, I. \quad (\text{C.49})$$

For subsequent use, the above quantities are considered to be the components of the $I \times I$ matrix:

$$\mathbf{D}_2 \equiv [d_2^{i,j}]_{I \times I} = \mathbf{0}. \quad (\text{C.50})$$

The derivatives of the liquid energy balance equations [cf. Eqs. (2.6) - (2.8)] with respect to m_a are:

1) For $\text{Re}_d < 2300$:

$$\frac{\partial N_2^{(i)}}{\partial m_a} \equiv e_2^i = 0; \quad i = 1, \dots, I; \quad (\text{C.51})$$

2) For $2,300 \leq \text{Re}_d \leq 10,000$:

$$\frac{\partial N_2^{(i)}}{\partial m_a} \equiv e_2^i = -(T_w^{(i+1)} - T_a^{(i)}) \cdot \frac{\partial H_2(m_a, \boldsymbol{\alpha})}{\partial m_a}; \quad i = 1, \dots, I; \quad (\text{C.52})$$

3) For $\text{Re}_d > 10,000$:

$$\frac{\partial N_2^{(i)}}{\partial m_a} \equiv e_2^i = -(T_w^{(i+1)} - T_a^{(i)}) \cdot \frac{\partial H_3(m_a, \boldsymbol{\alpha})}{\partial m_a}; \quad i = 1, \dots, I; \quad (\text{C.53})$$

APPENDIX C. DERIVATIVE MATRIX (JACOBIAN) OF THE MODEL EQUATIONS WITH RESPECT TO THE STATE FUNCTIONS

For subsequent use, the above quantities are considered to be the components of the I column vector \mathbf{E}_2 defined as follows:

$$\mathbf{E}_2 \equiv (e_2^i)_I = \begin{pmatrix} e_2^1 \\ e_2^2 \\ \vdots \\ e_2^{I-1} \\ e_2^I \end{pmatrix} \quad (\text{C.54})$$

C.1.3 Derivatives of the water vapor continuity equations with respect to the state variables

The derivatives of the water vapor continuity equations [cf. Eqs. (2.9) - (2.11)] with respect to $m_w^{(j)}$ are as follows:

$$\frac{\partial N_3^{(i)}}{\partial m_w^{(j+1)}} \equiv a_3^{i,j} = 0; \quad i = 1, \dots, I; \quad j = 1, \dots, I; \quad j \neq i - 1, \quad i; \quad (\text{C.55})$$

$$\frac{\partial N_3^{(i)}}{\partial m_w^{(i)}} \equiv a_3^{i,i-1} = \frac{1}{m_a}; \quad i = 2, \dots, I; \quad j = i - 1; \quad (\text{C.56})$$

$$\frac{\partial N_3^{(i)}}{\partial m_w^{(i+1)}} \equiv a_3^{i,i} = -\frac{1}{m_a}; \quad i = 1, \dots, I; \quad j = i. \quad (\text{C.57})$$

For subsequent use, the above quantities are considered to be the components of the $I \times I$ matrix \mathbf{A}_3 defined as follows:

APPENDIX C. DERIVATIVE MATRIX (JACOBIAN) OF THE MODEL EQUATIONS WITH RESPECT TO THE STATE FUNCTIONS

$$\mathbf{A}_3 \equiv (a_3^{i,j})_{I \times I} = \frac{1}{m_a} \begin{pmatrix} -1 & 0 & . & 0 & 0 \\ 1 & -1 & . & 0 & 0 \\ . & . & . & . & . \\ 0 & 0 & . & -1 & 0 \\ 0 & 0 & . & 1 & -1 \end{pmatrix}. \quad (\text{C.58})$$

The derivatives of the water vapor continuity equations [cf. Eqs. (2.9) - (2.11)] with respect to $T_w^{(j)}$ are as follows:

$$\frac{\partial N_3^{(i)}}{\partial T_w^{(j+1)}} \equiv b_3^{i,j} = 0; \quad i = 1, \dots, I; \quad j = 1, \dots, I. \quad (\text{C.59})$$

For subsequent use, the above quantities are considered to be the components of the $I \times I$ matrix

$$\mathbf{B}_3 \equiv [b_3^{i,j}]_{I \times I} = \mathbf{0}. \quad (\text{C.60})$$

The derivatives of the water vapor continuity equations [cf. Eqs. (2.9) - (2.11)] with respect to $T_a^{(j)}$ are as follows:

$$\frac{\partial N_3^{(i)}}{\partial T_a^{(j)}} \equiv c_3^{i,j} = 0; \quad i = 1, \dots, I; \quad j = 1, \dots, I. \quad (\text{C.61})$$

For subsequent use, the above quantities are considered to be the components of the $I \times I$ matrix

$$\mathbf{C}_3 \equiv [c_3^{i,j}]_{I \times I} = \mathbf{0}. \quad (\text{C.62})$$

The derivatives of the water vapor continuity equations [cf. Eqs. (2.9) - (2.11)] with respect to $\omega^{(j)}$ are:

$$\frac{\partial N_3^{(i)}}{\partial \omega^{(j)}} \equiv d_3^{i,j} = 0; \quad i = 1, \dots, I; \quad j = 1, \dots, I; \quad j \neq i, i+1; \quad (\text{C.63})$$

APPENDIX C. DERIVATIVE MATRIX (JACOBIAN) OF THE MODEL EQUATIONS WITH RESPECT TO THE STATE FUNCTIONS

$$\frac{\partial N_3^{(i)}}{\partial \omega^{(i)}} \equiv d_3^{i,i} = -1; \quad i = 1, \dots, I; j = i. \quad (\text{C.64})$$

$$\frac{\partial N_3^{(i)}}{\partial \omega^{(i+1)}} \equiv d_3^{i,i+1} = 1; \quad i = 1, \dots, I-1; j = i+1. \quad (\text{C.65})$$

For subsequent use, the above quantities are considered to be the components of the $I \times I$ matrix \mathbf{D}_3 defined as follows:

$$\mathbf{D}_3 \equiv (d_3^{i,j})_{I \times I} = \begin{pmatrix} -1 & 1 & . & 0 & 0 \\ 0 & -1 & . & 0 & 0 \\ . & . & . & . & . \\ 0 & 0 & . & -1 & 1 \\ 0 & 0 & . & 0 & -1 \end{pmatrix} \quad (\text{C.66})$$

The derivatives of the water vapor continuity equations [cf. Eqs. (2.9) - (2.11)] with respect to m_a are:

$$\frac{\partial N_3^{(i)}}{\partial m_a} \equiv e_3^i = -(m_w^{(i)} - m_w^{(i+1)}) \cdot \frac{\text{sgn}(m_a)}{m_a^2} = -\frac{(m_w^{(i)} - m_w^{(i+1)})}{m_a \cdot |m_a|}, \quad (\text{C.67})$$

$$i = 1, \dots, I;$$

For subsequent use, the above quantities are considered to be the components of the I column vector \mathbf{E}_3 defined as follows:

$$\mathbf{E}_3 \equiv (e_3^i)_I = \begin{pmatrix} e_3^1 \\ e_3^2 \\ \vdots \\ e_3^{I-1} \\ e_3^I \end{pmatrix} \quad (\text{C.68})$$

APPENDIX C. DERIVATIVE MATRIX (JACOBIAN) OF THE MODEL EQUATIONS WITH RESPECT TO THE STATE FUNCTIONS

C.1.4 Derivatives of the air/water vapor energy balance equations with respect to the state variables

The derivatives of the air/water vapor energy balance equations [cf. Eqs. (2.12) - (2.14)] with respect to $m_w^{(j)}$ are:

$$\frac{\partial N_4^{(i)}}{\partial m_w^{(j+1)}} \equiv a_4^{i,j} = 0; \quad i = 1, \dots, I; \quad j = 1, \dots, I; \quad j \neq i - 1, \quad i; \quad (C.69)$$

$$\frac{\partial N_4^{(i)}}{\partial m_w^{(i)}} \equiv a_4^{i,i-1} = \frac{h_{g,w}^{(i+1)}(T_w^{(i+1)}, \boldsymbol{\alpha})}{m_a}; \quad i = 2, \dots, I; \quad j = i - 1; \quad (C.70)$$

$$\frac{\partial N_4^{(i)}}{\partial m_w^{(i+1)}} \equiv a_4^{i,i} = -\frac{h_{g,w}^{(i+1)}(T_w^{(i+1)}, \boldsymbol{\alpha})}{m_a}; \quad i = 1, \dots, I; \quad j = i. \quad (C.71)$$

For subsequent use, the above quantities are considered to be the components of the $I \times I$ matrix \mathbf{A}_4 defined as follows:

$$\mathbf{A}_4 \equiv (a_4^{i,j})_{I \times I} = \begin{pmatrix} a_4^{1,1} & 0 & . & 0 & 0 \\ a_4^{2,1} & a_4^{2,2} & . & 0 & 0 \\ . & . & . & . & . \\ 0 & 0 & . & a_4^{I-1,I-1} & 0 \\ 0 & 0 & . & a_4^{I,I-1} & a_4^{I,I} \end{pmatrix} \quad (C.72)$$

Derivatives of the air/water vapor energy balance equations [cf. Eqs. (2.12) - (2.14)] with respect $T_w^{(j)}$:

$$\frac{\partial N_4^{(i)}}{\partial T_w^{(j+1)}} \equiv b_4^{i,j} = 0; \quad i = 1, \dots, I; \quad j \neq i; \quad (C.73)$$

$$\frac{\partial N_4^{(i)}}{\partial T_w^{(i+1)}} \equiv b_4^{i,i} = \frac{1}{m_a} \left[(m_w^{(i)} - m_w^{(i+1)}) \frac{\partial h_{g,w}^{(i+1)}}{\partial T_w^{(i+1)}} + H(m_a, \boldsymbol{\alpha}) \right]; \quad (C.74)$$

$$i = 1, \dots, I; \quad j = i.$$

APPENDIX C. DERIVATIVE MATRIX (JACOBIAN) OF THE MODEL EQUATIONS WITH RESPECT TO THE STATE FUNCTIONS

For subsequent use, the above quantities are considered to be the components of the $I \times I$ diagonal matrix \mathbf{B}_4 defined as follows:

$$\mathbf{B}_4 \equiv (b_4^{i,j})_{I \times I} = \begin{pmatrix} b_4^{1,1} & 0 & . & 0 & 0 \\ 0 & b_4^{2,2} & . & 0 & 0 \\ . & . & . & . & . \\ 0 & 0 & . & b_4^{I-1,I-1} & 0 \\ 0 & 0 & . & 0 & b_4^{I,I} \end{pmatrix} \quad (\text{C.75})$$

Derivatives of the air/water vapor energy balance equations [cf. Eqs. (2.12) - (2.14)] with respect to $T_a^{(j)}$:

$$c_4^{i,j} \equiv \frac{\partial N_4^{(i)}}{\partial T_a^{(j)}} = 0; \quad i = 1, \dots, I; \quad j \neq i, i+1; \quad (\text{C.76})$$

$$\begin{aligned} \frac{\partial N_4^{(i)}}{\partial T_a^{(i)}} \equiv c_4^{i,i} &= (T_a^{(i+1)} - T_a^{(i)}) \frac{\partial C_p^{(i)}}{\partial T_a^{(i)}} - C_p^{(i)} \left(\frac{T_a^{(i)} + 273.15}{2}, \boldsymbol{\alpha} \right) \\ &- \omega^{(i)} \frac{\partial h_{g,a}^{(i)}}{\partial T_a^{(i)}} - \frac{H(m_a, \boldsymbol{\alpha})}{m_a}; \quad i = 1, \dots, I; \quad j = i. \end{aligned} \quad (\text{C.77})$$

$$\frac{\partial N_4^{(i)}}{\partial T_a^{(i+1)}} \equiv c_4^{i,i+1} = C_p^{(i)} \left(\frac{T_a^{(i)} + 273.15}{2}, \boldsymbol{\alpha} \right) + \omega^{(i+1)} \frac{\partial h_{g,a}^{(i+1)}}{\partial T_a^{(i+1)}}; \quad (\text{C.78})$$

$$i = 1, \dots, I-1; \quad j = i+1.$$

For subsequent use, the above quantities are considered to be the components of the $I \times I$ diagonal matrix defined as follows:

APPENDIX C. DERIVATIVE MATRIX (JACOBIAN) OF THE MODEL EQUATIONS WITH RESPECT TO THE STATE FUNCTIONS

$$\mathbf{C}_4 \equiv (c_4^{i,j})_{I \times I} = \begin{pmatrix} c_4^{1,1} & c_4^{1,2} & . & 0 & 0 \\ 0 & c_4^{2,2} & . & 0 & 0 \\ . & . & . & . & . \\ 0 & 0 & . & c_4^{I-1,I-1} & c_4^{I-1,I} \\ 0 & 0 & . & 0 & c_4^{I,I} \end{pmatrix} \quad (\text{C.79})$$

Derivatives of the air/water vapor energy balance equations [cf. Eqs. (2.12) - (2.14)] with respect to $\omega^{(j)}$:

$$\frac{\partial N_4^{(i)}}{\partial \omega^{(j)}} \equiv d_4^{i,j} = 0; \quad i = 1, \dots, I; \quad j \neq i, i+1; \quad (\text{C.80})$$

$$\frac{\partial N_4^{(i)}}{\partial \omega^{(i)}} \equiv d_4^{i,i} = -h_{g,a}^{(i)}(T_a^{(i)}, \boldsymbol{\alpha}); \quad i = 1, \dots, I; \quad j = i; \quad (\text{C.81})$$

$$\frac{\partial N_4^{(i)}}{\partial \omega^{(i+1)}} \equiv d_4^{i,i+1} = h_{g,a}^{(i+1)}(T_a^{(i+1)}, \boldsymbol{\alpha}); \quad i = 1, \dots, I-1; \quad j = i+1. \quad (\text{C.82})$$

For subsequent use, the above quantities are considered to be the components of the $I \times I$ diagonal matrix \mathbf{D}_4 defined as follows:

$$\mathbf{D}_4 \equiv (d_4^{i,j})_{I \times I} = \begin{pmatrix} d_4^{1,1} & d_4^{1,2} & . & 0 & 0 \\ 0 & d_4^{2,2} & . & 0 & 0 \\ . & . & . & . & . \\ 0 & 0 & . & d_4^{I-1,I-1} & d_4^{I-1,I} \\ 0 & 0 & . & 0 & d_4^{I,I} \end{pmatrix} \quad (\text{C.83})$$

The derivatives of the air/water vapor energy balance equations [cf. Eqs. (2.12) - (2.14)] with respect to m_a are:

APPENDIX C. DERIVATIVE MATRIX (JACOBIAN) OF THE MODEL EQUATIONS WITH RESPECT TO THE STATE FUNCTIONS

1) For $\text{Re}_d < 2300$:

$$\begin{aligned} \frac{\partial N_4^{(i)}}{\partial m_a} \equiv e_4^i = & -\frac{(T_w^{(i+1)} - T_a^{(i)})}{m_a \cdot |m_a|} \cdot H(m_a, \boldsymbol{\alpha}) - \\ & \frac{(m_w^{(i)} - m_w^{(i+1)}) \cdot h_{g,w}^{(i+1)}(T_w^{(i+1)}, \boldsymbol{\alpha})}{m_a \cdot |m_a|}; \quad i = 1, \dots, I; \end{aligned} \quad (\text{C.84})$$

2) For $2,300 \leq \text{Re}_d \leq 10,000$:

$$\begin{aligned} \frac{\partial N_4^{(i)}}{\partial m_a} \equiv e_4^i = & \frac{(T_w^{(i+1)} - T_a^{(i)})}{|m_a|} \cdot \frac{\partial H_2(m_a, \boldsymbol{\alpha})}{\partial m_a} - \frac{(T_w^{(i+1)} - T_a^{(i)})}{m_a \cdot |m_a|} \cdot H(m_a, \boldsymbol{\alpha}) \\ & - \frac{(m_w^{(i)} - m_w^{(i+1)}) \cdot h_{g,w}^{(i+1)}(T_w^{(i+1)}, \boldsymbol{\alpha})}{m_a \cdot |m_a|}; \quad i = 1, \dots, I; \end{aligned} \quad (\text{C.85})$$

3) For $\text{Re}_d > 10,000$:

$$\begin{aligned} \frac{\partial N_4^{(i)}}{\partial m_a} \equiv e_4^i = & \frac{(T_w^{(i+1)} - T_a^{(i)})}{|m_a|} \cdot \frac{\partial H_3(m_a, \boldsymbol{\alpha})}{\partial m_a} - \frac{(T_w^{(i+1)} - T_a^{(i)})}{m_a \cdot |m_a|} \cdot H(m_a, \boldsymbol{\alpha}) \\ & - \frac{(m_w^{(i)} - m_w^{(i+1)}) \cdot h_{g,w}^{(i+1)}(T_w^{(i+1)}, \boldsymbol{\alpha})}{m_a \cdot |m_a|}; \quad i = 1, \dots, I; \end{aligned} \quad (\text{C.86})$$

For subsequent use, the above quantities are considered to be the components of the I column vector \mathbf{E}_4 defined as follows:

$$\mathbf{E}_4 \equiv (e_4^i)_I = \begin{pmatrix} e_4^1 \\ e_4^2 \\ \vdots \\ e_4^{I-1} \\ e_4^I \end{pmatrix} \quad (\text{C.87})$$

APPENDIX C. DERIVATIVE MATRIX (JACOBIAN) OF THE MODEL EQUATIONS WITH RESPECT TO THE STATE FUNCTIONS

C.1.5 Derivatives of the mechanical energy equation with respect to the state variables

The derivatives of the mechanical energy equation [cf. Eq. (2.15)] with respect to $m_w^{(j)}$ are:

$$a_5^j \equiv \frac{\partial N_5}{\partial m_w^{(j)}} = 0; \quad j = 1, \dots, I. \quad (\text{C.88})$$

For subsequent use, the above quantities are considered to be the components of the I row vector \mathbf{A}_5 defined as follows:

$$\mathbf{A}_5 \equiv (a_5^i)_I = (a_5^1 \quad a_5^2 \quad \dots \quad a_5^{I-1} \quad a_5^I) \quad (\text{C.89})$$

Derivatives of the mechanical energy equation [cf. Eq. (2.15)] with respect to $T_w^{(j)}$:

$$b_5^j \equiv \frac{\partial N_5}{\partial T_w^{(j)}} = 0; \quad j = 1, \dots, I. \quad (\text{C.90})$$

For subsequent use, the above quantities are considered to be the components of the I row vector \mathbf{B}_5 defined as follows:

$$\mathbf{B}_5 \equiv (b_5^i)_I = (b_5^1 \quad b_5^2 \quad \dots \quad b_5^{I-1} \quad b_5^I) \quad (\text{C.91})$$

Derivatives of the mechanical energy equation [cf. Eq. (2.15)] with respect to $T_a^{(j)}$:

$$c_5^j \equiv \frac{\partial N_5}{\partial T_a^{(j)}} = -\frac{P_{atm}g\Delta z}{R_{air} \left[T_a^{(j)} \right]^2}; \quad j = 2, \dots, I. \quad (\text{C.92})$$

$$c_5^1 \equiv \frac{\partial N_5}{\partial T_a^{(1)}} = -\frac{P_{atm}g \left(\frac{\Delta z}{2} + \Delta z_{4-2} \right)}{R_{air} \left[T_a^{(1)} \right]^2}; \quad j = 1. \quad (\text{C.93})$$

APPENDIX C. DERIVATIVE MATRIX (JACOBIAN) OF THE MODEL EQUATIONS WITH RESPECT TO THE STATE FUNCTIONS

For subsequent use, the above quantities are considered to be the components of the I row vector \mathbf{C}_5 defined as follows:

$$\mathbf{C}_5 \equiv (c_5^i)_I = (c_5^1 \quad c_5^2 \quad \dots \quad c_5^{I-1} \quad c_5^I) \quad (\text{C.94})$$

Derivatives of the mechanical energy equation [cf. Eq. (2.15)] with respect to $\omega^{(j)}$:

$$d_5^j \equiv \frac{\partial N_5}{\partial \omega^{(j)}} = 0; \quad j = 1, \dots, I. \quad (\text{C.95})$$

For subsequent use, the above quantities are considered to be the components of the I row vector \mathbf{D}_5 defined as follows:

$$\mathbf{D}_5 \equiv (d_5^i)_I = (d_5^1 \quad d_5^2 \quad \dots \quad d_5^{I-1} \quad d_5^I) \quad (\text{C.96})$$

Derivatives of the mechanical energy equation [cf. Eq. (2.15)] with respect to m_a :

$$\begin{aligned} e_5 \equiv \frac{\partial N_5}{\partial m_a} &= \frac{48f(\Delta z_{fill} + \Delta z_{de})}{\left(\frac{P_{atm}}{R_{air}T_{tdb}}\right)\left(\frac{D_h^2}{\mu_{air}}\right)A_{fill}} \\ &+ \frac{1}{2} \left[\frac{1}{(\pi r_{fan}^2)^2} - \frac{1}{(W_{dkx}W_{dky})^2} + \frac{k_{sum}}{A_{fill}^2} \right] \left(\frac{R_{air}T_{tdb}}{P_{atm}} \right) (2 \cdot |m_a|); \end{aligned} \quad (\text{C.97})$$

For subsequent use, the above quantities are considered to be the components of the 1-component row vector \mathbf{E}_5 defined as follows:

$$\mathbf{E}_5 \equiv (e_5) \quad (\text{C.98})$$

APPENDIX C. DERIVATIVE MATRIX (JACOBIAN) OF THE MODEL
EQUATIONS WITH RESPECT TO THE STATE FUNCTIONS

C.2 Jacobian Matrix of Case 1b: Fan Off, Saturated Outlet Air Conditions, with Inlet Air Saturated

As mentioned in Subsection 3.1.2, the Jacobian matrix of case 1b presents similarities with the Jacobian matrix of case 1a detailed above in Section C.1. More precisely, the sub-matrices $(\mathbf{A}_i, \mathbf{B}_i, \mathbf{C}_i, \mathbf{D}_i, \mathbf{E}_i; \quad i = 2, 3, 4, 5)$ whose elements represents the derivatives of Eqs. (2.28) - (2.37) with respect to the vector valued state function $\mathbf{u} \triangleq (\mathbf{m}_w, \mathbf{T}_w, \mathbf{T}_a, \boldsymbol{\omega}, m_a)^\dagger$ remain the same as in Section C.1, where those sub-matrices represents the same derivatives for Eqs. (2.6) - (2.15); for reasons of brevity, they have not been repeated for case 1b. On the other side, the sub-matrices $(\mathbf{A}_i^I, \mathbf{B}_i^I, \mathbf{C}_i^I, \mathbf{D}_i^I, \mathbf{E}_i^I; \quad i = 1)$ whose elements represents the derivatives of Eqs. (2.25) - (2.27) with respect to the vector valued state function $\mathbf{u} \triangleq (\mathbf{m}_w, \mathbf{T}_w, \mathbf{T}_a, \boldsymbol{\omega}, m_a)^\dagger$, are different from their respective formulations $(\mathbf{A}_i, \mathbf{B}_i, \mathbf{C}_i, \mathbf{D}_i, \mathbf{E}_i; \quad i = 1)$ in Section C.1.1, and therefore they will be hereby detailed.

C.2.1 Derivatives of the liquid continuity equations with respect to the state variables

The derivatives of the “liquid continuity equations” [cf. Eqs. (2.25) - (2.27)] with respect to $m_w^{(j)}$ are as follows:

$$\frac{\partial N_1^{(i)}}{\partial m_w^{(j+1)}} \equiv a_1^{i,j} = 0; \quad i = 1, \dots, I; \quad j = 1, \dots, I; \quad j \neq i - 1, \quad i; \quad (\text{C.99})$$

$$\frac{\partial N_1^{(i)}}{\partial m_w^{(i)}} \equiv a_1^{i,i-1} = -1; \quad i = 2, \dots, I; \quad j = i - 1; \quad (\text{C.100})$$

APPENDIX C. DERIVATIVE MATRIX (JACOBIAN) OF THE MODEL EQUATIONS WITH RESPECT TO THE STATE FUNCTIONS

$$\frac{\partial N_1^{(i)}}{\partial m_w^{(i+1)}} \equiv a_1^{i,i} = 1; \quad i = 1, \dots, I; \quad j = i. \quad (\text{C.101})$$

For subsequent use, the above quantities are considered to be the components of the $I \times I$ matrix \mathbf{A}_1^I defined as follows:

$$\mathbf{A}_1^I \equiv (a_1^{i,j})_{I \times I} = \begin{pmatrix} 1 & 0 & . & 0 & 0 \\ -1 & 1 & . & 0 & 0 \\ . & . & . & . & . \\ 0 & 0 & . & 1 & 0 \\ 0 & 0 & . & -1 & 1 \end{pmatrix} \quad (\text{C.102})$$

The derivatives of the “liquid continuity equations” [cf. Eqs. (2.25) - (2.27)] with respect to $T_w^{(j)}$ are as follows:

$$\frac{\partial N_1^{(i)}}{\partial T_w^{(j+1)}} \equiv b_1^{i,j} = 0; \quad i = 1, \dots, I; \quad j = 1, \dots, I; \quad j \neq i; \quad (\text{C.103})$$

$$\frac{\partial N_1^{(i)}}{\partial T_w^{(i+1)}} \equiv b_1^{i,i} = -\frac{M(m_a, \boldsymbol{\alpha})}{\bar{R}} \frac{P_{vs}^{(i+1)}(T_w^{(i+1)}, \boldsymbol{\alpha})}{[T_w^{(i+1)}]^2} \left\{ \frac{a_1}{T_w^{(i+1)}} + 1 \right\}; \quad (\text{C.104})$$

$$i = 1, \dots, I; \quad j = i.$$

For subsequent use, the above quantities are considered to be the components of the $I \times I$ diagonal matrix \mathbf{B}_1^I defined as follows:

$$\mathbf{B}_1^I \equiv (b_1^{i,j})_{I \times I} = \begin{pmatrix} b_1^{1,1} & 0 & . & 0 & 0 \\ 0 & b_1^{2,2} & . & 0 & 0 \\ . & . & . & . & . \\ 0 & 0 & . & b_1^{I-1,I-1} & 0 \\ 0 & 0 & . & 0 & b_1^{I,I} \end{pmatrix} \quad (\text{C.105})$$

APPENDIX C. DERIVATIVE MATRIX (JACOBIAN) OF THE MODEL EQUATIONS WITH RESPECT TO THE STATE FUNCTIONS

The derivatives of the “liquid continuity equations” [cf. Eqs. (2.25) - (2.27)] with respect to $T_a^{(j)}$ are as follows:

$$\frac{\partial N_1^{(i)}}{\partial T_a^{(j)}} \equiv c_1^{i,j} = 0; \quad i = 1, \dots, I; \quad j = 1, \dots, I; \quad j \neq i; \quad (\text{C.106})$$

$$\frac{\partial N_1^{(i)}}{\partial T_a^{(i)}} \equiv c_1^{i,i} = \frac{M(m_a, \boldsymbol{\alpha})}{\bar{R}} \frac{P_{vs}^{(i)}(T_a^{(i)}, \boldsymbol{\alpha})}{[T_a^{(i)}]^2} \left\{ \frac{a_1}{T_a^{(i)}} + 1 \right\}; \quad i = 1, \dots, I; \quad j = i. \quad (\text{C.107})$$

For subsequent use, the above quantities are considered to be the components of the $I \times I$ diagonal matrix \mathbf{C}_1^I defined as follows:

$$\mathbf{C}_1^I \equiv (c_1^{i,j})_{I \times I} = \begin{pmatrix} c_1^{1,1} & 0 & . & 0 & 0 \\ 0 & c_1^{2,2} & . & 0 & 0 \\ . & . & . & . & . \\ 0 & 0 & . & c_1^{I-1,I-1} & 0 \\ 0 & 0 & . & 0 & c_1^{I,I} \end{pmatrix} \quad (\text{C.108})$$

The derivatives of the “liquid continuity equations” [cf. Eqs. (2.25) - (2.27)] with respect to $\omega^{(j)}$ are as follows:

$$\frac{\partial N_1^{(i)}}{\partial \omega^{(j)}} \equiv d_1^{i,j} = 0; \quad i = 1, \dots, I; \quad j = 1, \dots, I; \quad j \neq i; \quad (\text{C.109})$$

$$\frac{\partial N_1^{(i)}}{\partial \omega^{(i)}} \equiv d_1^{i,i} = 0; \quad i = 1, \dots, I; \quad j = i. \quad (\text{C.110})$$

For subsequent use, the above quantities are considered to be the components of the $I \times I$ diagonal matrix \mathbf{D}_1^I defined as follows:

$$\mathbf{D}_1^I \equiv [d_1^{i,j}]_{I \times I} = \mathbf{0}. \quad (\text{C.111})$$

APPENDIX C. DERIVATIVE MATRIX (JACOBIAN) OF THE MODEL EQUATIONS WITH RESPECT TO THE STATE FUNCTIONS

The derivatives of the “liquid continuity equations” [cf. Eqs. (2.25) - (2.27)] with respect to m_a are:

1) For $\text{Re}_d < 2300$:

$$\frac{\partial N_1^{(i)}}{\partial m_a} \equiv e_1^i = 0; \quad i = 1, \dots, I; \quad (\text{C.112})$$

2) For $2,300 \leq \text{Re}_d \leq 10,000$:

$$\begin{aligned} \frac{\partial N_1^{(i)}}{\partial m_a} \equiv e_1^i &= \left[\frac{P_{vs}(T_w^{(i+1)}, \boldsymbol{\alpha})}{\bar{R} \cdot T_w^{(i+1)}} - \frac{P_{vs}^{(i)}(T_a^{(i)}, \boldsymbol{\alpha})}{\bar{R} \cdot T_a^{(i)}} \right] \cdot \frac{\partial M_2(m_a, \boldsymbol{\alpha})}{\partial m_a}; \\ i &= 1, \dots, I; \end{aligned} \quad (\text{C.113})$$

3) For $\text{Re}_d > 10,000$:

$$\begin{aligned} \frac{\partial N_1^{(i)}}{\partial m_a} \equiv e_1^i &= \left[\frac{P_{vs}(T_w^{(i+1)}, \boldsymbol{\alpha})}{\bar{R} \cdot T_w^{(i+1)}} - \frac{P_{vs}^{(i)}(T_a^{(i)}, \boldsymbol{\alpha})}{\bar{R} \cdot T_a^{(i)}} \right] \cdot \frac{\partial M_3(m_a, \boldsymbol{\alpha})}{\partial m_a}; \\ i &= 1, \dots, I; \end{aligned} \quad (\text{C.114})$$

For subsequent use, the above quantities are considered to be the components of the I column vector \mathbf{E}_1^I defined as follows:

$$\mathbf{E}_1^I \equiv (e_1^i)_I = \begin{pmatrix} e_1^1 \\ e_1^2 \\ \vdots \\ e_1^{I-1} \\ e_1^I \end{pmatrix} \quad (\text{C.115})$$

*APPENDIX C. DERIVATIVE MATRIX (JACOBIAN) OF THE MODEL
EQUATIONS WITH RESPECT TO THE STATE FUNCTIONS*

**C.2.2 Derivatives of the liquid energy balance equations
with respect to the state variables**

Derivatives of the liquid energy balance equations [cf. Eqs. (2.28) - (2.30)] with respect to the vector-values state function $\mathbf{u} \triangleq (\mathbf{m}_w, \mathbf{T}_w, \mathbf{T}_a, \boldsymbol{\omega}, m_a)^\dagger$ for case 1b are identical to the respective derivatives of Eqs. (2.6) - (2.8) detailed for case 1a.

See Eqs. (C.38) through (C.54) in Section C.1.2.

**C.2.3 Derivatives of the water vapor continuity equations
with respect to the state variables**

Derivatives of the water vapor continuity equations [cf. Eqs. (2.31) - (2.33)] with respect to the vector-values state function $\mathbf{u} \triangleq (\mathbf{m}_w, \mathbf{T}_w, \mathbf{T}_a, \boldsymbol{\omega}, m_a)^\dagger$ for case 1b are identical to the respective derivatives of Eqs. (2.9) - (2.11) detailed for case 1a. See Eqs. (C.55) through (C.68) in Section C.1.3.

**C.2.4 Derivatives of the air/water vapor energy balance
equations with respect to the state variables**

Derivatives of the air/water vapor balance equations [cf. Eqs. (2.34) - (2.36)] with respect to the vector-values state function $\mathbf{u} \triangleq (\mathbf{m}_w, \mathbf{T}_w, \mathbf{T}_a, \boldsymbol{\omega}, m_a)^\dagger$ for case 1b are identical to the respective derivatives of Eqs. (2.12) - (2.14) detailed for case 1a. See Eqs. (C.69) through (C.87) in Section C.1.4.

APPENDIX C. DERIVATIVE MATRIX (JACOBIAN) OF THE MODEL EQUATIONS WITH RESPECT TO THE STATE FUNCTIONS

C.2.5 Derivatives of the mechanical energy equation with respect to the state variables

Derivatives of mechanical energy equation [cf. Eq. (2.37)] with respect to the vector-values state function $\mathbf{u} \triangleq (\mathbf{m}_w, \mathbf{T}_w, \mathbf{T}_a, \boldsymbol{\omega}, m_a)^\dagger$ for case 1b are identical to the respective derivatives of Eq. (2.15) detailed for case 1a. See Eqs. (C.88) through (C.98) in Section C.1.5.

C.3 Jacobian Matrix of Case 2: Fan Off, Unsaturated Air Conditions

As mentioned in Subsection 3.1.3, the Jacobian matrix of case 2 presents similarities with the Jacobian matrix of case 1a detailed above in Section C.1. More precisely, the sub-matrices $(\mathbf{A}_i, \mathbf{B}_i, \mathbf{C}_i, \mathbf{D}_i, \mathbf{E}_i; \quad i = 2, 3, 4, 5)$ whose elements represents the derivatives of Eqs. (2.41) - (2.50) with respect to the vector valued state function $\mathbf{u} \triangleq (\mathbf{m}_w, \mathbf{T}_w, \mathbf{T}_a, \boldsymbol{\omega}, m_a)^\dagger$ remain the same as in Section C.1, where those sub-matrices represents the same derivatives for Eqs. (2.6) - (2.15); for reasons of brevity, they have not been repeated for case 2. On the other side, the sub-matrices $(\mathbf{A}_i^{II}, \mathbf{B}_i^{II}, \mathbf{C}_i^{II}, \mathbf{D}_i^{II}, \mathbf{E}_i^{II}; \quad i = 1)$ whose elements represents the derivatives of Eqs. (2.38) - (2.40) with respect to the vector valued state function $\mathbf{u} \triangleq (\mathbf{m}_w, \mathbf{T}_w, \mathbf{T}_a, \boldsymbol{\omega}, m_a)^\dagger$, are different from their respective formulations $(\mathbf{A}_i, \mathbf{B}_i, \mathbf{C}_i, \mathbf{D}_i, \mathbf{E}_i; \quad i = 1)$ in Section C.1.1, and therefore they will be hereby detailed.

APPENDIX C. DERIVATIVE MATRIX (JACOBIAN) OF THE MODEL
EQUATIONS WITH RESPECT TO THE STATE FUNCTIONS

**C.3.1 Derivatives of the liquid continuity equations with
respect to the state variables**

The derivatives of the “liquid continuity equations” [cf. Eqs. (2.38) - (2.40)] with respect to $m_w^{(j)}$ are as follows:

$$\frac{\partial N_1^{(i)}}{\partial m_w^{(j+1)}} \equiv a_1^{i,j} = 0; \quad i = 1, \dots, I; \quad j = 1, \dots, I; \quad j \neq i - 1, \quad i; \quad (C.116)$$

$$\frac{\partial N_1^{(i)}}{\partial m_w^{(i)}} \equiv a_1^{i,i-1} = -1; \quad i = 2, \dots, I; \quad j = i - 1; \quad (C.117)$$

$$\frac{\partial N_1^{(i)}}{\partial m_w^{(i+1)}} \equiv a_1^{i,i} = 1; \quad i = 1, \dots, I; \quad j = i. \quad (C.118)$$

For subsequent use, the above quantities are considered to be the components of the $I \times I$ matrix \mathbf{A}_1^{II} defined as follows:

$$\mathbf{A}_1^{II} \equiv (a_1^{i,j})_{I \times I} = \begin{pmatrix} 1 & 0 & . & 0 & 0 \\ -1 & 1 & . & 0 & 0 \\ . & . & . & . & . \\ 0 & 0 & . & 1 & 0 \\ 0 & 0 & . & -1 & 1 \end{pmatrix} \quad (C.119)$$

The derivatives of the “liquid continuity equations” [cf. Eqs. (2.38) - (2.40)] with respect to $T_w^{(j)}$ are as follows:

$$\frac{\partial N_1^{(i)}}{\partial T_w^{(j+1)}} \equiv b_1^{i,j} = 0; \quad i = 1, \dots, I; \quad j = 1, \dots, I; \quad j \neq i; \quad (C.120)$$

APPENDIX C. DERIVATIVE MATRIX (JACOBIAN) OF THE MODEL EQUATIONS WITH RESPECT TO THE STATE FUNCTIONS

$$\frac{\partial N_1^{(i)}}{\partial T_w^{(i+1)}} \equiv b_1^{i,i} = -\frac{M(m_a, \boldsymbol{\alpha})}{\bar{R}} \frac{P_{vs}^{(i+1)}(T_w^{(i+1)}, \boldsymbol{\alpha})}{[T_w^{(i+1)}]^2} \left\{ \frac{a_1}{T_w^{(i+1)}} + 1 \right\}; \quad (\text{C.121})$$

$$i = 1, \dots, I; \quad j = i.$$

For subsequent use, the above quantities are considered to be the components of the $I \times I$ diagonal matrix \mathbf{B}_1^{II} defined as follows:

$$\mathbf{B}_1^{II} \equiv (b_1^{i,j})_{I \times I} = \begin{pmatrix} b_1^{1,1} & 0 & . & 0 & 0 \\ 0 & b_1^{2,2} & . & 0 & 0 \\ . & . & . & . & . \\ 0 & 0 & . & b_1^{I-1,I-1} & 0 \\ 0 & 0 & . & 0 & b_1^{I,I} \end{pmatrix} \quad (\text{C.122})$$

The derivatives of the “liquid continuity equations” [cf. Eqs. (2.38) - (2.40)] with respect to $T_a^{(j)}$ are as follows:

$$\frac{\partial N_1^{(i)}}{\partial T_a^{(j)}} \equiv c_1^{i,j} = 0; \quad i = 1, \dots, I; \quad j = 1, \dots, I; \quad j \neq i; \quad (\text{C.123})$$

$$\frac{\partial N_1^{(i)}}{\partial T_a^{(i)}} \equiv c_1^{i,i} = \frac{M(m_a, \alpha)}{\bar{R}} \frac{\omega^{(i)} P_{atm}}{[T_a^{(i)}]^2 (0.622 + \omega^{(i)})}; \quad i = 1, \dots, I; \quad j = i. \quad (\text{C.124})$$

For subsequent use, the above quantities are considered to be the components of the $I \times I$ diagonal matrix \mathbf{C}_1^{II} defined as follows:

$$\mathbf{C}_1^{II} \equiv (c_1^{i,j})_{I \times I} = \begin{pmatrix} c_1^{1,1} & 0 & . & 0 & 0 \\ 0 & c_1^{2,2} & . & 0 & 0 \\ . & . & . & . & . \\ 0 & 0 & . & c_1^{I-1,I-1} & 0 \\ 0 & 0 & . & 0 & c_1^{I,I} \end{pmatrix}. \quad (\text{C.125})$$

APPENDIX C. DERIVATIVE MATRIX (JACOBIAN) OF THE MODEL EQUATIONS WITH RESPECT TO THE STATE FUNCTIONS

The derivatives of the “liquid continuity equations” [cf. Eqs. (2.38) - (2.40)] with respect to $\omega^{(j)}$ are as follows:

$$\frac{\partial N_1^{(i)}}{\partial \omega^{(j)}} \equiv d_1^{i,j} = 0; \quad i = 1, \dots, I; \quad j = 1, \dots, I; \quad j \neq i; \quad (\text{C.126})$$

$$\frac{\partial N_1^{(i)}}{\partial \omega^{(i)}} \equiv d_1^{i,i} = \frac{M(m_a, \alpha)}{\bar{R}} \frac{P_{atm}}{[0.622 + \omega^{(i)}] T_a^{(i)}} \left\{ \frac{\omega^{(i)}}{[0.622 + \omega^{(i)}]} - 1 \right\}; \quad (\text{C.127})$$

$$i = 1, \dots, I; \quad j = i.$$

For subsequent use, the above quantities are considered to be the components of the $I \times I$ diagonal matrix \mathbf{D}_1^{II} defined as follows:

$$\mathbf{D}_1^{II} \equiv (d_1^{i,j})_{I \times I} = \begin{pmatrix} d_1^{1,1} & 0 & . & 0 & 0 \\ 0 & d_1^{2,2} & . & 0 & 0 \\ . & . & . & . & . \\ 0 & 0 & . & d_1^{I-1,I-1} & 0 \\ 0 & 0 & . & 0 & d_1^{I,I} \end{pmatrix}. \quad (\text{C.128})$$

The derivatives of the “liquid continuity equations” [cf. Eqs. (2.38) - (2.40)] with respect to m_a are:

1) For $\text{Re}_d < 2300$:

$$\frac{\partial N_1^{(i)}}{\partial m_a} \equiv e_1^i = 0; \quad i = 1, \dots, I; \quad (\text{C.129})$$

2) For $2,300 \leq \text{Re}_d \leq 10,000$:

$$\frac{\partial N_1^{(i)}}{\partial m_a} \equiv e_1^i = \left[\frac{P_{vs}(T_w^{(i+1)}, \alpha)}{\bar{R} \cdot T_w^{(i+1)}} - \frac{\omega^{(i)} P_{atm}}{\bar{R} \cdot T_a^{(i)} (0.622 + \omega^{(i)})} \right] \cdot \frac{\partial M_2(m_a, \alpha)}{\partial m_a}; \quad (\text{C.130})$$

$$i = 1, \dots, I;$$

APPENDIX C. DERIVATIVE MATRIX (JACOBIAN) OF THE MODEL EQUATIONS WITH RESPECT TO THE STATE FUNCTIONS

3) For $\text{Re}_d > 10,000$:

$$\frac{\partial N_1^{(i)}}{\partial m_a} \equiv e_1^i = \left[\frac{P_{vs}(T_w^{(i+1)}, \boldsymbol{\alpha})}{\bar{R} \cdot T_w^{(i+1)}} - \frac{\omega^{(i)} P_{atm}}{\bar{R} \cdot T_a^{(i)} (0.622 + \omega^{(i)})} \right] \cdot \frac{\partial M_3(m_a, \boldsymbol{\alpha})}{\partial m_a}; \quad (\text{C.131})$$

$$i = 1, \dots, I;$$

For subsequent use, the above quantities are considered to be the components of the I column vector \mathbf{E}_1^{II} defined as follows:

$$\mathbf{E}_1^{II} \equiv (e_1^i)_I = \begin{pmatrix} e_1^1 \\ e_1^2 \\ \vdots \\ e_1^{I-1} \\ e_1^I \end{pmatrix}. \quad (\text{C.132})$$

C.3.2 Derivatives of the liquid energy balance equations with respect to the state variables

Derivatives of the liquid energy balance equations [cf. Eqs. (2.41) - (2.43)] with respect to the vector-values state function $\mathbf{u} \triangleq (\mathbf{m}_w, \mathbf{T}_w, \mathbf{T}_a, \boldsymbol{\omega}, m_a)^\dagger$ for case 2 are identical to the respective derivatives of Eqs. (2.6) - (2.8) detailed for case 1a. See Eqs. (C.38) through (C.54) in Section C.1.2.

C.3.3 Derivatives of the water vapor continuity equations with respect to the state variables

Derivatives of the water vapor continuity equations [cf. Eqs. (2.44) - (2.46)] with respect to the vector-values state function $\mathbf{u} \triangleq (\mathbf{m}_w, \mathbf{T}_w, \mathbf{T}_a, \boldsymbol{\omega}, m_a)^\dagger$ for

APPENDIX C. DERIVATIVE MATRIX (JACOBIAN) OF THE MODEL EQUATIONS WITH RESPECT TO THE STATE FUNCTIONS

case 2 are identical to the respective derivatives of Eqs. (2.9) - (2.11) detailed for case 1a. See Eqs. (C.55) through (C.68) in Section C.1.3.

C.3.4 Derivatives of the air/water vapor energy balance equations with respect to the state variables

Derivatives of the air/water vapor balance equations [cf. Eqs. (2.47) - (2.49)] with respect to the vector-values state function $\mathbf{u} \triangleq (\mathbf{m}_w, \mathbf{T}_w, \mathbf{T}_a, \boldsymbol{\omega}, m_a)^\dagger$ for case 2 are identical to the respective derivatives of Eqs. (2.12) - (2.14) detailed for case 1a. See Eqs. (C.69) through (C.87) in Section C.1.4.

C.3.5 Derivatives of the mechanical energy equation with respect to the state variables

Derivatives of mechanical energy equation [cf. Eq. (2.50)] with respect to the vector-values state function $\mathbf{u} \triangleq (\mathbf{m}_w, \mathbf{T}_w, \mathbf{T}_a, \boldsymbol{\omega}, m_a)^\dagger$ for case 2 are identical to the respective derivatives of Eq. (2.15) detailed for case 1a. See Eqs. (C.88) through (C.98) in Section C.1.5.

Appendix D

Verification of the Model Adjoint Functions

This appendix provides a complete display of the procedure followed to verify the numerical accuracy of the adjoint functions computed for all cases. Five specific adjoint functions $\left(\mu_a; o^{(49)}; \tau_a^{(49)}; \tau_w^{(1)}; \mu_w^{(1)}\right)$ have been selected for each of the five responses of the model $\left(T_a^{(1)}; T_w^{(50)}; RH^{(1)}; m_w^{(50)}; m_a\right)$ for the natural draft cases (case 1a, case 1b and case 2); four specific adjoint functions $\left(o^{(49)}; \tau_a^{(49)}; \tau_w^{(1)}; \mu_w^{(1)}\right)$ have been selected for each of the four responses of the model $\left(T_a^{(1)}; T_w^{(50)}; RH^{(1)}; m_w^{(50)}\right)$ for the mechanical draft cases (case 3a, case 3b and case 4). The adjoint functions have been selected in such a way that, once those have been verified, all the other adjoint functions would be consequently verified as well.

D.1 Verification of the Model Adjoint Functions for Case 1a: Fan Off, Saturated Outlet Air Conditions, with Inlet Air Unsaturated

The verification procedure of the adjoint functions for case 1a is reported in this section. For clarity reasons, the adjoint functions have been grouped based on the response they refer to.

D.1.1 Verification of the Adjoint Functions for the Outlet Air Temperature Response $T_a^{(1)}$

When $R = T_a^{(1)}$, the quantities $r_\ell^{(i)}$ defined in Eqs. (3.4) - (3.5) all vanish except for a single component, namely: $r_3^{(1)} \triangleq \partial R / \partial T_a^{(1)} = 1$. Thus, the adjoint functions corresponding to the outlet air temperature response $T_a^{(1)}$ are computed by solving the adjoint sensitivity system given in Eq. (3.10) using $r_3^{(1)} \triangleq \partial R / \partial T_a^{(1)} = 1$ as the only non-zero source term; for this case, the solution of Eq. (3.10) has been depicted in Figure 3.1.

D.1.1.1 Verification of the adjoint function μ_a

Note that the value of the adjoint function μ_a obtained by solving the adjoint sensitivity system given in Eq. (3.10) is $\mu_a = -0.24204 \text{ [K/(J/m}^3\text{)]}$, as indicated in Figure 3.1. Now select a variation δV_w in the wind speed V_w , and note that Eq. (3.22) yields the following expression for the sensitivity of the response $R = T_a^{(1)}$ to V_w :

APPENDIX D. VERIFICATION OF THE MODEL ADJOINT FUNCTIONS

$$\begin{aligned}
 S_5 &\triangleq \frac{\partial R}{\partial V_w} - \left[\sum_{i=1}^{49} \left(\mu_w^{(i)} \frac{\partial N_1^{(i)}}{\partial V_w} + \tau_w^{(i)} \frac{\partial N_2^{(i)}}{\partial V_w} + \tau_a^{(i)} \frac{\partial N_3^{(i)}}{\partial V_w} + o^{(i)} \frac{\partial N_4^{(i)}}{\partial V_w} \right) + \mu_a \frac{\partial N_5}{\partial V_w} \right] \\
 &= 0 - \mu_a \frac{\partial N_5}{\partial V_w} = -(\mu_a) [-V_w \cdot \rho(T_{tdb}, \boldsymbol{\alpha})].
 \end{aligned} \tag{D.1}$$

Re-writing Eq. (D.1) in the form

$$\mu_a = -\frac{S_5}{\partial N_5 / \partial V_w} \tag{D.2}$$

indicates that the value of the adjoint function μ_a could be computed independently if the sensitivity S_5 were available, since the quantity $\partial N_5 / \partial V_w = -2.1795 [J/(m^4/s)]$ is known. To first-order in the parameter perturbation, the finite-difference formula given in Eq. (3.23) can be used to compute the approximate sensitivity S_5^{FD} ; subsequently, this value can be used in conjunction with Eq. (D.2) to compute a “finite-difference sensitivity” value, denoted as $[\mu_a]^{SFD}$, for the respective adjoint, which would be accurate up to second-order in the respective parameter perturbation:

$$[\mu_a]^{SFD} = -\frac{S_5^{FD}}{\partial N_5 / \partial V_w} = -\left[\frac{T_{a,pert}^{(1)} - T_{a,nom}^{(1)}}{\delta V_w} \right] \left[\frac{\partial N_5}{\partial V_w} \right]^{-1} \tag{D.3}$$

Numerically, the wind speed V_w has the nominal (“base-case”) value of $V_w^0 = 1.353 [m/s]$. The corresponding nominal value $T_{a,nom}^{(1)}$ of the response $T_a^{(1)}$ is $T_{a,nom}^{(1)} = 298.4131 [K]$. Consider next a perturbation $\delta V_w = (0.017) V_w^0$, for which the perturbed value of the wind speed becomes $V_w^{pert} = V_w^0 - \delta V_w = 1.33 [m/s]$. Re-computing the perturbed response by solving Eqs. (2.2) - (2.15) with the value of V_w^{pert} yields the “perturbed response” value $T_{a,pert}^{(1)} = 298.4220 [K]$. Using now the nominal and perturbed response values together with the parameter perturbation in the finite-difference expression given in Eq. (3.23) yields the corresponding

APPENDIX D. VERIFICATION OF THE MODEL ADJOINT FUNCTIONS

“finite-difference-computed sensitivity” $S_5^{FD} \triangleq \frac{T_{a,pert}^{(1)} - T_{a,nom}^{(1)}}{\delta V_w} = -0.38757 \left[\frac{K}{m/s} \right]$.

Using this value together with the nominal values of the other quantities appearing in the expression on the right side of Eq. (D.3) yields $[\mu_a]^{SFD} = -0.23973 \left[K/(J/m^3) \right]$. This result compares well with the value $\mu_a = -0.24204 \left[K/(J/m^3) \right]$ obtained by solving the adjoint sensitivity system given in Eq. (3.10), cf., Figure 3.1.

D.1.1.2 Verification of the adjoint function $o^{(49)}$

Note that the value of the adjoint function $o^{(49)}$ obtained by solving the adjoint sensitivity system given in Eq. (3.10) is $o^{(49)} = -4.299 \times 10^{-5} \left[K/(J/kg) \right]$, as indicated in Figure 3.1. Now select a variation $\delta T_{a,in}$ in the inlet air temperature $T_{a,in}$, and note that Eq. (3.22) yields the following expression for the sensitivity of the response $R = T_a^{(1)}$ to $T_{a,in}$:

$$\begin{aligned} S_{45} &\triangleq \frac{\partial R}{\partial T_{a,in}} - \left[\sum_{i=1}^{49} \left(\mu_w^{(i)} \frac{\partial N_1^{(i)}}{\partial T_{a,in}} + \tau_w^{(i)} \frac{\partial N_2^{(i)}}{\partial T_{a,in}} + \tau_a^{(i)} \frac{\partial N_3^{(i)}}{\partial T_{a,in}} + o^{(i)} \frac{\partial N_4^{(i)}}{\partial T_{a,in}} \right) + \mu_a \frac{\partial N_5}{\partial T_{a,in}} \right] \\ &= 0 - \left[o^{(49)} \frac{\partial N_4^{(49)}}{\partial T_{a,in}} + \mu_a \frac{\partial N_5}{\partial T_{a,in}} \right] = -(o^{(49)}) \left[C_p \left(\frac{T_a^{(49)} + tK}{2} \right) + \omega_{in} \alpha_{1g} \right] \\ &\quad - (\mu_a) \cdot \left\{ \frac{R_{air}}{2 \cdot P_{atm}} \cdot |m_a| \cdot m_a \cdot \left[\left(\frac{1}{A_{out}^2} - \frac{1}{A_{in}^2} + \frac{k_{sum}}{A_{fill}^2} \right) + \frac{96f}{\text{Re}} \cdot \frac{L_{fill}}{A_{fill}^2 D_h} \right] \right. \\ &\quad \left. + \frac{g \cdot P_{atm}}{R_{air} \cdot T_{a,in}^2} \cdot \left(Z + \frac{V_w^2}{2g} - \Delta z_{rain} - \frac{\Delta z}{2} \right) \right\}. \end{aligned} \tag{D.4}$$

Re-writing Eq. (D.4) in the form

$$o^{(49)} = - \frac{S_{45} + \mu_a \frac{\partial N_5}{\partial T_{a,in}}}{\frac{\partial N_4^{(49)}}{\partial T_{a,in}}} \tag{D.5}$$

indicates that the value of the adjoint function $o^{(49)}$ could be computed independently if the sensitivity S_{45} were available, since the quantity $\partial N_4^{(49)} / \partial T_{a,in} =$

APPENDIX D. VERIFICATION OF THE MODEL ADJOINT FUNCTIONS

$1.03310 \times 10^3 [J/(kg \cdot K)]$ is known. To first-order in the parameter perturbation, the finite-difference formula given in Eq. (3.23) can be used to compute the approximate sensitivity S_{45}^{FD} ; subsequently, this value can be used in conjunction with Eq. (D.5) to compute a “finite-difference sensitivity” value, denoted as $[o^{(49)}]^{SFD}$, for the respective adjoint, which would be accurate up to second-order in the respective parameter perturbation:

$$[o^{(49)}]^{SFD} = -\frac{S_{45}^{FD} + \mu_a \frac{\partial N_5}{\partial T_{a,in}}}{\frac{\partial N_4^{(49)}}{\partial T_{a,in}}} = -\left[\frac{T_{a,pert}^{(1)} - T_{a,nom}^{(1)}}{\delta T_{a,in}} + \mu_a \frac{\partial N_5}{\partial T_{a,in}} \right] \left[\frac{\partial N_4^{(49)}}{\partial T_{a,in}} \right]^{-1} \quad (D.6)$$

Numerically, the inlet air temperature $T_{a,in}(=T_{db})$ has the nominal (“base-case”) value of $T_{a,in}^0 = 294.03 [K]$. The corresponding nominal value $T_{a,nom}^{(1)}$ of the response $T_a^{(1)}$ is $T_{a,nom}^{(1)} = 298.4131 [K]$. Consider next a perturbation $\delta T_{a,in} = (0.00102) T_{a,in}^0$, for which the perturbed value of the inlet air temperature becomes $T_{a,in}^{pert} = T_{a,in}^0 - \delta T_{a,in} = 294.00 [K]$. Re-computing the perturbed response by solving Eqs. (2.2) - (2.15) with the value of $T_{a,in}^{pert}$ yields the “perturbed response” value $T_{a,pert}^{(1)} = 298.4087 [K]$. Using now the nominal and perturbed response values together with the parameter perturbation in the finite-difference expression given in Eq. (3.23) yields the corresponding “finite-difference-computed sensitivity” $S_{45}^{FD} \triangleq \frac{T_{a,pert}^{(1)} - T_{a,nom}^{(1)}}{\delta T_{a,in}} = 0.14582$. Using this value together with the nominal values of the other quantities appearing in the expression on the right side of Eq. (D.6) yields $[o^{(49)}]^{SFD} = -4.307 \times 10^{-5} [K/(J/kg)]$. This result compares well with the value $o^{(49)} = -4.299 \times 10^{-5} [K/(J/kg)]$ obtained by solving the adjoint sensitivity system given in Eq. (3.10), cf., Figure 3.1. When solving this adjoint sensitivity system, the computation of $o^{(49)}$ depends on the previously computed adjoint functions $o^{(i)}$, $i = 1, \dots, I-1$; hence, the forgoing verification of the computational accuracy of $o^{(49)}$ also provides an indirect verification that the functions $o^{(i)}$, $i = 1, \dots, I-1$, were also computed accurately.

APPENDIX D. VERIFICATION OF THE MODEL ADJOINT FUNCTIONS

D.1.1.3 Verification of the adjoint function $\tau_a^{(49)}$

Note that the value of the adjoint function $\tau_a^{(49)}$ obtained by solving the adjoint sensitivity system given in Eq. (3.10) is $\tau_a^{(49)} = 95.392$ [K], as indicated in Figure 3.1. Now select a variation $\delta\omega_{in}$ in the inlet air humidity ratio ω_{in} , and note that Eq. (3.22) yields the following expression for the sensitivity of the response $R = T_a^{(1)}$ to ω_{in} :

$$\begin{aligned} S_{46} &\triangleq \frac{\partial R}{\partial \omega_{in}} - \left[\sum_{i=1}^{49} \left(\mu_w^{(i)} \frac{\partial N_1^{(i)}}{\partial \omega_{in}} + \tau_w^{(i)} \frac{\partial N_2^{(i)}}{\partial \omega_{in}} + \tau_a^{(i)} \frac{\partial N_3^{(i)}}{\partial \omega_{in}} + o^{(i)} \frac{\partial N_4^{(i)}}{\partial \omega_{in}} \right) + \mu_a \frac{\partial N_5}{\partial \omega_{in}} \right] \\ &= 0 - \left(\tau_a^{(49)} \frac{\partial N_3^{(49)}}{\partial \omega_{in}} + o^{(49)} \frac{\partial N_4^{(49)}}{\partial \omega_{in}} \right) = - \left[\tau_a^{(49)} \cdot (1) + o^{(49)} \cdot h_{g,a}^{(50)}(T_{a,in}, \boldsymbol{\alpha}) \right]. \end{aligned} \quad (\text{D.7})$$

Re-writing Eq. (D.7) in the form

$$\tau_a^{(49)} = -S_{46} - o^{(49)} \cdot h_{g,a}^{(50)}(T_{a,in}, \boldsymbol{\alpha}) \quad (\text{D.8})$$

indicates that the value of the adjoint function $\tau_a^{(49)}$ could be computed independently if the sensitivity S_{46} were available, since the $o^{(49)}$ has been verified in (the previous) Section D.1.1.2 and the quantity $h_{g,a}^{(50)}(T_{a,in}, \boldsymbol{\alpha})$ is known. To first-order in the parameter perturbation, the finite-difference formula given in Eq. (3.23) can be used to compute the approximate sensitivity S_{46}^{FD} ; subsequently, this value can be used in conjunction with Eq. (D.8) to compute a “finite-difference sensitivity” value, denoted as $[\tau_a^{(49)}]^{SFD}$, for the respective adjoint, which would be accurate up to second-order in the respective parameter perturbation:

$$[\tau_a^{(49)}]^{SFD} = -S_{46}^{FD} - o^{(49)} \cdot h_{g,a}^{(50)}(T_{a,in}, \boldsymbol{\alpha}) \quad (\text{D.9})$$

Numerically, the inlet air humidity ratio ω_{in} has the nominal (“base-case”) value of $\omega_{in}^0 = 0.015029407$. The corresponding nominal value $T_{a,nom}^{(1)}$ of the response $T_a^{(1)}$ is $T_{a,nom}^{(1)} = 298.4131$ [K]. Consider next a perturbation $\delta\omega_{in} =$

APPENDIX D. VERIFICATION OF THE MODEL ADJOINT FUNCTIONS

$(0.001243) \omega_{in}^0$, for which the perturbed value of the inlet air humidity ratio becomes $\omega_{in}^{pert} = \omega_{in}^0 - \delta\omega_{in} = 0.015010726$. Re-computing the perturbed response by solving Eqs. (2.2) - (2.15) with the value of ω_{in}^{pert} yields the “perturbed response” value $T_{a,pert}^{(1)} = 298.4128$ [K]. Using now the nominal and perturbed response values together with the parameter perturbation in the finite-difference expression given in Eq. (3.23) yields the corresponding “finite-difference-computed sensitivity” $S_{46}^{FD} \triangleq \frac{T_{a,pert}^{(1)} - T_{a,nom}^{(1)}}{\delta\omega_{in}} = 14.309$ [K]. Using this value together with the nominal values of the other quantities appearing in the expression on the right side of Eq. (D.9) yields $\left[\tau_a^{(49)}\right]^{SFD} = 94.837$ [K]. This result compares well with the value $\tau_a^{(49)} = 95.392$ [K] obtained by solving the adjoint sensitivity system given in Eq. (3.10), cf. Figure 3.1. When solving this adjoint sensitivity system, the computation of $\tau_a^{(49)}$ depends on the previously computed adjoint functions $\tau_a^{(i)}$, $i = 1, \dots, I-1$; hence, the forgoing verification of the computational accuracy of $\tau_a^{(49)}$ also provides an indirect verification that the functions $\tau_a^{(i)}$, $i = 1, \dots, I-1$ were also computed accurately.

D.1.1.4 Verification of the adjoint function $\tau_w^{(1)}$

Note that the value of the adjoint function $\tau_w^{(1)}$ obtained by solving the adjoint sensitivity system given in Eq. (3.10) is as follows: $\tau_w^{(1)} = -4.52 \times 10^{-6}$ [K/(J/s)], indicated in Figure 3.1. Now select a variation $\delta T_{w,in}$ in the inlet water temperature $T_{w,in}$, and note that Eq. (3.22) yields the following expression for the sensitivity of the response $R = T_a^{(1)}$ to $T_{w,in}$:

$$\begin{aligned} S_3 \triangleq \frac{\partial R}{\partial T_{w,in}} &= \left[\sum_{i=1}^{49} \left(\mu_w^{(i)} \frac{\partial N_1^{(i)}}{\partial T_{w,in}} + \tau_w^{(i)} \frac{\partial N_2^{(i)}}{\partial T_{w,in}} + \tau_a^{(i)} \frac{\partial N_3^{(i)}}{\partial T_{w,in}} + o^{(i)} \frac{\partial N_4^{(i)}}{\partial T_{w,in}} \right) + \mu_a \frac{\partial N_5}{\partial T_{w,in}} \right] \\ &= 0 - \tau_w^{(1)} \frac{\partial N_2^{(1)}}{\partial T_{w,in}} = 0 - \tau_w^{(1)} \cdot (m_{w,in} \cdot a_{1f}). \end{aligned} \tag{D.10}$$

APPENDIX D. VERIFICATION OF THE MODEL ADJOINT FUNCTIONS

Re-writing Eq. (D.10) in the form

$$\tau_w^{(1)} = -\frac{S_3}{(m_{w,in} \cdot a_{1f})} \quad (\text{D.11})$$

indicates that the value of the adjoint function $\tau_w^{(1)}$ could be computed independently if the sensitivity S_3 were available, since the quantity $m_{w,in} \cdot a_{1f}$ is known. To first-order in the parameter perturbation, the finite-difference formula given in Eq. (3.23) can be used to compute the approximate sensitivity S_3^{FD} ; subsequently, this value can be used in conjunction with Eq. (D.11) to compute a “finite-difference sensitivity” value, denoted as $[\tau_w^{(1)}]^{SFD}$, for the respective adjoint, which would be accurate up to second-order in the respective parameter perturbation:

$$[\tau_w^{(1)}]^{SFD} = -\frac{S_3^{FD}}{(m_{w,in} \cdot a_{1f})} \quad (\text{D.12})$$

Numerically, the inlet water temperature, $T_{w,in}$, has the nominal (“base-case”) value of $T_{w,in}^0 = 298.774$ [K]. As before, the corresponding nominal value $T_{a,nom}^{(1)}$ of the response $T_a^{(1)}$ is $T_{a,nom}^{(1)} = 298.4131$ [K]. Consider now a perturbation $\delta T_{w,in} = (0.0000669) T_{w,in}^0$, for which the perturbed value of the inlet water temperature becomes $T_{w,in}^{pert} = T_{w,in}^0 - \delta T_{w,in} = 298.754$ [K]. Re-computing the perturbed response by solving Eqs. (2.2) - (2.15) with the value of $T_{w,in}^{pert}$ yields the “perturbed response” value $T_{a,pert}^{(1)} = 298.3964$ [K]. Using now the nominal and perturbed response values together with the parameter perturbation in the finite-difference expression given in Eq. (3.23) yields the corresponding “finite-difference-computed sensitivity” $S_3^{FD} \triangleq \frac{T_{a,pert}^{(1)} - T_{a,nom}^{(1)}}{\delta T_{w,in}} = 0.83401$. Using this value together with the nominal values of the other quantities appearing in the expression on the right side of Eq. (D.12) yields $[\tau_w^{(1)}]^{SFD} = -4.53 \times 10^{-6}$ [K/(J/s)]. This result compares well with the value $\tau_w^{(1)} = -4.52 \times 10^{-6}$ [K/(J/s)] obtained by solving the adjoint sensitivity system given in Eq. (3.10), cf. Figure 3.1.

APPENDIX D. VERIFICATION OF THE MODEL ADJOINT FUNCTIONS

D.1.1.5 Verification of the adjoint function $\mu_w^{(1)}$

Note that the value of the adjoint function $\mu_w^{(1)}$ obtained by solving the adjoint sensitivity system given in Eq. (3.10) is as follows: $\mu_w^{(1)} = 11.0208 \text{ [K/(kg/s)]}$, respectively, as indicated in Figure 3.1. Now select a variation $\delta m_{w,in}$ in the inlet water mass flow rate $m_{w,in}$, and note that Eq. (3.22) yields the following expression for the sensitivity of the response $R = T_a^{(1)}$ to $m_{w,in}$:

$$\begin{aligned}
 S_{44} &\triangleq \frac{\partial R}{\partial m_{w,in}} - \left[\sum_{i=1}^{49} \left(\mu_w^{(i)} \frac{\partial N_1^{(i)}}{\partial m_{w,in}} + \tau_w^{(i)} \frac{\partial N_2^{(i)}}{\partial m_{w,in}} + \tau_a^{(i)} \frac{\partial N_3^{(i)}}{\partial m_{w,in}} + o^{(i)} \frac{\partial N_4^{(i)}}{\partial m_{w,in}} \right) \right. \\
 &\quad \left. + \mu_a \frac{\partial N_5}{\partial m_{w,in}} \right] = 0 - \left(\mu_w^{(1)} \frac{\partial N_1^{(1)}}{\partial m_{w,in}} + \tau_w^{(1)} \frac{\partial N_2^{(1)}}{\partial m_{w,in}} + \tau_a^{(1)} \frac{\partial N_3^{(1)}}{\partial m_{w,in}} + o^{(1)} \frac{\partial N_4^{(1)}}{\partial m_{w,in}} \right) \\
 &= - \left[\mu_w^{(1)} \cdot (-1) + \tau_w^{(1)} \cdot (T_{w,in} a_{1f} - a_{1g} T_w^{(2)} + a_{0f} - a_{0g}) \right. \\
 &\quad \left. + \tau_a^{(1)} \cdot \left(\frac{1}{m_a} \right) + o^{(1)} \cdot \left(\frac{a_{1g} T_w^{(2)} + a_{0g}}{m_a} \right) \right].
 \end{aligned} \tag{D.13}$$

Since the adjoint functions $\tau_a^{(49)}$ and $o^{(49)}$ have been already verified as described in Sections D.1.1.2 and D.1.1.3, it follows that the computed values of adjoint functions $\tau_a^{(1)} = 2156.57 \text{ [K]}$ and $o^{(1)} = -8.4654 \times 10^{-4} \text{ [K/(J/kg)]}$ can also be considered as being accurate, since they constitute the starting point for solving the adjoint sensitivity system in Eq. (3.10); $\tau_w^{(1)}$ was proved being accurate in Section D.1.1.4. Re-writing Eq. (D.13) in the form:

$$\begin{aligned}
 \mu_w^{(1)} &= S_{44} + \tau_w^{(1)} \cdot (T_{w,in} a_{1f} - a_{1g} T_w^{(2)} + a_{0f} - a_{0g}) \\
 &\quad + \tau_a^{(1)} \cdot \left(\frac{1}{m_a} \right) + o^{(1)} \cdot \left(\frac{a_{1g} T_w^{(2)} + a_{0g}}{m_a} \right)
 \end{aligned} \tag{D.14}$$

indicates that the value of the adjoint function $\mu_w^{(1)}$ could be computed independently if the sensitivity S_{44} were available, since all the other quantities are

APPENDIX D. VERIFICATION OF THE MODEL ADJOINT FUNCTIONS

known. To first-order in the parameter perturbation, the finite-difference formula given in Eq. (3.23) can be used to compute the approximate sensitivity S_{44}^{FD} ; subsequently, this value can be used in conjunction with Eq. (D.14) to compute a “finite-difference sensitivity” value, denoted as $[\mu_w^{(1)}]^{SFD}$, for the respective adjoint, which would be accurate up to second-order in the respective parameter perturbation:

$$\begin{aligned} [\mu_w^{(1)}]^{SFD} = \mu_w^{(1)} = S_{44}^{FD} + \tau_w^{(1)} \cdot (T_{w,in} a_{1f} - a_{1g} T_w^{(2)} + a_{0f} - a_{0g}) \\ + \tau_a^{(1)} \cdot \left(\frac{1}{m_a} \right) + o^{(1)} \cdot \left(\frac{a_{1g} T_w^{(2)} + a_{0g}}{m_a} \right) \end{aligned} \quad (D.15)$$

Numerically, the inlet water mass flow rate, $m_{w,in}$, has the nominal (“base-case”) value of $m_{w,in}^0 = 44.0213$ [kg/s]. As before, the corresponding nominal value $T_{a,nom}^{(1)}$ of the response $T_a^{(1)}$ is $T_{a,nom}^{(1)} = 298.4131$ [K]. Next, consider a perturbation $\delta m_{w,in} = (0.0004839) m_{w,in}^0$, for which the perturbed value of the inlet air temperature becomes $m_{w,in}^{pert} = m_{w,in}^0 - \delta m_{w,in} = 44.00$ [kg/s]. Re-computing the perturbed response by solving Eqs. (2.2) - (2.15) with the value of $m_{w,in}^{pert}$ yields the “perturbed response” value $T_{a,pert}^{(1)} = 298.4129$ [K]. Using now the nominal and perturbed response values together with the parameter perturbation in the finite-difference expression given in Eq. (3.23) yields the corresponding “finite-difference-computed sensitivity” $S_{44}^{FD} \triangleq \frac{T_{a,pert}^{(1)} - T_{a,nom}^{(1)}}{\delta m_{w,in}} = 0.00725$ $\left[\frac{K}{kg/s} \right]$. Using this value together with the nominal values of the other quantities appearing in the expression on the right side of Eq. (D.15) yields $[\mu_w^{(1)}]^{SFD} = 11.0208$ [K/(kg/s)]. This result compares well with the value $\mu_w^{(1)} = 11.0208$ [K/(kg/s)] obtained by solving the adjoint sensitivity system given in Eq. (3.10), cf. Figure 3.1.

D.1.2 Verification of the Adjoint Functions for the Outlet

Water Temperature Response $T_w^{(50)}$

When $R = T_w^{(50)}$, the quantities $r_\ell^{(i)}$ defined in Eqs. (3.4) - (3.5) all vanish except for a single component, namely: $r_2^{(49)} \triangleq \partial R / \partial T_w^{(50)} = 1$. Thus, the adjoint functions corresponding to the outlet air temperature response $T_w^{(50)}$ are computed by solving the adjoint sensitivity system given in Eq. (3.10) using $r_2^{(49)} \triangleq \partial R / \partial T_w^{(50)} = 1$ as the only non-zero source term; for this case, the solution of Eq. (3.10) has been depicted in Figure 3.2.

D.1.2.1 Verification of the adjoint function μ_a

Note that the value of the adjoint function μ_a obtained by solving the adjoint sensitivity system given in Eq. (3.10) is $\mu_a = -0.31664 \text{ [K/(J/m}^3\text{)]}$, as indicated in Figure 3.2. Now select a variation δV_w in the wind speed V_w , and note that Eq. (3.22) yields the following expression for the sensitivity of the response $R = T_w^{(50)}$ to V_w :

$$\begin{aligned} S_5 &\triangleq \frac{\partial R}{\partial V_w} - \left[\sum_{i=1}^{49} \left(\mu_w^{(i)} \frac{\partial N_1^{(i)}}{\partial V_w} + \tau_w^{(i)} \frac{\partial N_2^{(i)}}{\partial V_w} + \tau_a^{(i)} \frac{\partial N_3^{(i)}}{\partial V_w} + o^{(i)} \frac{\partial N_4^{(i)}}{\partial V_w} \right) + \mu_a \frac{\partial N_5}{\partial V_w} \right] \\ &= 0 - \mu_a \frac{\partial N_5}{\partial V_w} = -(\mu_a) [-V_w \cdot \rho(T_{tdb}, \boldsymbol{\alpha})]. \end{aligned} \tag{D.16}$$

Re-writing Eq. (D.16) in the form

$$\mu_a = -\frac{S_5}{\partial N_5 / \partial V_w} \tag{D.17}$$

indicates that the value of the adjoint function μ_a could be computed independently if the sensitivity S_5 were available, since the quantity $\partial N_5 / \partial V_w = -2.1795 \text{ [J/(m}^4\text{/s)]}$ is known. To first-order in the parameter perturbation, the finite-difference formula given in Eq. (3.23) can be used to compute the approx-

APPENDIX D. VERIFICATION OF THE MODEL ADJOINT FUNCTIONS

imate sensitivity S_5^{FD} ; subsequently, this value can be used in conjunction with Eq. (D.17) to compute a “finite-difference sensitivity” value, denoted as $[\mu_a]^{SFD}$, for the respective adjoint, which would be accurate up to second-order in the respective parameter perturbation:

$$[\mu_a]^{SFD} = -\frac{S_5^{FD}}{\partial N_5 / \partial V_w} = -\left[\frac{T_{a,pert}^{(1)} - T_{a,nom}^{(1)}}{\delta V_w} \right] \left[\frac{\partial N_5}{\partial V_w} \right]^{-1} \quad (D.18)$$

Numerically, the wind speed V_w has the nominal (“base-case”) value of $V_w^0 = 1.353$ [m/s]. The corresponding nominal value $T_{w,nom}^{(50)}$ of the response $T_w^{(50)}$ is $T_{w,nom}^{(50)} = 296.8570$ [K]. Consider next a perturbation $\delta V_w = (0.017) V_w^0$, for which the perturbed value of the wind speed becomes $V_w^{pert} = V_w^0 - \delta V_w = 1.33$ [m/s]. Re-computing the perturbed response by solving Eqs. (2.2) - (2.15) with the value of V_w^{pert} yields the “perturbed response” value $T_{w,pert}^{(50)} = 296.8687$ [K]. Using now the nominal and perturbed response values together with the parameter perturbation in the finite-difference expression given in Eq. (3.23) yields the corresponding “finite-difference-computed sensitivity” $S_5^{FD} \triangleq \frac{T_{w,pert}^{(50)} - T_{w,nom}^{(50)}}{\delta V_w} = -0.5109$ $\left[\frac{K}{m/s} \right]$. Using this value together with the nominal values of the other quantities appearing in the expression on the right side of Eq. (D.18) yields $[\mu_a]^{SFD} = -0.31602$ $[K/(J/m^3)]$. This result compares well with the value $\mu_a = -0.31664$ $[K/(J/m^3)]$ obtained by solving the adjoint sensitivity system given in Eq. (3.10), cf., Figure 3.2.

D.1.2.2 Verification of the adjoint function $o^{(49)}$

Note that the value of the adjoint function $o^{(49)}$ obtained by solving the adjoint sensitivity system given in Eq. (3.10) is $o^{(49)} = -1.1217 \times 10^{-4}$ $[K/(J/kg)]$, as indicated in Figure 3.2. Now select a variation $\delta T_{a,in}$ in the inlet air temperature $T_{a,in}$, and note that Eq. (3.22) yields the following expression for the sensitivity of the response $R = T_w^{(50)}$ to $T_{a,in}$:

APPENDIX D. VERIFICATION OF THE MODEL ADJOINT FUNCTIONS

$$\begin{aligned}
S_{45} &\triangleq \frac{\partial R}{\partial T_{a,in}} - \left[\sum_{i=1}^{49} \left(\mu_w^{(i)} \frac{\partial N_1^{(i)}}{\partial T_{a,in}} + \tau_w^{(i)} \frac{\partial N_2^{(i)}}{\partial T_{a,in}} + \tau_a^{(i)} \frac{\partial N_3^{(i)}}{\partial T_{a,in}} + o^{(i)} \frac{\partial N_4^{(i)}}{\partial T_{a,in}} \right) + \mu_a \frac{\partial N_5}{\partial T_{a,in}} \right] \\
&= 0 - \left[o^{(49)} \frac{\partial N_4^{(49)}}{\partial T_{a,in}} + \mu_a \frac{\partial N_5}{\partial T_{a,in}} \right] = -(o^{(49)}) \left[C_p \left(\frac{T_a^{(49)} + tK}{2} \right) + \omega_{in} \alpha_{1g} \right] \\
&\quad - (\mu_a) \cdot \left\{ \frac{R_{air}}{2 \cdot P_{atm}} \cdot |m_a| \cdot m_a \cdot \left[\left(\frac{1}{A_{out}^2} - \frac{1}{A_{in}^2} + \frac{k_{sum}}{A_{fill}^2} \right) + \frac{96f}{\text{Re}} \cdot \frac{L_{fill}}{A_{fill}^2 D_h} \right] \right. \\
&\quad \left. + \frac{g \cdot P_{atm}}{R_{air} \cdot T_{a,in}^2} \cdot \left(Z + \frac{V_w^2}{2g} - \Delta z_{rain} - \frac{\Delta z}{2} \right) \right\}.
\end{aligned} \tag{D.19}$$

Re-writing Eq. (D.19) in the form

$$o^{(49)} = - \frac{S_{45} + \mu_a \frac{\partial N_5}{\partial T_{a,in}}}{\frac{\partial N_4^{(49)}}{\partial T_{a,in}}} \tag{D.20}$$

indicates that the value of the adjoint function $o^{(49)}$ could be computed independently if the sensitivity S_{45} were available, since the quantity $\partial N_4^{(49)} / \partial T_{a,in} = 1.03310 \times 10^3 [J/(kg \cdot K)]$ is known. To first-order in the parameter perturbation, the finite-difference formula given in Eq. (3.23) can be used to compute the approximate sensitivity S_{45}^{FD} ; subsequently, this value can be used in conjunction with Eq. (D.20) to compute a “finite-difference sensitivity” value, denoted as $[o^{(49)}]^{SFD}$, for the respective adjoint, which would be accurate up to second-order in the respective parameter perturbation:

$$[o^{(49)}]^{SFD} = - \frac{S_{45}^{FD} + \mu_a \frac{\partial N_5}{\partial T_{a,in}}}{\frac{\partial N_4^{(49)}}{\partial T_{a,in}}} = - \left[\frac{T_{a,pert}^{(1)} - T_{a,nom}^{(1)}}{\delta T_{a,in}} + \mu_a \frac{\partial N_5}{\partial T_{a,in}} \right] \left[\frac{\partial N_4^{(49)}}{\partial T_{a,in}} \right]^{-1} \tag{D.21}$$

Numerically, the inlet air temperature $T_{a,in}(= T_{db})$ has the nominal (“base-case”) value of $T_{a,in}^0 = 294.03 [K]$. The corresponding nominal value $T_{w,nom}^{(50)}$ of the response $T_w^{(50)}$ is $T_{w,nom}^{(50)} = 296.8570 [K]$. Consider next a perturbation $\delta T_{a,in} = (0.00102) T_{a,in}^0$, for which the perturbed value of the inlet air temperature becomes $T_{a,in}^{pert} = T_{a,in}^0 - \delta T_{a,in} = 294.00 [K]$. Re-computing the perturbed

APPENDIX D. VERIFICATION OF THE MODEL ADJOINT FUNCTIONS

response by solving Eqs. (2.2) - (2.15) with the value of $T_{a,in}^{pert}$ yields the “perturbed response” value $T_{w,pert}^{(50)} = 296.8496$ [K]. Using now the nominal and perturbed response values together with the parameter perturbation in the finite-difference expression given in Eq. (3.23) yields the corresponding “finite-difference-computed sensitivity” $S_{45}^{FD} \triangleq \frac{T_{w,pert}^{(50)} - T_{w,nom}^{(50)}}{\delta T_{a,in}} = 0.24117$. Using this value together with the nominal values of the other quantities appearing in the expression on the right side of Eq. (D.21) yields $[o^{(49)}]^{SFD} = -1.1088 \times 10^{-4}$ [K/(J/kg)]. This result compares well with the value $o^{(49)} = -1.1217 \times 10^{-4}$ [K/(J/kg)] obtained by solving the adjoint sensitivity system given in Eq. (3.10), cf., Figure 3.2. When solving this adjoint sensitivity system, the computation of $o^{(49)}$ depends on the previously computed adjoint functions $o^{(i)}$, $i = 1, \dots, I - 1$; hence, the forgoing verification of the computational accuracy of $o^{(49)}$ also provides an indirect verification that the functions $o^{(i)}$, $i = 1, \dots, I - 1$, were also computed accurately.

D.1.2.3 Verification of the adjoint function $\tau_a^{(49)}$

Note that the value of the adjoint function $\tau_a^{(49)}$ obtained by solving the adjoint sensitivity system given in Eq. (3.10) is $\tau_a^{(49)} = 60.389$ [K], as indicated in Figure 3.2. Now select a variation $\delta\omega_{in}$ in the inlet air humidity ratio ω_{in} , and note that Eq. (3.22) yields the following expression for the sensitivity of the response $R = T_w^{(50)}$ to

$$\begin{aligned} S_{46} &\triangleq \frac{\partial R}{\partial \omega_{in}} - \left[\sum_{i=1}^{49} \left(\mu_w^{(i)} \frac{\partial N_1^{(i)}}{\partial \omega_{in}} + \tau_w^{(i)} \frac{\partial N_2^{(i)}}{\partial \omega_{in}} + \tau_a^{(i)} \frac{\partial N_3^{(i)}}{\partial \omega_{in}} + o^{(i)} \frac{\partial N_4^{(i)}}{\partial \omega_{in}} \right) + \mu_a \frac{\partial N_5}{\partial \omega_{in}} \right] \\ &= 0 - \left(\tau_a^{(49)} \frac{\partial N_3^{(49)}}{\partial \omega_{in}} + o^{(49)} \frac{\partial N_4^{(49)}}{\partial \omega_{in}} \right) = - [\tau_a^{(49)} \cdot (1) + o^{(49)} \cdot h_{g,a}^{(50)}(T_{a,in}, \boldsymbol{\alpha})] . \end{aligned} \quad (D.22)$$

Re-writing Eq. (D.22) in the form

$$\tau_a^{(49)} = -S_{46} - o^{(49)} \cdot h_{g,a}^{(50)}(T_{a,in}, \boldsymbol{\alpha}) \quad (D.23)$$

APPENDIX D. VERIFICATION OF THE MODEL ADJOINT FUNCTIONS

indicates that the value of the adjoint function $\tau_a^{(49)}$ could be computed independently if the sensitivity S_{46} were available, since the $o^{(49)}$ has been verified in (the previous) Section D.1.2.2 and the quantity $h_{g,a}^{(50)}(T_{a,in}, \boldsymbol{\alpha})$ is known. To first-order in the parameter perturbation, the finite-difference formula given in Eq. (3.23) can be used to compute the approximate sensitivity S_{46}^{FD} ; subsequently, this value can be used in conjunction with Eq. (D.23) to compute a “finite-difference sensitivity” value, denoted as $[\tau_a^{(49)}]^{SFD}$, for the respective adjoint, which would be accurate up to second-order in the respective parameter perturbation:

$$[\tau_a^{(49)}]^{SFD} = -S_{46}^{FD} - o^{(49)} \cdot h_{g,a}^{(50)}(T_{a,in}, \boldsymbol{\alpha}) \quad (\text{D.24})$$

Numerically, the inlet air humidity ratio ω_{in} has the nominal (“base-case”) value of $\omega_{in}^0 = 0.015029407$. The corresponding nominal value $T_{w,nom}^{(50)}$ of the response $T_w^{(50)}$ is $T_{w,nom}^{(50)} = 296.8570$ [K]. Consider next a perturbation $\delta\omega_{in} = (0.001243)\omega_{in}^0$, for which the perturbed value of the inlet air humidity ratio becomes $\omega_{in}^{pert} = \omega_{in}^0 - \delta\omega_{in} = 0.015010726$. Re-computing the perturbed response by solving Eqs. (2.2) - (2.15) with the value of ω_{in}^{pert} yields the “perturbed response” value $T_{w,pert}^{(50)} = 296.8528$ [K]. Using now the nominal and perturbed response values together with the parameter perturbation in the finite-difference expression given in Eq. (3.23) yields the corresponding “finite-difference-computed sensitivity” $S_{46}^{FD} \triangleq \frac{T_{w,pert}^{(50)} - T_{w,nom}^{(50)}}{\delta\omega_{in}} = 226.203$ [K]. Using this value together with the nominal values of the other quantities appearing in the expression on the right side of Eq. (D.24) yields $[\tau_a^{(49)}]^{SFD} = 58.656$ [K]. This result compares well with the value $\tau_a^{(49)} = 60.389$ [K] obtained by solving the adjoint sensitivity system given in Eq. (3.10), cf. Figure 3.2. When solving this adjoint sensitivity system, the computation of $\tau_a^{(49)}$ depends on the previously computed adjoint functions $\tau_a^{(i)}$, $i = 1, \dots, I - 1$; hence, the forgoing verification of the computational accuracy of $\tau_a^{(49)}$ also provides an indirect verification that the functions $\tau_a^{(i)}$, $i = 1, \dots, I - 1$ were also computed accurately.

APPENDIX D. VERIFICATION OF THE MODEL ADJOINT FUNCTIONS

D.1.2.4 Verification of the adjoint function $\tau_w^{(1)}$

Note that the value of the adjoint function $\tau_w^{(1)}$ obtained by solving the adjoint sensitivity system given in Eq. (3.10) is as follows: $\tau_w^{(1)} = -2.618 \times 10^{-6} \text{ [K/(J/s)]}$, indicated in Figure 3.2. Now select a variation $\delta T_{w,in}$ in the inlet water temperature $T_{w,in}$, and note that Eq. (3.22) yields the following expression for the sensitivity of the response $R = T_w^{(50)}$ to $T_{w,in}$:

$$\begin{aligned} S_3 &\triangleq \frac{\partial R}{\partial T_{w,in}} - \left[\sum_{i=1}^{49} \left(\mu_w^{(i)} \frac{\partial N_1^{(i)}}{\partial T_{w,in}} + \tau_w^{(i)} \frac{\partial N_2^{(i)}}{\partial T_{w,in}} + \tau_a^{(i)} \frac{\partial N_3^{(i)}}{\partial T_{w,in}} + o^{(i)} \frac{\partial N_4^{(i)}}{\partial T_{w,in}} \right) + \mu_a \frac{\partial N_5}{\partial T_{w,in}} \right] \\ &= 0 - \tau_w^{(1)} \frac{\partial N_2^{(1)}}{\partial T_{w,in}} = 0 - \tau_w^{(1)} \cdot (m_{w,in} \cdot a_{1f}). \end{aligned} \quad (\text{D.25})$$

Re-writing Eq. (D.25) in the form

$$\tau_w^{(1)} = - \frac{S_3}{(m_{w,in} \cdot a_{1f})} \quad (\text{D.26})$$

indicates that the value of the adjoint function $\tau_w^{(1)}$ could be computed independently if the sensitivity S_3 were available, since the quantity $m_{w,in} \cdot a_{1f}$ is known. To first-order in the parameter perturbation, the finite-difference formula given in Eq. (3.23) can be used to compute the approximate sensitivity S_3^{FD} ; subsequently, this value can be used in conjunction with Eq. (D.26) to compute a “finite-difference sensitivity” value, denoted as $[\tau_w^{(1)}]^{SFD}$, for the respective adjoint, which would be accurate up to second-order in the respective parameter perturbation:

$$[\tau_w^{(1)}]^{SFD} = - \frac{S_3^{FD}}{(m_{w,in} \cdot a_{1f})} \quad (\text{D.27})$$

Numerically, the inlet water temperature, $T_{w,in}$, has the nominal (“base-case”) value of $T_{w,in}^0 = 298.774 \text{ [K]}$. The corresponding nominal value $T_{w,nom}^{(50)}$ of the response $T_w^{(50)}$ is $T_{w,nom}^{(50)} = 296.8570 \text{ [K]}$. Consider now a perturbation $\delta T_{w,in} =$

APPENDIX D. VERIFICATION OF THE MODEL ADJOINT FUNCTIONS

$(0.0000669) T_{w,in}^0$, for which the perturbed value of the inlet water temperature becomes $T_{w,in}^{pert} = T_{w,in}^0 - \delta T_{w,in} = 298.754 [K]$. Re-computing the perturbed response by solving Eqs. (2.2) - (2.15) with the value of $T_{w,in}^{pert}$ yields the “perturbed response” value $T_{w,pert}^{(50)} = 296.8473 [K]$. Using now the nominal and perturbed response values together with the parameter perturbation in the finite-difference expression given in Eq. (3.23) yields the corresponding “finite-difference-computed sensitivity” $S_3^{FD} \triangleq \frac{T_{w,pert}^{(50)} - T_{w,nom}^{(50)}}{\delta T_{w,in}} = 0.48288$. Using this value together with the nominal values of the other quantities appearing in the expression on the right side of Eq. (D.27) yields $\left[\tau_w^{(1)} \right]^{SFD} = -2.620 \times 10^{-6} [K/(J/s)]$. This result compares well with the value $\tau_w^{(1)} = -2.618 \times 10^{-6} [K/(J/s)]$ obtained by solving the adjoint sensitivity system given in Eq. (3.10), cf. Figure 3.2.

D.1.2.5 Verification of the adjoint function $\mu_w^{(1)}$

Note that the value of the adjoint function $\mu_w^{(1)}$ obtained by solving the adjoint sensitivity system given in Eq. (3.10) is as follows: $\mu_w^{(1)} = 6.4310 [K/(kg/s)]$, respectively, as indicated in Figure 3.2. Now select a variation $\delta m_{w,in}$ in the inlet water mass flow rate $m_{w,in}$, and note that Eq. (3.22) yields the following expression for the sensitivity of the response $R = T_w^{(50)}$ to $m_{w,in}$:

$$\begin{aligned}
 S_{44} &\triangleq \frac{\partial R}{\partial m_{w,in}} - \left[\sum_{i=1}^{49} \left(\mu_w^{(i)} \frac{\partial N_1^{(i)}}{\partial m_{w,in}} + \tau_w^{(i)} \frac{\partial N_2^{(i)}}{\partial m_{w,in}} + \tau_a^{(i)} \frac{\partial N_3^{(i)}}{\partial m_{w,in}} + o^{(i)} \frac{\partial N_4^{(i)}}{\partial m_{w,in}} \right) \right. \\
 &\quad \left. + \mu_a \frac{\partial N_5}{\partial m_{w,in}} \right] = 0 - \left(\mu_w^{(1)} \frac{\partial N_1^{(1)}}{\partial m_{w,in}} + \tau_w^{(1)} \frac{\partial N_2^{(1)}}{\partial m_{w,in}} + \tau_a^{(1)} \frac{\partial N_3^{(1)}}{\partial m_{w,in}} + o^{(1)} \frac{\partial N_4^{(1)}}{\partial m_{w,in}} \right) \\
 &= - \left[\mu_w^{(1)} \cdot (-1) + \tau_w^{(1)} \cdot (T_{w,in} a_{1f} - a_{1g} T_w^{(2)} + a_{0f} - a_{0g}) \right. \\
 &\quad \left. + \tau_a^{(1)} \cdot \left(\frac{1}{m_a} \right) + o^{(1)} \cdot \left(\frac{a_{1g} T_w^{(2)} + a_{0g}}{m_a} \right) \right].
 \end{aligned} \tag{D.28}$$

APPENDIX D. VERIFICATION OF THE MODEL ADJOINT FUNCTIONS

Since the adjoint functions $\tau_a^{(49)}$ and $o^{(49)}$ have been already verified as described in Sections D.1.2.2 and D.1.2.3, it follows that the computed values of adjoint functions $\tau_a^{(1)} = -189.56 [K]$ and $o^{(1)} = 7.44 \times 10^{-5} [K/(J/kg)]$ can also be considered as being accurate, since they constitute the starting point for solving the adjoint sensitivity system in Eq. (3.10); $\tau_w^{(1)}$ was proved being accurate in Section D.1.2.4. Re-writing Eq. (D.28) in the form:

$$\begin{aligned} \mu_w^{(1)} = & S_{44} + \tau_w^{(1)} \cdot (T_{w,in}a_{1f} - a_{1g}T_w^{(2)} + a_{0f} - a_{0g}) \\ & + \tau_a^{(1)} \cdot \left(\frac{1}{m_a}\right) + o^{(1)} \cdot \left(\frac{a_{1g}T_w^{(2)} + a_{0g}}{m_a}\right) \end{aligned} \quad (D.29)$$

indicates that the value of the adjoint function $\mu_w^{(1)}$ could be computed independently if the sensitivity S_{44} were available, since all the other quantities are known. To first-order in the parameter perturbation, the finite-difference formula given in Eq. (3.23) can be used to compute the approximate sensitivity S_{44}^{FD} ; subsequently, this value can be used in conjunction with Eq. (D.29) to compute a “finite-difference sensitivity” value, denoted as $[\mu_w^{(1)}]^{SFD}$, for the respective adjoint, which would be accurate up to second-order in the respective parameter perturbation:

$$\begin{aligned} [\mu_w^{(1)}]^{SFD} = & \mu_w^{(1)} = S_{44}^{FD} + \tau_w^{(1)} \cdot (T_{w,in}a_{1f} - a_{1g}T_w^{(2)} + a_{0f} - a_{0g}) \\ & + \tau_a^{(1)} \cdot \left(\frac{1}{m_a}\right) + o^{(1)} \cdot \left(\frac{a_{1g}T_w^{(2)} + a_{0g}}{m_a}\right) \end{aligned} \quad (D.30)$$

Numerically, the inlet water mass flow rate, $m_{w,in}$, has the nominal (“base-case”) value of $m_{w,in}^0 = 44.0213 [kg/s]$. The corresponding nominal value $T_{w,nom}^{(50)}$ of the response $T_w^{(50)}$ is $T_{w,nom}^{(50)} = 296.8570 [K]$. Next, consider a perturbation $\delta m_{w,in} = (0.0004839) m_{w,in}^0$, for which the perturbed value of the inlet water mass flow rate becomes $m_{w,in}^{pert} = m_{w,in}^0 - \delta m_{w,in} = 44.00 [kg/s]$. Re-computing the perturbed response by solving Eqs. (2.2) - (2.15) with the value

APPENDIX D. VERIFICATION OF THE MODEL ADJOINT FUNCTIONS

of $m_{w,in}^{pert}$ yields the “perturbed response” value $T_{w,pert}^{(50)} = 296.8562$ [K]. Using now the nominal and perturbed response values together with the parameter perturbation in the finite-difference expression given in Eq. (3.23) yields the corresponding “finite-difference-computed sensitivity” $S_{44}^{FD} \triangleq \frac{T_{w,pert}^{(50)} - T_{w,nom}^{(50)}}{\delta m_{w,in}} = 0.03885$ $\left[\frac{K}{kg/s}\right]$. Using this value together with the nominal values of the other quantities appearing in the expression on the right side of Eq. (D.30) yields $\left[\mu_w^{(1)}\right]^{SFD} = 11.0208$ $[K/(kg/s)]$. This result compares well with the value $\mu_w^{(1)} = 11.0208$ $[K/(kg/s)]$ obtained by solving the adjoint sensitivity system given in Eq. (3.10), cf. Figure 3.2.

D.1.3 Verification of the Adjoint Functions for the Outlet

Air Relative Humidity $RH^{(1)}$

When $R = RH^{(1)}$, the quantities $r_\ell^{(i)}$ defined in Eqs. (3.4) - (3.5) all vanish except for two components, namely:

$$r_3^{(1)} \equiv \frac{\partial RH^{(1)}}{\partial T_a^{(1)}} = \frac{\partial}{\partial T_a^{(1)}} \left[\frac{P_v(\omega^{(1)}, \alpha)}{P_{vs}(T_a^{(1)}, \alpha)} \times 100 \right] = 100 \times \frac{P_v(\omega^{(1)}, \alpha)}{P_{vs}(T_a^{(1)}, \alpha)} \frac{a_1}{\left[T_a^{(1)}\right]^2} \quad (D.31)$$

$$r_4^{(1)} \equiv \frac{\partial RH^{(1)}}{\partial \omega^{(1)}} = \frac{\partial}{\partial \omega^{(1)}} \left[\frac{P_v(\omega^{(1)}, \alpha)}{P_{vs}(T_a^{(1)}, \alpha)} \times 100 \right] = \frac{0.622 P_{atm}}{(0.622 + \omega^{(1)})^2 e^{a_0 + \frac{a_1}{T_a^{(1)}}}} \times 100 \quad (D.32)$$

Thus, the adjoint functions corresponding to the outlet air temperature response $RH^{(1)}$ are computed by solving the adjoint sensitivity system given in Eq. (3.10) using $r_3^{(1)}$ and $r_4^{(1)}$ as the only non-zero source terms; for this case, the solution of Eq. (3.10) has been depicted in Figure 3.3.

APPENDIX D. VERIFICATION OF THE MODEL ADJOINT FUNCTIONS

D.1.3.1 Verification of the adjoint function μ_a

Note that the value of the adjoint function μ_a obtained by solving the adjoint sensitivity system given in Eq. (3.10) is $\mu_a = 0.00603 \left[(J/m^3)^{-1} \right]$, as indicated in Figure 3.3. Now select a variation δV_w in the wind speed V_w , and note that Eq. (3.22) yields the following expression for the sensitivity of the response $R = RH^{(1)}$ to V_w :

$$\begin{aligned} S_5 &\triangleq \frac{\partial R}{\partial V_w} - \left[\sum_{i=1}^{49} \left(\mu_w^{(i)} \frac{\partial N_1^{(i)}}{\partial V_w} + \tau_w^{(i)} \frac{\partial N_2^{(i)}}{\partial V_w} + \tau_a^{(i)} \frac{\partial N_3^{(i)}}{\partial V_w} + o^{(i)} \frac{\partial N_4^{(i)}}{\partial V_w} \right) + \mu_a \frac{\partial N_5}{\partial V_w} \right] \\ &= 0 - \mu_a \frac{\partial N_5}{\partial V_w} = -(\mu_a) [-V_w \cdot \rho(T_{tdb}, \boldsymbol{\alpha})]. \end{aligned} \quad (D.33)$$

Re-writing Eq. (D.33) in the form

$$\mu_a = -\frac{S_5}{\partial N_5 / \partial V_w} \quad (D.34)$$

indicates that the value of the adjoint function μ_a could be computed independently if the sensitivity S_5 were available, since the quantity $\partial N_5 / \partial V_w = -2.1795 [J/(m^4/s)]$ is known. To first-order in the parameter perturbation, the finite-difference formula given in Eq. (3.23) can be used to compute the approximate sensitivity S_5^{FD} ; subsequently, this value can be used in conjunction with Eq. (D.34) to compute a “finite-difference sensitivity” value, denoted as $[\mu_a]^{SFD}$, for the respective adjoint, which would be accurate up to second-order in the respective parameter perturbation:

$$[\mu_a]^{SFD} = -\frac{S_5^{FD}}{\partial N_5 / \partial V_w} = -\left[\frac{T_{a,pert}^{(1)} - T_{a,nom}^{(1)}}{\delta V_w} \right] \left[\frac{\partial N_5}{\partial V_w} \right]^{-1} \quad (D.35)$$

Numerically, the wind speed V_w has the nominal (“base-case”) value of $V_w^0 = 1.353 [m/s]$. The corresponding nominal value $RH_{nom}^{(1)}$ of the response $RH^{(1)}$ is

APPENDIX D. VERIFICATION OF THE MODEL ADJOINT FUNCTIONS

$RH_{nom}^{(1)} = 100.1052\%$. Consider next a perturbation $\delta V_w = (0.017) V_w^0$, for which the perturbed value of the wind speed becomes $V_w^{pert} = V_w^0 - \delta V_w = 1.33 \text{ [m/s]}$. Re-computing the perturbed response by solving Eqs. (2.2) - (2.15) with the value of V_w^{pert} yields the “perturbed response” value $RH_{pert}^{(1)} = 100.1049\%$. Using now the nominal and perturbed response values together with the parameter perturbation in the finite-difference expression given in Eq. (D.35) yields the corresponding “finite-difference-computed sensitivity” $S_5^{FD} \triangleq \frac{RH_{pert}^{(1)} - RH_{nom}^{(1)}}{\delta V_w} = 0.01078 \text{ [(m/s)}^{-1}\text{]}$. Using this value together with the nominal values of the other quantities appearing in the expression on the right side of Eq. (D.35) yields $[\mu_a]^{SFD} = 0.00667 \text{ [(J/m}^3\text{)}^{-1}\text{]}$. This result compares well with the value $\mu_a = 0.00603 \text{ [(J/m}^3\text{)}^{-1}\text{]}$ obtained by solving the adjoint sensitivity system given in Eq. (3.10), cf., Figure 3.3.

D.1.3.2 Verification of the adjoint function $o^{(49)}$

Note that the value of the adjoint function $o^{(49)}$ obtained by solving the adjoint sensitivity system given in Eq. (3.10) is $o^{(49)} = 6.692 \times 10^{-4} \text{ [(J/kg)}^{-1}\text{]}$, as indicated in Figure 3.3. Now select a variation $\delta T_{a,in}$ in the inlet air temperature $T_{a,in}$, and note that Eq. (3.22) yields the following expression for the sensitivity of the response $R = RH^{(1)}$ to $T_{a,in}$:

$$\begin{aligned}
 S_{45} &\triangleq \frac{\partial R}{\partial T_{a,in}} - \left[\sum_{i=1}^{49} \left(\mu_w^{(i)} \frac{\partial N_1^{(i)}}{\partial T_{a,in}} + \tau_w^{(i)} \frac{\partial N_2^{(i)}}{\partial T_{a,in}} + \tau_a^{(i)} \frac{\partial N_3^{(i)}}{\partial T_{a,in}} + o^{(i)} \frac{\partial N_4^{(i)}}{\partial T_{a,in}} \right) + \mu_a \frac{\partial N_5}{\partial T_{a,in}} \right] \\
 &= 0 - \left[o^{(49)} \frac{\partial N_4^{(49)}}{\partial T_{a,in}} + \mu_a \frac{\partial N_5}{\partial T_{a,in}} \right] = -(o^{(49)}) \left[C_p \left(\frac{T_a^{(49)} + tK}{2} \right) + \omega_{in} \alpha_{1g} \right] \\
 &\quad - (\mu_a) \cdot \left\{ \frac{R_{air}}{2 \cdot P_{atm}} \cdot |m_a| \cdot m_a \cdot \left[\left(\frac{1}{A_{out}^2} - \frac{1}{A_{in}^2} + \frac{k_{sum}}{A_{fill}^2} \right) + \frac{96f}{\text{Re}} \cdot \frac{L_{fill}}{A_{fill}^2 D_h} \right] \right. \\
 &\quad \left. + \frac{g \cdot P_{atm}}{R_{air} \cdot T_{a,in}^2} \cdot \left(Z + \frac{V_w^2}{2g} - \Delta z_{rain} - \frac{\Delta z}{2} \right) \right\}.
 \end{aligned} \tag{D.36}$$

APPENDIX D. VERIFICATION OF THE MODEL ADJOINT FUNCTIONS

Re-writing Eq. (D.36) in the form

$$o^{(49)} = -\frac{S_{45} + \mu_a \frac{\partial N_5}{\partial T_{a,in}}}{\frac{\partial N_4^{(49)}}{\partial T_{a,in}}} \quad (\text{D.37})$$

indicates that the value of the adjoint function $o^{(49)}$ could be computed independently if the sensitivity S_{45} were available, since the quantity $\partial N_4^{(49)}/\partial T_{a,in} = 1.03310 \times 10^3 [J/(kg \cdot K)]$ is known. To first-order in the parameter perturbation, the finite-difference formula given in Eq. (3.23) can be used to compute the approximate sensitivity S_{45}^{FD} ; subsequently, this value can be used in conjunction with Eq. (D.37) to compute a “finite-difference sensitivity” value, denoted as $[o^{(49)}]^{SFD}$, for the respective adjoint, which would be accurate up to second-order in the respective parameter perturbation:

$$[o^{(49)}]^{SFD} = -\frac{S_{45}^{FD} + \mu_a \frac{\partial N_5}{\partial T_{a,in}}}{\frac{\partial N_4^{(49)}}{\partial T_{a,in}}} = -\left[\frac{T_{a,pert}^{(1)} - T_{a,nom}^{(1)}}{\delta T_{a,in}} + \mu_a \frac{\partial N_5}{\partial T_{a,in}} \right] \left[\frac{\partial N_4^{(49)}}{\partial T_{a,in}} \right]^{-1} \quad (\text{D.38})$$

Numerically, the inlet air temperature $T_{a,in}(= T_{db})$ has the nominal (“base-case”) value of $T_{a,in}^0 = 294.03 [K]$. The corresponding nominal value $RH_{nom}^{(1)}$ of the response $RH^{(1)}$ is $RH_{nom}^{(1)} = 100.1052\%$. Consider next a perturbation $\delta T_{a,in} = (0.00102) T_{a,in}^0$, for which the perturbed value of the inlet air temperature becomes $T_{a,in}^{pert} = T_{a,in}^0 - \delta T_{a,in} = 294.00 [K]$. Re-computing the perturbed response by solving Eqs. (2.2) - (2.15) with the value of $T_{a,in}^{pert}$ yields the “perturbed response” value $RH_{pert}^{(1)} = 100.1260\%$. Using now the nominal and perturbed response values together with the parameter perturbation in the finite-difference expression given in Eq. (3.23) yields the corresponding “finite-difference-computed sensitivity” $S_{45}^{FD} \triangleq \frac{RH_{pert}^{(1)} - RH_{nom}^{(1)}}{\delta T_{a,in}} = -0.69388 [K^{-1}]$. Using this value together with the nominal values of the other quantities appearing in the expression on the right side of Eq. (D.38) yields $[o^{(49)}]^{SFD} = 6.932 \times 10^{-4} [(J/kg)^{-1}]$. This

APPENDIX D. VERIFICATION OF THE MODEL ADJOINT FUNCTIONS

result compares well with the value $o^{(49)} = 6.692 \times 10^{-4} \quad [(J/kg)^{-1}]$ obtained by solving the adjoint sensitivity system given in Eq. (3.10), cf., Figure 3.3. When solving this adjoint sensitivity system, the computation of $o^{(49)}$ depends on the previously computed adjoint functions $o^{(i)}$, $i = 1, \dots, I - 1$; hence, the forgoing verification of the computational accuracy of $o^{(49)}$ also provides an indirect verification that the functions $o^{(i)}$, $i = 1, \dots, I - 1$, were also computed accurately.

D.1.3.3 Verification of the adjoint function $\tau_a^{(49)}$

Note that the value of the adjoint function $\tau_a^{(49)}$ obtained by solving the adjoint sensitivity system given in Eq. (3.10) is $\tau_a^{(49)} = -2235.5 \text{ } [-]$, as indicated in Figure 3.3. Now select a variation $\delta\omega_{in}$ in the inlet air humidity ratio ω_{in} , and note that Eq. (3.22) yields the following expression for the sensitivity of the response $R = RH^{(1)}$ to ω_{in} :

$$\begin{aligned} S_{46} &\triangleq \frac{\partial R}{\partial \omega_{in}} - \left[\sum_{i=1}^{49} \left(\mu_w^{(i)} \frac{\partial N_1^{(i)}}{\partial \omega_{in}} + \tau_w^{(i)} \frac{\partial N_2^{(i)}}{\partial \omega_{in}} + \tau_a^{(i)} \frac{\partial N_3^{(i)}}{\partial \omega_{in}} + o^{(i)} \frac{\partial N_4^{(i)}}{\partial \omega_{in}} \right) + \mu_a \frac{\partial N_5}{\partial \omega_{in}} \right] \\ &= 0 - \left(\tau_a^{(49)} \frac{\partial N_3^{(49)}}{\partial \omega_{in}} + o^{(49)} \frac{\partial N_4^{(49)}}{\partial \omega_{in}} \right) = - \left[\tau_a^{(49)} \cdot (1) + o^{(49)} \cdot h_{g,a}^{(50)}(T_{a,in}, \boldsymbol{\alpha}) \right]. \end{aligned} \quad (D.39)$$

Re-writing Eq. (D.39) in the form

$$\tau_a^{(49)} = -S_{46} - o^{(49)} \cdot h_{g,a}^{(50)}(T_{a,in}, \boldsymbol{\alpha}) \quad (D.40)$$

indicates that the value of the adjoint function $\tau_a^{(49)}$ could be computed independently if the sensitivity S_{46} were available, since the $o^{(49)}$ has been verified in (the previous) Section D.1.3.2 and the quantity $h_{g,a}^{(50)}(T_{a,in}, \alpha)$ is known. To first-order in the parameter perturbation, the finite-difference formula given in Eq. (3.23) can be used to compute the approximate sensitivity S_{46}^{FD} ; subsequently, this value can be used in conjunction with Eq. (D.40) to compute a “finite-difference sen-

APPENDIX D. VERIFICATION OF THE MODEL ADJOINT FUNCTIONS

sitivity” value, denoted as $\left[\tau_a^{(49)}\right]^{SFD}$, for the respective adjoint, which would be accurate up to second-order in the respective parameter perturbation:

$$\left[\tau_a^{(49)}\right]^{SFD} = -S_{46}^{FD} - o^{(49)} \cdot h_{g,a}^{(50)}(T_{a,in}, \boldsymbol{\alpha}) \quad (\text{D.41})$$

Numerically, the inlet air humidity ratio ω_{in} has the nominal (“base-case”) value of $\omega_{in}^0 = 0.015029407$. The corresponding nominal value $RH_{nom}^{(1)}$ of the response $RH^{(1)}$ is $RH_{nom}^{(1)} = 100.1052\%$. Consider next a perturbation $\delta\omega_{in} = (0.001243)\omega_{in}^0$, for which the perturbed value of the inlet air humidity ratio becomes $\omega_{in}^{pert} = \omega_{in}^0 - \delta\omega_{in} = 0.015010726$. Re-computing the perturbed response by solving Eqs. (2.2) - (2.15) with the value of ω_{in}^{pert} yields the “perturbed response” value $RH_{pert}^{(1)} = 100.0951\%$. Using now the nominal and perturbed response values together with the parameter perturbation in the finite-difference expression given in Eq. (3.23) yields the corresponding “finite-difference-computed sensitivity” $S_{46}^{FD} \triangleq \frac{RH_{pert}^{(1)} - RH_{nom}^{(1)}}{\delta\omega_{in}} = 537.96 \quad [-]$. Using this value together with the nominal values of the other quantities appearing in the expression on the right side of Eq. (D.41) yields $\left[\tau_a^{(49)}\right]^{SFD} = -2298.3 \quad [-]$. This result compares well with the value $\tau_a^{(49)} = -2235.5 \quad [-]$ obtained by solving the adjoint sensitivity system given in Eq. (3.10), cf. Figure 3.3. When solving this adjoint sensitivity system, the computation of $\tau_a^{(49)}$ depends on the previously computed adjoint functions $\tau_a^{(i)}$, $i = 1, \dots, I - 1$; hence, the forgoing verification of the computational accuracy of $\tau_a^{(49)}$ also provides an indirect verification that the functions $\tau_a^{(i)}$, $i = 1, \dots, I - 1$ were also computed accurately.

D.1.3.4 Verification of the adjoint function $\tau_w^{(1)}$

Note that the value of the adjoint function $\tau_w^{(1)}$ obtained by solving the adjoint sensitivity system given in Eq. (3.10) is as follows: $\tau_w^{(1)} = -6.18 \times 10^{-7} \quad [(J/s)^{-1}]$, indicated in Figure 3.3. Now select a variation $\delta T_{w,in}$ in the inlet water tem-

APPENDIX D. VERIFICATION OF THE MODEL ADJOINT FUNCTIONS

perature $T_{w,in}$, and note that Eq. (3.22) yields the following expression for the sensitivity of the response $R = RH^{(1)}$ to $T_{w,in}$:

$$\begin{aligned} S_3 &\triangleq \frac{\partial R}{\partial T_{w,in}} - \left[\sum_{i=1}^{49} \left(\mu_w^{(i)} \frac{\partial N_1^{(i)}}{\partial T_{w,in}} + \tau_w^{(i)} \frac{\partial N_2^{(i)}}{\partial T_{w,in}} + \tau_a^{(i)} \frac{\partial N_3^{(i)}}{\partial T_{w,in}} + o^{(i)} \frac{\partial N_4^{(i)}}{\partial T_{w,in}} \right) + \mu_a \frac{\partial N_5}{\partial T_{w,in}} \right] \\ &= 0 - \tau_w^{(1)} \frac{\partial N_2^{(1)}}{\partial T_{w,in}} = 0 - \tau_w^{(1)} \cdot (m_{w,in} \cdot a_{1f}). \end{aligned} \quad (D.42)$$

Re-writing Eq. (D.42) in the form

$$\tau_w^{(1)} = - \frac{S_3}{(m_{w,in} \cdot a_{1f})} \quad (D.43)$$

indicates that the value of the adjoint function $\tau_w^{(1)}$ could be computed independently if the sensitivity S_3 were available, since the quantity $m_{w,in} \cdot a_{1f}$ is known. To first-order in the parameter perturbation, the finite-difference formula given in Eq. (3.23) can be used to compute the approximate sensitivity S_3^{FD} ; subsequently, this value can be used in conjunction with Eq. (D.43) to compute a “finite-difference sensitivity” value, denoted as $[\tau_w^{(1)}]^{SFD}$, for the respective adjoint, which would be accurate up to second-order in the respective parameter perturbation:

$$[\tau_w^{(1)}]^{SFD} = - \frac{S_3^{FD}}{(m_{w,in} \cdot a_{1f})} \quad (D.44)$$

Numerically, the inlet water temperature, $T_{w,in}$, has the nominal (“base-case”) value of $T_{w,in}^0 = 298.774$ [K]. The corresponding nominal value $RH_{nom}^{(1)}$ of the response $RH^{(1)}$ is $RH_{nom}^{(1)} = 100.1052\%$. Consider now a perturbation $\delta T_{w,in} = (0.0000669) T_{w,in}^0$, for which the perturbed value of the inlet water temperature becomes $T_{w,in}^{pert} = T_{w,in}^0 - \delta T_{w,in} = 298.754$ [K]. Re-computing the perturbed response by solving Eqs. (2.2) - (2.15) with the value of $T_{w,in}^{pert}$ yields the “perturbed response” value $RH_{pert}^{(1)} = 100.1029\%$. Using now the nominal and perturbed re-

APPENDIX D. VERIFICATION OF THE MODEL ADJOINT FUNCTIONS

sponse values together with the parameter perturbation in the finite-difference expression given in Eq. (3.23) yields the corresponding “finite-difference-computed sensitivity” $S_3^{FD} \triangleq \frac{RH_{pert}^{(1)} - RH_{nom}^{(1)}}{\delta T_{w,in}} = 0.48288 \text{ [K}^{-1}\text{]}$. Using this value together with the nominal values of the other quantities appearing in the expression on the right side of Eq. (D.44) yields $\left[\tau_w^{(1)}\right]^{SFD} = -6.16 \times 10^{-7} \text{ [(J/s)}^{-1}\text{]}$. This result compares well with the value $\tau_w^{(1)} = -6.18 \times 10^{-7} \text{ [(J/s)}^{-1}\text{]}$ obtained by solving the adjoint sensitivity system given in Eq. (3.10), cf. Figure 3.3.

D.1.3.5 Verification of the adjoint function $\mu_w^{(1)}$

Note that the value of the adjoint function $\mu_w^{(1)}$ obtained by solving the adjoint sensitivity system given in Eq. (3.10) is as follows: $\mu_w^{(1)} = -235.106 \text{ [(kg/s)}^{-1}\text{]}$, respectively, as indicated in Figure 3.3. Now select a variation $\delta m_{w,in}$ in the inlet water mass flow rate $m_{w,in}$, and note that Eq. (3.22) yields the following expression for the sensitivity of the response $R = RH^{(1)}$ to $m_{w,in}$:

$$\begin{aligned} S_{44} &\triangleq \frac{\partial R}{\partial m_{w,in}} - \left[\sum_{i=1}^{49} \left(\mu_w^{(i)} \frac{\partial N_1^{(i)}}{\partial m_{w,in}} + \tau_w^{(i)} \frac{\partial N_2^{(i)}}{\partial m_{w,in}} + \tau_a^{(i)} \frac{\partial N_3^{(i)}}{\partial m_{w,in}} + o^{(i)} \frac{\partial N_4^{(i)}}{\partial m_{w,in}} \right) \right. \\ &\quad \left. + \mu_a \frac{\partial N_5}{\partial m_{w,in}} \right] = 0 - \left(\mu_w^{(1)} \frac{\partial N_1^{(1)}}{\partial m_{w,in}} + \tau_w^{(1)} \frac{\partial N_2^{(1)}}{\partial m_{w,in}} + \tau_a^{(1)} \frac{\partial N_3^{(1)}}{\partial m_{w,in}} + o^{(1)} \frac{\partial N_4^{(1)}}{\partial m_{w,in}} \right) \\ &= - \left[\mu_w^{(1)} \cdot (-1) + \tau_w^{(1)} \cdot (T_{w,in} a_{1f} - a_{1g} T_w^{(2)} + a_{0f} - a_{0g}) \right. \\ &\quad \left. + \tau_a^{(1)} \cdot \left(\frac{1}{m_a} \right) + o^{(1)} \cdot \left(\frac{a_{1g} T_w^{(2)} + a_{0g}}{m_a} \right) \right]. \end{aligned} \tag{D.45}$$

Since the adjoint functions $\tau_a^{(49)}$ and $o^{(49)}$ have been already verified as described in Sections D.1.3.2 and D.1.3.3, it follows that the computed values of adjoint functions $\tau_a^{(1)} = -19110.5 \text{ [-]}$ and $o^{(1)} = 0.005632 \left[\left(\frac{J}{kg} \right)^{-1} \right]$ can also be considered as being accurate, since they constitute the starting point for solving

APPENDIX D. VERIFICATION OF THE MODEL ADJOINT FUNCTIONS

the adjoint sensitivity system in Eq. (3.10); $\tau_w^{(1)}$ was proved being accurate in Section D.1.3.4. Re-writing Eq. (D.45) in the form:

$$\begin{aligned} \mu_w^{(1)} = & S_{44} + \tau_w^{(1)} \cdot (T_{w,in}a_{1f} - a_{1g}T_w^{(2)} + a_{0f} - a_{0g}) \\ & + \tau_a^{(1)} \cdot \left(\frac{1}{m_a} \right) + o^{(1)} \cdot \left(\frac{a_{1g}T_w^{(2)} + a_{0g}}{m_a} \right) \end{aligned} \quad (D.46)$$

indicates that the value of the adjoint function $\mu_w^{(1)}$ could be computed independently if the sensitivity S_{44} were available, since all the other quantities are known. To first-order in the parameter perturbation, the finite-difference formula given in Eq. (3.23) can be used to compute the approximate sensitivity S_{44}^{FD} ; subsequently, this value can be used in conjunction with Eq. (D.46) to compute a “finite-difference sensitivity” value, denoted as $[\mu_w^{(1)}]^{SFD}$, for the respective adjoint, which would be accurate up to second-order in the respective parameter perturbation:

$$\begin{aligned} [\mu_w^{(1)}]^{SFD} = & \mu_w^{(1)} = S_{44}^{FD} + \tau_w^{(1)} \cdot (T_{w,in}a_{1f} - a_{1g}T_w^{(2)} + a_{0f} - a_{0g}) \\ & + \tau_a^{(1)} \cdot \left(\frac{1}{m_a} \right) + o^{(1)} \cdot \left(\frac{a_{1g}T_w^{(2)} + a_{0g}}{m_a} \right) \end{aligned} \quad (D.47)$$

Numerically, the inlet water mass flow rate, $m_{w,in}$, has the nominal (“base-case”) value of $m_{w,in}^0 = 44.0213$ [kg/s]. The corresponding nominal value $RH_{nom}^{(1)}$ of the response $RH^{(1)}$ is $RH_{nom}^{(1)} = 100.1052\%$. Next, consider a perturbation $\delta m_{w,in} = (0.0004839) m_{w,in}^0$, for which the perturbed value of the inlet water mass flow rate becomes $m_{w,in}^{pert} = m_{w,in}^0 - \delta m_{w,in} = 44.00$ [kg/s]. Re-computing the perturbed response by solving Eqs. (2.2) - (2.15) with the value of $m_{w,in}^{pert}$ yields the “perturbed response” value $RH_{pert}^{(1)} = 100.1052\%$. Using now the nominal and perturbed response values together with the parameter perturbation in the finite-difference expression given in Eq. (3.23) yields the corresponding “finite-difference-computed sensitivity” $S_{44}^{FD} \triangleq \frac{RH_{pert}^{(1)} - RH_{nom}^{(1)}}{\delta m_{w,in}} = -8.075 \times 10^{-4} \left[\left(\frac{kg}{s} \right)^{-1} \right]$.

APPENDIX D. VERIFICATION OF THE MODEL ADJOINT FUNCTIONS

Using this value together with the nominal values of the other quantities appearing in the expression on the right side of Eq. (D.47) yields $\left[\mu_w^{(1)}\right]^{SFD} = -235.106 \text{ [(kg/s)}^{-1}]$. This result compares well with the value $\mu_w^{(1)} = -235.106 \text{ [(kg/s)}^{-1}]$ obtained by solving the adjoint sensitivity system given in Eq. (3.10), cf. Figure 3.3.

D.1.4 Verification of the Adjoint Functions for the Outlet

Water Mass Flow Rate $m_w^{(50)}$

When $R = m_w^{(50)}$, the quantities $r_\ell^{(i)}$ defined in Eqs. (3.4) - (3.5) all vanish except for a single component, namely: $r_1^{(49)} \triangleq \partial R / \partial m_w^{(50)} = 1$. Thus, the adjoint functions corresponding to the outlet air temperature response $m_w^{(50)}$ are computed by solving the adjoint sensitivity system given in Eq. (3.10) using $r_1^{(49)} \triangleq \partial R / \partial m_w^{(50)} = 1$ as the only non-zero source term; for this case, the solution of Eq. (3.10) has been depicted in Figure 3.4.

D.1.4.1 Verification of the adjoint function μ_a

Note that the value of the adjoint function μ_a obtained by solving the adjoint sensitivity system given in Eq. (3.10) is $\mu_a = -0.017646 \text{ [(kg/s) / (J/m}^3\text{)]}$, as indicated in Figure 3.4. Now select a variation δV_w in the wind speed V_w , and note that Eq. (3.22) yields the following expression for the sensitivity of the response $R = m_w^{(50)}$ to V_w :

$$\begin{aligned} S_5 \triangleq \frac{\partial R}{\partial V_w} &= \left[\sum_{i=1}^{49} \left(\mu_w^{(i)} \frac{\partial N_1^{(i)}}{\partial V_w} + \tau_w^{(i)} \frac{\partial N_2^{(i)}}{\partial V_w} + \tau_a^{(i)} \frac{\partial N_3^{(i)}}{\partial V_w} + o^{(i)} \frac{\partial N_4^{(i)}}{\partial V_w} \right) + \mu_a \frac{\partial N_5}{\partial V_w} \right] \\ &= 0 - \mu_a \frac{\partial N_5}{\partial V_w} = -(\mu_a) [-V_w \cdot \rho(T_{tdb}, \boldsymbol{\alpha})]. \end{aligned} \tag{D.48}$$

APPENDIX D. VERIFICATION OF THE MODEL ADJOINT FUNCTIONS

Re-writing Eq. (D.48) in the form

$$\mu_a = -\frac{S_5}{\partial N_5 / \partial V_w} \quad (\text{D.49})$$

indicates that the value of the adjoint function μ_a could be computed independently if the sensitivity S_5 were available, since the quantity $\partial N_5 / \partial V_w = -2.1795 [J/(m^4/s)]$ is known. To first-order in the parameter perturbation, the finite-difference formula given in Eq. (3.23) can be used to compute the approximate sensitivity S_5^{FD} ; subsequently, this value can be used in conjunction with Eq. (D.49) to compute a “finite-difference sensitivity” value, denoted as $[\mu_a]^{SFD}$, for the respective adjoint, which would be accurate up to second-order in the respective parameter perturbation:

$$[\mu_a]^{SFD} = -\frac{S_5^{FD}}{\partial N_5 / \partial V_w} = -\left[\frac{T_{a,pert}^{(1)} - T_{a,nom}^{(1)}}{\delta V_w} \right] \left[\frac{\partial N_5}{\partial V_w} \right]^{-1} \quad (\text{D.50})$$

Numerically, the wind speed V_w has the nominal (“base-case”) value of $V_w^0 = 1.353 [m/s]$. The corresponding nominal value $m_{w,nom}^{(50)}$ of the response $m_w^{(50)}$ is $m_{w,nom}^{(50)} = 43.91418 [kg/s]$. Consider next a perturbation $\delta V_w = (0.017) V_w^0$, for which the perturbed value of the wind speed becomes $V_w^{pert} = V_w^0 - \delta V_w = 1.33 [m/s]$. Re-computing the perturbed response by solving Eqs. (2.2) - (2.15) with the value of V_w^{pert} yields the “perturbed response” value $m_{w,pert}^{(50)} = 43.91484 [kg/s]$. Using now the nominal and perturbed response values together with the parameter perturbation in the finite-difference expression given in Eq. (3.23) yields the corresponding value for the “finite-difference-computed sensitivity” $S_5^{FD} \triangleq \frac{m_{w,pert}^{(50)} - m_{w,nom}^{(50)}}{\delta V_w} = -0.02847 [(kg/s) / (m/s)]$. Using this value together with the nominal values of the other quantities appearing in the expression on the right side of Eq. (D.50) yields $[\mu_a]^{SFD} = -0.017612 [(kg/s) / (J/m^3)]$. This result compares well with the value $\mu_a = -0.017646 [(kg/s) / (J/m^3)]$ obtained by solving the adjoint sensitivity system given in Eq. (3.10), cf., Figure 3.4.

APPENDIX D. VERIFICATION OF THE MODEL ADJOINT FUNCTIONS

D.1.4.2 Verification of the adjoint function $o^{(49)}$

Note that the value of the adjoint function $o^{(49)}$ obtained by solving the adjoint sensitivity system given in Eq. (3.10) is $o^{(49)} = -9.08 \times 10^{-7} \quad [(kg/s) / (J/kg)]$, as indicated in Figure 3.4. Now select a variation $\delta T_{a,in}$ in the inlet air temperature $T_{a,in}$, and note that Eq. (3.22) yields the following expression for the sensitivity of the response $R = m_w^{(50)}$ to $T_{a,in}$:

$$\begin{aligned}
 S_{45} &\triangleq \frac{\partial R}{\partial T_{a,in}} - \left[\sum_{i=1}^{49} \left(\mu_w^{(i)} \frac{\partial N_1^{(i)}}{\partial T_{a,in}} + \tau_w^{(i)} \frac{\partial N_2^{(i)}}{\partial T_{a,in}} + \tau_a^{(i)} \frac{\partial N_3^{(i)}}{\partial T_{a,in}} + o^{(i)} \frac{\partial N_4^{(i)}}{\partial T_{a,in}} \right) + \mu_a \frac{\partial N_5}{\partial T_{a,in}} \right] \\
 &= 0 - \left[o^{(49)} \frac{\partial N_4^{(49)}}{\partial T_{a,in}} + \mu_a \frac{\partial N_5}{\partial T_{a,in}} \right] = -(o^{(49)}) \left[C_p \left(\frac{T_a^{(49)} + tK}{2} \right) + \omega_{in} \alpha_{1g} \right] \\
 &\quad - (\mu_a) \cdot \left\{ \frac{R_{air}}{2 \cdot P_{atm}} \cdot |m_a| \cdot m_a \cdot \left[\left(\frac{1}{A_{out}^2} - \frac{1}{A_{in}^2} + \frac{k_{sum}}{A_{fill}^2} \right) + \frac{96f}{Re} \cdot \frac{L_{fill}}{A_{fill}^2 D_h} \right] \right. \\
 &\quad \left. + \frac{g \cdot P_{atm}}{R_{air} \cdot T_{a,in}^2} \cdot \left(Z + \frac{V_w^2}{2g} - \Delta z_{rain} - \frac{\Delta z}{2} \right) \right\}.
 \end{aligned} \tag{D.51}$$

Re-writing Eq. (D.51) in the form

$$o^{(49)} = - \frac{S_{45} + \mu_a \frac{\partial N_5}{\partial T_{a,in}}}{\frac{\partial N_4^{(49)}}{\partial T_{a,in}}} \tag{D.52}$$

indicates that the value of the adjoint function $o^{(49)}$ could be computed independently if the sensitivity S_{45} were available, since the quantity $\partial N_4^{(49)} / \partial T_{a,in} = 1.03310 \times 10^3 [J/(kg \cdot K)]$ is known. To first-order in the parameter perturbation, the finite-difference formula given in Eq. (3.23) can be used to compute the approximate sensitivity S_{45}^{FD} ; subsequently, this value can be used in conjunction with Eq. (D.52) to compute a “finite-difference sensitivity” value, denoted as $[o^{(49)}]^{SFD}$, for the respective adjoint, which would be accurate up to second-

APPENDIX D. VERIFICATION OF THE MODEL ADJOINT FUNCTIONS

order in the respective parameter perturbation:

$$[o^{(49)}]^{SFD} = -\frac{S_{45}^{FD} + \mu_a \frac{\partial N_5}{\partial T_{a,in}}}{\frac{\partial N_4^{(49)}}{\partial T_{a,in}}} = -\left[\frac{T_{a,pert}^{(1)} - T_{a,nom}^{(1)}}{\delta T_{a,in}} + \mu_a \frac{\partial N_5}{\partial T_{a,in}} \right] \left[\frac{\partial N_4^{(49)}}{\partial T_{a,in}} \right]^{-1} \quad (D.53)$$

Numerically, the inlet air temperature $T_{a,in}(=T_{db})$ has the nominal (“base-case”) value of $T_{a,in}^0 = 294.03$ [K]. The corresponding nominal value $m_{w,nom}^{(50)}$ of the response $m_w^{(50)}$ is $m_{w,nom}^{(50)} = 43.91418$ [kg/s]. Consider next a perturbation $\delta T_{a,in} = (0.00102) T_{a,in}^0$, for which the perturbed value of the inlet air temperature becomes $T_{a,in}^{pert} = T_{a,in}^0 - \delta T_{a,in} = 294.00$ [K]. Re-computing the perturbed response by solving Eqs. (2.2) - (2.15) with the value of $T_{a,in}^{pert}$ yields the “perturbed response” value $m_{w,pert}^{(50)} = 43.91394$ [kg/s]. Using now the nominal and perturbed response values together with the parameter perturbation in the finite-difference expression given in Eq. (3.23) yields the corresponding “finite-difference-computed sensitivity” $S_{45}^{FD} \triangleq \frac{m_{w,pert}^{(50)} - m_{w,nom}^{(50)}}{\delta T_{a,in}} = 0.00821$ [$\frac{kg}{s \cdot K}$]. Using this value together with the nominal values of the other quantities appearing in the expression on the right side of Eq. (D.53) yields $[o^{(49)}]^{SFD} = -7.96 \times 10^{-7}$ [(kg/s) / (J/kg)]. This result compares well with the value $o^{(49)} = -9.08 \times 10^{-7}$ [(kg/s) / (J/kg)] obtained by solving the adjoint sensitivity system given in Eq. (3.10), cf., Figure 3.4. When solving this adjoint sensitivity system, the computation of $o^{(49)}$ depends on the previously computed adjoint functions $o^{(i)}$, $i = 1, \dots, I-1$; hence, the forgoing verification of the computational accuracy of $o^{(49)}$ also provides an indirect verification that the functions $o^{(i)}$, $i = 1, \dots, I-1$, were also computed accurately.

D.1.4.3 Verification of the adjoint function $\tau_a^{(49)}$

Note that the value of the adjoint function $\tau_a^{(49)}$ obtained by solving the adjoint sensitivity system given in Eq. (3.10) is $\tau_a^{(49)} = -14.812$ [kg/s], as indicated in

APPENDIX D. VERIFICATION OF THE MODEL ADJOINT FUNCTIONS

Figure 3.4. Now select a variation $\delta\omega_{in}$ in the inlet air humidity ratio ω_{in} , and note that Eq. (3.22) yields the following expression for the sensitivity of the response $R = m_w^{(50)}$ to ω_{in} :

$$\begin{aligned} S_{46} &\triangleq \frac{\partial R}{\partial \omega_{in}} - \left[\sum_{i=1}^{49} \left(\mu_w^{(i)} \frac{\partial N_1^{(i)}}{\partial \omega_{in}} + \tau_w^{(i)} \frac{\partial N_2^{(i)}}{\partial \omega_{in}} + \tau_a^{(i)} \frac{\partial N_3^{(i)}}{\partial \omega_{in}} + o^{(i)} \frac{\partial N_4^{(i)}}{\partial \omega_{in}} \right) + \mu_a \frac{\partial N_5}{\partial \omega_{in}} \right] \\ &= 0 - \left(\tau_a^{(49)} \frac{\partial N_3^{(49)}}{\partial \omega_{in}} + o^{(49)} \frac{\partial N_4^{(49)}}{\partial \omega_{in}} \right) = - \left[\tau_a^{(49)} \cdot (1) + o^{(49)} \cdot h_{g,a}^{(50)}(T_{a,in}, \boldsymbol{\alpha}) \right]. \end{aligned} \quad (D.54)$$

Re-writing Eq. (D.54) in the form

$$\tau_a^{(49)} = -S_{46} - o^{(49)} \cdot h_{g,a}^{(50)}(T_{a,in}, \boldsymbol{\alpha}) \quad (D.55)$$

indicates that the value of the adjoint function $\tau_a^{(49)}$ could be computed independently if the sensitivity S_{46} were available, since the $o^{(49)}$ has been verified in (the previous) Section 3.1.4.2 and the quantity $h_{g,a}^{(50)}(T_{a,in}, \alpha)$ is known. To first-order in the parameter perturbation, the finite-difference formula given in Eq. (3.23) can be used to compute the approximate sensitivity S_{46}^{FD} ; subsequently, this value can be used in conjunction with Eq. (D.55) to compute a “finite-difference sensitivity” value, denoted as $[\tau_a^{(49)}]^{SFD}$, for the respective adjoint, which would be accurate up to second-order in the respective parameter perturbation:

$$[\tau_a^{(49)}]^{SFD} = -S_{46}^{FD} - o^{(49)} \cdot h_{g,a}^{(50)}(T_{a,in}, \boldsymbol{\alpha}) \quad (D.56)$$

Numerically, the inlet air humidity ratio ω_{in} has the nominal (“base-case”) value of $\omega_{in}^0 = 0.015029407$. The corresponding nominal value $m_{w,nom}^{(50)}$ of the response $m_w^{(50)}$ is $m_{w,nom}^{(50)} = 43.91418 \text{ [kg/s]}$. Consider next a perturbation $\delta\omega_{in} = (0.001243)\omega_{in}^0$, for which the perturbed value of the inlet air humidity ratio becomes $\omega_{in}^{pert} = \omega_{in}^0 - \delta\omega_{in} = 0.015010726$. Re-computing the perturbed response by

APPENDIX D. VERIFICATION OF THE MODEL ADJOINT FUNCTIONS

solving Eqs. (2.2) - (2.15) with the value of ω_{in}^{pert} yields the “perturbed response” value $m_{w,pert}^{(50)} = 43.91386$ [kg/s]. Using now the nominal and perturbed response values together with the parameter perturbation in the finite-difference expression given in Eq. (3.23) yields the corresponding “finite-difference-computed sensitivity” $S_{46}^{FD} \triangleq \frac{m_{w,pert}^{(50)} - m_{w,nom}^{(50)}}{\delta\omega_{in}} = 17.254$ [kg/s]. Using this value together with the nominal values of the other quantities appearing in the expression on the right side of Eq. (D.56) yields $\left[\tau_a^{(49)}\right]^{SFD} = -14.948$ [kg/s]. This result compares well with the value $\tau_a^{(49)} = -14.812$ [kg/s] obtained by solving the adjoint sensitivity system given in Eq. (3.10), cf. Figure 3.4. When solving this adjoint sensitivity system, the computation of $\tau_a^{(49)}$ depends on the previously computed adjoint functions $\tau_a^{(i)}$, $i = 1, \dots, I - 1$; hence, the forgoing verification of the computational accuracy of $\tau_a^{(49)}$ also provides an indirect verification that the functions $\tau_a^{(i)}$, $i = 1, \dots, I - 1$ were also computed accurately.

D.1.4.4 Verification of the adjoint function $\tau_w^{(1)}$

Note that the value of the adjoint function $\tau_w^{(1)}$ obtained by solving the adjoint sensitivity system given in Eq. (3.10) is as follows: $\tau_w^{(1)} = 1.581 \times 10^{-7}$ [(J/kg)⁻¹], indicated in Figure 3.4. Now select a variation $\delta T_{w,in}$ in the inlet water temperature $T_{w,in}$, and note that Eq. (3.22) yields the following expression for the sensitivity of the response $R = m_w^{(50)}$ to $T_{w,in}$:

$$\begin{aligned} S_3 &\triangleq \frac{\partial R}{\partial T_{w,in}} - \left[\sum_{i=1}^{49} \left(\mu_w^{(i)} \frac{\partial N_1^{(i)}}{\partial T_{w,in}} + \tau_w^{(i)} \frac{\partial N_2^{(i)}}{\partial T_{w,in}} + \tau_a^{(i)} \frac{\partial N_3^{(i)}}{\partial T_{w,in}} + o^{(i)} \frac{\partial N_4^{(i)}}{\partial T_{w,in}} \right) + \mu_a \frac{\partial N_5}{\partial T_{w,in}} \right] \\ &= 0 - \tau_w^{(1)} \frac{\partial N_2^{(1)}}{\partial T_{w,in}} = 0 - \tau_w^{(1)} \cdot (m_{w,in} \cdot a_{1f}). \end{aligned} \tag{D.57}$$

Re-writing Eq. (D.57) in the form

$$\tau_w^{(1)} = - \frac{S_3}{(m_{w,in} \cdot a_{1f})} \tag{D.58}$$

APPENDIX D. VERIFICATION OF THE MODEL ADJOINT FUNCTIONS

indicates that the value of the adjoint function $\tau_w^{(1)}$ could be computed independently if the sensitivity S_3 were available, since the quantity $m_{w,in} \cdot a_{1f}$ is known. To first-order in the parameter perturbation, the finite-difference formula given in Eq. (3.23) can be used to compute the approximate sensitivity S_3^{FD} ; subsequently, this value can be used in conjunction with Eq. (D.58) to compute a “finite-difference sensitivity” value, denoted as $[\tau_w^{(1)}]^{SFD}$, for the respective adjoint, which would be accurate up to second-order in the respective parameter perturbation:

$$[\tau_w^{(1)}]^{SFD} = -\frac{S_3^{FD}}{(m_{w,in} \cdot a_{1f})} \quad (\text{D.59})$$

Numerically, the inlet water temperature, $T_{w,in}$, has the nominal (“base-case”) value of $T_{w,in}^0 = 298.774$ [K]. The corresponding nominal value $m_{w,nom}^{(50)}$ of the response $m_w^{(50)}$ is $m_{w,nom}^{(50)} = 43.91418$ [kg/s]. Consider now a perturbation $\delta T_{w,in} = (0.0000669) T_{w,in}^0$, for which the perturbed value of the inlet water temperature becomes $T_{w,in}^{pert} = T_{w,in}^0 - \delta T_{w,in} = 298.754$ [K]. Re-computing the perturbed response by solving Eqs. (2.2) - (2.15) with the value of $T_{w,in}^{pert}$ yields the “perturbed response” value $m_{w,pert}^{(50)} = 43.91477$ [kg/s]. Using now the nominal and perturbed response values together with the parameter perturbation in the finite-difference expression given in Eq. (3.23) yields the corresponding “finite-difference-computed sensitivity” $S_3^{FD} \triangleq \frac{m_{w,pert}^{(50)} - m_{w,nom}^{(50)}}{\delta T_{w,in}} = -0.031364$ [$\frac{\text{kg}}{\text{s} \cdot \text{K}}$]. Using this value together with the nominal values of the other quantities appearing in the expression on the right side of Eq. (D.59) yields $[\tau_w^{(1)}]^{SFD} = 1.580 \times 10^{-7}$ [(J/kg) $^{-1}$]. This result compares well with the value $\tau_w^{(1)} = 1.581 \times 10^{-7}$ [(J/kg) $^{-1}$] obtained by solving the adjoint sensitivity system given in Eq. (3.10), cf. Figure 3.4.

D.1.4.5 Verification of the adjoint function $\mu_w^{(1)}$

Note that the value of the adjoint function $\mu_w^{(1)}$ obtained by solving the adjoint sensitivity system given in Eq. (3.10) is as follows: $\mu_w^{(1)} = 0.61393$ [–], respec-

APPENDIX D. VERIFICATION OF THE MODEL ADJOINT FUNCTIONS

tively, as indicated in Figure 3.4. Now select a variation $\delta m_{w,in}$ in the inlet water mass flow rate $m_{w,in}$, and note that Eq. (3.22) yields the following expression for the sensitivity of the response $R = m_w^{(50)}$ to $m_{w,in}$:

$$\begin{aligned}
 S_{44} &\triangleq \frac{\partial R}{\partial m_{w,in}} - \left[\sum_{i=1}^{49} \left(\mu_w^{(i)} \frac{\partial N_1^{(i)}}{\partial m_{w,in}} + \tau_w^{(i)} \frac{\partial N_2^{(i)}}{\partial m_{w,in}} + \tau_a^{(i)} \frac{\partial N_3^{(i)}}{\partial m_{w,in}} + o^{(i)} \frac{\partial N_4^{(i)}}{\partial m_{w,in}} \right) \right. \\
 &\quad \left. + \mu_a \frac{\partial N_5}{\partial m_{w,in}} \right] = 0 - \left(\mu_w^{(1)} \frac{\partial N_1^{(1)}}{\partial m_{w,in}} + \tau_w^{(1)} \frac{\partial N_2^{(1)}}{\partial m_{w,in}} + \tau_a^{(1)} \frac{\partial N_3^{(1)}}{\partial m_{w,in}} + o^{(1)} \frac{\partial N_4^{(1)}}{\partial m_{w,in}} \right) \\
 &\quad = - \left[\mu_w^{(1)} \cdot (-1) + \tau_w^{(1)} \cdot (T_{w,in} a_{1f} - a_{1g} T_w^{(2)} + a_{0f} - a_{0g}) \right. \\
 &\quad \quad \left. + \tau_a^{(1)} \cdot \left(\frac{1}{m_a} \right) + o^{(1)} \cdot \left(\frac{a_{1g} T_w^{(2)} + a_{0g}}{m_a} \right) \right].
 \end{aligned} \tag{D.60}$$

Since the adjoint functions $\tau_a^{(49)}$ and $o^{(49)}$ have been already verified as described in Sections D.1.4.2 and D.1.4.3, it follows that the computed values of adjoint functions $\tau_a^{(1)} = -10.569 \text{ [kg/s]}$ and $o^{(1)} = 4.16 \times 10^{-6} \left[\left(\frac{\text{kg}}{\text{s}} \right) / \left(\frac{\text{J}}{\text{kg}} \right) \right]$ can also be considered as being accurate, since they constitute the starting point for solving the adjoint sensitivity system in Eq. (3.10); $\tau_w^{(1)}$ was proved being accurate in Section D.1.4.4. Re-writing Eq. (D.60) in the form:

$$\begin{aligned}
 \mu_w^{(1)} &= S_{44} + \tau_w^{(1)} \cdot (T_{w,in} a_{1f} - a_{1g} T_w^{(2)} + a_{0f} - a_{0g}) \\
 &\quad + \tau_a^{(1)} \cdot \left(\frac{1}{m_a} \right) + o^{(1)} \cdot \left(\frac{a_{1g} T_w^{(2)} + a_{0g}}{m_a} \right)
 \end{aligned} \tag{D.61}$$

indicates that the value of the adjoint function $\mu_w^{(1)}$ could be computed independently if the sensitivity S_{44} were available, since all the other quantities are known. To first-order in the parameter perturbation, the finite-difference formula given in Eq. (3.23) can be used to compute the approximate sensitivity S_{44}^{FD} ; subsequently, this value can be used in conjunction with Eq. (D.61) to compute a “finite-difference sensitivity” value, denoted as $\left[\mu_w^{(1)} \right]^{SFD}$, for the respective ad-

APPENDIX D. VERIFICATION OF THE MODEL ADJOINT FUNCTIONS

joint, which would be accurate up to second-order in the respective parameter perturbation:

$$\begin{aligned} [\mu_w^{(1)}]^{SFD} = \mu_w^{(1)} = S_{44}^{FD} + \tau_w^{(1)} \cdot (T_{w,in} a_{1f} - a_{1g} T_w^{(2)} + a_{0f} - a_{0g}) \\ + \tau_a^{(1)} \cdot \left(\frac{1}{m_a} \right) + o^{(1)} \cdot \left(\frac{a_{1g} T_w^{(2)} + a_{0g}}{m_a} \right) \end{aligned} \quad (D.62)$$

Numerically, the inlet water mass flow rate, $m_{w,in}$, has the nominal (“base-case”) value of $m_{w,in}^0 = 44.0213$ [kg/s]. The corresponding nominal value $m_{w,nom}^{(50)}$ of the response $m_w^{(50)}$ is $m_{w,nom}^{(50)} = 43.91418$ [kg/s]. Next, consider a perturbation $\delta m_{w,in} = (0.0004839) m_{w,in}^0$, for which the perturbed value of the inlet water mass flow rate becomes $m_{w,in}^{pert} = m_{w,in}^0 - \delta m_{w,in} = 44.00$ [kg/s]. Re-computing the perturbed response by solving Eqs. (2.2) - (2.15) with the value of $m_{w,in}^{pert}$ yields the “perturbed response” value $m_{w,pert}^{(50)} = 43.89289$ [kg/s]. Using now the nominal and perturbed response values together with the parameter perturbation in the finite-difference expression given in Eq. (3.23) yields the corresponding “finite-difference-computed sensitivity” $S_{44}^{FD} \triangleq \frac{m_{w,pert}^{(50)} - m_{w,nom}^{(50)}}{\delta m_{w,in}} = 0.99973$ [–]. Using this value together with the nominal values of the other quantities appearing in the expression on the right side of Eq. (D.62) yields $[\mu_w^{(1)}]^{SFD} = 0.61393$ [–]. This result compares well with the value $\mu_w^{(1)} = 0.61393$ [–] obtained by solving the adjoint sensitivity system given in Eq. (3.10), cf. Figure 3.4.

D.1.5 Verification of the Adjoint Functions for the Outlet

Air Mass Flow Rate m_a

When $R = m_w^{(50)}$, the quantities $r_\ell^{(i)}$ defined in Eqs. (3.4) - (3.5) all vanish except for a single component, namely: $R_5 \triangleq \partial R / \partial m_a = 1$. Thus, the adjoint functions corresponding to the outlet air temperature response $m_w^{(50)}$ are computed by solving the adjoint sensitivity system given in Eq. (3.10) using $R_5 \triangleq \partial R / \partial m_a = 1$

APPENDIX D. VERIFICATION OF THE MODEL ADJOINT FUNCTIONS

as the only non-zero source term; for this case, the solution of Eq. (3.10) has been depicted in Figure 3.5.

D.1.5.1 Verification of the adjoint function μ_a

Note that the value of the adjoint function μ_a obtained by solving the adjoint sensitivity system given in Eq. (3.10) is $\mu_a = 4.4364 \quad [(kg/s)/(J/m^3)]$, as indicated in Figure 3.5. Now select a variation δV_w in the wind speed V_w , and note that Eq. (3.22) yields the following expression for the sensitivity of the response $R = m_a$ to V_w :

$$\begin{aligned} S_5 &\triangleq \frac{\partial R}{\partial V_w} - \left[\sum_{i=1}^{49} \left(\mu_w^{(i)} \frac{\partial N_1^{(i)}}{\partial V_w} + \tau_w^{(i)} \frac{\partial N_2^{(i)}}{\partial V_w} + \tau_a^{(i)} \frac{\partial N_3^{(i)}}{\partial V_w} + o^{(i)} \frac{\partial N_4^{(i)}}{\partial V_w} \right) + \mu_a \frac{\partial N_5}{\partial V_w} \right] \\ &= 0 - \mu_a \frac{\partial N_5}{\partial V_w} = -(\mu_a) [-V_w \cdot \rho(T_{tdb}, \boldsymbol{\alpha})]. \end{aligned} \quad (D.63)$$

Re-writing Eq. (D.63) in the form

$$\mu_a = -\frac{S_5}{\partial N_5 / \partial V_w} \quad (D.64)$$

indicates that the value of the adjoint function μ_a could be computed independently if the sensitivity S_5 were available, since the quantity $\partial N_5 / \partial V_w = -2.1795 [J/(m^4/s)]$ is known. To first-order in the parameter perturbation, the finite-difference formula given in Eq. (3.23) can be used to compute the approximate sensitivity S_5^{FD} ; subsequently, this value can be used in conjunction with Eq. (D.64) to compute a “finite-difference sensitivity” value, denoted as $[\mu_a]^{SFD}$, for the respective adjoint, which would be accurate up to second-order in the respective parameter perturbation:

$$[\mu_a]^{SFD} = -\frac{S_5^{FD}}{\partial N_5 / \partial V_w} = -\left[\frac{T_{a,pert}^{(1)} - T_{a,nom}^{(1)}}{\delta V_w} \right] \left[\frac{\partial N_5}{\partial V_w} \right]^{-1} \quad (D.65)$$

APPENDIX D. VERIFICATION OF THE MODEL ADJOINT FUNCTIONS

Numerically, the wind speed V_w has the nominal (“base-case”) value of $V_w^0 = 1.353$ $[m/s]$. The corresponding nominal value $m_{a,nom}$ of the response m_a is $m_{a,nom} = 20.11022$ $[kg/s]$. Consider next a perturbation $\delta V_w = (0.017) V_w^0$, for which the perturbed value of the wind speed becomes $V_w^{pert} = V_w^0 - \delta V_w = 1.33$ $[m/s]$. Re-computing the perturbed response by solving Eqs. (2.2) - (2.15) with the value of V_w^{pert} yields the “perturbed response” value $m_{a,pert} = 19.94624$ $[kg/s]$. Using now the nominal and perturbed response values together with the parameter perturbation in the finite-difference expression given in Eq. (3.23) yields the corresponding “finite-difference-computed sensitivity” $S_5^{FD} \triangleq \frac{m_{a,pert} - m_{a,nom}}{\delta V_w} = 7.1295$ $[(kg/s) / (m/s)]$. Using this value together with the nominal values of the other quantities appearing in the expression on the right side of Eq. (D.65) yields $[\mu_a]^{SFD} = 4.4099$ $[(kg/s) / (J/m^3)]$. This result compares well with the value $\mu_a = 4.4364$ $[(kg/s) / (J/m^3)]$ obtained by solving the adjoint sensitivity system given in Eq. (3.10), cf., Figure 3.5.

D.1.5.2 Verification of the adjoint function $o^{(49)}$

Note that the value of the adjoint function $o^{(49)}$ obtained by solving the adjoint sensitivity system given in Eq. (3.10) is $o^{(49)} = -1.7873 \times 10^{-4}$ $[(kg/s) / (J/kg)]$, as indicated in Figure 3.5. Now select a variation $\delta T_{a,in}$ in the inlet air temperature $T_{a,in}$, and note that Eq. (3.22) yields the following expression for the sensitivity of the response $R = m_a$ to $T_{a,in}$:

APPENDIX D. VERIFICATION OF THE MODEL ADJOINT FUNCTIONS

$$\begin{aligned}
S_{45} &\triangleq \frac{\partial R}{\partial T_{a,in}} - \left[\sum_{i=1}^{49} \left(\mu_w^{(i)} \frac{\partial N_1^{(i)}}{\partial T_{a,in}} + \tau_w^{(i)} \frac{\partial N_2^{(i)}}{\partial T_{a,in}} + \tau_a^{(i)} \frac{\partial N_3^{(i)}}{\partial T_{a,in}} + o^{(i)} \frac{\partial N_4^{(i)}}{\partial T_{a,in}} \right) + \mu_a \frac{\partial N_5}{\partial T_{a,in}} \right] \\
&= 0 - \left[o^{(49)} \frac{\partial N_4^{(49)}}{\partial T_{a,in}} + \mu_a \frac{\partial N_5}{\partial T_{a,in}} \right] = -(o^{(49)}) \left[C_p \left(\frac{T_a^{(49)} + tK}{2} \right) + \omega_{in} \alpha_{1g} \right] \\
&\quad - (\mu_a) \cdot \left\{ \frac{R_{air}}{2 \cdot P_{atm}} \cdot |m_a| \cdot m_a \cdot \left[\left(\frac{1}{A_{out}^2} - \frac{1}{A_{in}^2} + \frac{k_{sum}}{A_{fill}^2} \right) + \frac{96f}{\text{Re}} \cdot \frac{L_{fill}}{A_{fill}^2 D_h} \right] \right. \\
&\quad \left. + \frac{g \cdot P_{atm}}{R_{air} \cdot T_{a,in}^2} \cdot \left(Z + \frac{V_w^2}{2g} - \Delta z_{rain} - \frac{\Delta z}{2} \right) \right\}.
\end{aligned} \tag{D.66}$$

Re-writing Eq. (D.66) in the form

$$o^{(49)} = - \frac{S_{45} + \mu_a \frac{\partial N_5}{\partial T_{a,in}}}{\frac{\partial N_4^{(49)}}{\partial T_{a,in}}} \tag{D.67}$$

indicates that the value of the adjoint function $o^{(49)}$ could be computed independently if the sensitivity S_{45} were available, since the quantity $\partial N_4^{(49)} / \partial T_{a,in} = 1.03310 \times 10^3 [J/(kg \cdot K)]$ is known. To first-order in the parameter perturbation, the finite-difference formula given in Eq. (3.23) can be used to compute the approximate sensitivity S_{45}^{FD} ; subsequently, this value can be used in conjunction with Eq. (D.67) to compute a “finite-difference sensitivity” value, denoted as $[o^{(49)}]^{SFD}$, for the respective adjoint, which would be accurate up to second-order in the respective parameter perturbation:

$$[o^{(49)}]^{SFD} = - \frac{S_{45}^{FD} + \mu_a \frac{\partial N_5}{\partial T_{a,in}}}{\frac{\partial N_4^{(49)}}{\partial T_{a,in}}} = - \left[\frac{T_{a,pert}^{(1)} - T_{a,nom}^{(1)}}{\delta T_{a,in}} + \mu_a \frac{\partial N_5}{\partial T_{a,in}} \right] \left[\frac{\partial N_4^{(49)}}{\partial T_{a,in}} \right]^{-1} \tag{D.68}$$

Numerically, the inlet air temperature $T_{a,in}(= T_{db})$ has the nominal (“base-case”) value of $T_{a,in}^0 = 294.03 [K]$. The corresponding nominal value $m_{a,nom}$ of the response m_a is $m_{a,nom} = 20.11022 [kg/s]$. Consider next a perturbation $\delta T_{a,in} =$

APPENDIX D. VERIFICATION OF THE MODEL ADJOINT FUNCTIONS

$(0.00102) T_{a,in}^0$, for which the perturbed value of the inlet air temperature becomes $T_{a,in}^{pert} = T_{a,in}^0 - \delta T_{a,in} = 294.00 [K]$. Re-computing the perturbed response by solving Eqs. (2.2) - (2.15) with the value of $T_{a,in}^{pert}$ yields the “perturbed response” value $m_{a,pert} = 20.16037 [kg/s]$. Using now the nominal and perturbed response values together with the parameter perturbation in the finite-difference expression given in Eq. (3.23) yields the corresponding “finite-difference-computed sensitivity” $S_{45}^{FD} \triangleq \frac{m_{a,pert} - m_{a,nom}}{\delta T_{a,in}} = -1.6714 \left[\frac{kg}{s \cdot K} \right]$. Using this value together with the nominal values of the other quantities appearing in the expression on the right side of Eq. (D.68) yields $[o^{(49)}]^{SFD} = -1.7992 \times 10^{-4} [(kg/s) / (J/kg)]$. This result compares well with the value $o^{(49)} = -1.7873 \times 10^{-4} [(kg/s) / (J/kg)]$ obtained by solving the adjoint sensitivity system given in Eq. (3.10), cf., Figure 3.5. When solving this adjoint sensitivity system, the computation of $o^{(49)}$ depends on the previously computed adjoint functions $o^{(i)}$, $i = 1, \dots, I - 1$; hence, the forgoing verification of the computational accuracy of $o^{(49)}$ also provides an indirect verification that the functions $o^{(i)}$, $i = 1, \dots, I - 1$, were also computed accurately.

D.1.5.3 Verification of the adjoint function $\tau_a^{(49)}$

Note that the value of the adjoint function $\tau_a^{(49)}$ obtained by solving the adjoint sensitivity system given in Eq. (3.10) is $\tau_a^{(49)} = 412.302 [kg/s]$, as indicated in Figure 3.5. Now select a variation $\delta \omega_{in}$ in the inlet air humidity ratio ω_{in} , and note that Eq. (3.22) yields the following expression for the sensitivity of the response $R = m_a$ to ω_{in} :

$$\begin{aligned} S_{46} &\triangleq \frac{\partial R}{\partial \omega_{in}} - \left[\sum_{i=1}^{49} \left(\mu_w^{(i)} \frac{\partial N_1^{(i)}}{\partial \omega_{in}} + \tau_w^{(i)} \frac{\partial N_2^{(i)}}{\partial \omega_{in}} + \tau_a^{(i)} \frac{\partial N_3^{(i)}}{\partial \omega_{in}} + o^{(i)} \frac{\partial N_4^{(i)}}{\partial \omega_{in}} \right) + \mu_a \frac{\partial N_5}{\partial \omega_{in}} \right] \\ &= 0 - \left(\tau_a^{(49)} \frac{\partial N_3^{(49)}}{\partial \omega_{in}} + o^{(49)} \frac{\partial N_4^{(49)}}{\partial \omega_{in}} \right) = - [\tau_a^{(49)} \cdot (1) + o^{(49)} \cdot h_{g,a}^{(50)}(T_{a,in}, \boldsymbol{\alpha})] . \end{aligned} \tag{D.69}$$

APPENDIX D. VERIFICATION OF THE MODEL ADJOINT FUNCTIONS

Re-writing Eq. (D.69) in the form

$$\tau_a^{(49)} = -S_{46} - o^{(49)} \cdot h_{g,a}^{(50)}(T_{a,in}, \boldsymbol{\alpha}) \quad (\text{D.70})$$

indicates that the value of the adjoint function $\tau_a^{(49)}$ could be computed independently if the sensitivity S_{46} were available, since the $o^{(49)}$ has been verified in (the previous) Section D.1.5.2 and the quantity $h_{g,a}^{(50)}(T_{a,in}, \alpha)$ is known. To first-order in the parameter perturbation, the finite-difference formula given in Eq. (3.23) can be used to compute the approximate sensitivity S_{46}^{FD} ; subsequently, this value can be used in conjunction with Eq. (D.70) to compute a “finite-difference sensitivity” value, denoted as $[\tau_a^{(49)}]^{SFD}$, for the respective adjoint, which would be accurate up to second-order in the respective parameter perturbation:

$$[\tau_a^{(49)}]^{SFD} = -S_{46}^{FD} - o^{(49)} \cdot h_{g,a}^{(50)}(T_{a,in}, \boldsymbol{\alpha}) \quad (\text{D.71})$$

Numerically, the inlet air humidity ratio ω_{in} has the nominal (“base-case”) value of $\omega_{in}^0 = 0.015029407$. The corresponding nominal value $m_{a,nom}$ of the response m_a is $m_{a,nom} = 20.11022$ [kg/s]. Consider next a perturbation $\delta\omega_{in} = (0.001243)\omega_{in}^0$, for which the perturbed value of the inlet air humidity ratio becomes $\omega_{in}^{pert} = \omega_{in}^0 - \delta\omega_{in} = 0.015010726$. Re-computing the perturbed response by solving Eqs. (2.2) - (2.15) with the value of ω_{in}^{pert} yields the “perturbed response” value $m_{a,pert} = 20.10942$ [kg/s]. Using now the nominal and perturbed response values together with the parameter perturbation in the finite-difference expression given in Eq. (3.23) yields the corresponding “finite-difference-computed sensitivity” $S_{46}^{FD} \triangleq \frac{m_{a,pert} - m_{a,nom}}{\delta\omega_{in}} = 42.865$ [kg/s]. Using this value together with the nominal values of the other quantities appearing in the expression on the right side of Eq. (D.71) yields $[\tau_a^{(49)}]^{SFD} = 411.031$ [kg/s]. This result compares well with the value $\tau_a^{(49)} = 412.302$ [kg/s] obtained by solving the adjoint sensitivity system given in Eq. (3.10), cf. Figure 3.5. When solving this adjoint sensitivity

APPENDIX D. VERIFICATION OF THE MODEL ADJOINT FUNCTIONS

system, the computation of $\tau_a^{(49)}$ depends on the previously computed adjoint functions $\tau_a^{(i)}$, $i = 1, \dots, I - 1$; hence, the forgoing verification of the computational accuracy of $\tau_a^{(49)}$ also provides an indirect verification that the functions $\tau_a^{(i)}$, $i = 1, \dots, I - 1$ were also computed accurately.

D.1.5.4 Verification of the adjoint function $\tau_w^{(1)}$

Note that the value of the adjoint function $\tau_w^{(1)}$ obtained by solving the adjoint sensitivity system given in Eq. (3.10) is as follows: $\tau_w^{(1)} = -8.111 \times 10^{-6} [(J/kg)^{-1}]$, indicated in Figure 3.5. Now select a variation $\delta T_{w,in}$ in the inlet water temperature $T_{w,in}$, and note that Eq. (3.22) yields the following expression for the sensitivity of the response $R = m_a$ to $T_{w,in}$:

$$\begin{aligned} S_3 &\triangleq \frac{\partial R}{\partial T_{w,in}} - \left[\sum_{i=1}^{49} \left(\mu_w^{(i)} \frac{\partial N_1^{(i)}}{\partial T_{w,in}} + \tau_w^{(i)} \frac{\partial N_2^{(i)}}{\partial T_{w,in}} + \tau_a^{(i)} \frac{\partial N_3^{(i)}}{\partial T_{w,in}} + o^{(i)} \frac{\partial N_4^{(i)}}{\partial T_{w,in}} \right) + \mu_a \frac{\partial N_5}{\partial T_{w,in}} \right] \\ &= 0 - \tau_w^{(1)} \frac{\partial N_2^{(1)}}{\partial T_{w,in}} = 0 - \tau_w^{(1)} \cdot (m_{w,in} \cdot a_{1f}). \end{aligned} \quad (D.72)$$

Re-writing Eq. (D.72) in the form

$$\tau_w^{(1)} = - \frac{S_3}{(m_{w,in} \cdot a_{1f})} \quad (D.73)$$

indicates that the value of the adjoint function $\tau_w^{(1)}$ could be computed independently if the sensitivity S_3 were available, since the quantity $m_{w,in} \cdot a_{1f}$ is known. To first-order in the parameter perturbation, the finite-difference formula given in Eq. (3.23) can be used to compute the approximate sensitivity S_3^{FD} ; subsequently, this value can be used in conjunction with Eq. (D.73) to compute a “finite-difference sensitivity” value, denoted as $[\tau_w^{(1)}]^{SFD}$, for the respective adjoint, which would be accurate up to second-order in the respective parameter perturbation:

$$[\tau_w^{(1)}]^{SFD} = - \frac{S_3^{FD}}{(m_{w,in} \cdot a_{1f})} \quad (D.74)$$

APPENDIX D. VERIFICATION OF THE MODEL ADJOINT FUNCTIONS

Numerically, the inlet water temperature, $T_{w,in}$, has the nominal (“base-case”) value of $T_{w,in}^0 = 298.774$ [K]. The corresponding nominal value $m_{a,nom}$ of the response m_a is $m_{a,nom} = 20.11022$ [kg/s]. Consider now a perturbation $\delta T_{w,in} = (0.0000669) T_{w,in}^0$, for which the perturbed value of the inlet water temperature becomes $T_{w,in}^{pert} = T_{w,in}^0 - \delta T_{w,in} = 298.754$ [K]. Re-computing the perturbed response by solving Eqs. (2.2) - (2.15) with the value of $T_{w,in}^{pert}$ yields the “perturbed response” value $m_{a,pert} = 20.08029$ [kg/s]. Using now the nominal and perturbed response values together with the parameter perturbation in the finite-difference expression given in Eq. (3.23) yields the corresponding “finite-difference-computed sensitivity” $S_3^{FD} \triangleq \frac{m_{a,pert} - m_{a,nom}}{\delta T_{w,in}} = 1.49647$ [$\frac{kg}{s \cdot K}$]. Using this value together with the nominal values of the other quantities appearing in the expression on the right side of Eq. (D.74) yields $\left[\tau_w^{(1)} \right]^{SFD} = -8.120 \times 10^{-6}$ [$(J/kg)^{-1}$]. This result compares well with the value $\tau_w^{(1)} = -8.111 \times 10^{-6}$ [$(J/kg)^{-1}$] obtained by solving the adjoint sensitivity system given in Eq. (3.10), cf. Figure 3.5.

D.1.5.5 Verification of the adjoint function $\mu_w^{(1)}$

Note that the value of the adjoint function $\mu_w^{(1)}$ obtained by solving the adjoint sensitivity system given in Eq. (3.10) is as follows: $\mu_w^{(1)} = 19.774$ [–], respectively, as indicated in Figure 3.5. Now select a variation $\delta m_{w,in}$ in the inlet water mass flow rate $m_{w,in}$, and note that Eq. (3.22) yields the following expression for the sensitivity of the response $R = m_a$ to $m_{w,in}$:

APPENDIX D. VERIFICATION OF THE MODEL ADJOINT FUNCTIONS

$$\begin{aligned}
S_{44} &\triangleq \frac{\partial R}{\partial m_{w,in}} - \left[\sum_{i=1}^{49} \left(\mu_w^{(i)} \frac{\partial N_1^{(i)}}{\partial m_{w,in}} + \tau_w^{(i)} \frac{\partial N_2^{(i)}}{\partial m_{w,in}} + \tau_a^{(i)} \frac{\partial N_3^{(i)}}{\partial m_{w,in}} + o^{(i)} \frac{\partial N_4^{(i)}}{\partial m_{w,in}} \right) \right. \\
&\quad \left. + \mu_a \frac{\partial N_5}{\partial m_{w,in}} \right] = 0 - \left(\mu_w^{(1)} \frac{\partial N_1^{(1)}}{\partial m_{w,in}} + \tau_w^{(1)} \frac{\partial N_2^{(1)}}{\partial m_{w,in}} + \tau_a^{(1)} \frac{\partial N_3^{(1)}}{\partial m_{w,in}} + o^{(1)} \frac{\partial N_4^{(1)}}{\partial m_{w,in}} \right) \\
&= - \left[\mu_w^{(1)} \cdot (-1) + \tau_w^{(1)} \cdot (T_{w,in} a_{1f} - a_{1g} T_w^{(2)} + a_{0f} - a_{0g}) \right. \\
&\quad \left. + \tau_a^{(1)} \cdot \left(\frac{1}{m_a} \right) + o^{(1)} \cdot \left(\frac{a_{1g} T_w^{(2)} + a_{0g}}{m_a} \right) \right].
\end{aligned} \tag{D.75}$$

Since the adjoint functions $\tau_a^{(49)}$ and $o^{(49)}$ have been already verified as described in Sections D.1.5.2 and D.1.5.3, it follows that the computed values of adjoint functions $\tau_a^{(1)} = 3308.26 \text{ [kg/s]}$ and $o^{(1)} = -0.001299 \left[\left(\frac{\text{kg}}{\text{s}} \right) / \left(\frac{\text{J}}{\text{kg}} \right) \right]$ can also be considered as being accurate, since they constitute the starting point for solving the adjoint sensitivity system in Eq. (3.10); $\tau_w^{(1)}$ was proved being accurate in Section D.1.5.4. Re-writing Eq. (D.75) in the form:

$$\begin{aligned}
\mu_w^{(1)} &= S_{44} + \tau_w^{(1)} \cdot (T_{w,in} a_{1f} - a_{1g} T_w^{(2)} + a_{0f} - a_{0g}) \\
&\quad + \tau_a^{(1)} \cdot \left(\frac{1}{m_a} \right) + o^{(1)} \cdot \left(\frac{a_{1g} T_w^{(2)} + a_{0g}}{m_a} \right)
\end{aligned} \tag{D.76}$$

indicates that the value of the adjoint function $\mu_w^{(1)}$ could be computed independently if the sensitivity S_{44} were available, since all the other quantities are known. To first-order in the parameter perturbation, the finite-difference formula given in Eq. (3.23) can be used to compute the approximate sensitivity S_{44}^{FD} ; subsequently, this value can be used in conjunction with Eq. (D.76) to compute a “finite-difference sensitivity” value, denoted as $\left[\mu_w^{(1)} \right]^{SFD}$, for the respective adjoint, which would be accurate up to second-order in the respective parameter perturbation:

APPENDIX D. VERIFICATION OF THE MODEL ADJOINT FUNCTIONS

$$\begin{aligned}
 [\mu_w^{(1)}]^{SFD} = \mu_w^{(1)} = S_{44}^{FD} + \tau_w^{(1)} \cdot (T_{w,in} a_{1f} - a_{1g} T_w^{(2)} + a_{0f} - a_{0g}) \\
 + \tau_a^{(1)} \cdot \left(\frac{1}{m_a} \right) + o^{(1)} \cdot \left(\frac{a_{1g} T_w^{(2)} + a_{0g}}{m_a} \right)
 \end{aligned} \tag{D.77}$$

Numerically, the inlet water mass flow rate, $m_{w,in}$, has the nominal (“base-case”) value of $m_{w,in}^0 = 44.0213$ [kg/s]. The corresponding nominal value $m_{a,nom}$ of the response m_a is $m_{a,nom} = 20.11022$ [kg/s]. Next, consider a perturbation $\delta m_{w,in} = (0.0004839) m_{w,in}^0$, for which the perturbed value of the inlet water mass flow rate becomes $m_{w,in}^{pert} = m_{w,in}^0 - \delta m_{w,in} = 44.00$ [kg/s]. Re-computing the perturbed response by solving Eqs. (2.2) - (2.15) with the value of $m_{w,in}^{pert}$ yields the “perturbed response” value $m_{a,pert} = 20.10986$ [kg/s]. Using now the nominal and perturbed response values together with the parameter perturbation in the finite-difference expression given in Eq. (3.23) yields the corresponding “finite-difference-computed sensitivity” $S_{44}^{FD} \triangleq \frac{m_{a,pert} - m_{a,nom}}{\delta m_{w,in}} = 0.01723$ [–]. Using this value together with the nominal values of the other quantities appearing in the expression on the right side of Eq. (D.77) yields $[\mu_w^{(1)}]^{SFD} = 19.774$ [–]. This result compares well with the value $\mu_w^{(1)} = 19.774$ [–] obtained by solving the adjoint sensitivity system given in Eq. (3.10), cf. Figure 3.5.

D.2 Verification of the Model Adjoint Functions for Case 1b: Fan Off, Saturated Outlet Air Conditions, with Inlet Air Saturated

The verification procedure of the adjoint functions for case 1b is reported in this section.

D.2.1 Verification of the adjoint function μ_a for all responses

When $R = T_a^{(1)}$, the quantities $r_\ell^{(i)}$ defined in Eqs. (3.27) - (3.28) all vanish except for a single component, namely: $r_3^{(1)} \triangleq \partial R / \partial T_a^{(1)} = 1$. Thus, the adjoint functions corresponding to the outlet air temperature response $T_a^{(1)}$ are computed by solving the adjoint sensitivity system given in Eq. (3.33) using $r_3^{(1)} \triangleq \partial R / \partial T_a^{(1)} = 1$ as the only non-zero source term; for this case, the solution of Eq. (3.33) has been depicted in Figure 3.6. Note that the value of the adjoint function μ_a obtained by solving the adjoint sensitivity system given in Eq. (3.33) is $\mu_a = -0.26270 \text{ [K/(J/m}^3\text{)]}$, as indicated in Figure 3.6. Now select a variation δV_w in the wind speed V_w , and note that Eq. (3.22) yields the following expression for the sensitivity of the response $R = T_a^{(1)}$ to V_w :

$$\begin{aligned} S_5 &\triangleq \frac{\partial R}{\partial V_w} - \left[\sum_{i=1}^{49} \left(\mu_w^{(i)} \frac{\partial N_1^{(i)}}{\partial V_w} + \tau_w^{(i)} \frac{\partial N_2^{(i)}}{\partial V_w} + \tau_a^{(i)} \frac{\partial N_3^{(i)}}{\partial V_w} + o^{(i)} \frac{\partial N_4^{(i)}}{\partial V_w} \right) + \mu_a \frac{\partial N_5}{\partial V_w} \right] \\ &= 0 - \mu_a \frac{\partial N_5}{\partial V_w} = -(\mu_a) [-V_w \cdot \rho(T_{tdb}, \boldsymbol{\alpha})]. \end{aligned} \tag{D.78}$$

Re-writing Eq. (D.78) in the form

$$\mu_a = -\frac{S_5}{\partial N_5 / \partial V_w} \tag{D.79}$$

APPENDIX D. VERIFICATION OF THE MODEL ADJOINT FUNCTIONS

indicates that the value of the adjoint function μ_a could be computed independently if the sensitivity S_5 were available, since the quantity $\partial N_5 / \partial V_w = -1.6392 [J/(m^4/s)]$ is known. To first-order in the parameter perturbation, the finite-difference formula given in Eq. (3.23) can be used to compute the approximate sensitivity S_5^{FD} ; subsequently, this value can be used in conjunction with Eq. (D.79) to compute a “finite-difference sensitivity” value, denoted as $[\mu_a]^{SFD}$, for the respective adjoint, which would be accurate up to second-order in the respective parameter perturbation:

$$[\mu_a]^{SFD} = -\frac{S_5^{FD}}{\partial N_5 / \partial V_w} = -\left[\frac{T_{a,pert}^{(1)} - T_{a,nom}^{(1)}}{\delta V_w} \right] \left[\frac{\partial N_5}{\partial V_w} \right]^{-1} \quad (D.80)$$

Numerically, the wind speed V_w has the nominal (“base-case”) value of $V_w^0 = 1.377 [m/s]$. The corresponding nominal value $T_{a,nom}^{(1)}$ of the response $T_a^{(1)}$ is $T_{a,nom}^{(1)} = 299.1041 [K]$. Consider next a perturbation $\delta T_{a,in} = (0.0196) V_w^0$, for which the perturbed value of the wind speed becomes $V_w^{pert} = V_w^0 - \delta V_w = 1.35 [m/s]$. Re-computing the perturbed response by solving Eqs. (2.25) - (2.37) with the value of V_w^{pert} yields the “perturbed response” value $T_{a,pert}^{(1)} = 299.1156 [K]$. Using now the nominal and perturbed response values together with the parameter perturbation in the finite-difference expression given in Eq. (3.23) yields the corresponding “finite-difference-computed sensitivity” $S_5^{FD} \triangleq \frac{T_{a,pert}^{(1)} - T_{a,nom}^{(1)}}{\delta V_w} = -0.42620 \left[\frac{K}{m/s} \right]$. Using this value together with the nominal values of the other quantities appearing in the expression on the right side of Eq. (D.80) yields $[\mu_a]^{SFD} = -0.26000 [K/(J/m^3)]$. This result compares well with the value $\mu_a = -0.26270 [K/(J/m^3)]$ obtained by solving the adjoint sensitivity system given in Eq. (3.33), cf., Figure 3.6. The same parameter perturbation was utilized to perform the same verification procedure for the adjoint function μ_a with respect to the other four responses; Table D.1 displays the obtained results, which compare well with the values in the bar plots in Figures 3.6 - 3.10.

APPENDIX D. VERIFICATION OF THE MODEL ADJOINT FUNCTIONS

Table D.1: Verification Table for adjoint function μ_a with respect to the responses $T_a^{(1)}$, $T_w^{(50)}$, $RH^{(1)}$, $m_w^{(50)}$ and m_a .

Response of interest		\mathbf{V}_w	$\mathbf{T}_a^{(1)}$	\mathbf{S}_5^{FD}	$[\mu_a]^{(\text{SFD})}$	μ_a
		$[m/s]$	$[K]$	$[K/(m/s)]$	$[K/(J/m^3)]$	
$\mathbf{T}_a^{(1)}$	Base case	1.377	299.1041	-0.42620	-0.26000	-0.26270
	Perturbed case	1.35	299.1156			
Response of interest		\mathbf{V}_w	$\mathbf{T}_w^{(50)}$	\mathbf{S}_5^{FD}	$[\mu_a]^{(\text{SFD})}$	μ_a
		$[m/s]$	$[K]$	$[K/(m/s)]$	$[K/(J/m^3)]$	
$\mathbf{T}_w^{(50)}$	Base case	1.377	297.4568	-0.49813	-0.30388	-0.30451
	Perturbed case	1.35	297.4703			
Response of interest		\mathbf{V}_w	$\mathbf{RH}^{(1)}$	\mathbf{S}_5^{FD}	$[\mu_a]^{(\text{SFD})}$	μ_a
		$[m/s]$	$[\%]$	$[(m/s)^{-1}]$	$[(J/m^3)^{-1}]$	
$\mathbf{RH}^{(1)}$	Base case	1.377	102.3758	-0.05731	-0.03496	-0.03451
	Perturbed case	1.35	102.3774			
Response of interest		\mathbf{V}_w	$\mathbf{m}_w^{(50)}$	\mathbf{S}_5^{FD}	$[\mu_a]^{(\text{SFD})}$	μ_a
		$[m/s]$	$[kg/s]$	$[(kg/s)/(m/s)]$	$[(kg/s)/(J/m^3)]$	
$\mathbf{m}_w^{(50)}$	Base case	1.377	43.89312	-0.02723	-0.016609	-0.016642
	Perturbed case	1.35	43.89386			
Response of interest		\mathbf{V}_w	\mathbf{m}_a	\mathbf{S}_5^{FD}	$[\mu_a]^{(\text{SFD})}$	μ_a
		$[m/s]$	$[kg/s]$	$[(kg/s)/(m/s)]$	$[(kg/s)/(J/m^3)]$	
\mathbf{m}_a	Base case	1.377	20.75415	6.9984	4.2692	4.2994
	Perturbed case	1.35	20.56520			

D.2.2 Verification of the adjoint function $o^{(49)}$ for all responses

When $R = T_a^{(1)}$, the quantities $r_\ell^{(i)}$ defined in Eqs. (3.27) - (3.28) all vanish except for a single component, namely: $r_3^{(1)} \triangleq \partial R / \partial T_a^{(1)} = 1$. Thus, the ad-

APPENDIX D. VERIFICATION OF THE MODEL ADJOINT FUNCTIONS

joint functions corresponding to the outlet air temperature response $T_a^{(1)}$ are computed by solving the adjoint sensitivity system given in Eq. (3.33) using $r_3^{(1)} \triangleq \partial R / \partial T_a^{(1)} = 1$ as the only non-zero source term; for this case, the solution of Eq. (3.33) has been depicted in Figure 3.6. Note that the value of the adjoint function $o^{(49)}$ obtained by solving the adjoint sensitivity system given in Eq. (3.33) is $o^{(49)} = -6.622 \times 10^{-5} \quad [K/(J/kg)]$, as indicated in Figure 3.6. Now select a variation $\delta T_{a,in}$ in the inlet air temperature $T_{a,in}$, and note that Eq. (3.22) yields the following expression for the sensitivity of the response $R = T_a^{(1)}$ to $T_{a,in}$:

$$\begin{aligned}
 S_{45} &\triangleq \frac{\partial R}{\partial T_{a,in}} - \left[\sum_{i=1}^{49} \left(\mu_w^{(i)} \frac{\partial N_1^{(i)}}{\partial T_{a,in}} + \tau_w^{(i)} \frac{\partial N_2^{(i)}}{\partial T_{a,in}} + \tau_a^{(i)} \frac{\partial N_3^{(i)}}{\partial T_{a,in}} + o^{(i)} \frac{\partial N_4^{(i)}}{\partial T_{a,in}} \right) + \mu_a \frac{\partial N_5}{\partial T_{a,in}} \right] \\
 &= 0 - \left[o^{(49)} \frac{\partial N_4^{(49)}}{\partial T_{a,in}} + \mu_a \frac{\partial N_5}{\partial T_{a,in}} \right] = -(o^{(49)}) \left[C_p \left(\frac{T_a^{(49)} + tK}{2} \right) + \omega_{in} \alpha_{1g} \right] \\
 &\quad - (\mu_a) \cdot \left\{ \frac{R_{air}}{2 \cdot P_{atm}} \cdot |m_a| \cdot m_a \cdot \left[\left(\frac{1}{A_{out}^2} - \frac{1}{A_{in}^2} + \frac{k_{sum}}{A_{fill}^2} \right) + \frac{96f}{\text{Re}} \cdot \frac{L_{fill}}{A_{fill}^2 D_h} \right] \right. \\
 &\quad \left. + \frac{g \cdot P_{atm}}{R_{air} \cdot T_{a,in}^2} \cdot \left(Z + \frac{V_w^2}{2g} - \Delta z_{rain} - \frac{\Delta z}{2} \right) \right\}.
 \end{aligned} \tag{D.81}$$

Re-writing Eq. (D.81) in the form

$$o^{(49)} = - \frac{S_{45} + \mu_a \frac{\partial N_5}{\partial T_{a,in}}}{\frac{\partial N_4^{(49)}}{\partial T_{a,in}}} \tag{D.82}$$

indicates that the value of the adjoint function $o^{(49)}$ could be computed independently if the sensitivity S_{45} were available, since the quantities $\partial N_4^{(49)} / \partial T_{a,in} = 1.03523 \times 10^3 [J/(kg \cdot K)]$ is known. To first-order in the parameter perturbation, the finite-difference formula given in Eq. (3.23) can be used to compute the approximate sensitivity S_{45}^{FD} ; subsequently, this value can be used in conjunction with Eq. (D.82) to compute a “finite-difference sensitivity” value, denoted as $[o^{(49)}]^{SFD}$, for the respective adjoint, which would be accurate up to second-

APPENDIX D. VERIFICATION OF THE MODEL ADJOINT FUNCTIONS

order in the respective parameter perturbation:

$$[o^{(49)}]^{SFD} = -\frac{S_{45}^{FD} + \mu_a \frac{\partial N_5}{\partial T_{a,in}}}{\frac{\partial N_4^{(49)}}{\partial T_{a,in}}} = -\left[\frac{T_{a,pert}^{(1)} - T_{a,nom}^{(1)}}{\delta T_{a,in}} + \mu_a \frac{\partial N_5}{\partial T_{a,in}} \right] \left[\frac{\partial N_4^{(49)}}{\partial T_{a,in}} \right]^{-1} \quad (D.83)$$

Numerically, the inlet air temperature $T_{a,in}(= T_{db})$ has the nominal (“base-case”) value of $T_{a,in}^0 = 294.4$ [K]. The corresponding nominal value $T_{a,nom}^{(1)}$ of the response $T_a^{(1)}$ is $T_{a,nom}^{(1)} = 299.1041$ [K]. Consider next a perturbation $\delta T_{a,in} = (0.000068) T_{a,in}^0$, for which the perturbed value of the inlet air temperature becomes $T_{a,in}^{pert} = T_{a,in}^0 - \delta T_{a,in} = 294.38$ [K]. Re-computing the perturbed response by solving Eqs. (2.25) - (2.37) with the value of $T_{a,in}^{pert}$ yields the “perturbed response” value $T_{a,pert}^{(1)} = 299.1005$ [K]. Using now the nominal and perturbed response values together with the parameter perturbation in the finite-difference expression given in Eq. (3.23) yields the corresponding “finite-difference-computed sensitivity” $S_{45}^{FD} \triangleq \frac{T_{a,pert}^{(1)} - T_{a,nom}^{(1)}}{\delta T_{a,in}} = 0.17720$. Using this value together with the nominal values of the other quantities appearing in the expression on the right side of Eq. (D.83) yields $[o^{(49)}]^{SFD} = -6.529 \times 10^{-5}$ [K/(J/kg)]. This result compares well with the value $o^{(49)} = -6.622 \times 10^{-5}$ [K/(J/kg)] obtained by solving the adjoint sensitivity system given in Eq. (3.33), cf., Figure 3.6. When solving this adjoint sensitivity system, the computation of $o^{(49)}$ depends on the previously computed adjoint functions $o^{(i)}$, $i = 1, \dots, I - 1$; hence, the forgoing verification of the computational accuracy of $o^{(49)}$ also provides an indirect verification that the functions $o^{(i)}$, $i = 1, \dots, I - 1$, were also computed accurately. The same parameter perturbation was utilized to perform the same verification procedure for the adjoint function $o^{(49)}$ with respect to the other four responses; Table D.2 displays the obtained results, which compare well with the values in the bar plots in Figures 3.6 - 3.10.

APPENDIX D. VERIFICATION OF THE MODEL ADJOINT FUNCTIONS

Table D.2: Verification Table for adjoint function $o^{(49)}$ with respect to the responses $T_a^{(1)}$, $T_w^{(50)}$, $RH^{(1)}$, $m_w^{(50)}$ and m_a .

Response of interest		$\mathbf{T}_{a,in}$	$\mathbf{T}_a^{(1)}$	\mathbf{S}_{45}^{FD}	$[\mathbf{o}^{(49)}]^{(SFD)}$	$\mathbf{o}^{(49)}$
		[K]	[K]	[-]	[K/(J/kg)]	
$\mathbf{T}_a^{(1)}$	Base case	294.40	299.1041	0.17720	$-6.53 \cdot 10^{-5}$	$-6.62 \cdot 10^{-5}$
	Perturbed case	294.38	299.1005			
Response of interest		$\mathbf{T}_{a,in}$	$\mathbf{T}_w^{(50)}$	\mathbf{S}_{45}^{FD}	$[\mathbf{o}^{(49)}]^{(SFD)}$	$\mathbf{o}^{(49)}$
		[K]	[K]	[-]	[K/(J/kg)]	
$\mathbf{T}_w^{(50)}$	Base case	294.40	297.4568	0.48509	$-3.46 \cdot 10^{-4}$	$-3.52 \cdot 10^{-4}$
	Perturbed case	294.38	297.4471			
Response of interest		$\mathbf{T}_{a,in}$	$\mathbf{RH}^{(1)}$	\mathbf{S}_{45}^{FD}	$[\mathbf{o}^{(49)}]^{(SFD)}$	$\mathbf{o}^{(49)}$
		[K]	[%]	$[K^{-1}]$	$[(J/kg)^{-1}]$	
$\mathbf{RH}^{(1)}$	Base case	294.40	102.3758	-4.8756	$4.72 \cdot 10^{-3}$	$4.83 \cdot 10^{-3}$
	Perturbed case	294.38	102.4734			
Response of interest		$\mathbf{T}_{a,in}$	$\mathbf{m}_w^{(50)}$	\mathbf{S}_{45}^{FD}	$[\mathbf{o}^{(49)}]^{(SFD)}$	$\mathbf{o}^{(49)}$
		[K]	[kg/s]	$[\frac{(kg/s)}{K}]$	$[\frac{(kg/s)}{(J/kg)}]$	
$\mathbf{m}_w^{(50)}$	Base case	294.40	43.89312	0.026119	$-1.85 \cdot 10^{-5}$	$-1.90 \cdot 10^{-5}$
	Perturbed case	294.38	43.89260			
Response of interest		$\mathbf{T}_{a,in}$	\mathbf{m}_a	\mathbf{S}_{45}^{FD}	$[\mathbf{o}^{(49)}]^{(SFD)}$	$\mathbf{o}^{(49)}$
		[K]	[kg/s]	$[\frac{(kg/s)}{K}]$	$[\frac{(kg/s)}{(J/kg)}]$	
\mathbf{m}_a	Base case	294.40	20.75415	-1.5528	$-2.33 \cdot 10^{-4}$	$-2.34 \cdot 10^{-4}$
	Perturbed case	294.38	20.78521			

D.2.3 Verification of the adjoint function $\tau_a^{(49)}$ for all responses

When $R = T_a^{(1)}$, the quantities $r_\ell^{(i)}$ defined in Eqs. (3.27) - (3.28) all vanish except for a single component, namely: $r_3^{(1)} \triangleq \partial R / \partial T_a^{(1)} = 1$. Thus, the adjoint functions corresponding to the outlet air temperature response $T_a^{(1)}$ are

APPENDIX D. VERIFICATION OF THE MODEL ADJOINT FUNCTIONS

computed by solving the adjoint sensitivity system given in Eq. (3.33) using $r_3^{(1)} \triangleq \partial R / \partial T_a^{(1)} = 1$ as the only non-zero source term; for this case, the solution of Eq. (3.33) has been depicted in Figure 3.6. Note that the value of the adjoint function $\tau_a^{(49)}$ obtained by solving the adjoint sensitivity system given in Eq. (3.33) is $\tau_a^{(49)} = 170.187$ [K], as indicated in Figure 3.6. Now select a variation $\delta\omega_{in}$ in the inlet air humidity ratio ω_{in} , and note that Eq. (3.22) yields the following expression for the sensitivity of the response $R = T_a^{(1)}$ to ω_{in} :

$$\begin{aligned} S_{46} &\triangleq \frac{\partial R}{\partial \omega_{in}} - \left[\sum_{i=1}^{49} \left(\mu_w^{(i)} \frac{\partial N_1^{(i)}}{\partial \omega_{in}} + \tau_w^{(i)} \frac{\partial N_2^{(i)}}{\partial \omega_{in}} + \tau_a^{(i)} \frac{\partial N_3^{(i)}}{\partial \omega_{in}} + o^{(i)} \frac{\partial N_4^{(i)}}{\partial \omega_{in}} \right) + \mu_a \frac{\partial N_5}{\partial \omega_{in}} \right] \\ &= 0 - \left(\tau_a^{(49)} \frac{\partial N_3^{(49)}}{\partial \omega_{in}} + o^{(49)} \frac{\partial N_4^{(49)}}{\partial \omega_{in}} \right) = - \left[\tau_a^{(49)} \cdot (1) + o^{(49)} \cdot h_{g,a}^{(50)}(T_{a,in}, \boldsymbol{\alpha}) \right]. \end{aligned} \quad (\text{D.84})$$

Re-writing Eq. (D.84) in the form

$$\tau_a^{(49)} = -S_{46} - o^{(49)} \cdot h_{g,a}^{(50)}(T_{a,in}, \boldsymbol{\alpha}) \quad (\text{D.85})$$

indicates that the value of the adjoint function $\tau_a^{(49)}$ could be computed independently if the sensitivity S_{46} were available, since the $o^{(49)}$ has been verified in Section D.1.1.2 and the quantity $h_{g,a}^{(50)}(T_{a,in}, \alpha)$ is known. To first-order in the parameter perturbation, the finite-difference formula given in Eq. (3.23) can be used to compute the approximate sensitivity S_{46}^{FD} ; subsequently, this value can be used in conjunction with Eq. (D.85) to compute a “finite-difference sensitivity” value, denoted as $\left[\tau_a^{(49)} \right]^{SFD}$, for the respective adjoint, which would be accurate up to second-order in the respective parameter perturbation:

$$\left[\tau_a^{(49)} \right]^{SFD} = -S_{46}^{FD} - o^{(49)} \cdot h_{g,a}^{(50)}(T_{a,in}, \boldsymbol{\alpha}) \quad (\text{D.86})$$

APPENDIX D. VERIFICATION OF THE MODEL ADJOINT FUNCTIONS

Numerically, the inlet air humidity ratio ω_{in} has the nominal (“base-case”) value of $\omega_{in}^0 = 0.0162008658$. The corresponding nominal value $T_{a,nom}^{(1)}$ of the response $T_a^{(1)}$ is $T_{a,nom}^{(1)} = 299.10408$ [K]. Consider next a perturbation $\delta\omega_{in} = (0.001236)\omega_{in}^0$, for which the perturbed value of the inlet air humidity ratio becomes $\omega_{in}^{pert} = \omega_{in}^0 - \delta\omega_{in} = 0.016180844$. Re-computing the perturbed response by solving Eqs. (2.25) - (2.37) with the value of ω_{in}^{pert} yields the “perturbed response” value $T_{a,pert}^{(1)} = 299.10412$ [K]. Using now the nominal and perturbed response values together with the parameter perturbation in the finite-difference expression given in Eq. (3.23) yields the corresponding “finite-difference-computed sensitivity” $S_{46}^{FD} \triangleq \frac{T_{a,pert}^{(1)} - T_{a,nom}^{(1)}}{\delta\omega_{in}} = -1.9686$ [K]. Using this value together with the nominal values of the quantities appearing in the expression on the right side of Eq. (D.86) yields $[\tau_a^{(49)}]^{SFD} = 170.185$ [K]. This result compares well with the value $\tau_a^{(49)} = 170.187$ [K] obtained by solving the adjoint sensitivity system given in Eq. (3.33), cf. Figure 3.6. When solving this adjoint sensitivity system, the computation of $\tau_a^{(49)}$ depends on the previously computed adjoint functions $\tau_a^{(i)}$, $i = 1, \dots, I-1$; hence, the forgoing verification of the computational accuracy of $\tau_a^{(49)}$ also provides an indirect verification that the functions $\tau_a^{(i)}$, $i = 1, \dots, I-1$ were also computed accurately. The same parameter perturbation was utilized to perform the same verification procedure for the adjoint function $\tau_a^{(49)}$ with respect to the other four responses; Table D.3 displays the obtained results, which compare well with the values in the bar plots in Figures 3.6 - 3.10.

Table D.3: Verification Table for adjoint function $\tau_a^{(49)}$ with respect to the responses $T_a^{(1)}$, $T_w^{(50)}$, $RH^{(1)}$, $m_w^{(50)}$ and m_a .

Response of interest		ω_{in}	$T_a^{(1)}$	S_{46}^{FD}	$[\tau_a^{(49)}]^{(SFD)}$	$\tau_a^{(49)}$
		[%]	[K]	[K]	[K]	
$T_a^{(1)}$	Base case	0.01620087	299.1041	-1.9686	170.185	170.187
	Perturbed case	0.01618084	298.10412			

APPENDIX D. VERIFICATION OF THE MODEL ADJOINT FUNCTIONS

Response of interest		ω_{in}	$\mathbf{T}_w^{(50)}$	$\mathbf{S}_{46}^{\text{FD}}$	$[\tau_a^{(49)}]^{(\text{SFD})}$	$\tau_a^{(49)}$
		[%]	[K]	[K]	[K]	
$\mathbf{T}_w^{(50)}$	Base case	0.01620087	297.4568	-2.2834	895.14	895.14
	Perturbed case	0.01618084	297.4569			
Response of interest		ω_{in}	$\mathbf{RH}^{(1)}$	$\mathbf{S}_{46}^{\text{FD}}$	$[\tau_a^{(49)}]^{(\text{SFD})}$	$\tau_a^{(49)}$
		[%]	[%]	[-]	[-]	
$\mathbf{RH}^{(1)}$	Base case	0.01620087	102.3758	4585.87	-16863	-16863
	Perturbed case	0.01618084	102.2841			
Response of interest		ω_{in}	$\mathbf{m}_w^{(50)}$	$\mathbf{S}_{46}^{\text{FD}}$	$[\tau_a^{(49)}]^{(\text{SFD})}$	$\tau_a^{(49)}$
		[%]	[kg/s]	[kg/s]	[kg/s]	
$\mathbf{m}_w^{(50)}$	Base case	0.01620087	43.89312	-0.1249	48.309	48.309
	Perturbed case	0.01618084	43.89314			
Response of interest		ω_{in}	\mathbf{m}_a	$\mathbf{S}_{46}^{\text{FD}}$	$[\tau_a^{(49)}]^{(\text{SFD})}$	$\tau_a^{(49)}$
		[%]	[kg/s]	[kg/s]	[kg/s]	
\mathbf{m}_a	Base case	0.01620087	20.75415	-4.1485	599.72	599.72
	Perturbed case	0.01618084	20.75424			

D.2.4 Verification of the adjoint function $\tau_w^{(1)}$ for all responses

When $R = T_a^{(1)}$, the quantities $r_\ell^{(i)}$ defined in Eqs. (3.27) - (3.28) all vanish except for a single component, namely: $r_3^{(1)} \triangleq \partial R / \partial T_a^{(1)} = 1$. Thus, the adjoint functions corresponding to the outlet air temperature response $T_a^{(1)}$ are computed by solving the adjoint sensitivity system given in Eq. (3.33) using $r_3^{(1)} \triangleq \partial R / \partial T_a^{(1)} = 1$ as the only non-zero source term; for this case, the solution of Eq. (3.33) has been depicted in Figure 3.6. Note that the values of the adjoint function $\tau_w^{(1)}$ obtained by solving the adjoint sensitivity system given in Eq. (3.33)

APPENDIX D. VERIFICATION OF THE MODEL ADJOINT FUNCTIONS

is as follows: $\tau_w^{(1)} = -4.42 \times 10^{-6} \text{ [K/(J/s)]}$, as indicated in Figure 3.6. Now select a variation $\delta T_{w,in}$ in the inlet water temperature $T_{w,in}$, and note that Eq. (3.22) yields the following expression for the sensitivity of the response $R = T_a^{(1)}$ to $T_{w,in}$:

$$\begin{aligned} S_3 &\triangleq \frac{\partial R}{\partial T_{w,in}} - \left[\sum_{i=1}^{49} \left(\mu_w^{(i)} \frac{\partial N_1^{(i)}}{\partial T_{w,in}} + \tau_w^{(i)} \frac{\partial N_2^{(i)}}{\partial T_{w,in}} + \tau_a^{(i)} \frac{\partial N_3^{(i)}}{\partial T_{w,in}} + o^{(i)} \frac{\partial N_4^{(i)}}{\partial T_{w,in}} \right) + \mu_a \frac{\partial N_5}{\partial T_{w,in}} \right] \\ &= 0 - \tau_w^{(1)} \frac{\partial N_2^{(1)}}{\partial T_{w,in}} = 0 - \tau_w^{(1)} \cdot (m_{w,in} \cdot a_{1f}). \end{aligned} \quad (\text{D.87})$$

Re-writing Eq. (D.87) in the form

$$\tau_w^{(1)} = - \frac{S_3}{(m_{w,in} \cdot a_{1f})} \quad (\text{D.88})$$

indicates that the value of the adjoint function $\tau_w^{(1)}$ could be computed independently if the sensitivity S_3 were available, since the quantity $m_{w,in} a_{1f}$ is known. To first-order in the parameter perturbation, the finite-difference formula given in Eq. (3.23) can be used to compute the approximate sensitivity S_3^{FD} ; subsequently, this value can be used in conjunction with Eq. (D.88) to compute a “finite-difference sensitivity” value, denoted as $[\tau_w^{(1)}]^{SFD}$, for the respective adjoint, which would be accurate up to second-order in the respective parameter perturbation:

$$[\tau_w^{(1)}]^{SFD} = - \frac{S_3^{FD}}{(m_{w,in} \cdot a_{1f})} \quad (\text{D.89})$$

Numerically, the inlet water temperature, $T_{w,in}$, has the nominal (“base-case”) value of $T_{w,in}^0 = 299.543 \text{ [K]}$. As before, the corresponding nominal value $T_{a,nom}^{(1)}$ of the response $T_a^{(1)}$ is $T_{a,nom}^{(1)} = 299.1041 \text{ [K]}$. Consider now a perturbation $\delta T_{w,in} = (0.0000668) T_{w,in}^0$, for which the perturbed value of the inlet water temperature becomes $T_{w,in}^{pert} = T_{w,in}^0 - \delta T_{w,in} = 299.523 \text{ [K]}$. Re-computing the perturbed response by solving Eqs. (2.25) - (2.37) with the value of $T_{w,in}^{pert}$ yields the “perturbed response” value $T_{a,pert}^{(1)} = 299.0878 \text{ [K]}$. Using now the nominal

APPENDIX D. VERIFICATION OF THE MODEL ADJOINT FUNCTIONS

and perturbed response values together with the parameter perturbation in the finite-difference expression given in Eq. (3.23) yields the corresponding “finite-difference-computed sensitivity” $S_3^{FD} \triangleq \frac{T_{a,pert}^{(1)} - T_{a,nom}^{(1)}}{\delta T_{w,in}} = 0.81533$. Using this value together with the nominal values of the other quantities appearing in the expression on the right side of Eq. (D.89) yields $\left[\tau_w^{(1)}\right]^{SFD} = -4.42 \times 10^{-6} [K/(J/s)]$. This result compares well with the value $\tau_w^{(1)} = -4.42 \times 10^{-6} [K/(J/s)]$ obtained by solving the adjoint sensitivity system given in Eq. (3.33), cf. Figure 3.6. The same parameter perturbation was utilized to perform the same verification procedure for the adjoint function $\tau_w^{(1)}$ with respect to the other four responses; Table D.4 displays the obtained results, which compare well with the values in the bar plots in Figures 3.6 - 3.10.

Table D.4: Verification Table for adjoint function $\tau_w^{(1)}$ with respect to the responses $T_a^{(1)}$, $T_w^{(50)}$, $RH^{(1)}$, $m_w^{(50)}$ and m_a .

Response of interest		$T_{w,in}$	$T_a^{(1)}$	S_3^{FD}	$\left[\tau_w^{(1)}\right]^{(SFD)}$	$\tau_w^{(1)}$
		[K]	[K]	[-]	[K/(J/s)]	
$T_a^{(1)}$	Base case	299.543	299.1041	0.81533	$-4.42 \cdot 10^{-6}$	$-4.42 \cdot 10^{-6}$
	Perturbed case	299.523	299.0878			
Response of interest		$T_{w,in}$	$T_w^{(50)}$	S_3^{FD}	$\left[\tau_w^{(1)}\right]^{(SFD)}$	$\tau_w^{(1)}$
		[K]	[K]	[-]	[K/(J/s)]	
$T_w^{(50)}$	Base case	299.543	297.4568	0.45398	$-2.464 \cdot 10^{-6}$	$-2.462 \cdot 10^{-6}$
	Perturbed case	299.523	297.4478			
Response of interest		$T_{w,in}$	$RH^{(1)}$	S_3^{FD}	$\left[\tau_w^{(1)}\right]^{(SFD)}$	$\tau_w^{(1)}$
		[K]	[%]	$[K^{-1}]$	$[(J/s)^{-1}]$	
$RH^{(1)}$	Base case	299.543	102.3758	0.22604	$-1.227 \cdot 10^{-6}$	$-1.228 \cdot 10^{-6}$
	Perturbed case	299.523	102.3713			

APPENDIX D. VERIFICATION OF THE MODEL ADJOINT FUNCTIONS

Response of interest		$T_{w,in}$	$m_w^{(50)}$	S_3^{FD}	$[\tau_w^{(1)}]^{(SFD)}$	$\tau_w^{(1)}$
		$[K]$	$[kg/s]$	$[\frac{(kg/s)}{K}]$	$[(J/kg)^{-1}]$	
$m_w^{(50)}$	Base case	299.543	43.89312	-0.03117	$1.692 \cdot 10^{-7}$	$1.693 \cdot 10^{-7}$
	Perturbed case	299.523	43.8937			
Response of interest		$T_{w,in}$	m_a	S_3^{FD}	$[\tau_w^{(1)}]^{(SFD)}$	$\tau_w^{(1)}$
		$[K]$	$[kg/s]$	$[\frac{(kg/s)}{K}]$	$[(J/kg)^{-1}]$	
m_a	Base case	299.543	20.75415	1.41412	$-7.669 \cdot 10^{-6}$	$-7.662 \cdot 10^{-6}$
	Perturbed case	299.523	20.72589			

D.2.5 Verification of the adjoint function $\mu_w^{(1)}$ for all responses

When $R = T_a^{(1)}$, the quantities $r_\ell^{(i)}$ defined in Eqs. (3.27) - (3.28) all vanish except for a single component, namely: $r_3^{(1)} \triangleq \partial R / \partial T_a^{(1)} = 1$. Thus, the adjoint functions corresponding to the outlet air temperature response $T_a^{(1)}$ are computed by solving the adjoint sensitivity system given in Eq. (3.33) using $r_3^{(1)} \triangleq \partial R / \partial T_a^{(1)} = 1$ as the only non-zero source term; for this case, the solution of Eq. (3.33) has been depicted in Figure 3.6. Note that the values of the adjoint function $\mu_w^{(1)}$ obtained by solving the adjoint sensitivity system given in Eq. (3.33) is as follows: $\mu_w^{(1)} = 10.765 [K/(kg/s)]$, as indicated in Figure 3.6. Now select a variation $\delta m_{w,in}$ in the inlet water mass flow rate $m_{w,in}$, and note that Eq. (3.22) yields the following expression for the sensitivity of the response $R = T_a^{(1)}$ to $m_{w,in}$:

APPENDIX D. VERIFICATION OF THE MODEL ADJOINT FUNCTIONS

$$\begin{aligned}
S_{44} &\triangleq \frac{\partial R}{\partial m_{w,in}} - \left[\sum_{i=1}^{49} \left(\mu_w^{(i)} \frac{\partial N_1^{(i)}}{\partial m_{w,in}} + \tau_w^{(i)} \frac{\partial N_2^{(i)}}{\partial m_{w,in}} + \tau_a^{(i)} \frac{\partial N_3^{(i)}}{\partial m_{w,in}} + o^{(i)} \frac{\partial N_4^{(i)}}{\partial m_{w,in}} \right) \right. \\
&\quad \left. + \mu_a \frac{\partial N_5}{\partial m_{w,in}} \right] = 0 - \left(\mu_w^{(1)} \frac{\partial N_1^{(1)}}{\partial m_{w,in}} + \tau_w^{(1)} \frac{\partial N_2^{(1)}}{\partial m_{w,in}} + \tau_a^{(1)} \frac{\partial N_3^{(1)}}{\partial m_{w,in}} + o^{(1)} \frac{\partial N_4^{(1)}}{\partial m_{w,in}} \right) \\
&= - \left[\mu_w^{(1)} \cdot (-1) + \tau_w^{(1)} \cdot (T_{w,in} a_{1f} - a_{1g} T_w^{(2)} + a_{0f} - a_{0g}) \right. \\
&\quad \left. + \tau_a^{(1)} \cdot \left(\frac{1}{m_a} \right) + o^{(1)} \cdot \left(\frac{a_{1g} T_w^{(2)} + a_{0g}}{m_a} \right) \right].
\end{aligned} \tag{D.90}$$

Since the adjoint functions $\tau_a^{(49)}$ and $o^{(49)}$ have been already verified as described in Sections D.1.1.3 and D.1.1.2, it follows that the computed values of adjoint functions $\tau_a^{(1)} = 2144.188 [K]$ $o^{(1)} = -8.4127 \times 10^{-4} [K/(J/kg)]$ can also be considered as being accurate, since they constitute the starting point for solving the adjoint sensitivity system in Eq. (3.33); $\tau_w^{(1)}$ was proved being accurate in Section D.1.1.4.

Re-writing Eq. (D.90) in the form

$$\begin{aligned}
\mu_w^{(1)} &= S_{44} + \tau_w^{(1)} \cdot (T_{w,in} a_{1f} - a_{1g} T_w^{(2)} + a_{0f} - a_{0g}) \\
&\quad + \tau_a^{(1)} \cdot \left(\frac{1}{m_a} \right) + o^{(1)} \cdot \left(\frac{a_{1g} T_w^{(2)} + a_{0g}}{m_a} \right)
\end{aligned} \tag{D.91}$$

indicates that the value of the adjoint function $\mu_w^{(1)}$ could be computed independently if the sensitivity S_{44} were available, since all the other quantities are known. To first-order in the parameter perturbation, the finite-difference formula given in Eq. (3.23) can be used to compute the approximate sensitivity S_{44}^{FD} ; subsequently, this value can be used in conjunction with Eq. (D.91) to compute a “finite-difference sensitivity” value, denoted as $\left[\mu_w^{(1)} \right]^{SFD}$, for the respective adjoint, which would be accurate up to second-order in the respective parameter

APPENDIX D. VERIFICATION OF THE MODEL ADJOINT FUNCTIONS

perturbation:

$$\begin{aligned} [\mu_w^{(1)}]^{SFD} = \mu_w^{(1)} = S_{44}^{FD} + \tau_w^{(1)} \cdot (T_{w,in} a_{1f} - a_{1g} T_w^{(2)} + a_{0f} - a_{0g}) \\ + \tau_a^{(1)} \cdot \left(\frac{1}{m_a} \right) + o^{(1)} \cdot \left(\frac{a_{1g} T_w^{(2)} + a_{0g}}{m_a} \right) \end{aligned} \quad (D.92)$$

Numerically, the inlet water mass flow rate, $m_{w,in}$, has the nominal (“base-case”) value of $m_{w,in}^0 = 44.0089 [kg/s]$. As before, the corresponding nominal value $T_{a,nom}^{(1)}$ of the response $T_a^{(1)}$ is $T_{a,nom}^{(1)} = 299.1041 [K]$. Consider now a perturbation $\delta m_{w,in} = (0.002475) m_{w,in}^0$, for which the perturbed value of the inlet water mass flow rate becomes $m_{w,in}^{pert} = m_{w,in}^0 - \delta m_{w,in} = 43.90 [kg/s]$. Re-computing the perturbed response by solving Eqs. (2.25) - (2.37) with the value of $m_{w,in}^{pert}$ yields the “perturbed response” value $T_{a,pert}^{(1)} = 299.1031 [K]$. Using now the nominal and perturbed response values together with the parameter perturbation in the finite-difference expression given in Eq. (3.23) yields the corresponding “finite-difference-computed sensitivity” $S_{44}^{FD} \triangleq \frac{T_{a,pert}^{(1)} - T_{a,nom}^{(1)}}{\delta m_{w,in}} = 0.00858 \left[\frac{K}{kg/s} \right]$. Using this value together with the nominal values of the other quantities appearing in the expression on the right side of Eq. (D.92) yields $[\mu_w^{(1)}]^{SFD} = 10.765 [K/(kg/s)]$. This result compares well with the value $\mu_w^{(1)} = 10.765 [K/(kg/s)]$ obtained by solving the adjoint sensitivity system given in Eq. (3.33), cf. Figure 3.6. The same parameter perturbation was utilized to perform the same verification procedure for the adjoint function $\mu_w^{(1)}$ with respect to the other four responses; Table D.5 displays the obtained results, which compare well with the values in the bar plots in Figures 3.6 - 3.10.

APPENDIX D. VERIFICATION OF THE MODEL ADJOINT FUNCTIONS

Table D.5: Verification Table for adjoint function $\mu_w^{(1)}$ with respect to the responses $T_a^{(1)}$, $T_w^{(50)}$, $RH^{(1)}$, $m_w^{(50)}$ and m_a .

Response of interest		$\mathbf{m}_{w,in}$	$\mathbf{T}_a^{(1)}$	\mathbf{S}_{44}^{FD}	$\left[\mu_w^{(1)}\right]^{(SFD)}$	$\mu_w^{(1)}$
		$[K/s]$	$[K]$	$\left[\frac{K}{kg/s}\right]$	$\left[\frac{K}{kg/s}\right]$	
$\mathbf{T}_a^{(1)}$	Base case	44.0089	299.1041	0.00858	10.765	10.765
	Perturbed case	43.90	299.1031			
Response of interest		$\mathbf{m}_{w,in}$	$\mathbf{T}_w^{(50)}$	\mathbf{S}_{44}^{FD}	$\left[\mu_w^{(1)}\right]^{(SFD)}$	$\mu_w^{(1)}$
		$[kg/s]$	$[K]$	$\left[\frac{K}{kg/s}\right]$	$\left[\frac{K}{kg/s}\right]$	
$\mathbf{T}_w^{(50)}$	Base case	44.0089	297.4568	0.04092	6.04792	6.04784
	Perturbed case	43.90	297.4524			
Response of interest		$\mathbf{m}_{w,in}$	$\mathbf{RH}^{(1)}$	\mathbf{S}_{44}^{FD}	$\left[\mu_w^{(1)}\right]^{(SFD)}$	$\mu_w^{(1)}$
		$[kg/s]$	$[\%]$	$\left[(kg/s)^{-1}\right]$	$\left[(kg/s)^{-1}\right]$	
$\mathbf{RH}^{(1)}$	Base case	44.0089	102.3758	0.01034	-215.61	-215.61
	Perturbed case	43.90	102.3747			
Response of interest		$\mathbf{m}_{w,in}$	$\mathbf{m}_w^{(50)}$	\mathbf{S}_{44}^{FD}	$\left[\mu_w^{(1)}\right]^{(SFD)}$	$\mu_w^{(1)}$
		$[kg/s]$	$[kg/s]$	$[-]$	$[-]$	
$\mathbf{m}_w^{(50)}$	Base case	44.0089	43.89312	0.99961	0.58679	0.58679
	Perturbed case	43.90	43.8937			
Response of interest		$\mathbf{m}_{w,in}$	\mathbf{m}_a	\mathbf{S}_{44}^{FD}	$\left[\mu_w^{(1)}\right]^{(SFD)}$	$\mu_w^{(1)}$
		$[kg/s]$	$[kg/s]$	$[-]$	$[-]$	
\mathbf{m}_a	Base case	44.0089	20.75415	0.01931	18.6601	18.6600
	Perturbed case	43.90	20.75205			

D.3 Verification of the Model Adjoint Functions for Case 2: Fan Off, Unsaturated Air Conditions

The verification procedure of the adjoint functions for case 2 is reported in this section.

D.3.1 Verification of the adjoint function μ_a for all responses

When $R = T_a^{(1)}$, the quantities $r_\ell^{(i)}$ defined in Eqs. (3.42) - (3.43) all vanish except for a single component, namely: $r_3^{(1)} \triangleq \partial R / \partial T_a^{(1)} = 1$. Thus, the adjoint functions corresponding to the outlet air temperature response $T_a^{(1)}$ are computed by solving the adjoint sensitivity system given in Eq. (3.40) using $r_3^{(1)} \triangleq \partial R / \partial T_a^{(1)} = 1$ as the only non-zero source term; for this case, the solution of Eq. (3.40) has been depicted in Figure 3.11. Note that the value of the adjoint function μ_a obtained by solving the adjoint sensitivity system given in Eq. (3.40) is $\mu_a = -0.12651 \quad [K/(J/m^3)]$, as indicated in Figure 3.11. Now select a variation δV_w in the wind speed V_w , and note that Eq. (3.22) yields the following expression for the sensitivity of the response $R = T_a^{(1)}$ to V_w :

$$\begin{aligned} S_5 &\triangleq \frac{\partial R}{\partial V_w} - \left[\sum_{i=1}^{49} \left(\mu_w^{(i)} \frac{\partial N_1^{(i)}}{\partial V_w} + \tau_w^{(i)} \frac{\partial N_2^{(i)}}{\partial V_w} + \tau_a^{(i)} \frac{\partial N_3^{(i)}}{\partial V_w} + o^{(i)} \frac{\partial N_4^{(i)}}{\partial V_w} \right) + \mu_a \frac{\partial N_5}{\partial V_w} \right] \\ &= 0 - \mu_a \frac{\partial N_5}{\partial V_w} = -(\mu_a) [-V_w \cdot \rho(T_{tdb}, \boldsymbol{\alpha})]. \end{aligned} \tag{D.93}$$

Re-writing Eq. (D.93) in the form

$$\mu_a = -\frac{S_5}{\partial N_5 / \partial V_w} \tag{D.94}$$

APPENDIX D. VERIFICATION OF THE MODEL ADJOINT FUNCTIONS

indicates that the value of the adjoint function μ_a could be computed independently if the sensitivity S_5 were available, since the quantity $\partial N_5 / \partial V_w = -2.1795 [J/(m^4/s)]$ is known. To first-order in the parameter perturbation, the finite-difference formula given in Eq. (3.23) can be used to compute the approximate sensitivity S_5^{FD} ; subsequently, this value can be used in conjunction with Eq. (D.94) to compute a “finite-difference sensitivity” value, denoted as $[\mu_a]^{SFD}$, for the respective adjoint, which would be accurate up to second-order in the respective parameter perturbation:

$$[\mu_a]^{SFD} = -\frac{S_5^{FD}}{\partial N_5 / \partial V_w} = -\left[\frac{T_{a,pert}^{(1)} - T_{a,nom}^{(1)}}{\delta V_w} \right] \left[\frac{\partial N_5}{\partial V_w} \right]^{-1} \quad (D.95)$$

Numerically, the wind speed V_w has the nominal (“base-case”) value of $V_w^0 = 1.859 [m/s]$. The corresponding nominal value $T_{a,nom}^{(1)}$ of the response $T_a^{(1)}$ is $T_{a,nom}^{(1)} = 298.7979 [K]$. Consider next a perturbation $\delta T_{a,in} = (0.01) V_w^0$, for which the perturbed value of the wind speed becomes $V_w^{pert} = V_w^0 - \delta V_w = 1.84041 [m/s]$. Re-computing the perturbed response by solving Eqs. (2.38) - (2.50) with the value of V_w^{pert} yields the “perturbed response” value $T_{a,pert}^{(1)} = 298.8029 [K]$. Using now the nominal and perturbed response values together with the parameter perturbation in the finite-difference expression given in Eq. (3.23) yields the corresponding “finite-difference-computed sensitivity” $S_5^{FD} \triangleq \frac{T_{a,pert}^{(1)} - T_{a,nom}^{(1)}}{\delta V_w} = -0.27219 \left[\frac{K}{m/s} \right]$. Using this value together with the nominal values of the other quantities appearing in the expression on the right side of Eq. (D.95) yields $[\mu_a]^{SFD} = -0.12489 [K/(J/m^3)]$. This result compares well with the value $\mu_a = -0.12651 [K/(J/m^3)]$ obtained by solving the adjoint sensitivity system given in Eq. (3.40), cf., Figure 3.11. The same parameter perturbation was utilized to perform the same verification procedure for the adjoint function μ_a with respect to the other four responses; Table D.6 displays the obtained results, which compare well with the values in the bar plots in Figures 3.11 - 3.15.

APPENDIX D. VERIFICATION OF THE MODEL ADJOINT FUNCTIONS

Table D.6: Verification Table for adjoint function μ_a with respect to the responses $T_a^{(1)}$, $T_w^{(50)}$, $RH^{(1)}$, $m_w^{(50)}$ and m_a .

Response of interest			$\mathbf{T}_a^{(1)}$	\mathbf{S}_5^{FD}	$[\mu_a]^{(\text{SFD})}$	μ_a
			$[m/s]$	$[K]$	$[K/(m/s)]$	$[K/(J/m^3)]$
$\mathbf{T}_a^{(1)}$	Base case	1.859	298.7979	-0.27219	-0.12489	-0.12651
	Perturbed case	1.84041	298.8029			
Response of interest			$\mathbf{T}_w^{(50)}$	\mathbf{S}_5^{FD}	$[\mu_a]^{(\text{SFD})}$	μ_a
			$[m/s]$	$[K]$	$[K/(m/s)]$	$[K/(J/m^3)]$
$\mathbf{T}_w^{(50)}$	Base case	1.859	297.4225	-0.95514	-0.43824	-0.43692
	Perturbed case	1.84041	297.4402			
Response of interest			$\mathbf{RH}^{(1)}$	\mathbf{S}_5^{FD}	$[\mu_a]^{(\text{SFD})}$	μ_a
			$[m/s]$	$[\%]$	$[(m/s)^{-1}]$	$[(J/m^3)^{-1}]$
$\mathbf{RH}^{(1)}$	Base case	1.859	99.79724	-0.71122	-0.32632	-0.33332
	Perturbed case	1.84041	99.81046			
Response of interest			$\mathbf{m}_w^{(50)}$	\mathbf{S}_5^{FD}	$[\mu_a]^{(\text{SFD})}$	μ_a
			$[m/s]$	$[kg/s]$	$\left[\frac{(kg/s)}{(m/s)}\right]$	$\left[\frac{(kg/s)}{(J/m^3)}\right]$
$\mathbf{m}_w^{(50)}$	Base case	1.859	43.90797	-0.073996	-0.033951	-0.033873
	Perturbed case	1.84041	43.90934			
Response of interest			\mathbf{m}_a	\mathbf{S}_5^{FD}	$[\mu_a]^{(\text{SFD})}$	μ_a
			$[m/s]$	$[kg/s]$	$\left[\frac{(kg/s)}{(m/s)}\right]$	$\left[\frac{(kg/s)}{(J/m^3)}\right]$
\mathbf{m}_a	Base case	1.859	15.83980	11.63149	5.33677	5.34064
	Perturbed case	1.84041	15.62357			

D.3.2 Verification of the adjoint function $o^{(49)}$ for all responses

When $R = T_a^{(1)}$, the quantities $r_\ell^{(i)}$ defined in Eqs. (3.42) - (3.43) all vanish except for a single component, namely: $r_3^{(1)} \triangleq \partial R / \partial T_a^{(1)} = 1$. Thus, the ad-

APPENDIX D. VERIFICATION OF THE MODEL ADJOINT FUNCTIONS

joint functions corresponding to the outlet air temperature response $T_a^{(1)}$ are computed by solving the adjoint sensitivity system given in Eq. (3.40) using $r_3^{(1)} \triangleq \partial R / \partial T_a^{(1)} = 1$ as the only non-zero source term; for this case, the solution of Eq. (3.40) has been depicted in Figure 3.11. Note that the value of the adjoint function $o^{(49)}$ obtained by solving the adjoint sensitivity system given in Eq. (3.40) is $o^{(49)} = -1.313 \times 10^{-5} \quad [K/(J/kg)]$, as indicated in Figure 3.11. Now select a variation $\delta T_{a,in}$ in the inlet air temperature $T_{a,in}$, and note that Eq. (3.22) yields the following expression for the sensitivity of the response $R = T_a^{(1)}$ to $T_{a,in}$:

$$\begin{aligned}
 S_{45} &\triangleq \frac{\partial R}{\partial T_{a,in}} - \left[\sum_{i=1}^{49} \left(\mu_w^{(i)} \frac{\partial N_1^{(i)}}{\partial T_{a,in}} + \tau_w^{(i)} \frac{\partial N_2^{(i)}}{\partial T_{a,in}} + \tau_a^{(i)} \frac{\partial N_3^{(i)}}{\partial T_{a,in}} + o^{(i)} \frac{\partial N_4^{(i)}}{\partial T_{a,in}} \right) + \mu_a \frac{\partial N_5}{\partial T_{a,in}} \right] \\
 &= 0 - \left[o^{(49)} \frac{\partial N_4^{(49)}}{\partial T_{a,in}} + \mu_a \frac{\partial N_5}{\partial T_{a,in}} \right] = -(o^{(49)}) \left[C_p \left(\frac{T_a^{(49)} + tK}{2} \right) + \omega_{in} \alpha_{1g} \right] \\
 &\quad - (\mu_a) \cdot \left\{ \frac{R_{air}}{2 \cdot P_{atm}} \cdot |m_a| \cdot m_a \cdot \left[\left(\frac{1}{A_{out}^2} - \frac{1}{A_{in}^2} + \frac{k_{sum}}{A_{fill}^2} \right) + \frac{96f}{\text{Re}} \cdot \frac{L_{fill}}{A_{fill}^2 D_h} \right] \right. \\
 &\quad \left. + \frac{g \cdot P_{atm}}{R_{air} \cdot T_{a,in}^2} \cdot \left(Z + \frac{V_w^2}{2g} - \Delta z_{rain} - \frac{\Delta z}{2} \right) \right\}.
 \end{aligned} \tag{D.96}$$

Re-writing Eq. (D.96) in the form

$$o^{(49)} = - \frac{S_{45} + \mu_a \frac{\partial N_5}{\partial T_{a,in}}}{\frac{\partial N_4^{(49)}}{\partial T_{a,in}}} \tag{D.97}$$

indicates that the value of the adjoint function $o^{(49)}$ could be computed independently if the sensitivity S_{45} were available, since the quantities $\partial N_4^{(49)} / \partial T_{a,in} = 1.0309 \times 10^3 [J/(kg \cdot K)]$ and $\partial N_5 / \partial T_{a,in} = 0.40491 [J/(m^3 \cdot K)]$ are known. To first-order in the parameter perturbation, the finite-difference formula given in Eq. (3.23) can be used to compute the approximate sensitivity S_{45}^{FD} ; subsequently, this value can be used in conjunction with Eq. (D.97) to compute a “finite-difference

APPENDIX D. VERIFICATION OF THE MODEL ADJOINT FUNCTIONS

sensitivity” value, denoted as $[o^{(49)}]^{SFD}$, for the respective adjoint, which would be accurate up to second-order in the respective parameter perturbation:

$$[o^{(49)}]^{SFD} = -\frac{S_{45}^{FD} + \mu_a \frac{\partial N_5}{\partial T_{a,in}}}{\frac{\partial N_4^{(49)}}{\partial T_{a,in}}} = -\left[\frac{T_{a,pert}^{(1)} - T_{a,nom}^{(1)}}{\delta T_{a,in}} + \mu_a \frac{\partial N_5}{\partial T_{a,in}} \right] \left[\frac{\partial N_4^{(49)}}{\partial T_{a,in}} \right]^{-1} \quad (D.98)$$

Numerically, the inlet air temperature $T_{a,in}(=T_{db})$ has the nominal (“base-case”) value of $T_{a,in}^0 = 298.882$ [K]. The corresponding nominal value $T_{a,nom}^{(1)}$ of the response $T_a^{(1)}$ is $T_{a,nom}^{(1)} = 298.7979$ [K]. Consider next a perturbation $\delta T_{a,in} = (0.0001) T_{a,in}^0$, for which the perturbed value of the inlet air temperature becomes $T_{a,in}^{pert} = T_{a,in}^0 - \delta T_{a,in} = 298.852$ [K]. Re-computing the perturbed response by solving Eqs. (2.38) - (2.50) with the value of $T_{a,in}^{pert}$ yields the “perturbed response” value $T_{a,pert}^{(1)} = 298.7960$ [K]. Using now the nominal and perturbed response values together with the parameter perturbation in the finite-difference expression given in Eq. (3.23) yields the corresponding “finite-difference-computed sensitivity” $S_{45}^{FD} \triangleq \frac{T_{a,pert}^{(1)} - T_{a,nom}^{(1)}}{\delta T_{a,in}} = 0.06555$. Using this value together with the nominal values of the other quantities appearing in the expression on the right side of Eq. (D.98) yields $[o^{(49)}]^{SFD} = -1.391 \times 10^{-5}$ [K/(J/kg)]. This result compares well with the value $o^{(49)} = -1.313 \times 10^{-5}$ [K/(J/kg)] obtained by solving the adjoint sensitivity system given in Eq. (3.40), cf., Figure 3.11. When solving this adjoint sensitivity system, the computation of $o^{(49)}$ depends on the previously computed adjoint functions $o^{(i)}$, $i = 1, \dots, I - 1$; hence, the forgoing verification of the computational accuracy of $o^{(49)}$ also provides an indirect verification that the functions $o^{(i)}$, $i = 1, \dots, I - 1$, were also computed accurately. The same parameter perturbation was utilized to perform the same verification procedure for the adjoint function $o^{(49)}$ with respect to the other four responses; Table D.7 displays the obtained results, which compare well with the values in the bar plots in Figures 3.11 - 3.15.

APPENDIX D. VERIFICATION OF THE MODEL ADJOINT FUNCTIONS

Table D.7: Verification Table for adjoint function $o^{(49)}$ with respect to the responses $T_a^{(1)}$, $T_w^{(50)}$, $RH^{(1)}$, $m_w^{(50)}$ and m_a .

Response of interest		$\mathbf{T}_{a,in}$	$\mathbf{T}_a^{(1)}$	\mathbf{S}_{45}^{FD}	$[\mathbf{o}^{(49)}]^{(SFD)}$	$\mathbf{o}^{(49)}$
		[K]	[K]	[-]	[K/(J/kg)]	
$\mathbf{T}_a^{(1)}$	Base case	298.882	298.7979	0.06555	$-1.39 \cdot 10^{-5}$	$-1.31 \cdot 10^{-5}$
	Perturbed case	298.852	298.7960			
Response of interest		$\mathbf{T}_{a,in}$	$\mathbf{T}_w^{(50)}$	\mathbf{S}_{45}^{FD}	$[\mathbf{o}^{(49)}]^{(SFD)}$	$\mathbf{o}^{(49)}$
		[K]	[K]	[-]	[K/(J/kg)]	
$\mathbf{T}_w^{(50)}$	Base case	298.882	297.4225	0.25125	$-7.21 \cdot 10^{-5}$	$-7.28 \cdot 10^{-5}$
	Perturbed case	298.852	297.4149			
Response of interest		$\mathbf{T}_{a,in}$	$\mathbf{RH}^{(1)}$	\mathbf{S}_{45}^{FD}	$[\mathbf{o}^{(49)}]^{(SFD)}$	$\mathbf{o}^{(49)}$
		[K]	[%]	$[K^{-1}]$	$[(J/kg)^{-1}]$	
$\mathbf{RH}^{(1)}$	Base case	298.882	99.79724	0.09039	$4.32 \cdot 10^{-5}$	$5.02 \cdot 10^{-5}$
	Perturbed case	298.852	99.79453			
Response of interest		$\mathbf{T}_{a,in}$	$\mathbf{m}_w^{(50)}$	\mathbf{S}_{45}^{FD}	$[\mathbf{o}^{(49)}]^{(SFD)}$	$\mathbf{o}^{(49)}$
		[K]	[kg/s]	$\left[\frac{(kg/s)}{K}\right]$	$\left[\frac{(kg/s)}{(J/kg)}\right]$	
$\mathbf{m}_w^{(50)}$	Base case	298.882	43.90797	0.012694	$9.91 \cdot 10^{-7}$	$9.18 \cdot 10^{-7}$
	Perturbed case	298.852	43.90758			
Response of interest		$\mathbf{T}_{a,in}$	\mathbf{m}_a	\mathbf{S}_{45}^{FD}	$[\mathbf{o}^{(49)}]^{(SFD)}$	$\mathbf{o}^{(49)}$
		[K]	[kg/s]	$\left[\frac{(kg/s)}{K}\right]$	$\left[\frac{(kg/s)}{(J/kg)}\right]$	
\mathbf{m}_a	Base case	298.882	15.83890	-2.03711	$-1.22 \cdot 10^{-4}$	$-1.18 \cdot 10^{-4}$
	Perturbed case	298.852	15.90091			

D.3.3 Verification of the adjoint function $\tau_a^{(49)}$ for all responses

When $R = T_a^{(1)}$, the quantities $r_\ell^{(i)}$ defined in Eqs. (3.42) - (3.43) all vanish except for a single component, namely: $r_3^{(1)} \triangleq \partial R / \partial T_a^{(1)} = 1$. Thus, the adjoint functions corresponding to the outlet air temperature response $T_a^{(1)}$ are

APPENDIX D. VERIFICATION OF THE MODEL ADJOINT FUNCTIONS

computed by solving the adjoint sensitivity system given in Eq. (3.40) using $r_3^{(1)} \triangleq \partial R / \partial T_a^{(1)} = 1$ as the only non-zero source term; for this case, the solution of Eq. (3.40) has been depicted in Figure 3.11. Note that the value of the adjoint function $\tau_a^{(49)}$ obtained by solving the adjoint sensitivity system given in Eq. (3.40) is $\tau_a^{(49)} = 21.555$ [K], as indicated in Figure 3.11. Now select a variation $\delta\omega_{in}$ in the inlet air humidity ratio ω_{in} , and note that Eq. (3.22) yields the following expression for the sensitivity of the response $R = T_a^{(1)}$ to ω_{in} :

$$\begin{aligned} S_{46} &\triangleq \frac{\partial R}{\partial \omega_{in}} - \left[\sum_{i=1}^{49} \left(\mu_w^{(i)} \frac{\partial N_1^{(i)}}{\partial \omega_{in}} + \tau_w^{(i)} \frac{\partial N_2^{(i)}}{\partial \omega_{in}} + \tau_a^{(i)} \frac{\partial N_3^{(i)}}{\partial \omega_{in}} + o^{(i)} \frac{\partial N_4^{(i)}}{\partial \omega_{in}} \right) + \mu_a \frac{\partial N_5}{\partial \omega_{in}} \right] \\ &= 0 - \left(\tau_a^{(49)} \frac{\partial N_3^{(49)}}{\partial \omega_{in}} + o^{(49)} \frac{\partial N_4^{(49)}}{\partial \omega_{in}} \right) = - \left[\tau_a^{(49)} \cdot (1) + o^{(49)} \cdot h_{g,a}^{(50)}(T_{a,in}, \boldsymbol{\alpha}) \right]. \end{aligned} \quad (\text{D.99})$$

Re-writing Eq. (D.99) in the form

$$\tau_a^{(49)} = -S_{46} - o^{(49)} \cdot h_{g,a}^{(50)}(T_{a,in}, \boldsymbol{\alpha}) \quad (\text{D.100})$$

indicates that the value of the adjoint function $\tau_a^{(49)}$ could be computed independently if the sensitivity S_{46} were available, since the $o^{(49)}$ has been verified in (the previous) Section D.1.1.2 and the quantity $h_{g,a}^{(50)}(T_{a,in}, \alpha)$ is known. To first-order in the parameter perturbation, the finite-difference formula given in Eq. (3.23) can be used to compute the approximate sensitivity S_{46}^{FD} ; subsequently, this value can be used in conjunction with Eq. (D.100) to compute a “finite-difference sensitivity” value, denoted as $[\tau_a^{(49)}]^{SFD}$, for the respective adjoint, which would be accurate up to second-order in the respective parameter perturbation:

$$[\tau_a^{(49)}]^{SFD} = -S_{46}^{FD} - o^{(49)} \cdot h_{g,a}^{(50)}(T_{a,in}, \boldsymbol{\alpha}) \quad (\text{D.101})$$

Numerically, the inlet air humidity ratio ω_{in} has the nominal (“base-case”) value of $\omega_{in}^0 = 0.0137976$. The corresponding nominal value $T_{a,nom}^{(1)}$ of the response

APPENDIX D. VERIFICATION OF THE MODEL ADJOINT FUNCTIONS

$T_a^{(1)}$ is $T_{a,nom}^{(1)} = 298.7979$ [K]. Consider next a perturbation $\delta\omega_{in} = (0.00125)\omega_{in}^0$, for which the perturbed value of the inlet air humidity ratio becomes $\omega_{in}^{pert} = \omega_{in}^0 - \delta\omega_{in} = 0.0137803$. Re-computing the perturbed response by solving Eqs. (2.38) - (2.50) with the value of ω_{in}^{pert} yields the “perturbed response” value $T_{a,pert}^{(1)} = 298.7977$ [K]. Using now the nominal and perturbed response values together with the parameter perturbation in the finite-difference expression given in Eq. (3.23) yields the corresponding “finite-difference-computed sensitivity” $S_{46}^{FD} \triangleq \frac{T_{a,pert}^{(1)} - T_{a,nom}^{(1)}}{\delta\omega_{in}} = 11.878$ [K]. Using this value together with the nominal values of the other quantities appearing in the expression on the right side of Eq. (D.101) yields $\left[\tau_a^{(49)}\right]^{SFD} = 21.5697$ [K]. This result compares well with the value $\tau_a^{(49)} = 21.555$ [K] obtained by solving the adjoint sensitivity system given in Eq. (3.40), cf. Figure 3.11. When solving this adjoint sensitivity system, the computation of $\tau_a^{(49)}$ depends on the previously computed adjoint functions $\tau_a^{(i)}$, $i = 1, \dots, I - 1$; hence, the forgoing verification of the computational accuracy of $\tau_a^{(49)}$ also provides an indirect verification that the functions $\tau_a^{(i)}$, $i = 1, \dots, I - 1$ were also computed accurately. The same parameter perturbation was utilized to perform the same verification procedure for the adjoint function $\tau_a^{(49)}$ with respect to the other four responses; Table D.8 displays the obtained results, which compare well with the values in the bar plots in Figures 3.11 - 3.15.

Table D.8: Verification Table for adjoint function $\tau_a^{(49)}$ with respect to the responses $T_a^{(1)}$, $T_w^{(50)}$, $RH^{(1)}$, $m_w^{(50)}$ and m_a .

Response of interest		ω_{in}	$T_a^{(1)}$	S_{46}^{FD}	$\left[\tau_a^{(49)}\right]^{(SFD)}$	$\tau_a^{(49)}$
		[%]	[K]	[K]	[K]	
$T_a^{(1)}$	Base case	0.0137976	298.7979	11.878	21.569	21.555
	Perturbed case	0.0137803	298.7977			

APPENDIX D. VERIFICATION OF THE MODEL ADJOINT FUNCTIONS

Response of interest		ω_{in}	$\mathbf{T}_w^{(50)}$	$\mathbf{S}_{46}^{\text{FD}}$	$[\tau_a^{(49)}]^{(\text{SFD})}$	$\tau_a^{(49)}$
		[%]	[K]	[K]	[K]	
$\mathbf{T}_w^{(50)}$	Base case	0.0137976	297.4225	201.180	-15.593	-15.799
	Perturbed case	0.0137803	297.4190			
Response of interest		ω_{in}	$\mathbf{RH}^{(1)}$	$\mathbf{S}_{46}^{\text{FD}}$	$[\tau_a^{(49)}]^{(\text{SFD})}$	$\tau_a^{(49)}$
		[%]	[%]	[-]	[-]	
$\mathbf{RH}^{(1)}$	Base case	0.0137976	99.79724	24.4676	-152.46	-152.50
	Perturbed case	0.0137803	99.79681			
Response of interest		ω_{in}	$\mathbf{m}_w^{(50)}$	$\mathbf{S}_{46}^{\text{FD}}$	$[\tau_a^{(49)}]^{(\text{SFD})}$	$\tau_a^{(49)}$
		[%]	[kg/s]	[kg/s]	[kg/s]	
$\mathbf{m}_w^{(50)}$	Base case	0.0137976	43.90797	15.1936	-17.533	-17.549
	Perturbed case	0.0137803	43.90770			
Response of interest		ω_{in}	\mathbf{m}_a	$\mathbf{S}_{46}^{\text{FD}}$	$[\tau_a^{(49)}]^{(\text{SFD})}$	$\tau_a^{(49)}$
		[%]	[kg/s]	[kg/s]	[kg/s]	
\mathbf{m}_a	Base case	0.0137976	15.83890	43.92139	256.109	256.059
	Perturbed case	0.0137803	15.83903			

D.3.4 Verification of the adjoint function $\tau_w^{(1)}$ for all responses

When $R = T_a^{(1)}$, the quantities $r_\ell^{(i)}$ defined in Eqs. (3.42) - (3.43) all vanish except for a single component, namely: $r_3^{(1)} \triangleq \partial R / \partial T_a^{(1)} = 1$. Thus, the adjoint functions corresponding to the outlet air temperature response $T_a^{(1)}$ are computed by solving the adjoint sensitivity system given in Eq. (3.40) using $r_3^{(1)} \triangleq \partial R / \partial T_a^{(1)} = 1$ as the only non-zero source term; for this case, the solution of Eq. (3.40) has been depicted in Figure 3.11. Note that the values of the adjoint function $\tau_w^{(1)}$ obtained by solving the adjoint sensitivity system given in Eq. (3.40)

APPENDIX D. VERIFICATION OF THE MODEL ADJOINT FUNCTIONS

is as follows: $\tau_w^{(1)} = -4.98 \times 10^{-6} \text{ [K/(J/s)]}$, as indicated in Figure 3.11. Now select a variation $\delta T_{w,in}$ in the inlet water temperature $T_{w,in}$, and note that Eq. (3.22) yields the following expression for the sensitivity of the response $R = T_a^{(1)}$ to $T_{w,in}$:

$$\begin{aligned} S_3 &\triangleq \frac{\partial R}{\partial T_{w,in}} - \left[\sum_{i=1}^{49} \left(\mu_w^{(i)} \frac{\partial N_1^{(i)}}{\partial T_{w,in}} + \tau_w^{(i)} \frac{\partial N_2^{(i)}}{\partial T_{w,in}} + \tau_a^{(i)} \frac{\partial N_3^{(i)}}{\partial T_{w,in}} + o^{(i)} \frac{\partial N_4^{(i)}}{\partial T_{w,in}} \right) + \mu_a \frac{\partial N_5}{\partial T_{w,in}} \right] \\ &= 0 - \tau_w^{(1)} \frac{\partial N_2^{(1)}}{\partial T_{w,in}} = 0 - \tau_w^{(1)} \cdot (m_{w,in} \cdot a_{1f}). \end{aligned} \quad (\text{D.102})$$

Re-writing Eq. (D.102) in the form

$$\tau_w^{(1)} = - \frac{S_3}{(m_{w,in} \cdot a_{1f})} \quad (\text{D.103})$$

indicates that the value of the adjoint function $\tau_w^{(1)}$ could be computed independently if the sensitivity S_3 were available, since the quantity $m_{w,in} a_{1f}$ is known. To first-order in the parameter perturbation, the finite-difference formula given in Eq. (3.23) can be used to compute the approximate sensitivity S_3^{FD} ; subsequently, this value can be used in conjunction with Eq. (D.103) to compute a “finite-difference sensitivity” value, denoted as $[\tau_w^{(1)}]^{SFD}$, for the respective adjoint, which would be accurate up to second-order in the respective parameter perturbation:

$$[\tau_w^{(1)}]^{SFD} = - \frac{S_3^{FD}}{(m_{w,in} \cdot a_{1f})} \quad (\text{D.104})$$

Numerically, the inlet water temperature, $T_{w,in}$, has the nominal (“base-case”) value of $T_{w,in}^0 = 298.893 \text{ [K]}$. As before, the corresponding nominal value $T_{a,nom}^{(1)}$ of the response $T_a^{(1)}$ is $T_{a,nom}^{(1)} = 298.7979 \text{ [K]}$. Consider now a perturbation $\delta T_{w,in} = (0.000067) T_{w,in}^0$, for which the perturbed value of the inlet water temperature becomes $T_{w,in}^{pert} = T_{w,in}^0 - \delta T_{w,in} = 298.873 \text{ [K]}$. Re-computing the perturbed response by solving Eqs. (2.38) - (2.50) with the value of $T_{w,in}^{pert}$ yields

APPENDIX D. VERIFICATION OF THE MODEL ADJOINT FUNCTIONS

the “perturbed response” value $T_{a,pert}^{(1)} = 298.7795$ [K]. Using now the nominal and perturbed response values together with the parameter perturbation in the finite-difference expression given in Eq. (3.23) yields the corresponding “finite-difference-computed sensitivity” $S_3^{FD} \triangleq \frac{T_{a,pert}^{(1)} - T_{a,nom}^{(1)}}{\delta T_{w,in}} = 0.91889$. Using this value together with the nominal values of the other quantities appearing in the expression on the right side of Eq. (D.104) yields $\left[\tau_w^{(1)}\right]^{SFD} = -4.99 \times 10^{-6}$ [K/(J/s)]. This result compares well with the value $\tau_w^{(1)} = -4.98 \times 10^{-6}$ [K/(J/s)] obtained by solving the adjoint sensitivity system given in Eq. (3.40), cf. Figure 3.11. The same parameter perturbation was utilized to perform the same verification procedure for the adjoint function $\tau_w^{(1)}$ with respect to the other four responses; Table D.9 displays the obtained results, which compare well with the values in the bar plots in Figures 3.11 - 3.15.

Table D.9: Verification Table for adjoint function $\tau_w^{(1)}$ with respect to the responses $T_a^{(1)}$, $T_w^{(50)}$, $RH^{(1)}$, $m_w^{(50)}$ and m_a .

Response of interest		$T_{w,in}$	$T_a^{(1)}$	S_3^{FD}	$\left[\tau_w^{(1)}\right]^{(SFD)}$	$\tau_w^{(1)}$
		[K]	[K]	[-]	[K/(J/s)]	
$T_a^{(1)}$	Base case	298.893	298.7979	0.91889	$-4.99 \cdot 10^{-6}$	$-4.98 \cdot 10^{-6}$
	Perturbed case	298.873	298.7795			
Response of interest		$T_{w,in}$	$T_w^{(50)}$	S_3^{FD}	$\left[\tau_w^{(1)}\right]^{(SFD)}$	$\tau_w^{(1)}$
		[K]	[K]	[-]	[K/(J/s)]	
$T_w^{(50)}$	Base case	298.893	297.4225	0.50358	$-2.73 \cdot 10^{-6}$	$-2.73 \cdot 10^{-6}$
	Perturbed case	298.873	297.4124			
Response of interest		$T_{w,in}$	$RH^{(1)}$	S_3^{FD}	$\left[\tau_w^{(1)}\right]^{(SFD)}$	$\tau_w^{(1)}$
		[K]	[%]	$[K^{-1}]$	$[(J/s)^{-1}]$	
$RH^{(1)}$	Base case	298.893	99.79724	-0.10693	$5.77 \cdot 10^{-7}$	$5.78 \cdot 10^{-7}$
	Perturbed case	298.873	99.7994			

APPENDIX D. VERIFICATION OF THE MODEL ADJOINT FUNCTIONS

Response of interest		$T_{w,in}$	$m_w^{(50)}$	S_3^{FD}	$[\tau_w^{(1)}]^{(SFD)}$	$\tau_w^{(1)}$
		[K]	[kg/s]	$\left[\frac{(kg/s)}{K}\right]$	$\left[(J/kg)^{-1}\right]$	
$m_w^{(50)}$	Base case	298.893	43.90797	-0.031364	$1.70 \cdot 10^{-7}$	$1.70 \cdot 10^{-7}$
	Perturbed case	298.873	43.90859			
Response of interest		$T_{w,in}$	m_a	S_3^{FD}	$[\tau_w^{(1)}]^{(SFD)}$	$\tau_w^{(1)}$
		[K]	[kg/s]	$\left[\frac{(kg/s)}{K}\right]$	$\left[(J/kg)^{-1}\right]$	
m_a	Base case	298.893	15.83980	1.91042	$-1.037 \cdot 10^{-5}$	$-1.035 \cdot 10^{-5}$
	Perturbed case	298.873	15.80159			

D.3.5 Verification of the adjoint function $\mu_w^{(1)}$ for all responses

When $R = T_a^{(1)}$, the quantities $r_\ell^{(i)}$ defined in Eqs. (3.42) - (3.43) all vanish except for a single component, namely: $r_3^{(1)} \triangleq \partial R / \partial T_a^{(1)} = 1$. Thus, the adjoint functions corresponding to the outlet air temperature response $T_a^{(1)}$ are computed by solving the adjoint sensitivity system given in Eq. (3.40) using $r_3^{(1)} \triangleq \partial R / \partial T_a^{(1)} = 1$ as the only non-zero source term; for this case, the solution of Eq. (3.40) has been depicted in Figure 3.11. Note that the values of the adjoint function $\mu_w^{(1)}$ obtained by solving the adjoint sensitivity system given in Eq. (3.40) is as follows: $\mu_w^{(1)} = 10.30109 \text{ [K/(kg/s)]}$, as indicated in Figure 3.11. Now select a variation $\delta m_{w,in}$ in the inlet water mass flow rate $m_{w,in}$, and note that Eq. (3.22) yields the following expression for the sensitivity of the response $R = T_a^{(1)}$ to $m_{w,in}$:

APPENDIX D. VERIFICATION OF THE MODEL ADJOINT FUNCTIONS

$$\begin{aligned}
S_{44} &\triangleq \frac{\partial R}{\partial m_{w,in}} - \left[\sum_{i=1}^{49} \left(\mu_w^{(i)} \frac{\partial N_1^{(i)}}{\partial m_{w,in}} + \tau_w^{(i)} \frac{\partial N_2^{(i)}}{\partial m_{w,in}} + \tau_a^{(i)} \frac{\partial N_3^{(i)}}{\partial m_{w,in}} + o^{(i)} \frac{\partial N_4^{(i)}}{\partial m_{w,in}} \right) \right. \\
&\quad \left. + \mu_a \frac{\partial N_5}{\partial m_{w,in}} \right] = 0 - \left(\mu_w^{(1)} \frac{\partial N_1^{(1)}}{\partial m_{w,in}} + \tau_w^{(1)} \frac{\partial N_2^{(1)}}{\partial m_{w,in}} + \tau_a^{(1)} \frac{\partial N_3^{(1)}}{\partial m_{w,in}} + o^{(1)} \frac{\partial N_4^{(1)}}{\partial m_{w,in}} \right) \\
&= - \left[\mu_w^{(1)} \cdot (-1) + \tau_w^{(1)} \cdot (T_{w,in} a_{1f} - a_{1g} T_w^{(2)} + a_{0f} - a_{0g}) \right. \\
&\quad \left. + \tau_a^{(1)} \cdot \left(\frac{1}{m_a} \right) + o^{(1)} \cdot \left(\frac{a_{1g} T_w^{(2)} + a_{0g}}{m_a} \right) \right].
\end{aligned} \tag{D.105}$$

Since the adjoint functions $\tau_a^{(49)}$ and $o^{(49)}$ have been already verified as described in Sections D.1.1.3 and D.1.1.2, it follows that the computed values of adjoint functions $\tau_a^{(1)} = 2128.24 [K]$ $o^{(1)} = -8.4254 \times 10^{-4} [K/(J/kg)]$ can also be considered as being accurate, since they constitute the starting point for solving the adjoint sensitivity system in Eq. (3.40); $\tau_w^{(1)}$ was proved being accurate in Section D.1.1.4. Re-writing Eq. (D.105) in the form

$$\begin{aligned}
\mu_w^{(1)} &= S_{44} + \tau_w^{(1)} \cdot (T_{w,in} a_{1f} - a_{1g} T_w^{(2)} + a_{0f} - a_{0g}) \\
&\quad + \tau_a^{(1)} \cdot \left(\frac{1}{m_a} \right) + o^{(1)} \cdot \left(\frac{a_{1g} T_w^{(2)} + a_{0g}}{m_a} \right)
\end{aligned} \tag{D.106}$$

indicates that the value of the adjoint function $\mu_w^{(1)}$ could be computed independently if the sensitivity S_{44} were available, since all the other quantities are known. To first-order in the parameter perturbation, the finite-difference formula given in Eq. (3.23) can be used to compute the approximate sensitivity S_{44}^{FD} ; subsequently, this value can be used in conjunction with Eq. (D.106) to compute a “finite-difference sensitivity” value, denoted as $\left[\mu_w^{(1)} \right]^{SFD}$, for the respective adjoint, which would be accurate up to second-order in the respective parameter

APPENDIX D. VERIFICATION OF THE MODEL ADJOINT FUNCTIONS

perturbation:

$$\begin{aligned} [\mu_w^{(1)}]^{SFD} = \mu_w^{(1)} = S_{44}^{FD} + \tau_w^{(1)} \cdot (T_{w,in} a_{1f} - a_{1g} T_w^{(2)} + a_{0f} - a_{0g}) \\ + \tau_a^{(1)} \cdot \left(\frac{1}{m_a} \right) + o^{(1)} \cdot \left(\frac{a_{1g} T_w^{(2)} + a_{0g}}{m_a} \right) \end{aligned} \quad (D.107)$$

Numerically, the inlet water mass flow rate, $m_{w,in}$, has the nominal (“base-case”) value of $m_{w,in}^0 = 44.0193 [kg/s]$. As before, the corresponding nominal value $T_{a,nom}^{(1)}$ of the response $T_a^{(1)}$ is $T_{a,nom}^{(1)} = 298.7979 [K]$. Consider now a perturbation $\delta m_{w,in} = (0.00068) m_{w,in}^0$, for which the perturbed value of the inlet water mass flow rate becomes $m_{w,in}^{pert} = m_{w,in}^0 - \delta m_{w,in} = 43.9893 [kg/s]$. Re-computing the perturbed response by solving Eqs. (2.38) - (2.50) with the value of $m_{w,in}^{pert}$ yields the “perturbed response” value $T_{a,pert}^{(1)} = 298.7978 [K]$. Using now the nominal and perturbed response values together with the parameter perturbation in the finite-difference expression given in Eq. (3.23) yields the corresponding “finite-difference-computed sensitivity” $S_{44}^{FD} \triangleq \frac{T_{a,pert}^{(1)} - T_{a,nom}^{(1)}}{\delta m_{w,in}} = 0.00328 \left[\frac{K}{kg/s} \right]$. Using this value together with the nominal values of the other quantities appearing in the expression on the right side of Eq. (D.107) yields $[\mu_w^{(1)}]^{SFD} = 10.9768 [K/(kg/s)]$. This result compares well with the value $\mu_w^{(1)} = 10.30109 [K/(kg/s)]$ obtained by solving Eq. (3.40), cf. Figure 3.11. The same parameter perturbation was utilized to perform the same verification procedure for the adjoint function $\mu_w^{(1)}$ with respect to the other four responses; Table D.10 displays the obtained results, which compare well with the values in the bar plots in Figures 3.11 - 3.15.

Table D.10: Verification Table for adjoint function $\mu_w^{(1)}$ with respect to the responses $T_a^{(1)}$, $T_w^{(50)}$, $RH^{(1)}$, $m_w^{(50)}$ and m_a .

Response of interest		$m_{w,in}$	$T_a^{(1)}$	S_{44}^{FD}	$[\mu_w^{(1)}]^{(SFD)}$	$\mu_w^{(1)}$
		$[K/s]$	$[K]$	$\left[\frac{K}{kg/s} \right]$	$\left[\frac{K}{kg/s} \right]$	
$T_a^{(1)}$	Base case	44.0193	298.7979	0.00328	10.977	10.301
	Perturbed case	43.9893	298.7978			

APPENDIX D. VERIFICATION OF THE MODEL ADJOINT FUNCTIONS

Response of interest			$\mathbf{T}_w^{(50)}$	$\mathbf{S}_{44}^{\text{FD}}$	$\left[\mu_w^{(1)}\right]^{(\text{SFD})}$	$\mu_w^{(1)}$
	$\mathbf{m}_{w,\text{in}}$					
			$[kg/s]$	$[K]$	$\left[\frac{K}{kg/s}\right]$	$\left[\frac{K}{kg/s}\right]$
$\mathbf{T}_w^{(50)}$	Base case	44.0193	297.4225	0.03142	6.0444	6.0443
	Perturbed case	43.9893	297.4215			
Response of interest	$\mathbf{m}_{w,\text{in}}$		$\mathbf{RH}^{(1)}$	$\mathbf{S}_{44}^{\text{FD}}$	$\left[\mu_w^{(1)}\right]^{(\text{SFD})}$	$\mu_w^{(1)}$
			$[kg/s]$	$[\%]$	$\left[(kg/s)^{-1}\right]$	$\left[(kg/s)^{-1}\right]$
$\mathbf{RH}^{(1)}$	Base case	44.0193	99.79724	-0.001267	-265.511	-265.511
	Perturbed case	43.9893	99.79728			
Response of interest	$\mathbf{m}_{w,\text{in}}$		$\mathbf{m}_w^{(50)}$	$\mathbf{S}_{44}^{\text{FD}}$	$\left[\mu_w^{(1)}\right]^{(\text{SFD})}$	$\mu_w^{(1)}$
			$[kg/s]$	$[kg/s]$	$[-]$	$[-]$
$\mathbf{m}_w^{(50)}$	Base case	44.0193	43.90797	0.99986	0.52753	0.52753
	Perturbed case	43.9893	43.87797			
Response of interest	$\mathbf{m}_{w,\text{in}}$		\mathbf{m}_a	$\mathbf{S}_{44}^{\text{FD}}$	$\left[\mu_w^{(1)}\right]^{(\text{SFD})}$	$\mu_w^{(1)}$
			$[kg/s]$	$[kg/s]$	$[-]$	$[-]$
\mathbf{m}_a	Base case	44.0193	15.38980	0.010543	22.807	22.807
	Perturbed case	43.9893	15.83948			

Appendix E

Derivatives of the Model Equations with respect to the Model Parameters

E.1 Derivatives of the Model Equations with respect to the Model Parameters for Case 1a: Fan Off, Saturated Outlet Air Conditions, with Inlet Air Unsaturated

The verification procedure of the adjoint functions for case 1a is reported in this section.

The following notation will be used for the derivatives of the above equations with respect to the parameters:

$$a_{\ell}^{i,j} \equiv \frac{\partial N_{\ell}^{(i)}}{\partial \alpha^{(j)}}; \ell = 1, 2, 3, 4, 5; i = 1, \dots, I; j = 1, \dots, N_{\alpha}. \quad (\text{E.1})$$

APPENDIX E. DERIVATIVES OF THE MODEL EQUATIONS WITH
RESPECT TO THE MODEL PARAMETERS

**E.1.1 Derivatives of the liquid continuity equations with
respect to the parameters**

The derivatives of the “liquid continuity equations” [cf. Eqs. (2.2) - (2.5)] with respect to the parameter $\alpha^{(1)} : T_{db}$ are as follows:

$$\begin{aligned} \frac{\partial N_1^{(i)}}{\partial \alpha^{(1)}} = \frac{\partial N_1^{(i)}}{\partial T_{db}} \equiv a_1^{i,1} = \frac{1}{\bar{R}} \left[\frac{P_{vs}^{(i+1)}(T_w^{(i+1)}, \boldsymbol{\alpha})}{T_w^{(i+1)}} - \frac{P_{vs}^{(i)}(T_a^{(i)}, \boldsymbol{\alpha})}{T_a^{(i)}} \right] \\ \cdot \frac{\partial M(m_a, \boldsymbol{\alpha})}{\partial D_{av}(T_{db}, \boldsymbol{\alpha})} \cdot \frac{\partial D_{av}(T_{db}, \boldsymbol{\alpha})}{\partial T_{db}}; \quad \ell = 1; \quad i = 1, \dots, K; \quad j = 1, \end{aligned} \quad (\text{E.2})$$

where K is the control volume at which its outlet air is saturated, and

$$\frac{\partial M(m_a, \boldsymbol{\alpha})}{\partial D_{av}(T_{db}, \boldsymbol{\alpha})} = \frac{2}{3} \cdot \frac{M(m_a, \boldsymbol{\alpha})}{D_{av}(T_{db}, \boldsymbol{\alpha})} \quad (\text{E.3})$$

$$\frac{\partial D_{av}(T_{db}, \boldsymbol{\alpha})}{\partial T_{db}} = \frac{1.5 \cdot a_{0,D_{av}} T_{db}^{0.5} - D_{av}(T_{db}, \boldsymbol{\alpha}) \cdot (a_{2,D_{av}} + 2 \cdot a_{3,D_{av}} T_{db})}{a_{1,D_{av}} + a_{2,D_{av}} T_{db} + a_{3,D_{av}} T_{db}^2} \quad (\text{E.4})$$

$$\begin{aligned} \frac{\partial N_1^{(i)}}{\partial \alpha^{(1)}} = \frac{\partial N_1^{(i)}}{\partial T_{db}} \equiv a_1^{i,1} = \frac{1}{\bar{R}} \left[\frac{P_{vs}^{(i+1)}(T_w^{(i+1)}, \boldsymbol{\alpha})}{T_w^{(i+1)}} - \frac{\omega^{(i)} P_{atm}}{(0.622 + \omega^{(i)}) T_a^{(i)}} \right] \\ \cdot \frac{\partial M(m_a, \boldsymbol{\alpha})}{\partial D_{av}(T_{db}, \boldsymbol{\alpha})} \cdot \frac{\partial D_{av}(T_{db}, \boldsymbol{\alpha})}{\partial T_{db}}. \quad \ell = 1; \quad i = K + 1, \dots, I; \quad j = 1, \end{aligned} \quad (\text{E.5})$$

The derivatives of the “liquid continuity equations” [cf. Eqs. (2.2) - (2.5)] with respect to the parameter $\alpha^{(2)} : T_{dp}$ are as follows:

$$\frac{\partial N_1^{(i)}}{\partial \alpha^{(2)}} = \frac{\partial N_1^{(i)}}{\partial T_{dp}} \equiv a_1^{i,2} = 0; \quad \ell = 1; \quad i = 1, \dots, I; \quad j = 2. \quad (\text{E.6})$$

The derivatives of the “liquid continuity equations” [cf. Eqs. (2.2) - (2.5)] with respect to the parameter $\alpha^{(3)} : T_{w,in}$ are as follows:

$$\frac{\partial N_1^{(1)}}{\partial \alpha^{(3)}} = \frac{\partial N_1^{(1)}}{\partial T_{w,in}} \equiv a_1^{1,3} = 0; \quad \ell = 1; \quad i = 1, \dots, I; \quad j = 3. \quad (\text{E.7})$$

APPENDIX E. DERIVATIVES OF THE MODEL EQUATIONS WITH RESPECT TO THE MODEL PARAMETERS

The derivatives of the “liquid continuity equations” [cf. Eqs. (2.2) - (2.5)] with respect to the parameter $\alpha^{(4)} : P_{atm}$ are as follows:

$$\frac{\partial N_1^{(i)}}{\partial \alpha^{(4)}} = \frac{\partial N_1^{(i)}}{\partial P_{atm}} \equiv a_1^{i,4} = 0; \quad \ell = 1; \quad i = 1, \dots, K; \quad j = 4, \quad (\text{E.8})$$

$$\frac{\partial N_1^{(i)}}{\partial \alpha^{(4)}} = \frac{\partial N_1^{(i)}}{\partial P_{atm}} \equiv a_1^{i,4} = -\frac{M(m_a, \boldsymbol{\alpha})}{\bar{R}} \frac{\omega^{(i)}}{T_a^{(i)}(0.622 + \omega^{(i)})}; \quad (\text{E.9})$$

$$\ell = 1; \quad i = K + 1, \dots, I; \quad j = 4.$$

The derivatives of the “liquid continuity equations” [cf. Eqs. (2.2) - (2.5)] with respect to the parameter $\alpha^{(5)} : V_w$ are as follows:

$$\frac{\partial N_1^{(i)}}{\partial \alpha^{(5)}} = \frac{\partial N_1^{(i)}}{\partial V_w} \equiv a_1^{i,5} = 0; \quad \ell = 1; \quad i = 1, \dots, I; \quad j = 5, \quad (\text{E.10})$$

The derivatives of the “liquid continuity equations” [cf. Eqs. (2.2) - (2.5)] with respect to the parameter $\alpha^{(6)} : k_{sum}$ are as follows:

$$\frac{\partial N_1^{(i)}}{\partial \alpha^{(6)}} = \frac{\partial N_1^{(i)}}{\partial k_{sum}} \equiv a_1^{i,6} = 0; \quad \ell = 1; \quad i = 1, \dots, I; \quad j = 6. \quad (\text{E.11})$$

The derivatives of the “liquid continuity equations” [cf. Eqs. (2.2) - (2.5)] with respect to the parameter $\alpha^{(7)} : \mu$ are as follows:

$$\frac{\partial N_1^{(i)}}{\partial \alpha^{(7)}} = \frac{\partial N_1^{(i)}}{\partial \mu} \equiv a_1^{i,7} = \frac{1}{\bar{R}} \left[\frac{P_{vs}^{(i+1)}(T_w^{(i+1)}, \boldsymbol{\alpha})}{T_w^{(i+1)}} - \frac{P_{vs}^{(i)}(T_a^{(i)}, \boldsymbol{\alpha})}{T_a^{(i)}} \right] \frac{\partial M(m_a, \boldsymbol{\alpha})}{\partial \mu};$$

$$\ell = 1; \quad i = 1, \dots, K; \quad j = 7, \quad (\text{E.12})$$

where

$$\frac{\partial M(m_a, \boldsymbol{\alpha})}{\partial \mu} = \begin{cases} 0 & \text{Re}_d < 2300 \\ -\frac{a_{1,Nu} \cdot M(m_a, \boldsymbol{\alpha}) \cdot \text{Re}(m_a, \boldsymbol{\alpha})}{Nu(\text{Re}, \boldsymbol{\alpha}) \cdot \mu} & 2300 \leq \text{Re}_d \leq 10000 \\ -0.8 \cdot \frac{M(m_a, \boldsymbol{\alpha})}{\mu} & \text{Re}_d > 10000 \end{cases} \quad (\text{E.13})$$

APPENDIX E. DERIVATIVES OF THE MODEL EQUATIONS WITH RESPECT TO THE MODEL PARAMETERS

$$\frac{\partial N_1^{(i)}}{\partial \alpha^{(7)}} = \frac{\partial N_1^{(i)}}{\partial \mu} \equiv a_1^{i,7} = \frac{1}{R} \left[\frac{P_{vs}^{(i+1)}(T_w^{(i+1)}, \boldsymbol{\alpha})}{T_w^{(i+1)}} - \frac{\omega^{(i)} P_{atm}}{(0.622 + \omega^{(i)}) T_a^{(i)}} \right] \frac{\partial M(m_a, \boldsymbol{\alpha})}{\partial \mu};$$

$$\ell = K + 1; \quad i = 1, \dots, I; \quad j = 7.$$
(E.14)

The derivatives of the “liquid continuity equations” [cf. Eqs. (2.2) - (2.5)] with respect to the parameter $\alpha^{(8)} : \nu$ are as follows:

$$\frac{\partial N_1^{(i)}}{\partial \alpha^{(8)}} = \frac{\partial N_1^{(i)}}{\partial \nu} \equiv a_1^{i,8} = \frac{1}{R} \left[\frac{P_{vs}^{(i+1)}(T_w^{(i+1)}, \boldsymbol{\alpha})}{T_w^{(i+1)}} - \frac{P_{vs}^{(i)}(T_a^{(i)}, \boldsymbol{\alpha})}{T_a^{(i)}} \right] \frac{\partial M(m_a, \boldsymbol{\alpha})}{\partial \nu};$$

$$\ell = 1; \quad i = 1, \dots, K; \quad j = 8,$$
(E.15)

where

$$\frac{\partial M(m_a, \boldsymbol{\alpha})}{\partial \nu} = \frac{1}{3} \frac{M(m_a, \boldsymbol{\alpha})}{\nu}$$

$$\frac{\partial N_1^{(i)}}{\partial \alpha^{(8)}} = \frac{\partial N_1^{(i)}}{\partial \nu} \equiv a_1^{i,8} = \frac{1}{R} \left[\frac{P_{vs}^{(i+1)}(T_w^{(i+1)}, \boldsymbol{\alpha})}{T_w^{(i+1)}} - \frac{\omega^{(i)} P_{atm}}{(0.622 + \omega^{(i)}) T_a^{(i)}} \right] \frac{\partial M(m_a, \boldsymbol{\alpha})}{\partial \nu};$$

$$\ell = 1; \quad i = K + 1, \dots, I; \quad j = 8.$$
(E.17)

The derivatives of the “liquid continuity equations” [cf. Eqs. (2.2) - (2.5)] with respect to the parameter $\alpha^{(9)} : k_{air}$ are as follows:

$$\frac{\partial N_1^{(i)}}{\partial \alpha^{(9)}} = \frac{\partial N_1^{(i)}}{\partial k_{air}} \equiv a_1^{i,9} = 0; \quad \ell = 1; \quad i = 1, \dots, I; \quad j = 9.$$
(E.18)

The derivatives of the “liquid continuity equations” [cf. Eqs. (2.2) - (2.5)] with respect to the parameter $\alpha^{(10)} : f_{ht}$ are as follows:

$$\frac{\partial N_1^{(i)}}{\partial \alpha^{(10)}} = \frac{\partial N_1^{(i)}}{\partial f_{ht}} \equiv a_1^{i,10} = 0; \quad \ell = 1; \quad i = 1, \dots, I; \quad j = 10.$$
(E.19)

The derivatives of the “liquid continuity equations” [cf. Eqs. (2.2) - (2.5)] with respect to the parameter $\alpha^{(11)} : f_{mt}$ are as follows:

APPENDIX E. DERIVATIVES OF THE MODEL EQUATIONS WITH RESPECT TO THE MODEL PARAMETERS

$$\frac{\partial N_1^{(i)}}{\partial \alpha^{(11)}} = \frac{\partial N_1^{(i)}}{\partial f_{mt}} \equiv a_1^{i,11} = \frac{1}{\bar{R}} \left[\frac{P_{vs}^{(i+1)}(T_w^{(i+1)}, \boldsymbol{\alpha})}{T_w^{(i+1)}} - \frac{P_{vs}^{(i)}(T_a^{(i)}, \boldsymbol{\alpha})}{T_a^{(i)}} \right] \frac{\partial M(m_a, \boldsymbol{\alpha})}{\partial f_{mt}};$$

$$\ell = 1; \quad i = 1, \dots, I; \quad j = 11,$$
(E.20)

where

$$\frac{\partial M(m_a, \boldsymbol{\alpha})}{\partial f_{mt}} = \frac{M_{H_2O} \text{Nu}(\text{Re}, \boldsymbol{\alpha}) \left(\frac{\nu}{\text{Pr}}\right)^{1/3} [D_{av}(T_{db}, \boldsymbol{\alpha})]^{2/3} w_{tsa} A_{surf}}{D_h I}$$
(E.21)

$$\frac{\partial N_1^{(i)}}{\partial \alpha^{(11)}} = \frac{\partial N_1^{(i)}}{\partial f_{mt}} \equiv a_1^{i,11} = \frac{1}{\bar{R}} \left[\frac{P_{vs}^{(i+1)}(T_w^{(i+1)}, \boldsymbol{\alpha})}{T_w^{(i+1)}} - \frac{\omega^{(i)} P_{atm}}{(0.622 + \omega^{(i)}) T_a^{(i)}} \right] \frac{\partial M(m_a, \boldsymbol{\alpha})}{\partial f_{mt}};$$

$$\ell = 1; \quad i = K + 1, \dots, I; \quad j = 11.$$
(E.22)

The derivatives of the “liquid continuity equations” [cf. Eqs. (2.2) - (2.5)] with respect to the parameter $\alpha^{(12)} : f$ are as follows:

$$\frac{\partial N_1^{(i)}}{\partial \alpha^{(12)}} = \frac{\partial N_1^{(i)}}{\partial f} \equiv a_1^{i,12} = 0; \quad \ell = 1; \quad i = 1, \dots, I; \quad j = 12.$$
(E.23)

The derivatives of the “liquid continuity equations” [cf. Eqs. (2.2) - (2.5)] with respect to the parameter $\alpha^{(13)} : a_0$ are as follows:

$$\frac{\partial N_1^{(i)}}{\partial \alpha^{(13)}} = \frac{\partial N_1^{(i)}}{\partial a_0} \equiv a_1^{i,13} = \frac{M(m_a, \boldsymbol{\alpha})}{\bar{R}} \left[\frac{P_{vs}^{(i+1)}(T_w^{(i+1)}, \boldsymbol{\alpha})}{T_w^{(i+1)}} - \frac{P_{vs}^{(i)}(T_a^{(i)}, \boldsymbol{\alpha})}{T_a^{(i)}} \right];$$

$$\ell = 1; \quad i = 1, \dots, K; \quad j = 13,$$
(E.24)

$$\frac{\partial N_1^{(i)}}{\partial \alpha^{(13)}} = \frac{\partial N_1^{(i)}}{\partial a_0} \equiv a_1^{i,13} = \frac{M(m_a, \boldsymbol{\alpha})}{\bar{R}} \frac{1}{T_w^{(i+1)}} \frac{\partial P_{vs}^{(i+1)}(T_w^{(i+1)}, \boldsymbol{\alpha})}{\partial a_0};$$
(E.25)

$$\ell = 1; \quad i = K + 1, \dots, I; \quad j = 13.$$

where

$$\frac{\partial P_{vs}^{(i+1)}(T_w^{(i+1)}, \boldsymbol{\alpha})}{\partial a_0} = P_{vs}^{(i+1)}(T_w^{(i+1)}, \boldsymbol{\alpha})$$
(E.26)

APPENDIX E. DERIVATIVES OF THE MODEL EQUATIONS WITH RESPECT TO THE MODEL PARAMETERS

The derivatives of the “liquid continuity equations” [cf. Eqs. (2.2) - (2.5)] with respect to the parameter $\alpha^{(14)} : a_1$ are as follows:

$$\frac{\partial N_1^{(i)}}{\partial \alpha^{(14)}} = \frac{\partial N_1^{(i)}}{\partial a_1} \equiv a_1^{i,14} = \frac{M(m_a, \boldsymbol{\alpha})}{\bar{R}} \left[\frac{P_{vs}^{(i+1)}(T_w^{(i+1)}, \boldsymbol{\alpha})}{(T_w^{(i+1)})^2} - \frac{P_{vs}^{(i)}(T_a^{(i)}, \boldsymbol{\alpha})}{(T_a^{(i)})^2} \right];$$

$$\ell = 1; \quad i = 1, \dots, K; \quad j = 14, \tag{E.27}$$

$$\frac{\partial N_1^{(i)}}{\partial \alpha^{(14)}} = \frac{\partial N_1^{(i)}}{\partial a_1} \equiv a_1^{i,14} = \frac{M(m_a, \boldsymbol{\alpha})}{\bar{R}} \frac{1}{T_w^{(i+1)}} \frac{\partial P_{vs}^{(i+1)}(T_w^{(i+1)}, \boldsymbol{\alpha})}{\partial a_1};$$

$$\ell = 1; \quad i = K + 1, \dots, I; \quad j = 14. \tag{E.28}$$

where

$$\frac{\partial P_{vs}^{(i+1)}(T_w^{(i+1)}, \boldsymbol{\alpha})}{\partial a_1} = \frac{P_{vs}^{(i+1)}(T_w^{(i+1)}, \boldsymbol{\alpha})}{T_w^{(i+1)}} \tag{E.29}$$

The derivatives of the “liquid continuity equations” [cf. Eqs. (2.2) - (2.5)] with respect to the parameter $\alpha^{(15)} : a_{0, c_{pa}}$ are as follows:

$$\frac{\partial N_1^{(i)}}{\partial \alpha^{(15)}} = \frac{\partial N_1^{(i)}}{\partial a_{0, c_{pa}}} \equiv a_1^{i,15} = 0; \quad \ell = 1; \quad i = 1, \dots, I; \quad j = 15. \tag{E.30}$$

The derivatives of the “liquid continuity equations” [cf. Eqs. (2.2) - (2.5)] with respect to the parameter $\alpha^{(16)} : a_{1, c_{pa}}$ are as follows:

$$\frac{\partial N_1^{(i)}}{\partial \alpha^{(16)}} = \frac{\partial N_1^{(i)}}{\partial a_{1, c_{pa}}} \equiv a_1^{i,16} = 0; \quad \ell = 1; \quad i = 1, \dots, I; \quad j = 16. \tag{E.31}$$

The derivatives of the “liquid continuity equations” [cf. Eqs. (2.2) - (2.5)] with respect to the parameter $\alpha^{(17)} : a_{2, c_{pa}}$ are as follows:

$$\frac{\partial N_1^{(i)}}{\partial \alpha^{(17)}} = \frac{\partial N_1^{(i)}}{\partial a_{2, c_{pa}}} \equiv a_1^{i,17} = 0; \quad \ell = 1; \quad i = 1, \dots, I; \quad j = 17. \tag{E.32}$$

APPENDIX E. DERIVATIVES OF THE MODEL EQUATIONS WITH RESPECT TO THE MODEL PARAMETERS

The derivatives of the “liquid continuity equations” [cf. Eqs. (2.2) - (2.5)] with respect to the parameter $\alpha^{(18)} : a_{0,D_{av}}$ are as follows:

$$\begin{aligned} \frac{\partial N_1^{(i)}}{\partial \alpha^{(18)}} = \frac{\partial N_1^{(i)}}{\partial a_{0,D_{av}}} \equiv a_1^{i,18} = \frac{1}{\bar{R}} \left[\frac{P_{vs}^{(i+1)}(T_w^{(i+1)}, \boldsymbol{\alpha})}{T_w^{(i+1)}} - \frac{P_{vs}^{(i)}(T_a^{(i)}, \boldsymbol{\alpha})}{T_a^{(i)}} \right] \\ \cdot \frac{\partial M(m_a, \boldsymbol{\alpha})}{\partial D_{av}(T_{db}, \boldsymbol{\alpha})} \cdot \frac{\partial D_{av}(T_{db}, \boldsymbol{\alpha})}{\partial a_{0,D_{av}}}; \quad \ell = 1; \quad i = 1, \dots, K; \quad j = 18, \end{aligned} \quad (\text{E.33})$$

where $\frac{\partial M(m_a, \boldsymbol{\alpha})}{\partial D_{av}(T_{db}, \boldsymbol{\alpha})}$ was defined previously in Eq. (E.3), and

$$\frac{\partial D_{av}(T_{db}, \boldsymbol{\alpha})}{\partial a_{0,D_{av}}} = \frac{T_{db}^{1.5}}{a_{1,D_{av}} + a_{2,D_{av}} T_{db} + a_{3,D_{av}} T_{db}^2} \quad (\text{E.34})$$

$$\begin{aligned} \frac{\partial N_1^{(i)}}{\partial \alpha^{(18)}} = \frac{\partial N_1^{(i)}}{\partial a_{0,D_{av}}} \equiv a_1^{i,18} = \frac{1}{\bar{R}} \left[\frac{P_{vs}^{(i+1)}(T_w^{(i+1)}, \boldsymbol{\alpha})}{T_w^{(i+1)}} - \frac{\omega^{(i)} P_{atm}}{(0.622 + \omega^{(i)}) T_a^{(i)}} \right] \\ \cdot \frac{\partial M(m_a, \boldsymbol{\alpha})}{\partial D_{av}(T_{db}, \boldsymbol{\alpha})} \cdot \frac{\partial D_{av}(T_{db}, \boldsymbol{\alpha})}{\partial a_{0,D_{av}}}; \quad \ell = 1; \quad i = K + 1, \dots, I; \quad j = 18. \end{aligned} \quad (\text{E.35})$$

The derivatives of the “liquid continuity equations” [cf. Eqs. (2.2) - (2.5)] with respect to the parameter $\alpha^{(19)} : a_{1,D_{av}}$ are as follows:

$$\begin{aligned} \frac{\partial N_1^{(i)}}{\partial \alpha^{(19)}} = \frac{\partial N_1^{(i)}}{\partial a_{1,D_{av}}} \equiv a_1^{i,19} = \frac{1}{\bar{R}} \left[\frac{P_{vs}^{(i+1)}(T_w^{(i+1)}, \boldsymbol{\alpha})}{T_w^{(i+1)}} - \frac{P_{vs}^{(i)}(T_a^{(i)}, \boldsymbol{\alpha})}{T_a^{(i)}} \right] \\ \cdot \frac{\partial M(m_a, \boldsymbol{\alpha})}{\partial D_{av}(T_{db}, \boldsymbol{\alpha})} \cdot \frac{\partial D_{av}(T_{db}, \boldsymbol{\alpha})}{\partial a_{1,D_{av}}}; \quad \ell = 1; \quad i = 1, \dots, K; \quad j = 19, \end{aligned} \quad (\text{E.36})$$

where $\frac{\partial M(m_a, \boldsymbol{\alpha})}{\partial D_{av}(T_{db}, \boldsymbol{\alpha})}$ was defined previously in Eq. (E.3), and

$$\frac{\partial D_{av}(T_{db}, \boldsymbol{\alpha})}{\partial a_{1,D_{av}}} = - \frac{a_{0,D_{av}} T_{db}^{1.5}}{(a_{1,D_{av}} + a_{2,D_{av}} T_{db} + a_{3,D_{av}} T_{db}^2)^2} \quad (\text{E.37})$$

$$\begin{aligned} \frac{\partial N_1^{(i)}}{\partial \alpha^{(19)}} = \frac{\partial N_1^{(i)}}{\partial a_{1,D_{av}}} \equiv a_1^{i,19} = \frac{1}{\bar{R}} \left[\frac{P_{vs}^{(i+1)}(T_w^{(i+1)}, \boldsymbol{\alpha})}{T_w^{(i+1)}} - \frac{\omega^{(i)} P_{atm}}{(0.622 + \omega^{(i)}) T_a^{(i)}} \right] \\ \cdot \frac{\partial M(m_a, \boldsymbol{\alpha})}{\partial D_{av}(T_{db}, \boldsymbol{\alpha})} \cdot \frac{\partial D_{av}(T_{db}, \boldsymbol{\alpha})}{\partial a_{1,D_{av}}}; \quad \ell = 1; \quad i = K + 1, \dots, I; \quad j = 19. \end{aligned} \quad (\text{E.38})$$

APPENDIX E. DERIVATIVES OF THE MODEL EQUATIONS WITH RESPECT TO THE MODEL PARAMETERS

The derivatives of the “liquid continuity equations” [cf. Eqs. (2.2) - (2.5)] with respect to the parameter $\alpha^{(20)} : a_{2,D_{av}}$ are as follows:

$$\begin{aligned} \frac{\partial N_1^{(i)}}{\partial \alpha^{(20)}} = \frac{\partial N_1^{(i)}}{\partial a_{2,D_{av}}} &\equiv a_1^{i,20} = \frac{1}{\overline{R}} \left[\frac{P_{vs}^{(i+1)}(T_w^{(i+1)}, \boldsymbol{\alpha})}{T_w^{(i+1)}} - \frac{P_{vs}^{(i)}(T_a^{(i)}, \boldsymbol{\alpha})}{T_a^{(i)}} \right] \\ &\cdot \frac{\partial M(m_a, \boldsymbol{\alpha})}{\partial D_{av}(T_{db}, \boldsymbol{\alpha})} \cdot \frac{\partial D_{av}(T_{db}, \boldsymbol{\alpha})}{\partial a_{2,D_{av}}}; \quad \ell = 1; \quad i = 1, \dots, K; \quad j = 20, \end{aligned} \quad (\text{E.39})$$

where $\frac{\partial M(m_a, \boldsymbol{\alpha})}{\partial D_{av}(T_{db}, \boldsymbol{\alpha})}$ was defined previously in Eq. (E.3), and

$$\frac{\partial D_{av}(T_{db}, \boldsymbol{\alpha})}{\partial a_{2,D_{av}}} = - \frac{a_{0,D_{av}} T_{db}^{2.5}}{(a_{1,D_{av}} + a_{2,D_{av}} T_{db} + a_{3,D_{av}} T_{db}^2)^2} \quad (\text{E.40})$$

$$\begin{aligned} \frac{\partial N_1^{(i)}}{\partial \alpha^{(20)}} = \frac{\partial N_1^{(i)}}{\partial a_{2,D_{av}}} &\equiv a_1^{i,20} = \frac{1}{\overline{R}} \left[\frac{P_{vs}^{(i+1)}(T_w^{(i+1)}, \boldsymbol{\alpha})}{T_w^{(i+1)}} - \frac{\omega^{(i)} P_{atm}}{(0.622 + \omega^{(i)}) T_a^{(i)}} \right] \\ &\cdot \frac{\partial M(m_a, \boldsymbol{\alpha})}{\partial D_{av}(T_{db}, \boldsymbol{\alpha})} \cdot \frac{\partial D_{av}(T_{db}, \boldsymbol{\alpha})}{\partial a_{2,D_{av}}}; \quad \ell = 1; \quad i = K + 1, \dots, I; \quad j = 20. \end{aligned} \quad (\text{E.41})$$

The derivatives of the “liquid continuity equations” [cf. Eqs. (2.2) - (2.5)] with respect to the parameter $\alpha^{(21)} : a_{3,D_{av}}$ are as follows:

$$\begin{aligned} \frac{\partial N_1^{(i)}}{\partial \alpha^{(21)}} = \frac{\partial N_1^{(i)}}{\partial a_{3,D_{av}}} &\equiv a_1^{i,21} = \frac{1}{\overline{R}} \left[\frac{P_{vs}^{(i+1)}(T_w^{(i+1)}, \boldsymbol{\alpha})}{T_w^{(i+1)}} - \frac{P_{vs}^{(i)}(T_a^{(i)}, \boldsymbol{\alpha})}{T_a^{(i)}} \right] \\ &\cdot \frac{\partial M(m_a, \boldsymbol{\alpha})}{\partial D_{av}(T_{db}, \boldsymbol{\alpha})} \cdot \frac{\partial D_{av}(T_{db}, \boldsymbol{\alpha})}{\partial a_{3,D_{av}}}; \quad \ell = 1; \quad i = 1, \dots, K; \quad j = 21, \end{aligned} \quad (\text{E.42})$$

where $\frac{\partial M(m_a, \boldsymbol{\alpha})}{\partial D_{av}(T_{db}, \boldsymbol{\alpha})}$ was defined previously in Eq. (E.3), and

$$\frac{\partial D_{av}(T_{db}, \boldsymbol{\alpha})}{\partial a_{3,D_{av}}} = - \frac{a_{0,D_{av}} T_{db}^{3.5}}{(a_{1,D_{av}} + a_{2,D_{av}} T_{db} + a_{3,D_{av}} T_{db}^2)^2} \quad (\text{E.43})$$

$$\begin{aligned} \frac{\partial N_1^{(i)}}{\partial \alpha^{(21)}} = \frac{\partial N_1^{(i)}}{\partial a_{3,D_{av}}} &\equiv a_1^{i,21} = \frac{1}{\overline{R}} \left[\frac{P_{vs}^{(i+1)}(T_w^{(i+1)}, \boldsymbol{\alpha})}{T_w^{(i+1)}} - \frac{\omega^{(i)} P_{atm}}{(0.622 + \omega^{(i)}) T_a^{(i)}} \right] \\ &\cdot \frac{\partial M(m_a, \boldsymbol{\alpha})}{\partial D_{av}(T_{db}, \boldsymbol{\alpha})} \cdot \frac{\partial D_{av}(T_{db}, \boldsymbol{\alpha})}{\partial a_{3,D_{av}}}; \quad \ell = 1; \quad i = K + 1, \dots, I; \quad j = 21. \end{aligned} \quad (\text{E.44})$$

APPENDIX E. DERIVATIVES OF THE MODEL EQUATIONS WITH RESPECT TO THE MODEL PARAMETERS

The derivatives of the “liquid continuity equations” [cf. Eqs. (2.2) - (2.5)] with respect to the parameter $\alpha^{(22)} : a_{0f}$ are as follows:

$$\frac{\partial N_1^{(i)}}{\partial \alpha^{(22)}} = \frac{\partial N_1^{(i)}}{\partial a_{0f}} \equiv a_1^{i,22} = 0; \quad \ell = 1; \quad i = 1, \dots, I; \quad j = 22. \quad (\text{E.45})$$

The derivatives of the “liquid continuity equations” [cf. Eqs. (2.2) - (2.5)] with respect to the parameter $\alpha^{(23)} : a_{1f}$ are as follows:

$$\frac{\partial N_1^{(i)}}{\partial \alpha^{(23)}} = \frac{\partial N_1^{(i)}}{\partial a_{1f}} \equiv a_1^{i,23} = 0; \quad \ell = 1; \quad i = 1, \dots, I; \quad j = 23. \quad (\text{E.46})$$

The derivatives of the “liquid continuity equations” [cf. Eqs. (2.2) - (2.5)] with respect to the parameter $\alpha^{(24)} : a_{0g}$ are as follows:

$$\frac{\partial N_1^{(i)}}{\partial \alpha^{(24)}} = \frac{\partial N_1^{(i)}}{\partial a_{0g}} \equiv a_1^{i,24} = 0; \quad \ell = 1; \quad i = 1, \dots, I; \quad j = 24. \quad (\text{E.47})$$

The derivatives of the “liquid continuity equations” [cf. Eqs. (2.2) - (2.5)] with respect to the parameter $\alpha^{(25)} : a_{1g}$ are as follows:

$$\frac{\partial N_1^{(i)}}{\partial \alpha^{(25)}} = \frac{\partial N_1^{(i)}}{\partial a_{1g}} \equiv a_1^{i,25} = 0; \quad \ell = 1; \quad i = 1, \dots, I; \quad j = 25. \quad (\text{E.48})$$

The derivatives of the “liquid continuity equations” [cf. Eqs. (2.2) - (2.5)] with respect to the parameter $\alpha^{(26)} : a_{0,Nu}$ are as follows:

$$\begin{aligned} \frac{\partial N_1^{(i)}}{\partial \alpha^{(26)}} = \frac{\partial N_1^{(i)}}{\partial a_{0,Nu}} \equiv a_1^{i,26} = \frac{1}{\bar{R}} \left[\frac{P_{vs}^{(i+1)}(T_w^{(i+1)}, \boldsymbol{\alpha})}{T_w^{(i+1)}} - \frac{P_{vs}^{(i)}(T_a^{(i)}, \boldsymbol{\alpha})}{T_a^{(i)}} \right] \\ \cdot \frac{\partial M(m_a, \boldsymbol{\alpha})}{\partial Nu(\text{Re}, \boldsymbol{\alpha})} \cdot \frac{\partial Nu(\text{Re}, \boldsymbol{\alpha})}{\partial a_{0,Nu}}; \quad \ell = 1; \quad i = 1, \dots, K; \quad j = 26, \end{aligned} \quad (\text{E.49})$$

where

$$\frac{\partial M(\text{Re}, \boldsymbol{\alpha})}{\partial Nu(\text{Re}, \boldsymbol{\alpha})} = \frac{M(m_a, \boldsymbol{\alpha})}{Nu(\text{Re}, \boldsymbol{\alpha})} \quad (\text{E.50})$$

APPENDIX E. DERIVATIVES OF THE MODEL EQUATIONS WITH RESPECT TO THE MODEL PARAMETERS

$$\frac{\partial Nu(\text{Re}, \boldsymbol{\alpha})}{\partial a_{0,Nu}} = \begin{cases} 1 & \text{Re}_d < 2300 \\ 0 & 2300 \leq \text{Re}_d \leq 10000 \\ 0 & \text{Re}_d > 10000 \end{cases} \quad (\text{E.51})$$

$$\begin{aligned} \frac{\partial N_1^{(i)}}{\partial \alpha^{(26)}} = \frac{\partial N_1^{(i)}}{\partial a_{0,Nu}} \equiv a_1^{i,26} &= \frac{1}{\overline{R}} \left[\frac{P_{vs}^{(i+1)}(T_w^{(i+1)}, \boldsymbol{\alpha})}{T_w^{(i+1)}} - \frac{\omega^{(i)} P_{atm}}{(0.622 + \omega^{(i)}) T_a^{(i)}} \right] \\ &\cdot \frac{\partial M(m_a, \boldsymbol{\alpha})}{\partial Nu(\text{Re}, \boldsymbol{\alpha})} \cdot \frac{\partial Nu(\text{Re}, \boldsymbol{\alpha})}{\partial a_{0,Nu}}; \quad \ell = 1; \quad i = K + 1, \dots, I; \quad j = 26. \end{aligned} \quad (\text{E.52})$$

The derivatives of the “liquid continuity equations” [cf. Eqs. (2.2) - (2.5)] with respect to the parameter $\alpha^{(27)} : a_{1,Nu}$ are as follows:

$$\begin{aligned} \frac{\partial N_1^{(i)}}{\partial \alpha^{(27)}} = \frac{\partial N_1^{(i)}}{\partial a_{1,Nu}} \equiv a_1^{i,27} &= \frac{1}{\overline{R}} \left[\frac{P_{vs}^{(i+1)}(T_w^{(i+1)}, \boldsymbol{\alpha})}{T_w^{(i+1)}} - \frac{P_{vs}^{(i)}(T_a^{(i)}, \boldsymbol{\alpha})}{T_a^{(i)}} \right] \\ &\cdot \frac{\partial M(m_a, \boldsymbol{\alpha})}{\partial Nu(\text{Re}, \boldsymbol{\alpha})} \cdot \frac{\partial Nu(\text{Re}, \boldsymbol{\alpha})}{\partial a_{1,Nu}}; \quad \ell = 1; \quad i = 1, \dots, K; \quad j = 27, \end{aligned} \quad (\text{E.53})$$

where $\frac{\partial M(m_a, \boldsymbol{\alpha})}{\partial Nu(\text{Re}, \boldsymbol{\alpha})}$ was defined previously in Eq. (E.50), and

$$\frac{\partial Nu(\text{Re}, \boldsymbol{\alpha})}{\partial a_{1,Nu}} = \begin{cases} 0 & \text{Re}_d < 2300 \\ \text{Re}(m_a, \boldsymbol{\alpha}) & 2300 \leq \text{Re}_d \leq 10000 \\ 0 & \text{Re}_d > 10000 \end{cases} \quad (\text{E.54})$$

$$\begin{aligned} \frac{\partial N_1^{(i)}}{\partial \alpha^{(27)}} = \frac{\partial N_1^{(i)}}{\partial a_{1,Nu}} \equiv a_1^{i,27} &= \frac{1}{\overline{R}} \left[\frac{P_{vs}^{(i+1)}(T_w^{(i+1)}, \boldsymbol{\alpha})}{T_w^{(i+1)}} - \frac{\omega^{(i)} P_{atm}}{(0.622 + \omega^{(i)}) T_a^{(i)}} \right] \\ &\cdot \frac{\partial M(m_a, \boldsymbol{\alpha})}{\partial Nu(\text{Re}, \boldsymbol{\alpha})} \cdot \frac{\partial Nu(\text{Re}, \boldsymbol{\alpha})}{\partial a_{1,Nu}}; \quad \ell = 1; \quad i = K + 1, \dots, I; \quad j = 27. \end{aligned} \quad (\text{E.55})$$

The derivatives of the “liquid continuity equations” [cf. Eqs. (2.2) - (2.5)] with respect to the parameter $\alpha^{(28)} : a_{2,Nu}$ are as follows:

$$\begin{aligned} \frac{\partial N_1^{(i)}}{\partial \alpha^{(28)}} = \frac{\partial N_1^{(i)}}{\partial a_{2,Nu}} \equiv a_1^{i,28} &= \frac{1}{\overline{R}} \left[\frac{P_{vs}^{(i+1)}(T_w^{(i+1)}, \boldsymbol{\alpha})}{T_w^{(i+1)}} - \frac{P_{vs}^{(i)}(T_a^{(i)}, \boldsymbol{\alpha})}{T_a^{(i)}} \right] \\ &\cdot \frac{\partial M(m_a, \boldsymbol{\alpha})}{\partial Nu(\text{Re}, \boldsymbol{\alpha})} \cdot \frac{\partial Nu(\text{Re}, \boldsymbol{\alpha})}{\partial a_{2,Nu}}; \quad \ell = 1; \quad i = 1, \dots, K; \quad j = 28, \end{aligned} \quad (\text{E.56})$$

APPENDIX E. DERIVATIVES OF THE MODEL EQUATIONS WITH RESPECT TO THE MODEL PARAMETERS

where $\frac{\partial M(m_a, \boldsymbol{\alpha})}{\partial Nu(\text{Re}, \boldsymbol{\alpha})}$ was defined previously in Eq. (E.50), and

$$\frac{\partial Nu(\text{Re}, \boldsymbol{\alpha})}{\partial a_{2, Nu}} = \begin{cases} 0 & \text{Re}_d < 2300 \\ 1 & 2300 \leq \text{Re}_d \leq 10000 \\ 0 & \text{Re}_d > 10000 \end{cases} \quad (\text{E.57})$$

$$\frac{\partial N_1^{(i)}}{\partial \alpha^{(28)}} = \frac{\partial N_1^{(i)}}{\partial a_{2, Nu}} \equiv a_1^{i, 28} = \frac{1}{\overline{R}} \left[\frac{P_{vs}^{(i+1)}(T_w^{(i+1)}, \boldsymbol{\alpha})}{T_w^{(i+1)}} - \frac{\omega^{(i)} P_{atm}}{(0.622 + \omega^{(i)}) T_a^{(i)}} \right] \quad (\text{E.58})$$

$$\cdot \frac{\partial M(m_a, \boldsymbol{\alpha})}{\partial Nu(\text{Re}, \boldsymbol{\alpha})} \cdot \frac{\partial Nu(\text{Re}, \boldsymbol{\alpha})}{\partial a_{2, Nu}}; \quad \ell = 1; \quad i = K + 1, \dots, I; \quad j = 28.$$

The derivatives of the “liquid continuity equations” [cf. Eqs. (2.2) - (2.5)] with respect to the parameter $\alpha^{(29)} : a_{3, Nu}$ are as follows:

$$\frac{\partial N_1^{(i)}}{\partial \alpha^{(29)}} = \frac{\partial N_1^{(i)}}{\partial a_{3, Nu}} \equiv a_1^{i, 29} = \frac{1}{\overline{R}} \left[\frac{P_{vs}^{(i+1)}(T_w^{(i+1)}, \boldsymbol{\alpha})}{T_w^{(i+1)}} - \frac{P_{vs}^{(i)}(T_a^{(i)}, \boldsymbol{\alpha})}{T_a^{(i)}} \right] \quad (\text{E.59})$$

$$\cdot \frac{\partial M(m_a, \boldsymbol{\alpha})}{\partial Nu(\text{Re}, \boldsymbol{\alpha})} \cdot \frac{\partial Nu(\text{Re}, \boldsymbol{\alpha})}{\partial a_{3, Nu}}; \quad \ell = 1; \quad i = 1, \dots, K; \quad j = 29,$$

where $\frac{\partial M(m_a, \boldsymbol{\alpha})}{\partial Nu(\text{Re}, \boldsymbol{\alpha})}$ was defined previously in Eq. (E.50), and

$$\frac{\partial Nu(\text{Re}, \boldsymbol{\alpha})}{\partial a_{3, Nu}} = \begin{cases} 0 & \text{Re}_d < 2300 \\ 0 & 2300 \leq \text{Re}_d \leq 10000 \\ [\text{Re}(m_a, \boldsymbol{\alpha})]^{0.8} \cdot \text{Pr}^{\frac{1}{3}} & \text{Re}_d > 10000 \end{cases} \quad (\text{E.60})$$

$$\frac{\partial N_1^{(i)}}{\partial \alpha^{(29)}} = \frac{\partial N_1^{(i)}}{\partial a_{3, Nu}} \equiv a_1^{i, 29} = \frac{1}{\overline{R}} \left[\frac{P_{vs}^{(i+1)}(T_w^{(i+1)}, \boldsymbol{\alpha})}{T_w^{(i+1)}} - \frac{\omega^{(i)} P_{atm}}{(0.622 + \omega^{(i)}) T_a^{(i)}} \right] \quad (\text{E.61})$$

$$\cdot \frac{\partial M(m_a, \boldsymbol{\alpha})}{\partial Nu(\text{Re}, \boldsymbol{\alpha})} \cdot \frac{\partial Nu(\text{Re}, \boldsymbol{\alpha})}{\partial a_{3, Nu}}; \quad \ell = 1; \quad i = K + 1, \dots, I; \quad j = 29.$$

The derivatives of the “liquid continuity equations” [cf. Eqs. (2.2) - (2.5)] with respect to the parameter $\alpha^{(30)} : W_{dkx}$ are as follows:

$$\frac{\partial N_1^{(i)}}{\partial \alpha^{(30)}} = \frac{\partial N_1^{(i)}}{\partial W_{dkx}} \equiv a_1^{i, 30} = 0; \quad \ell = 1; \quad i = 1, \dots, I; \quad j = 30. \quad (\text{E.62})$$

APPENDIX E. DERIVATIVES OF THE MODEL EQUATIONS WITH RESPECT TO THE MODEL PARAMETERS

The derivatives of the “liquid continuity equations” [cf. Eqs. (2.2) - (2.5)] with respect to the parameter $\alpha^{(31)} : W_{dky}$ are as follows:

$$\frac{\partial N_1^{(i)}}{\partial \alpha^{(31)}} = \frac{\partial N_1^{(i)}}{\partial W_{dky}} \equiv a_1^{i,31} = 0; \quad \ell = 1; \quad i = 1, \dots, I; \quad j = 31. \quad (\text{E.63})$$

The derivatives of the “liquid continuity equations” [cf. Eqs. (2.2) - (2.5)] with respect to the parameter $\alpha^{(32)} : \Delta z_{dk}$ are as follows:

$$\frac{\partial N_1^{(i)}}{\partial \alpha^{(32)}} = \frac{\partial N_1^{(i)}}{\partial \Delta z_{dk}} \equiv a_1^{i,32} = 0; \quad \ell = 1; \quad i = 1, \dots, I; \quad j = 32. \quad (\text{E.64})$$

The derivatives of the “liquid continuity equations” [cf. Eqs. (2.2) - (2.5)] with respect to the parameter $\alpha^{(33)} : \Delta z_{fan}$ are as follows:

$$\frac{\partial N_1^{(i)}}{\partial \alpha^{(33)}} = \frac{\partial N_1^{(i)}}{\partial \Delta z_{fan}} \equiv a_1^{i,33} = 0; \quad \ell = 1; \quad i = 1, \dots, I; \quad j = 33. \quad (\text{E.65})$$

The derivatives of the “liquid continuity equations” [cf. Eqs. (2.2) - (2.5)] with respect to the parameter $\alpha^{(34)} : D_{fan}$ are as follows:

$$\frac{\partial N_1^{(i)}}{\partial \alpha^{(34)}} = \frac{\partial N_1^{(i)}}{\partial D_{fan}} \equiv a_1^{i,34} = 0; \quad \ell = 1; \quad i = 1, \dots, I; \quad j = 34. \quad (\text{E.66})$$

The derivatives of the “liquid continuity equations” [cf. Eqs. (2.2) - (2.5)] with respect to the parameter $\alpha^{(35)} : \Delta z_{fill}$ are as follows:

$$\frac{\partial N_1^{(i)}}{\partial \alpha^{(35)}} = \frac{\partial N_1^{(i)}}{\partial \Delta z_{fill}} \equiv a_1^{i,35} = 0; \quad \ell = 1; \quad i = 1, \dots, I; \quad j = 35. \quad (\text{E.67})$$

The derivatives of the “liquid continuity equations” [cf. Eqs. (2.2) - (2.5)] with respect to the parameter $\alpha^{(36)} : \Delta z_{rain}$ are as follows:

$$\frac{\partial N_1^{(i)}}{\partial \alpha^{(36)}} = \frac{\partial N_1^{(i)}}{\partial \Delta z_{rain}} \equiv a_1^{i,36} = 0; \quad \ell = 1; \quad i = 1, \dots, I; \quad j = 36. \quad (\text{E.68})$$

APPENDIX E. DERIVATIVES OF THE MODEL EQUATIONS WITH
RESPECT TO THE MODEL PARAMETERS

The derivatives of the “liquid continuity equations” [cf. Eqs. (2.2) - (2.5)] with respect to the parameter $\alpha^{(37)} : \Delta z_{bs}$ are as follows:

$$\frac{\partial N_1^{(i)}}{\partial \alpha^{(37)}} = \frac{\partial N_1^{(i)}}{\partial \Delta z_{bs}} \equiv a_1^{i,37} = 0; \quad \ell = 1; \quad i = 1, \dots, I; \quad j = 37. \quad (\text{E.69})$$

The derivatives of the “liquid continuity equations” [cf. Eqs. (2.2) - (2.5)] with respect to the parameter $\alpha^{(38)} : \Delta z_{de}$ are as follows:

$$\frac{\partial N_1^{(i)}}{\partial \alpha^{(38)}} = \frac{\partial N_1^{(i)}}{\partial \Delta z_{de}} \equiv a_1^{i,38} = 0; \quad \ell = 1; \quad i = 1, \dots, I; \quad j = 38. \quad (\text{E.70})$$

The derivatives of the “liquid continuity equations” [cf. Eqs. (2.2) - (2.5)] with respect to the parameter $\alpha^{(39)} : D_h$ are as follows:

$$\begin{aligned} \frac{\partial N_1^{(i)}}{\partial \alpha^{(39)}} = \frac{\partial N_1^{(i)}}{\partial D_h} \equiv a_1^{i,39} &= \frac{1}{\bar{R}} \left[\frac{P_{vs}^{(i+1)}(T_w^{(i+1)}, \boldsymbol{\alpha})}{T_w^{(i+1)}} - \frac{P_{vs}^{(i)}(T_a^{(i)}, \boldsymbol{\alpha})}{T_a^{(i)}} \right] \frac{\partial M(m_a, \boldsymbol{\alpha})}{\partial D_h}; \\ \ell &= 1; \quad i = 1, \dots, K; \quad j = 39, \end{aligned} \quad (\text{E.71})$$

where

$$\frac{\partial M(m_a, \boldsymbol{\alpha})}{\partial D_h} = \begin{cases} -M(m_a, \boldsymbol{\alpha})/D_h & \text{Re}_d < 2300 \\ -\frac{a_{2,Nu} M(m_a, \boldsymbol{\alpha})}{Nu(\text{Re}, \boldsymbol{\alpha}) D_h} & 2300 \leq \text{Re}_d \leq 10000 \\ -0.2 \cdot M(m_a, \boldsymbol{\alpha})/D_h & \text{Re}_d > 10000 \end{cases} \quad (\text{E.72})$$

$$\begin{aligned} \frac{\partial N_1^{(i)}}{\partial \alpha^{(39)}} = \frac{\partial N_1^{(i)}}{\partial D_h} \equiv a_1^{i,39} &= \frac{1}{\bar{R}} \left[\frac{P_{vs}^{(i+1)}(T_w^{(i+1)}, \boldsymbol{\alpha})}{T_w^{(i+1)}} - \frac{\omega^{(i)} P_{atm}}{(0.622 + \omega^{(i)}) T_a^{(i)}} \right] \frac{\partial M(m_a, \boldsymbol{\alpha})}{\partial D_h}; \\ \ell &= 1; \quad i = K + 1, \dots, I; \quad j = 39. \end{aligned} \quad (\text{E.73})$$

APPENDIX E. DERIVATIVES OF THE MODEL EQUATIONS WITH RESPECT TO THE MODEL PARAMETERS

The derivatives of the “liquid continuity equations” [cf. Eqs. (2.2) - (2.5)] with respect to the $\alpha^{(40)} : A_{fill}$ are as follows:

$$\frac{\partial N_1^{(i)}}{\partial \alpha^{(40)}} = \frac{\partial N_1^{(i)}}{\partial A_{fill}} \equiv a_1^{i,40} = \frac{1}{\overline{R}} \left[\frac{P_{vs}^{(i+1)}(T_w^{(i+1)}, \boldsymbol{\alpha})}{T_w^{(i+1)}} - \frac{P_{vs}^{(i)}(T_a^{(i)}, \boldsymbol{\alpha})}{T_a^{(i)}} \right] \frac{\partial M(m_a, \boldsymbol{\alpha})}{\partial A_{fill}};$$

$$\ell = 1; \quad i = 1, \dots, K; \quad j = 40,$$
(E.74)

where

$$\frac{\partial M(m_a, \boldsymbol{\alpha})}{\partial A_{fill}} = \begin{cases} 0 & \text{Re}_d < 2300 \\ -\frac{a_{1,Nu} M(m_a, \boldsymbol{\alpha}) \text{Re}(m_a, \boldsymbol{\alpha})}{Nu(\text{Re}, \boldsymbol{\alpha}) A_{fill}} & 2300 \leq \text{Re}_d \leq 10000 \\ -0.8 \cdot M(m_a, \boldsymbol{\alpha}) / A_{fill} & \text{Re}_d > 10000 \end{cases} \quad (\text{E.75})$$

$$\frac{\partial N_1^{(i)}}{\partial \alpha^{(40)}} = \frac{\partial N_1^{(i)}}{\partial A_{fill}} \equiv a_1^{i,40} = \frac{1}{\overline{R}} \left[\frac{P_{vs}^{(i+1)}(T_w^{(i+1)}, \boldsymbol{\alpha})}{T_w^{(i+1)}} - \frac{\omega^{(i)} P_{atm}}{(0.622 + \omega^{(i)}) T_a^{(i)}} \right] \frac{\partial M(m_a, \boldsymbol{\alpha})}{\partial A_{fill}};$$

$$\ell = 1; \quad i = K + 1, \dots, I; \quad j = 40.$$
(E.76)

The derivatives of the “liquid continuity equations” [cf. Eqs. (2.2) - (2.5)] with respect to the parameter $\alpha^{(41)} : A_{surf}$ are as follows:

$$\frac{\partial N_1^{(i)}}{\partial \alpha^{(41)}} = \frac{\partial N_1^{(i)}}{\partial A_{surf}} \equiv a_1^{i,41} = \frac{1}{\overline{R}} \left[\frac{P_{vs}^{(i+1)}(T_w^{(i+1)}, \boldsymbol{\alpha})}{T_w^{(i+1)}} - \frac{P_{vs}^{(i)}(T_a^{(i)}, \boldsymbol{\alpha})}{T_a^{(i)}} \right] \frac{\partial M(m_a, \boldsymbol{\alpha})}{\partial A_{surf}};$$

$$\ell = 1; \quad i = 1, \dots, K; \quad j = 41,$$
(E.77)

where

$$\frac{\partial M(m_a, \boldsymbol{\alpha})}{\partial A_{surf}} = \frac{M(m_a, \boldsymbol{\alpha})}{A_{surf}} \quad (\text{E.78})$$

$$\frac{\partial N_1^{(i)}}{\partial \alpha^{(41)}} = \frac{\partial N_1^{(i)}}{\partial A_{surf}} \equiv a_1^{i,41} = \frac{1}{\overline{R}} \left[\frac{P_{vs}^{(i+1)}(T_w^{(i+1)}, \boldsymbol{\alpha})}{T_w^{(i+1)}} - \frac{\omega^{(i)} P_{atm}}{(0.622 + \omega^{(i)}) T_a^{(i)}} \right] \frac{\partial M(m_a, \boldsymbol{\alpha})}{\partial A_{surf}};$$

$$\ell = 1; \quad i = K + 1, \dots, I; \quad j = 41.$$
(E.79)

APPENDIX E. DERIVATIVES OF THE MODEL EQUATIONS WITH RESPECT TO THE MODEL PARAMETERS

The derivatives of the “liquid continuity equations” [cf. Eqs. (2.2) - (2.5)] with respect to the parameter $\alpha^{(42)} : \text{Pr}$ are as follows:

$$\frac{\partial N_1^{(i)}}{\partial \alpha^{(42)}} = \frac{\partial N_1^{(i)}}{\partial \text{Pr}} \equiv a_1^{i,42} = \frac{1}{\bar{R}} \left[\frac{P_{vs}^{(i+1)}(T_w^{(i+1)}, \boldsymbol{\alpha})}{T_w^{(i+1)}} - \frac{P_{vs}^{(i)}(T_a^{(i)}, \boldsymbol{\alpha})}{T_a^{(i)}} \right] \frac{\partial M(m_a, \boldsymbol{\alpha})}{\partial \text{Pr}};$$

$$\ell = 1; \quad i = 1, \dots, K; \quad j = 42,$$
(E.80)

where

$$\frac{\partial M(m_a, \boldsymbol{\alpha})}{\partial \text{Pr}} = \begin{cases} -\frac{M(m_a, \boldsymbol{\alpha})}{3 \cdot \text{Pr}} & \text{Re}_d \leq 10000 \\ 0 & \text{Re}_d > 10000 \end{cases}$$
(E.81)

$$\frac{\partial N_1^{(i)}}{\partial \alpha^{(42)}} = \frac{\partial N_1^{(i)}}{\partial \text{Pr}} \equiv a_1^{i,42} = \frac{1}{\bar{R}} \left[\frac{P_{vs}^{(i+1)}(T_w^{(i+1)}, \boldsymbol{\alpha})}{T_w^{(i+1)}} - \frac{\omega^{(i)} P_{atm}}{(0.622 + \omega^{(i)}) T_a^{(i)}} \right] \frac{\partial M(m_a, \boldsymbol{\alpha})}{\partial \text{Pr}};$$

$$\ell = 1; \quad i = K + 1, \dots, I; \quad j = 42.$$
(E.82)

The derivatives of the “liquid continuity equations” [cf. Eqs. (2.2) - (2.5)] with respect to the parameter $\alpha^{(43)} : w_{tsa}$ are as follows:

$$\frac{\partial N_1^{(i)}}{\partial \alpha^{(43)}} = \frac{\partial N_1^{(i)}}{\partial w_{tsa}} \equiv a_1^{i,43} = \frac{1}{\bar{R}} \left[\frac{P_{vs}^{(i+1)}(T_w^{(i+1)}, \boldsymbol{\alpha})}{T_w^{(i+1)}} - \frac{P_{vs}^{(i)}(T_a^{(i)}, \boldsymbol{\alpha})}{T_a^{(i)}} \right] \frac{\partial M(m_a, \boldsymbol{\alpha})}{\partial w_{tsa}};$$

$$\ell = 1; \quad i = 1, \dots, K; \quad j = 43,$$
(E.83)

where

$$\frac{\partial M(m_a, \boldsymbol{\alpha})}{\partial w_{tsa}} = \frac{M_{H_2O} f_{mt} \text{Nu}(\text{Re}, \boldsymbol{\alpha}) \left(\frac{\nu}{\text{Pr}}\right)^{1/3} [D_{av}(T_{db}, \boldsymbol{\alpha})]^{2/3} A_{surf}}{D_h I}$$
(E.84)

$$\frac{\partial N_1^{(i)}}{\partial \alpha^{(43)}} = \frac{\partial N_1^{(i)}}{\partial w_{tsa}} \equiv a_1^{i,43} = \frac{1}{\bar{R}} \left[\frac{P_{vs}^{(i+1)}(T_w^{(i+1)}, \boldsymbol{\alpha})}{T_w^{(i+1)}} - \frac{\omega^{(i)} P_{atm}}{(0.622 + \omega^{(i)}) T_a^{(i)}} \right] \frac{\partial M(m_a, \boldsymbol{\alpha})}{\partial w_{tsa}};$$

$$\ell = 1; \quad i = K + 1, \dots, I; \quad j = 43.$$
(E.85)

APPENDIX E. DERIVATIVES OF THE MODEL EQUATIONS WITH RESPECT TO THE MODEL PARAMETERS

The derivatives of the “liquid continuity equations” [cf. Eqs. (2.2) - (2.5)] with respect to the parameter $\alpha^{(44)} : m_{w,in}$ are as follows:

$$\frac{\partial N_1^{(1)}}{\partial \alpha^{(44)}} = \frac{\partial N_1^{(1)}}{\partial m_{w,in}} \equiv a_1^{1,44} = -1; \quad \ell = 1; \quad i = 1; \quad j = 44, \quad (\text{E.86})$$

$$\frac{\partial N_1^{(i)}}{\partial \alpha^{(44)}} = \frac{\partial N_1^{(i)}}{\partial m_{w,in}} \equiv a_1^{i,44} = 0; \quad \ell = 1; \quad i = 2, \dots, I; \quad j = 44. \quad (\text{E.87})$$

The derivatives of the “liquid continuity equations” [cf. Eqs. (2.2) - (2.5)] with respect to the parameter $\alpha^{(45)} : T_{a,in}$ are as follows:

$$\frac{\partial N_1^{(i)}}{\partial \alpha^{(45)}} = \frac{\partial N_1^{(i)}}{\partial T_{a,in}} \equiv a_1^{i,45} = 0; \quad \ell = 1; \quad i = 1, \dots, I; \quad j = 45. \quad (\text{E.88})$$

The derivatives of the “liquid continuity equations” [cf. Eqs. (2.2) - (2.5)] with respect to the parameter $\alpha^{(46)} : \omega_{in}$ are as follows:

$$\frac{\partial N_1^{(i)}}{\partial \alpha^{(46)}} = \frac{\partial N_1^{(i)}}{\partial \omega_{in}} \equiv a_1^{i,46} = 0; \quad \ell = 1; \quad i = 1, \dots, I; \quad j = 46. \quad (\text{E.89})$$

The derivatives of the “liquid continuity equations” [cf. Eqs. (2.2) - (2.5)] with respect to the parameter $\alpha^{(47)} : Sc$ are as follows:

$$\begin{aligned} \frac{\partial N_1^{(i)}}{\partial \alpha^{(47)}} = \frac{\partial N_1^{(i)}}{\partial Sc} \equiv a_1^{i,47} &= \frac{1}{\bar{R}} \left[\frac{P_{vs}^{(i+1)}(T_w^{(i+1)}, \boldsymbol{\alpha})}{T_w^{(i+1)}} - \frac{P_{vs}^{(i)}(T_a^{(i)}, \boldsymbol{\alpha})}{T_a^{(i)}} \right] \frac{\partial M(m_a, \boldsymbol{\alpha})}{\partial Sc}; \\ \ell &= 1; \quad i = 1, \dots, K; \quad j = 47, \end{aligned} \quad (\text{E.90})$$

where

$$\frac{\partial M(m_a, \boldsymbol{\alpha})}{\partial Sc} = \frac{1}{3} \frac{M(m_a, \boldsymbol{\alpha})}{Sc} \quad (\text{E.91})$$

$$\frac{\partial N_1^{(i)}}{\partial \alpha^{(47)}} = \frac{\partial N_1^{(i)}}{\partial Sc} \equiv a_1^{i,47} = \frac{1}{\bar{R}} \left[\frac{P_{vs}^{(i+1)}(T_w^{(i+1)}, \boldsymbol{\alpha})}{T_w^{(i+1)}} - \frac{\omega^{(i)} P_{atm}}{(0.622 + \omega^{(i)}) T_a^{(i)}} \right] \frac{\partial M(m_a, \boldsymbol{\alpha})}{\partial Sc};$$

$$\ell = 1; \quad i = K + 1, \dots, I; \quad j = 47. \quad (\text{E.92})$$

APPENDIX E. DERIVATIVES OF THE MODEL EQUATIONS WITH
RESPECT TO THE MODEL PARAMETERS

**E.1.2 Derivatives of the liquid energy balance equations
with respect to the parameters**

The derivatives of the liquid energy balance equations [cf. Eqs. (2.6) - (2.8)]
with respect to the parameter $\alpha^{(1)} : T_{db}$ are as follows:

$$\frac{\partial N_2^{(i)}}{\partial \alpha^{(1)}} = \frac{\partial N_2^{(i)}}{\partial T_{db}} \equiv a_2^{i,1} = 0; \quad \ell = 2; \quad i = 1, \dots, I; \quad j = 1. \quad (\text{E.93})$$

The derivatives of the liquid energy balance equations [cf. Eqs. (2.6) - (2.8)]
with respect to the parameter $\alpha^{(2)} : T_{dp}$ are as follows:

$$\frac{\partial N_2^{(i)}}{\partial \alpha^{(2)}} = \frac{\partial N_2^{(i)}}{\partial T_{dp}} \equiv a_2^{i,2} = 0; \quad \ell = 2; \quad i = 1, \dots, I; \quad j = 2. \quad (\text{E.94})$$

The derivatives of the liquid energy balance equations [cf. Eqs. (2.6) - (2.8)]
with respect to the parameter $\alpha^{(3)} : T_{w,in}$ are as follows:

$$\frac{\partial N_2^{(1)}}{\partial \alpha^{(3)}} = \frac{\partial N_2^{(1)}}{\partial T_{w,in}} \equiv a_2^{1,3} = m_{w,in} \frac{\partial h_f^{(1)}(T_{w,in}, \boldsymbol{\alpha})}{\partial T_{w,in}}; \quad \ell = 2; \quad i = 1; \quad j = 3, \quad (\text{E.95})$$

where

$$\frac{\partial h_f^{(1)}(T_{w,in}, \boldsymbol{\alpha})}{\partial T_{w,in}} = a_{1f}, \quad (\text{E.96})$$

$$\frac{\partial N_2^{(i)}}{\partial \alpha^{(3)}} = \frac{\partial N_2^{(i)}}{\partial T_{w,in}} \equiv a_2^{i,3} = 0; \quad \ell = 2; \quad i = 2, \dots, I; \quad j = 3. \quad (\text{E.97})$$

The derivatives of the liquid energy balance equations [cf. Eqs. (2.6) - (2.8)]
with respect to the parameter $\alpha^{(4)} : P_{atm}$ are as follows:

$$\frac{\partial N_2^{(i)}}{\partial \alpha^{(4)}} = \frac{\partial N_2^{(i)}}{\partial P_{atm}} \equiv a_2^{i,4} = 0; \quad \ell = 2; \quad i = 1, \dots, I; \quad j = 4, \quad (\text{E.98})$$

APPENDIX E. DERIVATIVES OF THE MODEL EQUATIONS WITH RESPECT TO THE MODEL PARAMETERS

The derivatives of the liquid energy balance equations [cf. Eqs. (2.6) - (2.8)] with respect to the parameter $\alpha^{(5)} : V_w$ are as follows:

$$\frac{\partial N_2^{(i)}}{\partial \alpha^{(5)}} = \frac{\partial N_2^{(i)}}{\partial V_w} \equiv a_2^{i,5} = 0; \quad \ell = 2; \quad i = 1, \dots, I; \quad j = 5, \quad (\text{E.99})$$

The derivatives of the liquid energy balance equations [cf. Eqs. (2.6) - (2.8)] with respect to the parameter $\alpha^{(6)} : k_{sum}$ are as follows:

$$\frac{\partial N_2^{(i)}}{\partial \alpha^{(6)}} = \frac{\partial N_2^{(i)}}{\partial k_{sum}} \equiv a_2^{i,6} = 0; \quad \ell = 2; \quad i = 1, \dots, I; \quad j = 6. \quad (\text{E.100})$$

The derivatives of the liquid energy balance equations [cf. Eqs. (2.6) - (2.8)] with respect to the parameter $\alpha^{(7)} : \mu$ are as follows:

$$\frac{\partial N_2^{(i)}}{\partial \alpha^{(7)}} = \frac{\partial N_2^{(i)}}{\partial \mu} \equiv a_2^{i,7} = - (T_w^{(i+1)} - T_a^{(i)}) \frac{\partial H(m_a, \boldsymbol{\alpha})}{\partial \mu}; \quad \ell = 2; \quad i = 1, \dots, I; \quad j = 7, \quad (\text{E.101})$$

where

$$\frac{\partial H(m_a, \boldsymbol{\alpha})}{\partial \mu} = \begin{cases} 0 & \text{Re}_d < 2300 \\ -\frac{a_{1,Nu} \cdot H(m_a, \boldsymbol{\alpha}) \cdot \text{Re}(m_a, \boldsymbol{\alpha})}{Nu(\text{Re}, \boldsymbol{\alpha}) \cdot \mu} & 2300 \leq \text{Re}_d \leq 10000 \\ -0.8 \cdot \frac{H(m_a, \boldsymbol{\alpha})}{\mu} & \text{Re}_d > 10000 \end{cases} \quad (\text{E.102})$$

The derivatives of the liquid energy balance equations [cf. Eqs. (2.6) - (2.8)] with respect to the parameter $\alpha^{(8)} : \nu$ are as follows:

$$\frac{\partial N_2^{(i)}}{\partial \alpha^{(8)}} = \frac{\partial N_2^{(i)}}{\partial \nu} \equiv a_2^{i,8} = 0; \quad \ell = 2; \quad i = 1, \dots, I; \quad j = 8. \quad (\text{E.103})$$

The derivatives of the liquid energy balance equations [cf. Eqs. (2.6) - (2.8)] with respect to the parameter $\alpha^{(9)} : k_{air}$ are as follows:

$$\frac{\partial N_2^{(i)}}{\partial \alpha^{(9)}} = \frac{\partial N_2^{(i)}}{\partial k_{air}} \equiv a_2^{i,9} = - (T_w^{(i+1)} - T_a^{(i)}) \frac{\partial H(m_a, \boldsymbol{\alpha})}{\partial k_{air}}; \quad \ell = 2; \quad i = 1, \dots, I; \quad j = 9, \quad (\text{E.104})$$

APPENDIX E. DERIVATIVES OF THE MODEL EQUATIONS WITH
RESPECT TO THE MODEL PARAMETERS

where

$$\frac{\partial H(m_a, \boldsymbol{\alpha})}{\partial k_{air}} = \frac{H(m_a, \boldsymbol{\alpha})}{k_{air}} = \frac{f_{ht} Nu(\text{Re}, \boldsymbol{\alpha}) w_{tsa} A_{surf}}{D_h I}. \quad (\text{E.105})$$

The derivatives of the liquid energy balance equations [cf. Eqs. (2.6) - (2.8)] with respect to the parameter $\alpha^{(10)} : f_{ht}$ are as follows:

$$\frac{\partial N_2^{(i)}}{\partial \alpha^{(10)}} = \frac{\partial N_2^{(i)}}{\partial f_{ht}} \equiv a_2^{i,10} = - (T_w^{(i+1)} - T_a^{(i)}) \frac{\partial H(m_a, \boldsymbol{\alpha})}{\partial f_{ht}}; \quad \ell = 2; \quad i = 1, \dots, I; \quad j = 10, \quad (\text{E.106})$$

where

$$\frac{\partial H(m_a, \boldsymbol{\alpha})}{\partial f_{ht}} = \frac{H(m_a, \boldsymbol{\alpha})}{f_{ht}} = \frac{k_{air} Nu(\text{Re}, \boldsymbol{\alpha}) w_{tsa} A_{surf}}{D_h I}. \quad (\text{E.107})$$

The derivatives of the liquid energy balance equations [cf. Eqs. (2.6) - (2.8)] with respect to the parameter $\alpha^{(11)} : f_{mt}$ are as follows:

$$\frac{\partial N_2^{(i)}}{\partial \alpha^{(11)}} = \frac{\partial N_2^{(i)}}{\partial f_{mt}} \equiv a_2^{i,11} = 0; \quad \ell = 2; \quad i = 1, \dots, I; \quad j = 11. \quad (\text{E.108})$$

The derivatives of the liquid energy balance equations [cf. Eqs. (2.6) - (2.8)] with respect to the parameter $\alpha^{(12)} : f$ are as follows:

$$\frac{\partial N_2^{(i)}}{\partial \alpha^{(12)}} = \frac{\partial N_2^{(i)}}{\partial f} \equiv a_2^{i,12} = 0; \quad \ell = 2; \quad i = 1, \dots, I; \quad j = 12. \quad (\text{E.109})$$

The derivatives of the liquid energy balance equations [cf. Eqs. (2.6) - (2.8)] with respect to the parameter $\alpha^{(13)} : a_0$ are as follows:

$$\frac{\partial N_2^{(i)}}{\partial \alpha^{(13)}} = \frac{\partial N_2^{(i)}}{\partial a_0} \equiv a_2^{i,13} = 0; \quad \ell = 2; \quad i = 1, \dots, I; \quad j = 13. \quad (\text{E.110})$$

APPENDIX E. DERIVATIVES OF THE MODEL EQUATIONS WITH RESPECT TO THE MODEL PARAMETERS

The derivatives of the liquid energy balance equations [cf. Eqs. (2.6) - (2.8)] with respect to the parameter $\alpha^{(14)} : a_1$ are as follows:

$$\frac{\partial N_2^{(i)}}{\partial \alpha^{(14)}} = \frac{\partial N_2^{(i)}}{\partial a_1} \equiv a_2^{i,14} = 0; \quad \ell = 2; \quad i = 1, \dots, I; \quad j = 14. \quad (\text{E.111})$$

The derivatives of the liquid energy balance equations [cf. Eqs. (2.6) - (2.8)] with respect to the parameter $\alpha^{(15)} : a_{0,c_{pa}}$ are as follows:

$$\frac{\partial N_2^{(i)}}{\partial \alpha^{(15)}} = \frac{\partial N_2^{(i)}}{\partial a_{0,c_{pa}}} \equiv a_2^{i,15} = 0; \quad \ell = 2; \quad i = 1, \dots, I; \quad j = 15. \quad (\text{E.112})$$

The derivatives of the liquid energy balance equations [cf. Eqs. (2.6) - (2.8)] with respect to the parameter $\alpha^{(16)} : a_{1,c_{pa}}$ are as follows:

$$\frac{\partial N_2^{(i)}}{\partial \alpha^{(16)}} = \frac{\partial N_2^{(i)}}{\partial a_{1,c_{pa}}} \equiv a_2^{i,16} = 0; \quad \ell = 2; \quad i = 1, \dots, I; \quad j = 16. \quad (\text{E.113})$$

The derivatives of the liquid energy balance equations [cf. Eqs. (2.6) - (2.8)] with respect to the parameter $\alpha^{(17)} : a_{2,c_{pa}}$ are as follows:

$$\frac{\partial N_2^{(i)}}{\partial \alpha^{(17)}} = \frac{\partial N_2^{(i)}}{\partial a_{2,c_{pa}}} \equiv a_2^{i,17} = 0; \quad \ell = 2; \quad i = 1, \dots, I; \quad j = 17. \quad (\text{E.114})$$

The derivatives of the liquid energy balance equations [cf. Eqs. (2.6) - (2.8)] with respect to the parameter $\alpha^{(18)} : a_{0,D_{av}}$ are as follows:

$$\frac{\partial N_2^{(i)}}{\partial \alpha^{(18)}} = \frac{\partial N_2^{(i)}}{\partial a_{0,D_{av}}} \equiv a_2^{i,18} = 0; \quad \ell = 2; \quad i = 1, \dots, I; \quad j = 18. \quad (\text{E.115})$$

The derivatives of the liquid energy balance equations [cf. Eqs. (2.6) - (2.8)] with respect to the parameter $\alpha^{(19)} : a_{1,D_{av}}$ are as follows:

$$\frac{\partial N_2^{(i)}}{\partial \alpha^{(19)}} = \frac{\partial N_2^{(i)}}{\partial a_{1,D_{av}}} \equiv a_2^{i,19} = 0; \quad \ell = 2; \quad i = 1, \dots, I; \quad j = 19. \quad (\text{E.116})$$

APPENDIX E. DERIVATIVES OF THE MODEL EQUATIONS WITH RESPECT TO THE MODEL PARAMETERS

The derivatives of the liquid energy balance equations [cf. Eqs. (2.6) - (2.8)] with respect to the parameter $\alpha^{(20)} : a_{2,D_{av}}$ are as follows:

$$\frac{\partial N_2^{(i)}}{\partial \alpha^{(20)}} = \frac{\partial N_2^{(i)}}{\partial a_{2,D_{av}}} \equiv a_2^{i,20} = 0; \quad \ell = 2; \quad i = 1, \dots, I; \quad j = 20. \quad (\text{E.117})$$

The derivatives of the liquid energy balance equations [cf. Eqs. (2.6) - (2.8)] with respect to the parameter $\alpha^{(21)} : a_{3,D_{av}}$ are as follows:

$$\frac{\partial N_2^{(i)}}{\partial \alpha^{(21)}} = \frac{\partial N_2^{(i)}}{\partial a_{3,D_{av}}} \equiv a_2^{i,21} = 0; \quad \ell = 2; \quad i = 1, \dots, I; \quad j = 21. \quad (\text{E.118})$$

The derivatives of the liquid energy balance equations [cf. Eqs. (2.6) - (2.8)] with respect to the parameter $\alpha^{(22)} : a_{0f}$ are as follows:

$$\begin{aligned} \frac{\partial N_2^{(i)}}{\partial \alpha^{(22)}} &= \frac{\partial N_2^{(i)}}{\partial a_{0f}} \equiv a_2^{i,22} = m_w^{(i)} \frac{\partial h_f^{(i)}(T_w^{(i)}, \boldsymbol{\alpha})}{\partial a_{0f}} - m_w^{(i+1)} \frac{\partial h_f^{(i+1)}(T_w^{(i+1)}, \boldsymbol{\alpha})}{\partial a_{0f}} \\ &= m_w^{(i)} - m_w^{(i+1)}; \quad \ell = 2; \quad i = 1, \dots, I; \quad j = 22. \end{aligned} \quad (\text{E.119})$$

The derivatives of the liquid energy balance equations [cf. Eqs. (2.6) - (2.8)] with respect to the parameter $\alpha^{(23)} : a_{1f}$ are as follows:

$$\begin{aligned} \frac{\partial N_2^{(i)}}{\partial \alpha^{(23)}} &= \frac{\partial N_2^{(i)}}{\partial a_{1f}} \equiv a_2^{i,23} = m_w^{(i)} \frac{\partial h_f^{(i)}(T_w^{(i)}, \boldsymbol{\alpha})}{\partial a_{1f}} - m_w^{(i+1)} \frac{\partial h_f^{(i+1)}(T_w^{(i+1)}, \boldsymbol{\alpha})}{\partial a_{1f}} \\ &= T_w^{(i)} m_w^{(i)} - T_w^{(i+1)} m_w^{(i+1)}; \quad \ell = 2; \quad i = 1, \dots, I; \quad j = 23. \end{aligned} \quad (\text{E.120})$$

The derivatives of the liquid energy balance equations [cf. Eqs. (2.6) - (2.8)] with respect to the parameter $\alpha^{(24)} : a_{0g}$ are as follows:

$$\begin{aligned} \frac{\partial N_2^{(i)}}{\partial \alpha^{(24)}} &= \frac{\partial N_2^{(i)}}{\partial a_{0g}} \equiv a_2^{i,24} = -(m_w^{(i)} - m_w^{(i+1)}) \frac{\partial h_{g,w}^{(i+1)}(T_w^{(i+1)}, \boldsymbol{\alpha})}{\partial a_{0g}} \\ &= m_w^{(i+1)} - m_w^{(i)}; \quad \ell = 2; \quad i = 1, \dots, I; \quad j = 24. \end{aligned} \quad (\text{E.121})$$

APPENDIX E. DERIVATIVES OF THE MODEL EQUATIONS WITH RESPECT TO THE MODEL PARAMETERS

The derivatives of the liquid energy balance equations [cf. Eqs. (2.6) - (2.8)] with respect to the parameter $\alpha^{(25)} : a_{1g}$ are as follows:

$$\begin{aligned} \frac{\partial N_2^{(i)}}{\partial \alpha^{(25)}} &= \frac{\partial N_2^{(i)}}{\partial a_{1g}} \equiv a_2^{i,25} = -(m_w^{(i)} - m_w^{(i+1)}) \frac{\partial h_{g,w}^{(i+1)}(T_w^{(i+1)}, \boldsymbol{\alpha})}{\partial a_{1g}} \\ &= - (m_w^{(i)} - m_w^{(i+1)}) T_w^{(i+1)}; \quad \ell = 2; \quad i = 1, \dots, I; \quad j = 25. \end{aligned} \quad (\text{E.122})$$

The derivatives of the liquid energy balance equations [cf. Eqs. (2.6) - (2.8)] with respect to the parameter $\alpha^{(26)} : a_{0,Nu}$ are as follows:

$$\begin{aligned} \frac{\partial N_2^{(i)}}{\partial \alpha^{(26)}} &= \frac{\partial N_2^{(i)}}{\partial a_{0,Nu}} \equiv a_2^{i,26} = - (T_w^{(i+1)} - T_a^{(i)}) \frac{\partial H(m_a, \boldsymbol{\alpha})}{\partial Nu(\text{Re}, \boldsymbol{\alpha})} \frac{\partial Nu(\text{Re}, \boldsymbol{\alpha})}{\partial a_{0,Nu}}; \\ \ell &= 2; \quad i = 1, \dots, I; \quad j = 26, \end{aligned} \quad (\text{E.123})$$

where

$$\frac{\partial H(m_a, \boldsymbol{\alpha})}{\partial Nu(\text{Re}, \boldsymbol{\alpha})} = \frac{H(m_a, \boldsymbol{\alpha})}{Nu(\text{Re}, \boldsymbol{\alpha})} \quad (\text{E.124})$$

and $\frac{\partial Nu(\text{Re}, \boldsymbol{\alpha})}{\partial a_{0,Nu}}$ was defined in Eq. (E.51).

The derivatives of the liquid energy balance equations [cf. Eqs. (2.6) - (2.8)] with respect to the parameter $\alpha^{(27)} : a_{1,Nu}$ are as follows:

$$\begin{aligned} \frac{\partial N_2^{(i)}}{\partial \alpha^{(27)}} &= \frac{\partial N_2^{(i)}}{\partial a_{1,Nu}} \equiv a_2^{i,27} = - (T_w^{(i+1)} - T_a^{(i)}) \frac{\partial H(m_a, \boldsymbol{\alpha})}{\partial Nu(\text{Re}, \boldsymbol{\alpha})} \frac{\partial Nu(\text{Re}, \boldsymbol{\alpha})}{\partial a_{1,Nu}}; \\ \ell &= 2; \quad i = 1, \dots, I; \quad j = 27, \end{aligned} \quad (\text{E.125})$$

where $\frac{\partial H(m_a, \boldsymbol{\alpha})}{\partial Nu(\text{Re}, \boldsymbol{\alpha})}$ was defined in Eq. (E.124) and $\frac{\partial Nu(\text{Re}, \boldsymbol{\alpha})}{\partial a_{1,Nu}}$ was defined in Eq. (E.54).

The derivatives of the liquid energy balance equations [cf. Eqs. (2.6) - (2.8)] with respect to the parameter $\alpha^{(28)} : a_{2,Nu}$ are as follows:

$$\begin{aligned} \frac{\partial N_2^{(i)}}{\partial \alpha^{(28)}} &= \frac{\partial N_2^{(i)}}{\partial a_{2,Nu}} \equiv a_2^{i,28} = - (T_w^{(i+1)} - T_a^{(i)}) \frac{\partial H(m_a, \boldsymbol{\alpha})}{\partial Nu(\text{Re}, \boldsymbol{\alpha})} \frac{\partial Nu(\text{Re}, \boldsymbol{\alpha})}{\partial a_{2,Nu}}; \\ \ell &= 2; \quad i = 1, \dots, I; \quad j = 28, \end{aligned} \quad (\text{E.126})$$

APPENDIX E. DERIVATIVES OF THE MODEL EQUATIONS WITH RESPECT TO THE MODEL PARAMETERS

where $\frac{\partial H(m_a, \boldsymbol{\alpha})}{\partial Nu(\text{Re}, \boldsymbol{\alpha})}$ was defined in Eq. (E.124) and $\frac{\partial Nu(\text{Re}, \boldsymbol{\alpha})}{\partial a_{2, Nu}}$ was defined in Eq. (E.57).

The derivatives of the liquid energy balance equations [cf. Eqs. (2.6) - (2.8)] with respect to the parameter $\alpha^{(29)} : a_{3, Nu}$ are as follows:

$$\frac{\partial N_2^{(i)}}{\partial \alpha^{(29)}} = \frac{\partial N_2^{(i)}}{\partial a_{3, Nu}} \equiv a_2^{i, 29} = - (T_w^{(i+1)} - T_a^{(i)}) \frac{\partial H(m_a, \boldsymbol{\alpha})}{\partial Nu(\text{Re}, \boldsymbol{\alpha})} \frac{\partial Nu(\text{Re}, \boldsymbol{\alpha})}{\partial a_{3, Nu}}; \quad (\text{E.127})$$

$$\ell = 2; \quad i = 1, \dots, I; \quad j = 29,$$

where $\frac{\partial H(m_a, \boldsymbol{\alpha})}{\partial Nu(\text{Re}, \boldsymbol{\alpha})}$ was defined in Eq. (E.124) and $\frac{\partial Nu(\text{Re}, \boldsymbol{\alpha})}{\partial a_{3, Nu}}$ was defined in Eq. (E.60).

The derivatives of the liquid energy balance equations [cf. Eqs. (2.6) - (2.8)] with respect to the parameter $\alpha^{(30)} : W_{dkx}$ are as follows:

$$\frac{\partial N_2^{(i)}}{\partial \alpha^{(30)}} = \frac{\partial N_2^{(i)}}{\partial W_{dkx}} \equiv a_2^{i, 30} = 0; \quad \ell = 2; \quad i = 1, \dots, I; \quad j = 30. \quad (\text{E.128})$$

The derivatives of the liquid energy balance equations [cf. Eqs. (2.6) - (2.8)] with respect to the parameter $\alpha^{(31)} : W_{dky}$ are as follows:

$$\frac{\partial N_2^{(i)}}{\partial \alpha^{(31)}} = \frac{\partial N_2^{(i)}}{\partial W_{dky}} \equiv a_2^{i, 31} = 0; \quad \ell = 2; \quad i = 1, \dots, I; \quad j = 31. \quad (\text{E.129})$$

The derivatives of the liquid energy balance equations [cf. Eqs. (2.6) - (2.8)] with respect to the parameter $\alpha^{(32)} : \Delta z_{dk}$ are as follows:

$$\frac{\partial N_2^{(i)}}{\partial \alpha^{(32)}} = \frac{\partial N_2^{(i)}}{\partial \Delta z_{dk}} \equiv a_2^{i, 32} = 0; \quad \ell = 2; \quad i = 1, \dots, I; \quad j = 32. \quad (\text{E.130})$$

The derivatives of the liquid energy balance equations [cf. Eqs. (2.6) - (2.8)] with respect to the parameter $\alpha^{(33)} : \Delta z_{fan}$ are as follows:

$$\frac{\partial N_2^{(i)}}{\partial \alpha^{(33)}} = \frac{\partial N_2^{(i)}}{\partial \Delta z_{fan}} \equiv a_2^{i, 33} = 0; \quad \ell = 2; \quad i = 1, \dots, I; \quad j = 33. \quad (\text{E.131})$$

APPENDIX E. DERIVATIVES OF THE MODEL EQUATIONS WITH RESPECT TO THE MODEL PARAMETERS

The derivatives of the liquid energy balance equations [cf. Eqs. (2.6) - (2.8)] with respect to the parameter $\alpha^{(34)} : D_{fan}$ are as follows:

$$\frac{\partial N_2^{(i)}}{\partial \alpha^{(34)}} = \frac{\partial N_2^{(i)}}{\partial D_{fan}} \equiv a_2^{i,34} = 0; \ell = 2; \quad i = 1, \dots, I; \quad j = 34, \quad (\text{E.132})$$

The derivatives of the liquid energy balance equations [cf. Eqs. (2.6) - (2.8)] with respect to the parameter $\alpha^{(35)} : \Delta z_{fill}$ are as follows:

$$\frac{\partial N_2^{(i)}}{\partial \alpha^{(35)}} = \frac{\partial N_2^{(i)}}{\partial \Delta z_{fill}} \equiv a_2^{i,35} = 0; \quad \ell = 2; \quad i = 1, \dots, I; \quad j = 35. \quad (\text{E.133})$$

The derivatives of the liquid energy balance equations [cf. Eqs. (2.6) - (2.8)] with respect to the parameter $\alpha^{(36)} : \Delta z_{rain}$ are as follows:

$$\frac{\partial N_2^{(i)}}{\partial \alpha^{(36)}} = \frac{\partial N_2^{(i)}}{\partial \Delta z_{rain}} \equiv a_2^{i,36} = 0; \quad \ell = 2; \quad i = 1, \dots, I; \quad j = 36. \quad (\text{E.134})$$

The derivatives of the liquid energy balance equations [cf. Eqs. (2.6) - (2.8)] with respect to the parameter $\alpha^{(37)} : \Delta z_{bs}$ are as follows:

$$\frac{\partial N_2^{(i)}}{\partial \alpha^{(37)}} = \frac{\partial N_2^{(i)}}{\partial \Delta z_{bs}} \equiv a_2^{i,37} = 0; \quad \ell = 2; \quad i = 1, \dots, I; \quad j = 37. \quad (\text{E.135})$$

The derivatives of the liquid energy balance equations [cf. Eqs. (2.6) - (2.8)] with respect to the parameter $\alpha^{(38)} : \Delta z_{de}$ are as follows:

$$\frac{\partial N_2^{(i)}}{\partial \alpha^{(38)}} = \frac{\partial N_2^{(i)}}{\partial \Delta z_{de}} \equiv a_2^{i,38} = 0; \quad \ell = 2; \quad i = 1, \dots, I; \quad j = 38. \quad (\text{E.136})$$

The derivatives of the liquid energy balance equations [cf. Eqs. (2.6) - (2.8)] with respect to the parameter $\alpha^{(39)} : D_h$ are as follows:

$$\begin{aligned} \frac{\partial N_2^{(i)}}{\partial \alpha^{(39)}} = \frac{\partial N_2^{(i)}}{\partial D_h} &\equiv a_2^{i,39} = - (T_w^{(i+1)} - T_a^{(i)}) \frac{\partial H(m_a, \boldsymbol{\alpha})}{\partial D_h}; \\ &\ell = 2; \quad i = 1, \dots, I; \quad j = 39, \end{aligned} \quad (\text{E.137})$$

APPENDIX E. DERIVATIVES OF THE MODEL EQUATIONS WITH
RESPECT TO THE MODEL PARAMETERS

where

$$\frac{\partial H(m_a, \boldsymbol{\alpha})}{\partial D_h} = \begin{cases} -H(m_a, \boldsymbol{\alpha})/D_h & \text{Re}_d < 2300 \\ -\frac{a_{2,Nu}H(m_a, \boldsymbol{\alpha})}{Nu(\text{Re}, \boldsymbol{\alpha})D_h} & 2300 \leq \text{Re}_d \leq 10000 \\ -0.2 \cdot H(m_a, \boldsymbol{\alpha})/D_h & \text{Re}_d > 10000 \end{cases} \quad (\text{E.138})$$

The derivatives of the liquid energy balance equations [cf. Eqs. (2.6) - (2.8)]
with respect to the parameter $\alpha^{(40)} : A_{fill}$ are as follows:

$$\frac{\partial N_2^{(i)}}{\partial \alpha^{(40)}} = \frac{\partial N_2^{(i)}}{\partial A_{fill}} \equiv a_2^{i,40} = - (T_w^{(i+1)} - T_a^{(i)}) \frac{\partial H(m_a, \boldsymbol{\alpha})}{\partial A_{fill}}; \quad (\text{E.139})$$

$$\ell = 2; \quad i = 1, \dots, I; \quad j = 40,$$

where

$$\frac{\partial H(m_a, \boldsymbol{\alpha})}{\partial A_{fill}} = \begin{cases} 0 & \text{Re}_d < 2300 \\ -\frac{a_{1,Nu}H(m_a, \boldsymbol{\alpha})\text{Re}(m_a, \boldsymbol{\alpha})}{Nu(\text{Re}, \boldsymbol{\alpha})A_{fill}} & 2300 \leq \text{Re}_d \leq 10000 \\ -0.8 \cdot H(m_a, \boldsymbol{\alpha})/A_{fill} & \text{Re}_d > 10000 \end{cases} \quad (\text{E.140})$$

The derivatives of the liquid energy balance equations [cf. Eqs. (2.6) - (2.8)]
with respect to the parameter $\alpha^{(41)} : A_{surf}$ are as follows:

$$\frac{\partial N_2^{(i)}}{\partial \alpha^{(41)}} = \frac{\partial N_2^{(i)}}{\partial A_{surf}} \equiv a_2^{i,41} = - (T_w^{(i+1)} - T_a^{(i)}) \frac{\partial H(m_a, \boldsymbol{\alpha})}{\partial A_{surf}}; \quad (\text{E.141})$$

$$\ell = 2; \quad i = 1, \dots, I; \quad j = 41,$$

where

$$\frac{\partial H(m_a, \boldsymbol{\alpha})}{\partial A_{surf}} = \frac{H(m_a, \boldsymbol{\alpha})}{A_{surf}} = \frac{f_{ht}k_{air}Nu(\text{Re}, \boldsymbol{\alpha})w_{tsa}}{D_h I}. \quad (\text{E.142})$$

The derivatives of the liquid energy balance equations [cf. Eqs. (2.6) - (2.8)]
with respect to the parameter $\alpha^{(42)} : \text{Pr}$ are as follows:

$$\frac{\partial N_2^{(i)}}{\partial \alpha^{(42)}} = \frac{\partial N_2^{(i)}}{\partial \text{Pr}} \equiv a_2^{i,42} = - (T_w^{(i+1)} - T_a^{(i)}) \frac{\partial H(m_a, \boldsymbol{\alpha})}{\partial \text{Pr}}; \quad (\text{E.143})$$

$$\ell = 2; \quad i = 1, \dots, I; \quad j = 42,$$

APPENDIX E. DERIVATIVES OF THE MODEL EQUATIONS WITH RESPECT TO THE MODEL PARAMETERS

where

$$\frac{\partial H(m_a, \boldsymbol{\alpha})}{\partial \text{Pr}} = \begin{cases} 0 & \text{Re}_d \leq 10000 \\ H(m_a, \boldsymbol{\alpha})/(3 \cdot \text{Pr}) & \text{Re}_d > 10000 \end{cases} \quad (\text{E.144})$$

The derivatives of the liquid energy balance equations [cf. Eqs. (2.6) - (2.8)] with respect to the parameter $\alpha^{(43)} : w_{tsa}$ are as follows:

$$\begin{aligned} \frac{\partial N_2^{(i)}}{\partial \alpha^{43}} &= \frac{\partial N_2^{(i)}}{\partial w_{tsa}} \equiv a_2^{i,43} = - (T_w^{(i+1)} - T_a^{(i)}) \frac{\partial H(m_a, \boldsymbol{\alpha})}{\partial w_{tsa}}; \\ \ell &= 2; \quad i = 1, \dots, I; \quad j = 43, \end{aligned} \quad (\text{E.145})$$

where

$$\frac{\partial H(m_a, \boldsymbol{\alpha})}{\partial w_{tsa}} = \frac{f_{ht} Nu(\text{Re}, \boldsymbol{\alpha}) k_{air} A_{surf}}{D_h I}. \quad (\text{E.146})$$

The derivatives of the liquid energy balance equations [cf. Eqs. (2.6) - (2.8)] with respect to the parameter $\alpha^{(44)} : m_{w,in}$ are as follows:

$$\begin{aligned} \frac{\partial N_2^{(1)}}{\partial \alpha^{(44)}} &= \frac{\partial N_2^{(1)}}{\partial m_{w,in}} \equiv a_2^{1,44} = h_f^{(1)}(T_{w,in}, \boldsymbol{\alpha}) - h_{g,w}^{(2)}(T_w^{(2)}, \boldsymbol{\alpha}) \\ &= T_{w,in} a_{1f} - a_{1g} T_w^{(2)} + a_{0f} - a_{0g}, \quad \ell = 2; \quad i = 1; \quad j = 44, \end{aligned} \quad (\text{E.147})$$

$$\frac{\partial N_2^{(i)}}{\partial \alpha^{(44)}} = \frac{\partial N_2^{(i)}}{\partial m_{w,in}} \equiv a_2^{i,44} = 0; \quad \ell = 2; \quad i = 2, \dots, I; \quad j = 44. \quad (\text{E.148})$$

The derivatives of the liquid energy balance equations [cf. Eqs. (2.6) - (2.8)] with respect to the parameter $\alpha^{(45)} : T_{a,in}$ are as follows:

$$\frac{\partial N_2^{(i)}}{\partial \alpha^{(45)}} = \frac{\partial N_2^{(i)}}{\partial T_{a,in}} \equiv a_2^{i,45} = 0; \quad \ell = 2; \quad i = 1, \dots, I; \quad j = 45. \quad (\text{E.149})$$

The derivatives of the liquid energy balance equations [cf. Eqs. (2.6) - (2.8)] with respect to the parameter $\alpha^{(46)} : \omega_{in}$ are as follows:

$$\frac{\partial N_2^{(i)}}{\partial \alpha^{(46)}} = \frac{\partial N_2^{(i)}}{\partial \omega_{in}} \equiv a_2^{i,46} = 0; \quad \ell = 2; \quad i = 1, \dots, I; \quad j = 46. \quad (\text{E.150})$$

APPENDIX E. DERIVATIVES OF THE MODEL EQUATIONS WITH RESPECT TO THE MODEL PARAMETERS

The derivatives of the liquid energy balance equations [cf. Eqs. (2.6) - (2.8)] with respect to the parameter $\alpha^{(47)} : Sc$ are as follows:

$$\frac{\partial N_2^{(i)}}{\partial \alpha^{(47)}} = \frac{\partial N_2^{(i)}}{\partial Sc} \equiv a_2^{i,47} = 0; \quad \ell = 2; \quad i = 1, \dots, I; \quad j = 47. \quad (\text{E.151})$$

E.1.3 Derivatives of the water vapor continuity equations with respect to the parameters

The derivatives of the water vapor continuity equations [cf. Eqs. (2.9) - (2.11)] with respect to the parameter $\alpha^{(1)} : T_{db}$ are as follows:

$$\frac{\partial N_3^{(i)}}{\partial \alpha^{(1)}} = \frac{\partial N_3^{(i)}}{\partial T_{db}} \equiv a_3^{i,1} = 0; \quad \ell = 3; \quad i = 1, \dots, I; \quad j = 1. \quad (\text{E.152})$$

The derivatives of the water vapor continuity equations [cf. Eqs. (2.9) - (2.11)] with respect to the parameter $\alpha^{(2)} : T_{dp}$ are as follows:

$$\frac{\partial N_3^{(i)}}{\partial \alpha^{(2)}} = \frac{\partial N_3^{(i)}}{\partial T_{dp}} \equiv a_3^{i,2} = 0; \quad \ell = 3; \quad i = 1, \dots, I - 1; \quad j = 2, \quad (\text{E.153})$$

$$\frac{\partial N_3^{(I)}}{\partial \alpha^{(2)}} = \frac{\partial N_3^{(I)}}{\partial T_{dp}} \equiv a_3^{I,2} = \frac{\partial \omega_{in}}{\partial T_{dp}}; \quad \ell = 3; \quad i = I; \quad j = 2, \quad (\text{E.154})$$

where

$$\frac{\partial \omega_{in}}{\partial T_{dp}} = - \frac{0.622 a_1 P_{atm} e^{a_0 + \frac{a_1}{T_{dp}}}}{T_{dp}^2 \left(P_{atm} - e^{a_0 + \frac{a_1}{T_{dp}}} \right)^2}. \quad (\text{E.155})$$

The derivatives of the water vapor continuity equations [cf. Eqs. (2.9) - (2.11)] with respect to the parameter $\alpha^{(3)} : T_{w,in}$ are as follows:

$$\frac{\partial N_3^{(1)}}{\partial \alpha^{(3)}} = \frac{\partial N_3^{(1)}}{\partial T_{w,in}} \equiv a_3^{1,3} = 0; \quad \ell = 3; \quad i = I; \quad j = 3, \quad (\text{E.156})$$

APPENDIX E. DERIVATIVES OF THE MODEL EQUATIONS WITH RESPECT TO THE MODEL PARAMETERS

The derivatives of the water vapor continuity equations [cf. Eqs. (2.9) - (2.11)] with respect to the parameter $\alpha^{(4)} : P_{atm}$ are as follows:

$$\frac{\partial N_3^{(i)}}{\partial \alpha^{(4)}} = \frac{\partial N_3^{(i)}}{\partial P_{atm}} \equiv a_3^{i,4} = 0; \quad \ell = 3; \quad i = 1, \dots, I-1; \quad j = 4, \quad (\text{E.157})$$

$$\frac{\partial N_3^{(I)}}{\partial \alpha^{(4)}} = \frac{\partial N_3^{(I)}}{\partial P_{atm}} \equiv a_3^{I,4} = \frac{\partial \omega_{in}}{\partial P_{atm}}; \quad \ell = 3; \quad i = I; \quad j = 4, \quad (\text{E.158})$$

where

$$\frac{\partial \omega_{in}}{\partial P_{atm}} = -\frac{0.622e^{a_0 + \frac{a_1}{T_{dp}}}}{\left(P_{atm} - e^{a_0 + \frac{a_1}{T_{dp}}}\right)^2}. \quad (\text{E.159})$$

The derivatives of the water vapor continuity equations [cf. Eqs. (2.9) - (2.11)] with respect to the parameter $\alpha^{(5)} : V_w$ are as follows:

$$\frac{\partial N_3^{(i)}}{\partial \alpha^{(5)}} = \frac{\partial N_3^{(i)}}{\partial V_w} \equiv a_3^{i,5} = 0; \quad \ell = 3; \quad i = 1, \dots, I; \quad j = 5. \quad (\text{E.160})$$

The derivatives of the water vapor continuity equations [cf. Eqs. (2.9) - (2.11)] with respect to the parameter $\alpha^{(6)} : k_{sum}$ are as follows:

$$\frac{\partial N_3^{(i)}}{\partial \alpha^{(6)}} = \frac{\partial N_3^{(i)}}{\partial k_{sum}} \equiv a_3^{i,6} = 0; \quad \ell = 3; \quad i = 1, \dots, I; \quad j = 6. \quad (\text{E.161})$$

The derivatives of the water vapor continuity equations [cf. Eqs. (2.9) - (2.11)] with respect to the parameter $\alpha^{(7)} : \mu$ are as follows:

$$\frac{\partial N_3^{(i)}}{\partial \alpha^{(7)}} = \frac{\partial N_3^{(i)}}{\partial \mu} \equiv a_3^{i,7} = 0; \quad \ell = 3; \quad i = 1, \dots, I; \quad j = 7. \quad (\text{E.162})$$

The derivatives of the water vapor continuity equations [cf. Eqs. (2.9) - (2.11)] with respect to the parameter $\alpha^{(8)} : \nu$ are as follows:

$$\frac{\partial N_3^{(i)}}{\partial \alpha^{(8)}} = \frac{\partial N_3^{(i)}}{\partial \nu} \equiv a_3^{i,8} = 0; \quad \ell = 3; \quad i = 1, \dots, I; \quad j = 8. \quad (\text{E.163})$$

APPENDIX E. DERIVATIVES OF THE MODEL EQUATIONS WITH RESPECT TO THE MODEL PARAMETERS

The derivatives of the water vapor continuity equations [cf. Eqs. (2.9) - (2.11)] with respect to the parameter $\alpha^{(9)} : k_{air}$ are as follows:

$$\frac{\partial N_3^{(i)}}{\partial \alpha^{(9)}} = \frac{\partial N_3^{(i)}}{\partial k_{air}} \equiv a_3^{i,9} = 0; \quad \ell = 3; \quad i = 1, \dots, I; \quad j = 9. \quad (\text{E.164})$$

The derivatives of the water vapor continuity equations [cf. Eqs. (2.9) - (2.11)] with respect to the parameter $\alpha^{(10)} : f_{ht}$ are as follows:

$$\frac{\partial N_3^{(i)}}{\partial \alpha^{(10)}} = \frac{\partial N_3^{(i)}}{\partial f_{ht}} \equiv a_3^{i,10} = 0; \quad \ell = 3; \quad i = 1, \dots, I; \quad j = 10. \quad (\text{E.165})$$

The derivatives of the water vapor continuity equations [cf. Eqs. (2.9) - (2.11)] with respect to the parameter $\alpha^{(11)} : f_{mt}$ are as follows:

$$\frac{\partial N_3^{(i)}}{\partial \alpha^{(11)}} = \frac{\partial N_3^{(i)}}{\partial f_{mt}} \equiv a_3^{i,11} = 0; \quad \ell = 3; \quad i = 1, \dots, I; \quad j = 11. \quad (\text{E.166})$$

The derivatives of the water vapor continuity equations [cf. Eqs. (2.9) - (2.11)] with respect to the parameter $\alpha^{(12)} : f$ are as follows:

$$\frac{\partial N_3^{(i)}}{\partial \alpha^{(12)}} = \frac{\partial N_3^{(i)}}{\partial f} \equiv a_3^{i,12} = 0; \quad \ell = 3; \quad i = 1, \dots, I; \quad j = 12. \quad (\text{E.167})$$

The derivatives of the water vapor continuity equations [cf. Eqs. (2.9) - (2.11)] with respect to the parameter $\alpha^{(13)} : a_0$ are as follows:

$$\frac{\partial N_3^{(i)}}{\partial \alpha^{(13)}} = \frac{\partial N_3^{(i)}}{\partial a_0} \equiv a_3^{i,13} = 0; \quad \ell = 3; \quad i = 1, \dots, I-1; \quad j = 13, \quad (\text{E.168})$$

$$\frac{\partial N_3^{(I)}}{\partial \alpha^{(13)}} = \frac{\partial N_3^{(I)}}{\partial a_0} \equiv a_3^{I,13} = \frac{\partial \omega_{in}}{\partial a_0}; \quad \ell = 3; \quad i = I; \quad j = 13, \quad (\text{E.169})$$

where

$$\frac{\partial \omega_{in}}{\partial a_0} = \frac{0.622 P_{atm} e^{a_0 + \frac{a_1}{T_{dp}}}}{\left(P_{atm} - e^{a_0 + \frac{a_1}{T_{dp}}} \right)^2}; \quad (\text{E.170})$$

APPENDIX E. DERIVATIVES OF THE MODEL EQUATIONS WITH RESPECT TO THE MODEL PARAMETERS

The derivatives of the water vapor continuity equations [cf. Eqs. (2.9) - (2.11)] with respect to the parameter $\alpha^{(14)} : a_1$ are as follows:

$$\frac{\partial N_3^{(i)}}{\partial \alpha^{(14)}} = \frac{\partial N_3^{(i)}}{\partial a_1} \equiv a_3^{i,14} = 0; \quad \ell = 3; \quad i = 1, \dots, I-1; \quad j = 14, \quad (\text{E.171})$$

$$\frac{\partial N_3^{(I)}}{\partial \alpha^{(14)}} = \frac{\partial N_3^{(I)}}{\partial a_1} \equiv a_3^{I,14} = \frac{\partial \omega_{in}}{\partial a_1}; \quad \ell = 3; \quad i = I; \quad j = 14, \quad (\text{E.172})$$

where

$$\frac{\partial \omega_{in}}{\partial a_1} = \frac{0.622 P_{atm} e^{a_0 + \frac{a_1}{T_{dp}}}}{T_{dp} \left(P_{atm} - e^{a_0 + \frac{a_1}{T_{dp}}} \right)^2}. \quad (\text{E.173})$$

The derivatives of the water vapor continuity equations [cf. Eqs. (2.9) - (2.11)] with respect to the parameter $\alpha^{(15)} : a_{0,c_{pa}}$ are as follows:

$$\frac{\partial N_3^{(i)}}{\partial \alpha^{(15)}} = \frac{\partial N_3^{(i)}}{\partial a_{0,c_{pa}}} \equiv a_3^{i,15} = 0; \quad \ell = 3; \quad i = 1, \dots, I; \quad j = 15. \quad (\text{E.174})$$

The derivatives of the water vapor continuity equations [cf. Eqs. (2.9) - (2.11)] with respect to the parameter $\alpha^{(16)} : a_{1,c_{pa}}$ are as follows:

$$\frac{\partial N_3^{(i)}}{\partial \alpha^{(16)}} = \frac{\partial N_3^{(i)}}{\partial a_{1,c_{pa}}} \equiv a_3^{i,16} = 0; \quad \ell = 3; \quad i = 1, \dots, I; \quad j = 16. \quad (\text{E.175})$$

The derivatives of the water vapor continuity equations [cf. Eqs. (2.9) - (2.11)] with respect to the parameter $\alpha^{(17)} : a_{2,c_{pa}}$ are as follows:

$$\frac{\partial N_3^{(i)}}{\partial \alpha^{(17)}} = \frac{\partial N_3^{(i)}}{\partial a_{2,c_{pa}}} \equiv a_3^{i,17} = 0; \quad \ell = 3; \quad i = 1, \dots, I; \quad j = 17. \quad (\text{E.176})$$

The derivatives of the water vapor continuity equations [cf. Eqs. (2.9) - (2.11)] with respect to the parameter $\alpha^{(18)} : a_{0,D_{av}}$ are as follows:

$$\frac{\partial N_3^{(i)}}{\partial \alpha^{(18)}} = \frac{\partial N_3^{(i)}}{\partial a_{0,D_{av}}} \equiv a_3^{i,18} = 0; \quad \ell = 3; \quad i = 1, \dots, I; \quad j = 18. \quad (\text{E.177})$$

APPENDIX E. DERIVATIVES OF THE MODEL EQUATIONS WITH
RESPECT TO THE MODEL PARAMETERS

The derivatives of the water vapor continuity equations [cf. Eqs. (2.9) - (2.11)] with respect to the parameter $\alpha^{(19)} : a_{1,D_{av}}$ are as follows:

$$\frac{\partial N_3^{(i)}}{\partial \alpha^{(19)}} = \frac{\partial N_3^{(i)}}{\partial a_{1,D_{av}}} \equiv a_3^{i,19} = 0; \quad \ell = 3; \quad i = 1, \dots, I; \quad j = 19. \quad (\text{E.178})$$

The derivatives of the water vapor continuity equations [cf. Eqs. (2.9) - (2.11)] with respect to the parameter $\alpha^{(20)} : a_{2,D_{av}}$ are as follows:

$$\frac{\partial N_3^{(i)}}{\partial \alpha^{(20)}} = \frac{\partial N_3^{(i)}}{\partial a_{2,D_{av}}} \equiv a_3^{i,20} = 0; \quad \ell = 3; \quad i = 1, \dots, I; \quad j = 20. \quad (\text{E.179})$$

The derivatives of the water vapor continuity equations [cf. Eqs. (2.9) - (2.11)] with respect to the parameter $\alpha^{(21)} : a_{3,D_{av}}$ are as follows:

$$\frac{\partial N_3^{(i)}}{\partial \alpha^{(21)}} = \frac{\partial N_3^{(i)}}{\partial a_{3,D_{av}}} \equiv a_3^{i,21} = 0; \quad \ell = 3; \quad i = 1, \dots, I; \quad j = 21. \quad (\text{E.180})$$

The derivatives of the water vapor continuity equations [cf. Eqs. (2.9) - (2.11)] with respect to the parameter $\alpha^{(22)} : a_{0f}$ are as follows:

$$\frac{\partial N_3^{(i)}}{\partial \alpha^{(22)}} = \frac{\partial N_3^{(i)}}{\partial a_{0f}} \equiv a_3^{i,22} = 0; \quad \ell = 3; \quad i = 1, \dots, I; \quad j = 22. \quad (\text{E.181})$$

The derivatives of the water vapor continuity equations [cf. Eqs. (2.9) - (2.11)] with respect to the parameter $\alpha^{(23)} : a_{1f}$ are as follows:

$$\frac{\partial N_3^{(i)}}{\partial \alpha^{(23)}} = \frac{\partial N_3^{(i)}}{\partial a_{1f}} \equiv a_3^{i,23} = 0; \quad \ell = 3; \quad i = 1, \dots, I; \quad j = 23. \quad (\text{E.182})$$

The derivatives of the water vapor continuity equations [cf. Eqs. (2.9) - (2.11)] with respect to the parameter $\alpha^{(24)} : a_{0g}$ are as follows:

$$\frac{\partial N_3^{(i)}}{\partial \alpha^{(24)}} = \frac{\partial N_3^{(i)}}{\partial a_{0g}} \equiv a_3^{i,24} = 0; \quad \ell = 3; \quad i = 1, \dots, I; \quad j = 24. \quad (\text{E.183})$$

APPENDIX E. DERIVATIVES OF THE MODEL EQUATIONS WITH
RESPECT TO THE MODEL PARAMETERS

The derivatives of the water vapor continuity equations [cf. Eqs. (2.9) - (2.11)] with respect to the parameter $\alpha^{(25)} : a_{1g}$ are as follows:

$$\frac{\partial N_3^{(i)}}{\partial \alpha^{(25)}} = \frac{\partial N_3^{(i)}}{\partial a_{1g}} \equiv a_3^{i,25} = 0; \quad \ell = 3; \quad i = 1, \dots, I; \quad j = 25. \quad (\text{E.184})$$

The derivatives of the water vapor continuity equations [cf. Eqs. (2.9) - (2.11)] with respect to the parameter $\alpha^{(26)} : a_{0,Nu}$ are as follows:

$$\frac{\partial N_3^{(i)}}{\partial \alpha^{(26)}} = \frac{\partial N_3^{(i)}}{\partial a_{0,Nu}} \equiv a_3^{i,26} = 0; \quad \ell = 3; \quad i = 1, \dots, I; \quad j = 26. \quad (\text{E.185})$$

The derivatives of the water vapor continuity equations [cf. Eqs. (2.9) - (2.11)] with respect to the parameter $\alpha^{(27)} : a_{1,Nu}$ are as follows:

$$\frac{\partial N_3^{(i)}}{\partial \alpha^{(27)}} = \frac{\partial N_3^{(i)}}{\partial a_{1,Nu}} \equiv a_3^{i,27} = 0; \quad \ell = 3; \quad i = 1, \dots, I; \quad j = 27. \quad (\text{E.186})$$

The derivatives of the water vapor continuity equations [cf. Eqs. (2.9) - (2.11)] with respect to the parameter $\alpha^{(28)} : a_{2,Nu}$ are as follows:

$$\frac{\partial N_3^{(i)}}{\partial \alpha^{(28)}} = \frac{\partial N_3^{(i)}}{\partial a_{2,Nu}} \equiv a_3^{i,28} = 0; \quad \ell = 3; \quad i = 1, \dots, I; \quad j = 28. \quad (\text{E.187})$$

The derivatives of the water vapor continuity equations [cf. Eqs. (2.9) - (2.11)] with respect to the parameter $\alpha^{(29)} : a_{3,Nu}$ are as follows:

$$\frac{\partial N_3^{(i)}}{\partial \alpha^{(29)}} = \frac{\partial N_3^{(i)}}{\partial a_{3,Nu}} \equiv a_3^{i,29} = 0; \quad \ell = 3; \quad i = 1, \dots, I; \quad j = 29. \quad (\text{E.188})$$

The derivatives of the water vapor continuity equations [cf. Eqs. (2.9) - (2.11)] with respect to the parameter $\alpha^{(30)} : W_{dkx}$ are as follows:

$$\frac{\partial N_3^{(i)}}{\partial \alpha^{(30)}} = \frac{\partial N_3^{(i)}}{\partial W_{dkx}} \equiv a_3^{i,30} = 0; \quad \ell = 3; \quad i = 1, \dots, I; \quad j = 30. \quad (\text{E.189})$$

APPENDIX E. DERIVATIVES OF THE MODEL EQUATIONS WITH
RESPECT TO THE MODEL PARAMETERS

The derivatives of the water vapor continuity equations [cf. Eqs. (2.9) - (2.11)] with respect to the parameter $\alpha^{(31)} : W_{dky}$ are as follows:

$$\frac{\partial N_3^{(i)}}{\partial \alpha^{(31)}} = \frac{\partial N_3^{(i)}}{\partial W_{dky}} \equiv a_3^{i,31} = 0; \quad \ell = 3; \quad i = 1, \dots, I; \quad j = 31. \quad (\text{E.190})$$

The derivatives of the water vapor continuity equations [cf. Eqs. (2.9) - (2.11)] with respect to the parameter $\alpha^{(32)} : \Delta z_{dk}$ are as follows:

$$\frac{\partial N_3^{(i)}}{\partial \alpha^{(32)}} = \frac{\partial N_3^{(i)}}{\partial \Delta z_{dk}} \equiv a_3^{i,32} = 0; \quad \ell = 3; \quad i = 1, \dots, I; \quad j = 32. \quad (\text{E.191})$$

The derivatives of the water vapor continuity equations [cf. Eqs. (2.9) - (2.11)] with respect to the parameter $\alpha^{(33)} : \Delta z_{fan}$ are as follows:

$$\frac{\partial N_3^{(i)}}{\partial \alpha^{(33)}} = \frac{\partial N_3^{(i)}}{\partial \Delta z_{fan}} \equiv a_3^{i,33} = 0; \quad \ell = 3; \quad i = 1, \dots, I; \quad j = 33. \quad (\text{E.192})$$

The derivatives of the water vapor continuity equations [cf. Eqs. (2.9) - (2.11)] with respect to the parameter $\alpha^{(34)} : D_{fan}$ are as follows:

$$\frac{\partial N_3^{(i)}}{\partial \alpha^{(34)}} = \frac{\partial N_3^{(i)}}{\partial D_{fan}} \equiv a_3^{i,34} = 0; \quad \ell = 3; \quad i = 1, \dots, I; \quad j = 34, \quad (\text{E.193})$$

The derivatives of the water vapor continuity equations [cf. Eqs. (2.9) - (2.11)] with respect to the parameter $\alpha^{(35)} : \Delta z_{fill}$ are as follows:

$$\frac{\partial N_3^{(i)}}{\partial \alpha^{(35)}} = \frac{\partial N_3^{(i)}}{\partial \Delta z_{fill}} \equiv a_3^{i,35} = 0; \quad \ell = 3; \quad i = 1, \dots, I; \quad j = 35. \quad (\text{E.194})$$

The derivatives of the water vapor continuity equations [cf. Eqs. (2.9) - (2.11)] with respect to the parameter $\alpha^{(36)} : \Delta z_{rain}$ are as follows:

$$\frac{\partial N_3^{(i)}}{\partial \alpha^{(36)}} = \frac{\partial N_3^{(i)}}{\partial \Delta z_{rain}} \equiv a_3^{i,36} = 0; \quad \ell = 3; \quad i = 1, \dots, I; \quad j = 36. \quad (\text{E.195})$$

APPENDIX E. DERIVATIVES OF THE MODEL EQUATIONS WITH
RESPECT TO THE MODEL PARAMETERS

The derivatives of the water vapor continuity equations [cf. Eqs. (2.9) - (2.11)] with respect to the parameter $\alpha^{(37)} : \Delta z_{bs}$ are as follows:

$$\frac{\partial N_3^{(i)}}{\partial \alpha^{(37)}} = \frac{\partial N_3^{(i)}}{\partial \Delta z_{bs}} \equiv a_3^{i,37} = 0; \quad \ell = 3; \quad i = 1, \dots, I; \quad j = 37. \quad (\text{E.196})$$

The derivatives of the water vapor continuity equations [cf. Eqs. (2.9) - (2.11)] with respect to the parameter $\alpha^{(38)} : \Delta z_{de}$ are as follows:

$$\frac{\partial N_3^{(i)}}{\partial \alpha^{(38)}} = \frac{\partial N_3^{(i)}}{\partial \Delta z_{de}} \equiv a_3^{i,38} = 0; \quad \ell = 3; \quad i = 1, \dots, I; \quad j = 38. \quad (\text{E.197})$$

The derivatives of the water vapor continuity equations [cf. Eqs. (2.9) - (2.11)] with respect to the parameter $\alpha^{(39)} : D_h$ are as follows:

$$\frac{\partial N_3^{(i)}}{\partial \alpha^{(39)}} = \frac{\partial N_3^{(i)}}{\partial D_h} \equiv a_3^{i,39} = 0; \quad \ell = 3; \quad i = 1, \dots, I; \quad j = 39. \quad (\text{E.198})$$

The derivatives of the water vapor continuity equations [cf. Eqs. (2.9) - (2.11)] with respect to the parameter $\alpha^{(40)} : A_{fill}$ are as follows:

$$\frac{\partial N_3^{(i)}}{\partial \alpha^{(40)}} = \frac{\partial N_3^{(i)}}{\partial A_{fill}} \equiv a_3^{i,40} = 0; \quad \ell = 3; \quad i = 1, \dots, I; \quad j = 40. \quad (\text{E.199})$$

The derivatives of the water vapor continuity equations [cf. Eqs. (2.9) - (2.11)] with respect to the parameter $\alpha^{(41)} : A_{surf}$ are as follows:

$$\frac{\partial N_3^{(i)}}{\partial \alpha^{(41)}} = \frac{\partial N_3^{(i)}}{\partial A_{surf}} \equiv a_3^{i,41} = 0; \quad \ell = 3; \quad i = 1, \dots, I; \quad j = 41. \quad (\text{E.200})$$

The derivatives of the water vapor continuity equations [cf. Eqs. (2.9) - (2.11)] with respect to the parameter $\alpha^{(42)} : \text{Pr}$ are as follows:

$$\frac{\partial N_3^{(i)}}{\partial \alpha^{(42)}} = \frac{\partial N_3^{(i)}}{\partial \text{Pr}} \equiv a_3^{i,42} = 0; \quad \ell = 3; \quad i = 1, \dots, I; \quad j = 42. \quad (\text{E.201})$$

APPENDIX E. DERIVATIVES OF THE MODEL EQUATIONS WITH RESPECT TO THE MODEL PARAMETERS

The derivatives of the water vapor continuity equations [cf. Eqs. (2.9) - (2.11)] with respect to the parameter $\alpha^{(43)} : w_{tsa}$ are as follows:

$$\frac{\partial N_3^{(i)}}{\partial \alpha^{(43)}} = \frac{\partial N_3^{(i)}}{\partial w_{tsa}} \equiv a_3^{i,43} = 0; \quad \ell = 3; \quad i = 1, \dots, I; \quad j = 43. \quad (\text{E.202})$$

The derivatives of the water vapor continuity equations [cf. Eqs. (2.9) - (2.11)] with respect to the parameter $\alpha^{(44)} : m_{w,in}$ are as follows:

$$\frac{\partial N_3^{(1)}}{\partial \alpha^{(44)}} = \frac{\partial N_3^{(1)}}{\partial m_{w,in}} \equiv a_3^{1,44} = \frac{1}{m_a}; \quad \ell = 3; \quad i = 1; \quad j = 44, \quad (\text{E.203})$$

$$\frac{\partial N_3^{(i)}}{\partial \alpha^{(44)}} = \frac{\partial N_3^{(i)}}{\partial m_{w,in}} \equiv a_3^{i,44} = 0; \quad \ell = 3; \quad i = 2, \dots, I; \quad j = 44. \quad (\text{E.204})$$

The derivatives of the water vapor continuity equations [cf. Eqs. (2.9) - (2.11)] with respect to the parameter $\alpha^{(45)} : T_{a,in}$ are as follows:

$$\frac{\partial N_3^{(i)}}{\partial \alpha^{(45)}} = \frac{\partial N_3^{(i)}}{\partial T_{a,in}} \equiv a_3^{i,45} = 0; \quad \ell = 3; \quad i = 1, \dots, I; \quad j = 45. \quad (\text{E.205})$$

The derivatives of the water vapor continuity equations [cf. Eqs. (2.9) - (2.11)] with respect to the parameter $\alpha^{(46)} : \omega_{in}$ are as follows:

$$\frac{\partial N_3^{(i)}}{\partial \alpha^{(46)}} = \frac{\partial N_3^{(i)}}{\partial \omega_{in}} \equiv a_3^{i,46} = 0; \quad \ell = 3; \quad i = 1, \dots, I-1; \quad j = 46, \quad (\text{E.206})$$

$$\frac{\partial N_3^{(I)}}{\partial \alpha^{(46)}} = \frac{\partial N_3^{(I)}}{\partial \omega_{in}} \equiv a_3^{I,46} = 1; \quad \ell = 3; \quad i = I; \quad j = 46. \quad (\text{E.207})$$

The derivatives of the water vapor continuity equations [cf. Eqs. (2.9) - (2.11)] with respect to the parameter $\alpha^{(47)} : Sc$ are as follows:

$$\frac{\partial N_3^{(i)}}{\partial \alpha^{(47)}} = \frac{\partial N_3^{(i)}}{\partial Sc} \equiv a_3^{i,47} = 0; \quad \ell = 3; \quad i = 1, \dots, I; \quad j = 47. \quad (\text{E.208})$$

APPENDIX E. DERIVATIVES OF THE MODEL EQUATIONS WITH
RESPECT TO THE MODEL PARAMETERS

**E.1.4 Derivatives of the air/water vapor energy balance
equations with respect to the parameters**

The derivatives of the air/water vapor energy balance equations [cf. Eqs. (2.12) - (2.14)] with respect to the parameter $\alpha^{(1)} : T_{db}$ are as follows:

$$\frac{\partial N_4^{(i)}}{\partial \alpha^{(1)}} = \frac{\partial N_4^{(i)}}{\partial T_{db}} \equiv a_4^{i,1} = 0; \quad \ell = 4; \quad i = 1, \dots, I-1; \quad j = 1, \quad (\text{E.209})$$

$$\begin{aligned} \frac{\partial N_4^{(I)}}{\partial \alpha^{(1)}} &= \frac{\partial N_4^{(I)}}{\partial T_{db}} \equiv a_4^{I,1} = C_p^{(I)} \left(\frac{T_a^{(I)} + 273.15}{2}, \boldsymbol{\alpha} \right) + \omega_{in} \frac{\partial h_{g,a}^{(I+1)}(T_{a,in}, \boldsymbol{\alpha})}{\partial T_{a,in}} \\ &= C_p^{(I)} \left(\frac{T_a^{(I)} + 273.15}{2}, \boldsymbol{\alpha} \right) + \omega_{in} a_{1g}; \quad \ell = 4; \quad i = I; \quad j = 1. \end{aligned} \quad (\text{E.210})$$

Note: The value of the inlet air temperature is set equal to dry-bulb temperature, although these quantities are treated as two different parameters in the model. The dry-bulb temperature is used in mass diffusivity calculations. The relation between the two parameters, i.e., $T_{a,in} = T_{db}$, needs to be accounted for when computing the respective derivatives: the derivative of Eq. (2.13) with respect to the dry-bulb temperature must be the same as the derivative of Eq. (2.13) with respect to the inlet air temperature.

The derivatives of the air/water vapor energy balance equations [cf. Eqs. (2.12) - (2.14)] with respect to the parameter $\alpha^{(2)} : T_{dp}$ are as follows:

$$\frac{\partial N_4^{(i)}}{\partial \alpha^{(2)}} = \frac{\partial N_4^{(i)}}{\partial T_{dp}} \equiv a_4^{i,2} = 0; \quad \ell = 4; \quad i = 1, \dots, I-1; \quad j = 2, \quad (\text{E.211})$$

$$\frac{\partial N_4^{(I)}}{\partial \alpha^{(2)}} = \frac{\partial N_4^{(I)}}{\partial T_{dp}} \equiv a_4^{I,2} = \frac{\partial \omega_{in}}{\partial T_{dp}} (a_{1g} T_{a,in} + a_{0g}); \quad \ell = 4; \quad i = I; \quad j = 2, \quad (\text{E.212})$$

where $\frac{\partial \omega_{in}}{\partial T_{dp}}$ was defined in Eq. (E.155).

APPENDIX E. DERIVATIVES OF THE MODEL EQUATIONS WITH
RESPECT TO THE MODEL PARAMETERS

The derivatives of the air/water vapor energy balance equations [cf. Eqs. (2.12) - (2.14)] with respect to the parameter $\alpha^{(3)} : T_{w,in}$ are as follows:

$$\frac{\partial N_4^{(1)}}{\partial \alpha^{(3)}} = \frac{\partial N_4^{(1)}}{\partial T_{w,in}} \equiv a_4^{1,3} = 0; \ell = 4; i = 1; j = 3, \quad (\text{E.213})$$

The derivatives of the air/water vapor energy balance equations [cf. Eqs. (2.12) - (2.14)] with respect to the parameter $\alpha^{(4)} : P_{atm}$ are as follows:

$$\frac{\partial N_4^{(i)}}{\partial \alpha^{(4)}} = \frac{\partial N_4^{(i)}}{\partial P_{atm}} \equiv a_4^{i,4} = 0; \quad \ell = 4; i = 1, \dots, I-1; j = 4, \quad (\text{E.214})$$

$$\frac{\partial N_4^{(I)}}{\partial \alpha^{(4)}} = \frac{\partial N_4^{(I)}}{\partial P_{atm}} \equiv a_4^{I,4} = \frac{\partial \omega_{in}}{\partial P_{atm}} (a_{1g} T_{a,in} + a_{0g}); \quad \ell = 4; i = I; j = 4, \quad (\text{E.215})$$

where $\frac{\partial \omega_{in}}{\partial P_{atm}}$ was defined in Eq. (E.159).

The derivatives of the air/water vapor energy balance equations [cf. Eqs. (2.12) - (2.14)] with respect to the parameter $\alpha^{(5)} : V_w$ are as follows:

$$\frac{\partial N_4^{(i)}}{\partial \alpha^{(5)}} = \frac{\partial N_4^{(i)}}{\partial V_w} \equiv a_4^{i,5} = 0; \quad \ell = 4; i = 1, \dots, I; j = 5, \quad (\text{E.216})$$

The derivatives of the air/water vapor energy balance equations [cf. Eqs. (2.12) - (2.14)] with respect to the parameter $\alpha^{(6)} : k_{sum}$ are as follows:

$$\frac{\partial N_4^{(i)}}{\partial \alpha^{(6)}} = \frac{\partial N_4^{(i)}}{\partial k_{sum}} \equiv a_4^{i,6} = 0; \quad \ell = 4; i = 1, \dots, I; j = 6. \quad (\text{E.217})$$

The derivatives of the air/water vapor energy balance equations [cf. Eqs. (2.12) - (2.14)] with respect to the parameter $\alpha^{(7)} : \mu$ are as follows:

$$\frac{\partial N_4^{(i)}}{\partial \alpha^{(7)}} = \frac{\partial N_4^{(i)}}{\partial \mu} \equiv a_4^{i,7} = \frac{(T_w^{(i+1)} - T_a^{(i)})}{m_a} \frac{\partial H(m_a, \boldsymbol{\alpha})}{\partial \mu}; \quad \ell = 4; i = 1, \dots, I; j = 7, \quad (\text{E.218})$$

APPENDIX E. DERIVATIVES OF THE MODEL EQUATIONS WITH RESPECT TO THE MODEL PARAMETERS

where $\frac{\partial H(m_a, \boldsymbol{\alpha})}{\partial \mu}$ was defined in Eq. (E.102).

The derivatives of the air/water vapor energy balance equations [cf. Eqs. (2.12) - (2.14)] with respect to the parameter $\alpha^{(8)} : \nu$ are as follows:

$$\frac{\partial N_4^{(i)}}{\partial \alpha^{(8)}} = \frac{\partial N_4^{(i)}}{\partial \nu} \equiv a_4^{i,8} = 0; \quad \ell = 4; \quad i = 1, \dots, I; \quad j = 8. \quad (\text{E.219})$$

The derivatives of the air/water vapor energy balance equations [cf. Eqs. (2.12) - (2.14)] with respect to the parameter $\alpha^{(9)} : k_{air}$ are as follows:

$$\frac{\partial N_4^{(i)}}{\partial \alpha^{(9)}} = \frac{\partial N_4^{(i)}}{\partial k_{air}} \equiv a_4^{i,9} = \frac{(T_w^{(i+1)} - T_a^{(i)})}{m_a} \frac{\partial H(m_a, \boldsymbol{\alpha})}{\partial k_{air}}; \quad \ell = 4; \quad i = 1, \dots, I; \quad j = 9, \quad (\text{E.220})$$

where $\frac{\partial H(m_a, \boldsymbol{\alpha})}{\partial k_{air}}$ was defined in Eq. (E.105).

The derivatives of the air/water vapor energy balance equations [cf. Eqs. (2.12) - (2.14)] with respect to the parameter $\alpha^{(10)} : f_{ht}$ are as follows:

$$\frac{\partial N_4^{(i)}}{\partial \alpha^{(10)}} = \frac{\partial N_4^{(i)}}{\partial f_{ht}} \equiv a_4^{i,10} = \frac{(T_w^{(i+1)} - T_a^{(i)})}{m_a} \frac{\partial H(m_a, \boldsymbol{\alpha})}{\partial f_{ht}}; \quad \ell = 4; \quad i = 1, \dots, I; \quad j = 10, \quad (\text{E.221})$$

where $\frac{\partial H(m_a, \boldsymbol{\alpha})}{\partial f_{ht}}$ was defined in Eq. (E.107).

The derivatives of the air/water vapor energy balance equations [cf. Eqs. (2.12) - (2.14)] with respect to the parameter $\alpha^{(11)} : f_{mt}$ are as follows:

$$\frac{\partial N_4^{(i)}}{\partial \alpha^{(11)}} = \frac{\partial N_4^{(i)}}{\partial f_{mt}} \equiv a_4^{i,11} = 0; \quad \ell = 4; \quad i = 1, \dots, I; \quad j = 11. \quad (\text{E.222})$$

The derivatives of the air/water vapor energy balance equations [cf. Eqs. (2.12) - (2.14)] with respect to the parameter $\alpha^{(12)} : f$ are as follows:

$$\frac{\partial N_4^{(i)}}{\partial \alpha^{(12)}} = \frac{\partial N_4^{(i)}}{\partial f} \equiv a_4^{i,12} = 0; \quad \ell = 4; \quad i = 1, \dots, I; \quad j = 12. \quad (\text{E.223})$$

APPENDIX E. DERIVATIVES OF THE MODEL EQUATIONS WITH RESPECT TO THE MODEL PARAMETERS

The derivatives of the air/water vapor energy balance equations [cf. Eqs. (2.12) - (2.14)] with respect to the parameter $\alpha^{(13)} : a_0$ are as follows:

$$\frac{\partial N_4^{(i)}}{\partial \alpha^{(13)}} = \frac{\partial N_4^{(i)}}{\partial a_0} \equiv a_4^{i,13} = 0; \quad \ell = 4; \quad i = 1, \dots, I-1; \quad j = 13, \quad (\text{E.224})$$

$$\frac{\partial N_4^{(I)}}{\partial \alpha^{(13)}} = \frac{\partial N_4^{(I)}}{\partial a_0} \equiv a_4^{I,13} = \frac{\partial \omega_{in}}{\partial a_0} (a_1 g T_{a,in} + a_0 g); \quad \ell = 4; \quad i = I; \quad j = 13, \quad (\text{E.225})$$

where $\frac{\partial \omega_{in}}{\partial a_0}$ was defined in Eq. (E.170).

The derivatives of the air/water vapor energy balance equations [cf. Eqs. (2.12) - (2.14)] with respect to the parameter $\alpha^{(14)} : a_1$ are as follows:

$$\frac{\partial N_4^{(i)}}{\partial \alpha^{(14)}} = \frac{\partial N_4^{(i)}}{\partial a_1} \equiv a_4^{i,14} = 0; \quad \ell = 4; \quad i = 1, \dots, I-1; \quad j = 14, \quad (\text{E.226})$$

$$\frac{\partial N_4^{(I)}}{\partial \alpha^{(14)}} = \frac{\partial N_4^{(I)}}{\partial a_1} \equiv a_4^{I,14} = \frac{\partial \omega_{in}}{\partial a_1} (a_1 g T_{a,in} + a_0 g); \quad \ell = 4; \quad i = I; \quad j = 14, \quad (\text{E.227})$$

where $\frac{\partial \omega_{in}}{\partial a_1}$ was defined in Eq. (E.173).

The derivatives of the air/water vapor energy balance equations [cf. Eqs. (2.12) - (2.14)] with respect to the parameter $\alpha^{(15)} : a_{0,c_{pa}}$ are as follows:

$$\begin{aligned} \frac{\partial N_4^{(i)}}{\partial \alpha^{(15)}} &= \frac{\partial N_4^{(i)}}{\partial a_{0,c_{pa}}} \equiv a_4^{i,15} = (T_a^{(i+1)} - T_a^{(i)}) \frac{\partial C_p^{(i)} \left(\frac{T_a^{(i)} + 273.15}{2}, \boldsymbol{\alpha} \right)}{\partial a_{0,c_{pa}}} \\ &= T_a^{(i+1)} - T_a^{(i)}; \quad \ell = 4; \quad i = 1, \dots, I; \quad j = 15. \end{aligned} \quad (\text{E.228})$$

The derivatives of the air/water vapor energy balance equations [cf. Eqs. (2.12) - (2.14)] with respect to the parameter $\alpha^{(16)} : a_{1,c_{pa}}$ are as follows:

$$\begin{aligned} \frac{\partial N_4^{(i)}}{\partial \alpha^{(16)}} &= \frac{\partial N_4^{(i)}}{\partial a_{1,c_{pa}}} \equiv a_4^{i,16} = (T_a^{(i+1)} - T_a^{(i)}) \frac{\partial C_p^{(i)} \left(\frac{T_a^{(i)} + 273.15}{2}, \boldsymbol{\alpha} \right)}{\partial a_{1,c_{pa}}} \\ &= 0.5 (T_a^{(i+1)} - T_a^{(i)}) (T_a^{(i)} + 273.15); \quad \ell = 4; \quad i = 1, \dots, I; \quad j = 16. \end{aligned} \quad (\text{E.229})$$

APPENDIX E. DERIVATIVES OF THE MODEL EQUATIONS WITH
RESPECT TO THE MODEL PARAMETERS

The derivatives of the air/water vapor energy balance equations [cf. Eqs. (2.12) - (2.14)] with respect to the parameter $\alpha^{(17)} : a_{2,c_{pa}}$ are as follows:

$$\begin{aligned} \frac{\partial N_4^{(i)}}{\partial \alpha^{(17)}} &= \frac{\partial N_4^{(i)}}{\partial a_{2,c_{pa}}} \equiv a_4^{i,17} = (T_a^{(i+1)} - T_a^{(i)}) \frac{\partial C_p^{(i)} \left(\frac{T_a^{(i)} + 273.15}{2}, \boldsymbol{\alpha} \right)}{\partial a_{2,c_{pa}}} \\ &= 0.25 (T_a^{(i+1)} - T_a^{(i)}) [T_a^{(i)} + 273.15]^2; \quad \ell = 4; \quad i = 1, \dots, I; \quad j = 17. \end{aligned} \quad (\text{E.230})$$

The derivatives of the air/water vapor energy balance equations [cf. Eqs. (2.12) - (2.14)] with respect to the parameter $\alpha^{(18)} : a_{0,D_{av}}$ are as follows:

$$\frac{\partial N_4^{(i)}}{\partial \alpha^{(18)}} = \frac{\partial N_4^{(i)}}{\partial a_{0,D_{av}}} \equiv a_4^{i,18} = 0; \quad \ell = 4; \quad i = 1, \dots, I; \quad j = 18. \quad (\text{E.231})$$

The derivatives of the air/water vapor energy balance equations [cf. Eqs. (2.12) - (2.14)] with respect to the parameter $\alpha^{(19)} : a_{1,D_{av}}$ are as follows:

$$\frac{\partial N_4^{(i)}}{\partial \alpha^{(19)}} = \frac{\partial N_4^{(i)}}{\partial a_{1,D_{av}}} \equiv a_4^{i,19} = 0; \quad \ell = 4; \quad i = 1, \dots, I; \quad j = 19. \quad (\text{E.232})$$

The derivatives of the air/water vapor energy balance equations [cf. Eqs. (2.12) - (2.14)] with respect to the parameter $\alpha^{(20)} : a_{2,D_{av}}$ are as follows:

$$\frac{\partial N_4^{(i)}}{\partial \alpha^{(20)}} = \frac{\partial N_4^{(i)}}{\partial a_{2,D_{av}}} \equiv a_4^{i,20} = 0; \quad \ell = 4; \quad i = 1, \dots, I; \quad j = 20. \quad (\text{E.233})$$

The derivatives of the air/water vapor energy balance equations [cf. Eqs. (2.12) - (2.14)] with respect to the parameter $\alpha^{(21)} : a_{3,D_{av}}$ are as follows:

$$\frac{\partial N_4^{(i)}}{\partial \alpha^{(21)}} = \frac{\partial N_4^{(i)}}{\partial a_{3,D_{av}}} \equiv a_4^{i,21} = 0; \quad \ell = 4; \quad i = 1, \dots, I; \quad j = 21. \quad (\text{E.234})$$

APPENDIX E. DERIVATIVES OF THE MODEL EQUATIONS WITH
RESPECT TO THE MODEL PARAMETERS

The derivatives of the air/water vapor energy balance equations [cf. Eqs. (2.12) - (2.14)] with respect to the parameter $\alpha^{(22)} : a_{0f}$ are as follows:

$$\frac{\partial N_4^{(i)}}{\partial \alpha^{(22)}} = \frac{\partial N_4^{(i)}}{\partial a_{0f}} \equiv a_4^{i,22} = 0; \quad \ell = 4; \quad i = 1, \dots, I; \quad j = 22. \quad (\text{E.235})$$

The derivatives of the air/water vapor energy balance equations [cf. Eqs. (2.12) - (2.14)] with respect to the parameter $\alpha^{(23)} : a_{1f}$ are as follows:

$$\frac{\partial N_4^{(i)}}{\partial \alpha^{(23)}} = \frac{\partial N_4^{(i)}}{\partial a_{1f}} \equiv a_4^{i,23} = 0; \quad \ell = 4; \quad i = 1, \dots, I; \quad j = 23. \quad (\text{E.236})$$

The derivatives of the air/water vapor energy balance equations [cf. Eqs. (2.12) - (2.14)] with respect to the parameter $\alpha^{(24)} : a_{0g}$ are as follows:

$$\begin{aligned} \frac{\partial N_4^{(i)}}{\partial \alpha^{(24)}} = \frac{\partial N_4^{(i)}}{\partial a_{0g}} &\equiv a_4^{i,24} = \omega^{(i+1)} - \omega^{(i)} + \frac{m_w^{(i)} - m_w^{(i+1)}}{m_a}; \\ \ell = 4; \quad i = 1, \dots, I; \quad j = 24. \end{aligned} \quad (\text{E.237})$$

The derivatives of the air/water vapor energy balance equations [cf. Eqs. (2.12) - (2.14)] with respect to the parameter $\alpha^{(25)} : a_{1g}$ are as follows:

$$\begin{aligned} \frac{\partial N_4^{(i)}}{\partial \alpha^{(25)}} = \frac{\partial N_4^{(i)}}{\partial a_{1g}} &\equiv a_4^{i,25} = \omega^{(i+1)} T_a^{(i+1)} - \omega^{(i)} T_a^{(i)} + \frac{(m_w^{(i)} - m_w^{(i+1)}) T_w^{(i+1)}}{m_a}; \\ \ell = 4; \quad i = 1, \dots, I; \quad j = 25. \end{aligned} \quad (\text{E.238})$$

The derivatives of the air/water vapor energy balance equations [cf. Eqs. (2.12) - (2.14)] with respect to the parameter $\alpha^{(26)} : a_{0,Nu}$ are as follows:

$$\begin{aligned} \frac{\partial N_4^{(i)}}{\partial \alpha^{(26)}} = \frac{\partial N_4^{(i)}}{\partial a_{0,Nu}} &\equiv a_4^{i,26} = \frac{(T_w^{(i+1)} - T_a^{(i)})}{m_a} \frac{\partial H(m_a, \boldsymbol{\alpha})}{\partial Nu(\text{Re}, \boldsymbol{\alpha})} \frac{\partial Nu(\text{Re}, \boldsymbol{\alpha})}{\partial a_{0,Nu}}; \\ \ell = 4; \quad i = 1, \dots, I; \quad j = 26, \end{aligned} \quad (\text{E.239})$$

APPENDIX E. DERIVATIVES OF THE MODEL EQUATIONS WITH RESPECT TO THE MODEL PARAMETERS

where $\frac{\partial H(m_a, \boldsymbol{\alpha})}{\partial Nu(\text{Re}, \boldsymbol{\alpha})}$ and $\frac{\partial Nu(\text{Re}, \boldsymbol{\alpha})}{\partial a_{0, Nu}}$ were defined previously in Eqs. (E.124) and (E.51) respectively.

The derivatives of the air/water vapor energy balance equations [cf. Eqs. (2.12) - (2.14)] with respect to the parameter $\alpha^{(27)} : a_{1, Nu}$ are as follows:

$$\frac{\partial N_4^{(i)}}{\partial \alpha^{(27)}} = \frac{\partial N_4^{(i)}}{\partial a_{1, Nu}} \equiv a_4^{i, 27} = \frac{(T_w^{(i+1)} - T_a^{(i)})}{m_a} \frac{\partial H(m_a, \boldsymbol{\alpha})}{\partial Nu(\text{Re}, \boldsymbol{\alpha})} \frac{\partial Nu(\text{Re}, \boldsymbol{\alpha})}{\partial a_{1, Nu}}; \quad (\text{E.240})$$

$$\ell = 4; \quad i = 1, \dots, I; \quad j = 27,$$

where $\frac{\partial H(m_a, \boldsymbol{\alpha})}{\partial Nu(\text{Re}, \boldsymbol{\alpha})}$ and $\frac{\partial Nu(\text{Re}, \boldsymbol{\alpha})}{\partial a_{1, Nu}}$ were defined previously in Eqs. (E.124) and (E.54), respectively.

The derivatives of the air/water vapor energy balance equations [cf. Eqs. (2.12) - (2.14)] with respect to the parameter $\alpha^{(28)} : a_{2, Nu}$ are as follows:

$$\frac{\partial N_4^{(i)}}{\partial \alpha^{(28)}} = \frac{\partial N_4^{(i)}}{\partial a_{2, Nu}} \equiv a_4^{i, 28} = \frac{(T_w^{(i+1)} - T_a^{(i)})}{m_a} \frac{\partial H(m_a, \boldsymbol{\alpha})}{\partial Nu(\text{Re}, \boldsymbol{\alpha})} \frac{\partial Nu(\text{Re}, \boldsymbol{\alpha})}{\partial a_{2, Nu}}; \quad (\text{E.241})$$

$$\ell = 4; \quad i = 1, \dots, I; \quad j = 28,$$

where $\frac{\partial H(m_a, \boldsymbol{\alpha})}{\partial Nu(\text{Re}, \boldsymbol{\alpha})}$ and $\frac{\partial Nu(\text{Re}, \boldsymbol{\alpha})}{\partial a_{2, Nu}}$ were defined previously in Eqs. (E.124) and (E.57), respectively.

The derivatives of the air/water vapor energy balance equations [cf. Eqs. (2.12) - (2.14)] with respect to the parameter $\alpha^{(29)} : a_{3, Nu}$ are as follows:

$$\frac{\partial N_4^{(i)}}{\partial \alpha^{(29)}} = \frac{\partial N_4^{(i)}}{\partial a_{3, Nu}} \equiv a_4^{i, 29} = \frac{(T_w^{(i+1)} - T_a^{(i)})}{m_a} \frac{\partial H(m_a, \boldsymbol{\alpha})}{\partial Nu(\text{Re}, \boldsymbol{\alpha})} \frac{\partial Nu(\text{Re}, \boldsymbol{\alpha})}{\partial a_{3, Nu}}; \quad (\text{E.242})$$

$$\ell = 4; \quad i = 1, \dots, I; \quad j = 29,$$

where $\frac{\partial H(m_a, \boldsymbol{\alpha})}{\partial Nu(\text{Re}, \boldsymbol{\alpha})}$ and $\frac{\partial Nu(\text{Re}, \boldsymbol{\alpha})}{\partial a_{3, Nu}}$ were defined previously in Eqs. (E.124) and (E.60), respectively.

APPENDIX E. DERIVATIVES OF THE MODEL EQUATIONS WITH
RESPECT TO THE MODEL PARAMETERS

The derivatives of the air/water vapor energy balance equations [cf. Eqs. (2.12) - (2.14)] with respect to the parameter $\alpha^{(30)} : W_{dkx}$ are as follows:

$$\frac{\partial N_4^{(i)}}{\partial \alpha^{(30)}} = \frac{\partial N_4^{(i)}}{\partial W_{dkx}} \equiv a_4^{i,30} = 0; \quad \ell = 4; \quad i = 1, \dots, I; \quad j = 30. \quad (\text{E.243})$$

The derivatives of the air/water vapor energy balance equations [cf. Eqs. (2.12) - (2.14)] with respect to the parameter $\alpha^{(31)} : W_{dky}$ are as follows:

$$\frac{\partial N_4^{(i)}}{\partial \alpha^{(31)}} = \frac{\partial N_4^{(i)}}{\partial W_{dky}} \equiv a_4^{i,31} = 0; \quad \ell = 4; \quad i = 1, \dots, I; \quad j = 31. \quad (\text{E.244})$$

The derivatives of the air/water vapor energy balance equations [cf. Eqs. (2.12) - (2.14)] with respect to the parameter $\alpha^{(32)} : \Delta z_{dk}$ are as follows:

$$\frac{\partial N_4^{(i)}}{\partial \alpha^{(32)}} = \frac{\partial N_4^{(i)}}{\partial \Delta z_{dk}} \equiv a_4^{i,32} = 0; \quad \ell = 4; \quad i = 1, \dots, I; \quad j = 32. \quad (\text{E.245})$$

The derivatives of the air/water vapor energy balance equations [cf. Eqs. (2.12) - (2.14)] with respect to the parameter $\alpha^{(33)} : \Delta z_{fan}$ are as follows:

$$\frac{\partial N_4^{(i)}}{\partial \alpha^{(33)}} = \frac{\partial N_4^{(i)}}{\partial \Delta z_{fan}} \equiv a_4^{i,33} = 0; \quad \ell = 4; \quad i = 1, \dots, I; \quad j = 33. \quad (\text{E.246})$$

The derivatives of the air/water vapor energy balance equations [cf. Eqs. (2.12) - (2.14)] with respect to the parameter $\alpha^{(34)} : D_{fan}$ are as follows:

$$\frac{\partial N_4^{(i)}}{\partial \alpha^{(34)}} = \frac{\partial N_4^{(i)}}{\partial D_{fan}} \equiv a_4^{i,34} = 0; \quad \ell = 4; \quad i = 1, \dots, I; \quad j = 34, \quad (\text{E.247})$$

The derivatives of the air/water vapor energy balance equations [cf. Eqs. (2.12) - (2.14)] with respect to the parameter $\alpha^{(35)} : \Delta z_{fill}$ are as follows:

$$\frac{\partial N_4^{(i)}}{\partial \alpha^{(35)}} = \frac{\partial N_4^{(i)}}{\partial \Delta z_{fill}} \equiv a_4^{i,35} = 0; \quad \ell = 4; \quad i = 1, \dots, I; \quad j = 35. \quad (\text{E.248})$$

APPENDIX E. DERIVATIVES OF THE MODEL EQUATIONS WITH RESPECT TO THE MODEL PARAMETERS

The derivatives of the air/water vapor energy balance equations [cf. Eqs. (2.12) - (2.14)] with respect to the parameter $\alpha^{(36)} : \Delta z_{rain}$ are as follows:

$$\frac{\partial N_4^{(i)}}{\partial \alpha^{(36)}} = \frac{\partial N_4^{(i)}}{\partial \Delta z_{rain}} \equiv a_4^{i,36} = 0; \quad \ell = 4; \quad i = 1, \dots, I; \quad j = 36. \quad (\text{E.249})$$

The derivatives of the air/water vapor energy balance equations [cf. Eqs. (2.12) - (2.14)] with respect to the parameter $\alpha^{(37)} : \Delta z_{bs}$ are as follows:

$$\frac{\partial N_4^{(i)}}{\partial \alpha^{(37)}} = \frac{\partial N_4^{(i)}}{\partial \Delta z_{bs}} \equiv a_4^{i,37} = 0; \quad \ell = 4; \quad i = 1, \dots, I; \quad j = 37. \quad (\text{E.250})$$

The derivatives of the air/water vapor energy balance equations [cf. Eqs. (2.12) - (2.14)] with respect to the parameter $\alpha^{(38)} : \Delta z_{de}$ are as follows:

$$\frac{\partial N_4^{(i)}}{\partial \alpha^{(38)}} = \frac{\partial N_4^{(i)}}{\partial \Delta z_{de}} \equiv a_4^{i,38} = 0; \quad \ell = 4; \quad i = 1, \dots, I; \quad j = 38. \quad (\text{E.251})$$

The derivatives of the air/water vapor energy balance equations [cf. Eqs. (2.12) - (2.14)] with respect to the parameter $\alpha^{(39)} : D_h$ are as follows:

$$\frac{\partial N_4^{(i)}}{\partial \alpha^{(39)}} = \frac{\partial N_4^{(i)}}{\partial D_h} \equiv a_4^{i,39} = \frac{(T_w^{(i+1)} - T_a^{(i)})}{m_a} \frac{\partial H(m_a, \boldsymbol{\alpha})}{\partial D_h}; \quad (\text{E.252})$$

$$\ell = 4; \quad i = 1, \dots, I; \quad j = 39,$$

where $\frac{\partial H(m_a, \boldsymbol{\alpha})}{\partial D_h}$ was defined in Eq. (E.138).

The derivatives of the air/water vapor energy balance equations [cf. Eqs. (2.12) - (2.14)] with respect to the parameter $\alpha^{(40)} : A_{fill}$ are as follows:

$$\frac{\partial N_4^{(i)}}{\partial \alpha^{(40)}} = \frac{\partial N_4^{(i)}}{\partial A_{fill}} \equiv a_4^{i,40} = \frac{(T_w^{(i+1)} - T_a^{(i)})}{m_a} \frac{\partial H(m_a, \boldsymbol{\alpha})}{\partial A_{fill}}; \quad (\text{E.253})$$

$$\ell = 4; \quad i = 1, \dots, I; \quad j = 40,$$

where $\frac{\partial H(m_a, \boldsymbol{\alpha})}{\partial A_{fill}}$ was defined in Eq. (E.140).

APPENDIX E. DERIVATIVES OF THE MODEL EQUATIONS WITH RESPECT TO THE MODEL PARAMETERS

The derivatives of the air/water vapor energy balance equations [cf. Eqs. (2.12) - (2.14)] with respect to the parameter $\alpha^{(41)} : A_{surf}$ are as follows:

$$\frac{\partial N_4^{(i)}}{\partial \alpha^{(41)}} = \frac{\partial N_4^{(i)}}{\partial A_{surf}} \equiv a_4^{i,41} = \frac{(T_w^{(i+1)} - T_a^{(i)})}{m_a} \frac{\partial H(m_a, \boldsymbol{\alpha})}{\partial A_{surf}}; \quad (\text{E.254})$$

$$\ell = 4; \quad i = 1, \dots, I; \quad j = 41,$$

where $\frac{\partial H(m_a, \boldsymbol{\alpha})}{\partial A_{surf}}$ was defined in Eq. (E.142).

The derivatives of the air/water vapor energy balance equations [cf. Eqs. (2.12) - (2.14)] with respect to the parameter $\alpha^{(42)} : \text{Pr}$ are as follows:

$$\frac{\partial N_4^{(i)}}{\partial \alpha^{(42)}} = \frac{\partial N_4^{(i)}}{\partial \text{Pr}} \equiv a_4^{i,42} = \frac{(T_w^{(i+1)} - T_a^{(i)})}{m_a} \frac{\partial H(m_a, \boldsymbol{\alpha})}{\partial \text{Pr}}; \quad (\text{E.255})$$

$$\ell = 4; \quad i = 1, \dots, I; \quad j = 42,$$

where $\frac{\partial H(m_a, \boldsymbol{\alpha})}{\partial \text{Pr}}$ was defined in Eq. (E.144).

The derivatives of the air/water vapor energy balance equations [cf. Eqs. (2.12) - (2.14)] with respect to the parameter $\alpha^{(43)} : w_{tsa}$ are as follows:

$$\frac{\partial N_4^{(i)}}{\partial \alpha^{(43)}} = \frac{\partial N_4^{(i)}}{\partial w_{tsa}} \equiv a_4^{i,43} = \frac{(T_w^{(i+1)} - T_a^{(i)})}{m_a} \frac{\partial H(m_a, \boldsymbol{\alpha})}{\partial w_{tsa}}; \quad (\text{E.256})$$

$$\ell = 4; \quad i = 1, \dots, I; \quad j = 43,$$

where

$$\frac{\partial H(m_a, \boldsymbol{\alpha})}{\partial w_{tsa}} = \frac{f_{ht} Nu(\text{Re}, \boldsymbol{\alpha}) k_{air} A_{surf}}{D_h I} \quad (\text{E.257})$$

The derivatives of the air/water vapor energy balance equations [cf. Eqs. (2.12) - (2.14)] with respect to the parameter $\alpha^{(44)} : m_{w,in}$ are as follows:

$$\frac{\partial N_4^{(1)}}{\partial \alpha^{(44)}} = \frac{\partial N_4^{(1)}}{\partial m_{w,in}} \equiv a_4^{1,44} = \frac{h_{g,w}^{(2)}(T_w^{(2)}, \boldsymbol{\alpha})}{m_a} = \frac{a_{1g} T_w^{(2)} + a_{0g}}{m_a}; \quad (\text{E.258})$$

$$\ell = 4; \quad i = 1; \quad j = 44,$$

APPENDIX E. DERIVATIVES OF THE MODEL EQUATIONS WITH
RESPECT TO THE MODEL PARAMETERS

$$\frac{\partial N_4^{(i)}}{\partial \alpha^{(44)}} = \frac{\partial N_4^{(i)}}{\partial m_{w,in}} \equiv a_4^{i,44} = 0; \quad \ell = 4; \quad i = 2, \dots, I; \quad j = 44. \quad (\text{E.259})$$

The derivatives of the air/water vapor energy balance equations [cf. Eqs. (2.12) - (2.14)] with respect to the parameter $\alpha^{(45)} : T_{a,in}$ are as follows:

$$\frac{\partial N_4^{(i)}}{\partial \alpha^{(45)}} = \frac{\partial N_4^{(i)}}{\partial T_{a,in}} \equiv a_4^{i,45} = 0; \quad \ell = 4; \quad i = 1, \dots, I - 1; \quad j = 45, \quad (\text{E.260})$$

$$\begin{aligned} \frac{\partial N_4^{(I)}}{\partial \alpha^{(45)}} &= \frac{\partial N_4^{(I)}}{\partial T_{a,in}} \equiv a_4^{I,45} = C_p^{(I)} \left(\frac{T_a^{(I)} + 273.15}{2}, \boldsymbol{\alpha} \right) + \omega_{in} \frac{\partial h_{g,a}^{(I+1)}(T_{a,in}, \boldsymbol{\alpha})}{\partial T_{a,in}} \\ &= C_p^{(I)} \left(\frac{T_a^{(I)} + 273.15}{2}, \boldsymbol{\alpha} \right) + \omega_{in} a_{1g}; \quad \ell = 4; \quad i = I; \quad j = 45. \end{aligned} \quad (\text{E.261})$$

The derivatives of the air/water vapor energy balance equations [cf. Eqs. (2.12) - (2.14)] with respect to the parameter $\alpha^{(46)} : \omega_{in}$ are as follows:

$$\frac{\partial N_4^{(i)}}{\partial \alpha^{(46)}} = \frac{\partial N_4^{(i)}}{\partial \omega_{in}} \equiv a_4^{i,46} = 0; \quad \ell = 4; \quad i = 1, \dots, I - 1; \quad j = 46, \quad (\text{E.262})$$

$$\frac{\partial N_4^{(I)}}{\partial \alpha^{(46)}} = \frac{\partial N_4^{(I)}}{\partial \omega_{in}} \equiv a_4^{I,46} = h_{g,a}^{(I+1)}(T_{a,in}, \boldsymbol{\alpha}); \quad \ell = 4; \quad i = I; \quad j = 46. \quad (\text{E.263})$$

The derivatives of the air/water vapor energy balance equations [cf. Eqs. (2.12) - (2.14)] with respect to the parameter $\alpha^{(47)} : Sc$ are as follows:

$$\frac{\partial N_4^{(i)}}{\partial \alpha^{(47)}} = \frac{\partial N_4^{(i)}}{\partial Sc} \equiv a_4^{i,47} = 0; \quad \ell = 4; \quad i = 1, \dots, I; \quad j = 47. \quad (\text{E.264})$$

APPENDIX E. DERIVATIVES OF THE MODEL EQUATIONS WITH
RESPECT TO THE MODEL PARAMETERS

**E.1.5 Derivatives of the mechanical energy equations with
respect to the parameters**

The derivatives of the mechanical energy equation [cf. Eq. (2.15)] with respect to the parameter $\alpha^{(1)} : T_{db}$ are as follows:

$$\begin{aligned} \frac{\partial N_5}{\partial \alpha^{(1)}} = \frac{\partial N_5}{\partial T_{db}} &\equiv a_5^1 \equiv \frac{R_{air}}{2 \cdot P_{atm}} \cdot |m_a| \cdot m_a \\ &\cdot \left[\left(\frac{1}{A_{out}^2} - \frac{1}{A_{in}^2} + \frac{k_{sum}}{A_{fill}^2} \right) + \frac{96f}{\text{Re}} \cdot \frac{L_{fill}}{A_{fill}^2 D_h} \right] + \\ &+ \frac{g \cdot P_{atm}}{R_{air} \cdot T_{db}^2} \cdot \left(Z + \frac{V_w^2}{2g} - \Delta z_{rain} - \frac{\Delta z}{2} \right); \quad \ell = 5; \quad j = 1. \end{aligned} \quad (\text{E.265})$$

since

$$T_{db} = T_{a,in}. \quad (\text{E.266})$$

The derivatives of the mechanical energy equation [cf. Eq. (2.15)] with respect to the parameter $\alpha^{(2)} : T_{dp}$ are as follows:

$$\frac{\partial N_5}{\partial \alpha^{(2)}} = \frac{\partial N_5}{\partial T_{dp}} \equiv a_5^2 = 0; \quad \ell = 5; \quad j = 2. \quad (\text{E.267})$$

The derivatives of the mechanical energy equation [cf. Eq. (2.15)] with respect to the parameter $\alpha^{(3)} : T_{w,in}$ are as follows:

$$\frac{\partial N_5}{\partial \alpha^{(3)}} = \frac{\partial N_5}{\partial T_{w,in}} \equiv a_5^3 = 0; \quad \ell = 5; \quad j = 3. \quad (\text{E.268})$$

APPENDIX E. DERIVATIVES OF THE MODEL EQUATIONS WITH RESPECT TO THE MODEL PARAMETERS

The derivatives of the mechanical energy equation [cf. Eq. (2.15)] with respect to the parameter $\alpha^{(4)} : P_{atm}$ are as follows:

$$\begin{aligned} \frac{\partial N_5}{\partial \alpha^{(4)}} &= \frac{\partial N_5}{\partial P_{atm}} \equiv a_5^4 \equiv -\frac{R_{air} \cdot T_{tdb}}{2 \cdot P_{atm}^2} \cdot |m_a| \cdot m_a \\ &\cdot \left[\left(\frac{1}{A_{out}^2} - \frac{1}{A_{in}^2} + \frac{k_{sum}}{A_{fill}^2} \right) + \frac{96f}{\text{Re}} \cdot \frac{L_{fill}}{A_{fill}^2 D_h} \right] + \frac{g}{R_{air} \cdot T_{tdb}} \\ &\cdot \left[-Z - \frac{V_w^2}{2g} + \Delta z_{rain} + \Delta z_{4-2} \frac{T_{tdb}}{T_a^{(1)}} + \Delta z \cdot T_{tdb} \cdot \left(\frac{1}{2T_{a,in}} + \frac{1}{2T_a^{(1)}} + \sum_{i=2}^I \frac{1}{T_a^{(i)}} \right) \right]; \\ &\ell = 5; \quad j = 4. \end{aligned} \tag{E.269}$$

The derivatives of the mechanical energy equation [cf. Eq. (2.15)] with respect to the parameter $\alpha^{(5)} : V_w$ are as follows:

$$\frac{\partial N_5}{\partial \alpha^{(5)}} = \frac{\partial N_5}{\partial V_w} \equiv a_5^5 = -V_w \cdot \rho(T_{db}, \boldsymbol{\alpha}); \quad \ell = 5; \quad j = 5. \tag{E.270}$$

The derivatives of the mechanical energy equation [cf. Eq. (2.15)] with respect to the parameter $\alpha^{(6)} : k_{sum}$ are as follows:

$$\frac{\partial N_5}{\partial \alpha^{(6)}} = \frac{\partial N_5}{\partial k_{sum}} \equiv a_5^6 = \frac{|m_a| \cdot m_a}{2\rho(T_{db}, \boldsymbol{\alpha}) \cdot A_{fill}^2}; \quad \ell = 5; \quad j = 6. \tag{E.271}$$

The derivatives of the mechanical energy equation [cf. Eq. (2.15)] with respect to the parameter $\alpha^{(7)} : \mu$ are as follows:

$$\frac{\partial N_5}{\partial \alpha^{(7)}} = \frac{\partial N_5}{\partial \mu} \equiv a_5^7 = \frac{96f \cdot L_{fill}}{2\rho(T_{db}, \boldsymbol{\alpha}) \cdot A_{fill} \cdot D_h^2} \cdot m_a; \quad \ell = 5; \quad j = 7. \tag{E.272}$$

The derivatives of the mechanical energy equation [cf. Eq. (2.15)] with respect to the parameter $\alpha^{(8)} : \nu$ are as follows:

$$\frac{\partial N_5}{\partial \alpha^{(8)}} = \frac{\partial N_5}{\partial \nu} \equiv a_5^8 = 0; \quad \ell = 5; \quad j = 8. \tag{E.273}$$

APPENDIX E. DERIVATIVES OF THE MODEL EQUATIONS WITH
RESPECT TO THE MODEL PARAMETERS

The derivatives of the mechanical energy equation [cf. Eq. (2.15)] with respect to the parameter $\alpha^{(9)} : k_{air}$ are as follows:

$$\frac{\partial N_5}{\partial \alpha^{(9)}} = \frac{\partial N_5}{\partial k_{air}} \equiv a_5^9 = 0; \quad \ell = 5; \quad j = 9. \quad (\text{E.274})$$

The derivatives of the mechanical energy equation [cf. Eq. (2.15)] with respect to the parameter $\alpha^{(10)} : f_{ht}$ are as follows:

$$\frac{\partial N_5}{\partial \alpha^{(10)}} = \frac{\partial N_5}{\partial f_{ht}} \equiv a_5^{10} = 0; \quad \ell = 5; \quad j = 10. \quad (\text{E.275})$$

The derivatives of the mechanical energy equation [cf. Eq. (2.15)] with respect to the parameter $\alpha^{(11)} : f_{mt}$ are as follows:

$$\frac{\partial N_5}{\partial \alpha^{(11)}} = \frac{\partial N_5}{\partial f_{mt}} \equiv a_5^{11} = 0; \quad \ell = 5; \quad j = 11. \quad (\text{E.276})$$

The derivatives of the mechanical energy equation [cf. Eq. (2.15)] with respect to the parameter $\alpha^{(12)} : f$ are as follows:

$$\frac{\partial N_5}{\partial \alpha^{(12)}} = \frac{\partial N_5}{\partial f} \equiv a_5^{12} = \frac{96 \cdot L_{fill} \cdot |m_a| \cdot m_a}{2\rho(T_{db}, \boldsymbol{\alpha}) \cdot \text{Re} \cdot A_{fill}^2 \cdot D_h}; \quad \ell = 5; \quad j = 12. \quad (\text{E.277})$$

The derivatives of the mechanical energy equation [cf. Eq. (2.15)] with respect to the parameter $\alpha^{(13)} : a_0$ are as follows:

$$\frac{\partial N_5}{\partial \alpha^{(13)}} = \frac{\partial N_5}{\partial a_0} \equiv a_5^{13} = 0; \quad \ell = 5; \quad j = 13. \quad (\text{E.278})$$

The derivatives of the mechanical energy equation [cf. Eq. (2.15)] with respect to the parameter $\alpha^{(14)} : a_1$ are as follows:

$$\frac{\partial N_5}{\partial \alpha^{(14)}} = \frac{\partial N_5}{\partial a_1} \equiv a_5^{14} = 0; \quad \ell = 5; \quad j = 14. \quad (\text{E.279})$$

APPENDIX E. DERIVATIVES OF THE MODEL EQUATIONS WITH
RESPECT TO THE MODEL PARAMETERS

The derivatives of the mechanical energy equation [cf. Eq. (2.15)] with respect to the parameter $\alpha^{(15)} : a_{0,c_{pa}}$ are as follows:

$$\frac{\partial N_5}{\partial \alpha^{(15)}} = \frac{\partial N_5}{\partial a_{0,c_{pa}}} \equiv a_5^{15} = 0; \quad \ell = 5; \quad j = 15. \quad (\text{E.280})$$

The derivatives of the mechanical energy equation [cf. Eq. (2.15)] with respect to the parameter $\alpha^{(16)} : a_{1,c_{pa}}$ are as follows:

$$\frac{\partial N_5}{\partial \alpha^{(16)}} = \frac{\partial N_5}{\partial a_{1,c_{pa}}} \equiv a_5^{16} = 0; \quad \ell = 5; \quad j = 16. \quad (\text{E.281})$$

The derivatives of the mechanical energy equation [cf. Eq. (2.15)] with respect to the parameter $\alpha^{(17)} : a_{2,c_{pa}}$ are as follows:

$$\frac{\partial N_5}{\partial \alpha^{(17)}} = \frac{\partial N_5}{\partial a_{2,c_{pa}}} \equiv a_5^{17} = 0; \quad \ell = 5; \quad j = 17. \quad (\text{E.282})$$

The derivatives of the mechanical energy equation [cf. Eq. (2.15)] with respect to the parameter $\alpha^{(18)} : a_{0,D_{av}}$ are as follows:

$$\frac{\partial N_5}{\partial \alpha^{(18)}} = \frac{\partial N_5}{\partial a_{0,D_{av}}} \equiv a_5^{18} = 0; \quad \ell = 5; \quad j = 18. \quad (\text{E.283})$$

The derivatives of the mechanical energy equation [cf. Eq. (2.15)] with respect to the parameter $\alpha^{(19)} : a_{1,D_{av}}$ are as follows:

$$\frac{\partial N_5}{\partial \alpha^{(19)}} = \frac{\partial N_5}{\partial a_{1,D_{av}}} \equiv a_5^{19} = 0; \quad \ell = 5; \quad j = 19. \quad (\text{E.284})$$

The derivatives of the mechanical energy equation [cf. Eq. (2.15)] with respect to the parameter $\alpha^{(20)} : a_{2,D_{av}}$ are as follows:

$$\frac{\partial N_5}{\partial \alpha^{(20)}} = \frac{\partial N_5}{\partial a_{2,D_{av}}} \equiv a_5^{20} = 0; \quad \ell = 5; \quad j = 20. \quad (\text{E.285})$$

APPENDIX E. DERIVATIVES OF THE MODEL EQUATIONS WITH RESPECT TO THE MODEL PARAMETERS

The derivatives of the mechanical energy equation [cf. Eq. (2.15)] with respect to the parameter $\alpha^{(21)} : a_{3,D_{av}}$ are as follows:

$$\frac{\partial N_5}{\partial \alpha^{(21)}} = \frac{\partial N_5}{\partial a_{3,D_{av}}} \equiv a_5^{21} = 0; \quad \ell = 5; \quad j = 21. \quad (\text{E.286})$$

The derivatives of the mechanical energy equation [cf. Eq. (2.15)] with respect to the parameter $\alpha^{(22)} : a_{0f}$ are as follows:

$$\frac{\partial N_5}{\partial \alpha^{(22)}} = \frac{\partial N_5}{\partial a_{0f}} \equiv a_5^{22} = 0; \quad \ell = 5; \quad j = 22. \quad (\text{E.287})$$

The derivatives of the mechanical energy equation [cf. Eq. (2.15)] with respect to the parameter $\alpha^{(23)} : a_{1f}$ are as follows:

$$\frac{\partial N_5}{\partial \alpha^{(23)}} = \frac{\partial N_5}{\partial a_{1f}} \equiv a_5^{23} = 0; \quad \ell = 5; \quad j = 23. \quad (\text{E.288})$$

The derivatives of the mechanical energy equation [cf. Eq. (2.15)] with respect to the parameter $\alpha^{(24)} : a_{0g}$ are as follows:

$$\frac{\partial N_5}{\partial \alpha^{(24)}} = \frac{\partial N_5}{\partial a_{0g}} \equiv a_5^{24} = 0; \quad \ell = 5; \quad j = 24. \quad (\text{E.289})$$

The derivatives of the mechanical energy equation [cf. Eq. (2.15)] with respect to the parameter $\alpha^{(25)} : a_{1g}$ are as follows:

$$\frac{\partial N_5}{\partial \alpha^{(25)}} = \frac{\partial N_5}{\partial a_{1g}} \equiv a_5^{25} = 0; \quad \ell = 5; \quad j = 25. \quad (\text{E.290})$$

The derivatives of the mechanical energy equation [cf. Eq. (2.15)] with respect to the parameter $\alpha^{(26)} : a_{0,Nu}$ are as follows:

$$\frac{\partial N_5}{\partial \alpha^{(26)}} = \frac{\partial N_5}{\partial a_{0,Nu}} \equiv a_5^{26} = 0; \quad \ell = 5; \quad j = 26. \quad (\text{E.291})$$

APPENDIX E. DERIVATIVES OF THE MODEL EQUATIONS WITH
RESPECT TO THE MODEL PARAMETERS

The derivatives of the mechanical energy equation [cf. Eq. (2.15)] with respect to the parameter $\alpha^{(27)} : a_{1,Nu}$ are as follows:

$$\frac{\partial N_5}{\partial \alpha^{(27)}} = \frac{\partial N_5}{\partial a_{1,Nu}} \equiv a_5^{27} = 0; \quad \ell = 5; \quad j = 27. \quad (\text{E.292})$$

The derivatives of the mechanical energy equation [cf. Eq. (2.15)] with respect to the parameter $\alpha^{(28)} : a_{2,Nu}$ are as follows:

$$\frac{\partial N_5}{\partial \alpha^{(28)}} = \frac{\partial N_5}{\partial a_{1,Nu}} \equiv a_5^{28} = 0; \quad \ell = 5; \quad j = 28. \quad (\text{E.293})$$

The derivatives of the mechanical energy equation [cf. Eq. (2.15)] with respect to the parameter $\alpha^{(29)} : a_{3,Nu}$ are as follows:

$$\frac{\partial N_5}{\partial \alpha^{(29)}} = \frac{\partial N_5}{\partial a_{1,Nu}} \equiv a_5^{29} = 0; \quad \ell = 5; \quad j = 29. \quad (\text{E.294})$$

The derivatives of the mechanical energy equation [cf. Eq. (2.15)] with respect to the parameter $\alpha^{(30)} : W_{dkx}$ are as follows:

$$\frac{\partial N_5}{\partial \alpha^{(30)}} = \frac{\partial N_5}{\partial W_{dkx}} \equiv a_5^{30} = \frac{|m_a| \cdot m_a}{\rho(T_{db}, \boldsymbol{\alpha}) \cdot W_{dkx}^3 \cdot W_{dky}^2}; \quad \ell = 5; \quad j = 30. \quad (\text{E.295})$$

The derivatives of the mechanical energy equation [cf. Eq. (2.15)] with respect to the parameter $\alpha^{(31)} : W_{dky}$ are as follows:

$$\frac{\partial N_5}{\partial \alpha^{(31)}} = \frac{\partial N_5}{\partial W_{dky}} \equiv a_5^{31} = \frac{|m_a| \cdot m_a}{\rho(T_{db}, \boldsymbol{\alpha}) \cdot W_{dkx}^2 \cdot W_{dky}^3}; \quad \ell = 5; \quad j = 31. \quad (\text{E.296})$$

The derivatives of the mechanical energy equation [cf. Eq. (2.15)] with respect to the parameter $\alpha^{(32)} : \Delta z_{dk}$ are as follows:

$$\frac{\partial N_5}{\partial \alpha^{(32)}} = \frac{\partial N_5}{\partial \Delta z_{dk}} \equiv a_5^{32} = g \frac{P_{atm}}{R_{air}} \left[\frac{1}{T_a^{(1)}} - \frac{1}{T_{db}} \right]; \quad \ell = 5; \quad j = 32. \quad (\text{E.297})$$

APPENDIX E. DERIVATIVES OF THE MODEL EQUATIONS WITH RESPECT TO THE MODEL PARAMETERS

The derivatives of the mechanical energy equation [cf. Eq. (2.15)] with respect to the parameter $\alpha^{(33)} : \Delta z_{fan}$ are as follows:

$$\frac{\partial N_5}{\partial \alpha^{(33)}} = \frac{\partial N_5}{\partial \Delta z_{fan}} \equiv a_5^{33} = g \frac{P_{atm}}{R_{air}} \left[\frac{1}{T_a^{(1)}} - \frac{1}{T_{db}} \right]; \quad \ell = 5; \quad j = 33. \quad (\text{E.298})$$

The derivatives of the mechanical energy equation [cf. Eq. (2.15)] with respect to the parameter $\alpha^{(34)} : D_{fan}$ are as follows:

$$\frac{\partial N_5}{\partial \alpha^{(34)}} = \frac{\partial N_5}{\partial D_{fan}} \equiv a_5^{34} = -\frac{32 \cdot |m_a| \cdot m_a}{\rho(T_{db}, \boldsymbol{\alpha}) \cdot \pi^2 \cdot D_{fan}^5}; \quad \ell = 5; \quad j = 34. \quad (\text{E.299})$$

The derivatives of the mechanical energy equation [cf. Eq. (2.15)] with respect to the parameter $\alpha^{(35)} : \Delta z_{fill}$ are as follows:

$$\begin{aligned} \frac{\partial N_5}{\partial \alpha^{(35)}} = \frac{\partial N_5}{\partial \Delta z_{fill}} \equiv a_5^{35} = & \frac{96f \cdot |m_a| \cdot m_a}{2\rho(T_{db}, \boldsymbol{\alpha}) \cdot \text{Re} \cdot A_{fill}^2 \cdot D_h} - g \frac{P_{atm}}{R_{air} \cdot T_a^{(1)}} \\ & + g \frac{P_{atm}}{R_{air} \cdot I} \cdot \left[\frac{1}{2T_{a,in}} + \frac{1}{2T_a^{(1)}} + \sum_{i=2}^I \frac{1}{T_a^{(i)}} \right]; \quad \ell = 5; \quad j = 35. \end{aligned} \quad (\text{E.300})$$

The derivatives of the mechanical energy equation [cf. Eq. (2.15)] with respect to the parameter $\alpha^{(36)} : \Delta z_{rain}$ are as follows:

$$\frac{\partial N_5}{\partial \alpha^{(36)}} = \frac{\partial N_5}{\partial \Delta z_{rain}} \equiv a_5^{36} = g \frac{P_{atm}}{R_{air}} \left[\frac{1}{T_{db}} - \frac{1}{T_a^{(1)}} \right]; \quad \ell = 5; \quad j = 36. \quad (\text{E.301})$$

The derivatives of the mechanical energy equation [cf. Eq. (2.15)] with respect to the parameter $\alpha^{(37)} : \Delta z_{bs}$ are as follows:

$$\frac{\partial N_5}{\partial \alpha^{(37)}} = \frac{\partial N_5}{\partial \Delta z_{bs}} \equiv a_5^{37} = g \frac{P_{atm}}{R_{air}} \left[\frac{1}{T_{db}} - \frac{1}{T_a^{(1)}} \right]; \quad \ell = 5; \quad j = 37. \quad (\text{E.302})$$

APPENDIX E. DERIVATIVES OF THE MODEL EQUATIONS WITH RESPECT TO THE MODEL PARAMETERS

The derivatives of the mechanical energy equation [cf. Eq. (2.15)] with respect to the parameter $\alpha^{(38)} : \Delta z_{de}$ are as follows:

$$\frac{\partial N_5}{\partial \alpha^{(38)}} = \frac{\partial N_5}{\partial \Delta z_{de}} \equiv a_5^{38} = \frac{96f \cdot |m_a| \cdot m_a}{2\rho(T_{db}, \boldsymbol{\alpha}) \cdot \text{Re} \cdot A_{fill}^2 \cdot D_h}; \quad \ell = 5; \quad j = 38. \quad (\text{E.303})$$

The derivatives of the mechanical energy equation [cf. Eq. (2.15)] with respect to the parameter $\alpha^{(39)} : D_h$ are as follows:

$$\frac{\partial N_5}{\partial \alpha^{(39)}} = \frac{\partial N_5}{\partial D_h} \equiv a_5^{39} = -\frac{96f \cdot \mu_{air} \cdot L_{fill} \cdot m_a}{\rho(T_{db}, \boldsymbol{\alpha}) \cdot A_{fill} \cdot D_h^3}; \quad \ell = 5; \quad j = 39. \quad (\text{E.304})$$

The derivatives of the mechanical energy equation [cf. Eq. (2.15)] with respect to the parameter $\alpha^{(40)} : A_{fill}$ are as follows:

$$\frac{\partial N_5}{\partial \alpha^{(40)}} = \frac{\partial N_5}{\partial A_{fill}} \equiv a_5^{40} = -\frac{k_{sum} \cdot |m_a| \cdot m_a}{\rho(T_{db}, \boldsymbol{\alpha}) \cdot A_{fill}^3} - \frac{96f \cdot \mu_{air} \cdot L_{fill} \cdot m_a}{2\rho(T_{db}, \boldsymbol{\alpha}) \cdot A_{fill}^2 \cdot D_h^2}; \quad \ell = 5; \quad j = 40. \quad (\text{E.305})$$

The derivatives of the mechanical energy equation [cf. Eq. (2.15)] with respect to the parameter $\alpha^{(41)} : A_{surf}$ are as follows:

$$\frac{\partial N_5}{\partial \alpha^{(41)}} = \frac{\partial N_5}{\partial A_{surf}} \equiv a_5^{41} = 0; \quad \ell = 5; \quad j = 41. \quad (\text{E.306})$$

The derivatives of the mechanical energy equation [cf. Eq. (2.15)] with respect to the parameter $\alpha^{(42)} : \text{Pr}$ are as follows:

$$\frac{\partial N_5}{\partial \alpha^{(42)}} = \frac{\partial N_5}{\partial \text{Pr}} \equiv a_5^{42} = 0; \quad \ell = 5; \quad j = 42. \quad (\text{E.307})$$

The derivatives of the mechanical energy equation [cf. Eq. (2.15)] with respect to the parameter $\alpha^{(43)} : w_{tsa}$ are as follows:

$$\frac{\partial N_5}{\partial \alpha^{(43)}} = \frac{\partial N_5}{\partial w_{tsa}} \equiv a_5^{43} = 0; \quad \ell = 5; \quad j = 43. \quad (\text{E.308})$$

APPENDIX E. DERIVATIVES OF THE MODEL EQUATIONS WITH
RESPECT TO THE MODEL PARAMETERS

The derivatives of the mechanical energy equation [cf. Eq. (2.15)] with respect to the parameter $\alpha^{(44)} : m_{w,in}$ are as follows:

$$\frac{\partial N_5}{\partial \alpha^{(44)}} = \frac{\partial N_5}{\partial m_{w,in}} \equiv a_5^{44} = 0; \quad \ell = 5; \quad j = 44. \quad (\text{E.309})$$

The derivatives of the mechanical energy equation [cf. Eq. (2.15)] with respect to the parameter $\alpha^{(45)} : T_{a,in}$ are as follows:

$$\begin{aligned} \frac{\partial N_5}{\partial \alpha^{(45)}} = \frac{\partial N_5}{\partial T_{a,in}} \equiv a_5^{45} = & \frac{R_{air}}{2 \cdot P_{atm}} \cdot |m_a| \cdot m_a \\ & \cdot \left[\left(\frac{1}{A_{out}^2} - \frac{1}{A_{in}^2} + \frac{k_{sum}}{A_{fill}^2} \right) + \frac{96f}{\text{Re}} \cdot \frac{L_{fill}}{A_{fill}^2 D_h} \right] \\ & + \frac{g \cdot P_{atm}}{R_{air} \cdot T_{a,in}^2} \cdot \left(Z + \frac{V_w^2}{2g} - \Delta z_{rain} - \frac{\Delta z}{2} \right); \quad \ell = 5; \quad j = 45. \end{aligned} \quad (\text{E.310})$$

The derivatives of the mechanical energy equation [cf. Eq. (2.15)] with respect to the parameter $\alpha^{(46)} : \omega_{in}$ are as follows:

$$\frac{\partial N_5}{\partial \alpha^{(46)}} = \frac{\partial N_5}{\partial \omega_{in}} \equiv a_5^{46} = 0; \quad \ell = 5; \quad j = 46. \quad (\text{E.311})$$

The derivatives of the mechanical energy equation [cf. Eq. (2.15)] with respect to the parameter $\alpha^{(47)} : Sc$ are as follows:

$$\frac{\partial N_5}{\partial \alpha^{(47)}} = \frac{\partial N_5}{\partial Sc} \equiv a_5^{47} = 0; \quad \ell = 5; \quad j = 47. \quad (\text{E.312})$$

E.2 Derivatives of the Model Equations with respect to the Model Parameters for Case 1b: Fan Off, Saturated Outlet Air Conditions, with Inlet Air Saturated

The differences between the governing equations for case 1a and case 1b are only in the “liquid continuity equations”. Other governing equations (i.e., liquid energy balance equations; water vapor continuity equations; air/water vapor energy balance equations; mechanical energy equation) are the same for both cases, and their derivatives in Subsections E.1.2 through E.1.5. Therefore for case 1b, only the derivatives of the “liquid continuity equations” with respect to parameters are derived as follows, since the derivatives of other governing equations with respect to parameters are the same as that of case 1a. The notation used will be the following:

$$a_1^{i,j} \equiv \frac{\partial N_1^{(i)}}{\partial \alpha^{(j)}}; \quad i = 1, \dots, I; \quad j = 1, \dots, N_\alpha. \quad (\text{E.313})$$

E.2.1 Derivatives of the liquid continuity equations with respect to the parameters

The derivatives of the “liquid continuity equations” [cf. Eqs. (2.25) - (2.27)] with respect to the parameter $\alpha^{(1)} : T_{db}$ are as follows:

$$\begin{aligned} \frac{\partial N_1^{(i)}}{\partial \alpha^{(1)}} = \frac{\partial N_1^{(i)}}{\partial T_{db}} \equiv a_1^{i,1} = \frac{1}{R} \left[\frac{P_{vs}^{(i+1)}(T_w^{(i+1)}, \boldsymbol{\alpha})}{T_w^{(i+1)}} - \frac{P_{vs}^{(i)}(T_a^{(i)}, \boldsymbol{\alpha})}{T_a^{(i)}} \right] \\ \cdot \frac{\partial M(m_a, \boldsymbol{\alpha})}{\partial D_{av}(T_{db}, \boldsymbol{\alpha})} \cdot \frac{\partial D_{av}(T_{db}, \boldsymbol{\alpha})}{\partial T_{db}}; \quad \ell = 1; \quad i = 1, \dots, I; \quad j = 1, \end{aligned} \quad (\text{E.314})$$

where $\frac{\partial M(m_a, \boldsymbol{\alpha})}{\partial D_{av}(T_{db}, \boldsymbol{\alpha})}$ and $\frac{\partial D_{av}(T_{db}, \boldsymbol{\alpha})}{\partial T_{db}}$ were defined in Eqs. (E.3) and (E.4), respectively.

APPENDIX E. DERIVATIVES OF THE MODEL EQUATIONS WITH RESPECT TO THE MODEL PARAMETERS

The derivatives of the “liquid continuity equations” [cf. Eqs. (2.25) - (2.27)] with respect to the parameter $\alpha^{(2)} : T_{dp}$ are as follows:

$$\frac{\partial N_1^{(i)}}{\partial \alpha^{(2)}} = \frac{\partial N_1^{(i)}}{\partial T_{dp}} \equiv a_1^{i,2} = 0; \quad \ell = 1; \quad i = 1, \dots, I; \quad j = 2. \quad (\text{E.315})$$

The derivatives of the “liquid continuity equations” [cf. Eqs. (2.25) - (2.27)] with respect to the parameter $\alpha^{(3)} : T_{w,in}$ are as follows:

$$\frac{\partial N_1^{(1)}}{\partial \alpha^{(3)}} = \frac{\partial N_1^{(1)}}{\partial T_{w,in}} \equiv a_1^{1,3} = 0; \quad \ell = 1; \quad i = 1; \quad j = 3, \quad (\text{E.316})$$

The derivatives of the “liquid continuity equations” [cf. Eqs. (2.25) - (2.27)] with respect to the parameter $\alpha^{(4)} : P_{atm}$ are as follows:

$$\frac{\partial N_1^{(i)}}{\partial \alpha^{(4)}} = \frac{\partial N_1^{(i)}}{\partial P_{atm}} \equiv a_1^{i,4} = 0; \quad \ell = 1; \quad i = 1, \dots, I; \quad j = 4, \quad (\text{E.317})$$

The derivatives of the “liquid continuity equations” [cf. Eqs. (2.25) - (2.27)] with respect to the parameter $\alpha^{(5)} : V_w$ are as follows:

$$\frac{\partial N_1^{(i)}}{\partial \alpha^{(5)}} = \frac{\partial N_1^{(i)}}{\partial V_w} \equiv a_1^{i,5} = 0; \quad \ell = 1; \quad i = 1, \dots, I; \quad j = 5, \quad (\text{E.318})$$

The derivatives of the “liquid continuity equations” [cf. Eqs. (2.25) - (2.27)] with respect to the parameter $\alpha^{(6)} : k_{sum}$ are as follows:

$$\frac{\partial N_1^{(i)}}{\partial \alpha^{(6)}} = \frac{\partial N_1^{(i)}}{\partial k_{sum}} \equiv a_1^{i,6} = 0; \quad \ell = 1; \quad i = 1, \dots, I; \quad j = 6. \quad (\text{E.319})$$

The derivatives of the “liquid continuity equations” [cf. Eqs. (2.25) - (2.27)] with respect to the parameter $\alpha^{(7)} : \mu$ are as follows:

$$\begin{aligned} \frac{\partial N_1^{(i)}}{\partial \alpha^{(7)}} = \frac{\partial N_1^{(i)}}{\partial \mu} \equiv a_1^{i,7} &= \frac{1}{R} \left[\frac{P_{vs}^{(i+1)}(T_w^{(i+1)}, \boldsymbol{\alpha})}{T_w^{(i+1)}} - \frac{P_{vs}^{(i)}(T_a^{(i)}, \boldsymbol{\alpha})}{T_a^{(i)}} \right] \frac{\partial M(m_a, \boldsymbol{\alpha})}{\partial \mu}; \\ &\ell = 1; \quad i = 1, \dots, I; \quad j = 7, \end{aligned} \quad (\text{E.320})$$

APPENDIX E. DERIVATIVES OF THE MODEL EQUATIONS WITH RESPECT TO THE MODEL PARAMETERS

where $\frac{\partial M(m_a, \boldsymbol{\alpha})}{\partial \mu}$ was defined in Eq. (E.13).

The derivatives of the “liquid continuity equations” [cf. Eqs. (2.25) - (2.27)] with respect to the parameter $\alpha^{(8)} : \nu$ are as follows:

$$\begin{aligned} \frac{\partial N_1^{(i)}}{\partial \alpha^{(8)}} = \frac{\partial N_1^{(i)}}{\partial \nu} \equiv a_1^{i,8} &= \frac{1}{R} \left[\frac{P_{vs}^{(i+1)}(T_w^{(i+1)}, \boldsymbol{\alpha})}{T_w^{(i+1)}} - \frac{P_{vs}^{(i)}(T_a^{(i)}, \boldsymbol{\alpha})}{T_a^{(i)}} \right] \frac{\partial M(m_a, \boldsymbol{\alpha})}{\partial \nu}; \\ \ell &= 1; \quad i = 1, \dots, I; \quad j = 8, \end{aligned} \quad (\text{E.321})$$

where $\frac{\partial M(m_a, \boldsymbol{\alpha})}{\partial \nu}$ was defined in Eq. (E.16).

The derivatives of the “liquid continuity equations” [cf. Eqs. (2.25) - (2.27)] with respect to the parameter $\alpha^{(9)} : k_{air}$ are as follows:

$$\frac{\partial N_1^{(i)}}{\partial \alpha^{(9)}} = \frac{\partial N_1^{(i)}}{\partial k_{air}} \equiv a_1^{i,9} = 0; \quad \ell = 1; \quad i = 1, \dots, I; \quad j = 9. \quad (\text{E.322})$$

The derivatives of the “liquid continuity equations” [cf. Eqs. (2.25) - (2.27)] with respect to the parameter $\alpha^{(10)} : f_{ht}$ are as follows:

$$\frac{\partial N_1^{(i)}}{\partial \alpha^{(10)}} = \frac{\partial N_1^{(i)}}{\partial f_{ht}} \equiv a_1^{i,10} = 0; \quad \ell = 1; \quad i = 1, \dots, I; \quad j = 10. \quad (\text{E.323})$$

The derivatives of the “liquid continuity equations” [cf. Eqs. (2.25) - (2.27)] with respect to the parameter $\alpha^{(11)} : f_{mt}$ are as follows:

$$\begin{aligned} \frac{\partial N_1^{(i)}}{\partial \alpha^{(11)}} = \frac{\partial N_1^{(i)}}{\partial f_{mt}} \equiv a_1^{i,11} &= \frac{1}{R} \left[\frac{P_{vs}^{(i+1)}(T_w^{(i+1)}, \boldsymbol{\alpha})}{T_w^{(i+1)}} - \frac{P_{vs}^{(i)}(T_a^{(i)}, \boldsymbol{\alpha})}{T_a^{(i)}} \right] \frac{\partial M(m_a, \boldsymbol{\alpha})}{\partial f_{mt}}; \\ \ell &= 1; \quad i = 1, \dots, I; \quad j = 11, \end{aligned} \quad (\text{E.324})$$

where $\frac{\partial M(m_a, \boldsymbol{\alpha})}{\partial f_{mt}}$ was defined in Eq. (E.21).

APPENDIX E. DERIVATIVES OF THE MODEL EQUATIONS WITH RESPECT TO THE MODEL PARAMETERS

The derivatives of the “liquid continuity equations” [cf. Eqs. (2.25) - (2.27)] with respect to the parameter $\alpha^{(12)} : f$ are as follows:

$$\frac{\partial N_1^{(i)}}{\partial \alpha^{(12)}} = \frac{\partial N_1^{(i)}}{\partial f} \equiv a_1^{i,12} = 0; \quad \ell = 1; \quad i = 1, \dots, I; \quad j = 12. \quad (\text{E.325})$$

The derivatives of the “liquid continuity equations” [cf. Eqs. (2.25) - (2.27)] with respect to the parameter $\alpha^{(13)} : a_0$ are as follows:

$$\begin{aligned} \frac{\partial N_1^{(i)}}{\partial \alpha^{(13)}} = \frac{\partial N_1^{(i)}}{\partial a_0} \equiv a_1^{i,13} &= \frac{M(m_a, \boldsymbol{\alpha})}{\bar{R}} \left[\frac{P_{vs}^{(i+1)}(T_w^{(i+1)}, \boldsymbol{\alpha})}{T_w^{(i+1)}} - \frac{P_{vs}^{(i)}(T_a^{(i)}, \boldsymbol{\alpha})}{T_a^{(i)}} \right]; \\ \ell &= 1; \quad i = 1, \dots, I; \quad j = 13, \end{aligned} \quad (\text{E.326})$$

The derivatives of the “liquid continuity equations” [cf. Eqs. (2.25) - (2.27)] with respect to the parameter $\alpha^{(14)} : a_1$ are as follows:

$$\begin{aligned} \frac{\partial N_1^{(i)}}{\partial \alpha^{(14)}} = \frac{\partial N_1^{(i)}}{\partial a_1} \equiv a_1^{i,14} &= \frac{M(m_a, \boldsymbol{\alpha})}{\bar{R}} \left[\frac{P_{vs}^{(i+1)}(T_w^{(i+1)}, \boldsymbol{\alpha})}{\left(T_w^{(i+1)}\right)^2} - \frac{P_{vs}^{(i)}(T_a^{(i)}, \boldsymbol{\alpha})}{\left(T_a^{(i)}\right)^2} \right]; \\ \ell &= 1; \quad i = 1, \dots, I; \quad j = 14, \end{aligned} \quad (\text{E.327})$$

The derivatives of the “liquid continuity equations” [cf. Eqs. (2.25) - (2.27)] with respect to the parameter $\alpha^{(15)} : a_{0,c_{pa}}$ are as follows:

$$\frac{\partial N_1^{(i)}}{\partial \alpha^{(15)}} = \frac{\partial N_1^{(i)}}{\partial a_{0,c_{pa}}} \equiv a_1^{i,15} = 0; \quad \ell = 1; \quad i = 1, \dots, I; \quad j = 15. \quad (\text{E.328})$$

The derivatives of the “liquid continuity equations” [cf. Eqs. (2.25) - (2.27)] with respect to the parameter $\alpha^{(16)} : a_{1,c_{pa}}$ are as follows:

$$\frac{\partial N_1^{(i)}}{\partial \alpha^{(16)}} = \frac{\partial N_1^{(i)}}{\partial a_{1,c_{pa}}} \equiv a_1^{i,16} = 0; \quad \ell = 1; \quad i = 1, \dots, I; \quad j = 16. \quad (\text{E.329})$$

APPENDIX E. DERIVATIVES OF THE MODEL EQUATIONS WITH RESPECT TO THE MODEL PARAMETERS

The derivatives of the “liquid continuity equations” [cf. Eqs. (2.25) - (2.27)] with respect to the parameter $\alpha^{(17)} : a_{2,c_{pa}}$ are as follows:

$$\frac{\partial N_1^{(i)}}{\partial \alpha^{(17)}} = \frac{\partial N_1^{(i)}}{\partial a_{2,c_{pa}}} \equiv a_1^{i,17} = 0; \quad \ell = 1; \quad i = 1, \dots, I; \quad j = 17. \quad (\text{E.330})$$

The derivatives of the “liquid continuity equations” [cf. Eqs. (2.25) - (2.27)] with respect to the parameter $\alpha^{(18)} : a_{0,D_{av}}$ are as follows:

$$\begin{aligned} \frac{\partial N_1^{(i)}}{\partial \alpha^{(18)}} = \frac{\partial N_1^{(i)}}{\partial a_{0,D_{av}}} \equiv a_1^{i,18} = \frac{1}{\bar{R}} & \left[\frac{P_{vs}^{(i+1)}(T_w^{(i+1)}, \boldsymbol{\alpha})}{T_w^{(i+1)}} - \frac{P_{vs}^{(i)}(T_a^{(i)}, \boldsymbol{\alpha})}{T_a^{(i)}} \right] \\ & \cdot \frac{\partial M(m_a, \boldsymbol{\alpha})}{\partial D_{av}(T_{db}, \boldsymbol{\alpha})} \cdot \frac{\partial D_{av}(T_{db}, \boldsymbol{\alpha})}{\partial a_{0,D_{av}}}; \quad \ell = 1; \quad i = 1, \dots, I; \quad j = 18, \end{aligned} \quad (\text{E.331})$$

where $\frac{\partial M(m_a, \boldsymbol{\alpha})}{\partial D_{av}(T_{db}, \boldsymbol{\alpha})}$ was defined previously in Eq. (E.3), and $\frac{\partial D_{av}(T_{db}, \boldsymbol{\alpha})}{\partial a_{0,D_{av}}}$ was defined previously in Eq. (E.34).

The derivatives of the “liquid continuity equations” [cf. Eqs. (2.25) - (2.27)] with respect to the parameter $\alpha^{(19)} : a_{1,D_{av}}$ are as follows:

$$\begin{aligned} \frac{\partial N_1^{(i)}}{\partial \alpha^{(19)}} = \frac{\partial N_1^{(i)}}{\partial a_{1,D_{av}}} \equiv a_1^{i,19} = \frac{1}{\bar{R}} & \left[\frac{P_{vs}^{(i+1)}(T_w^{(i+1)}, \boldsymbol{\alpha})}{T_w^{(i+1)}} - \frac{P_{vs}^{(i)}(T_a^{(i)}, \boldsymbol{\alpha})}{T_a^{(i)}} \right] \\ & \cdot \frac{\partial M(m_a, \boldsymbol{\alpha})}{\partial D_{av}(T_{db}, \boldsymbol{\alpha})} \cdot \frac{\partial D_{av}(T_{db}, \boldsymbol{\alpha})}{\partial a_{1,D_{av}}}; \quad \ell = 1; \quad i = 1, \dots, I; \quad j = 19, \end{aligned} \quad (\text{E.332})$$

where $\frac{\partial M(m_a, \boldsymbol{\alpha})}{\partial D_{av}(T_{db}, \boldsymbol{\alpha})}$ was defined previously in Eq. (E.3), and $\frac{\partial D_{av}(T_{db}, \boldsymbol{\alpha})}{\partial a_{1,D_{av}}}$ was defined previously in Eq. (E.37).

The derivatives of the “liquid continuity equations” [cf. Eqs. (2.25) - (2.27)] with respect to the parameter $\alpha^{(20)} : a_{2,D_{av}}$ are as follows:

$$\begin{aligned} \frac{\partial N_1^{(i)}}{\partial \alpha^{(20)}} = \frac{\partial N_1^{(i)}}{\partial a_{2,D_{av}}} \equiv a_1^{i,20} = \frac{1}{\bar{R}} & \left[\frac{P_{vs}^{(i+1)}(T_w^{(i+1)}, \boldsymbol{\alpha})}{T_w^{(i+1)}} - \frac{P_{vs}^{(i)}(T_a^{(i)}, \boldsymbol{\alpha})}{T_a^{(i)}} \right] \\ & \cdot \frac{\partial M(m_a, \boldsymbol{\alpha})}{\partial D_{av}(T_{db}, \boldsymbol{\alpha})} \cdot \frac{\partial D_{av}(T_{db}, \boldsymbol{\alpha})}{\partial a_{2,D_{av}}}; \quad \ell = 1; \quad i = 1, \dots, I; \quad j = 20, \end{aligned} \quad (\text{E.333})$$

APPENDIX E. DERIVATIVES OF THE MODEL EQUATIONS WITH RESPECT TO THE MODEL PARAMETERS

where $\frac{\partial M(m_a, \boldsymbol{\alpha})}{\partial D_{av}(T_{db}, \boldsymbol{\alpha})}$ was defined previously in Eq. (E.3), and $\frac{\partial D_{av}(T_{db}, \boldsymbol{\alpha})}{\partial a_{2, D_{av}}}$ was defined previously in Eq. (E.40).

The derivatives of the “liquid continuity equations” [cf. Eqs. (2.25) - (2.27)] with respect to the parameter $\alpha^{(21)} : a_{3, D_{av}}$ are as follows:

$$\begin{aligned} \frac{\partial N_1^{(i)}}{\partial \alpha^{(21)}} = \frac{\partial N_1^{(i)}}{\partial a_{3, D_{av}}} \equiv a_1^{i, 21} = \frac{1}{\bar{R}} \left[\frac{P_{vs}^{(i+1)}(T_w^{(i+1)}, \boldsymbol{\alpha})}{T_w^{(i+1)}} - \frac{P_{vs}^{(i)}(T_a^{(i)}, \boldsymbol{\alpha})}{T_a^{(i)}} \right] \\ \cdot \frac{\partial M(m_a, \boldsymbol{\alpha})}{\partial D_{av}(T_{db}, \boldsymbol{\alpha})} \cdot \frac{\partial D_{av}(T_{db}, \boldsymbol{\alpha})}{\partial a_{3, D_{av}}}; \quad \ell = 1; \quad i = 1, \dots, I; \quad j = 21, \end{aligned} \quad (\text{E.334})$$

where $\frac{\partial M(m_a, \boldsymbol{\alpha})}{\partial D_{av}(T_{db}, \boldsymbol{\alpha})}$ was defined previously in Eq. (E.3), and $\frac{\partial D_{av}(T_{db}, \boldsymbol{\alpha})}{\partial a_{3, D_{av}}}$ was defined previously in Eq. (E.43).

The derivatives of the “liquid continuity equations” [cf. Eqs. (2.25) - (2.27)] with respect to the parameter $\alpha^{(22)} : a_{0f}$ are as follows:

$$\frac{\partial N_1^{(i)}}{\partial \alpha^{(22)}} = \frac{\partial N_1^{(i)}}{\partial a_{0f}} \equiv a_1^{i, 22} = 0; \quad \ell = 1; \quad i = 1, \dots, I; \quad j = 22. \quad (\text{E.335})$$

The derivatives of the “liquid continuity equations” [cf. Eqs. (2.25) - (2.27)] with respect to the parameter $\alpha^{(23)} : a_{1f}$ are as follows:

$$\frac{\partial N_1^{(i)}}{\partial \alpha^{(23)}} = \frac{\partial N_1^{(i)}}{\partial a_{1f}} \equiv a_1^{i, 23} = 0; \quad \ell = 1; \quad i = 1, \dots, I; \quad j = 23. \quad (\text{E.336})$$

The derivatives of the “liquid continuity equations” [cf. Eqs. (2.25) - (2.27)] with respect to the parameter $\alpha^{(24)} : a_{0g}$ are as follows:

$$\frac{\partial N_1^{(i)}}{\partial \alpha^{(24)}} = \frac{\partial N_1^{(i)}}{\partial a_{0g}} \equiv a_1^{i, 24} = 0; \quad \ell = 1; \quad i = 1, \dots, I; \quad j = 24. \quad (\text{E.337})$$

APPENDIX E. DERIVATIVES OF THE MODEL EQUATIONS WITH RESPECT TO THE MODEL PARAMETERS

The derivatives of the “liquid continuity equations” [cf. Eqs. (2.25) - (2.27)] with respect to the parameter $\alpha^{(25)} : a_{1g}$ are as follows:

$$\frac{\partial N_1^{(i)}}{\partial \alpha^{(25)}} = \frac{\partial N_1^{(i)}}{\partial a_{1g}} \equiv a_1^{i,25} = 0; \quad \ell = 1; \quad i = 1, \dots, I; \quad j = 25. \quad (\text{E.338})$$

The derivatives of the “liquid continuity equations” [cf. Eqs. (2.25) - (2.27)] with respect to the parameter $\alpha^{(26)} : a_{0,Nu}$ are as follows:

$$\begin{aligned} \frac{\partial N_1^{(i)}}{\partial \alpha^{(26)}} = \frac{\partial N_1^{(i)}}{\partial a_{0,Nu}} \equiv a_1^{i,26} = \frac{1}{R} \left[\frac{P_{vs}^{(i+1)}(T_w^{(i+1)}, \boldsymbol{\alpha})}{T_w^{(i+1)}} - \frac{P_{vs}^{(i)}(T_a^{(i)}, \boldsymbol{\alpha})}{T_a^{(i)}} \right] \\ \cdot \frac{\partial M(m_a, \boldsymbol{\alpha})}{\partial Nu(\text{Re}, \boldsymbol{\alpha})} \frac{\partial Nu(\text{Re}, \boldsymbol{\alpha})}{\partial a_{0,Nu}}; \quad \ell = 1; \quad i = 1, \dots, I; \quad j = 26, \end{aligned} \quad (\text{E.339})$$

where $\frac{\partial M(m_a, \boldsymbol{\alpha})}{\partial Nu(\text{Re}, \boldsymbol{\alpha})}$ was defined previously in Eq. (E.50) and $\frac{\partial Nu(\text{Re}, \boldsymbol{\alpha})}{\partial a_{0,Nu}}$ was defined previously in Eq. (E.51).

The derivatives of the “liquid continuity equations” [cf. Eqs. (2.25) - (2.27)] with respect to the parameter $\alpha^{(27)} : a_{1,Nu}$ are as follows:

$$\begin{aligned} \frac{\partial N_1^{(i)}}{\partial \alpha^{(27)}} = \frac{\partial N_1^{(i)}}{\partial a_{1,Nu}} \equiv a_1^{i,27} = \frac{1}{R} \left[\frac{P_{vs}^{(i+1)}(T_w^{(i+1)}, \boldsymbol{\alpha})}{T_w^{(i+1)}} - \frac{P_{vs}^{(i)}(T_a^{(i)}, \boldsymbol{\alpha})}{T_a^{(i)}} \right] \\ \cdot \frac{\partial M(m_a, \boldsymbol{\alpha})}{\partial Nu(\text{Re}, \boldsymbol{\alpha})} \frac{\partial Nu(\text{Re}, \boldsymbol{\alpha})}{\partial a_{1,Nu}}; \quad \ell = 1; \quad i = 1, \dots, I; \quad j = 27, \end{aligned} \quad (\text{E.340})$$

where $\frac{\partial M(m_a, \boldsymbol{\alpha})}{\partial Nu(\text{Re}, \boldsymbol{\alpha})}$ was defined previously in Eq. (E.50) and $\frac{\partial Nu(\text{Re}, \boldsymbol{\alpha})}{\partial a_{1,Nu}}$ was defined previously in Eq. (E.54).

The derivatives of the “liquid continuity equations” [cf. Eqs. (2.25) - (2.27)] with respect to the parameter $\alpha^{(28)} : a_{2,Nu}$ are as follows:

$$\begin{aligned} \frac{\partial N_1^{(i)}}{\partial \alpha^{(28)}} = \frac{\partial N_1^{(i)}}{\partial a_{2,Nu}} \equiv a_1^{i,28} = \frac{1}{R} \left[\frac{P_{vs}^{(i+1)}(T_w^{(i+1)}, \boldsymbol{\alpha})}{T_w^{(i+1)}} - \frac{P_{vs}^{(i)}(T_a^{(i)}, \boldsymbol{\alpha})}{T_a^{(i)}} \right] \\ \cdot \frac{\partial M(m_a, \boldsymbol{\alpha})}{\partial Nu(\text{Re}, \boldsymbol{\alpha})} \frac{\partial Nu(\text{Re}, \boldsymbol{\alpha})}{\partial a_{2,Nu}}; \quad \ell = 1; \quad i = 1, \dots, I; \quad j = 28, \end{aligned} \quad (\text{E.341})$$

APPENDIX E. DERIVATIVES OF THE MODEL EQUATIONS WITH RESPECT TO THE MODEL PARAMETERS

where $\frac{\partial M(m_a, \alpha)}{\partial Nu(\text{Re}, \alpha)}$ was defined previously in Eq. (E.50) and $\frac{\partial Nu(\text{Re}, \alpha)}{\partial a_{2, Nu}}$ was defined previously in Eq. (E.57).

The derivatives of the “liquid continuity equations” [cf. Eqs. (2.25) - (2.27)] with respect to the parameter $\alpha^{(29)} : a_{3, Nu}$ are as follows:

$$\begin{aligned} \frac{\partial N_1^{(i)}}{\partial \alpha^{(29)}} = \frac{\partial N_1^{(i)}}{\partial a_{3, Nu}} &\equiv a_1^{i, 29} = \frac{1}{R} \left[\frac{P_{vs}^{(i+1)}(T_w^{(i+1)}, \alpha)}{T_w^{(i+1)}} - \frac{P_{vs}^{(i)}(T_a^{(i)}, \alpha)}{T_a^{(i)}} \right] \\ &\cdot \frac{\partial M(m_a, \alpha)}{\partial Nu(\text{Re}, \alpha)} \frac{\partial Nu(\text{Re}, \alpha)}{\partial a_{3, Nu}}; \quad \ell = 1; \quad i = 1, \dots, I; \quad j = 29, \end{aligned} \quad (\text{E.342})$$

where $\frac{\partial M(m_a, \alpha)}{\partial Nu(\text{Re}, \alpha)}$ was defined previously in Eq. (E.50) and $\frac{\partial Nu(\text{Re}, \alpha)}{\partial a_{3, Nu}}$ was defined previously in Eq. (E.60).

The derivatives of the “liquid continuity equations” [cf. Eqs. (2.25) - (2.27)] with respect to the parameter $\alpha^{(30)} : W_{dkx}$ are as follows:

$$\frac{\partial N_1^{(i)}}{\partial \alpha^{(30)}} = \frac{\partial N_1^{(i)}}{\partial W_{dkx}} \equiv a_1^{i, 30} = 0; \quad \ell = 1; \quad i = 1, \dots, I; \quad j = 30. \quad (\text{E.343})$$

The derivatives of the “liquid continuity equations” [cf. Eqs. (2.25) - (2.27)] with respect to the parameter $\alpha^{(31)} : W_{dky}$ are as follows:

$$\frac{\partial N_1^{(i)}}{\partial \alpha^{(31)}} = \frac{\partial N_1^{(i)}}{\partial W_{dky}} \equiv a_1^{i, 31} = 0; \quad \ell = 1; \quad i = 1, \dots, I; \quad j = 31. \quad (\text{E.344})$$

The derivatives of the “liquid continuity equations” [cf. Eqs. (2.25) - (2.27)] with respect to the parameter $\alpha^{(32)} : \Delta z_{dk}$ are as follows:

$$\frac{\partial N_1^{(i)}}{\partial \alpha^{(32)}} = \frac{\partial N_1^{(i)}}{\partial \Delta z_{dk}} \equiv a_1^{i, 32} = 0; \quad \ell = 1; \quad i = 1, \dots, I; \quad j = 32. \quad (\text{E.345})$$

APPENDIX E. DERIVATIVES OF THE MODEL EQUATIONS WITH
RESPECT TO THE MODEL PARAMETERS

The derivatives of the “liquid continuity equations” [cf. Eqs. (2.25) - (2.27)] with respect to the parameter $\alpha^{(33)} : \Delta z_{fan}$ are as follows:

$$\frac{\partial N_1^{(i)}}{\partial \alpha^{(33)}} = \frac{\partial N_1^{(i)}}{\partial \Delta z_{fan}} \equiv a_1^{i,33} = 0; \quad \ell = 1; \quad i = 1, \dots, I; \quad j = 33. \quad (\text{E.346})$$

The derivatives of the “liquid continuity equations” [cf. Eqs. (2.25) - (2.27)] with respect to the parameter $\alpha^{(34)} : D_{fan}$ are as follows:

$$\frac{\partial N_1^{(i)}}{\partial \alpha^{(34)}} = \frac{\partial N_1^{(i)}}{\partial D_{fan}} \equiv a_1^{i,34} = 0; \quad \ell = 1; \quad i = 1, \dots, I; \quad j = 34, \quad (\text{E.347})$$

The derivatives of the “liquid continuity equations” [cf. Eqs. (2.25) - (2.27)] with respect to the parameter $\alpha^{(35)} : \Delta z_{fill}$ are as follows:

$$\frac{\partial N_1^{(i)}}{\partial \alpha^{(35)}} = \frac{\partial N_1^{(i)}}{\partial \Delta z_{fill}} \equiv a_1^{i,35} = 0; \quad \ell = 1; \quad i = 1, \dots, I; \quad j = 35. \quad (\text{E.348})$$

The derivatives of the “liquid continuity equations” [cf. Eqs. (2.25) - (2.27)] with respect to the parameter $\alpha^{(36)} : \Delta z_{rain}$ are as follows:

$$\frac{\partial N_1^{(i)}}{\partial \alpha^{(36)}} = \frac{\partial N_1^{(i)}}{\partial \Delta z_{rain}} \equiv a_1^{i,36} = 0; \quad \ell = 1; \quad i = 1, \dots, I; \quad j = 36. \quad (\text{E.349})$$

The derivatives of the “liquid continuity equations” [cf. Eqs. (2.25) - (2.27)] with respect to the parameter $\alpha^{(37)} : \Delta z_{bs}$ are as follows:

$$\frac{\partial N_1^{(i)}}{\partial \alpha^{(37)}} = \frac{\partial N_1^{(i)}}{\partial \Delta z_{bs}} \equiv a_1^{i,37} = 0; \quad \ell = 1; \quad i = 1, \dots, I; \quad j = 37. \quad (\text{E.350})$$

The derivatives of the “liquid continuity equations” [cf. Eqs. (2.25) - (2.27)] with respect to the parameter $\alpha^{(38)} : \Delta z_{de}$ are as follows:

$$\frac{\partial N_1^{(i)}}{\partial \alpha^{(38)}} = \frac{\partial N_1^{(i)}}{\partial \Delta z_{de}} \equiv a_1^{i,38} = 0; \quad \ell = 1; \quad i = 1, \dots, I; \quad j = 38. \quad (\text{E.351})$$

APPENDIX E. DERIVATIVES OF THE MODEL EQUATIONS WITH RESPECT TO THE MODEL PARAMETERS

The derivatives of the “liquid continuity equations” [cf. Eqs. (2.25) - (2.27)] with respect to the parameter $\alpha^{(39)} : D_h$ are as follows:

$$\frac{\partial N_1^{(i)}}{\partial \alpha^{(39)}} = \frac{\partial N_1^{(i)}}{\partial D_h} \equiv a_1^{i,39} = \frac{1}{\bar{R}} \left[\frac{P_{vs}^{(i+1)}(T_w^{(i+1)}, \boldsymbol{\alpha})}{T_w^{(i+1)}} - \frac{P_{vs}^{(i)}(T_a^{(i)}, \boldsymbol{\alpha})}{T_a^{(i)}} \right] \frac{\partial M(m_a, \boldsymbol{\alpha})}{\partial D_h};$$

$$\ell = 1; \quad i = 1, \dots, I; \quad j = 39,$$
(E.352)

where $\frac{\partial M(m_a, \boldsymbol{\alpha})}{\partial D_h}$ was defined previously in Eq. (E.72).

The derivatives of the “liquid continuity equations” [cf. Eqs. (2.25) - (2.27)] with respect to the parameter $\alpha^{(40)} : A_{fill}$ are as follows:

$$\frac{\partial N_1^{(i)}}{\partial \alpha^{(40)}} = \frac{\partial N_1^{(i)}}{\partial A_{fill}} \equiv a_1^{i,40} = \frac{1}{\bar{R}} \left[\frac{P_{vs}^{(i+1)}(T_w^{(i+1)}, \boldsymbol{\alpha})}{T_w^{(i+1)}} - \frac{P_{vs}^{(i)}(T_a^{(i)}, \boldsymbol{\alpha})}{T_a^{(i)}} \right] \frac{\partial M(m_a, \boldsymbol{\alpha})}{\partial A_{fill}};$$

$$\ell = 1; \quad i = 1, \dots, I; \quad j = 40,$$
(E.353)

where $\frac{\partial M(m_a, \boldsymbol{\alpha})}{\partial A_{fill}}$ was defined previously in Eq. (E.75).

The derivatives of the “liquid continuity equations” [cf. Eqs. (2.25) - (2.27)] with respect to the parameter $\alpha^{(41)} : A_{surf}$ are as follows:

$$\frac{\partial N_1^{(i)}}{\partial \alpha^{(41)}} = \frac{\partial N_1^{(i)}}{\partial A_{surf}} \equiv a_1^{i,41} = \frac{1}{\bar{R}} \left[\frac{P_{vs}^{(i+1)}(T_w^{(i+1)}, \boldsymbol{\alpha})}{T_w^{(i+1)}} - \frac{P_{vs}^{(i)}(T_a^{(i)}, \boldsymbol{\alpha})}{T_a^{(i)}} \right] \frac{\partial M(m_a, \boldsymbol{\alpha})}{\partial A_{surf}};$$

$$\ell = 1; \quad i = 1, \dots, I; \quad j = 41,$$
(E.354)

where $\frac{\partial M(m_a, \boldsymbol{\alpha})}{\partial A_{surf}}$ was defined previously in Eq. (E.78).

The derivatives of the “liquid continuity equations” [cf. Eqs. (2.25) - (2.27)] with respect to the parameter $\alpha^{(42)} : \text{Pr}$ are as follows:

$$\frac{\partial N_1^{(i)}}{\partial \alpha^{(42)}} = \frac{\partial N_1^{(i)}}{\partial \text{Pr}} \equiv a_1^{i,42} = \frac{1}{\bar{R}} \left[\frac{P_{vs}^{(i+1)}(T_w^{(i+1)}, \boldsymbol{\alpha})}{T_w^{(i+1)}} - \frac{P_{vs}^{(i)}(T_a^{(i)}, \boldsymbol{\alpha})}{T_a^{(i)}} \right] \frac{\partial M(m_a, \boldsymbol{\alpha})}{\partial \text{Pr}};$$

$$\ell = 1; \quad i = 1, \dots, I; \quad j = 42,$$
(E.355)

APPENDIX E. DERIVATIVES OF THE MODEL EQUATIONS WITH RESPECT TO THE MODEL PARAMETERS

where $\frac{\partial M(m_a, \boldsymbol{\alpha})}{\partial \text{Pr}}$ was defined previously in Eq. (E.81).

The derivatives of the “liquid continuity equations” [cf. Eqs. (2.25) - (2.27)] with respect to the parameter $\alpha^{(43)} : w_{tsa}$ are as follows:

$$\frac{\partial N_1^{(i)}}{\partial \alpha^{(43)}} = \frac{\partial N_1^{(i)}}{\partial w_{tsa}} \equiv a_1^{i,43} = \frac{1}{R} \left[\frac{P_{vs}^{(i+1)}(T_w^{(i+1)}, \boldsymbol{\alpha})}{T_w^{(i+1)}} - \frac{P_{vs}^{(i)}(T_a^{(i)}, \boldsymbol{\alpha})}{T_a^{(i)}} \right] \frac{\partial M(m_a, \boldsymbol{\alpha})}{\partial w_{tsa}};$$

$$\ell = 1; \quad i = 1, \dots, I; \quad j = 43,$$
(E.356)

where $\frac{\partial M(m_a, \boldsymbol{\alpha})}{\partial w_{tsa}}$ was defined in Eq. (E.84).

The derivatives of the “liquid continuity equations” [cf. Eqs. (2.25) - (2.27)] with respect to the parameter $\alpha^{(44)} : m_{w,in}$ are as follows:

$$\frac{\partial N_1^{(1)}}{\partial \alpha^{(44)}} = \frac{\partial N_1^{(1)}}{\partial m_{w,in}} \equiv a_1^{1,44} = -1; \quad \ell = 1; \quad i = 1; \quad j = 44,$$
(E.357)

$$\frac{\partial N_1^{(i)}}{\partial \alpha^{(44)}} = \frac{\partial N_1^{(i)}}{\partial m_{w,in}} \equiv a_1^{i,44} = 0; \quad \ell = 1; \quad i = 2, \dots, I; \quad j = 44.$$
(E.358)

The derivatives of the “liquid continuity equations” [cf. Eqs. (2.25) - (2.27)] with respect to the parameter $\alpha^{(45)} : T_{a,in}$ are as follows:

$$\frac{\partial N_1^{(i)}}{\partial \alpha^{(45)}} = \frac{\partial N_1^{(i)}}{\partial T_{a,in}} \equiv a_1^{i,45} = 0; \quad \ell = 1; \quad i = 1, \dots, I; \quad j = 45.$$
(E.359)

The derivatives of the “liquid continuity equations” [cf. Eqs. (2.25) - (2.27)] with respect to the parameter $\alpha^{(46)} : \omega_{in}$ are as follows:

$$\frac{\partial N_1^{(i)}}{\partial \alpha^{(46)}} = \frac{\partial N_1^{(i)}}{\partial \omega_{in}} \equiv a_1^{i,46} = 0; \quad \ell = 1; \quad i = 1, \dots, I; \quad j = 46.$$
(E.360)

APPENDIX E. DERIVATIVES OF THE MODEL EQUATIONS WITH RESPECT TO THE MODEL PARAMETERS

The derivatives of the “liquid continuity equations” [cf. Eqs. (2.25) - (2.27)] with respect to the parameter $\alpha^{(47)} : Sc$ are as follows:

$$\frac{\partial N_1^{(i)}}{\partial \alpha^{(47)}} = \frac{\partial N_1^{(i)}}{\partial Sc} \equiv a_1^{i,47} = \frac{1}{\bar{R}} \left[\frac{P_{vs}^{(i+1)}(T_w^{(i+1)}, \boldsymbol{\alpha})}{T_w^{(i+1)}} - \frac{P_{vs}^{(i)}(T_a^{(i)}, \boldsymbol{\alpha})}{T_a^{(i)}} \right] \frac{\partial M(m_a, \boldsymbol{\alpha})}{\partial Sc};$$

$$\ell = 1; \quad i = 1, \dots, I; \quad j = 47,$$
(E.361)

where $\frac{\partial M(m_a, \boldsymbol{\alpha})}{\partial Sc}$ was defined previously in Eq. (E.91).

E.3 Derivatives of the Model Equations with respect to the Model Parameters for Case 2: Fan Off, Unsaturated Air Conditions

The differences between the governing equations for case 1a and case 2 are only in the “liquid continuity equations”. Other governing equations (i.e., liquid energy balance equations; water vapor continuity equations; air/water vapor energy balance equations; mechanical energy equation) are the same for both cases, and their derivatives in Subsections E.1.2 through E.1.5. Therefore for case 2, only the derivatives of the “liquid continuity equations” with respect to parameters are derived as follows, since the derivatives of other governing equations with respect to parameters are the same as that of case 1a.

The notation used will be the following:

$$a_1^{i,j} \equiv \frac{\partial N_1^{(i)}}{\partial \alpha^{(j)}}; \quad i = 1, \dots, I; \quad j = 1, \dots, N_\alpha. \quad (E.362)$$

APPENDIX E. DERIVATIVES OF THE MODEL EQUATIONS WITH
RESPECT TO THE MODEL PARAMETERS

**E.3.1 Derivatives of the liquid continuity equations with
respect to the parameters**

The derivatives of the “liquid continuity equations” [cf. Eqs. (2.38) - (2.40)]
with respect to the parameter $\alpha^{(1)} : T_{db}$ are as follows:

$$\begin{aligned} \frac{\partial N_1^{(i)}}{\partial \alpha^{(1)}} = \frac{\partial N_1^{(i)}}{\partial T_{db}} \equiv a_1^{i,1} = \frac{1}{R} \left[\frac{P_{vs}^{(i+1)}(T_w^{(i+1)}, \boldsymbol{\alpha})}{T_w^{(i+1)}} - \frac{\omega^{(i)} P_{atm}}{(0.622 + \omega^{(i)}) T_a^{(i)}} \right] \\ \cdot \frac{\partial M(m_a, \boldsymbol{\alpha})}{\partial D_{av}(T_{db}, \boldsymbol{\alpha})} \cdot \frac{\partial D_{av}(T_{db}, \boldsymbol{\alpha})}{\partial T_{db}}. \quad \ell = 1; \quad i = 1, \dots, I; \quad j = 1, \end{aligned} \quad (\text{E.363})$$

where $\frac{\partial M(m_a, \boldsymbol{\alpha})}{\partial D_{av}(T_{db}, \boldsymbol{\alpha})}$ and $\frac{\partial D_{av}(T_{db}, \boldsymbol{\alpha})}{\partial T_{db}}$ were defined in Eqs. (E.3) and (E.4), respectively.

The derivatives of the “liquid continuity equations” [cf. Eqs. (2.38) - (2.40)]
with respect to the parameter $\alpha^{(2)} : T_{dp}$ are as follows:

$$\frac{\partial N_1^{(i)}}{\partial \alpha^{(2)}} = \frac{\partial N_1^{(i)}}{\partial T_{dp}} \equiv a_1^{i,2} = 0; \quad \ell = 1; \quad i = 1, \dots, I; \quad j = 2. \quad (\text{E.364})$$

The derivatives of the “liquid continuity equations” [cf. Eqs. (2.38) - (2.40)]
with respect to the parameter $\alpha^{(3)} : T_{w,in}$ are as follows:

$$\frac{\partial N_1^{(1)}}{\partial \alpha^{(3)}} = \frac{\partial N_1^{(1)}}{\partial T_{w,in}} \equiv a_1^{1,3} = 0; \quad \ell = 1; \quad i = 1; \quad j = 3, \quad (\text{E.365})$$

The derivatives of the “liquid continuity equations” [cf. Eqs. (2.38) - (2.40)]
with respect to the parameter $\alpha^{(4)} : P_{atm}$ are as follows:

$$\begin{aligned} \frac{\partial N_1^{(i)}}{\partial \alpha^{(4)}} = \frac{\partial N_1^{(i)}}{\partial P_{atm}} \equiv a_1^{i,4} = -\frac{M(m_a, \boldsymbol{\alpha})}{R} \frac{\omega^{(i)}}{T_a^{(i)}(0.622 + \omega^{(i)})}; \\ \ell = 1; \quad i = 1, \dots, I; \quad j = 4, \end{aligned} \quad (\text{E.366})$$

APPENDIX E. DERIVATIVES OF THE MODEL EQUATIONS WITH RESPECT TO THE MODEL PARAMETERS

The derivatives of the “liquid continuity equations” [cf. Eqs. (2.38) - (2.40)] with respect to the parameter $\alpha^{(5)} : V_w$ are as follows:

$$\frac{\partial N_1^{(i)}}{\partial \alpha^{(5)}} = \frac{\partial N_1^{(i)}}{\partial V_w} \equiv a_1^{i,5} = 0; \quad \ell = 1; \quad i = 1, \dots, I; \quad j = 5, \quad (\text{E.367})$$

The derivatives of the “liquid continuity equations” [cf. Eqs. (2.38) - (2.40)] with respect to the parameter $\alpha^{(6)} : k_{sum}$ are as follows:

$$\frac{\partial N_1^{(i)}}{\partial \alpha^{(6)}} = \frac{\partial N_1^{(i)}}{\partial k_{sum}} \equiv a_1^{i,6} = 0; \quad \ell = 1; \quad i = 1, \dots, I; \quad j = 6. \quad (\text{E.368})$$

The derivatives of the “liquid continuity equations” [cf. Eqs. (2.38) - (2.40)] with respect to the parameter $\alpha^{(7)} : \mu$ are as follows:

$$\begin{aligned} \frac{\partial N_1^{(i)}}{\partial \alpha^{(7)}} = \frac{\partial N_1^{(i)}}{\partial \mu} \equiv a_1^{i,7} &= \frac{1}{\bar{R}} \left[\frac{P_{vs}^{(i+1)}(T_w^{(i+1)}, \boldsymbol{\alpha})}{T_w^{(i+1)}} - \frac{\omega^{(i)} P_{atm}}{(0.622 + \omega^{(i)}) T_a^{(i)}} \right] \frac{\partial M(m_a, \boldsymbol{\alpha})}{\partial \mu}; \\ \ell &= 1; \quad i = 1, \dots, I; \quad j = 7. \end{aligned} \quad (\text{E.369})$$

where $\frac{\partial M(m_a, \boldsymbol{\alpha})}{\partial \mu}$ was defined in Eq. (E.13).

The derivatives of the “liquid continuity equations” [cf. Eqs. (2.38) - (2.40)] with respect to the parameter $\alpha^{(8)} : \nu$ are as follows:

$$\begin{aligned} \frac{\partial N_1^{(i)}}{\partial \alpha^{(8)}} = \frac{\partial N_1^{(i)}}{\partial \nu} \equiv a_1^{i,8} &= \frac{1}{\bar{R}} \left[\frac{P_{vs}^{(i+1)}(T_w^{(i+1)}, \boldsymbol{\alpha})}{T_w^{(i+1)}} - \frac{\omega^{(i)} P_{atm}}{(0.622 + \omega^{(i)}) T_a^{(i)}} \right] \frac{\partial M(m_a, \boldsymbol{\alpha})}{\partial \nu}; \\ \ell &= 1; \quad i = 1, \dots, I; \quad j = 8. \end{aligned} \quad (\text{E.370})$$

where $\frac{\partial M(m_a, \boldsymbol{\alpha})}{\partial \nu}$ was defined in Eq. (E.16).

The derivatives of the “liquid continuity equations” [cf. Eqs. (2.38) - (2.40)] with respect to the parameter $\alpha^{(9)} : k_{air}$ are as follows:

$$\frac{\partial N_1^{(i)}}{\partial \alpha^{(9)}} = \frac{\partial N_1^{(i)}}{\partial k_{air}} \equiv a_1^{i,9} = 0; \quad \ell = 1; \quad i = 1, \dots, I; \quad j = 9. \quad (\text{E.371})$$

APPENDIX E. DERIVATIVES OF THE MODEL EQUATIONS WITH RESPECT TO THE MODEL PARAMETERS

The derivatives of the “liquid continuity equations” [cf. Eqs. (2.38) - (2.40)] with respect to the parameter $\alpha^{(10)} : f_{ht}$ are as follows:

$$\frac{\partial N_1^{(i)}}{\partial \alpha^{(10)}} = \frac{\partial N_1^{(i)}}{\partial f_{ht}} \equiv a_1^{i,10} = 0; \quad \ell = 1; \quad i = 1, \dots, I; \quad j = 10. \quad (\text{E.372})$$

The derivatives of the “liquid continuity equations” [cf. Eqs. (2.38) - (2.40)] with respect to the parameter $\alpha^{(11)} : f_{mt}$ are as follows:

$$\begin{aligned} \frac{\partial N_1^{(i)}}{\partial \alpha^{(11)}} = \frac{\partial N_1^{(i)}}{\partial f_{mt}} \equiv a_1^{i,11} &= \frac{1}{\bar{R}} \left[\frac{P_{vs}^{(i+1)}(T_w^{(i+1)}, \boldsymbol{\alpha})}{T_w^{(i+1)}} - \frac{\omega^{(i)} P_{atm}}{(0.622 + \omega^{(i)}) T_a^{(i)}} \right] \frac{\partial M(m_a, \boldsymbol{\alpha})}{\partial f_{mt}}, \\ \ell &= 1; \quad i = 1, \dots, I; \quad j = 11. \end{aligned} \quad (\text{E.373})$$

where $\frac{\partial M(m_a, \boldsymbol{\alpha})}{\partial f_{mt}}$ was defined in Eq. (E.21).

The derivatives of the “liquid continuity equations” [cf. Eqs. (2.38) - (2.40)] with respect to the parameter $\alpha^{(12)} : f$ are as follows:

$$\frac{\partial N_1^{(i)}}{\partial \alpha^{(12)}} = \frac{\partial N_1^{(i)}}{\partial f} \equiv a_1^{i,12} = 0; \quad \ell = 1; \quad i = 1, \dots, I; \quad j = 12. \quad (\text{E.374})$$

The derivatives of the “liquid continuity equations” [cf. Eqs. (2.38) - (2.40)] with respect to the parameter $\alpha^{(13)} : a_0$ are as follows:

$$\begin{aligned} \frac{\partial N_1^{(i)}}{\partial \alpha^{(13)}} = \frac{\partial N_1^{(i)}}{\partial a_0} \equiv a_1^{i,13} &= \frac{M(m_a, \boldsymbol{\alpha})}{\bar{R}} \frac{1}{T_w^{(i+1)}} \frac{\partial P_{vs}^{(i+1)}(T_w^{(i+1)}, \boldsymbol{\alpha})}{\partial a_0}, \\ \ell &= 1; \quad i = 1, \dots, I; \quad j = 13. \end{aligned} \quad (\text{E.375})$$

where

$$\frac{\partial P_{vs}^{(i+1)}(T_w^{(i+1)}, \boldsymbol{\alpha})}{\partial a_0} = P_{vs}^{(i+1)}(T_w^{(i+1)}, \boldsymbol{\alpha}). \quad (\text{E.376})$$

APPENDIX E. DERIVATIVES OF THE MODEL EQUATIONS WITH RESPECT TO THE MODEL PARAMETERS

The derivatives of the “liquid continuity equations” [cf. Eqs. (2.38) - (2.40)] with respect to the parameter $\alpha^{(14)} : a_1$ are as follows:

$$\frac{\partial N_1^{(i)}}{\partial \alpha^{(14)}} = \frac{\partial N_1^{(i)}}{\partial a_1} \equiv a_1^{i,14} = \frac{M(m_a, \alpha)}{\bar{R}} \frac{1}{T_w^{(i+1)}} \frac{\partial P_{vs}^{(i+1)}(T_w^{(i+1)}, \alpha)}{\partial a_1}; \quad (\text{E.377})$$

$$\ell = 1; \quad i = 1, \dots, I; \quad j = 14.$$

where

$$\frac{\partial P_{vs}^{(i+1)}(T_w^{(i+1)}, \alpha)}{\partial a_1} = \frac{P_{vs}^{(i+1)}(T_w^{(i+1)}, \alpha)}{T_w^{(i+1)}}. \quad (\text{E.378})$$

The derivatives of the “liquid continuity equations” [cf. Eqs. (2.38) - (2.40)] with respect to the parameter $\alpha^{(15)} : a_{0,c_{pa}}$ are as follows:

$$\frac{\partial N_1^{(i)}}{\partial \alpha^{(15)}} = \frac{\partial N_1^{(i)}}{\partial a_{0,c_{pa}}} \equiv a_1^{i,15} = 0; \quad \ell = 1; \quad i = 1, \dots, I; \quad j = 15. \quad (\text{E.379})$$

The derivatives of the “liquid continuity equations” [cf. Eqs. (2.38) - (2.40)] with respect to the parameter $\alpha^{(16)} : a_{1,c_{pa}}$ are as follows:

$$\frac{\partial N_1^{(i)}}{\partial \alpha^{(16)}} = \frac{\partial N_1^{(i)}}{\partial a_{1,c_{pa}}} \equiv a_1^{i,16} = 0; \quad \ell = 1; \quad i = 1, \dots, I; \quad j = 16. \quad (\text{E.380})$$

The derivatives of the “liquid continuity equations” [cf. Eqs. (2.38) - (2.40)] with respect to the parameter $\alpha^{(17)} : a_{2,c_{pa}}$ are as follows:

$$\frac{\partial N_1^{(i)}}{\partial \alpha^{(17)}} = \frac{\partial N_1^{(i)}}{\partial a_{2,c_{pa}}} \equiv a_1^{i,17} = 0; \quad \ell = 1; \quad i = 1, \dots, I; \quad j = 17. \quad (\text{E.381})$$

The derivatives of the “liquid continuity equations” [cf. Eqs. (2.38) - (2.40)] with respect to the parameter $\alpha^{(18)} : a_{0,D_{av}}$ are as follows:

$$\begin{aligned} \frac{\partial N_1^{(i)}}{\partial \alpha^{(18)}} = \frac{\partial N_1^{(i)}}{\partial a_{0,D_{av}}} \equiv a_1^{i,18} = \frac{1}{\bar{R}} \left[\frac{P_{vs}^{(i+1)}(T_w^{(i+1)}, \alpha)}{T_w^{(i+1)}} - \frac{\omega^{(i)} P_{atm}}{(0.622 + \omega^{(i)}) T_a^{(i)}} \right] \\ \cdot \frac{\partial M(m_a, \alpha)}{\partial D_{av}(T_{db}, \alpha)} \cdot \frac{\partial D_{av}(T_{db}, \alpha)}{\partial a_{0,D_{av}}}; \quad \ell = 1; \quad i = 1, \dots, I; \quad j = 18. \end{aligned} \quad (\text{E.382})$$

APPENDIX E. DERIVATIVES OF THE MODEL EQUATIONS WITH RESPECT TO THE MODEL PARAMETERS

where $\frac{\partial M(m_a, \boldsymbol{\alpha})}{\partial D_{av}(T_{db}, \boldsymbol{\alpha})}$ was defined previously in Eq. (E.3), and $\frac{\partial D_{av}(T_{db}, \boldsymbol{\alpha})}{\partial a_{0, D_{av}}}$ was defined previously in Eq. (E.34).

The derivatives of the “liquid continuity equations” [cf. Eqs. (2.38) - (2.40)] with respect to the parameter $\alpha^{(19)} : a_{1, D_{av}}$ are as follows:

$$\begin{aligned} \frac{\partial N_1^{(i)}}{\partial \alpha^{(19)}} = \frac{\partial N_1^{(i)}}{\partial a_{1, D_{av}}} \equiv a_1^{i, 19} = \frac{1}{R} \left[\frac{P_{vs}^{(i+1)}(T_w^{(i+1)}, \boldsymbol{\alpha})}{T_w^{(i+1)}} - \frac{\omega^{(i)} P_{atm}}{(0.622 + \omega^{(i)}) T_a^{(i)}} \right] \\ \cdot \frac{\partial M(m_a, \boldsymbol{\alpha})}{\partial D_{av}(T_{db}, \boldsymbol{\alpha})} \cdot \frac{\partial D_{av}(T_{db}, \boldsymbol{\alpha})}{\partial a_{1, D_{av}}}; \quad \ell = 1; \quad i = 1, \dots, I; \quad j = 19. \end{aligned} \quad (\text{E.383})$$

where $\frac{\partial M(m_a, \boldsymbol{\alpha})}{\partial D_{av}(T_{db}, \boldsymbol{\alpha})}$ was defined previously in Eq. (E.3), and $\frac{\partial D_{av}(T_{db}, \boldsymbol{\alpha})}{\partial a_{1, D_{av}}}$ was defined previously in Eq. (E.37).

The derivatives of the “liquid continuity equations” [cf. Eqs. (2.38) - (2.40)] with respect to the parameter $\alpha^{(20)} : a_{2, D_{av}}$ are as follows:

$$\begin{aligned} \frac{\partial N_1^{(i)}}{\partial \alpha^{(20)}} = \frac{\partial N_1^{(i)}}{\partial a_{2, D_{av}}} \equiv a_1^{i, 20} = \frac{1}{R} \left[\frac{P_{vs}^{(i+1)}(T_w^{(i+1)}, \boldsymbol{\alpha})}{T_w^{(i+1)}} - \frac{\omega^{(i)} P_{atm}}{(0.622 + \omega^{(i)}) T_a^{(i)}} \right] \\ \cdot \frac{\partial M(m_a, \boldsymbol{\alpha})}{\partial D_{av}(T_{db}, \boldsymbol{\alpha})} \cdot \frac{\partial D_{av}(T_{db}, \boldsymbol{\alpha})}{\partial a_{2, D_{av}}}; \quad \ell = 1; \quad i = 1, \dots, I; \quad j = 20. \end{aligned} \quad (\text{E.384})$$

where $\frac{\partial M(m_a, \boldsymbol{\alpha})}{\partial D_{av}(T_{db}, \boldsymbol{\alpha})}$ was defined previously in Eq. (E.3), and $\frac{\partial D_{av}(T_{db}, \boldsymbol{\alpha})}{\partial a_{2, D_{av}}}$ was defined previously in Eq. (E.40).

The derivatives of the “liquid continuity equations” [cf. Eqs. (2.38) - (2.40)] with respect to the parameter $\alpha^{(21)} : a_{3, D_{av}}$ are as follows:

$$\begin{aligned} \frac{\partial N_1^{(i)}}{\partial \alpha^{(21)}} = \frac{\partial N_1^{(i)}}{\partial a_{3, D_{av}}} \equiv a_1^{i, 21} = \frac{1}{R} \left[\frac{P_{vs}^{(i+1)}(T_w^{(i+1)}, \boldsymbol{\alpha})}{T_w^{(i+1)}} - \frac{\omega^{(i)} P_{atm}}{(0.622 + \omega^{(i)}) T_a^{(i)}} \right] \\ \cdot \frac{\partial M(m_a, \boldsymbol{\alpha})}{\partial D_{av}(T_{db}, \boldsymbol{\alpha})} \cdot \frac{\partial D_{av}(T_{db}, \boldsymbol{\alpha})}{\partial a_{3, D_{av}}}; \quad \ell = 1; \quad i = 1, \dots, I; \quad j = 21. \end{aligned} \quad (\text{E.385})$$

where $\frac{\partial M(m_a, \boldsymbol{\alpha})}{\partial D_{av}(T_{db}, \boldsymbol{\alpha})}$ was defined previously in Eq. (E.3), and $\frac{\partial D_{av}(T_{db}, \boldsymbol{\alpha})}{\partial a_{3, D_{av}}}$ was defined previously in Eq. (E.43).

APPENDIX E. DERIVATIVES OF THE MODEL EQUATIONS WITH
RESPECT TO THE MODEL PARAMETERS

The derivatives of the “liquid continuity equations” [cf. Eqs. (2.38) - (2.40)] with respect to the parameter $\alpha^{(22)} : a_{0f}$ are as follows:

$$\frac{\partial N_1^{(i)}}{\partial \alpha^{(22)}} = \frac{\partial N_1^{(i)}}{\partial a_{0f}} \equiv a_1^{i,22} = 0; \quad \ell = 1; \quad i = 1, \dots, I; \quad j = 22. \quad (\text{E.386})$$

The derivatives of the “liquid continuity equations” [cf. Eqs. (2.38) - (2.40)] with respect to the parameter $\alpha^{(23)} : a_{1f}$ are as follows:

$$\frac{\partial N_1^{(i)}}{\partial \alpha^{(23)}} = \frac{\partial N_1^{(i)}}{\partial a_{1f}} \equiv a_1^{i,23} = 0; \quad \ell = 1; \quad i = 1, \dots, I; \quad j = 23. \quad (\text{E.387})$$

The derivatives of the “liquid continuity equations” [cf. Eqs. (2.38) - (2.40)] with respect to the parameter $\alpha^{(24)} : a_{0g}$ are as follows:

$$\frac{\partial N_1^{(i)}}{\partial \alpha^{(24)}} = \frac{\partial N_1^{(i)}}{\partial a_{0g}} \equiv a_1^{i,24} = 0; \quad \ell = 1; \quad i = 1, \dots, I; \quad j = 24. \quad (\text{E.388})$$

The derivatives of the “liquid continuity equations” [cf. Eqs. (2.38) - (2.40)] with respect to the parameter $\alpha^{(25)} : a_{1g}$ are as follows:

$$\frac{\partial N_1^{(i)}}{\partial \alpha^{(25)}} = \frac{\partial N_1^{(i)}}{\partial a_{1g}} \equiv a_1^{i,25} = 0; \quad \ell = 1; \quad i = 1, \dots, I; \quad j = 25. \quad (\text{E.389})$$

The derivatives of the “liquid continuity equations” [cf. Eqs. (2.38) - (2.40)] with respect to the parameter $\alpha^{(26)} : a_{0,Nu}$ are as follows:

$$\begin{aligned} \frac{\partial N_1^{(i)}}{\partial \alpha^{(26)}} = \frac{\partial N_1^{(i)}}{\partial a_{0,Nu}} \equiv a_1^{i,26} = \frac{1}{R} & \left[\frac{P_{vs}^{(i+1)}(T_w^{(i+1)}, \boldsymbol{\alpha})}{T_w^{(i+1)}} - \frac{\omega^{(i)} P_{atm}}{(0.622 + \omega^{(i)}) T_a^{(i)}} \right] \\ & \cdot \frac{\partial M(m_a, \boldsymbol{\alpha})}{\partial Nu(\text{Re}, \boldsymbol{\alpha})} \frac{\partial Nu(\text{Re}, \boldsymbol{\alpha})}{\partial a_{0,Nu}}; \quad \ell = 1; \quad i = 1, \dots, I; \quad j = 26. \end{aligned} \quad (\text{E.390})$$

where $\frac{\partial M(m_a, \boldsymbol{\alpha})}{\partial Nu(\text{Re}, \boldsymbol{\alpha})}$ was defined previously in Eq. (E.50), and $\frac{\partial Nu(\text{Re}, \boldsymbol{\alpha})}{\partial a_{0,Nu}}$ was defined previously in Eq. (E.51).

APPENDIX E. DERIVATIVES OF THE MODEL EQUATIONS WITH RESPECT TO THE MODEL PARAMETERS

The derivatives of the “liquid continuity equations” [cf. Eqs. (2.38) - (2.40)] with respect to the parameter $\alpha^{(27)} : a_{1,Nu}$ are as follows:

$$\begin{aligned} \frac{\partial N_1^{(i)}}{\partial \alpha^{(27)}} = \frac{\partial N_1^{(i)}}{\partial a_{1,Nu}} \equiv a_1^{i,27} = \frac{1}{\bar{R}} \left[\frac{P_{vs}^{(i+1)}(T_w^{(i+1)}, \boldsymbol{\alpha})}{T_w^{(i+1)}} - \frac{\omega^{(i)} P_{atm}}{(0.622 + \omega^{(i)}) T_a^{(i)}} \right] \\ \cdot \frac{\partial M(m_a, \boldsymbol{\alpha})}{\partial Nu(\text{Re}, \boldsymbol{\alpha})} \frac{\partial Nu(\text{Re}, \boldsymbol{\alpha})}{\partial a_{1,Nu}}; \quad \ell = 1; \quad i = 1, \dots, I; \quad j = 27. \end{aligned} \quad (\text{E.391})$$

where $\frac{\partial M(m_a, \boldsymbol{\alpha})}{\partial Nu(\text{Re}, \boldsymbol{\alpha})}$ was defined previously in Eq. (E.50), and $\frac{\partial Nu(\text{Re}, \boldsymbol{\alpha})}{\partial a_{1,Nu}}$ was defined previously in Eq. (E.54).

The derivatives of the “liquid continuity equations” [cf. Eqs. (2.38) - (2.40)] with respect to the parameter $\alpha^{(28)} : a_{2,Nu}$ are as follows:

$$\begin{aligned} \frac{\partial N_1^{(i)}}{\partial \alpha^{(28)}} = \frac{\partial N_1^{(i)}}{\partial a_{2,Nu}} \equiv a_1^{i,28} = \frac{1}{\bar{R}} \left[\frac{P_{vs}^{(i+1)}(T_w^{(i+1)}, \boldsymbol{\alpha})}{T_w^{(i+1)}} - \frac{\omega^{(i)} P_{atm}}{(0.622 + \omega^{(i)}) T_a^{(i)}} \right] \\ \cdot \frac{\partial M(m_a, \boldsymbol{\alpha})}{\partial Nu(\text{Re}, \boldsymbol{\alpha})} \frac{\partial Nu(\text{Re}, \boldsymbol{\alpha})}{\partial a_{2,Nu}}; \quad \ell = 1; \quad i = 1, \dots, I; \quad j = 28. \end{aligned} \quad (\text{E.392})$$

where $\frac{\partial M(m_a, \boldsymbol{\alpha})}{\partial Nu(\text{Re}, \boldsymbol{\alpha})}$ was defined previously in Eq. (E.50), and $\frac{\partial Nu(\text{Re}, \boldsymbol{\alpha})}{\partial a_{2,Nu}}$ was defined previously in Eq. (E.57)

The derivatives of the “liquid continuity equations” [cf. Eqs. (2.38) - (2.40)] with respect to the parameter $\alpha^{(29)} : a_{3,Nu}$ are as follows:

$$\begin{aligned} \frac{\partial N_1^{(i)}}{\partial \alpha^{(29)}} = \frac{\partial N_1^{(i)}}{\partial a_{3,Nu}} \equiv a_1^{i,29} = \frac{1}{\bar{R}} \left[\frac{P_{vs}^{(i+1)}(T_w^{(i+1)}, \boldsymbol{\alpha})}{T_w^{(i+1)}} - \frac{\omega^{(i)} P_{atm}}{(0.622 + \omega^{(i)}) T_a^{(i)}} \right] \\ \cdot \frac{\partial M(m_a, \boldsymbol{\alpha})}{\partial Nu(\text{Re}, \boldsymbol{\alpha})} \frac{\partial Nu(\text{Re}, \boldsymbol{\alpha})}{\partial a_{3,Nu}}; \quad \ell = 1; \quad i = 1, \dots, I; \quad j = 29. \end{aligned} \quad (\text{E.393})$$

where $\frac{\partial M(m_a, \boldsymbol{\alpha})}{\partial Nu(\text{Re}, \boldsymbol{\alpha})}$ was defined previously in Eq. (E.50), and $\frac{\partial Nu(\text{Re}, \boldsymbol{\alpha})}{\partial a_{3,Nu}}$ was defined previously in Eq. (E.60).

APPENDIX E. DERIVATIVES OF THE MODEL EQUATIONS WITH
RESPECT TO THE MODEL PARAMETERS

The derivatives of the “liquid continuity equations” [cf. Eqs. (2.38) - (2.40)] with respect to the parameter $\alpha^{(30)} : W_{dkx}$ are as follows:

$$\frac{\partial N_1^{(i)}}{\partial \alpha^{(30)}} = \frac{\partial N_1^{(i)}}{\partial W_{dkx}} \equiv a_1^{i,30} = 0; \quad \ell = 1; \quad i = 1, \dots, I; \quad j = 30. \quad (\text{E.394})$$

The derivatives of the “liquid continuity equations” [cf. Eqs. (2.38) - (2.40)] with respect to the parameter $\alpha^{(31)} : W_{dky}$ are as follows:

$$\frac{\partial N_1^{(i)}}{\partial \alpha^{(31)}} = \frac{\partial N_1^{(i)}}{\partial W_{dky}} \equiv a_1^{i,31} = 0; \quad \ell = 1; \quad i = 1, \dots, I; \quad j = 31. \quad (\text{E.395})$$

The derivatives of the “liquid continuity equations” [cf. Eqs. (2.38) - (2.40)] with respect to the parameter $\alpha^{(32)} : \Delta z_{dk}$ are as follows:

$$\frac{\partial N_1^{(i)}}{\partial \alpha^{(32)}} = \frac{\partial N_1^{(i)}}{\partial \Delta z_{dk}} \equiv a_1^{i,32} = 0; \quad \ell = 1; \quad i = 1, \dots, I; \quad j = 32. \quad (\text{E.396})$$

The derivatives of the “liquid continuity equations” [cf. Eqs. (2.38) - (2.40)] with respect to the parameter $\alpha^{(33)} : \Delta z_{fan}$ are as follows:

$$\frac{\partial N_1^{(i)}}{\partial \alpha^{(33)}} = \frac{\partial N_1^{(i)}}{\partial \Delta z_{fan}} \equiv a_1^{i,33} = 0; \quad \ell = 1; \quad i = 1, \dots, I; \quad j = 33. \quad (\text{E.397})$$

The derivatives of the “liquid continuity equations” [cf. Eqs. (2.38) - (2.40)] with respect to the parameter $\alpha^{(34)} : D_{fan}$ are as follows:

$$\frac{\partial N_1^{(i)}}{\partial \alpha^{(34)}} = \frac{\partial N_1^{(i)}}{\partial D_{fan}} \equiv a_1^{i,34} = 0; \quad \ell = 1; \quad i = 1, \dots, I; \quad j = 34, \quad (\text{E.398})$$

The derivatives of the “liquid continuity equations” [cf. Eqs. (2.38) - (2.40)] with respect to the parameter $\alpha^{(35)} : \Delta z_{fill}$ are as follows:

$$\frac{\partial N_1^{(i)}}{\partial \alpha^{(35)}} = \frac{\partial N_1^{(i)}}{\partial \Delta z_{fill}} \equiv a_1^{i,35} = 0; \quad \ell = 1; \quad i = 1, \dots, I; \quad j = 35. \quad (\text{E.399})$$

APPENDIX E. DERIVATIVES OF THE MODEL EQUATIONS WITH RESPECT TO THE MODEL PARAMETERS

The derivatives of the “liquid continuity equations” [cf. Eqs. (2.38) - (2.40)] with respect to the parameter $\alpha^{(36)} : \Delta z_{rain}$ are as follows:

$$\frac{\partial N_1^{(i)}}{\partial \alpha^{(36)}} = \frac{\partial N_1^{(i)}}{\partial \Delta z_{rain}} \equiv a_1^{i,36} = 0; \quad \ell = 1; \quad i = 1, \dots, I; \quad j = 36. \quad (\text{E.400})$$

The derivatives of the “liquid continuity equations” [cf. Eqs. (2.38) - (2.40)] with respect to the parameter $\alpha^{(37)} : \Delta z_{bs}$ are as follows:

$$\frac{\partial N_1^{(i)}}{\partial \alpha^{(37)}} = \frac{\partial N_1^{(i)}}{\partial \Delta z_{bs}} \equiv a_1^{i,37} = 0; \quad \ell = 1; \quad i = 1, \dots, I; \quad j = 37. \quad (\text{E.401})$$

The derivatives of the “liquid continuity equations” [cf. Eqs. (2.38) - (2.40)] with respect to the parameter $\alpha^{(38)} : \Delta z_{de}$ are as follows:

$$\frac{\partial N_1^{(i)}}{\partial \alpha^{(38)}} = \frac{\partial N_1^{(i)}}{\partial \Delta z_{de}} \equiv a_1^{i,38} = 0; \quad \ell = 1; \quad i = 1, \dots, I; \quad j = 38. \quad (\text{E.402})$$

The derivatives of the “liquid continuity equations” [cf. Eqs. (2.38) - (2.40)] with respect to the parameter $\alpha^{(39)} : D_h$ are as follows:

$$\begin{aligned} \frac{\partial N_1^{(i)}}{\partial \alpha^{(39)}} = \frac{\partial N_1^{(i)}}{\partial D_h} \equiv a_1^{i,39} &= \frac{1}{\bar{R}} \left[\frac{P_{vs}^{(i+1)}(T_w^{(i+1)}, \alpha)}{T_w^{(i+1)}} - \frac{\omega^{(i)} P_{atm}}{(0.622 + \omega^{(i)}) T_a^{(i)}} \right] \frac{\partial M(m_a, \alpha)}{\partial D_h}; \\ \ell &= 1; \quad i = 1, \dots, I; \quad j = 39. \end{aligned} \quad (\text{E.403})$$

where $\frac{\partial M(m_a, \alpha)}{\partial D_h}$ was defined previously in Eq. (E.72).

The derivatives of the “liquid continuity equations” [cf. Eqs. (2.38) - (2.40)] with respect to the parameter $\alpha^{(40)} : A_{fill}$ are as follows:

$$\begin{aligned} \frac{\partial N_1^{(i)}}{\partial \alpha^{(40)}} = \frac{\partial N_1^{(i)}}{\partial A_{fill}} \equiv a_1^{i,40} &= \frac{1}{\bar{R}} \left[\frac{P_{vs}^{(i+1)}(T_w^{(i+1)}, \alpha)}{T_w^{(i+1)}} - \frac{\omega^{(i)} P_{atm}}{(0.622 + \omega^{(i)}) T_a^{(i)}} \right] \frac{\partial M(m_a, \alpha)}{\partial A_{fill}}; \\ \ell &= 1; \quad i = 1, \dots, I; \quad j = 40. \end{aligned} \quad (\text{E.404})$$

APPENDIX E. DERIVATIVES OF THE MODEL EQUATIONS WITH RESPECT TO THE MODEL PARAMETERS

where $\frac{\partial M(m_a, \alpha)}{\partial A_{fill}}$ was defined previously in Eq. (E.75).

The derivatives of the “liquid continuity equations” [cf. Eqs. (2.38) - (2.40)] with respect to the parameter $\alpha^{(41)} : A_{surf}$ are as follows:

$$\frac{\partial N_1^{(i)}}{\partial \alpha^{(41)}} = \frac{\partial N_1^{(i)}}{\partial A_{surf}} \equiv a_1^{i,41} = \frac{1}{\bar{R}} \left[\frac{P_{vs}^{(i+1)}(T_w^{(i+1)}, \alpha)}{T_w^{(i+1)}} - \frac{\omega^{(i)} P_{atm}}{(0.622 + \omega^{(i)}) T_a^{(i)}} \right] \frac{\partial M(m_a, \alpha)}{\partial A_{surf}};$$

$$\ell = 1; \ i = 1, \dots, I; \ j = 41.$$
(E.405)

where $\frac{\partial M(m_a, \alpha)}{\partial A_{surf}}$ was defined previously in Eq. (E.78).

The derivatives of the “liquid continuity equations” [cf. Eqs. (2.38) - (2.40)] with respect to the parameter $\alpha^{(42)} : \text{Pr}$ are as follows:

$$\frac{\partial N_1^{(i)}}{\partial \alpha^{(42)}} = \frac{\partial N_1^{(i)}}{\partial \text{Pr}} \equiv a_1^{i,42} = \frac{1}{\bar{R}} \left[\frac{P_{vs}^{(i+1)}(T_w^{(i+1)}, \alpha)}{T_w^{(i+1)}} - \frac{\omega^{(i)} P_{atm}}{(0.622 + \omega^{(i)}) T_a^{(i)}} \right] \frac{\partial M(m_a, \alpha)}{\partial \text{Pr}};$$

$$\ell = 1; \ i = 1, \dots, I; \ j = 42.$$
(E.406)

where $\frac{\partial M(m_a, \alpha)}{\partial \text{Pr}}$ was defined previously in Eq. (E.81).

The derivatives of the “liquid continuity equations” [cf. Eqs. (2.38) - (2.40)] with respect to the parameter $\alpha^{(43)} : w_{tsa}$ are as follows:

$$\frac{\partial N_1^{(i)}}{\partial \alpha^{(43)}} = \frac{\partial N_1^{(i)}}{\partial w_{tsa}} \equiv a_1^{i,43} = \frac{1}{\bar{R}} \left[\frac{P_{vs}^{(i+1)}(T_w^{(i+1)}, \alpha)}{T_w^{(i+1)}} - \frac{\omega^{(i)} P_{atm}}{(0.622 + \omega^{(i)}) T_a^{(i)}} \right] \frac{\partial M(m_a, \alpha)}{\partial w_{tsa}};$$

$$\ell = 1; \ i = 1, \dots, I; \ j = 43.$$
(E.407)

where $\frac{\partial M(m_a, \alpha)}{\partial w_{tsa}}$ was defined in Eq. (E.84).

The derivatives of the “liquid continuity equations” [cf. Eqs. (2.38) - (2.40)] with respect to the parameter $\alpha^{(44)} : m_{w,in}$ are as follows:

$$\frac{\partial N_1^{(1)}}{\partial \alpha^{(44)}} = \frac{\partial N_1^{(1)}}{\partial m_{w,in}} \equiv a_1^{1,44} = -1; \quad \ell = 1; \ i = 1; \ j = 44,$$
(E.408)

APPENDIX E. DERIVATIVES OF THE MODEL EQUATIONS WITH
RESPECT TO THE MODEL PARAMETERS

$$\frac{\partial N_1^{(i)}}{\partial \alpha^{(44)}} = \frac{\partial N_1^{(i)}}{\partial m_{w,in}} \equiv a_1^{i,44} = 0; \quad \ell = 1; \quad i = 2, \dots, I; \quad j = 44. \quad (\text{E.409})$$

The derivatives of the “liquid continuity equations” [cf. Eqs. (2.38) - (2.40)] with respect to the parameter $\alpha^{(45)} : T_{a,in}$ are as follows:

$$\frac{\partial N_1^{(i)}}{\partial \alpha^{(45)}} = \frac{\partial N_1^{(i)}}{\partial T_{a,in}} \equiv a_1^{i,45} = 0; \quad \ell = 1; \quad i = 1, \dots, I; \quad j = 45. \quad (\text{E.410})$$

The derivatives of the “liquid continuity equations” [cf. Eqs. (2.38) - (2.40)] with respect to the parameter $\alpha^{(46)} : \omega_{in}$ are as follows:

$$\frac{\partial N_1^{(i)}}{\partial \alpha^{(46)}} = \frac{\partial N_1^{(i)}}{\partial \omega_{in}} \equiv a_1^{i,46} = 0; \quad \ell = 1; \quad i = 1, \dots, I; \quad j = 46. \quad (\text{E.411})$$

The derivatives of the “liquid continuity equations” [cf. Eqs. (2.38) - (2.40)] with respect to the parameter $\alpha^{(47)} : Sc$ are as follows:

$$\begin{aligned} \frac{\partial N_1^{(i)}}{\partial \alpha^{(47)}} = \frac{\partial N_1^{(i)}}{\partial Sc} \equiv a_1^{i,47} = \frac{1}{R} \left[\frac{P_{vs}^{(i+1)}(T_w^{(i+1)}, \alpha)}{T_w^{(i+1)}} - \frac{\omega^{(i)} P_{atm}}{(0.622 + \omega^{(i)}) T_a^{(i)}} \right] \frac{\partial M(m_a, \alpha)}{\partial Sc}; \\ \ell = 1; \quad i = 1, \dots, I; \quad j = 47. \end{aligned} \quad (\text{E.412})$$

where $\frac{\partial M(m_a, \alpha)}{\partial Sc}$ was defined previously in Eq. (E.91).

Bibliography

- [1] CACUCI, D.G., *Sensitivity theory for nonlinear systems: I. Nonlinear functional analysis approach*, J. Math. Phys., **22**, pp. 2794-2802, 1981;
- [2] CACUCI, D.G., *Sensitivity theory for nonlinear systems: II. Extensions to Additional Classes of Responses*, J. Math. Phys., **22**, pp. 2803-2812, 1981;
- [3] CACUCI, D.G., *Sensitivity and Uncertainty Analysis: Theory*, **Vol. 1**, Chapman & Hall/CRC, Boca Raton, USA, 2003;
- [4] CACUCI, D.G.; IONESCU-BUJOR, M.; NAVON, I.M., *Sensitivity and Uncertainty Analysis: Applications to Large Scale Systems*, **Vol. 2**, Chapman & Hall/CRC, Boca Raton, USA, 2005;
- [5] CACUCI, D.G., *Second-order adjoint sensitivity analysis methodology (2^{nd} -ASAM) for computing exactly and efficiently first-and second-order sensitivities in large-scale linear systems: I. Computational methodology*, J. Comp. Phys., **284**, pp. 687-699, 2015;
- [6] CACUCI, D.G., *Second-order adjoint sensitivity analysis methodology (2^{nd} -ASAM) for computing exactly and efficiently first-and second-order sensitivities in large-scale linear systems: II. Illustrative application to a paradigm particle diffusion problem*, J. Comp. Phys., **284**, pp. 700-717, 2015;

BIBLIOGRAPHY

- [7] CACUCI, D.G., *The Second-Order Adjoint Sensitivity Analysis Methodology for Nonlinear Systems - I: Theory*, Nucl. Sci. Eng., **184**, pp. 16-30, 2016;
- [8] CACUCI, D.G., *The Second-Order Adjoint Sensitivity Analysis Methodology for Nonlinear Systems - II: Illustrative Application to a Nonlinear Heat Conduction Problem*, Nucl. Sci. Eng., **184**, pp. 31-52, 2016;
- [9] CECCHINI, G.; FARINELLI, U.; GANDINI, A.; SALVATORE, M., *Analysis of integral data for few-group parameter evaluation of fast reactors*, Proc. 3rd Int. Conf. on Peaceful Uses of Atomic Energy, **Vol. 2**, pp. 388-397, Geneva, 1964;
- [10] HUMI, M.; WAGCSCHAL, J.J.; YEIVIN, Y., *Multi-group Constants From Integral Data*, Proc. 3rd Int. Conf. on Peaceful Uses of Atomic Energy, **Vol. 2**, p. 398, Geneva, 1964;
- [11] USACHHEV, L.N., *Perturbation Theory for the Breeding Ratio and for Other Number Ratios Pertaining to Various Reactor Processes*, J. Nuc. Energy Part A/B, **18**, p. 571, 1964;
- [12] ROWLANDS, J., et al., *The Production and Performance of the Adjusted Cross-Section Set FGL5*, Proc. Int. Symposium "Physics of Fast Reactors", Tokyo, 1973;
- [13] GANDINI, A.; PETILLI, M., *A Code Using the Lagrange Multipliers Method for Nuclear Data Adjustment*, CNEN-RI/FI(73)39, Comitato Nazionale Energia Nucleare, Casaccia/Rome, Italy, 1973;
- [14] KUROI, H.; MITANI, H., *Adjustment to Cross-Section Data to Fit Integral Experiments by Least Squares Method*, J. Nuc. Sci. Technology, **12**, p. 663, 1975;

BIBLIOGRAPHY

- [15] DRAGT, J.B, et al., *Methods of Adjustment and Error Evaluation of Neutron Capture Cross Sections*, Nucl. Sci. Eng., **62**, p. 117, 1977;
- [16] WEISBIN, C.R, et al., *Application of Sensitivity and Uncertainty Methodology to Fast Reactor Integral Experiment Analysis*, Nucl. Sci. Eng., **66**, p. 307, 1978;
- [17] BARHEN, J.; CACUCI, D.G., et al., *Uncertainty Analysis of Time-Dependent Nonlinear Systems: Theory and Application to Transient Thermal Hydraulics*, Nucl. Sci. Eng., **81**, pp. 23-44, 1982;
- [18] LEWIS, J.M.; LAKSHMIVARAHAN, S.; DHALL, S.K, *Dynamic Data Assimilation: A Least Square Approach*, Cambridge University Press, Cambridge, 1978;
- [19] LAHOZ, W.; KHATTATOV, B.; MÉNARD R., Editors, *Data Assimilation: Making Sense of Observations*, Springer Verlag, 2010;
- [20] CACUCI, D.G.; NAVON, M.I.; IONESCU-BUJOR, M., *Computational Methods for Data Analysis and Assimilation*, Nucl. Sci. Eng., Chapman & Hall/CRC, Boca Raton, 2011;
- [21] CACUCI, D.G.; IONESCU-BUJOR, M., *Model Calibration and Best-Estimate Prediction Through Experimental Data Assimilation: I. Mathematical Framework*, Nucl. Sci. Eng., **165**, pp. 18-44, 2010;
- [22] CACUCI, D.G.; BADEA, M.C., *Predictive Modeling of Coupled Multi-Physics Systems: II. Illustrative Applications to Reactor Physics*, Ann. Nucl. Energy, **70**, pp. 279-291, 2014;
- [23] LATTEN, C.; CACUCI, D. G., *Predictive Modeling of Coupled Systems: Uncertainty Reduction Using Multiple Reactor Physics Benchmarks*, Nucl. Sci. Eng., **178**, pp. 156-171, 2014;

BIBLIOGRAPHY

- [24] CACUCI, D.G.; ARSLAN, E., *Reducing Uncertainties via Predictive Modeling: FLICA4 Calibration Using BFBT Benchmarks*, Nucl. Sci. Eng., **176**, pp. 339-349, 2014;
- [25] ARSLAN, E.; CACUCI, D. G., *Predictive Modeling of Liquid-Sodium Thermal-Hydraulics Experiments and Computations*, Ann. Nucl. Energy, **63C**, pp. 355-370, 2014;
- [26] ALEMAN, S.E.; GARRETT, A.J., *Operational Cooling Tower Model (CT-Tool v1.0)*, SRNL-STI-2015-00039, Revision 0, Savannah River National Laboratory, Savannah River, SC, USA, January 2015;
- [27] CACUCI, D. G., *Predictive Modeling of Coupled Multi-Physics Systems: I. Theory*, Ann. Nucl. Energy, **70**, pp. 266-278, 2014;
- [28] CACUCI, D.G.; DI ROCCO F., *Predictive Modeling of a Buoyancy-Operated Cooling Tower Under Saturated Conditions - I: Adjoint Sensitivity Model*, Nucl. Sci. Eng., **185**, pp. 484-548, 2017;
- [29] DI ROCCO, F.; CACUCI, D.G.; BADEA M.C., *Predictive Modeling of a Buoyancy-Operated Cooling Tower Under Saturated Conditions - II: Optimal Best-Estimate Results with Reduced Predicted Uncertainties*, Nucl. Sci. Eng., **185**, pp. 549-603, 2017;
- [30] DI ROCCO F.; CACUCI D.G., *Predictive Modeling of a Buoyancy-Operated Cooling Tower Under Saturated Conditions: Adjoint Sensitivity Model and Optimal Best-Estimate Results with Reduced Predicted Uncertainties*, Energies, **9**, p. 1028, 2016;
- [31] FANG, R.; CACUCI, D.G.; BADEA, M.C., *Predictive Modeling of a Paradigm Mechanical Cooling Tower: II. Optimal Best-Estimate Results with Reduced Predicted Uncertainties*, Energies, **9**, p. 747, 2016;

BIBLIOGRAPHY

- [32] FANG, R.; CACUCI, D.G.; BADEA, M.C., *Sensitivity and Uncertainty Analysis of Counter-Flow Mechanical Draft Cooling Towers - II: Predictive Modeling*, Nuclear Technology, **198**, pp. 132-192, 2017;
- [33] GARRETT, A.J.; PARKER M. J.; VILLA-ALEMAN E., 2004 *Savannah River site Cooling Tower Collection*, SRNL-DOD-2005-07, Atmospheric Technologies Group, Savannah River National Laboratory, Aiken, SC, USA, May 2005;
- [34] COLLIER, M.; HINDMARSH, A.C.; SERBAN R.; WOODWARD, C. S., *User Documentation for KINSOL v2.8.2*, Center for Applied Scientific Computing of Lawrence Livermore National Laboratory, CA, USA, 2015;
- [35] OPPE, T.C.; JOUBERT, W.D.; KINCAID, D.R., *A Package for Solving Large Sparse Linear Systems by Various Iterative Methods*, NSPCG User's Guide, Version 1.0. Center for Numerical Analysis, the University of Texas at Austin, April 1988;
- [36] SAAD, Y.; SCHULTZ, M.H., *GMRES: A Generalized Minimal Residual Algorithm for Solving Nonsymmetric Linear Systems*, SIAM J. Sci. Stat. Comp., **7**, No. 3, pp. 856-869, 1986;
- [37] CACUCI, D.G.; IONESCU-BUJOR, M., *On the Evaluation of Discrepant Scientific Data with Unrecognized Errors*, Nucl. Sci. Eng., **165**, pp. 1-17, 2010;
- [38] FARAGÓ, I.; HAVASI, A.; ZLATEV, Z., Editors, *Advanced Numerical Methods for Complex Environmental Models: Needs and Availability*, Bentham Science Publishers, Oak Park, IL 60301-0446, USA, 2014;

BIBLIOGRAPHY

- [39] CACUCI, D.G.; NAVON, M.I.; IONESCU-BUJOR, M., *Computational Methods for Data Evaluation and Assimilation*, Chapman & Hall/CRC, Boca Raton, 2014;